



Dominion[®]

**North Anna
Early Site Permit
Application**

September 2003

Revision 1
October 2003

NRC is granted permission to place copies of this information on its public document database and make as many copies as necessary to fulfill its internal and public dissemination requirements.

EARLY SITE PERMIT APPLICATION Contents

Part 1: Administrative Information

Chapter 1	Introduction	1-1-1
1.1	Purpose of an Early Site Permit Application.	1-1-3
1.2	Early Site Permit Application Format and Content	1-1-4
	1.2.1 Format and Content	1-1-4
	1.2.2 Labeling Conventions	1-1-5
	1.2.3 Industry Coordination	1-1-6
1.3	Information Required by 10 CFR 50.33(a) through (d)	1-1-7

Part 2: Site Safety Analysis Report

Chapter 1	Introduction and General Description	2-1-1
1.1	Introduction	2-1-1
1.2	General Site Description.	2-1-3
	1.2.1 Site Location	2-1-3
	1.2.2 Site Development	2-1-3
1.3	Plant Parameters Envelope	2-1-9
	1.3.1 Plant Parameters Envelope Approach	2-1-9
	1.3.2 Overview of Reactor Types Used for PPE Development	2-1-10
	1.3.3 Use of the PPE Tables	2-1-13
1.4	Identification of Agents and Contractors	2-1-41
	1.4.1 Bechtel Power Corporation	2-1-41
	1.4.2 Other Contractors	2-1-41
1.5	Requirements for Further Technical Information.	2-1-43
1.6	Material Incorporated by Reference.	2-1-44
1.7	Drawings and Other Detailed Information.	2-1-45
1.8	Conformance to NRC Regulations and Regulatory Guidance	2-1-46
	1.8.1 Conformance with NRC Regulations	2-1-46
	1.8.2 Conformance to NRC Regulatory Guides	2-1-57
	1.8.3 Conformance to NRC Review Standard	2-1-69
Chapter 2	Site Characteristics	2-2-1
2.1	Introduction	2-2-1
	2.1.1 Site Location and Description	2-2-1

Contents

2.1.2	Exclusion Area Authority and Control	2-2-3
2.1.3	Population Distribution	2-2-4
2.2	Nearby Industrial, Transportation, and Military Facilities	2-2-28
2.2.1	Location and Routes	2-2-28
2.2.2	Descriptions	2-2-28
2.2.3	Evaluation of Potential Accidents	2-2-30
2.3	Meteorology	2-2-36
2.3.1	Regional Climatology	2-2-36
2.3.2	Local Meteorology	2-2-41
2.3.3	Onsite Meteorological Measurements Program	2-2-45
2.3.4	Short-Term (Accident) Diffusion Estimates	2-2-49
2.3.5	Long-Term (Routine) Diffusion Estimates	2-2-52
2.4	Hydrology	2-2-98
2.4.1	Hydrologic Description	2-2-98
2.4.2	Floods	2-2-104
2.4.3	Probable Maximum Flood on Streams and Rivers	2-2-106
2.4.4	Potential Dam Failures	2-2-111
2.4.5	Probable Maximum Surge and Seiche Flooding	2-2-111
2.4.6	Probable Maximum Tsunami Flooding	2-2-112
2.4.7	Ice Effects	2-2-112
2.4.8	Cooling Water Canals and Reservoirs	2-2-116
2.4.9	Channel Diversions	2-2-118
2.4.10	Flooding Protection Requirements	2-2-118
2.4.11	Low Water Considerations	2-2-119
2.4.12	Groundwater	2-2-122
2.4.13	Accidental Releases of Liquid Effluents to Ground and Surface Waters	2-2-133
2.5	Geology, Seismology, and Geotechnical Engineering	2-2-169
2.5.1	Basic Geologic and Seismic Information	2-2-169
2.5.2	Vibratory Ground Motion	2-2-226
2.5.3	Surface Faulting	2-2-263
2.5.4	Stability of Subsurface Materials and Foundations	2-2-271
	Appendix 2.5.4A Triaxial and Consolidation Tests of Soils at SWR	2-5.4A-1

Contents

	Appendix 2.5.4B Final Report, Results of Geotechnical Exploration and Testing, North Anna ESP Project, Louisa County, Virginia, Prepared by MACTEC Engineering and Consulting, MACTEC Project Number 30720-2-5400, February 2003	2-5.4A-1
	2.5.5 Stability of Slopes	2-2-304
	2.5.6 Embankments and Dams	2-2-310
Chapter 3	Design of Structures, Components, Equipment, and Systems	2-3-1
Chapter 13	Conduct of Operations	2-13-1
13.3	Emergency Planning	2-13-1
13.3.1	Emergency Planning Overview	2-13-1
13.3.2	Major Features Emergency Plan	2-13-1
13.3.3	Contracts and Arrangements	2-13-33
13.3.4	Conformance with NUREG-0652, Supplement 2	2-13-34
13.6	Industrial Security	2-13-39
Chapter 15	Accident Analyses	2-15-1
15.1	Selection of Accidents	2-15-1
15.2	Evaluation Methodology	2-15-3
15.3	Source Terms	2-15-5
15.4	Radiological Consequences	2-15-6
Chapter 17	Quality Assurance	2-17-1
17.1	ESP Quality Assurance	2-17-1
Part 3: Environmental Report		
Chapter 1	Introduction	3-1-1
1.1	The Proposed Action	3-1-1
1.1.1	The Applicant and Owner	3-1-2
1.1.2	Site Location	3-1-2
1.1.3	Reactor Information	3-1-2
1.1.4	Cooling System Information	3-1-3
1.1.5	Transmission System Information	3-1-3
1.1.6	Pre-Application Public Involvement	3-1-3
1.1.7	Construction Start Date	3-1-4

Contents

	1.2 Status of Reviews, Approvals, and Consultations	3-1-6
Chapter 2	Environmental Description	3-2-1
	2.1 Site Location	3-2-1
	2.2 Land	3-2-6
	2.2.1 The Site and Vicinity	3-2-6
	2.2.2 Transmission Corridors and Offsite Areas	3-2-9
	2.2.3 The Region	3-2-10
	2.3 Water	3-2-20
	2.3.1 Hydrology	3-2-20
	2.3.2 Water Use	3-2-27
	2.3.3 Water Quality	3-2-33
	2.4 Ecology	3-2-65
	2.4.1 Terrestrial Ecology	3-2-65
	2.4.2 Aquatic Ecology	3-2-68
	2.5 Socioeconomics	3-2-90
	2.5.1 Demography	3-2-90
	2.5.2 Community Characteristics	3-2-98
	2.5.3 Historic Properties	3-2-105
	2.5.4 Environmental Justice	3-2-108
	2.6 Geology	3-2-147
	2.6.1 Geological Conditions	3-2-147
	2.6.2 Seismological Conditions	3-2-149
	2.6.3 Geotechnical Conditions	3-2-151
	2.6.4 Environmental Impact Evaluation	3-2-152
	2.7 Meteorology and Air Quality	3-2-170
	2.7.1 General Climate	3-2-170
	2.7.2 Regional Air Quality	3-2-172
	2.7.3 Severe Weather	3-2-173
	2.7.4 Local Meteorology	3-2-176
	2.7.5 Short-Term Diffusion Estimates	3-2-180
	2.7.6 Long-Term (Routine) Diffusion Estimates	3-2-181
	2.8 Related Federal Project Activities	3-2-246

Contents

Chapter 3	Plant Description	3-3-1
3.1	External Appearance and Plant Layout	3-3-2
3.1.1	Existing Site Development	3-3-2
3.1.2	Power Plant Design	3-3-2
3.1.3	Plant Parameters Envelope	3-3-4
3.1.4	Plant Appearance	3-3-4
3.1.5	Site Development and Improvements	3-3-5
3.2	Reactor Power Conversion System	3-3-37
3.2.1	Reactor Description	3-3-37
3.2.2	Engineered Safety Features	3-3-37
3.2.3	Power Conversion Systems	3-3-38
3.3	Plant Water Use	3-3-39
3.3.1	Water Consumption	3-3-39
3.3.2	Water Treatment	3-3-40
3.4	Cooling System	3-3-47
3.4.1	Description and Operational Modes	3-3-47
3.4.2	Component Descriptions	3-3-51
3.5	Radioactive Waste Management System	3-3-65
3.5.1	Liquid Radioactive Waste Management System	3-3-65
3.5.2	Gaseous Radioactive Waste Management System	3-3-66
3.5.3	Solid Radioactive Waste Management System	3-3-66
3.6	Nonradioactive Waste Systems	3-3-68
3.6.1	Effluents Containing Chemicals or Biocides	3-3-68
3.6.2	Sanitary System Effluents	3-3-68
3.6.3	Other Effluents	3-3-69
3.7	Power Transmission System	3-3-70
3.7.1	Switchyard Interfaces	3-3-70
3.7.2	Transmission System	3-3-70
3.8	Transportation of Radioactive Materials	3-3-72
3.8.1	Light-Water-Cooled Reactors	3-3-72
3.8.2	Gas-Cooled Reactors	3-3-75
3.8.3	Methodology Assessment	3-3-82

Contents

Chapter 4	Environmental Impacts of Construction	3-4-1
4.1	Land-Use Impacts	3-4-1
4.1.1	The Site and Vicinity	3-4-1
4.1.2	Transmission Corridors and Offsite Areas	3-4-5
4.1.3	Historic Properties and Cultural Resources	3-4-6
4.2	Water-Related Impacts	3-4-9
4.2.1	Hydrologic Alterations	3-4-9
4.2.2	Water-Use Impacts	3-4-11
4.3	Ecological Impacts	3-4-14
4.3.1	Terrestrial Ecosystems	3-4-14
4.3.2	Aquatic Ecosystems	3-4-16
4.4	Socioeconomic Impacts	3-4-21
4.4.1	Physical Impacts	3-4-21
4.4.2	Social and Economic Impacts	3-4-27
4.4.3	Environmental Justice Impacts	3-4-34
4.5	Radiation Exposure to Construction Workers	3-4-36
4.5.1	Site Layout	3-4-36
4.5.2	Radiation Sources	3-4-36
4.5.3	Measured and Calculated Dose Rates	3-4-36
4.5.4	Construction Worker Doses	3-4-37
4.6	Measures and Controls to Limit Adverse Impacts During Construction	3-4-42
Chapter 5	Environmental Impacts of Station Operation	3-5-1
5.1	Land-Use Impacts	3-5-2
5.1.1	The Site and Vicinity	3-5-2
5.1.2	Transmission Corridors and Offsite Areas	3-5-3
5.1.3	Historic Properties	3-5-3
5.2	Water-Related Impacts	3-5-4
5.2.1	Hydrologic Alterations and Plant Water Supply	3-5-4
5.2.2	Water-Use Impacts	3-5-8
5.3	Cooling System Impacts	3-5-19
5.3.1	Intake System	3-5-19
5.3.2	Discharge System	3-5-39
5.3.3	Heat-Discharge System	3-5-60

Contents

	5.3.4 Impacts to Members of the Public	3-5-65
5.4	Radiological Impacts of Normal Operation	3-5-98
	5.4.1 Exposure Pathways	3-5-98
	5.4.2 Radiation Doses to Members of the Public	3-5-99
	5.4.3 Impacts to Members of the Public	3-5-100
	5.4.4 Impacts to Biota Other than Members of the Public	3-5-100
5.5	Environmental Impact of Waste	3-5-114
	5.5.1 Nonradioactive-Waste-System Impacts	3-5-114
	5.5.2 Mixed Waste Impacts	3-5-116
	5.5.3 Conclusions	3-5-119
5.6	Transmission System Impacts	3-5-121
	5.6.1 Terrestrial Ecosystems	3-5-121
	5.6.2 Aquatic Ecosystems	3-5-123
	5.6.3 Impacts to Members of the Public	3-5-124
5.7	Uranium Fuel Cycle Impacts	3-5-128
	5.7.1 Light-Water-Cooled Reactors	3-5-128
	5.7.2 Gas-cooled Reactors	3-5-129
	5.7.3 Methodology Assessment	3-5-136
5.8	Socioeconomic Impacts	3-5-146
	5.8.1 Physical Impacts of Station Operation	3-5-146
	5.8.2 Social and Economic Impacts of Station Operation	3-5-149
	5.8.3 Environmental Justice Impacts	3-5-155
5.9	Decommissioning	3-5-159
5.10	Measures and Controls to Limit Adverse Impacts During Operation	3-5-161
Chapter 6	Environmental Measurements and Monitoring Programs	3-6-1
6.1	Thermal Monitoring	3-6-1
	6.1.1 Existing Thermal Monitoring Program	3-6-1
	6.1.2 Pre-Application, Pre-Operational, and Operational Thermal Monitoring ...	3-6-2
6.2	Radiological Monitoring	3-6-6
	6.2.1 Radiological Environmental Monitoring Program Basis	3-6-6
	6.2.2 Radiological Environmental Monitoring Program Contents	3-6-6
	6.2.3 Radiological Environmental Monitoring Program Reporting	3-6-7
	6.2.4 Quality Assurance Program	3-6-7

Contents

6.3	Hydrological Monitoring	3-6-10
	6.3.1 Existing Hydrological Monitoring	3-6-10
	6.3.2 Construction and Pre-Operational Monitoring	3-6-10
	6.3.3 Operational Monitoring	3-6-11
6.4	Meteorological Monitoring	3-6-13
	6.4.1 General Description – Onsite Meteorological Monitoring Program	3-6-13
	6.4.2 Instrument Calibration and Maintenance	3-6-16
	6.4.3 Data Recording Systems	3-6-16
	6.4.4 Meteorological Data Analysis Procedure	3-6-17
	6.4.5 Preoperational and Operational Monitoring	3-6-17
6.5	Ecological Monitoring	3-6-21
	6.5.1 Terrestrial Ecology and Land Use	3-6-21
	6.5.2 Aquatic Ecology	3-6-23
6.6	Chemical Monitoring	3-6-28
	6.6.1 Pre-Application Monitoring	3-6-28
	6.6.2 Construction and Pre-Operational Monitoring	3-6-29
	6.6.3 Operational Monitoring	3-6-30
6.7	Summary of Monitoring Programs	3-6-38
	6.7.1 Pre-Application Monitoring	3-6-38
	6.7.2 Construction and Pre-Operational Monitoring	3-6-38
	6.7.3 Operational Monitoring	3-6-38
Chapter 7	Environmental Impacts of Postulated Accidents Involving Radioactive Materials	3-7-1
7.1	Design Basis Accidents	3-7-1
	7.1.1 Selection of Accidents	3-7-1
	7.1.2 Evaluation Methodology	3-7-2
	7.1.3 Source Terms	3-7-3
	7.1.4 Radiological Consequences	3-7-3
7.2	Severe Accidents	3-7-30
	7.2.1 Applicability of Existing Generic Severe Accident Studies	3-7-30
	7.2.2 Evaluation of Potential Severe Accident Releases	3-7-32
	7.2.3 Evaluation of Economic Impacts of Severe Accidents	3-7-36
	7.2.4 Consideration of Commission Severe Accident Policy	3-7-37

Contents

	7.2.5 Conclusion	3-7-38
7.3	Severe Accident Mitigation Alternatives	3-7-40
7.4	Transportation Accidents	3-7-41
Chapter 8	Need for Power	3-8-1
Chapter 9	Alternatives to the Proposed Action	3-9-1
9.1	No-Action Alternative	3-9-1
9.2	Energy Alternatives	3-9-1
9.3	Alternative Sites	3-9-1
	9.3.1 Technical Approach	3-9-1
	9.3.2 Region Of Interest	3-9-1
	9.3.3 Identification of Candidate Sites	3-9-2
	9.3.4 Alternative Sites Evaluation	3-9-6
9.4	Alternative Plant and Transmission Systems	3-9-12
	9.4.1 Heat Dissipation Systems	3-9-12
	9.4.2 Circulating Water Systems	3-9-20
	9.4.3 Transmission Systems	3-9-23
Chapter 10	Environmental Consequences of the Proposed Action	3-10-1
10.1	Unavoidable Adverse Environmental Impacts	3-10-1
	10.1.1 Unavoidable Adverse Environmental Impacts During Construction	3-10-1
	10.1.2 Unavoidable Adverse Environmental Impacts During Operation	3-10-2
	10.1.3 Summary of Adverse Environmental Impacts	3-10-2
	10.1.4 Irreversible and Irretrievable Commitment of Resources	3-10-3
10.2	Irreversible and Irretrievable Commitments of Resources	3-10-18
	10.2.1 Irreversible Environmental Commitments	3-10-18
	10.2.2 Irretrievable Commitments of Resources	3-10-20
10.3	Relationship Between Short-Term Uses and Long-Term Productivity of the Human Environment	3-10-22
	10.3.1 Construction of New Units at ESP Site and Long-Term Productivity	3-10-22
	10.3.2 Operation of the New Units and Long-Term Productivity	3-10-23
	10.3.3 Summary of Relationship Between Short-Term Uses and Long-Term Productivity	3-10-24
10.4	Benefit – Cost Balance	3-10-26

Contents

Part 4: Programs and Plans

Chapter 1	Site Redress	4-1-1
1.1	Description of Site Preparation Activities	4-1-1
1.2	Site Redress Plan	4-1-3
1.2.1	Site Redress Plan Objective and Considerations	4-1-3
1.2.2	Description of Site Redress	4-1-4
1.2.3	NRC Notification Upon Completion	4-1-9

Tables

Part 1: Administrative Information

Table 1.3-1	Dominion Nuclear North Anna, LLC, Officers and Directors	1-1-8
-------------	--	-------

Part 2: Site Safety Analysis Report

Table 1.3-1	Plant Parameters Envelope.	2-1-14
Table 1.3-2	Bounding Value Notes for Table 1.3-1	2-1-35
Table 1.3-3	Blowdown Constituents and Concentrations.	2-1-36
Table 1.3-4	Yearly Emissions Auxiliary Boilers	2-1-37
Table 1.3-5	Yearly Emissions From Standby Diesel Generators	2-1-37
Table 1.3-6	Standby Power System Gas Turbine Flue Gas Effluents	2-1-38
Table 1.3-7	Radionuclides in Annual Normal Liquid Releases (ci/yr).	2-1-39
Table 1.3-8	Radionuclides in Annual Normal Gaseous Releases (ci/yr)	2-1-40
Table 2.1-1	Lake Anna Recreational Facilities.	2-2-12
Table 2.1-2	Tourist Attractions, Parks and Recreational Areas	2-2-13
Table 2.1-3	Schools Within 10 Miles of ESP Site.	2-2-13
Table 2.2-1	Airports Within 15 Miles of the ESP Site	2-2-34
Table 2.2-2	Toxic Chemicals– Largest Single Container Stored at the NAPS Site	2-2-34
Table 2.3-1	ESP Site Tornado Parameters	2-2-39
Table 2.3-2	NWS Stations Near ESP Site	2-2-41
Table 2.3-3	PAVAN Results (0.5% Limiting Case, 1996-98 Meteorological Data).	2-2-52
Table 2.3-4	Extreme 1-Mile Wind Passage at Richmond, Virginia.	2-2-57
Table 2.3-5	Selected National Weather Service Stations for Meteorological Extremes in the ESP Site Region (Date of Occurrence).	2-2-57
Table 2.3-6	Richmond Climatological Data	2-2-58
Table 2.3-7	Mean Annual Meteorological Data for Stations in the Site Region	2-2-59
Table 2.3-8	ESP Site Mean Wind Speeds (MPH) 1974-1987	2-2-59
Table 2.3-9	ESP Site Vertical Stability (ΔT) and Low Level Wind Speed Distribution 1974-1987.	2-2-60
Table 2.3-10	Meteorological Data Recovery Rates (percent) (ESP Site, January 1, 1996 – December 31, 2001)	2-2-61
Table 2.3-11	Primary Tower Parameters	2-2-61
Table 2.3-12	Backup Tower Parameters	2-2-62
Table 2.3-13	PAVAN Results for χ/Q Values at the EAB.	2-2-63
Table 2.3-14	PAVAN Results for χ/Q Values at the LPZ	2-2-65
Table 2.3-15	ESP Application Nearby Sensitive Receptors.	2-2-67
Table 2.3-16	XOQDOQ Predicted Maximum χ/Q and D/Q Values at Specific Points of Interest	2-2-68
Table 2.3-17	XOQDOQ Predicted Maximum Annual Averages (Ground-Level Release)	2-2-69

Table 2.4-1	Lake Anna Storage Allocation	2-2-101
Table 2.4-2	Mean Monthly Hydrologic Statistics for Lake Anna	2-2-103
Table 2.4-3	North Anna Power Station Local Probable Maximum Precipitation Values	2-2-105
Table 2.4-4	Maximum Precipitation Depths.	2-2-107
Table 2.4-5	Lake Anna Annual Minimum Water Level	2-2-120
Table 2.4-6	Lake Anna Low Water Level Durations	2-2-122
Table 2.4-7	Probable Maximum Precipitation Temporal Distribution	2-2-139
Table 2.4-8	February 1979 Rainfall Data	2-2-140
Table 2.4-9	March 1994 Rainfall Data	2-2-141
Table 2.4-10	June 1995 Rainfall Data	2-2-142
Table 2.4-11	Lake Anna Watershed HEC-1 Precipitation Loss Rates	2-2-142
Table 2.4-12	Historic Minimum Intake Water Temperature of Less Than 4°C (39.2°F) During The Operation of North Anna Units 1 and 2 from 1978 to 2001	2-2-143
Table 2.4-13	Historic Winter Minimum and Mean Low Daily Temperature with Durations Equal to or Exceeding 5 Days in Richmond, Virginia, for the Period of 1961 to 1995 (Reference 24)	2-2-143
Table 2.4-14	Annual Peak Discharges On the North Anna River.	2-2-145
Table 2.4-15	Quarterly Groundwater Level Elevations.	2-2-146
Table 2.4-16	Hydraulic Conductivity Values.	2-2-147
Table 2.4-17	North Anna Power Station Water Supply Wells	2-2-148
Table 2.4-18	North Anna Power Station Groundwater Use January 1, 2002 to December 31, 2002 (Millions of Gallons)	2-2-149
Table 2.4-19	Public Groundwater Supplies In Louisa County	2-2-150
Table 2.5-1	Definitions of Classes Used in the Compilation of Quaternary Faults, Liquefaction Features, and Deformation in the Central and Eastern United States (After Crone and Wheeler, 2000)	2-2-328
Table 2.5-2	Quaternary Faults, Liquefaction Features, and Possible Tectonic Features Within the Site Region (200-Mile Radius) (Modified from Crone)	2-2-329
Table 2.5-3	Site Area Stratigraphic Column (5-Mile Radius)	2-2-330
Table 2.5-4	Earthquakes 1985-2001, $m \geq 3.0$, within 35°N–41°N and 74°W–82°W	2-2-331
Table 2.5-5	Summary of Bechtel Seismic Sources	2-2-332
Table 2.5-6	Summary of Dames & Moore Seismic Sources	2-2-334
Table 2.5-7	Summary of Law Engineering Seismic Sources	2-2-336
Table 2.5-8	Summary of Rondout Seismic Sources.	2-2-339
Table 2.5-9	Summary of Weston Seismic Sources	2-2-341
Table 2.5-10	Summary of Woodward-Clyde Seismic Sources.	2-2-345
Table 2.5-11	Comparison of EPRI Characterizations of the Central Virginia Seismic Zone	2-2-348
Table 2.5-12	Seismic Source Zone Parameters from Bollinger Study (Reference 125)	2-2-349

Table 2.5-13	Seismic Source Zone Parameters from Chapman and Krimgold Study (Reference 126)	2-2-350
Table 2.5-14	Summary of Selected USGS Seismic Sources (Reference 127)	2-2-351
Table 2.5-15	1989 EPRI PSHA Study Models	2-2-351
Table 2.5-16	Comparison of PGA Results for North Anna Using 1989 EPRI Sources and Ground Motion Models	2-2-352
Table 2.5-17	Comparison of Spectral Velocity Results for North Anna Using 1989 EPRI Sources and Ground Motion Models	2-2-352
Table 2.5-18	Seismic Sources Contributing to 99% of Hazard for Each 1989 EPRI Team	2-2-353
Table 2.5-19	Significant Seismic Source at North Anna by 1989 EPRI Team	2-2-353
Table 2.5-20	Controlling Earthquake Magnitude and Distances 1989 EPRI Sources and Ground Motion Models	2-2-353
Table 2.5-21	Spectral Amplitudes Using 1989 EPRI Sources And Ground Motion Models	2-2-354
Table 2.5-22	Updated Seismic Hazard Results at ESP Site	2-2-354
Table 2.5-23	Controlling Earthquake Magnitude and Distances, Updated Models	2-2-354
Table 2.5-24	Summary of Performance-Based Spectrum Calculations, Base Case	2-2-355
Table 2.5-25	Spectral Accelerations Corresponding to Mean 5×10^{-5} Annual Frequency	2-2-355
Table 2.5-26	Controlling Earthquake Magnitudes and Distances Corresponding to Mean 5×10^{-5} Annual Frequency	2-2-355
Table 2.5-27	Summary of Spectrum Calculations for Sensitivity Study with Increased Alternate Minimum Magnitude.	2-2-356
Table 2.5-28	Summary of Spectrum Calculations for Sensitivity Study with Alternate Aleatory Ground Motion Uncertainties	2-2-356
Table 2.5-29	Zone IIA Constituents	2-2-357
Table 2.5-30	Summary of Units 1&2 Borings—Soils	2-2-358
Table 2.5-31	Summary of Units 1 & 2 Borings—Rock	2-2-361
Table 2.5-32	Summary of Units 3 & 4 Borings—Soils	2-2-364
Table 2.5-33	Summary of Units 3 & 4 Borings—Rock	2-2-366
Table 2.5-34	Summary of Service Water Reservoir Borings—Soils	2-2-368
Table 2.5-35	Summary of Service Water Reservoir Borings—Rock	2-2-369
Table 2.5-36	Summary of ISFSI Borings—Soils	2-2-370
Table 2.5-37	Summary of ISFSI Borings—Rock	2-2-371
Table 2.5-38	Summary of ESP Borings, Observation Wells, and CPTs—Soils.	2-2-372
Table 2.5-39	Summary of ESP Borings, Observation Wells, and CPTs—Rock.	2-2-373
Table 2.5-40	Summary of Soil Sampling Results	2-2-374
Table 2.5-41	Summary of Rock Coring Results	2-2-374
Table 2.5-42	Summary of Laboratory Tests Performed	2-2-375
Table 2.5-43	Summary of ESP Laboratory Test Results	2-2-376

Table 2.5-44	Summary of ESP Laboratory Test Results—Rock	2-2-377
Table 2.5-45	Summary of Geotechnical Engineering Properties	2-2-378
Table 2.5-46	ZPA Results from SHAKE Analysis.	2-2-380
Table 2.5-47	Allowable Bearing Capacity Values.	2-2-382
Table 13.3-1	Dose Limit Guidelines	2-13-26
Table 13.3-2	Cross Reference to NUREG-0654, Supplement 2	2-13-32
Table 15.4-1	Summary of Design Basis Accident Doses.	2-15-8
Table 15.4-2	Activity Releases for AP1000 Main Steam Line Break, Pre-Existing Iodine Spike.	2-15-9
Table 15.4-3	Doses for AP1000 Main Steam Line Break, Pre-Existing Iodine Spike.	2-15-10
Table 15.4-4	Activity Releases for AP1000 Main Steam Line Break, Accident-Initiated Iodine Spike.	2-15-11
Table 15.4-5	Doses for AP1000 Main Steam Line Break, Accident-Initiated Iodine Spike	2-15-12
Table 15.4-6	Activity Releases for AP1000 Locked Rotor Accident.	2-15-13
Table 15.4-7	Doses for AP1000 Locked Rotor Accident	2-15-14
Table 15.4-8	Activity Releases for AP1000 Rod Ejection Accident	2-15-15
Table 15.4-9	Doses for AP1000 Rod Ejection Accident.	2-15-16
Table 15.4-10	Doses for AP1000 Failure of Small Lines Carrying Primary Coolant Outside Containment	2-15-16
Table 15.4-11	Activity Releases for ABWR Failure of Small Lines Carrying Primary Coolant Outside Containment.	2-15-17
Table 15.4-12	Doses for ABWR Failure of Small Lines Carrying Primary Coolant Outside Containment	2-15-17
Table 15.4-13	Activity Releases for AP1000 Steam Generator Tube Rupture, Pre-Existing Iodine Spike.	2-15-18
Table 15.4-14	Doses for AP1000 Steam Generator Tube Rupture, Pre-Existing Iodine Spike . .	2-15-19
Table 15.4-15	Activity Releases for AP1000 Steam Generator Tube Rupture, Accident-Initiated Iodine Spike	2-15-20
Table 15.4-16	Doses for AP1000 Steam Generator Tube Rupture, Accident-Initiated Iodine Spike.	2-15-21
Table 15.4-17	Activity Releases for ABWR Main Steam Line Break	2-15-22
Table 15.4-18	Doses for ABWR Main Steam Line Break, Pre-Existing Iodine Spike.	2-15-23
Table 15.4-19	Doses for ABWR Main Steam Line Break, Accident-Initiated Iodine Spike	2-15-23
Table 15.4-20	Activity Releases for AP1000 Loss-of-Coolant Accident.	2-15-24
Table 15.4-21	Doses for AP1000 Loss-of-Coolant Accident	2-15-26
Table 15.4-22	Activity Releases for ABWR Loss-of-Coolant Accident.	2-15-27
Table 15.4-23	Doses for ABWR Loss-of-Coolant Accident	2-15-28
Table 15.4-24	Activity Releases for AP1000 Fuel Handling Accident	2-15-28
Table 15.4-25	Doses for AP1000 Fuel Handling Accident.	2-15-29

Table 15.4-26	Activity Releases for ABWR Fuel Handling Accident	2-15-30
Table 15.4-27	Doses for ABWR Fuel Handling Accident	2-15-31

Part 3: Environmental Report

Table 1.2-1	Federal, State, and Local Authorizations	3-1-8
Table 2.2-1	North Anna Transmission Rights-of-Way	3-2-13
Table 2.2-2	Land Use in Louisa, Orange and Spotsylvania Counties	3-2-14
Table 2.2-3	Virginia Statewide Land Use Summary	3-2-15
Table 2.3-1	Lake Anna Storage Allocation	3-2-22
Table 2.3-2	USGS Stream Gauge Data	3-2-23
Table 2.3-3	Monthly Water Level Statistics for Lake Anna, August 1978 through March 2003 (ft msl)	3-2-23
Table 2.3-4	Consumptive Surface Water Users in the Affected Hydrologic System	3-2-28
Table 2.3-5	Consumptive Surface Water Use Statistics for the Affected Hydrologic System	3-2-29
Table 2.3-6	North Anna Power Station Water Supply Wells	3-2-32
Table 2.3-7	Daily Water Temperature Statistics for Lake Anna	3-2-34
Table 2.3-8	Monthly Streamflow Statistics (cfs)	3-2-40
Table 2.3-9	Quarterly Groundwater Level Elevations	3-2-41
Table 2.3-10	Hydraulic Conductivity Values	3-2-42
Table 2.3-11	Public Groundwater Supplies In Louisa County	3-2-43
Table 2.3-12	North Anna Power Station Groundwater Use January 1, 2002 to December 31, 2002	3-2-45
Table 2.3-13	Water Quality Statistics for Lake Anna	3-2-46
Table 2.3-14	Water Quality Data for the Piedmont Crystalline Aquifers	3-2-50
Table 2.5-1	Population Distribution from 2000 to 2040 Within 16-km (10-mi) of the ESP Site	3-2-112
Table 2.5-2	Estimated Sex Distribution of Population in 2000 Within 16-km (10-mi.) of the ESP Site	3-2-112
Table 2.5-3	Sex Distribution of Population in the Major Employee-Contributing Counties and Virginia	3-2-112
Table 2.5-4	Estimated Age Distribution of Population in 2000 Within 16-km (10-mi.) of the ESP Site	3-2-113
Table 2.5-5	Estimated Income Distribution of Population Within 16-km (10-mi) of the ESP Site (for ages greater than 15)	3-2-113
Table 2.5-6	Racial & Ethnic Distribution of Population in 2000 Within 16-km (10-mi.) of the ESP Site	3-2-114
Table 2.5-7	Income Distribution of Population in the Major Employee-Contributing Counties and Virginia (For Ages Greater Than 15)	3-2-114

Table 2.5-8	Population Distribution from 2000 to 2040 Within 80-km (50-mi) of the ESP Site	3-2-115
Table 2.5-9	Estimated Sex Distribution of Population in 2000 Within 80-km (50-mi.) of the ESP Site	3-2-115
Table 2.5-10	Estimated Age Distribution of Population in 2000 Within 80-km (50-mi) of the ESP Site	3-2-115
Table 2.5-11	Racial & Ethnic Distribution of Population in 2000 Within 80-km (50-mi) of the Site	3-2-116
Table 2.5-12	Racial and Ethnic Distribution of Population in the Major Employee-Contributing Counties and Virginia.	3-2-116
Table 2.5-13	Estimated Income Distribution of Population Within 80-km (50-mi) of the ESP Site (For Ages Greater Than 15).	3-2-117
Table 2.5-14	Age Distribution of Population in the Major Employee-Contributing Counties and Virginia	3-2-117
Table 2.5-15	Population Distribution Table	3-2-118
Table 2.5-16	Lake Anna Recreational Facilities	3-2-121
Table 2.5-17	Tourist Attractions, Parks and Recreational Areas	3-2-122
Table 2.5-18	Employment and Income Statistics by State, County, and City	3-2-123
Table 2.5-19	Major Employers in Louisa County, Virginia	3-2-123
Table 2.5-20	Major Private Employers in Orange County, Virginia	3-2-123
Table 2.5-21	Major Private Employers in Spotsylvania County, Virginia	3-2-124
Table 2.5-22	Vacant Housing Units by County During 2000	3-2-125
Table 2.5-23	Regional Fire Stations and Emergency Service Centers	3-2-125
Table 2.5-24	Historic Sites in Counties Near the ESP Site	3-2-126
Table 2.5-25	Historic Sites within the Vicinity.	3-2-127
Table 2.6-1	Summary of Geotechnical Engineering Properties	3-2-161
Table 2.7-1	NWS Stations Near ESP Site	3-2-176
Table 2.7-2	Summary of Virginia Tornado Intensities	3-2-186
Table 2.7-3	Extreme 1-Mile Wind Passage at Richmond, Virginia.	3-2-187
Table 2.7-4	Richmond Climatological Data	3-2-188
Table 2.7-5	Mean Annual Meteorological Data for Stations in the Site Region	3-2-189
Table 2.7-6	Comparison of Mean Temperature Data for North Anna, Richmond, Partlow, and Louisa (°F) (September 16, 1971–September 15, 1972).	3-2-189
Table 2.7-7	North Anna Mean Wind Speeds (mph) 1974-1987	3-2-190
Table 2.7-8	North Anna Vertical Stability (ΔT) and Low-Level Wind Speed Distribution 1974-1987.	3-2-190
Table 2.7-9	1996-98 NAPS Meteorological Data (33-ft Level).	3-2-191
Table 2.7-10	Shortest Distances from the ESP Plant Envelope Boundary to the EAB	3-2-195
Table 2.7-11	PAVAN Results for χ/Q Values at the EAB.	3-2-196

Table 2.7-12	PAVAN Results for χ/Q Values at the LPZ	3-2-200
Table 2.7-13	ESP Application Nearby Sensitive Receptors	3-2-201
Table 2.7-14	XOQDOQ Predicted Maximum χ/Q and D/Q Values at Specific Points of Interest	3-2-202
Table 2.7-15	XOQDOQ Predicted Maximum Annual Averages (Ground-Level Release)	3-2-203
Table 2.7-16	Long-Term Average χ/Q (sec/m^3) for Routine Releases at Specific Points of Interest (1996-98 Meteorological Data)	3-2-205
Table 2.7-17	Long-Term Average χ/Q (sec/m^3) for Routine Releases at Distances Between 0.25 to 50 Miles No Decay, Undepleted	3-2-207
Table 2.7-18	Long-Term Average χ/Q (sec/m^3) for Routine Releases at Distances Between 0.25 to 50 Miles 2.260-Day Decay, Undepleted	3-2-210
Table 2.7-19	Long-Term Average χ/Q (sec/m^3) for Routine Releases at Distances Between 0.25 to 50 Miles 8.000-Day Decay, Depleted	3-2-213
Table 2.7-20	Long-Term Average D/Q ($1/\text{m}^3$) for Routine Releases at Distances Between 0.25 to 50 Miles	3-2-216
Table 3.1-1	Plant Parameters Envelope	3-3-10
Table 3.1-2	Bounding Value Notes for Table 3.1-1	3-3-31
Table 3.1-3	Blowdown Constituents and Concentrations	3-3-32
Table 3.1-4	Yearly Emissions Auxiliary Boilers	3-3-33
Table 3.1-5	Yearly Emissions From Standby Diesel Generators	3-3-33
Table 3.1-6	Standby Power System Gas Turbine Flue Gas Effluents	3-3-34
Table 3.1-7	Radionuclides in Annual Normal Liquid Releases (ci/yr)	3-3-35
Table 3.1-8	Radionuclides in Annual Normal Gaseous Releases (ci/yr)	3-3-36
Table 3.3-1	Unit 3 Water Consumption	3-3-42
Table 3.3-2	Unit 4 Water Consumption	3-3-43
Table 3.8-1	LWR-S4 Transportation Impact Evaluation	3-3-84
Table 3.8-2	Gas-cooled Reactor Transportation Impact Evaluation	3-3-86
Table 3.8-3	Summary Table S-4: Environmental Impact of Transportation of Fuel and Waste to and from One Light-Water-Cooled Nuclear Power Reactor	3-3-90
Table 4.1-1	Land Use within the ESP Site and Vicinity	3-4-3
Table 4.1-2	Construction Areas	3-4-3
Table 4.3-1	Peak and Attenuated Noise (in dba) Levels Expected from Operations of Construction Equipment	3-4-16
Table 4.4-2	Distances from Construction Site to EAB	3-4-25
Table 4.4-1	Equipment and Approximate Noise Level	3-4-25
Table 4.4-3	Level-of-Service Designation Characteristics	3-4-31
Table 4.5-1	TLD Dose Measurements at West Protected Area Fence of Existing Units	3-4-40
Table 4.5-2	Annual Construction Worker Doses	3-4-40

Table 4.5-3	Comparison with 10 CFR 20.1301 Criteria for Doses to Members of the Public	3-4-40
Table 4.5-4	Comparison with 40 CFR 190 Criteria for Doses to Members of the Public	3-4-41
Table 4.5-5	Comparison with 10 CFR 50, Appendix I Criteria for Effluent Doses	3-4-41
Table 4.6-1	Summary of Measures and Controls to Limit Adverse Impacts During Construction	3-4-43
Table 5.2-1	Available Water Supply Versus Plant Water Needs	3-5-7
Table 5.2-2	Data Input for Water Balance Model	3-5-10
Table 5.2-3	Lake Anna Low Outflow Frequency	3-5-12
Table 5.2-4	Lake Anna Low Water Level Frequency	3-5-14
Table 5.3-1	Mean Number of Representative Important Fish Species Estimated Impinged per Month at the Existing Units from 1979–1983	3-5-26
Table 5.3-2	Mean Number of Representative Important Fish Species Estimated Impinged per Month at NAPS With New Unit 3 Using a Once-Through Cooling System	3-5-28
Table 5.3-3	Mean Number of Representative Important Fish Species Estimated Impinged per Month with Existing Units and a New Unit 3 Using a Once-Through Cooling System.	3-5-29
Table 5.3-4	Mean Number of Representative Important Fish Species Estimated Impinged per Month With the Operation of a New Unit 4 with Cooling Towers Using Makeup Water from North Anna Reservoir	3-5-30
Table 5.3-5	Mean Number of Representative Important Fish Species Estimated Entrained per Month From 1979-1983 With Existing Units Operating	3-5-34
Table 5.3-6	Mean Number of Representative Important Fish Species Estimated Entrained per Month With New Unit 3 Using a Once-Through Cooling System	3-5-35
Table 5.3-7	Mean Number of Representative Important Fish Species Estimated Entrained per Month With Existing Units And a New Unit 3 Using a Once-Through Cooling System	3-5-35
Table 5.3-8	Mean Number of Representative Important Fish Species Estimated Entrained per Month with the Operation of a New Unit 4 with Cooling Towers Using Makeup Water from North Anna Reservoir	3-5-37
Table 5.3-9	Lake Anna Reservoir Temperature Measurements	3-5-67
Table 5.3-10	Physical Attributes of North Anna Reservoir and WHTF	3-5-73
Table 5.3-11	Maximum, Minimum, and Average Daily Observed Surface Temperatures at Four Monitoring Stations in WHTF and North Anna Reservoir from 7/26/1978 to 4/10/2003	3-5-74
Table 5.3-12	Exceedence Frequency of Observed Daily Surface Temperatures at Four Monitoring Stations in WHTF and North Anna Reservoir from 7/26/1978 to 4/10/2003	3-5-74
Table 5.3-13	Monthly Maximum and Average Observed Surface Temperature Near Intake from 7/26/1978 to 4/10/2003	3-5-75

Table 5.3-14	Maximum and Minimum Daily Surface Temperature at Six Locations in the WHTF and the Reservoir Based on 42-years of Model Prediction from January 1961 to May 2003	3-5-76
Table 5.3-15	Mean Surface Temperature and Mean Surface Temperature During July and August at Six Locations in the WHTF and the North Anna Reservoir Based on 42-years of Model Prediction from January 1961 to May 2003.	3-5-76
Table 5.3-16	Exceedence Frequency of Daily Surface Temperatures at Six Locations in the WHTF and the North Anna Reservoir Based on 42-years of Model Prediction from January 1961 to May 2003.	3-5-77
Table 5.3-17	Predicted Maximum Daily Surface Temperature Increase Due to One and Two New Once-through Cooling System Units On the Lake	3-5-77
Table 5.3-18	North Anna Cooling Pond Model Areas	3-5-78
Table 5.3-19	Average Daily Water Temperatures at Burrus Point with 3-Unit Operation	3-5-79
Table 5.3-20	Average Daily Water Temperatures at Thurman Island with 3-Unit Operation	3-5-79
Table 5.3-21	Average Daily Water Temperatures in Intake Area with 3-Unit Operation	3-5-80
Table 5.3-22	Temperature (°F) Requirements of Important Fish Species of Lake Anna	3-5-81
Table 5.4-1	Liquid Pathway Parameters	3-5-104
Table 5.4-2	Liquid Pathway Consumption Factors for Maximally Exposed Individual	3-5-104
Table 5.4-3	Gaseous Pathway Parameters	3-5-105
Table 5.4-4	Gaseous Pathway Receptor Locations	3-5-105
Table 5.4-5	Gaseous Pathway Consumption Factors for Maximally Exposed Individual.	3-5-105
Table 5.4-6	Release of Activities in Liquid Effluent	3-5-106
Table 5.4-7	Release of Activities in Gaseous Effluent	3-5-107
Table 5.4-8	Liquid Pathway Doses for Maximally Exposed Individuals at Lake Anna	3-5-108
Table 5.4-9	Gaseous Pathway Doses for Maximally Exposed Individuals.	3-5-109
Table 5.4-10	Comparison of Maximally Exposed Individual Doses with 10 CFR 50, Appendix I Criteria	3-5-110
Table 5.4-11	Comparison of Maximally Exposed Individual Doses with 40 CFR 190 Criteria	3-5-110
Table 5.4-12	Collective Total Body Doses Within 50 Miles	3-5-111
Table 5.4-13	Important Biota Species and Analytical Surrogates	3-5-111
Table 5.4-14	Terrestrial Biota Parameters	3-5-112
Table 5.4-15	Parameters for Shoreline and Swimming Exposure to Biota	3-5-112
Table 5.4-16	Biota Doses from Liquid and Gaseous Effluents.	3-5-113
Table 5.6-1	Results of Induced Current Analysis	3-5-125
Table 5.7-1	Gas-Cooled Fuel Cycle Impact Evaluation	3-5-138
Table 5.7-2	SWU and Feed Calculation Results	3-5-141
Table 5.7-3	10 CFR 51.51, Table S-3- of Uranium Fuel Cycle Environmental Data	3-5-142
Table 5.8-1	VEC Preliminary Local Population Projections, 2000–2030	3-5-152

Table 5.10-1	Summary of Impacts and Measures and Controls to Limit Adverse Impacts During Operations	3-5-162
Table 6.1-1	Water Temperature Recorder Station Locations.	3-6-3
Table 6.2-1	Radiation Pathway Monitoring.	3-6-8
Table 6.3-1	VPDES Hydrological Monitoring Program.	3-6-12
Table 6.4-1	Meteorological Data Recovery Rates (percent) (North Anna, January 1, 1996–December 31, 2001)	3-6-19
Table 6.4-2	Primary Tower Meteorological Parameters	3-6-20
Table 6.4-3	Backup Tower Parameters	3-6-20
Table 6.6-1	VPDES Water Quality Monitoring Program.	3-6-31
Table 6.7-1	Pre-Application, Construction/Pre-Operational, and Operational Thermal Monitoring Program.	3-6-39
Table 6.7-2	Pre-Application, Construction/Pre-Operational, and Operational Radiological Monitoring Program.	3-6-39
Table 6.7-3	Pre-Application, Construction/Pre-Operational, and Operational Hydrological Monitoring Program.	3-6-40
Table 6.7-4	Pre-Application, Construction/Pre-Operational, and Operational Meteorological Monitoring Program.	3-6-41
Table 6.7-5	Pre-Application, Construction/Pre-Operational, and Operational Ecological Monitoring Program.	3-6-42
Table 6.7-6	VPDES Water Quality Monitoring Program.	3-6-43
Table 7.1-1	Design Certification γ/Q Values	3-7-3
Table 7.1-2	Summary of Design Basis Accident Doses	3-7-6
Table 7.1-3	Activity Releases for AP1000 Main Steam Line Break, Pre-Existing Iodine Spike.	3-7-7
Table 7.1-4	Doses for AP1000 Main Steam Line Break, Pre-Existing Iodine Spike.	3-7-8
Table 7.1-5	Activity Releases for AP1000 Main Steam Line Break, Accident-Initiated Iodine Spike.	3-7-9
Table 7.1-6	Doses for AP1000 Main Steam Line Break, Accident-Initiated Iodine Spike	3-7-10
Table 7.1-7	Activity Releases for AP1000 Locked Rotor Accident.	3-7-11
Table 7.1-8	Doses for AP1000 Locked Rotor Accident	3-7-12
Table 7.1-9	Activity Releases for AP1000 Rod Ejection Accident	3-7-13
Table 7.1-10	Doses for AP1000 Rod Ejection Accident.	3-7-14
Table 7.1-11	Doses for AP1000 Failure of Small Lines Carrying Primary Coolant Outside Containment	3-7-14
Table 7.1-12	Activity Releases for ABWR Failure of Small Lines Carrying Primary Coolant Outside Containment.	3-7-15
Table 7.1-13	Doses for ABWR Failure of Small Lines Carrying Primary Coolant Outside Containment	3-7-15

Table 7.1-14	Activity Releases for AP1000 Steam Generator Tube Rupture, Pre-Existing Iodine Spike.	3-7-16
Table 7.1-15	Doses for AP1000 Steam Generator Tube Rupture, Pre-Existing Iodine Spike . .	3-7-17
Table 7.1-16	Activity Releases for AP1000 Steam Generator Tube Rupture, Accident-Initiated Iodine Spike	3-7-18
Table 7.1-17	Doses for AP1000 Steam Generator Tube Rupture, Accident-Initiated Iodine Spike.	3-7-19
Table 7.1-18	Activity Releases for ABWR Main Steam Line Break	3-7-20
Table 7.1-19	Doses for ABWR Main Steam Line Break, Pre-Existing Iodine Spike.	3-7-21
Table 7.1-20	Doses for ABWR Main Steam Line Break, Accident-Initiated Iodine Spike	3-7-21
Table 7.1-21	Activity Releases for AP1000 Loss-of-Coolant Accident.	3-7-22
Table 7.1-22	Doses for AP1000 Loss-of-Coolant Accident	3-7-24
Table 7.1-23	Activity Releases for ABWR Loss-of-Coolant Accident.	3-7-25
Table 7.1-24	Doses for ABWR Loss-of-Coolant Accident	3-7-26
Table 7.1-25	Activity Releases for AP1000 Fuel Handling Accident	3-7-26
Table 7.1-26	Doses for AP1000 Fuel Handling Accident	3-7-27
Table 7.1-27	Activity Releases for ABWR Fuel Handling Accident	3-7-28
Table 7.1-28	Doses for ABWR Fuel Handling Accident	3-7-29
Table 9.3-1	Summary of Environment Impacts For New Nuclear Units	3-9-8
Table 9.3-2	Suitability Criteria	3-9-9
Table 9.3-3	Site Merit Scores for the Four Alternative Sites	3-9-10
Table 9.4-1	Screening of Unit 3 Alternative Heat Dissipation Systems (Base Case & Alternatives 1–2)	3-9-24
Table 9.4-2	Screening of Unit 3 Alternative Heat Dissipation Systems (Alternatives 3–5).	3-9-27
Table 9.4-3	Summary Comparison of Unit 3 Heat Dissipation Systems Impacts.	3-9-31
Table 9.4-4	Initial Screening of Alternative Heat Dissipation Systems - Unit 4 (Base Case & Alternatives 6–8)	3-9-32
Table 9.4-5	Screening of Unit 4 Alternative Heat Dissipation Systems (Alternatives 9 & 10)	3-9-36
Table 9.4-6	Summary Comparison of Unit 4 Heat Dissipation Systems Impacts.	3-9-38
Table 9.4-7	Screening of Alternatives to the Proposed Intake System (Base Case & Alternative 1)	3-9-39
Table 9.4-8	Screening of Alternatives to the Proposed Intake System (Base Case & Alternatives 2 & 3)	3-9-40
Table 9.4-9	Screening of Alternatives to the Proposed Discharge System (Base Case & Alternative 4)	3-9-42
Table 9.4-10	Screening of Alternatives to the Proposed Discharge System Location (Base Case & Alternatives 5 & 6)	3-9-43

Figures

Part 1: Administrative Information

Figure 1.0-1	ESP Site Layout	1-1-2
--------------	---------------------------	-------

Part 2: Site Safety Analysis Report

Figure 1.2-1	Site Location – 10 Mile Radius	2-1-5
Figure 1.2-2	Site Location – 50 Mile Radius	2-1-6
Figure 1.2-3	Site Layout – Current Development	2-1-7
Figure 1.2-4	Site Layout – New Development	2-1-8
Figure 2.1-1	Site Boundary	2-2-14
Figure 2.1-2	Ten-Mile Surrounding Area	2-2-15
Figure 2.1-3	Fifty-Mile Surrounding Area	2-2-16
Figure 2.1-4	16-Kilometer (10-Mile) Resident and Transient Population Distribution–2000 . .	2-2-17
Figure 2.1-5	16-Kilometer (10-Mile) Resident and Transient Population Distribution–2010 . .	2-2-18
Figure 2.1-6	16-Kilometer (10-Mile) Resident and Transient Population Distribution–2020 . .	2-2-19
Figure 2.1-7	16-Kilometer (10-Mile) Resident and Transient Population Distribution–2030 . .	2-2-20
Figure 2.1-8	16-Kilometer (10-Mile) Resident and Transient Population Distribution–2040 . .	2-2-21
Figure 2.1-9	80-Kilometer (50-Mile) Resident and Transient Population Distribution–2000 . .	2-2-22
Figure 2.1-10	80-Kilometer (50-Mile) Resident and Transient Population Distribution–2010 . .	2-2-23
Figure 2.1-11	80-Kilometer (50-Mile) Resident and Transient Population Distribution–2020 . .	2-2-24
Figure 2.1-12	80-Kilometer (50-Mile) Resident and Transient Population Distribution–2030 . .	2-2-25
Figure 2.1-13	80-Kilometer (50-Mile) Resident and Transient Population Distribution–2040 . .	2-2-26
Figure 2.1-14	Population Density	2-2-27
Figure 2.2-1	Location of Airports And Airways	2-2-35
Figure 2.3-1	North Anna Seasonal Wind Direction Roses: Low-Level Winds: 1974–1987: Season = Spring	2-2-71
Figure 2.3-2	North Anna Seasonal Wind Direction Roses: High-Level Winds: 1974–1987: Season = Spring	2-2-72
Figure 2.3-3	North Anna Seasonal Wind Direction Roses: Low-Level Winds: 1974–1987: Season = Summer	2-2-73
Figure 2.3-4	North Anna Seasonal Wind Direction Roses: High-Level Winds: 1974–1987: Season = Summer	2-2-74
Figure 2.3-5	North Anna Seasonal Wind Direction Roses: Low-Level Winds: 1974–1987: Season = Fall	2-2-75
Figure 2.3-6	North Anna Seasonal Wind Direction Roses: High-Level Winds: 1974–1987: Season = Fall	2-2-76
Figure 2.3-7	North Anna Seasonal Wind Direction Roses: Low-Level Winds: 1974–1987: Season = Winter	2-2-77

Figures

Figure 2.3-8	North Anna Seasonal Wind Direction Roses: High-Level Winds: 1974–1987: Season = Winter	2-2-78
Figure 2.3-9	North Anna Seasonal Wind Direction Roses: Low-Level Winds: 1974–1987: Season = Overall.	2-2-79
Figure 2.3-10	North Anna Seasonal Wind Direction Roses: High-Level Winds: 1974–1987: Season = Overall.	2-2-80
Figure 2.3-11	North Anna Seasonal Wind Persistence Roses: Low-Level Winds: 1974–1987: Season = Spring	2-2-81
Figure 2.3-12	North Anna Seasonal Wind Persistence Roses: High-Level Winds: 1974–1987: Season = Spring	2-2-82
Figure 2.3-13	North Anna Seasonal Wind Persistence Roses: Low-Level Winds: 1974–1987: Season = Summer	2-2-83
Figure 2.3-14	North Anna Seasonal Wind Persistence Roses: High-Level Winds: 1974–1987: Season = Summer	2-2-84
Figure 2.3-15	North Anna Seasonal Wind Persistence Roses: Low-Level Winds: 1974–1987: Season = Fall	2-2-85
Figure 2.3-16	North Anna Seasonal Wind Persistence Roses: High-Level Winds: 1974–1987: Season = Fall	2-2-86
Figure 2.3-17	North Anna Seasonal Wind Persistence Roses: Low-Level Winds: 1974–1987: Season = Winter	2-2-87
Figure 2.3-18	North Anna Seasonal Wind Persistence Roses: High-Level Winds: 1974–1987: Season = Winter	2-2-88
Figure 2.3-19	North Anna Seasonal Wind Persistence Roses: Low-Level Winds: 1974–1987: Season = Overall.	2-2-89
Figure 2.3-20	North Anna Seasonal Wind Persistence Roses: High-Level Winds: 1974–1987: Season = Overall.	2-2-90
Figure 2.3-21	Topographic Map	2-2-91
Figure 2.3-22	Vertical Profiles	2-2-92
Figure 2.3-23	Location of Meteorological Tower	2-2-96
Figure 2.3-24	Location of Meteorological Tower Relative to Local Ground Features	2-2-97
Figure 2.4-1	Lake Anna Hydrologic Features	2-2-152
Figure 2.4-2	Deleted	2-2-153
Figure 2.4-3	Spillway and Discharge Capacity (One Gate of Three) North Anna Dam.	2-2-154
Figure 2.4-4	Skimmer Gate Discharge Capacity North Anna Dam	2-2-155
Figure 2.4-5	Combined Lake Anna and WHTF Drainage Area	2-2-156
Figure 2.4-6	Combined North Anna Reservoir and WHTF Watershed: 3-Hour Unit Hydrograph	2-2-157
Figure 2.4-7	1979 Storm Outflow Hydrograph Comparison	2-2-158
Figure 2.4-8	1994 Storm Outflow Hydrograph Comparison	2-2-159

Figures

Figure 2.4-9	1995 Storm Outflow Hydrograph Comparison	2-2-160
Figure 2.4-10	North Anna Reservoir & WHTF Combined Stage-Storage	2-2-161
Figure 2.4-11	Combined North Anna Reservoir & WHTF PMF Inflow Hydrograph.	2-2-162
Figure 2.4-12	North Anna Site - Fetch Diagram	2-2-163
Figure 2.4-13	Existing Cooling Water Canals and Reservoirs.	2-2-164
Figure 2.4-14	Schematic Cross-Sectional Diagram of Water Discharge System at Dike 3 WHTF.	2-2-165
Figure 2.4-15	Groundwater Level Hydrographs	2-2-166
Figure 2.4-16	Piezometric Head Contour Map	2-2-167
Figure 2.4-17	Existing North Anna Water Supply Wells	2-2-168
Figure 2.5-4B-1	Sub-Surface Investigation Location Plan	2-2-396
Figure 2.5-1	Regional Physiographic Map (200-Mile Radius).	2-2-383
Figure 2.5-2	Evolution of the Appalachian Orogen (after Hatcher, 1987)	2-2-384
Figure 2.5-3	Regional Geologic Map (200-Mile Radius)	2-2-385
Figure 2.5-4	Lithotectonic Belts of the Piedmont Province	2-2-387
Figure 2.5-5	Simplified Tectonostratigraphic Map	2-2-388
Figure 2.5-6	Simplified Tectonic Map of Virginia	2-2-389
Figure 2.5-7	Evolution of the Appalachian Orogen (after Glover and others, 1995)	2-2-390
Figure 2.5-8	Crustal Section Through Appalachian Orogen (200-mile radius)	2-2-391
Figure 2.5-9	Tectonic Features Map (200-mile radius)	2-2-392
Figure 2.5-10	Site Vicinity Geologic Map (25-Mile Radius)	2-2-393
Figure 2.5-11	Site Area Geologic Map (5-Mile Radius)	2-2-395
Figure 2.5-12	Quaternary Features Map	2-2-397
Figure 2.5-13	Northern, Central, and Southern Segments of the East Coast Fault System . . .	2-2-398
Figure 2.5-14	Seismic Source Zones and Seismicity in Central and Eastern North America . .	2-2-399
Figure 2.5-15	Site Area Topographic Map (5-Mile Radius)	2-2-400
Figure 2.5-16	Site Topographic Map (0.6-Mile Radius)	2-2-401
Figure 2.5-17	Site Area Geologic Cross Section A-A' (5-Mile Radius)	2-2-402
Figure 2.5-18	Site Geologic Map (0.6-Mile Radius)	2-2-403
Figure 2.5-19	Bechtel Group EPRI Sources	2-2-404
Figure 2.5-20	Dames & Moore EPRI Sources.	2-2-405
Figure 2.5-21	Law Engineering EPRI Sources	2-2-406
Figure 2.5-22	Rondout Associates EPRI Sources.	2-2-407
Figure 2.5-23	Woodward-Clyde EPRI Sources	2-2-408
Figure 2.5-24	Weston EPRI Sources.	2-2-409
Figure 2.5-25	Various EPRI Geometries of the Central Virginia Seismic Zone.	2-2-410
Figure 2.5-26	Low-Frequency, 10 ⁻⁵ Median, Magnitude-Distance Deaggregation Using 1989 EPRI Sources and Ground Motion.	2-2-411

Figures

Figure 2.5-27	High-Frequency, 10^{-5} Median, Magnitude-Distance Deaggregation Using 1989 EPRI Sources and Ground Motion	2-2-412
Figure 2.5-28	1989 EPRI 1 Hz Mean Hazard Contribution by Source (Bechtel); Sources Contributing Most to ESP Site Hazard Are Emphasized	2-2-413
Figure 2.5-29	1989 EPRI Hazard 1 Hz Mean Contribution by Source (Dames & Moore); Sources Contributing Most to ESP Site Hazard Are Emphasized	2-2-414
Figure 2.5-30	1989 EPRI 1 Hz Mean Hazard Contribution by Source (Law Engineering); Sources Contributing Most to ESP Site Hazard Are Emphasized	2-2-415
Figure 2.5-31	1989 EPRI 1 Hz Hazard Contribution by Source (Rondout Team); Sources Contributing Most to ESP Site Hazard Are Emphasized	2-2-416
Figure 2.5-32	1989 EPRI 1 Hz Hazard Contribution by Source (Woodward-Clyde); Sources Contributing Most to ESP Site Hazard Are Emphasized	2-2-417
Figure 2.5-33	1989 EPRI 1 Hz Hazard Contribution by Source (Weston Geophysical); Sources Contributing Most to ESP Site Hazard Are Emphasized	2-2-418
Figure 2.5-34	Logic Tree for ECFS Northern Segment	2-2-419
Figure 2.5-35	Logic Tree for the Updated Charleston Source (ECFS Southern Segment)	2-2-419
Figure 2.5-36	Bechtel and Rondout Team Representations of Central Virginia Seismic Zone, and Seismicity in the Region Recorded from 1985 to 2001	2-2-420
Figure 2.5-37	Comparison of Seismic Activity Rates for Bechtel Source E Considering Original EPRI (through 1984) and Updated (through 2001) Earthquake Catalogs	2-2-421
Figure 2.5-38	Comparison of Seismic Activity for Rondout Source 29 Considering Original EPRI (through 1984) and Updated (through 2001) Earthquake Catalogs	2-2-422
Figure 2.5-39	Comparison of Seismic Activity for 200-Mile Radius Source Around North Anna Considering Original EPRI (through 1984) and Updated (through 2001) Earthquake Catalogs	2-2-423
Figure 2.5-40	Effect of ECFS Faults on Median, 1 Hz Seismic Hazard	2-2-424
Figure 2.5-41	Effect of ECFS Faults on Mean, 1 Hz Seismic Hazard	2-2-425
Figure 2.5-42	Effect of ECFS Faults on Median, 10 Hz Seismic Hazard	2-2-426
Figure 2.5-43	Effect of ECFS Faults on Mean, 10 Hz Seismic Hazard	2-2-427
Figure 2.5-44	Sensitivity of 10 Hz Seismic Hazard to 1989 and 2003 Ground Motion Models	2-2-428
Figure 2.5-45	Sensitivity of 1 Hz Seismic Hazard to 1989 and 2003 Ground Motion Models	2-2-429
Figure 2.5-46	Low-Frequency, 10^{-5} Median, Magnitude-Distance Deaggregation Using Updated Source and Ground Motion Models	2-2-430
Figure 2.5-47	High-Frequency, 10^{-5} Median, Magnitude-Distance Deaggregation Using Updated Source and Ground Motion Models	2-2-431
Figure 2.5-48	Selected Performance-Based Horizontal SSE Response Spectrum, As Scaled from Mean 10^{-4} Ground Motion Spectrum, Compared to RG 1.60 Spectrum Anchored to 0.3g.	2-2-432

Figures

Figure 2.5-49	Magnitude-Distance Deaggregation for Low-Frequencies (1 and 2.5 Hz) at a Mean Annual Frequency of 5×10^{-5} Using Updated Source and Ground Motion Models.	2-2-433
Figure 2.5-50	Magnitude-Distance Deaggregation for High-Frequencies (5 and 10 Hz) at a Mean Annual Frequency of 5×10^{-5} Using Updated Source and Ground Motion Models.	2-2-434
Figure 2.5-51	Horizontal Ground Motion Spectrum Calculated for Reference Probability of Mean 5×10^{-5} , Compared to RG 1.60 Spectrum Anchored to 0.3g and to Selected SSE Spectrum	2-2-435
Figure 2.5-52	Sensitivity Plot of Scaled Spectrum Calculated Using Alternative Lower-Bound M of 5.0 and Scaling Factors in Table 2.5-27, Compared to RG 1.60 Spectrum Anchored to 0.3g and to Selected SSE Spectrum	2-2-436
Figure 2.5-53	Comparison of Aleatory Sigmas Reported for California with Weighted Average Aleatory Sigma from EPRI Ground Motion 2003 Models for $M = 5.5$, $R_{CD} = 20$ km	2-2-437
Figure 2.5-54	Sensitivity Plot of Scaled Spectrum Calculated Using Alternative Ground Motion Aleatory Uncertainties and Scaling Factors in Table 2.5-28, Compared to RG 1.60 Spectrum Anchored to 0.3g and to Selected SSE Spectrum	2-2-438
Figure 2.5-55	Horizontal SSE and OBE Response Spectra Based on Updated Models (5% of Critical Damping)	2-2-439
Figure 2.5-56	Site Vicinity Geologic Map and Seismicity (25-Mile Radius)	2-2-440
Figure 2.5-57	Subsurface Profile A-A'	2-2-441
Figure 2.5-58	Subsurface Profile B-B'	2-2-442
Figure 2.5-59	Locations of Previous Boreholes.	2-2-443
Figure 2.5-60	ESP Borehole Locations	2-2-444
Figure 2.5-61	Locations of All Exploration Points	2-2-445
Figure 2.5-62	Zone IIA Shear Wave Velocity Profile (a) Full-Depth Shear Wave Velocity Profile (b).	2-2-446
Figure 2.5-63	Variation of Normalized Shear Modulus with Cycle Shear Strain	2-2-447
Figure 2.5-64	Variation of Damping Ratio with Cyclic Shear Strain	2-2-448
Figure 2.5-65	Plan View of Slope North of the SWR	2-2-449
Figure 2.5-66	Photograph of Plan View of Slope North of the SWR	2-2-450
Figure 2.5-67	Photograph of Slope North of the SWR	2-2-451
Figure 2.5-68	Cross-Section of Existing Slope North of the SWR.	2-2-452
Figure 2.5-69	SLOPE/W Analysis of Long-Term Static Case	2-2-453
Figure 2.5-70	SLOPE/W Analysis of Seismic Case.	2-2-454
Figure 2.5-71	Log of Boring B-15	2-2-455
Figure 2.5-72	Log of Boring B-18	2-2-456

Figures

Figure 13.3-1	Plume Exposure Pathway Emergency Planning Zone	2-13-4
Figure 13.3-2	Ingestion Exposure Pathway Emergency Planning Zone	2-13-5
Figure 13.3-3	Onsite-Offsite Interface	2-13-11
Figure 13.3-4	Remote Assembly Areas	2-13-24

Part 3: Environmental Report

Figure 1.1-1	ESP Site	3-1-5
Figure 2.1-1	North Anna ESP Site Boundaries	3-2-3
Figure 2.1-2	10 Mile North Anna Vicinity Map	3-2-4
Figure 2.1-3	North Anna Power Station 50 Mile View	3-2-5
Figure 2.2-1	Existing NAPS Site Detail Map	3-2-16
Figure 2.2-2	Land Use Classifications for Louisa County, Virginia (Site and Vicinity)	3-2-17
Figure 2.2-3	Land Use Classifications for Spotsylvania County, Virginia (Site and Vicinity)	3-2-18
Figure 2.2-4	Existing Transmission Line Corridors	3-2-19
Figure 2.3-1	Lake Anna	3-2-51
Figure 2.3-2	Elevation-Area Curves for North Anna Reservoir and Waste Heat Treatment Facility	3-2-52
Figure 2.3-3	Deleted	3-2-53
Figure 2.3-4	Spillway Discharge Capacity (One Gate of Three) North Anna Dam	3-2-54
Figure 2.3-5	Skimmer Gate Discharge Capacity for North Anna Dam	3-2-55
Figure 2.3-6	Locations of USGS Stream Gauging Stations in the North Anna River Watershed	3-2-56
Figure 2.3-7	Ground Water Level Hydrographs	3-2-57
Figure 2.3-8	Piezometric Head Contour Map	3-2-58
Figure 2.3-9	Surface Water Bodies That Could Affect or Be Affected by Plant Water Use	3-2-59
Figure 2.3-10	Surface Water Bodies Within 10 Kilometers (6.2 Miles)	3-2-60
Figure 2.3-11	Existing Water Supply Wells	3-2-61
Figure 2.3-12	Temperature and Water Quality Sampling Stations	3-2-62
Figure 2.3-13	Temporal Variation in Lake Anna Water Temperature at Selected Locations	3-2-63
Figure 2.3-14	Water Quality in Crystalline Terrane (Pittsylvania and Halifax Counties, Virginia)	3-2-64
Figure 2.4-1	Lake Anna and the North Anna River	3-2-86
Figure 2.4-2	North Anna River; Northeast Creek; Contrary Creek	3-2-87
Figure 2.4-3	Schematic Cross-Sectional Diagram of Water-Discharge System at Dike 3 WHTF	3-2-88
Figure 2.4-4	Location of Temperature Sensors - Lake Anna	3-2-89
Figure 2.5-1	10-Mile Surrounding Area	3-2-128
Figure 2.5-2	50-Mile Surrounding Area	3-2-129

Figures

Figure 2.5-3	16-Kilometer (10-Mile) Resident and Transient Population Distribution–2000 . . .	3-2-130
Figure 2.5-4	16-Kilometer (10-Mile) Resident and Transient Population Distribution–2010 . . .	3-2-131
Figure 2.5-5	16-Kilometer (10-Mile) Resident and Transient Population Distribution–2020 . . .	3-2-132
Figure 2.5-6	16-Kilometer (10-Mile) Resident and Transient Population Distribution–2030 . . .	3-2-133
Figure 2.5-7	16-Kilometer (10-Mile) Resident and Transient Population Distribution–2040 . . .	3-2-134
Figure 2.5-8	80-Kilometer (50-Mile) Resident and Transient Population Distribution–2000 . . .	3-2-135
Figure 2.5-9	80-Kilometer (50-Mile) Resident and Transient Population Distribution–2010 . . .	3-2-136
Figure 2.5-10	80-Kilometer (50-Mile) Resident and Transient Population Distribution–2020 . . .	3-2-137
Figure 2.5-11	80-Kilometer (50-Mile) Resident and Transient Population Distribution–2030 . . .	3-2-138
Figure 2.5-12	80-Kilometer (50-Mile) Resident and Transient Population Distribution–2040 . . .	3-2-139
Figure 2.5-13	Population Density	3-2-140
Figure 2.5-14	Minority Population	3-2-141
Figure 2.5-15	Low-Income Population.	3-2-142
Figure 2.5-16	50-Mile Vicinity Map Showing Counties and Important Towns and Cities	3-2-143
Figure 2.5-17	Area Potentials for Yielding Archeological Resources Within the Study Area . . .	3-2-144
Figure 2.5-18	Cemeteries Within the NAPS Site Boundary.	3-2-145
Figure 2.5-19	Location of Historic Sites in the Vicinity of NAPS	3-2-146
Figure 2.6-1	Regional Physiographic Map (200-Mile Radius).	3-2-163
Figure 2.6-2	Site Topographic Map (0.6-Mile Radius).	3-2-164
Figure 2.6-3	Lithotectonic Belts of the Piedmont Province	3-2-165
Figure 2.6-4	Site Area Geologic Map (5-Mile Radius).	3-2-166
Figure 2.6-5	Site Area Geologic Cross Section (5-Mile Radius)	3-2-168
Figure 2.6-6	Seismic Source Zones and Seismicity in Central and Eastern North America . . .	3-2-169
Figure 2.7-1	Location of Meteorological Tower	3-2-219
Figure 2.7-2	Location of Meteorological Tower Relative to Local Ground Features	3-2-220
Figure 2.7-3	North Anna Seasonal Wind Direction Roses: Low-Level Winds: 1974–1987: Season = Spring	3-2-221
Figure 2.7-4	North Anna Seasonal Wind Direction Roses: High-Level Winds: 1974–1987: Season = Spring	3-2-222
Figure 2.7-5	North Anna Seasonal Wind Direction Roses: Low-Level Winds: 1974–1987: Season = Summer	3-2-223
Figure 2.7-6	North Anna Seasonal Wind Direction Roses: High-Level Winds: 1974–1987: Season = Summer	3-2-224
Figure 2.7-7	North Anna Seasonal Wind Direction Roses: Low-Level Winds: 1974–1987: Season = Fall	3-2-225
Figure 2.7-8	North Anna Seasonal Wind Direction Roses: High-Level Winds: 1974–1987: Season = Fall	3-2-226

Figures

Figure 2.7-9	North Anna Seasonal Wind Direction Roses: Low-Level Winds: 1974–1987: Season = Winter	3-2-227
Figure 2.7-10	North Anna Seasonal Wind Direction Roses: High-Level Winds: 1974–1987: Season = Winter	3-2-228
Figure 2.7-11	North Anna Seasonal Wind Direction Roses: Low-Level Winds: 1974–1987: Season = Overall.	3-2-229
Figure 2.7-12	North Anna Seasonal Wind Direction Roses: High-Level Winds: 1974–1987: Season = Overall.	3-2-230
Figure 2.7-13	North Anna Seasonal Wind Persistence Roses: Low-Level Winds: 1974–1987: Season = Spring	3-2-231
Figure 2.7-14	North Anna Seasonal Wind Persistence Roses: High-Level Winds: 1974–1987: Season = Spring	3-2-232
Figure 2.7-15	North Anna Seasonal Wind Persistence Roses: Low-Level Winds: 1974–1987: Season = Summer	3-2-233
Figure 2.7-16	North Anna Seasonal Wind Persistence Roses: High-Level Winds: 1974–1987: Season = Summer	3-2-234
Figure 2.7-17	North Anna Seasonal Wind Persistence Roses: Low-Level Winds: 1974–1987: Season = Fall	3-2-235
Figure 2.7-18	North Anna Seasonal Wind Persistence Roses: High-Level Winds: 1974–1987: Season = Fall	3-2-236
Figure 2.7-19	North Anna Seasonal Wind Persistence Roses: Low-Level Winds: 1974–1987: Season = Winter	3-2-237
Figure 2.7-20	North Anna Seasonal Wind Persistence Roses: High-Level Winds: 1974–1987: Season = Winter	3-2-238
Figure 2.7-21	North Anna Seasonal Wind Persistence Roses: Low-Level Winds: 1974–1987: Season = Overall.	3-2-239
Figure 2.7-22	North Anna Seasonal Wind Persistence Roses: High-Level Winds: 1974–1987: Season = Overall.	3-2-240
Figure 2.7-23	Topographic Map	3-2-241
Figure 2.7-24	Vertical Profiles	3-2-242
Figure 3.1-1	Existing North Anna Power Station Site	3-3-7
Figure 3.1-2	Artist’s Conception of New Units Adjacent to Existing Units	3-3-8
Figure 3.1-3	ESP Site Utilization Plan	3-3-9
Figure 3.3-1	Unit 3 Cooling Water Use	3-3-44
Figure 3.3-2	Unit 4 Cooling Water Use	3-3-45
Figure 3.3-3	Power Block Water Use	3-3-46
Figure 3.4-1	Proposed Location of the Intake Structure and Discharge Structures for the New Units 3 and 4	3-3-55
Figure 3.4-2	North Anna Plant - Reservoir and WHTF of Lake Anna	3-3-56

Figures

Figure 3.4-3	Layout of Screenwell/Pump Intake for New Units 3 and 4	3-3-57
Figure 3.4-4	Schematic View of Pump Intake	3-3-58
Figure 3.4-5	Discharge Outfall at Head of the Discharge Canal for New Units 3 and 4	3-3-59
Figure 3.4-6	Discharge Channel and Dike 3 Outlet Structure	3-3-60
Figure 3.4-7	Schematic Diagram of the Discharge System.	3-3-61
Figure 3.4-8	Location of Discharge Structure in Dike 3 and Bottom Topography of the North Anna Reservoir	3-3-62
Figure 3.4-9	Water Discharge System from WHTF to North Anna Reservoir	3-3-63
Figure 3.4-10	Water Discharge System from WHTF to North Anna Reservoir	3-3-64
Figure 4.1-1	Vicinity Highways, Railroads, and Utility Rights-of-Way	3-4-8
Figure 4.2-1	Ephemeral Stream Locations	3-4-13
Figure 5.2-1	Lake Anna Water Balance Model	3-5-9
Figure 5.2-2	Lake Anna Outflow Hydrographs	3-5-17
Figure 5.2-3	Lake Anna Water Level Hydrographs	3-5-18
Figure 5.3-1	Generalized Map of North Anna Power Station Environs	3-5-82
Figure 5.3-2	Intake Structure and Approach Channel for the New Units and the Existing Units	3-5-83
Figure 5.3-3	Observed Seasonal Average Vertical Temperature Profiles at Monitoring Station A Near North Anna Dam	3-5-84
Figure 5.3-4	Observed Seasonal Average Vertical Temperature Profiles at Monitoring Station I near the Intake	3-5-85
Figure 5.3-5	Predicted Monthly Temperature for Scenario 1.	3-5-86
Figure 5.3-6	Predicted Monthly Temperature for Scenario 2.	3-5-87
Figure 5.3-7	Predicted Seasonal Average Vertical Temperature Profiles at Intake for Existing Units (Scenario 1)	3-5-88
Figure 5.3-8	Predicted Seasonal Average Vertical Temperature Profiles at North Anna Dam for Existing Units (Scenario 1)	3-5-89
Figure 5.3-9	Predicted Seasonal Average Vertical Temperature Profiles at Intake for Existing Units and One New Once-through Unit (Scenario 2).	3-5-90
Figure 5.3-10	Predicted Seasonal Average Vertical Temperature Profiles at North Anna Dam for Existing Units and One New Once-through Unit (Scenario 2).	3-5-91
Figure 5.3-11	Schematization of the North Anna Cooling Lake System Used in the Segmented Model	3-5-92
Figure 5.3-12	Schematization of Convective Circulation in a Dead-End Side Arm	3-5-93
Figure 5.3-13	Measured and Predicted Surface Temperature at Discharge for Calibration Run from 1/1996 to 12/2001	3-5-94
Figure 5.3-14	Measured and Predicted Surface Temperature at Burrus Point for Calibration Run from 1/1996 to 12/2001	3-5-95

Figures

Figure 5.3-15	Measured and Predicted Surface Temperature at Discharge for Validation Run from 7/1978 to 9/1983	3-5-96
Figure 5.3-16	Measured and Predicted Surface Temperature at Burrus Point for Validation Run from 7/1978 to 9/1983	3-5-97
Figure 5.8-1	Site Boundary and Cooling Tower Envelope Area	3-5-158
Figure 6.1-1	Locations of Water Temperature Monitoring Stations	3-6-4
Figure 6.1-2	Temperature Profiling Stations A Through N	3-6-5
Figure 6.2-1	Preoperational Radiological Environmental Sampling Program Sample Station Locations.	3-6-9
Figure 6.6-1	Location of Temperature Sensors – Lake Anna	3-6-35
Figure 6.6-2	Location of Thermal Plume Sampling Stations – Lake Anna	3-6-36
Figure 6.6-3	Location of Monitored VPDES Permit Outfalls	3-6-37
Figure 9.3-1	Region of Interest	3-9-11

Part 4: Programs and Plans

Figure 1.2-1	Ephemeral Steam Locations	4-1-8
--------------	-------------------------------------	-------

Acronyms/Abbreviations/Initialisms

ABWR	Advanced BWR
ANS	Alert and Notification System
BWR	Boiling Water Reactor
CEDE	Committed Effective Dose Equivalent
CEQ	Council of Environmental Quality
CFR	Code of Federal Regulations
cfs	Cubic Feet per Second
Ci	Curies
cm	Centimeter
COL	Combined License
CWA	Clean Water Act
CWIS	Cooling Water Intake System
DBA	Design Basis Accident
DDE	Deep Dose Equivalent
DEI	Dominion Energy, Inc.
DEM	Virginia Department of Emergency Management
DHS	United States Department of Homeland Security
DNP	Dominion Nuclear Projects, Inc.
DOE	United States Department of Energy
DRI	Dominion Resources, Inc.
EAB	Exclusion Area Boundary
EAC	Evacuation Assembly Center
EAL	Emergency Action Level
EAS	Emergency Alert System
EI	Exposure Index
EMI	Emergency Management Institute
EOC	Emergency Operations Center
EOF	Emergency Operations Facility
EPA	U.S Environmental Protection Agency
EPZ	Emergency Planning Zone
ERDS	Emergency Response Data System
ERO	Emergency Response Organization
ESBWR	Economic Simplified BWR
ESF	Engineered Safety Features
ESP	Early Site Permit
ETE	Evacuation time estimate
FCO	Federal Coordinating Officer
FES	Final Environmental Statements
FRERP	Federal Radiological Emergency Response Plan
FRMAC	Federal Radiological Monitoring and Assessment Center
FRP	Federal Response Plan
GEIS	Generic Impact Environmental Statement
gpd	Gallons per Day

Acronyms/Abbreviations/Initialisms

gpm	Gallons per Minute
GT-MHR	Gas Turbine Modular Helium Reactor
HMR	Hydro-Meteorological Report
INPO	Institute of Nuclear Power Operations
IPZ	Ingestion Exposure Pathway Emergency Planning Zone
IRIS	International Reactor Innovative and Secure
ISFSI	Independent Spent Fuel Storage Installation
LOCA	Loss-of-Coolant Accident
LOS	Level of Service
LPGS	Liquid Pathway Generic Study
LPZ	Low Population Zone
LWR	Light-Water-Cooled Reactor
MCV	Medical College of Virginia
MEI	Maximally Exposed Individual
mg/kg	Milligrams Per Kilogram
mgpd	Million Gallons per Day
MSA	Metropolitan Statistical Area
msl	Mean Sea Level
MT	Metric Tons
MTU	Metric Tons Uranium
MW	Megawatts
MWd	Megawatt Days
NAEP	North Anna Power Station Emergency Plan
NANIC	North Anna Nuclear Information Center
NAPS	North Anna Power Station
NEI	Nuclear Energy Institute
NEP	Nuclear Emergency Preparedness
NEPA	National Environmental Policy Act
NOAA	National Oceanic and Atmospheric Administration
NPSEPT	Nuclear Power Station Emergency Preparedness Training
NRC	United States Nuclear Regulatory Commission
NRHP	National Register of Historic Places
NRP	National Response Plan
NWS	National Weather Service
ODEC	Old Dominion Electric Cooperative
OOM	Order-of-Magnitude
OSC	Operational Support Center (Onsite Operations Assembly Area)
PAZ	Protective Action Zone
PBMR	Pebble Bed Modular Reactor
PMF	Probable Maximum Flood
PMP	Probable Maximum Precipitation
PPE	Plant Parameter Envelope
ppm	Parts Per Million

Acronyms/Abbreviations/Initialisms

PWR	Pressurized Water Reactor
RAA	Remote Assembly Area
RAP	Radiological Assistance Program
RERP	Radiological Emergency Response Plan
RG	Regulatory Guide
ROI	Region of Interest
SAMA	Severe Accident Mitigation Alternatives
SCC	State Corporation Commission
SEIS	Supplemental Environmental Impact Statement
SHPO	State Historic Preservation Officer
SRP	Standard Review Plan
SSAR	Site Safety Analysis Report
SWPPP	Storm Water Pollution Prevention Plan
SWR	Service Water Reservoir
SWU	Separative Work Units
TEDE	Total Effective Dose Equivalent
TSC	Technical Support Center
UFSAR	Updated Final Safety Analysis Report
UHS	Ultimate Heat Sink
USACE	U.S. Army Corps of Engineers
USFWS	U.S. Fish and Wildlife Service
USGS	U.S. Geological Survey
VCU	Virginia Commonwealth University
VDCR	Virginia Department of Conservation and Recreation
VDEQ	Virginia Department of Environmental Quality
VDGIF	Virginia Department of Game and Inland Fisheries
VDH	Virginia Department of Health
VDHR	Virginia Division of Historic Resources
VDOT	Virginia Department of Transportation
VEC	Virginia Employment Commission
VMRC	Virginia Marine Resource Commission
VPDES	Virginia Pollutant Discharge Elimination System
VSP	Commonwealth of Virginia State Police
WHTF	Waste Heat Treatment Facility

Changed Pages

Pages changed/added after initial publication (Revision 0) are listed here.

Revision	Date	Affected Pages
1	October 2003	Cover, xxiii-xxxii, xxxvii, 2-2-100, 2-2-153, 3-2-21, 3-2-53

PART 1 - ADMINISTRATIVE INFORMATION

Contents

Chapter 1	Introduction	1-1-1
1.1	Purpose of an Early Site Permit Application.	1-1-3
1.2	Early Site Permit Application Format and Content	1-1-4
1.2.1	Format and Content	1-1-4
1.2.2	Labeling Conventions	1-1-5
1.2.3	Industry Coordination	1-1-6
1.3	Information Required by 10 CFR 50.33(a) through (d)	1-1-7

PART 1: ADMINISTRATIVE INFORMATION

Chapter 1 Introduction

Dominion Nuclear North Anna, LLC (“Dominion”) submits this application for an early site permit (ESP) to the U.S. Nuclear Regulatory Commission (NRC) in accordance with the requirements of Title 10 of the Code of Federal Regulations, Part 52, (10 CFR 52) Subpart A, Early Site Permits. Dominion requests that the NRC issue an ESP to Dominion having a duration of twenty years for the site described herein. The information in this application has been developed to support the issuance of that permit.

The site selected for the ESP is a parcel of land on the North Anna Power Station (NAPS) site in Louisa County, Virginia, approximately 40 miles north-northwest of Richmond, Virginia. Other, existing nuclear facilities licensed by the NRC are located on the NAPS site. Those other facilities are NAPS Units 1 and 2 (Docket Nos. 50-338/339; NRC Facility Operating License Nos. NPF-4/7) and the North Anna Independent Spent Fuel Storage Installation (ISFSI) (NRC Docket No. 72-16; Materials License No. SNM-2507). NAPS Units 1 and 2 have been producing electricity for customers since 1978 and 1980, respectively. The site selected for the ESP, called the ESP site, is located within the NAPS site. It is adjacent to and generally west of the existing units and is illustrated in Figure 1.0-1.

The NAPS site, which includes the existing facilities and the ESP site, is owned by Virginia Electric and Power Company (Virginia Power) and Old Dominion Electric Cooperative (ODEC), as tenants in common. Virginia Power is the licensed operator of the existing facilities, with control of the existing facilities and the authority to act as ODEC’s agent. Virginia Power supports this application.

Both Virginia Power and Dominion are direct and indirect wholly-owned subsidiaries, respectively, of Dominion Resources, Inc. (DRI). If Dominion decides to proceed with the development of new nuclear units on the ESP site, it would enter into and obtain, to the extent necessary, appropriate state public utility commission approval(s) of an agreement to purchase or lease the ESP site. Similarly, if Dominion decides to conduct any pre-construction activities authorized by the ESP pursuant to 10 CFR 52.17(c), it would enter into and obtain, to the extent necessary, appropriate state public utility commission approval(s) of site redress or related agreement(s) with Virginia Power, before conducting the activities. The agreement would authorize Dominion to conduct the pre-construction activities and confirm Dominion’s obligation to perform any site redress as may be required pursuant to the site redress plan approved by the NRC. Dominion’s site redress obligation would be supported by a guaranty provided by its ultimate parent, DRI (see Part 4, Programs and Plans).

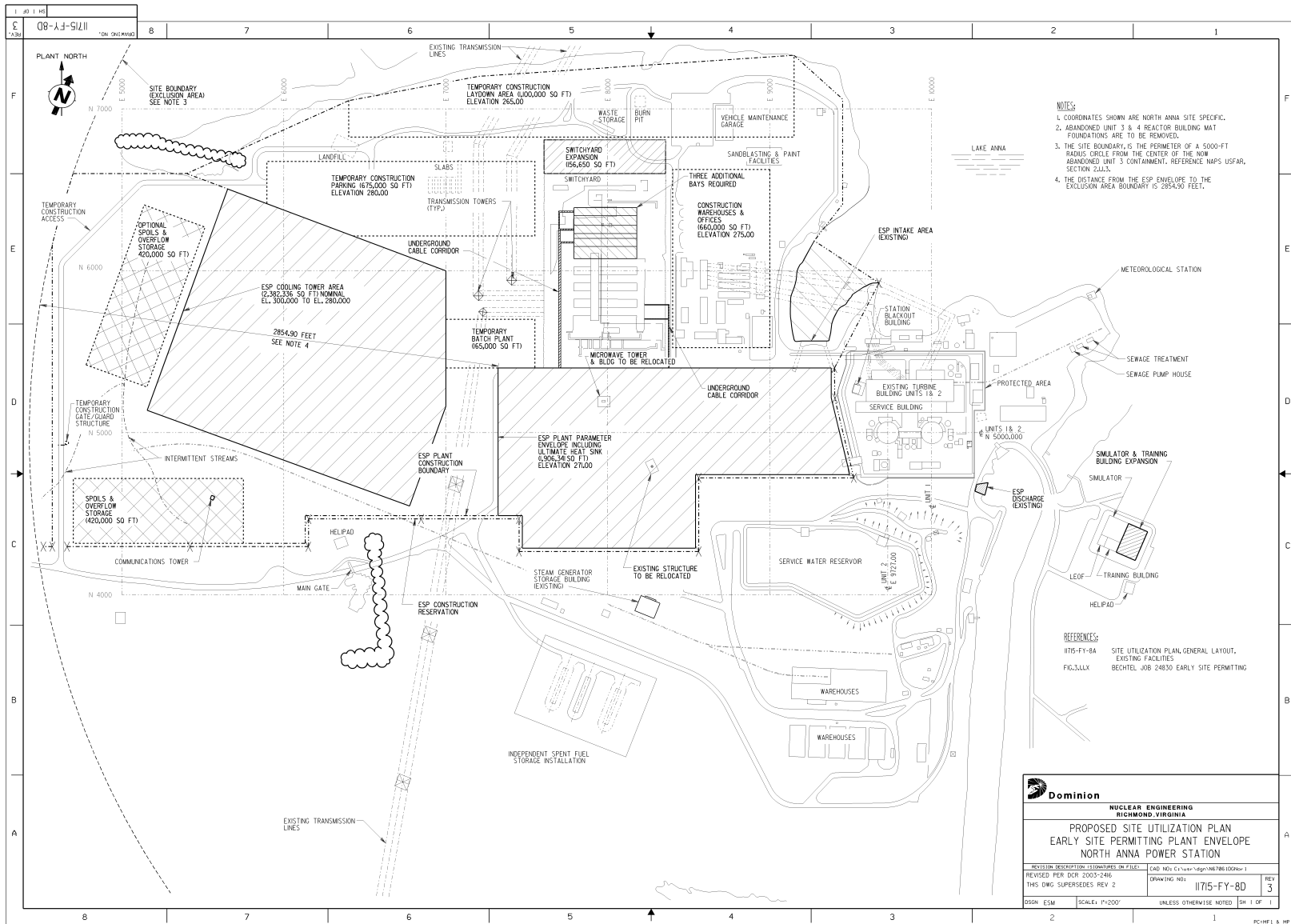


Figure 1.0-1 ESP Site Layout

1.1 Purpose of an Early Site Permit Application

For a commercial nuclear power plant to operate in the United States, it has to obtain a license from the NRC. Over the decades, the NRC and its predecessor agency, the Atomic Energy Commission, have issued more than a hundred operating licenses.

In the past, nuclear power plants were licensed under a two-step licensing process set forth in Part 50 of NRC's regulations. That process required the NRC to first issue a construction permit and later, an operating license. In 1989, the NRC established an alternative licensing process, designated Part 52, that essentially combined the construction permit and operating license processes, with certain conditions, into a single "combined license (COL)." Other licensing actions governed by Part 52 include the ESP, which allows an applicant to obtain approval for a site and "bank" it for future use, and the certified standard plant design, which can be used by an interested applicant as an "off-the-shelf" design already approved by the NRC.

Under Part 52, the NRC can issue an ESP approving one or more sites separate from any other licensing action contained in NRC's regulations. Such permits are valid for ten to twenty years and can be renewed for an additional ten to twenty years.

Site safety issues, environmental issues, and certain aspects of emergency preparedness are addressed as part of the ESP process. Those issues are addressed independent from NRC's review of any specific reactor design. Licensing issues are resolved with finality under the ESP process and are not re-examined in any subsequent licensing action involving the permitted site, absent information meeting certain standards established by the NRC (Reference 1).

Section 1.1 References

1. 10 CFR 52.39, Finality of Early Site Permit Determinations.

1.2 Early Site Permit Application Format and Content

1.2.1 Format and Content

This application contains the information required by NRC regulations (Reference 1) for an ESP application. The application has been submitted to the NRC in accordance with NRC guidance (Reference 2).

The application is organized as follows:

- **Part 1 – Administrative Information.** This part contains general corporate information about Dominion and an overview of the application format and content.
- **Part 2 – Site Safety Analysis Report (SSAR).** This part contains information about site safety, emergency preparedness, and quality assurance. The site safety section includes a description of the ESP site and proposed facilities, an assessment of the site features affecting the facility design, and meteorological, hydrologic, geologic, and seismic characteristics of the site.

Regarding the description of the facilities for which the proposed site may be used, Dominion has not selected a particular reactor design to be constructed at the ESP site. Thus, in order to provide sufficient design information to enable the NRC to determine that the proposed site is suitable for new units, a surrogate design has been provided as part of the application. The surrogate plant is in the form of a set of bounding plant parameters termed the “plant parameters envelope (PPE).” The PPE approach has been accepted by the NRC (Reference 3). The combination of PPE values and site characteristics that would form the licensing basis for NRC’s issuance of an ESP are identified in the application.

This part also discusses the capability of the facilities to withstand the natural and man-made environmental hazards of the site. The emergency preparedness information includes an assessment of any impediments to implementing an emergency plan at the ESP site and describes the major features of an emergency plan. The quality assurance program under which ESP-related activities have been performed is provided.

Where possible, the SSAR section numbers correspond to the section numbers identified in draft NRC Part 52 guidance (Reference 4). Consistent with that guidance, there are some gaps in the numbering sequence. This is intentional. Also, in a few instances, information has been located elsewhere in the application because it was deemed more appropriate for ESP purposes. However, to the extent practical, the numbering sequence in this ESP application has been maintained consistent with NRC guidance. This approach is intended to facilitate any subsequent integration of the information in this ESP application with a design certification and/or COL activity in which the complete numbering sequence would be used.

- **Part 3 – Environmental Report.** This part contains information about site environmental issues. It focuses on the environmental impacts to the ESP site from the construction and operation of one or more reactors having characteristics that fall within the plant parameters envelope.

- **Part 4 – Programs and Plans.** This part contains information about site redress. Site redress describes the actions that would be taken by Dominion to ensure that the ESP site is restored to an environmentally stable and aesthetically acceptable condition if certain limited pre-construction activities are conducted and the ESP expires before it is referenced in an application for a COL.

Each part is intended to stand alone to the extent practical. That is, information appearing within one part may be referenced elsewhere within the same part to minimize duplication. However, if the same information is used in more than one part, that information may be replicated so that each part may be used without reliance on another part. In the electronic format, references between parts may be “hyperlinked.”

1.2.2 Labeling Conventions

Each page of this application, except Appendix 2.5.4B (a third-party report), has a header that indicates the Part of this application to which it belongs. Other content identity is established as follows.

1.2.2.1 Pagination

Content pages are numbered to indicate their Part, Chapter, and page within a chapter. For example, page 3-2-36 is the 36th page in Part 3, Chapter 2.

Page numbers on part-level supporting pages, such as tables of contents, indicate the associated part number and sequential page number (in lower-case roman numerals). Page numbers on overall supporting pages, such as the table of contents for the entire application, consist only of lower-case roman numerals.

1.2.2.2 Paragraph Numbering

Within each Part, chapters are numbered sequentially. Subtier content is numbered based on the chapter number. For example, Chapter 2, Section 2.1, Section 2.1.1, etc. References to sections are within a Part unless otherwise specified.

1.2.2.3 References

Reference lists appear at the end of each Section, i.e., the first subdivision within chapters. For example, the References list for Part 3, Section 2.5 appears at the end of Section 2.5.

1.2.2.4 Tables and Figures

Table and figure numbers consist of the Section number, and a sequential number. For example, Figure 2.3-10 is the 10th figure for Section 2.3. See the lists of Tables and Figures at the beginning of this application for a complete inventory.

1.2.3 Industry Coordination

As part of the activities undertaken in the preparation of this application, another DRI subsidiary, Dominion Energy, Inc. (DEI), participated in the Nuclear Energy Institute's (NEI) Early Site Permit Task Force. The task force included the other lead applicants involved in demonstrating the Part 52 ESP process. The task force met periodically with the NRC staff over a two-year period. A number of generic issues related to the ESP process were identified and resolved through those interactions. In addition, DEI worked in concert with the other lead applicants to optimize commonality among the lead applicants. The results of those issue resolutions and the common approaches are reflected in this application.

Section 1.2 References

1. 10 CFR 52.17, Content of Applications.
2. NRC Regulatory Issues Summary 2001-05, "Guidance on Submitting Documents to the NRC by Electronic Information Exchange or on CD-ROM," January 25, 2001.
3. February 5, 2003 NRC letter to NEI, J. E. Lyons to R. L. Simard, titled "Resolution of Early Site Permit Topic 6 (ESP-6), Use of Plant Parameter Envelope (PPE) Approach."
4. NRC Review Standard RS-002, Processing Applications for Early Site Permits: Draft for Interim Use and Public Comment, December 23, 2002, as supplemented.

1.3 Information Required by 10 CFR 50.33(a) through (d)

Dominion Nuclear North Anna, LLC (Dominion) is the applicant for this ESP. Dominion Nuclear North Anna, LLC is an indirect wholly-owned subsidiary of DRI. DRI is one of the nation's leading energy companies, serving five million retail energy customers in nine states. DRI is the largest fully-integrated natural gas and electric provider in the United States, with over \$37 billion in assets, over \$10 billion in annual revenue, and over \$2 billion in annual cash flow. DRI's energy base includes 24,000 megawatts (MW) of electric generation, 6.1 trillion cubic feet equivalent of proved gas and oil reserves, and nearly 7,900 miles of natural gas transmission pipeline. Virginia Electric and Power Company (Virginia Power), a subsidiary of DRI, is the NRC-licensed operator of NAPS, the Surry Power Station, and their associated ISFSIs. Dominion Nuclear Connecticut, Inc., also an indirect, wholly-owned subsidiary of DRI, is the licensed operator of the Millstone Power Station.

NRC regulations (Reference 1) require that an ESP application contain certain corporate information about the applicant. The required information is provided in Table 1.3-1.

Section 1.3 References

1. 10 CFR 50.33(a) through (d), Contents of Applications, general information.

Table 1.3-1 Dominion Nuclear North Anna, LLC, Officers and Directors

Name of Applicant	Dominion Nuclear North Anna, LLC, a Virginia limited liability company
Address	120 Tredegar Street Richmond, Virginia 23219
Description of Business	Entity seeking to obtain an early site permit for new nuclear generation at the North Anna site
Principal business location	120 Tredegar Street, Richmond, Virginia 23219

Names, addresses, and citizenship of member:			
Name	Title	Address	Citizenship
Dominion Nuclear Projects, Inc.	Sole Member	120 Tredegar Street Richmond, VA 23219	USA

Names, addresses, and citizenship of directors and officers:			
Name	Title	Address	Citizenship
Mark F. McGettrick	President and Chief Executive Officer – Generation	120 Tredegar Street Third Floor Richmond, VA 23219	USA
David A. Christian	Senior Vice President - Nuclear Operations and Chief Nuclear Officer	Innsbrook Technical Center - 2SW 5000 Dominion Boulevard Glen Allen, VA 23060	USA
G. Scott Hetzer	Senior Vice President and Treasurer	100 Tredegar Street Third Floor Richmond, VA 23219	USA
William R. Matthews	Senior Vice President - Nuclear Operations	Millstone Power Station Rope Ferry Road Waterford, CT 06385	USA
Martin L. Bowling, Jr.	Vice President - Technical Services	Innsbrook Technical Center, 1NE 5000 Dominion Boulevard Glen Allen, VA 23060	USA
Pamela F. Faggert	Vice President - Chief Environmental Officer	Innsbrook Technical Center, 1SE 5000 Dominion Boulevard Glen Allen, VA 23060	USA
Eugene S. Grecheck	Vice President - Nuclear Support Services	Innsbrook Technical Center, 2SE 5000 Dominion Boulevard Glen Allen, VA 23060	USA
Leslie N. Hartz	Vice President - Nuclear Engineering	Innsbrook Technical Center, 2SE 5000 Dominion Boulevard Glen Allen, VA 23060	USA

Table 1.3-1 Dominion Nuclear North Anna, LLC, Officers and Directors

James K. Martin	Vice President - Business Development	120 Tredegar Street Third Floor Richmond, VA 23219	USA
Patricia A. Wilkerson	Vice President and Corporate Secretary	100 Tredegar Street Third Floor Richmond, VA 23219	USA
Lee D. Katz	Controller	120 Tredegar Street Third Floor Richmond, VA 23219	USA
James P. Carney	Assistant Treasurer	100 Tredegar Street Second Floor Richmond, VA 23219	USA
E. J. Marks, III	Assistant Secretary	100 Tredegar Street Second Floor Richmond, VA 23219	USA
Jerry G. Overman	Assistant Treasurer	100 Tredegar Street Third Floor Richmond, VA 23219	USA

No Foreign Ownership, Control or Influence:

Dominion Nuclear North Anna, LLC, is wholly-owned by Dominion Nuclear Projects, Inc. (DNP). DNP is a wholly-owned subsidiary of Dominion Energy, Inc., which in turn is wholly-owned by Dominion Resources, Inc. (DRI). None of the aforementioned entities is owned, controlled, or dominated by an alien, foreign corporation, or foreign government.

PART 2 - SITE SAFETY ANALYSIS REPORT

Contents

Chapter 1	Introduction and General Description	2-1-1
1.1	Introduction	2-1-1
1.2	General Site Description	2-1-3
1.2.1	Site Location	2-1-3
1.2.2	Site Development	2-1-3
1.3	Plant Parameters Envelope	2-1-9
1.3.1	Plant Parameters Envelope Approach	2-1-9
1.3.2	Overview of Reactor Types Used for PPE Development	2-1-10
1.3.3	Use of the PPE Tables	2-1-13
1.4	Identification of Agents and Contractors	2-1-41
1.4.1	Bechtel Power Corporation	2-1-41
1.4.2	Other Contractors	2-1-41
1.5	Requirements for Further Technical Information	2-1-43
1.6	Material Incorporated by Reference	2-1-44
1.7	Drawings and Other Detailed Information	2-1-45
1.8	Conformance to NRC Regulations and Regulatory Guidance	2-1-46
1.8.1	Conformance with NRC Regulations	2-1-46
1.8.2	Conformance to NRC Regulatory Guides	2-1-57
1.8.3	Conformance to NRC Review Standard	2-1-69
Chapter 2	Site Characteristics	2-2-1
2.1	Introduction	2-2-1
2.1.1	Site Location and Description	2-2-1
2.1.2	Exclusion Area Authority and Control	2-2-3
2.1.3	Population Distribution	2-2-4
2.2	Nearby Industrial, Transportation, and Military Facilities	2-2-28
2.2.1	Location and Routes	2-2-28
2.2.2	Descriptions	2-2-28
2.2.3	Evaluation of Potential Accidents	2-2-30
2.3	Meteorology	2-2-36
2.3.1	Regional Climatology	2-2-36
2.3.2	Local Meteorology	2-2-41
2.3.3	Onsite Meteorological Measurements Program	2-2-45
2.3.4	Short-Term (Accident) Diffusion Estimates	2-2-49

Contents

2.3.5	Long-Term (Routine) Diffusion Estimates	2-2-52
2.4	Hydrology	2-2-98
2.4.1	Hydrologic Description	2-2-98
2.4.2	Floods	2-2-104
2.4.3	Probable Maximum Flood on Streams and Rivers	2-2-106
2.4.4	Potential Dam Failures	2-2-111
2.4.5	Probable Maximum Surge and Seiche Flooding	2-2-111
2.4.6	Probable Maximum Tsunami Flooding	2-2-112
2.4.7	Ice Effects	2-2-112
2.4.8	Cooling Water Canals and Reservoirs	2-2-116
2.4.9	Channel Diversions	2-2-118
2.4.10	Flooding Protection Requirements	2-2-118
2.4.11	Low Water Considerations	2-2-119
2.4.12	Groundwater	2-2-122
2.4.13	Accidental Releases of Liquid Effluents to Ground and Surface Waters	2-2-133
2.5	Geology, Seismology, and Geotechnical Engineering	2-2-169
2.5.1	Basic Geologic and Seismic Information	2-2-169
2.5.2	Vibratory Ground Motion	2-2-226
2.5.3	Surface Faulting	2-2-263
2.5.4	Stability of Subsurface Materials and Foundations	2-2-271
	Appendix 2.5.4A Triaxial and Consolidation Tests of Soils at SWR	2-5.4A-1
	Appendix 2.5.4B Final Report, Results of Geotechnical Exploration and Testing, North Anna ESP Project, Louisa County, Virginia, Prepared by MACTEC Engineering and Consulting, MACTEC Project Number 30720-2-5400, February 2003	2-5.4B-1
2.5.5	Stability of Slopes	2-2-304
2.5.6	Embankments and Dams	2-2-310
Chapter 3	Design of Structures, Components, Equipment, and Systems	2-3-1
Chapter 13	Conduct of Operations	2-13-1
13.3	Emergency Planning	2-13-1
13.3.1	Emergency Planning Overview	2-13-1
13.3.2	Major Features Emergency Plan	2-13-1
13.3.3	Contracts and Arrangements	2-13-33

Contents

13.3.4 Conformance with NUREG-0652, Supplement 2 2-13-34

13.6 Industrial Security 2-13-39

Chapter 15 Accident Analyses. 2-15-1

15.1 Selection of Accidents 2-15-1

15.2 Evaluation Methodology 2-15-3

15.3 Source Terms. 2-15-5

15.4 Radiological Consequences. 2-15-6

Chapter 17 Quality Assurance 2-17-1

17.1 ESP Quality Assurance. 2-17-1

PART 2: SITE SAFETY ANALYSIS REPORT

Chapter 1 Introduction and General Description

1.1 Introduction

This Site Safety Analysis Report (SSAR) supports Dominion's application for its ESP site. The SSAR addresses site suitability issues and complies with the applicable portions of 10 CFR 52, Subpart A, Early Site Permits.

The site selected for the Early Site Permit (ESP) is a parcel of land on the North Anna Power Station (NAPS) site in Louisa County, Virginia, approximately 40 miles north-northwest of Richmond, Virginia. Other, existing nuclear facilities licensed by the U. S. Nuclear Regulatory Commission (NRC) are located on the NAPS site. Those other facilities are NAPS Units 1 and 2 (Docket Nos. 50-338/339; NRC Facility Operating License Nos. NPF-4/7) and the North Anna Independent Spent Fuel Storage Installation (ISFSI) (NRC Docket No. 72-16; Materials License No. SNM-2507). NAPS Units 1 and 2 have been producing electricity for customers since 1978 and 1980, respectively. The site selected for the ESP, called the ESP site, is located within the NAPS site. It is adjacent to and generally west of the existing units and is illustrated in Figure 1.2-4.

The NAPS site, which includes the existing facilities and the ESP site, is owned by Virginia Electric and Power Company (Virginia Power) and Old Dominion Electric Cooperative (ODEC), as tenants in common. Virginia Power is the licensed operator of the existing facilities, with control of the existing facilities and the authority to act as ODEC's agent. Virginia Power supports this application.

Dominion has not selected a particular reactor design to be constructed at the ESP site. Thus, in order to provide sufficient design information to enable the NRC to determine that the site is suitable for new units, a surrogate design has been provided. The surrogate design is in the form of a set of bounding plant parameters termed the "plant parameters envelope (PPE)." The PPE approach has been accepted by the NRC (Reference 1). The combination of PPE values and site characteristics that would form the permit basis for NRC's issuance of an ESP are identified in this SSAR.

The SSAR contains information about site safety, emergency preparedness, and quality assurance. The following paragraphs briefly describe the contents of the SSAR:

Chapter 1, Introduction and General Description, includes a general site description, an overview of reactor types, and the PPE approach.

Chapter 2, Site Characteristics, includes geography and demography, nearby industrial installations, transportation and military facilities, and meteorologic, hydrologic, geologic, and seismic characteristics of the site, including information about aircraft hazards. It also includes descriptions of effluents, thermal discharges, and conformance with 10 CFR 100, Reactor Site

Criteria, requirements. This chapter provides the anticipated maximum levels of radiological and thermal effluents the new units would produce.

Chapter 3, Design of Structures, Components, Equipment, and Systems contains a pointer to information on air craft hazards located in Chapter 2.

Chapter 13, Conduct of Operations, includes the major features of the emergency plan and other emergency preparedness information.

Chapter 15, Accident Analyses, includes accident and dose consequence analyses required by 10 CFR 52.17(a)(1), 50.34(a)(1) and 100.21(c)(2), applying the PPE approach.

Chapter 17, Quality Assurance, includes the Quality Assurance Program under which the ESP application has been prepared.

Where possible, the SSAR section numbers correspond to the section numbers identified in draft NRC Part 52 guidance (Reference 2). Consistent with that guidance, there are some gaps in the numbering sequence. This is intentional. Also, in a few instances, information has been located elsewhere in the application because it was deemed more appropriate for ESP purposes. However, to the extent practical, the numbering sequence in this ESP application has been maintained consistent with NRC guidance. This approach is intended to facilitate any subsequent integration of the information in this ESP application with a design certification and/or combined license (COL) activity in which the complete numbering sequence would be used.

Section 1.1 References

1. February 5, 2003 NRC letter to NEI, J. E. Lyons to R. L. Simard, titled "Resolution of Early Site Permit Topic 6 (ESP-6), Use of Plant Parameter Envelope (PPE) Approach."
2. NRC Review Standard RS-002, Processing Applications for Early Site Permits: Draft for Interim Use and Public Comment, December 23, 2002, as supplemented.

1.2 General Site Description

1.2.1 Site Location

The ESP site is situated on a peninsula on the south shore of Lake Anna, at the end of State Route 700 in Louisa County, in northeastern Virginia (see Figure 1.2-2). The ESP site is approximately 40 miles north-northwest of Richmond, Virginia; 36 miles east of Charlottesville, Virginia; and 22 miles southwest of Fredericksburg, Virginia. Interstates 95 and 64 pass within 16 miles to the east and 18 miles to the south of the ESP site, respectively.

The NAPS site comprises 1803 acres, of which about 760 acres are covered by water. The NAPS site is laid out according to the site plan as shown in Figure 1.2-3. Virginia Power and ODEC own, and Virginia Power controls, all of the land within the NAPS site boundary, including those portions of the North Anna Reservoir and Waste Heat Treatment Facility (WHTF) that lie within the site boundary. These companies also own all land outside the NAPS site boundary that forms Lake Anna, up to the expected high-water marks. The NAPS site and all supporting facilities, including the North Anna Reservoir, the WHTF, the earth dam, dikes, railroad spur, and roads constitute approximately 18,643 acres. Lake Anna, which includes the North Anna Reservoir and the WHTF, was created to serve the needs of the power station.

A more detailed description of the site can be found in Section 2.2.

1.2.2 Site Development

The NAPS site currently has two Westinghouse pressurized water reactors (PWR), rated at 2893 MWth and their supporting structures. These structures include a circulating water pumphouse and discharge structure, water treatment building, switchyard, and training center. In addition, an ISFSI is located on the site. Figure 1.2-3 shows the current NAPS site development.

The site selected for the ESP is a parcel of land on the NAPS site. The ESP site is adjacent to and generally to the west of the existing units, and is illustrated in Figure 1.2-4.

No specific plant design has been chosen for the ESP site within the NAPS site. Instead, a set of bounding plant parameters is presented to envelop future ESP site development. This PPE is based on the addition of power generation from two distinct units, to be designated North Anna Units 3 and 4. (The PPE is described in Section 1.3.) Each unit represents a portion of the total generation capacity to be added and would consist of one or more reactors or reactor modules. These multiple reactors or modules (the number of which may vary depending on the reactor type selected) would be grouped into distinct operating units. Each unit would consist of a plant of one or more modules that would not exceed 4300 MWth of nuclear generating capacity. Because a specific design has not been selected, boundaries have been established for the placement of the new units. The boundaries are shown in Figure 1.2-4.

Section 1.2 References

None

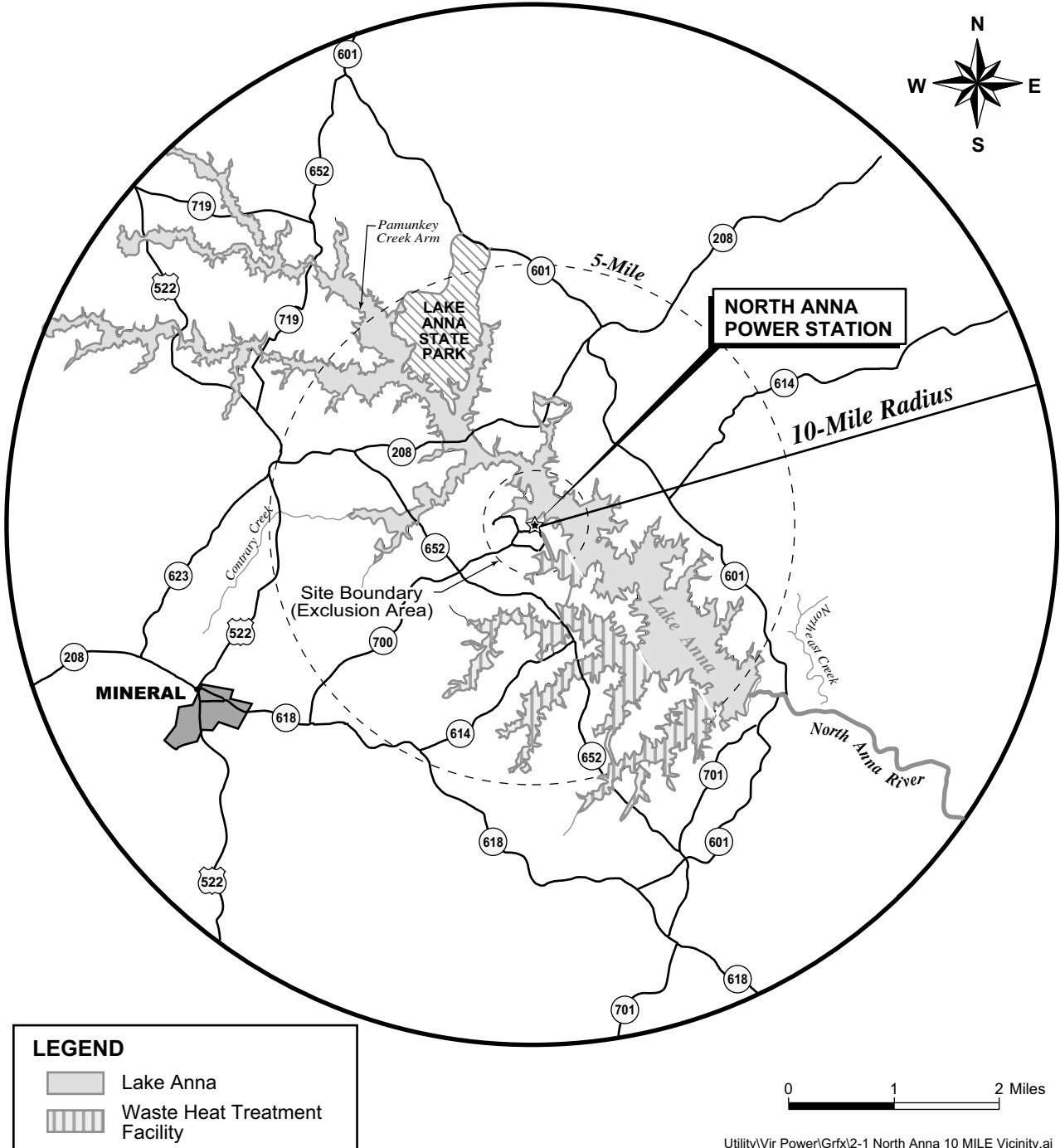


Figure 1.2-1 Site Location – 10 Mile Radius

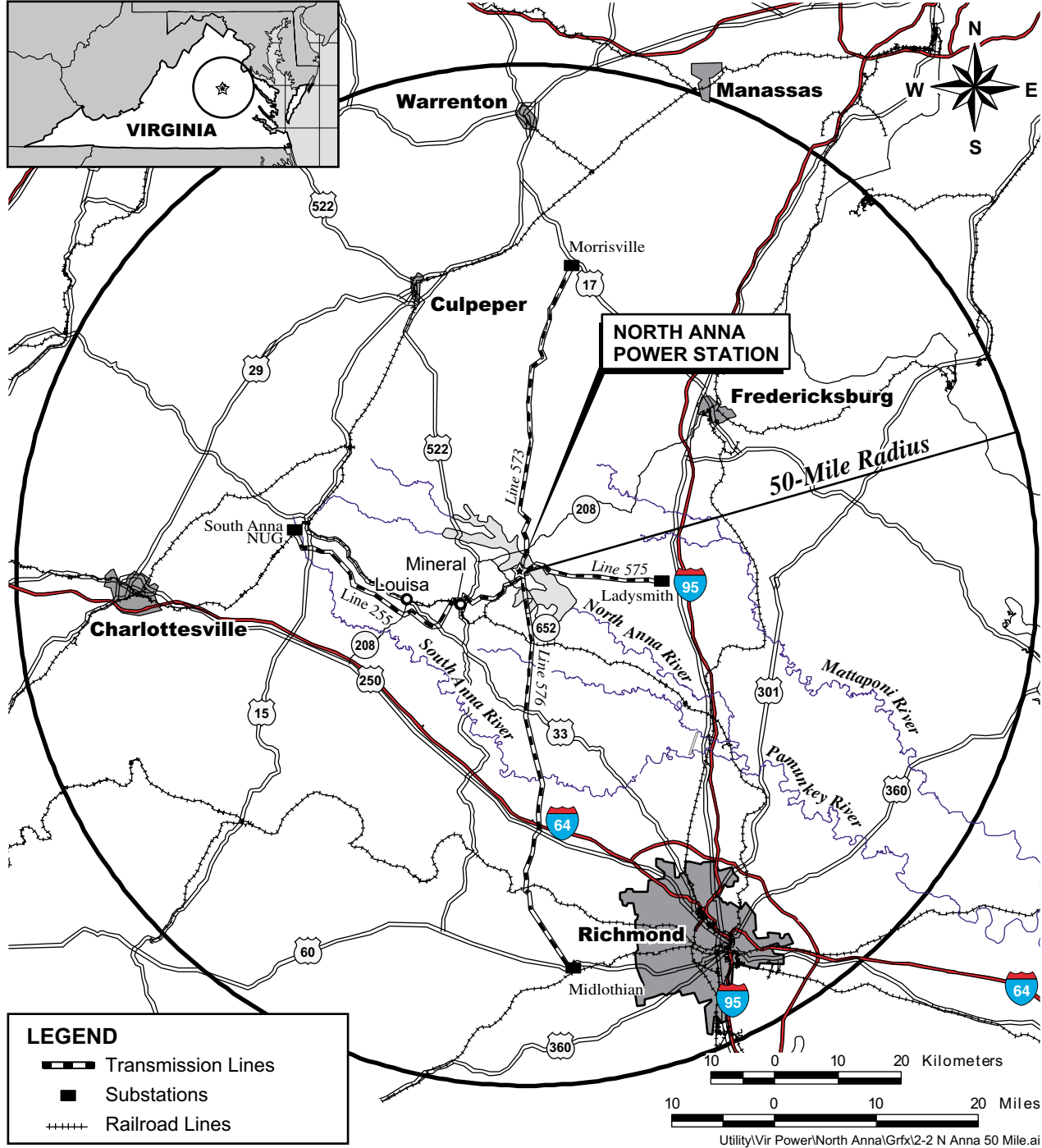


Figure 1.2-2 Site Location – 50 Mile Radius

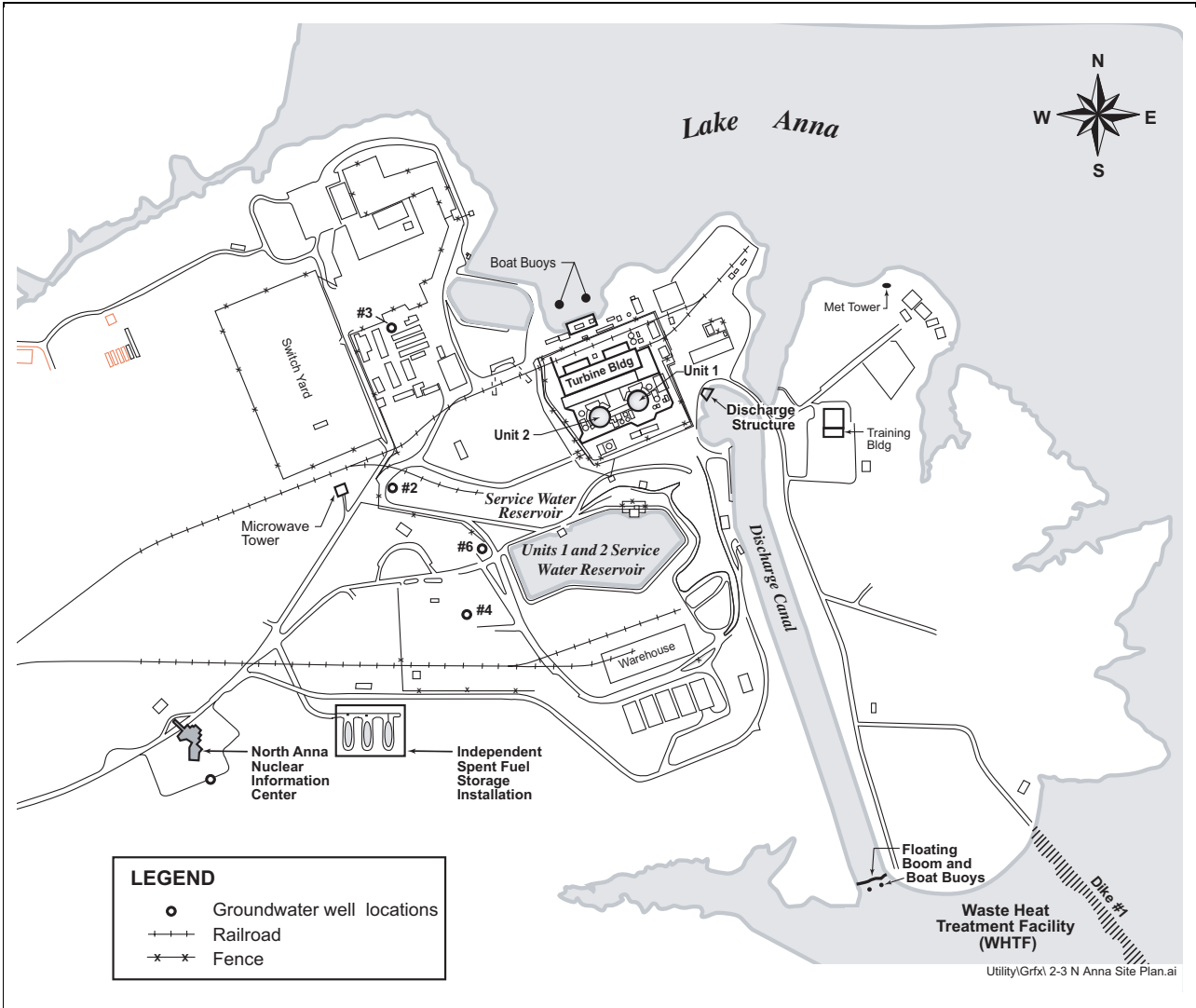


Figure 1.2-3 Site Layout – Current Development

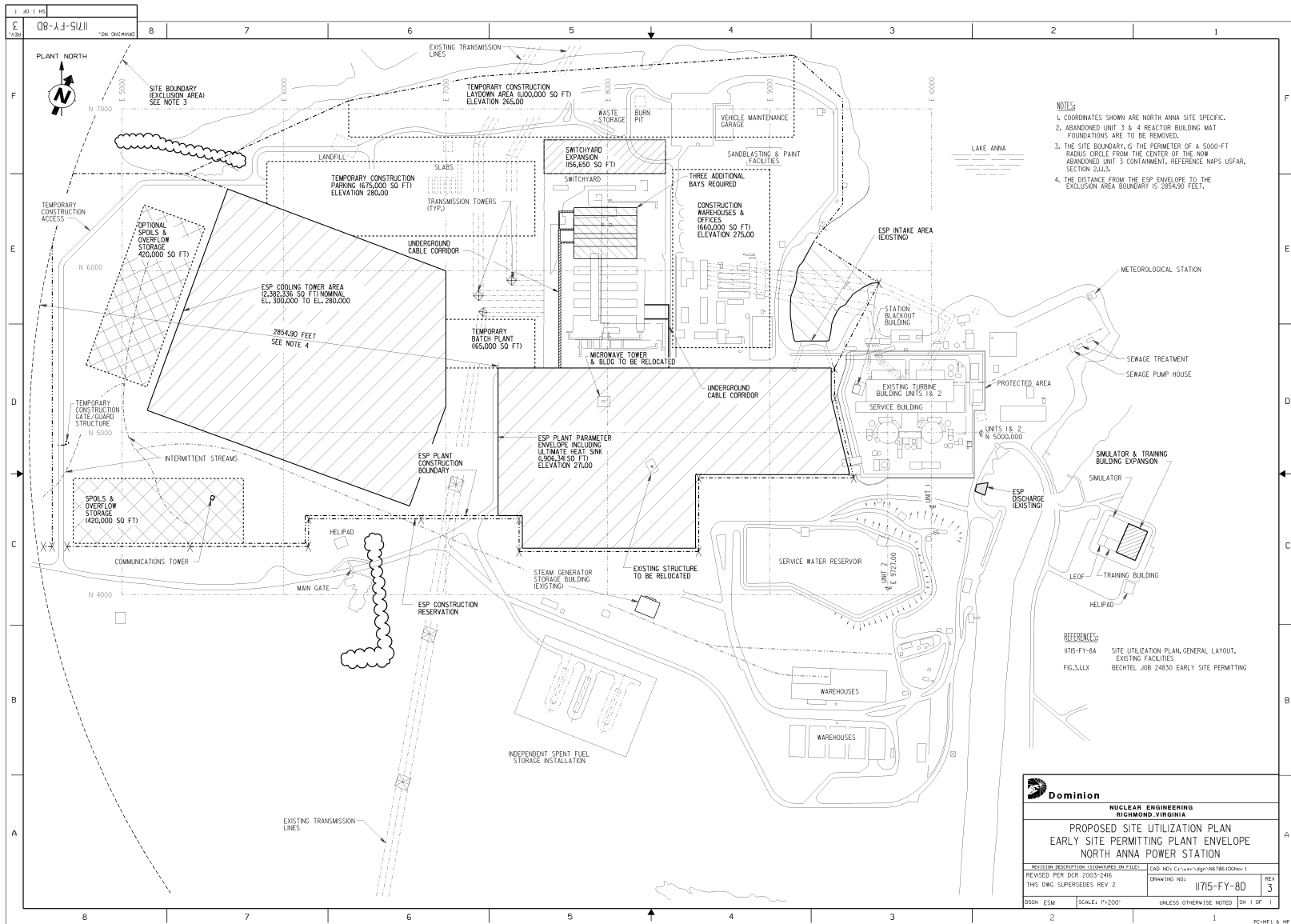


Figure 1.2-4 Site Layout – New Development

1.3 Plant Parameters Envelope

The required contents of an ESP application are specified in 10 CFR 52.17. The application should specify the number, type and thermal power level of the facilities for which the ESP site may be used [10 CFR 52.17(a)(1)(I)]. The concept of a PPE to describe the bounding plant for which the ESP site is suitable has been accepted by the NRC (Reference 1). The PPE, its development, and its use in this application is discussed in the following sections. This PPE approach provides sufficient design details to support NRC review of the ESP application while also recognizing that technological developments may result in new reactor technologies becoming available that may not have been envisioned at the time of ESP application submittal. The actual design selected would be reviewed at the time of a COL application to ensure that the design fits within the PPE envelope. Any differences would be addressed in the COL application.

1.3.1 Plant Parameters Envelope Approach

The listing of plant parameters necessary to define the plant-site interface – the PPE - was developed in the early 1990s based on work sponsored by the U.S. Department of Energy (DOE) and the nuclear industry, which included reactor vendors and utilities. The effort was intended to provide a comprehensive list of plant parameters to accurately characterize a plant at a site. Over time, this list has evolved to encompass information needed to support development of an ESP application, including the SSAR and the Environmental Report.

The PPE was developed based on data from selected reactor designs of two types (light-water-cooled reactors (LWRs) and helium-cooled reactors). To ensure that the resulting PPE has the flexibility to bound multiple reactor designs, these designs were selected to provide a broad cross section of available reactors. Brief descriptions of each of these reactor types are included in Section 1.3.2.

The resulting PPE Table, Table 1.3-1, lists both the single and two unit values for each parameter. The bounding parameters are the single largest (or smallest) value for each category, using engineering, safety and environmental conservatism to select the appropriate value. As noted in Section 1.3.2.2, a single unit may consist of more than one reactor for purposes of developing the PPE. Definitions for each PPE parameter are supplied on this table. Additional supporting information to support this table is included in Table 1.3-3 through Table 1.3-7. The PPE is not intended to be limited to the designs selected to create the envelope, but rather to provide a broad overall outline of a design concept and to include other potential designs if they can be demonstrated to fall within the parameter values provided in the PPE.

1.3.2 Overview of Reactor Types Used for PPE Development

Seven reactor designs have been used to develop the PPE bounding values.

- ACR-700, LWR, developed by Atomic Energy Canada Limited
- Advanced Boiling Water Reactor, developed by General Electric (ABWR)
- AP-1000, PWR, developed by Westinghouse Electric Company
- Economic Simplified Boiling Water Reactor, developed by General Electric (ESBWR)
- Gas Turbine Modular Helium Reactor (GT-MHR), developed by General Atomics.
- International Reactor Innovative and Secure (IRIS) next generation PWR, developed by a consortium led by Westinghouse Electric Company
- Pebble Bed Modular Reactor (PBMR), developed by PBMR (Pty) Ltd.

1.3.2.1 ACR-700

The ACR-700 is designed by Atomic Energy Canada Limited (AECL) and is based on the CANDU 6 design. The ACR-700 is a 1983 MWth light-water-cooled, heavy-water-moderated reactor. It uses four heat transport pumps circulating light water through two steam generators to remove the heat from the horizontal reactor vessel, called a calandria. This light water primary coolant circulates through individual pressurized fuel channels in the calandria. On the other side of these fuel channels, the calandria contains a heavy water moderator at low temperature and pressure, which allows increased neutron efficiency.

The CANDU 6 design is a natural uranium fueled reactor; a design attained by using heavy water as the primary heat removal fluid. For ACR-700, the primary coolant has been changed to light water, reducing the cost and complexity of the plant. The resulting reduction in neutron efficiency requires that the fuel be slightly enriched, to approximately 2 percent U^{235} . The fuel elements, however, are similar to those used in CANDU 6 with minor improvements to increase thermal efficiency.

Unlike the ABWR and AP1000, the use of individual pressurized fuel channels in the ACR-700 allows the ACR-700 to be continuously refueled on power. Fueling machines are designed to isolate an individual fuel channel, remove a selected number of fuel assemblies (which are only about 20 inches long) and return the channel to service. Electrical power generation would be through the use of a standard steam turbine cycle.

The CANDU reactor design has been inservice in a variety of countries. Thirty-four CANDU units have been constructed worldwide. The ACR-700 design is configured in a two-reactor block, with shared systems between the two reactors. This two-reactor block makes up one unit for purposes of developing the PPE.

1.3.2.2 **Advanced Boiling Water Reactor**

The ABWR is an evolutionary design of the boiling water reactor (BWR) design developed by the General Electric Company. The ABWR design has been certified by the NRC (under 10 CFR 52, Appendix A). The certified design is rated at 3926 MWth and is a single cycle, forced circulation BWR. The design is based on existing BWR designs, similar to the ones operating in the United States at Clinton and Grand Gulf, but incorporates several advanced features, including vessel-mounted recirculation pumps, fine motion control rod drives and an advanced digital and multiplexed instrumentation and control system. Additional changes have added a third division of safety-related equipment and improved the containment design.

Studies performed by General Electric indicate that this design has sufficient operating margins to allow uprate of the core thermal power. Based on this analysis, the PPE data supplied for this design is based on the uprated, 4300 MWth design of this plant. Other than a thermal power uprate, no other significant design changes are required. Electrical power generation is through the use of a standard steam turbine cycle.

To date, two ABWR units have been constructed and are currently in operation in Japan. Additional units are under construction in Taiwan (two) and Japan (two), with six others in various stages of design in Japan. The ABWR is designed as a single-unit, stand-alone configuration.

1.3.2.3 **AP1000**

The Westinghouse AP1000 is a 3400 MWth PWR. Its design is based on the NRC design certified AP600 (under 10 CFR 52, Appendix C), with design changes to accommodate the increase in power output. The AP1000 is a two-loop, four-reactor-coolant-pump design that uses fuel, reactor vessel, and internals similar to those in service today at South Texas. The reactor coolant pumps are canned-type pumps to reduce the probability of leakage and to improve reliability. The design is functionally similar to that of the AP600, with the containment building, reactor vessel, steam generators, reactor coolant pumps and pressurizer increased in size to accommodate the increase in thermal power.

The AP1000 is designed to use passive features for accident mitigation. An externally cooled steel containment building, In-containment refueling water storage tank, rapid depressurizing capability and other design features allow the elimination of all safety-related alternating current powered equipment. Electrical power generation would be through the use of a standard steam turbine cycle.

The AP1000 is designed in a single-unit, stand-alone configuration.

1.3.2.4 **Economic Simplified Boiling Water Reactor**

The ESBWR is a further evolution from the ABWR and is designed by the General Electric Company. The ESBWR is a 4000 MWth single cycle BWR with a rated electrical output of 1390 MWe. The ESBWR relies on the use of natural circulation and passive safety features to

enhance plant performance and simplify the design. The use of natural circulation has allowed the elimination of several BWR systems. This has also increased plant accident reliability by eliminating active safety systems for emergency plant cooling.

The ESBWR has achieved its plant simplification by using innovative adaptations of operating plant systems, for example combining shutdown cooling and reactor water cleanup systems. The only major new concept or system is the passive containment cooling system (PCCS). In other cases, key components such as depressurization valves and isolation condensers are new, but utilize proven concepts.

The ESBWR is designed as a single, stand-alone unit.

1.3.2.5 Gas Turbine – Modular Helium Reactor

The Gas Turbine – Modular Helium Reactor (GT-MHR) is under development by General Atomics Corporation. The GT-MHR is a modular, medium sized helium cooled graphite moderated reactor using helium as the coolant. Each 600 MWth module includes a reactor and gas turbine, operating in a high temperature (900°C) Brayton cycle. The fuel for the GT-MHR consists of triple coated small uranium spheres formed into compacts and inserted into hexagonal graphite blocks. These blocks, along with those without fuel, are assembled inside the reactor to form a reactor core. The helium removes the heat from the reactor and is expanded across a gas turbine to generate electricity. Low and high pressure turbines, located on the same shaft as the power turbine, compress the gas and return it to the reactor.

Four GT-MHR modules are grouped together to make one unit for purposes of developing the PPE.

1.3.2.6 International Reactor Innovative and Secure

The IRIS is being designed by a consortium lead by Westinghouse Electric Company. The IRIS design is a modular, medium-power, light-water reactor under development to meet DOE Generation IV reactor design criteria. Using light water for both a coolant and moderator, the IRIS design eliminates all loss of coolant accidents by placing the entire reactor coolant system within a single reactor vessel. The components used for the design of IRIS are not new technology but some of them are employed in nuclear power for the first time. The steam generators are of a helical tube design, the reactor coolant pumps are spool type and require eight pumps per reactor, and the pressurizer is located in the upper head of the vessel.

The reactor core is designed for long burns between refueling outages, with outages planned for 4-year to 6-year intervals. The fuel assemblies are similar to that used by Westinghouse in U.S. and European reactors. Electrical power generation would be through the use of a standard steam turbine cycle.

Individual IRIS modules are rated at 1000 MWth and are grouped two or three modules to each power block. Three IRIS reactors make up one unit for purposes of developing the PPE.

1.3.2.7 Pebble Bed Modular Reactor

The PBMR is designed as a small modular graphite moderated helium cooled gas turbine reactor. PBMR (Pty) Ltd. of South Africa is developing the design. Each module is designed as a 400 MWth reactor and gas turbine assembly. The reactor uses low enriched uranium fuel encased in small triple coated spheres and then assembled into spheres, or pebbles. These pebbles are then loaded into a graphite shielded and moderated reactor vessel. Heat generated in the reactor is removed using the helium coolant and converted to electricity through a gas turbine operating on a high temperature (900°C) Brayton cycle. Individual low-pressure and high-pressure gas turbines compress the gas and return it to the reactor.

Specialized systems remove the pebbles one at a time, assay them to determine burnup, and then replace or return the pebble to the reactor. This design allows on power refueling with the fuel continuously replaced as needed. The PBMR design also stores all of its spent fuel (for its 40-year operating life) on site in specially designed tanks.

The design of the PBMR groups one or more of these modules together using a common service building. Eight PBMR modules are grouped together to make one unit for purposes of developing the PPE.

1.3.3 Use of the PPE Tables

The PPE tables are based on information supplied by the reactor vendors for the plant designs listed above. Site dependant PPE data was based on a typical site (not a specific site and not the ESP site) and chosen to bound approximately 85 percent of all existing sites. Site specific information is not listed on these tables.

The data included in this table is not to be taken as final design specific information. In some cases, where designs are not mature, the data supplied is based on engineering judgement, prior experience, or a calculation based on non-site specific assumptions. The data is reasonable and would bound most applications. An example of this is in the design of the circulating water system, which is based on site specific water supplies and temperature. Additionally, site specific environmental data is used to design the condenser and circulating water heat removal systems. The listed circulating water designs, which include once through cooling and both mechanical and natural draft towers, are based on a bounding plant design and location and would be modified to meet site characteristics when required. However, the data provided are reasonable and can be used until site-specific design data is available.

Section 1.3 References

1. Letter from James E. Lyons of USNRC to Dr. Ronald L. Simard of NEI, dated February 5, 2003.

Table 1.3-1 Plant Parameters Envelope

PPE Section	Bounding Value ^a [Value for 2 Units in brackets] ^b	Bound Notes See Table 1.3-2	Comments	Definition
1. Structures			c	
1.1 Building Characteristics				
1.1.1 Height	234 ft-0 in. [Same for 2nd unit/group]	1		The height from finished grade to the top of the tallest power block structure, excluding cooling towers.
1.1.2 Foundation Embedment	140 ft [Same for 2nd unit/group]	2		The depth from finished grade to the bottom of the basemat for the most deeply embedded power block structure.
1.2 Precipitation (for Roof Design)				
1.2.1 Maximum Rainfall Rate	19.4 in/hr (6.2 in/5 min) [Same for 2nd unit/group]	2, 3, 4, 5		The probable maximum precipitation (PMP) value that can be accommodated by a plant design. Expressed as maximum precipitation for 1 hour in 1 square mile with a ratio for five minutes to the 1 hour PMP of 0.32 as found in National Weather Service Publication HMR No. 52. A site specific value is used for this parameter.
1.2.2 Snow and Ice Load	50 lb/sq ft [Same for 2nd unit/group]	2, 3, 4		The maximum load on structure roofs due to the accumulation of snow and ice that can be accommodated by a plant design.
1.3 Safe Shutdown Earthquake (SSE)				
1.3.1 Design Response Spectra	RG 1.60 [Same for 2nd unit/group]	6		The assumed design response spectra used to establish a plant's seismic design. A site specific value is used for this parameter.
1.3.2 Peak Ground Acceleration	0.30g [Same for 2nd unit/group]	6		The maximum earthquake ground acceleration for which a plant is designed; this is defined as the acceleration which corresponds to the zero period in the response spectra taken in the free field at plant grade elevation. A site specific value is used for this parameter.
1.3.3 Time History	Envelope SSE Response Spectra [Same for 2nd unit/group]	6		The plot of earthquake ground motion as a function of time used to establish a plant's seismic design. A site specific value is used for this parameter.
1.3.4 Capable Tectonic Structures or Sources	No fault displacement potential within the investigative area [Same for 2nd unit/group]	1		The assumption made in a plant design about the presence of capable faults or earthquake sources in the vicinity of the plant site (e.g., no fault displacement potential within the investigative area).

Table 1.3-1 Plant Parameters Envelope

PPE Section	Bounding Value ^a [Value for 2 Units in brackets] ^b	Bound Notes See Table 1.3-2	Comments	Definition
1.4 Site Water Level (Allowable)				
1.4.1 Maximum Flood (or Tsunami)	1 ft below plant grade [Same for 2nd unit/group]	2, 3, 4		Design assumption regarding the difference in elevation between finished plant grade and the water level due to the probable maximum flood and probable maximum precipitation (defined in ANSI/ANS 2.8-1992) used in the plant design. A site specific value is used for this parameter.
1.4.2 Maximum Ground Water	1 meter below grade (i.e., 3.3 feet below grade) [Same for 2nd unit/group]	7		Design assumption regarding the difference in elevation between finished plant grade and the maximum site ground water level used in the plant design. A site specific value is used for this parameter.
1.5 Soil Properties Design Bases				
1.5.1 Liquefaction	None at Site-Specific SSE [Same for 2nd unit/group]	6		Design assumption regarding the presence of potentially liquefying soils at a site (e.g., none at Site-Specific SSE). A site specific value is used for this parameter.
1.5.2 Minimum Bearing Capacity (Static)	15 ksf [Same for 2nd unit/group]	2, 3		Design assumption regarding the capacity of the competent load-bearing layer required to support the loads exerted by plant structures used in the plant design. A site specific value is used for this parameter.
1.5.3 Minimum Shear Wave Velocity	≥3,500 fps [Same for 2nd unit/group.]	1		The assumed limiting propagation velocity of shear waves through the foundation materials used in the plant design. A site specific value is used for this parameter.
1.6 Tornado (Design Bases)				
1.6.1 Maximum Pressure Drop	2.0 psi [Same for 2nd unit/group]	6		The design assumption for the decrease in ambient pressure from normal atmospheric pressure due to the passage of the tornado. A site specific value is used for this parameter.
1.6.2 Maximum Rotational Speed	240 mph [Same for 2nd unit/group]	6		The design assumption for the component of tornado wind speed due to the rotation within the tornado. A site specific value is used for this parameter.
1.6.3 Maximum Translational Speed	60 mph [Same for 2nd unit/group]	6		The design assumption for the component of tornado wind speed due to the movement of the tornado over the ground. A site specific value is used for this parameter.

Table 1.3-1 Plant Parameters Envelope

PPE Section	Bounding Value ^a [Value for 2 Units in brackets] ^b	Bound Notes See Table 1.3-2	Comments	Definition
1.6.4 Maximum Wind Speed	300 MPH [Same for 2nd unit/group]	6		The design assumption for the sum of maximum rotational and maximum translational wind speed components. A site specific value is used for this parameter.
1.6.5 Missile Spectra	Spectrum II from NUREG-0800 SRP Section 3.5.1.4 [Same for 2nd unit/group]	4, 8		The design assumptions regarding missiles that could be ejected either horizontally or vertically from a tornado. The spectra identify mass, dimensions and velocity of credible missiles.
1.6.6 Radius of Maximum Rotational Speed	150 ft [Same for 2nd unit/group]	6		The design assumption for distance from the center of the tornado at which the maximum rotational wind speed occurs.
1.6.7 Rate of Pressure Drop	1.2 psi/sec [Same for 2nd unit/group]	6		The assumed design rate at which the pressure drops due to the passage of the tornado. A site specific value is used for this parameter.
1.7 Wind				
1.7.1 Basic Wind Speed	110 mph [Same for 2nd unit/group]	2, 3, 4		The design wind, or “fastest mile of wind” with a 100-year return period (NUREG-0800, Sections 2.3.1 and 3.3.1) for which the facility is designed. A site specific value is used for this parameter.
1.7.2 Importance Factors	1.0 (non-safety related)/ 1.11 (safety related) [Same for 2nd unit/group]	2, 3		Multiplication factors (as defined in ANSI A58.1-1982) applied to basic wind speed to develop the plant design. A site specific value is used for this parameter.
2. Normal Plant Heat Sink				
2.1 Ambient Air Requirements				
2.1.1 Normal Shutdown Max Ambient Temp (1% Exceed)	100°F db / 77°F wb coincident [Same for 2nd unit/group]	6		Assumption used for the maximum ambient temperature that will be exceeded no more than 1% of the time, to design plant systems capable of effecting normal shutdown under the assumed temperature condition.
2.1.2 Normal Shutdown Max Wet Bulb Temp (1% Exceed)	80°F wb non-coincident [Same for 2nd unit/group]	6		Assumption used for the maximum wet bulb temperature that will be exceeded no more than 1% of the time – used in design of plant systems that must be capable of effecting normal shutdown under the assumed temperature condition.

Table 1.3-1 Plant Parameters Envelope

PPE Section	Bounding Value ^a [Value for 2 Units in brackets] ^b	Bound Notes See Table 1.3-2	Comments	Definition
2.1.3 Normal Shutdown Min Ambient Temp (1% Exceed)	-10°F [Same for 2nd unit/group]	6		Assumption used for the minimum ambient temperature that will be exceeded no more than 1% of the time to design of plant systems that must be capable of effecting normal shutdown under the assumed temperature condition.
2.1.4 Rx Thermal Power Max Ambient Temp (0% Exceed)	115°F db/80°F wb coincident [Same for 2nd unit/group]	6		Assumption used for the maximum ambient temperature that will never be exceeded – used in design of plant systems that must be capable of supporting full power operation under the assumed temperature condition.
2.1.5 Rx Thermal Power Max Wet Bulb Temp (0% Exceed)	81°F wb non-coincident [Same for 2nd unit/group]	6		Assumption used for the maximum wet bulb temperature that will never be exceeded – used in design of plant systems that must be capable of supporting full power operation under the assumed temperature condition.
2.1.6 Rx Thermal Power Min Ambient Temp (0% Exceed)	-40°F [Same for 2nd unit/group]	6		Assumption used for the minimum ambient temperature that will never be exceeded – used in design of plant systems that must be capable of supporting full power operation under the assumed temperature condition.
2.2 Condenser				
2.2.1 Max Inlet Temp Condenser/ Heat Exchanger	91°F [Same for 2nd unit/group.]	1, 7		Design assumption for the maximum acceptable circulating water temperature at the inlet to the condenser or cooling water system heat exchangers. A site specific value is used for this parameter.
2.2.2 Condenser / Heat Exchanger Duty	9.7 E9 btu/hr [Additional 9.7 E9 btu/hr for 2nd unit/group]	3, 5		Design value for the waste heat rejected to the circulating water system across the condensers.
2.3 Mechanical Draft Cooling Towers				
2.3.1 Acreage	50 acres [100 acres]	3, 5	e	The land required for cooling towers or ponds, including support facilities such as equipment sheds, basins, canals, or shoreline buffer areas. A site specific value is used for this parameter.
2.3.2 Approach Temperature	10°F [Same for 2nd unit/group]	1, 4, 7		The difference between the cold water temperature and the ambient wet bulb temperature. A site specific value is used for this parameter.

Table 1.3-1 Plant Parameters Envelope

PPE Section	Bounding Value ^a [Value for 2 Units in brackets] ^b	Bound Notes See Table 1.3-2	Comments	Definition
2.3.3 Blowdown Constituents and Concentrations	See Table 1.3-3 [Twice that shown in table]		f	The maximum expected concentrations for anticipated constituents in the cooling water systems blowdown to the receiving water body. A site specific value is used for this parameter.
2.3.4 Blowdown Flow Rate	6400 gpm expected (24,500 gpm max) [12,800 gpm expected (49,000 gpm max)]	1, 5	g	The normal (and maximum) flow rate of the blowdown stream from the cooling water systems to the receiving water body for closed system designs. A site specific value is used for this parameter.
2.3.5 Blowdown Temperature	100°F [Same for 2nd unit/group]	1, 2, 3, 4, 5	g	The maximum expected blowdown temperature at the point of discharge to the receiving water body.
2.3.6 Cycles of Concentration	4 [Same for 2nd unit/group]	6	f	The ratio of total dissolved solids in the cooling water blowdown streams to the total dissolved solids in the makeup water streams. A site specific value is used for this parameter.
2.3.7 Evaporation Rate	17,550 gpm expected (19,500 gpm max) [35,100 gpm expected (39,000 gpm max)]	3	h	The expected (and maximum) rate at which water is lost by evaporation from the cooling water systems. A site specific value is used for this parameter.
2.3.8 Height	60 ft [Same for 2nd unit/group]	1, 3, 4, 5, 7	c	The vertical height above finished grade of either natural draft or mechanical draft cooling towers associated with the cooling water systems.
2.3.9 Makeup Flow Rate	23,950 gpm expected (44,000 gpm max) [47,900 gpm expected (88,000 gpm max)]	9	g	The expected (and maximum) rate of removal of water from a natural source to replace water losses from closed cooling water system. A site specific value is used for this parameter.
2.3.10 Noise	55 dba at 1000 ft [Same for 2nd unit/group]	6	i	The maximum expected sound level produced by operation of cooling towers, measured at 1000 feet from the noise source.
2.3.11 Cooling Tower Temperature Range	23°F [Same for 2nd unit/group]	7		The temperature difference between the cooling water entering and leaving the towers or ponds. A site specific value is used for this parameter.
2.3.12 Cooling Water Flow Rate	800,000 gpm [1,600,000 gpm]	5		The total cooling water flow rate through the condenser/heat exchangers.

Table 1.3-1 Plant Parameters Envelope

PPE Section	Bounding Value ^a [Value for 2 Units in brackets] ^b	Bound Notes See Table 1.3-2	Comments	Definition
2.3.13 Heat Rejection Rate (Blowdown)	6,400 gpm expected (19,500 gpm max) @100°F [12,800 gpm expected (39,000 gpm max)]	3, 5		The expected heat rejection rate to a receiving water body, expressed as flow rate in gallons per minute at a temperature in degrees Fahrenheit. A site specific value is used for this parameter.
2.3.14 Maximum Consumption of Raw Water	30,000 gpm [60,000 gpm]	1		The expected maximum short-term consumptive use of water by the cooling water systems (evaporation and drift losses).
2.3.15 Monthly Average Consumption of Raw Water	23,000 gpm [46,000 gpm]	10		The expected normal operating consumption of water by the cooling water systems (evaporation and drift losses). A site specific value is used for this parameter.
2.3.16 Stored Water Volume	11,800,000 gal [23,600,000 gal]	5		The quantity of water stored in cooling water system impoundments, basins, tanks and/or ponds.
2.4 Natural Draft Cooling Towers			d	
2.4.1 Acreage	34.5 acres [69 acres]	7		The land required for cooling towers or ponds, including support facilities such as equipment sheds, basins, canals, or shoreline buffer areas. A site specific value is used for this parameter.
2.4.2 Approach Temperature	10°F [Same for 2nd unit/group.]	1, 4, 7		The difference between the cold water temperature and the ambient wet bulb temperature. A site specific value is used for this parameter.
2.4.3 Blowdown Constituents and Concentrations	See Table 1.3-3 [Twice that shown in table]		f	The maximum expected concentrations for anticipated constituents in the cooling water systems blowdown to the receiving water body. A site specific value is used for this parameter.
2.4.4 Blowdown Flow Rate	6,400 gpm expected (24,500 gpm max) [12,800 gpm expected (49,000 gpm max)]	1, 5	g	The normal (and maximum) flow rate of the blowdown stream from the cooling water systems to the receiving water body for closed system designs. A site specific value is used for this parameter.
2.4.5 Blowdown Temperature	100°F [Same for 2nd unit/group]	1, 3, 4, 5	g	The maximum expected blowdown temperature at the point of discharge to the receiving water body.

Table 1.3-1 Plant Parameters Envelope

PPE Section	Bounding Value ^a [Value for 2 Units in brackets] ^b	Bound Notes See Table 1.3-2	Comments	Definition
2.4.6 Cycles of Concentration	4 [Same for 2nd unit/group]	1, 3, 4, 5, 7	f	The ratio of total dissolved solids in the cooling water blowdown streams to the total dissolved solids in the makeup water streams. A site specific value is used for this parameter.
2.4.7 Evaporation Rate	17,550 gpm expected (19,500 gpm max) [35,100 gpm expected (39,000 gpm max)]	3	h	The expected (and maximum) rate at which water is lost by evaporation from the cooling water systems. A site specific value is used for this parameter.
2.4.8 Height	550 ft [Same for 2nd unit/group]	3, 5, 7	j	The vertical height above finished grade of either natural draft or mechanical draft cooling towers associated with the cooling water systems.
2.4.9 Makeup Flow Rate	23,950 gpm expected (44,000 gpm max) [47,900 gpm expected (88,000 gpm max)]	9	g	The expected (and maximum) rate of removal of water from a natural source to replace water losses from closed cooling water systems. A site specific value is used for this parameter.
2.4.10 Noise	55 dba at 1000 ft [Same for 2nd unit/group]	1, 3, 4, 5, 7	i	The maximum expected sound level produced by operation of cooling towers, measured at 1000 feet from the noise source.
2.4.11 Cooling Tower Temperature Range	23°F [Same for 2nd unit/group]	7		The temperature difference between the cooling water entering and leaving the towers or ponds. A site specific value is used for this parameter.
2.4.12 Cooling Water Flow Rate	800,000 gpm [1,600,000 gpm]	5		The total cooling water flow rate through the condenser/heat exchangers.
2.4.13 Heat Rejection Rate (Blowdown)	6,400 gpm expected (19,500 gpm max) @ 100°F [12,800 gpm expected (39,000 gpm max) @ 100°F]	3, 5		The expected heat rejection rate to a receiving water body, expressed as flow rate in gallons per minute at a temperature in degrees Fahrenheit.
2.4.14 Maximum Consumption of Raw Water	33,720 gpm [67,440 gpm]	4		The expected maximum short-term consumptive use of water by the cooling water systems (evaporation and drift losses).

Table 1.3-1 Plant Parameters Envelope

PPE Section	Bounding Value ^a [Value for 2 Units in brackets] ^b	Bound Notes See Table 1.3-2	Comments	Definition
2.4.15 Monthly Average Consumption of Raw Water	23,000 gpm [46,000 gpm]	10		The expected normal operating consumption of water by the cooling water systems (evaporation and drift losses).
2.4.16 Stored Water Volume	11,800,000 gal [23,600,000 gal]	5		The quantity of water stored in cooling water system impoundments, basins, tanks and/or ponds.
2.5 Once-Through Cooling			d	
2.5.1 Cooling Water Discharge Temperature	127°F [Same for 2nd unit/group.]	2	g	Expected temperature of the cooling water at the exit of the condenser/heat exchangers. A site specific value is used for this parameter.
2.5.2 Cooling Water Flow Rate	1,140,000 gpm [2,280,000 gpm]	5	g	Total cooling water flow rate through the condenser (also the rate of withdrawal from and return to the water source).
2.5.3 Cooling Water Temperature Rise	18°F [Same for 2nd unit/group.]	1, 3, 5	g	Temperature rise across the condenser (temperature of water out minus temperature of water in).
2.5.4 Evaporation Rate	10,550 gpm expected (11,700 gpm max) [21,100 gpm expected (23,400 gpm max)]	3	h	The expected (and maximum) rate at which water is lost by evaporation from the receiving water body as a result of heating in the condenser. A site specific value is used for this parameter.
2.5.5 Heat Rejection Rate	9.7 E9 Btu/hr [19.4 E9 Btu/hr]	3, 5		The expected heat rejection rate to a receiving water body.
3. Ultimate Heat Sink			k	
3.1 Ambient Air Requirements				
3.1.1 Maximum Ambient Temp (0% Exceedance)	115°F db/80°F wb coincident [Same for 2nd unit/group]	2, 3, 5, 7		Assumption used for the maximum ambient temperature in designing the UHS system to provide heat rejection for 30 days under the assumed temperature condition.

Table 1.3-1 Plant Parameters Envelope

PPE Section	Bounding Value ^a [Value for 2 Units in brackets] ^b	Bound Notes See Table 1.3-2	Comments	Definition
3.1.2 Maximum Wet Bulb Temp (0% Exceedance)	81°F wb (non-coincident) [Same for 2nd unit/group]	2, 3, 5, 7		Assumption used for the maximum wet bulb temperature in designing the UHS system to provide heat rejection for 30 days under the assumed temperature condition.
3.1.3 Minimum Ambient Temp (0% Exceedance)	-40°F [Same for 2nd unit/group]	2, 3, 5, 7		Assumption used for the minimum ambient temperature in designing the UHS system to provide heat rejection for 30 days under the assumed temperature condition.
3.2 CCW Heat Exchanger				
3.2.1 Maximum Inlet Temp to CCW Heat Exchanger	95°F [Same for 2nd unit/group]	3, 5, 7		The maximum temperature of safety-related service water at the inlet of the UHS component cooling water heat exchanger.
3.2.2 CCW Heat Exchanger Duty	420 E6 Btu/hr (shutdown) [Additional 420 E6 Btu/hr (shutdown) for 2nd unit]	3		The heat transferred to the safety-related service water system for rejection to the environment in UHS heat removal devices.
3.3 Mech Draft Cooling Towers				
3.3.1 Acreage	0.5 acre [1.0 acre]	3, 5	k	The land required for UHS cooling towers or ponds, including support facilities such as equipment sheds, basins, canals, or shoreline buffer areas.
3.3.2 Approach Temperature	15°F [Same for 2nd unit/group]	3, 5		The difference between the cold water temperature and the ambient wet bulb temperature.
3.3.3 Blowdown Constituents and Concentrations	See Table 1.3-3 [Twice that shown in table]		k	The maximum expected concentrations for anticipated constituents in the UHS blowdown to the receiving water body.
3.3.4 Blowdown Flow Rate	144 gpm expected (850 gpm max) [288 gpm expected (1700 gpm max)]	3, 7	k	The normal (and maximum) flow rate of the blowdown stream from the UHS system to receiving water body for closed system designs.
3.3.5 Blowdown Temperature	95°F [Same for 2nd unit/group]	3, 5	k	The maximum expected UHS blowdown temperature at the point of discharge to the receiving water body.
3.3.6 Cycles of Concentration	4 (2 Minimum) [Same for 2nd unit/group]	3, 5, 7	k	The ratio of total dissolved solids in the UHS system blowdown streams to the total dissolved solids in the makeup water streams.

Table 1.3-1 Plant Parameters Envelope

PPE Section	Bounding Value ^a [Value for 2 Units in brackets] ^b	Bound Notes See Table 1.3-2	Comments	Definition
3.3.7 Evaporation Rate	411 gpm normal 850 gpm shutdown [822 gpm normal 1700 gpm shutdown]	3, 7	k	The expected (and maximum) rate at which water is lost by evaporation from the UHS system.
3.3.8 Height	60 ft [Same for 2nd unit/group]	3, 5, 7	k	The vertical height above finished grade of mechanical draft cooling towers associated with the UHS system.
3.3.9 Makeup Flow Rate	555 gpm 1700 gpm max [1,110 gpm, 3,400 gpm max]	3, 7, 9	k	The expected (and maximum) rate of removal of water from a natural source to replace water losses from the UHS system.
3.3.10 Noise	55 dba at 1000 ft [Same for 2nd unit/group]	2, 3, 5, 7	k	The maximum expected sound level produced by operation of mechanical draft UHS cooling towers, measured at 1000 feet from the noise source.
3.3.11 Cooling Tower Temperature Range	16°F [Same for 2nd unit/group]	5		The temperature difference between the cooling water entering and leaving the UHS system.
3.3.12 Cooling Water Flow Rate	26,125 gpm (normal) 52,250 gpm (shutdown/ accident) [52,250 gpm (normal), 104,500 (shutdown/ accident)]	3		The total cooling water flow rate through the UHS system.
3.3.13 Heat Rejection Rate (Blowdown)	100 gpm expected (850 gpm max) @95°F [200 gpm expected (1,700 gpm max) @95°F]	3		The expected heat rejection rate to a receiving water body, expressed as flow rate in gallons per minute at a temperature in degrees Fahrenheit.
3.3.14 Maximum Consumption of Raw Water	900 gpm [1800 gpm]	7		The expected maximum short-term consumptive use of water by the UHS system (evaporation and drift losses).
3.3.15 Monthly Average Consumption of Raw Water	533 gpm [1066 gpm]	10		The expected normal operating consumption of water by the UHS system (evaporation and drift losses).

Table 1.3-1 Plant Parameters Envelope

PPE Section	Bounding Value ^a [Value for 2 Units in brackets] ^b	Bound Notes See Table 1.3-2	Comments	Definition
3.3.16 Stored Water Volume	30,600,000 gal [61,200,000 gal]	3		The quantity of water stored in UHS impoundments, basins, tanks and/or ponds.
4. Containment Heat Removal System (Post-Accident)				
4.1 Ambient Air Requirements				
4.1.1 Maximum Ambient Air Temperature (0% Exceedance)	115°F db/80°F wb coincident [Same for 2nd unit/group]	1, 7		Assumed maximum ambient temperature used in designing the containment heat removal system.
4.1.2 Minimum Ambient Temperature (0% Exceedance)	-40°F [Same for 2nd unit/group]	1, 7		Assumed minimum ambient temperature used in designing the containment heat removal system.
5. Potable Water/Sanitary Waste System				
5.1 Discharge to Site Water Bodies				
5.1.1 Flow Rate	60 gpm expected (105 gpm max) [120 gpm expected (210 gpm max)]	7	I	The expected (and maximum) effluent flow rate from the potable and sanitary waste water systems to the receiving water body.
5.2 Raw Water Requirements				
5.2.1 Maximum Use	120 gpm [240 gpm]	5	I	The maximum short-term rate of withdrawal from the water source for the potable and sanitary waste water systems.
5.2.2 Monthly Average Use	90 gpm [180 gpm]	5	I	The average rate of withdrawal from the water source for the potable and sanitary waste water systems.
6. Demineralized Water System				
6.1 Discharge to Site Water Bodies				

Table 1.3-1 Plant Parameters Envelope

PPE Section	Bounding Value ^a [Value for 2 Units in brackets] ^b	Bound Notes See Table 1.3-2	Comments	Definition
6.1.1 Flow Rate	110 gpm expected (150 gpm max) [220 gpm expected (300 gpm max)]	5, 7	I	The expected (and maximum) effluent flow rate from the demineralized system to the receiving water body.
6.2 Raw Water Requirements				
6.2.1 Maximum Use	720 gpm [1440 gpm]	5	I	The maximum short-term rate of withdrawal from the water source for the demineralized water system.
6.2.2 Monthly Average Use	550 gpm [1100 gpm]	5	I	The average rate of withdrawal from the water source for the demineralized water system.
7. Fire Protection System				
7.1 Raw Water Requirements				
7.1.1 Maximum Use	2,500 gpm [5,000 gpm]	11	I	The maximum short-term rate of withdrawal from the water source for the fire protection water system.
7.1.2 Monthly Average Use	675,000 gal/mo [1,350,000 gal/mo]	7	I	The average rate of withdrawal from the water source for the fire protection water system.
7.1.3 Stored Water Volume	2,325,000 gallons [4,650,000 gallons]	7		The quantity of water stored in fire protection system impoundments, basins or tanks.
8. Miscellaneous Drain				
8.1 Discharge to Site Water Bodies				
8.1.1 Flow Rate	100 gpm expected (150 gpm max) [200 gpm expected (300 gpm max)]	3, 7	I	The expected (and maximum) effluent flow rate from miscellaneous drains to the receiving water body.

Table 1.3-1 Plant Parameters Envelope

PPE Section	Bounding Value ^a [Value for 2 Units in brackets] ^b	Bound Notes See Table 1.3-2	Comments	Definition
9. Unit Vent/Airborne Effluent Release Point				
9.1 Atmospheric Dispersion (CHI/Q) (Accident)				The atmospheric dispersion coefficients used in the design safety analysis to estimate dose consequences of accident airborne releases.
9.1.1 0-2 hr @EAB	0.61 E-3 sec/m ³ [Same for 2nd unit/group]	1		A site specific value is used for this parameter.
9.1.2 0-8 hr @LPZ	1.30 E-4 sec/m ³ [Same for 2nd unit/group]	5		A site specific value is used for this parameter.
9.1.3 8-24 hr @LPZ	1.0 E-4 sec/m ³ [Same for 2nd unit/group]	1, 5		A site specific value is used for this parameter.
9.1.4 1-4 day @LPZ	4.18 E-5 sec/m ³ [Same for 2nd unit/group]	3		A site specific value is used for this parameter.
9.1.5 4-30 day @LPZ	9.24 E-6 sec/m ³ [Same for 2nd unit/group]	3		A site specific value is used for this parameter.
9.2 Atmospheric Dispersion (X/Q) (Annual Average)	1.17 E-6 sec/m ³ [Same for 2nd unit/group]	3		The atmospheric dispersion coefficients used in the safety analysis for the dose consequences of normal airborne releases. A site specific value is used for this parameter.
9.3 Dose Consequences			m	
9.3.1 Normal	10 CFR 20, 10 CFR 50 App I [Same for 2nd unit/group]	6		The estimated design radiological dose consequences due to gaseous releases from normal operation of the plant.
9.3.2 Post-Accident	10 CFR 20, 10 CFR 50 APP I, 10 CFR 100 [Same for 2nd unit/group]	1, 3, 4, 5, 7		The estimated design radiological dose consequences due to gaseous releases from postulated accidents.
9.3.3 Severe Accidents	25 rem wb in 24 hr 0.5 mi <1E-6/rx-yr [Same for 2nd unit/group]	1, 3, 7		

Table 1.3-1 Plant Parameters Envelope

PPE Section	Bounding Value ^a [Value for 2 Units in brackets] ^b	Bound Notes See Table 1.3-2	Comments	Definition
9.4 Release Point			n	
9.4.1 Configuration (Horiz vs. Vert)	Horizontal	2		The orientation of the release point discharge flow.
9.4.2 Elevation (Normal)	95.5 ft [Same for 2nd unit/group]	2		The elevation above finished grade of the release point for routine operational releases.
9.4.3 Elevation (Post Accident)	Ground level [Same for 2nd unit/group]	1, 2, 3, 5, 7		The elevation above finished grade of the release point for accident sequence releases.
9.4.4 Minimum Distance to Site Boundary	0.5 mi exclusion area [Same for 2nd unit/group]	1, 3, 7		The minimum lateral distance from the release point to the site boundary.
9.4.5 Temperature	No value bounds, overall range is 35-120°F [Same for 2nd unit/group]			The temperature of the airborne effluent stream at the release point.
9.4.6 Volumetric Flow Rate	118,000 scfm for 2 units (normal operation) [for 2 units]	5		The volumetric flow rate of the airborne effluent stream at the release point.
9.5 Source Term			o	
9.5.1 Gaseous (Normal)	13,070 Ci/yr [26,140 Ci/yr] See Table 1.3-8 for isotopic breakdown	12		The annual activity, by isotope, contained in routine plant airborne effluent streams.
9.5.2 Gaseous (Post-Accident)	See Chap 15 Tables RG 1.70 [Same for 2nd unit/group]	1, 3	p	The activity, by isotope, contained in post-accident airborne effluents.
9.5.3 Tritium	3530 ci/yr [7060 ci/yr]	5		The annual activity of tritium contained in routine plant airborne effluent streams.

Table 1.3-1 Plant Parameters Envelope

PPE Section	Bounding Value ^a [Value for 2 Units in brackets] ^b	Bound Notes See Table 1.3-2	Comments	Definition
10. Liquid Radwaste System				
10.1 Dose Consequences			q	
10.1.1 Normal	10 CFR 50, Appendix I, 10 CFR 20	1, 3, 4, 5		The estimated design radiological dose consequences due to liquid effluent releases from normal operation of the plant.
10.1.2 Post-Accident	10 CFR 20, 10 CFR 100 [Same for 2nd unit/group]	1, 3, 4, 5		The estimated design radiological dose consequences due to liquid effluent releases from postulated accidents.
10.2 Release Point				
10.2.1 Flow Rate	100 gpm + 10,000 gpm dilution [200 gpm + 20,000 gpm dilution]	3		The discharge (including minimum dilution flow, if any) of liquid potentially radioactive effluent streams from plant systems to the receiving water body.
10.3 Source Term				
10.3.1 Liquid	0.313 ci/yr [0.626 ci/yr] See Table 1.3-7 for isotopic breakdown	13		The annual activity, by isotope, contained in routine plant liquid effluent streams.
10.3.2 Tritium	3100 ci/yr [6200 ci/yr]	5		The annual activity of tritium contained in routine plant liquid effluent streams.
11. Solid Radwaste System				
11.1 Acreage				
11.1.1 Low Level Radwaste Storage	2 years in radwaste building @ expected generation rate [Same for 2nd unit/group]	1		The land usage required to provide onsite storage of low level radioactive wastes.

Table 1.3-1 Plant Parameters Envelope

PPE Section	Bounding Value ^a [Value for 2 Units in brackets] ^b	Bound Notes See Table 1.3-2	Comments	Definition
11.2 Solid Radwaste				
11.2.1 Activity	2700 ci/yr [5400 ci/yr]	3		The annual activity contained in solid radioactive wastes generated during routine plant operations.
11.2.2 Volume	9041 cu ft/yr [18,646 cu ft/yr]	4		The expected volume of solid radioactive wastes generated during routine plant operations.
12. Auxiliary Boiler System				
12.1 Exhaust Elevation	110 ft above plant grade [Same for 2nd unit/group]	5	u	The height above finished plant grade at which the flue gas effluents are released to the environment.
12.2 Flue Gas Effluents	See Table 1.3-4 [Twice that shown in table]		u	The expected combustion products and anticipated quantities released to the environment due to operation of the auxiliary boilers, diesel engines and gas turbines.
12.3 Fuel Type	No. 2 [Same for 2nd unit/group]	1, 3, 5, 7	u	The type of fuel oil required for proper operation of the auxiliary boilers, diesel engines and gas turbines.
12.4 Heat Input Rate (btu/hr)	156,000,000 Btu/hr [312,000,000 Btu/hr]	1		The average heat input rate due to the periodic operation of the auxiliary boilers.
13. Heating, Ventilation and Air Conditioning System				
13.1 Ambient Air Requirements				
13.1.1 Non-safety HVAC max ambient temp (1% Exceed)	100°F db/77°F wb coincident [Same for 2nd unit/group]	6		Assumption used for the maximum ambient temperature that will be exceeded no more than 1% of the time, to design the non-safety HVAC systems.
13.1.2 Non-safety HVAC min ambient temp (1% Exceed)	-10°F [Same for 2nd unit/group]	6		Assumption used for the minimum ambient temperature that will be exceeded no more than 1% of the time, to design the non-safety HVAC systems.
13.1.3 Safety HVAC max ambient temp (0% Exceed)	115°F db/80°F wb coincident [Same for 2nd unit/group]	1, 3, 5, 7		Assumption used for the maximum ambient temperature that will never be exceeded, to design the safety-related HVAC systems.

Table 1.3-1 Plant Parameters Envelope

PPE Section	Bounding Value ^a [Value for 2 Units in brackets] ^b	Bound Notes See Table 1.3-2	Comments	Definition
13.1.4 Safety HVAC min ambient temp (0% Exceed)	-40°F [Same for 2nd unit/group]	1, 3, 5, 7		Assumption used for the minimum ambient temperature that will never be exceeded, to design the safety-related HVAC systems.
13.1.5 Vent System max ambient temp (5% Exceed)	95°F dry bulb/ 77°F wb coincident), 79°F wb (non-coincident) [Same for 2nd unit/group]	3, 5		Assumption used for the maximum ambient temperature that will be exceeded no more than 5% of the time to design the non-HVAC ventilation systems.
13.1.6 Vent System min ambient temp (5% Exceed)	- 5°F [Same for 2nd unit/group]	3		Assumption used for the minimum ambient temperature that will be exceeded no more than 5% of the time to design the non-HVAC ventilation systems.
14. Onsite/Offsite Electrical Power System				
14.1 Acreage				
14.1.1 Switchyard	15 acres [30 acres]	7	e	The land usage required for the high voltage switchyard used to connect the plant to the transmission grid.
15. Standby Power System				
15.1 Diesels				
15.1.1 Diesel Capacity	4 x 6500 kw [8 x 6500 kw]	5		The capacity of diesel engines used for generation of standby electrical power.
15.1.2 Diesel Exhaust Elevation	30 ft [Same for 2nd unit/group]	4	u	The elevation above finished grade of the release point for standby diesel exhaust releases.
15.1.3 Diesel Flue Gas Effluents	See Table 1.3-5 [Twice that shown in table]		u	The expected combustion products and anticipated quantities released to the environment due to operation of the emergency standby diesel generators.
15.1.4 Diesel Noise	55 dba at 1000 ft [Same for 2nd unit/group.]	1, 3, 4, 5, 7	i	The maximum expected sound level produced by operation of diesel engines turbines, measured at 1000 feet from the noise source.

Table 1.3-1 Plant Parameters Envelope

PPE Section	Bounding Value ^a [Value for 2 Units in brackets] ^b	Bound Notes See Table 1.3-2	Comments	Definition
15.1.5 Diesel Fuel Type	No. 2 per ASTM D975-1974 [Same for 2nd unit/group]	1, 3, 4, 5, 7		The type of fuel oil required for proper operation of the diesel engines.
15.2 Gas Turbines				
15.2.1 Gas Turbine Capacity (kw)	20 MWe at limiting site conditions [40 MWe at limiting site conditions]	3		The capacity of gas turbines used for generation of standby electrical power.
15.2.2 Gas Turbine Exhaust Elevation	60 ft [Same for 2nd unit/group]	3	u	The elevation above finished grade of the release point for standby gas turbine exhaust releases.
15.2.3 Gas Turbine Flue Gas Effluents	See Table 1.3-6 [Twice that shown in table]		u	The expected combustion products and anticipated quantities released to the environment due to operation of the emergency standby gas-turbine generators.
15.2.4 Gas Turbine Noise	55 dba at 1000 ft [Same for 2nd unit/group]	2, 3	i	The maximum expected sound level produced by operation of gas turbines, measured at 1000 feet from the noise source.
15.2.5 Gas Turbine Fuel Type	Distillate [Same for 2nd unit/group]	2, 3	u	The type of fuel oil required for proper operation of the gas turbines.
16. Plant Characteristics				
16.1 Access Routes				
16.1.1 Heavy Haul Routes	7 acres [Same for 2nd unit/group]	3, 7	e	The land usage required for permanent heavy haul routes to support normal operations and refueling.
16.1.2 Spent Fuel Cask Weight	150 tons [Same for 2nd unit/group]	3	v	The weight of the heaviest expected shipment during normal plant operations and refueling.

Table 1.3-1 Plant Parameters Envelope

PPE Section	Bounding Value ^a [Value for 2 Units in brackets] ^b	Bound Notes See Table 1.3-2	Comments	Definition
16.2 Acreage	87 acres [174 acres]	2	w	The land area required to provide space for plant facilities. A site specific value is used for this parameter.
16.2.1 Office Facilities	1.8 acres [2.18 acre (95,200 sq ft)]	2		A site specific value is used for this parameter.
16.2.2 Parking Lots	3.86 acres [7.72 acres]	3		A site specific value is used for this parameter.
16.2.3 Permanent Support Facilities	12 acres [8.4 acres]	2		A site specific value is used for this parameter.
16.2.4 Power Block	11.64 acres [23.3 acres]	7		A site specific value is used for this parameter.
16.2.5 Protected Area	40 acres [80 acres]	7		A site specific value is used for this parameter.
16.3 Megawatts Thermal	4300 MWt [8600 MWt.]	3		The thermal power generated by one unit (may be the total of several modules).
16.4 Plant Design Life	60 years [Same for 2nd unit/group]	1, 2, 3, 5, 7	x	The operational life for which the plant is designed.
16.5 Plant Population				
16.5.1 Operation	580 people [1160 people]	5	x	The number of people required to operate and maintain the plant. A site specific value is used for this parameter.
16.5.2 Refueling / Major Maintenance	1000 people [Same for 2nd unit/group]	1	x	The additional number of temporary staff required to conduct refueling and major maintenance activities. A site specific value is used for this parameter.
16.6 Station Capacity Factor	96% [Same for 2nd unit/group]	2		The percentage of time that a plant is capable of providing power to the grid.

Table 1.3-1 Plant Parameters Envelope

PPE Section	Bounding Value ^a [Value for 2 Units in brackets] ^b	Bound Notes See Table 1.3-2	Comments	Definition
17. Construction				
17.1 Access Routes				
17.1.1 Construction Module Dimensions	90' (H) x 82' (W) x 93' (L) or 130' (Dia) x 51' (H) [Same for 2nd unit/group]	1, 7	v	The maximum expected length, width, and height of the largest construction modules or components and delivery vehicles to be transported to the site during construction.
17.1.2 Heaviest Construction Shipment	2,200,00 lb. [Same for 2nd unit/group]	2	v	The maximum expected weight of the heaviest construction shipment to the site.
17.2 Acreage				
The land area required to provide space for construction support facilities.				
17.2.1 Laydown Area	29 acres [58 acres]	3	e	A site specific value is used for this parameter.
17.2.2 Temporary Construction Facilities	52 acres [104 acres]	3	e	A site specific value is used for this parameter.
17.3 Construction				
17.3.1 Noise	76-101 db @ 50 ft [Same for 2nd unit/group]	1, 3, 4, 5, 7	i	The maximum expected sound level due to construction activities, measured at 50 feet from the noise source.
17.4 Plant Population				
17.4.1 Construction	3150 people max [5,355 for unit simultaneous construction]	3, 14	x	Peak employment during plant construction. A site specific value is used for this parameter.
17.5 Site Preparation Duration	18 months [Same for 2nd unit/group]	1, 3, 7	x	Length of time required to prepare the site for construction.

Comments:

a. PPE values should be based on plant designs being considered. The Bounding PPE values provide an envelope (most restrictive values selected) for the ABWR, ESBWR, AP1000, IRIS, GT-MHR, PBMR and ACR-700 designs. A composite PPE should be used for the actual set of plant designs under consideration for the site.

- b. The values in brackets reflects the values corresponding to a plant that is twice the vendor's specified standard size plant, i.e., two ABWR units, two ESBWR units, two AP1000 units, six IRIS units, two sets of four GT-MHR modules, two sets of eight PBMR modules and two ACR-700 twin unit plants.
- c. Visual resources impacts.
- d. Applicants must identify main condenser cooling system alternatives (e.g., mechanical or natural draft cooling towers, cooling ponds, or once-through cooling). To maintain multiple options, the most restrictive value for each cooling system PPE section should be used in the ESP application (e.g., 550-foot cooling tower height selected if both mechanical and natural draft towers are being considered).
- e. Construction impacts on ecological resources.
- f. Operational impacts on water quality and ecological resources.
- g. Operational impacts on water quality and ecological resources. An NPDES permit must be obtained for this blowdown rate, blowdown temperature, withdrawal rate or temperature rise.
- h. Operational impacts on water quality and local climatology.
- i. Noise impacts.
- j. Visual impacts.
- k. Impacts of the main condenser cooling system will usually bound impacts from operation of the Ultimate Heat Sink.
- l. Operational impacts on water quality and aquatic ecological resources.
- m. Values listed for Section 9.3 are regulatory standards for effluent concentrations, doses from routine operations, and doses from postulated accidents. The applicant must demonstrate that the plant is capable of meeting these standards considering the plant design and, for the dose standards, dilution and dispersion conditions at the site.
- n. Release point characteristics (Section 9.4.1 - Section 9.4.6) are used to calculate atmospheric dispersion factors used: S - In the Site SAR to demonstrate compliance with requirements listed in Section 9.3, and, E - In the ER to estimate impacts from routine and accident-scenario atmospheric releases.
- o. Source term data (Section 9.5.1 -Section 9.5.3) are used to calculate dose consequences used: S - In the Site SAR to demonstrate compliance with requirements listed in Section 9.3, and, E - In the ER to estimate impacts from routine and accident-scenario atmospheric releases.
- p. See Section 9.5. Tables in Chapter 15 of RG 1.70 list the design and accident sequence parameters necessary to derive these source terms. Applicants must obtain calculated release values from the vendor/A-E for designs under consideration.
- q. Values listed for Section 10.1 are regulatory standards for effluent concentrations, doses from routine operations, and doses from postulated accidents. The applicant must demonstrate that the plant is capable of meeting these standards considering the plant design and, for the dose standards, dilution and dispersion conditions at the site.
- r. Flow rate and dilution characteristics (Section 10.2) are used to calculate dilution factors used: S - In the Site SAR to demonstrate compliance with requirements listed in Section 10.1, and, E - In the ER to estimate impacts from liquid effluents.
- s. Liquid discharge data (Section 10.3.1 - Section 10.3.2) are used to calculate dose consequences used: S - In the Site SAR to demonstrate compliance with requirements listed in Section 10.1, and, E - In the ER to estimate impacts from liquid effluents.
- t. Environmental effects of the uranium fuel cycle, including solid waste management, are set forth in Table S-3 of 10 CFR 51.20. Reference to this Table is made in the applicant's ER.
- u. Operational impacts of non-radiological atmospheric emissions.
- v. Transport requirements for component delivery.
- w. Total acreage footprint for site facilities is used to estimate construction impacts on ecological resources.
- x. Socio-economic impacts of plant construction and operation.

Table 1.3-2 Bounding Value Notes for Table 1.3-1

1. Bounding value from AP1000 criteria.
2. Bounding value from GT-MHR criteria.
3. Bounding value from ABWR/ESBWR criteria.
4. Bounding value from PBMR criteria.
5. Bounding value from ACR-700 criteria.
6. Bounding value common for the seven designs.
7. Bounding value from IRIS criteria.
8. The Spectrum A missiles were for plants that used the November 24, 1975 version of the SRP; for all plants since, the Spectrum I or II of the July 1981 version of the SRP was to be used.
9. The bounding Makeup Flow Rate is a calculated value based on the sum of the bounding Evaporation rate plus the bounding Blowdown Flow Rate.
10. The bounding value for the Monthly Average Consumption of Raw Water is a calculated value based on the maximum bounding makeup flow rate times the bounding capacity factor (PPE Section 16.6).
11. Bounding value from ESBWR criteria.
12. The Gaseous (Normal) source term bounding value is the sum of the bounding values of the yearly released activity for each nuclide type for each reactor (ABWR, AP1000, ACR-700). These were the only reactor types with adequate information available. See Table 1.3-8.
13. The liquid waste source term bounding value is the sum of the bounding values of the yearly released activity for each nuclide type for each reactor (ABWR, AP1000, ACR-700). These were the only reactor types with adequate information available. The PBMR value was not supported by isotopic data and was not used in the evaluation. See Table 1.3-7.
14. Two-unit simultaneous construction staffing is based on 170% of single unit build. This assumes optimum timing between units and is based on rough estimates by Bechtel. Refined information will be contingent upon type of plant built, and plant location.

Table 1.3-3 Blowdown Constituents and Concentrations^a

Constituent	Bounding Value			Notes
	Concentration (ppm) ^b			
	River Source	Well/Treated Water	Envelope	
Chlorine demand	10.1	--	10.1	c, d, e
Free available chlorine	0.5	--	0.5	f
Chromium	--	--	--	
Copper	--	6	6	f
Iron	0.9	3.5	3.5	f
Zinc	--	0.6	0.6	f
Phosphate	--	7.2	7.2	c, d, e
Sulfate	599	3500	3500	f
Oil and grease	--	--	--	
Total dissolved solids	--	17,000	--	c, d, e
Total suspended solids	49.5	150	150	f
BOD, 5-day	--	--	--	

- a. See PPE Section 2.3.3, 2.4.3, and 3.3.3.
- b. Assumed cycles of concentration equals 4.
- c. Bounding value from ABWR/ESBWR criteria.
- d. Bounding value from AP1000 criteria.
- e. Bounding value from PBMR criteria.
- f. Bounding value common for the seven designs.

Table 1.3-4 Yearly Emissions Auxiliary Boilers^a

Bounding Value		
Pollutant Discharged ^b	Quantity (lb.)	Notes
Particulates	9,900	c
Sulfur oxides	31,703	d
Carbon monoxide	1749	d
Hydrocarbons	50,100	e
Nitrogen oxides	19,022	d

- a. See PPE Section 12.2.
- b. Emissions are based on 30 days/yr operation for each of the generators.
- c. Bounding value from ABWR/ESBWR criteria.
- d. Bounding value from ACR-700 criteria.
- e. Bounding value from AP1000 criteria.

Table 1.3-5 Yearly Emissions From Standby Diesel Generators^a

Bounding Value		
Pollutant Discharged ^b	Quantity (lb.)	Notes
Particulates	<1,230	c
Sulfur oxides	4,608	d
Carbon monoxide	4,600	e
Hydrocarbons	3,070	e
Nitrogen oxides	28,968	d

- a. See PPE Section 15.1.
- b. Emissions are based on 4 hrs/month operation for each of the generators.
- c. Bounding value from IRIS criteria.
- d. Bounding value from ABWR/ESBWR criteria.
- e. Bounding value from ACR-700 criteria.

Table 1.3-6 Standby Power System Gas Turbine Flue Gas Effluents^a

Fuel: Distillate 20°F Ambient
9,890 BTU/kWH (LHV)
10,480 BTU/KWH (HHV)

Bounding Value		
Fuel Consumption Rate	121,200 lb/hr^b	
Effluent	Quantity^c (lb.)	Notes
NO _x (PPMVD @15% O ₂)	42	d
NO _x as NO ₂	2016	d
CO (PPMVD)	31	d
CO	912	d
UHC (PPMVD)	3	d
UHC	48	d
VOC	10	b
SO ₂	1882	d
SO ₃	30	b
Sulfur Mist	50	b
Particulates	22	b
Exhaust Analysis	% Vol	
Argon	0.87	d
Nitrogen	72.56	b
Oxygen	12.52	d
Carbon Dioxide	5.19	b
Water	9.87	b

- a. See PPE Section 15.2.
- b. Bounding value from GT-MHR criteria.
- c. Emissions are based on 4 hrs/month operation for each of the generators.
- d. Bounding value from ABWR criteria.

Table 1.3-7 Radionuclides in Annual Normal Liquid Releases (ci/yr)^a

Corrosion and Activation Products	Bounding Value	Notes	Fission Products	Bounding Value	Notes	Fission Products	Bounding Value	Notes	Fission Products	Bounding Value	Notes
C-14	0.000440	b	Br-84	0.00002	d	Rh-103m	0.00493	d	Cs-136	0.00063	d
Na-24	0.00281	c	Rb-88	0.00027	d	Ru-106	0.07352	d	Cs-137	0.01332	d
P-32	0.00018	c	Rb-89	0.0000441	c	Rh-106	0.07352	d	Ba-137m	0.01245	d
Cr-51	0.00770	c	Sr-89	0.00011	c	Ag-110m	0.00105	d	Cs-138	0.00019	c
Mn-54	0.0026	c	Sr-90	0.0000351	c	Ag-110	0.00014	d	Ba-140	0.00552	d
Fe-55	0.00581	c	Y-90	0.0000031	c	Sb-124	0.000679	b	La-140	0.00743	d
Mn-56	0.00381	c	Sr-91	0.0009	c	Te-129m	0.00012	d	Ce-141	0.00012	c
Co-56	0.00519	c	Y-91	0.00011	c	Te-129	0.00015	d	Ce-143	0.00019	d
Co-57	0.0000719	c	Y-91m	0.00001	d	Te-131m	0.00009	d	Pr-143	0.00013	d
Fe-59	0.00020	d	Sr-92	0.0008	c	Te-131	0.00003	d	Ce-144	0.00316	d
Co-58	0.00336	d	Y-92	0.0006	c	I-131	0.01413	d	Pr-144	0.00316	d
Co-60	0.00911	c	Y-93	0.0009	c	Te-132	0.00024	d	All others	0.00002	d
Ni-63	0.00014	c	Zr-95	0.00104	b	I-132	0.0026	c	Total (except tritium)	0.313	
Cu-64	0.00751	c	Nb-95	0.00191	b	I-133	0.01	c			
Zn-65	0.00041	d	Mo-99	0.000830	c	I-134	0.0017	c	Tritium release	3100	b
W-187	0.00013	d	Tc-99m	0.0008	c	Cs-134	0.00993	d			
Np-239	0.00311	c	Ru-103	0.00493	d	I-135	0.00751	c			

- a. See PPE Section 10.3.
- b. Bounding Value from twin ACR-700 criteria.
- c. Bounding Value from design certified ABWR.
- d. Bounding Value from AP1000 criteria.

Table 1.3-8 Radionuclides in Annual Normal Gaseous Releases (ci/yr)^a

Bounding			Bounding			Bounding			Bounding		
Radionuclide	Value	Notes	Radionuclide	Value	Notes	Radionuclide	Value	Notes	Radionuclide	Value	Notes
Noble Gases			Iodines			Cu-64	1.00E-02	c	Ag-110m	2.00E-06	c
Ar-41	3.03E+02	b	I-131	2.59E-01	c	Zn-65	1.11E-02	c	Sb-124	1.81E-04	c
Kr-83m	8.38E-04	c	I-132	2.19E+00	c	Rb-89	4.32E-05	c	Sb-125	6.1E-05	d
Kr-85m	3.6E+01	d	I-133	1.70E+00	c	Sr-89	5.68E-03	c	Te-129m	2.19E-04	c
Kr-85	4.1E+03	d	I-134	3.78E+00	c	Sr-90	1.2E-03	d	Te-131m	7.57E-05	c
Kr-87	2.51E+01	c	I-135	2.41E+00	c	Y-90	4.59E-05	c	Te-132	1.89E-05	c
Kr-88	4.6E+01	d	Others			Sr-91	1.00E-03	c	Cs-134	6.22E-03	c
Kr-89	2.41E+02	c	C-14	9.19E+00	c	Sr-92	7.84E-04	c	Cs-136	5.95E-04	c
Kr-90	3.24E-04	c	Na-24	4.05E-03	c	Y-91	2.41E-04	c	Cs-137	9.46E-03	c
Xe-131m	1.8E+03	d	P-32	9.19E-04	c	Y-92	6.22E-04	c	Cs-138	1.70E-04	c
Xe-133m	8.7E+01	d	Cr-51	3.51E-02	c	Y-93	1.11E-03	c	Ba-140	2.70E-02	c
Xe-133	4.6E+03	d	Mn-54	5.41E-03	c	Zr-95	1.59E-03	c	La-140	1.81E-03	c
Xe-135m	4.05E+02	c	Mn-56	3.51E-03	c	Nb-95	8.38E-03	c	Ce-141	9.19E-03	c
Xe-135	4.59E+02	c	Fe-55	6.49E-03	c	Mo-99	5.95E-02	c	Ce-144	1.89E-05	c
Xe-137	5.14E+02	c	Co-57	8.2E-06	d	Tc-99m	2.97E-04	c	Pr-144	1.89E-05	c
Xe-138	4.32E+02	c	Co-58	2.3E-02	d	Ru-103	3.51E-03	c	W-187	1.89E-04	c
Xe-139	4.05E-04	c	Co-60	1.30E-02	c	Rh-103m	1.11E-04	c	Np-239	1.19E-02	c
			Fe-59	8.11E-04	c	Ru-106	7.8E-05	d	Total	1.307E+04	
			Ni-63	6.49E-06	c	Rh-106	1.89E-05	c			

- a. See Table 1 Section 9.5.1.
- b. Bounding Value from twin ACR700 criteria.
- c. Bounding Value from ABWR criteria.
- d. Bounding Value from AP1000 criteria.

1.4 Identification of Agents and Contractors

Dominion selected Bechtel Power Corporation (Bechtel) as its primary contractor to assist with the preparation of the ESP application. In this role, Bechtel supplied personnel, systems, project management, and resources to work on an integrated team with Dominion.

1.4.1 Bechtel Power Corporation

Bechtel is the nation's largest power contractor, headquartered in San Francisco. Bechtel has a history of supporting the nuclear power industry, beginning with the construction in 1950 of the EBR-1 reactor. Since then, Bechtel has engineered and constructed more than 60,000 MWe of nuclear power capacity worldwide. Currently, Bechtel has 50,000 employees working on 1,100 projects in 66 different countries around the globe.

1.4.2 Other Contractors

In addition to Bechtel, contractual relationships were established with several specialized consultants to assist in developing the ESP application.

1.4.2.1 Tetra Tech NUS, Inc.

Tetra Tech NUS, Inc. performed data collection and analysis, and prepared several sections of the Environmental Report, including the ecological description of the site and vicinity, environmental impacts of construction, and plant cooling system impacts on terrestrial and aquatic ecosystems.

1.4.2.2 MACTEC Engineering and Consulting, Inc.

MACTEC Engineering and Consulting, Inc. performed geotechnical field investigations and laboratory testing in support of SSAR Section 2.5, Geology, Seismology, and Geotechnical Engineering. That effort included performing standard penetration tests; obtaining core samples and rock cores; performing cone penetrometer tests, cross-hole seismic tests, and laboratory tests of soil and rock samples; installing ground water observation wells; and preparing a data report.

1.4.2.3 William Lettis & Associates, Inc.

William Lettis & Associates, Inc. performed geologic mapping and the characterization of seismic sources in support of SSAR Section 2.5, including literature review, geologic field reconnaissance, review and evaluation of existing seismic source characterization models, identification and characterization of any new or different sources, and preparation of the related SSAR sections.

1.4.2.4 Risk Engineering, Inc.

Risk Engineering, Inc. performed probabilistic seismic hazard assessments and related sensitivity analyses in support of SSAR Section 2.5. These assignments included sensitivity analyses of seismic source parameters and updated ground motion attenuation relationships, development of

updated safe shutdown earthquake ground motion values, and preparation of the related SSAR sections.

Section 1.4 References

None

1.5 Requirements for Further Technical Information

There are no technical information development programs remaining to be performed to support this application.

Section 1.5 References

None

1.6 Material Incorporated by Reference

No material has been incorporated by reference in this application.

Section 1.6 References

None

1.7 Drawings and Other Detailed Information

No such information has been submitted separately as part of this application.

Section 1.7 References

None

1.8 Conformance to NRC Regulations and Regulatory Guidance

This section discusses the conformance of the ESP application SSAR with applicable NRC regulations and guidance. NRC regulations are contained in Title 10 of the Code of Federal Regulations. NRC guidance is contained in NRC Regulatory Guides (RGs) and the draft NRC review standard for ESP applications (Reference 1). Exemptions, exceptions, and clarifications to the requirements and guidance are described below.

NRC regulations are legally binding requirements. If a legally binding requirement applicable to ESP can not be met, an *exemption* from the applicable regulation is needed. No *exemptions* to NRC regulations are required to support this ESP application. In certain instances, a regulation is listed because it could have applied under certain conditions. If the conditions are not met, conformance is specified as “not required” or “not applicable” and an explanation provided.

Exceptions are identified when the guidance can not be met as stated, but the intent or objective can be achieved by acceptable alternatives.

Clarifications are identified when guidance is met, but additional information is needed to provide complete understanding of the method of conformance.

Conformance with NRC regulations is described in Section 1.8.1, conformance with NRC RGs is described in Section 1.8.2, and conformance with NRC Review Standard RS-002 is described in Section 1.8.3.

1.8.1 Conformance with NRC Regulations

This section describes conformance with the applicable requirements of NRC regulations. Conformance with the regulation was determined using the acceptance criteria sections of NUREG-0800, as modified by draft RS-002 (Reference 1, Attachment 2). The NRC regulation number, title, description of applicable requirements, affected SSAR sections, and statement of conformance are provided. Exceptions and clarifications to conformance with the regulation are noted, as appropriate.

Regulation	10 CFR 20
Title	Standards for Protection Against Radiation
Description	Describe the restricted area boundaries in order to determine whether releases in excess of limits may occur.
Affected Section	2.1.1
Conformance	Conforms
Exceptions	None
Clarifications	None

Regulation	10 CFR 20, Appendix B, Table 2
Title	Annual Limits on Intake and Derived Air Concentrations of Radionuclides for Occupational Exposure; Effluent Concentrations; Concentrations for Release to Sewerage
Description	Provides radionuclide-specific concentration limits for ingestion of water.
Affected Section	2.4.13
Conformance	Conforms
Exceptions	None
Clarifications	Defer to the COL application. The types of facilities that would be used to store radioactive liquids and any associated inventory are unique to each design. Therefore, it is not feasible to complete this evaluation until a reactor design is selected.

Regulation	10 CFR 50.33(a) through (d)
Title	Contents of Applications; General Information
Description	Provide the name, address, description, and citizenship of applicant.
Affected Sections	Part 1 of the ESP Application
Conformance	Conforms
Exceptions	None
Clarifications	None

Regulation	10 CFR 50.34(a)(1)
Title	Contents of Applications; Technical Information
Description	Requires that reactors reflect an extremely low probability for accidents that could result in the release of significant quantities of radioactive fission products. Section (a)(1)(ii)(D) further states that EAB and LPZ accident doses should be within 25 Rem TEDE.
Affected Section	Chapter 15
Conformance	Conforms
Exceptions	None
Clarifications	None

Regulation	10 CFR 50.34(a)(12) [referenced in 52.17]
Title	Contents of Applications; Technical Information
Description	Requires conformance to current (i.e., probabilistic) NRC seismic criteria
Affected Section	2.4.5
Conformance	Conforms
Exceptions	None
Clarifications	None

Regulation	10 CFR 50.34(b)(10) [referenced in 52.17]
Title	Contents of Applications; Technical Information
Description	This section of the regulation requires conformance to current (i.e., probabilistic) NRC seismic criteria
Affected Section	2.4.5
Conformance	Conforms
Exceptions	None
Clarifications	None

Regulation	10 CFR 50.47
Title	Emergency Plans
Description	Describe additional meteorological measurements taken for emergency preparedness planning.
Affected Section	2.3.3
Conformance	Conforms
Exceptions	None
Clarifications	None

Regulation	10 CFR 50.55a
Title	Codes and Standards
Description	Requires structures, systems, and components to be designed and constructed to quality standards commensurate with the importance of the safety function to be provided.
Affected Sections	2.4.8, 2.4.10, 2.5.5
Conformance	Conforms
Exceptions	None
Clarifications	None

Regulation	10 CFR 50, Appendix A, GDC 2
Title	Design Bases for Protection Against Natural Phenomena
Description	Requires structures, systems, and components important to safety to be designed to withstand the effects of natural phenomena.
Affected Sections	2.3.1, 2.3.2, 2.4.1, 2.4.8, 2.4.10, 2.4.11, 2.5.1, 2.5.3
Conformance	Conforms
Exceptions	None
Clarifications	Section 2.5.3 – This section evaluates the potential for surface deformation only.

Regulation	10 CFR 50, Appendix A, GDC 4
Title	Environmental and Dynamic Effects Design Bases
Description	Provide information on tornadoes that could generate missiles.
Affected Section	2.3.1
Conformance	Conforms
Exceptions	None
Clarifications	None

Regulation 10 CFR 50, Appendix A, GDC 44

Title	Cooling Water
Description	Requires an ultimate heat sink capable of accepting the plant's heat load under normal and accident conditions.
Affected Sections	2.4.8, 2.4.9, 2.4.11, 2.5.4, 2.5.5
Conformance	Conforms
Exceptions	None
Clarifications	None

Regulation 10 CFR 50, Appendix E

Title	Emergency Planning and Preparedness for Production and Utilization Facilities
Description	Describe additional meteorological measurements taken for emergency preparedness planning.
Affected Section	2.3.3
Conformance	Conforms
Exceptions	None
Clarifications	None

Regulation 10 CFR 50, Appendix I

Title	Numerical Guides for Design Objectives and Limiting Conditions for Operation to Meet the Criterion "As Low As Reasonably Achievable" for Radioactive Material in Light-Water-Cooled Nuclear Power Reactor Effluents
Description	Section 2.3.3 – Describe meteorological data used in the compliance with the numerical guides for doses to meet the criterion of ALARA. Section 2.3.5 – Demonstrate compliance by characterizing atmospheric transport and diffusion conditions in order to estimate the radiological consequences of routine releases of materials to the atmosphere.
Affected Sections	2.3.3, 2.3.5
Conformance	Conforms
Exceptions	None
Clarifications	None

Regulation 10 CFR 50, Appendix S IV(a)

Title	Earthquake Engineering Criteria for Nuclear Power Plants
Description	The SSE ground motion must be characterized by free-field ground motion response spectra at the free ground surface. The OBE must be characterized by response spectra.
Affected Section	2.5.2
Conformance	Conforms
Exceptions	None
Clarifications	Surface rock conditions are assumed. The OBE has been defined as one third of the SSE ground motion design response spectra.

Regulation	10 CFR 50, Appendix S IV(b)
Title	Earthquake Engineering Criteria for Nuclear Power Plants
Description	The potential for surface deformation must be taken into account in the design of the nuclear power plant by providing reasonable assurance that in the event of deformation, certain structures, systems, and components will remain functional.
Affected Section	2.5.3
Conformance	Conforms
Exceptions	None
Clarifications	This section evaluates the potential for surface deformation only.

Regulation	10 CFR 50, Appendix S IV(c)
Title	Earthquake Engineering Criteria for Nuclear Power Plants
Description	Account for seismically induced floods and water waves from either locally or distantly generated seismic activity and other design conditions.
Affected Sections	2.4.2, 2.4.5
Conformance	Conforms
Exceptions	None
Clarifications	None

Regulation	10 CFR 52, Subpart A
Title	Early Site Permits
Description	Describe the seismic and geologic characteristics of the proposed site.
Affected Sections	2.5.1, 2.5.2
Conformance	Conforms
Exceptions	None
Clarifications	None

Regulation	10 CFR 52.17(a)
Title	Contents of Applications
Description	Section 2.4.1, 2.4.2, 2.4.5, 2.4.6, 2.4.10, 2.4.12 – Describe the hydrologic characteristics of the site. Section 2.4.7 – Provide a description of any icing phenomena with the potential to result in adverse effects to the intake structure or other safety-related facilities for a nuclear power plant or plants of specified type that might be constructed on the proposed site. Section 2.4.9 – Requires that physical characteristics of the site are taken into account to determine acceptability of site for nuclear power plants.
Affected Sections	2.4.1, 2.4.2, 2.4.5, 2.4.6, 2.4.7, 2.4.9, 2.4.10, 2.4.12
Conformance	Conforms
Exceptions	None
Clarifications	Section 2.4.6 – The North Anna Site is not located in a coastal region and not subject to tsunami flooding.

Regulation	10 CFR 52.17(a)(1)
<hr/>	
Title	Contents of Applications
Description	Provide an analysis and evaluation of the major structures, systems, and components of the facility that bear significantly on the acceptability of the site under the radiological consequence evaluation factors identified in 10 CFR 50.34(a)(1).
Affected Section	Chapter 15
Conformance	Conforms
Exceptions	None
Clarifications	The PPE provides this information. Results conform to 50.34(a)(1).

Regulation	10 CFR 52.17(a)(1)(ii)
<hr/>	
Title	Contents of Applications
Description	Provide the site boundaries.
Affected Section	2.1.1
Conformance	Conforms
Exceptions	None
Clarifications	None

Regulation	10 CFR 52.17(a)(1)(vi)
<hr/>	
Title	Contents of Applications
Description	Describe the hydrologic characteristics of the proposed site.
Affected Sections	2.4.3, 2.4.4
Conformance	Conforms
Exceptions	None
Clarifications	None

Regulation	10 CFR 52.17(a)(1)(vii)
<hr/>	
Title	Contents of Applications
Description	Provide the location and description of any nearby industrial, military, or transportation facilities and routes.
Affected Sections	2.2.1, 2.2.2
Conformance	Conforms
Exceptions	None
Clarifications	None

Regulation	10 CFR 52.17(a)(1)(viii)
<hr/>	
Title	Contents of Applications
Description	Provide the existing and projected population profiles for the area around the site.
Affected Section	2.1.3
Conformance	Conforms
Exceptions	None
Clarifications	None

Regulation	10 CFR 52.17(a)(2)
Title	Contents of Applications
Description	This section of the regulation requires that a complete environmental report be submitted in accordance with 10 CFR 51.45 and 51.50.
Affected Section	Part 3
Conformance	Conforms
Exceptions	None
Clarifications	None

Regulation	10 CFR 52.17(b)(1)
Title	Contents of Applications
Description	This section of the regulation requires that certain emergency preparedness information be submitted. The application must identify physical characteristics unique to the proposed site that could pose a significant impediment to the development of emergency plans.
Affected Section	13.3
Conformance:	Conforms
Exceptions:	None
Clarifications:	None

Regulation	10 CFR 52.17(b)(2)
Title	Contents of Applications
Description	Provides an option in the regulation to submit a major features emergency plan as part of an ESP application.
Affected Section	13.3
Conformance	Conforms
Exceptions	Certain EP criteria are not implementable at the ESP stage. See Section 4.0 of the Major Features Emergency Plan
Clarifications	The applicant has the option to submit the Major Features of an Emergency Plan or a complete and integrated Emergency Plan. Dominion has elected to exercise the major features option and has included the required information.

Regulation	10 CFR 52.17(b)(3)
Title	Contents of Applications
Description	Requires the applicant to identify contacts and arrangements with local, state and federal agencies with emergency preparedness responsibilities.
Affected Section	13.3
Conformance	Conforms
Exceptions	None
Clarifications	None

Regulation	10 CFR 52.17(c)
Title	Contents of Applications
Description	This section of the regulation specifies information the applicant must submit as part of its ESP application if it later wishes to perform activities at the site allowed for under 10 CFR 50.10(e)(1) [typically referred to as Limited Work Authorization-1] without first obtaining separation authorization required by that section.
Affected Section	Part 4 of the ESP Application
Conformance	Conforms
Exceptions	None
Clarifications	None
Regulation	10 CFR 100
Title	Reactor Site Criteria
Description	All Sections Not Listed Below – Evaluate the hydrologic characteristics of the site. Sections 2.5.2, 2.5.4, 2.5.5 – Provides general criteria that guide the evaluation of the suitability of the site for nuclear power reactors.
Affected Sections	2.4.1, 2.4.5, 2.4.6, 2.4.7, 2.4.8, 2.4.9, 2.4.11, 2.4.13, 2.5.2, 2.5.4, 2.5.5
Conformance	Conforms
Exceptions	None
Clarifications	Section 2.4.13 – Defer to the COL application. The types of facilities that would be used to store radioactive liquids and any associated inventory are unique to each design. Therefore, it is not feasible to complete this evaluation until a reactor design is selected.
Regulation	10 CFR 100.3
Title	Definitions
Description	Defines exclusion area, low population zone and population center distance as they apply to 10 CFR 100.
Affected Section	2.1.2, 2.1.3
Conformance	Conforms
Exceptions	None
Clarifications	None
Regulation	10 CFR 100, Subpart B
Title	Evaluation Factors for Stationary Power Reactor Site Applications on or After January 10, 1997
Description	Provide information on the exclusion area, low population zone, and population center distance to the site.
Affected Sections	2.1.1, 2.1.3
Conformance	Conforms
Exceptions	None
Clarifications	None

Regulation	10 CFR 100.20
Title	Reactor Site Criteria
Description	Sections 2.2.1, 2.2.2 - Provide details of the use characteristics of the site environs. Section 2.2.3 - The nature and proximity of man-made hazards must be evaluated to establish site parameters for use in determining whether a plant design can accommodate commonly occurring hazards, and whether the risk of others hazards is low.
Affected Sections	2.2.1, 2.2.2, 2.2.3
Conformance	Conforms
Exceptions	None
Clarifications	None
Regulation	10 CFR 100.20(c)
Title	Reactor Site Criteria
Description	Sections 2.3.1, 2.3.2 – Describe the consideration that has been given the meteorological characteristics of the site. Section 2.3.3 – Describe meteorological data collected for use in characterizing the meteorological conditions of the site. Sections 2.4.1, 2.4.2, 2.4.3, 2.4.5, 2.4.6, 2.4.10 – Describe the hydrologic characteristics of the proposed site. Section 2.4.4 – Requires that the physical characteristics of the site, including hydrology, be taken into account when determining site acceptability. 2.4.5 – Provide a description of the surface and subsurface hydrologic characteristics of the region and an analysis of the potential for flooding due to surges and seiches. 2.4.6 – Provide a description of the hydrologic characteristics of the coastal region in which the proposed site is located and an analysis of severe seismically induced waves. Section 2.4.7 – Provide a description of any icing phenomena with the potential to result in adverse effects to the intake structure or other safety-related facilities for a nuclear power plant or plants of specified type that might be constructed on the proposed site. Section 2.4.9, 2.4.12 – Requires that physical characteristics of the site be taken into account to determine acceptability of site for nuclear power plants.
Affected Sections	2.3.1, 2.3.2, 2.3.3, 2.4.1, 2.4.2, 2.4.3, 2.4.4, 2.4.5, 2.4.6, 2.4.7, 2.4.9, 2.4.10, 2.4.12
Conformance	Conforms
Exceptions	None
Clarifications	Section 2.4.6 – The North Anna Site is not located in a coastal region and, therefore, not subject to tsunami flooding.
Regulation	10 CFR 100.21
Title	Non-seismic Siting Criteria
Description	Discuss meteorological considerations used in the evaluation to determine an acceptable EA and LPZ.
Affected Section	2.3.4
Conformance	Conforms
Exceptions	None
Clarifications	None

Regulation	10 CFR 100.21(c)(2)
Title	Non-seismic Siting Criteria
Description	Radiological dose consequences of postulated accidents shall meet the criteria in 50.34(a)(1).
Affected Section	Chapter 15
Conformance	Conforms
Exceptions	None
Clarifications	None
Regulation	10 CFR 100.21(d)
Title	Non-seismic Siting Criteria
Description	Sections 2.3.1, 2.3.2 – Describe the consideration that has been given the meteorological characteristics of the site. Section 2.3.3 – Describe meteorological data collected for use in characterizing the meteorological conditions of the site.
Affected Sections	2.3.1, 2.3.2, 2.3.3
Conformance	Conforms
Exceptions	None
Clarifications	None
Regulation	10 CFR 100.23
Title	Geologic and Seismic Siting Criteria
Description	Section 2.4.12 - Sets forth the criteria to determine the suitability of design bases with respect to seismic characteristics of the site. Section 2.5.5 - Obtain the seismic and geologic data necessary to address site suitability and identify seismic and geologic factors to be taken into account in the siting and design of the nuclear power plant.
Affected Section	2.4.12, 2.5.5
Conformance	Conforms
Exceptions	None
Clarifications	None

Regulation	10 CFR 100.23(c)
Title	Geologic and Seismic Siting Criteria
Description	<p>Section 2.4.4 – Requires an investigation to obtain geologic and seismic data for evaluating seismically induced floods, including failure of an upstream dam during an earthquake or low water levels from failure of a downstream dam.</p> <p>Section 2.4.6 – Investigate distantly and locally generated waves or tsunamis that have affected or could affect the proposed site, including available evidence regarding the runup or drawdown associated with historic tsunamis in the same coastal region and local features of coastal topography that might modify runup or drawdown.</p> <p>Section 2.4.7 – Provide a description of any icing phenomena with the potential to result in adverse effects to the intake structure or other safety-related facilities for a nuclear power plant or plants of specified type that might be constructed on the proposed site.</p> <p>Section 2.4.11, 2.4.12 – Requires that physical characteristics of the site be taken into account to determine acceptability of site for nuclear power plants.</p> <p>Sections 2.5.1, 2.5.2, 2.5.3 – Determine the SSE and its uncertainty, the potential for surface tectonic and nontectonic deformations, the design bases for seismically induced floods and water waves, and other design conditions.</p> <p>Section 2.5.4, 2.5.5 – Consider the geologic and seismic conditions at the site during the siting and design of the nuclear plant. Investigate the geological and seismological characteristics of the site in sufficient scope and detail to permit an adequate evaluation of the proposed site.</p>
Affected Sections	2.4.4, 2.4.6, 2.4.7, 2.4.11, 2.4.12, 2.5.1, 2.5.2, 2.5.3, 2.5.4, 2.5.5
Conformance	Conforms
Exceptions	None
Clarifications	Section 2.4.6 – Since the site is inland and not subject to tsunami flooding, no wave analysis was performed or investigated. The site is protected from tsunami flooding.
Regulation	10 CFR 100.23(d)(4)
Title	Geologic and seismic siting factors
Description	Section 2.4.12 – Requires that the physical properties of materials underlying the site be considered when designing a system to supply cooling water for emergency and long-term shutdown decay heat removal.
Affected Section	2.4.12
Exceptions	None
Clarifications	None
Regulation	10 CFR 100, Appendix A
Title	Seismic and Geologic Siting Criteria for Nuclear Power Plants
Description	Investigate the seismic and geologic data necessary to determine site suitability and identify seismic and geologic factors to be taken into account in the siting and design of the nuclear power plant.
Affected Sections	2.5.5
Conformance	Conforms
Exceptions	None
Clarifications	None

1.8.2 Conformance to NRC Regulatory Guides

This section describes conformance with the applicable guidance in published NRC RGs, as specified in the acceptance criteria sections of NUREG-0800, as modified by draft RS-002 Reference 1, Attachment 2. The RG title, description of applicable guidance, revision number, date, affected SSAR sections, and statement of conformance are provided. Exceptions and clarifications to conformance with the guidance in the RG are noted, as appropriate.

Document	Regulatory Guide 1.5
----------	-----------------------------

Title	Assumptions Used for Evaluating the Potential Radiological Consequences of a Steam Line Break Accident for Boiling Water Reactors
Description	Provides information, recommendations, and guidance and in general describes an acceptable basis to implement the requirements of 10 CFR 100.
Revision	Rev. 0
Date	March 1971
Affected Section	2.3.4
Conformance	Conforms
Exceptions	None
Clarifications	None

Document	Regulatory Guide 1.23
----------	------------------------------

Title	Onsite Meteorological Programs
Description	Provides the criteria for an acceptable onsite meteorological measurements program.
Revision	Rev. 0/Rev. 1
Date	1972/1986
Affected Sections	2.3.2, 2.3.3, 2.3.4, 2.7
Conformance	Conforms
Exceptions	None
Clarifications	None

Document	Regulatory Guide 1.24
----------	------------------------------

Title	Assumptions Used for Evaluating the Potential Radiological Consequences of a Pressurized Water Reactor Radioactive Gas Storage Tank Failure
Description	Provides information, recommendations, and guidance and in general describes an acceptable basis to implement the requirements of 10 CFR 100.
Revision	Rev. 0
Date	March 1972
Affected Section	2.3.4
Conformance	Conforms
Exceptions	None
Clarifications	None

Document **Regulatory Guide 1.59**

Title	Flood Design Basis for Nuclear Power Plants
Description	Provides guidance for estimating the design basis for flooding, considering the worst single phenomenon and combinations for less severe phenomena.
Revision	Rev. 2
Date	August 1977
Affected Sections	2.4.2, 2.4.3, 2.4.4, 2.4.5, 2.4.6, 2.4.7, 2.4.8, 2.4.10
Conformance	Conforms
Exceptions	None
Clarifications	None

Document **Regulatory Guide 1.60**

Title	Design Response for Seismic Design of Nuclear Power Plants
Description	Smoothed response spectra are generally used for design purposes -- for example, a standard spectral shape that has been used in the past is presented in RG 1.60. These smoothed spectra are still acceptable when the smoothed design spectra compare favorably with site-specific response spectra.
Revision	Rev. 1
Date	December 1973
Affected Section	2.5.2
Conformance	Not Required
Exceptions	Site-specific response spectra are lower than RG 1.60 for low frequencies and exceed RG 1.60 spectra for high frequencies.
Clarifications	None

Document **Regulatory Guide 1.70**

Title	Standard Format and Content of Safety Analysis Reports for Nuclear Power Plants – LWR Edition
Description	<p>Section 2.0 – Provide information on the geological, seismological, hydrological and meteorological characteristics of the site and vicinity, in conjunction with present and projected population distribution and land use and site activities and controls.</p> <p>Section 2.1.1 – Specify the location of each reactor at the site. Provide a site area map that shows property lines, site boundary, principal plant structures, other structures within the site area, exclusion area boundary, and highways, railways, and waterways that traverse the site. Describe the boundaries of the restricted area (per 10 CFR 20) and how access to this area will be controlled.</p> <p>Section 2.1.2 – Address ownership of all lands within the exclusion area. Describe any activities unrelated to plant operation that may be permitted within the exclusion area. Describe how traffic on any highways, railways, or waterways that traverse the exclusion area will be controlled in the event of an emergency.</p> <p>Section 2.1.3 – Describe the population distributions within 50 miles of the site, including any seasonal or transient populations. Specify the low population zone. Identify the nearest population center and the projected cumulative population density.</p> <p>Section 2.2.1 – Provide maps showing the location and distance from the nuclear plant of all significant industrial facilities, military installations, oil and gas pipelines, etc. Also show any nearby air traffic patterns or transportation routes.</p> <p>Section 2.2.2 – Describe all significant industrial facilities, military installations, oil and gas pipelines, etc. Detail products manufactured and shipped of a hazardous nature, relationship of shipping to the intake structure, and airport operations. Also provide a project of future growth of existing and new types of activities in the vicinity of the plant.</p> <p>Section 2.2.3 – Determine the design basis external events considering explosions, flammable vapor clouds, toxic chemical, fires, collisions with the intake structure, and liquid spills and evaluate the effects of these events on safety-related SSCs.</p> <p>Section 2.3.1 – Describe the: 1) general climate of the region, 2) seasonal and annual frequencies of severe weather phenomena, 3) meteorological data used for evaluating the performance of the ultimate heat sink, 4) design basis tornado, and 5) all other regional meteorological and air quality conditions used for design and operating basis considerations.</p> <p>Section 2.3.2 – Provide monthly and annual summaries of: 1) wind roses and wind persistence, 2) air/dewpoint temperatures, 3) extremes of atmospheric water vapor, 4) precipitation, 5) fog and smog, and 6) atmospheric stability, 7) monthly mixing height data, 8) and hourly averages of wind speed and direction. Discuss and evaluate the potential impact of the plant on the meteorological parameters. Provide all local meteorological and air quality conditions used for design and operating basis considerations.</p> <p>Section 2.3.3 – Describe the preoperational and operational programs for meteorological measurements at the site. Provide joint frequency distributions of wind speed and direction by atmospheric stability class.</p> <p>Section 2.3.4 – Provide conservative and realistic estimates of atmospheric diffusion (X/Q) at the EA and LPZ. Base diffusion estimates on the most representative meteorological data. Discuss any impacts due to local topography.</p> <p>Section 2.3.5 – Provide realistic estimates of annual average atmospheric transport and diffusion characteristic to a distance of 50 miles from the plant. Provide a detailed description of the model used to calculate realistic annual average X/Q values. Provide a calculation of the maximum annual average X/Q at or beyond the site boundary for each venting location.</p>

(continued)

Description
(continued)

Section 2.4.1 – Describe the site and all safety-related elevations, structures, exterior accesses, equipment, and systems from the standpoint of hydrologic considerations. Describe the location, size, shape, and other hydrologic characteristics of streams, lakes, shore regions, and ground water environments influencing plant siting. Include a description of existing and proposed water control structures, both upstream and downstream, that may influence conditions at the site.

Section 2.4.2 – Provide date, level, peak discharge, and related information for major historical flood events in the site region. The considerations taken to determine the design basis flood elevation, as well as the elevation itself should be discussed. The effects of local intense precipitation at the site should be discussed.

Section 2.4.3 – Indicate the methodology and approach used to determine the PMF level. Include discussion on development of PMP, precipitation losses, runoff models, PMF flow hydrograph, water level determination, and coincident wave activity.

Section 2.4.4 – Discuss the investigation of seismically induced floods including results for seismically induced dam failures and antecedent flood flows coincident with the flood peak.

Section 2.4.5 – Discuss the maximum water levels associated with the probable maximum surge and seiche flooding at the site. Areas to be considered include the probable maximum hurricane or other probable maximum wind, antecedent water levels, coincident wave action and run-up and resonance.

Section 2.4.6 – Discuss historical tsunamis, either recorded or translated and inferred, that provide information for use in determining the probable maximum water levels and the geoseismic generating mechanisms available.

Section 2.4.7 – Describe potential icing effects and design criteria for protecting safety-related facilities from the most severe ice jam flood, wind-driven ice ridges, or other ice-produced effects and forces that are reasonably possible and could affect safety-related facilities with respect to adjacent streams, lakes, etc., for both high and low water levels.

Section 2.4.8 – Present the design basis for the capacity and operating plan for safety-related cooling water canals and reservoirs.

Section 2.4.9 – Discuss the potential for upstream diversion or rerouting of the source of cooling water.

Section 2.4.10 – Describe the static and dynamic consequences of all types of flooding on each pertinent safety-related facility. Present the design bases required to ensure that the safety-related facilities will be capable of surviving all design flood conditions.

Section 2.4.11 – Discuss the impact of low water conditions on safety-related facilities as well as cooling water and service water systems. For safety-related structures demonstrate ability to perform adequately with probable minimum flow rate and level. For non-safety-related water supplies, demonstrate that the supply will be adequate during a 100-year drought.

Section 2.4.12 – Describe ability of the surface water environment to disperse, dilute, or concentrate accidental liquid releases of radioactive effluents as related to existing or potential future water users.

Section 2.4.13 (except 2.4.13.3) – Describe the regional and local groundwater aquifers, formations, sources and sinks and onsite groundwater use, including present and projected future use. Describe the effects of present and projected groundwater use on gradients and groundwater or piezometric levels beneath the site. Note any potential groundwater recharge areas. Indicate the range of values and method of determination for vertical and horizontal permeability and total and effective porosity (specific yield). Discuss the potential for reversibility of groundwater flow resulting from local areas of pumping for both plant and non-plant use. Discuss plans, procedures, safeguards, and monitoring programs to be used to protect present and projected groundwater use. Identify existing groundwater users. Discuss the history of groundwater or piezometric level fluctuations beneath and in the vicinity of the site. Provide groundwater or piezometric contour maps of aquifers beneath and in the vicinity of the site.

(continued)

Description (continued)	<p>Section 2.4.13.3 – Provide a conservative analysis of a postulated accidental release of liquid radioactive material at the site.</p> <p>Section 2.5.1 – Discuss the regional and site geology including: All geologic and man-made hazards within the site region and relate them to the regional tectonic structures and tectonic provinces, and geomorphology. Identify and describe tectonic structures underlying the region surrounding the site and discuss their geologic history. Detailed discussions of regional tectonic structures of significance to the site. Structural geology in the vicinity of the site. The relationship of the site structure to regional tectonics, with particular attention to specific structural units such as folds, faults, anticlines, synclines, domes, and basins.</p> <p>Section 2.5.2 – Determine the SSE and OBE design ground motion based on identification of tectonic provinces or active geologic structures with which earthquake activity in the region can be associated.</p> <p>Section 2.5.3 – Information should be provided to describe whether there exists a potential for surface faulting at the site.</p> <p>Section 2.5.4 – Present information that thoroughly defines the conditions and engineering properties of both soil and/or rock supporting nuclear power plants. The stability of the soils and rock under plant structures should be evaluated both for static and dynamic loading conditions. Both the operating and safe shutdown earthquakes should be used in the dynamic stability evaluation.</p> <p>Section 2.5.5 – Present information concerning the static and dynamic stability of all soil or rock slopes, both natural and man-made. Evaluate the stability of the slopes using classic and contemporary methods of analyses. Include in the evaluation, comparative field performance of similar slopes. Include in the stability evaluation of man-made slopes summary data and a discussion of construction procedures, record testing, and instrumentation monitoring.</p> <p>Section 2.5.6 – Include information related to the investigation, engineering design, proposed construction, and performance of all earth, rock, or earth and rock fill embankments used for plant flood protection or for impounding cooling water required for the operation of the nuclear power plant.</p> <p>Chapter 15 – Evaluate the response of the plant to postulated disturbances in process variables, malfunctions, or failures of equipment. Examine the effects of anticipated process disturbances and postulated component failures to determine their consequences and to evaluate the capability of the plant to control or accommodate such failures and situations.</p>
Revision	Rev. 3
Date	November 1, 1978
Affected SSAR Sections	1.1, 1.4, 1.5, 1.6, 1.7, 1.8, 2.0, 2.1.1, 2.1.2, 2.1.3, 2.2.1, 2.2.2, 2.2.3, 2.3.1, 2.3.2, 2.3.3, 2.3.4, 2.3.5, 2.4.1, 2.4.2, 2.4.3, 2.4.4, 2.4.5, 2.4.6, 2.4.7, 2.4.8, 2.4.9, 2.4.10, 2.4.11, 2.4.12, 2.4.13, 2.5.1, 2.5.2, 2.5.3, 2.5.4, 2.5.5, 2.5.6, Chapter 15
Conformance	<p>Conforms (all except those listed below)</p> <p>Partial Conformance (Sections 2.3.5, 2.4.11, 2.5.4, Chapter 15)</p> <p>Not Required (Section 2.4.13.3)</p> <p>Not Applicable (Sections 2.4.8, 2.5.6)</p>

Exceptions Specific design information is not provided.
 Section 2.3.5 – As the venting locations would not be fixed until at the COL stage, the calculation of the maximum annual average χ/Q at or beyond the site boundary for each venting location will be provided in the COL application.
 Section 2.4.11 – Since the Lake Anna water level during drought conditions is determined by many factors in addition to inflow rate (i.e. air temperature and rejected heat load) the 100-year drought condition does not directly apply to Lake Anna and has not been determined. Historic and predicted low water levels and durations are presented.
 Section 2.4.13.3 – Defer to the COL application. The types of facilities that would be used to store radioactive liquids and any associated inventory are unique to each design. Therefore, it is not feasible to complete this evaluation until a reactor design is selected.
 Section 2.5.4 – Discussed excavation and backfill in general terms – specific locations, quantities etc. would be addressed in the COL application when details are known. A brief summary of the derivation of the SSE and OBE is provided. Discussed subsurface instrumentation in overall terms – specific locations, types of instrumentation, reading schedule would be addressed in the COL application when details are known.
 Chapter 15 – Most but not all the accidents listed in RG 1.70 are analyzed (e.g., waste gas decay tank failure not analyzed). The main criteria for selecting the accidents are RG 1.183 and NUREG-0800, as suggested in Chapter 15 of RS-002.

Clarifications The guidance is written for Part 50 applicants with a known plant design. It is followed to the extent feasible for an ESP application submitted in accordance with Part 52 using the PPE approach.
 Section 2.4.8 – The cooling water canals and reservoirs at the ESP site are not safety-related.
 Section 2.5.2 – Per RG 1.165, EPRI 1989, evaluated for any needed updating, provides an acceptable basis for source model description.
 Section 2.5.6 – No embankments or dams for plant flood protection or cooling water will be constructed.

Document	Regulatory Guide 1.76, Including March 25, 1988 Interim Staff Position, ALWR Design Basis Tornado
Title	Design Basis Tornado for Nuclear Power Plants
Description	Defines the design basis tornado.
Revision	Rev. 0
Date	April 1974
Affected Section	2.3.1
Conformance	Conforms
Exception	None
Clarifications	None

Document **Regulatory Guide 1.77**

Title Evaluating the Habitability of a Nuclear Power Plant Control Room During a Postulated Hazardous Chemical Release

Description Provides information, recommendations, and guidance and in general describes an acceptable basis to implement the requirements of 10 CFR 100.

Revision Rev. 0

Date May 1974

Affected Section 2.3.4

Conformance Not Required

Exceptions Control room impacts would be evaluated in the COL application.

Clarifications None

Document **Regulatory Guide 1.78**

Title Assumptions for Evaluating the Habitability of a Nuclear Power Plant Control Room During a Postulated Hazardous Chemical Release

Description Sections 2.2.1, 2.2.2 – Provides guidance for evaluating the habitability of the control room during a postulated hazardous chemical release.
Section 2.3.4 – Provides information, recommendations, and guidance and in general describes an acceptable basis to implement the requirements of 10 CFR 100.

Revision Rev. 1

Date December 2001

Affected Sections 2.2.1, 2.2.2, 2.3.4

Conformance Not Required

Exceptions Control room impacts would be evaluated in the COL application.

Clarifications None

Document **Regulatory Guide 1.91**

Title Evaluations of Explosions Postulated to Occur on Transportation Routes Near Nuclear Power Plants

Description Describes methods for ensuring that the risk of damage due to an explosion on a nearby transportation route is sufficiently low.

Revision Rev. 1

Date February 1978

Affected Sections 2.2.1, 2.2.2

Conformance Conforms

Exceptions None

Clarifications None

Document **Regulatory Guide 1.102**

Title Flood Protection for Nuclear Power Plants
Description Provides guidance on flood protection measures.
Revision Rev. 1
Date September 1976
Affected Sections 2.4.2, 2.4.3, 2.4.4, 2.4.5, 2.4.6, 2.4.7, 2.4.8, 2.4.10
Conformance Conforms
Exceptions None
Clarifications None

Document **Regulatory Guide 1.111**

Title Methods for Estimating Atmospheric Transport and Dispersion of Gaseous Effluents in Routine Releases from Light-Water-Cooled Reactors
Description Provides criteria for characterizing atmospheric transport and diffusion conditions for evaluating the consequences of routine releases.
Revision Rev. 1
Date July 1977
Affected Sections 2.3.5, 2.7
Conformance Conforms
Exceptions None
Clarifications None

Document **Regulatory Guide 1.113**

Title Estimating Aquatic Dispersion of Effluents from Accidental and Routine Reactor Releases for the Purpose of Implementing Appendix I
Description Provides guidance in selecting and using surface water models.
Revision Rev. 1
Date April 1977
Affected Sections 2.4.13
Conformance Not Required
Exceptions Defer to the COL application. The types of facilities that would be used to store radioactive liquids and any associated inventory are unique to each design. Therefore, it is not feasible to complete this evaluation until a reactor design is selected.

Document Regulatory Guide 1.125

Title	Physical Models for Design and Operation of Hydraulic Structures and Systems for Nuclear Power Plants
Description	Provides guidance on the use of physical models of hydraulic structures and systems.
Revision	Rev. 1
Date	October 1978
Affected Sections	2.4.5, 2.4.6, 2.4.8, 2.4.10
Conformance	Not Required
Exceptions	None
Clarifications	Physical modeling of hydraulic structures is not necessary for the ESP.

Document Regulatory Guide 1.132

Title	Site Investigations for Foundations of Nuclear Power Plants
Description	Provides guidance for site investigation programs.
Revision	Rev. 1 Proposed Rev. 2 (Draft RG DG-1101)
Date	March 1979
Affected Sections	2.5.1, 2.5.2, 2.5.3, 2.5.4, 2.5.5
Conformance	Conforms (all except those listed below) Partial (Section 2.5.4, 2.5.5)
Exceptions	Section 2.5.4 – Only borings used for cross-hole seismic tests were surveyed for deviation. Only split-spoon and rock core samples were taken. Soil sampling was continuous to 5 m depth and rock coring was continuous in all borings. Appendix D Borings were spaced further apart than recommended because of the general nature of the investigation. Section 2.5.5 – 4.3.1.2 Only borings used for cross-hole seismic tests were surveyed for deviation. 4.3.2 Only split-spoon and rock core samples were taken. 4.3.2.2 Soil sampling was continuous to 5 m depth and rock coring was continuous in all borings. Appendix D Borings were spaced further apart than recommended because of general nature of investigation.
Clarifications	None

Document Regulatory Guide 1.138

Title	Laboratory Investigations of Soils for Engineering Analysis and Design of Nuclear Power Plants
Description	Describes laboratory investigations and testing practices acceptable for determining soil and rock properties and characteristics needed for engineering analysis and design for foundations and earthwork.
Revision	Proposed Rev. 1 (Draft RG DG-1109)
Date	April 1978
Affected Sections	2.5.4, 2.5.5
Conformance	Partial Conformance
Exceptions	No new cyclic triaxial tests were performed since a large number of high quality cyclic triaxial tests had been performed previously. No resonant column tests were performed.
Clarifications	None

Document Regulatory Guide 1.145

Title Atmospheric Dispersion Models for Potential Accident Consequence Assessments at Nuclear Power Plants

Description Identifies acceptable methods for choosing X/Q values for evaluations.

Revision Rev. 1

Date November 1982

Affected Sections 2.3.4, 2.7

Conformance Conforms

Exceptions None

Clarifications None

Document Regulatory Guide 1.165

Title Identification and Characterization of Seismic Sources and Determination of Safe Shutdown Earthquake Ground Motion

Description Describes acceptable methods to: 1) conduct geological seismological, and geophysical investigations of the site and region around the site, 2) identify and characterize seismic sources, 3) perform PSHA, and 4) determine the SSE for the site.

Revision Rev. 0

Date March 1997

Affected Sections 2.5.1, 2.5.2, 2.5.3

Conformance Conforms (2.5.1, 2.5.3)
Partial Conformance (2.5.2)

Exceptions Section 2.5.2 – The evaluation of vibratory ground motion conformance to RG 1.165 with the exception of the development of the selected SSE ground motion spectrum. The selected spectrum was developed in accordance with an alternate approach as described in Sections 2.5.2 and 2.5.2.6.7.

Clarifications None

Document Draft Regulatory Guide DG-1105

Title Procedures and Criteria for Assessing Seismic Soil Liquefaction at Nuclear Power Plant Sites

Description Provides guidance for evaluation of the behavior of soils subjected to earthquake shaking.

Revision

Date March 2001

Affected Sections 2.5.2, 2.5.4, 2.5.5

Conformance Conforms (Section 2.5.2)
Partial Conformance (Sections 2.5.4, 2.5.5)

Exceptions Sections 2.5.4, 2.5.5 – For updated analysis for ESP, SPT and CPT values were used. The original analyses using cyclic triaxial test results were modified using newly generated peak accelerations.

Clarifications None

1.8.3 Conformance to NRC Review Standard

This section describes conformance to the published draft NRC review standard RS-002 (Reference 1). Draft RS-002, Attachment 2 incorporates and clarifies NRC guidance from the Standard Review Plan (SRP). For each applicable SRP section listed, the corresponding SSAR section(s), and a statement of conformance are provided. Exceptions and clarifications are noted, as appropriate.

RS-002 Section and Title	2.1.1 Site Location and Description
Section	2.1.1
Conformance	Conforms (except as noted below)
Exceptions	For security reasons, UTM coordinates not provided
Clarifications	None
RS-002 Section and Title	2.1.2 Exclusion Area Authority and Control
Section	2.1.2
Conformance	Conforms
Exceptions	None
Clarifications	None
RS-002 Section and Title	2.1.3 Population Distribution
Section	2.1.3
Conformance	Conforms
Exceptions	None
Clarifications	None
RS-002 Section and Title	2.2.1-2.2.2 Identification of Potential Hazards in Site Vicinity
Sections	2.2.1-2.2.2
Conformance	Conforms
Exceptions	None
Clarifications	None
RS-002 Section and Title	2.2.3 Evaluation of Potential Accidents
Section	2.2.3
Conformance	Conforms
Exceptions	None
Clarifications	None
RS-002 Section and Title	2.3.1 Regional Climatology
Section	2.3.1
Conformance	Conforms
Exceptions	None
Clarifications	None

RS-002 Section and Title **2.3.2 Local Meteorology**

Section 2.3.2
 Conformance Conforms
 Exceptions None
 Clarifications None

RS-002 Section and Title **2.3.3 Onsite Meteorological Measurements Program**

Section 2.3.3
 Conformance Conforms
 Exceptions None
 Clarifications None

RS-002 Section and Title **2.3.4 Short-Term Dispersion Estimates for Accidental Atmospheric Releases**

Section 2.3.4
 Conformance Conforms (except as noted below)
 Exceptions Atmospheric dispersion estimates for the Control Room from radiological and onsite hazardous material releases would be evaluated in the COL application.
 Clarifications None

RS-002 Section and Title **2.3.5 Long-Term Diffusion Estimates**

Section 2.3.5
 Conformance Conforms
 Exceptions None
 Clarifications None

RS-002 Section and Title **2.4.1 Hydrologic Description**

Section 2.4.1
 Conformance Conforms
 Exceptions: None
 Clarifications None

RS-002 Section and Title **2.4.2 Floods**

Section 2.4.2
 Conformance Conforms
 Exceptions None
 Clarifications None

RS-002 Section and Title **2.4.3 Probable Maximum Flood (PMF) on Streams and Rivers**

Section 2.4.3
 Conformance Conforms
 Exceptions None
 Clarifications None

RS-002 Section and Title **2.4.4 Potential Dam Failures**

Section 2.4.4
Conformance Conforms
Exceptions None
Clarifications None

RS-002 Section and Title **2.4.5 Probable Maximum Surge and Seiche Flooding**

Section 2.4.5
Conformance Conforms
Exceptions None
Clarifications None

RS-002 Section and Title **2.4.6 Probable Maximum Tsunami Flooding**

Section 2.4.6
Conformance Conforms
Exceptions None
Clarifications None

RS-002 Section and Title **2.4.7 Ice Effects**

Section 2.4.7
Conformance Conforms
Exceptions None
Clarifications None

RS-002 Section and Title **2.4.9 Channel Diversions**

Section 2.4.9
Conformance Conforms
Exceptions None
Clarifications None

RS-002 Section and Title **2.4.11 Low Water Considerations**

Section 2.4.11
Conformance Conforms
Exceptions None
Clarifications None

RS-002 Section and Title **2.4.12 Groundwater**

Section 2.4.12
Conformance Conforms
Exceptions None
Clarifications None

RS-002 Section and Title **2.4.13 Accidental Releases of Liquid Effluents in Ground and Surface Waters**

Section 2.4.13

Conformance Not Required

Exceptions Defer to the COL application. The types of facilities that would be used to store radioactive liquids and any associated inventory are unique to each design. Therefore, it is not feasible to complete this evaluation until a reactor design is selected.

Clarifications None

RS-002 Section and Title **2.5.4 Stability of Subsurface Materials and Foundations**

Section 2.4.4

Conformance Conforms

Exceptions None

Clarifications None

RS-002 Section and Title **2.5.5 Stability of Slopes**

Section 2.4.5

Conformance Conforms

Exceptions None

Clarifications None

RS-002 Section and Title **3.5.1.6 Aircraft Hazards**

Section 3.5.1.6

Conformance Conforms

Exceptions None

Clarifications None

RS-002 Section and Title **13.3 Emergency Planning**

Section 13.3

Conformance Conforms

Exceptions See Section 13.3.4

Clarifications See Section 13.3.4

RS-002 Section and Title **15.0 Radiological Consequences of Design Basis Accidents**

Section Chapter 15

Conformance Conforms

Exceptions None

Clarifications The PPE approach in RS-002 was used for the evaluation.

RS-002 Section and Title **17.1.1 Early Site Permit Quality Assurance Controls**

SSAR Section 17

Conformance Conforms

Exceptions See Section 17.1, Appendix B

Clarifications None

Section 1.8 References

1. NRC Draft Review Standard RS-002, Processing Applications for Early Site Permits, December 23, 2002, as supplemented.

Chapter 2 Site Characteristics

Chapter 2 describes the characteristics of the ESP site.

This section is divided into the following subsections:

- Geography and demography
- Nearby industrial, transportation, and military facilities
- Meteorology
- Hydrology
- Geology and seismology

2.1 Introduction

2.1.1 Site Location and Description

2.1.1.1 Site Location

The ESP site is located within the existing NAPS site. The location of the new units would be confined to the plant envelope area shown in Figure 2.1-1 and Figure 1.2-4. The eastern boundary of the plant envelope area is approximately 570 feet west of the center of the existing Unit 1 containment building.

The ESP site is located in the northeastern portion of Virginia in rural Louisa County. The site is on a peninsula on the southern shore of Lake Anna at the end of State Route 700. The earth dam that creates Lake Anna is about 5 miles southeast of the site. The North Anna River flows southeasterly, joining the South Anna River to form the Pamunkey River about 27 miles southeast of the site.

Louisa County includes two incorporated towns, Louisa and Mineral. According to the 2000 Census survey, the Town of Mineral, which has a population of 424 located within about 1 square mile (incorporated), is the largest community within 10 miles of the ESP site (Reference 1). Figure 2.1-2 shows the general location of the ESP site and localities surrounding the site within 10 miles.

Regionally, as indicated in Figure 2.1-3, the site is about 40 miles north-northwest of Richmond, Virginia; 36 miles east of Charlottesville, Virginia; and 22 miles southwest of Fredericksburg, Virginia. Highways U.S. Route 1 and I-95, the two principal eastern corridor highways passing through Richmond, pass within 15 and 16 miles, respectively, east of the site.

2.1.1.2 Site Description

The topography surrounding the ESP site is characteristic of the central Piedmont Plateau with a gently rolling surface varying from 200 to 500 feet above sea level.

Lake Anna was created to serve the needs of the power station. It is about 17 miles long and has 272 miles of irregular shoreline with various contour and scenic views (Reference 2, Section 2.1).

The ESP site lies along the lake shoreline. The land adjacent to Lake Anna is becoming increasingly residential as the area is developed.

Lake Anna is divided into two separate impoundments: the North Anna Reservoir and the WHTF. The North Anna Reservoir covers 9600 acres and functions as a storage impoundment for plant cooling. The smaller 3400-acre WHTF, consisting of three cooling ponds, is separated from the North Anna Reservoir by a series of dikes.

The NAPS property comprises 1803 acres, of which about 760 acres are covered by water. NAPS is laid out according to the site plan shown in Figure 2.1-1. Virginia Power and ODEC own, and Virginia Power controls, all of the land within the NAPS site boundary, including those portions of the North Anna Reservoir and WHTF that lie within the site boundary. These companies also own all land outside the NAPS site boundary that forms Lake Anna up to the expected high-water marks. The NAPS site and all supporting facilities, including the North Anna Reservoir, the WHTF, the earth dam, dikes, railroad spur, and roads constitute approximately 18,643 acres (Reference 3, Section 2.1.1.2).

If Dominion decides to proceed with the development of new units at the ESP site, it would first enter into and obtain appropriate regulatory approvals of an agreement with the NAPS owners to purchase or lease the ESP site. The agreement or conveyance documents would provide for mutual use of the NAPS site as a single exclusion area and single restricted area for all nuclear units within the NAPS property including the new units located within the ESP site.

2.1.1.3 Boundary For Establishing Effluent Release Limits

The ESP exclusion area, shown in Figure 2.1-1, is the perimeter of a 5000-ft-radius circle from the center of the abandoned Unit 3 containment. This is the same as the exclusion area for the existing units. There are no residents in this exclusion area. The new units would be located within the ESP plant envelope area west of the existing units protected area and would be well within the exclusion area.

Consistent with the licenses for the existing units, the gaseous effluent release limits for the new units would apply at or beyond the ESP exclusion area, as shown in Figure 2.1-1. The liquid effluent release limits for the new units would apply at the end of the discharge canal, which is designated as the release point to unrestricted areas.

All areas outside the exclusion area would be unrestricted areas in the context of 10 CFR 20. Additionally, the guidelines provided in 10 CFR 50, Appendix I for radiation exposures to meet the criterion "as low as is reasonable achievable" would be applied at the 5000-ft-radius exclusion area boundary (EAB).

2.1.2 Exclusion Area Authority and Control

2.1.2.1 Authority

As discussed in Section 2.1.1.2, if Dominion decides to proceed with the development of new units, it would enter into and obtain appropriate regulatory approvals to purchase or lease the ESP site from Virginia Power and ODEC. The agreement or conveyance documents would provide for the mutual use of the NAPS site as a single exclusion area. As part of this arrangement, each party would agree to immediately notify the other in the event of an emergency and to abide by the reasonable requests of the party declaring an emergency to exclude non-plant personnel and property from the exclusion area. The parties would also agree to work cooperatively to control third party activity that might otherwise present an unacceptable hazard to nuclear operations. Because the appropriate regulatory approvals of the conveyance and agreement (pursuant to Virginia Code, 56-77 and 56-580) would be a prerequisite to Dominion's development of the new units, such arrangements would be in place before issuance of a COL for the new units.

The perimeter of the existing NAPS EAB on land is adequately posted with "No Trespassing" signs. Also, floating bottom-moored buoys supporting the "No Trespassing" signs have been implanted, with suitable spacing, across the entrance to the small inlet of the North Anna Reservoir immediately north of the existing units. All markers conform to Virginia state standards. Also, a log-type boom arrangement and a small number of bottom-moored floating buoys supporting "No Trespassing" signs have been placed across the entrance to the main cooling water canal (Canal C). No additional posting would be necessary for the new units.

Along Lake Anna, outside the exclusion area, Virginia Power has granted each land owner an easement to use a portion of Virginia Power's property above the fluctuating water line for the erection of piers, jetties, or other recreational structures for access to the lake. Such structures require Virginia Power approval as to type and location and are permitted only to the extent that they would not be detrimental to the development, operation, and maintenance of the electric generating facilities, the dam, the reservoir, the dikes, and the cooling lagoons. With respect to the land bordering the cooling lagoons, Virginia Power has granted each land owner a permit to use the Virginia Power-owned land above the fluctuating water level; however, this permission is expressly revocable by Virginia Power to the extent necessary to preserve the character and maintain the operation of the WHTF (cooling lagoons) as a private water treatment facility. A limited number of landowners have been granted permissions to erect docks on the shoreline within the exclusion area. Since the ESP plant envelope (as shown in Figure 2.1-1) is located close to the existing units, Dominion intends to maintain the above practices for the new units in order to safeguard the proper use of the lake and the cooling lagoons.

2.1.2.2 Control of Activities Unrelated to Plant Operation

A portion of the smallest cooling lagoon, where recreational use is primarily for fishing, lies within the EAB. Water skiing and recreational boating are more prevalent in the other two, much larger cooling lagoons, which are entirely outside the exclusion area. Access to the cooling lagoons is restricted to property owners and their guests, as there is no means of access by boat from the North Anna Reservoir to any of the cooling lagoons.

Boaters on the North Anna Reservoir also have access to the portion of the lake within the exclusion area. Such use is largely transient as boaters from the marinas and boat ramps north and west of the NAPS site access the area between the existing units and the dam.

Should an event that necessitates implementing boating and water use restrictions on Lake Anna occur, the restrictions would be under the direction and authority of the Virginia Department of Game and Inland Fisheries (VDGIF), and the Sheriffs' Departments of Louisa, Spotsylvania, and Orange Counties. Such arrangements would be documented in the new units' emergency plan. In parallel, the appropriate portions of the emergency plan would be implemented in support of those state and local actions.

2.1.2.3 Arrangements for Traffic Control

No state or county roads, railways or waterways traverse the ESP exclusion area; therefore, no traffic control would be required. State Routes 700 and 652 provide access for NAPS staff and access by the general public to the North Anna Visitor Center. These same routes would provide similar access to the ESP site.

2.1.3 Population Distribution

The population distribution surrounding the ESP site, up to an 80-kilometer (50-mile) radius, has been estimated, based on the most recent United States Census Bureau decennial census data (Reference 4). The population distribution encompasses 9 concentric rings at 2 km (1.2 mi.), 4 km (2.5 mi.), 6 km (3.7 mi.), 8 km (5.0 mi.), 10 km (6.2 mi.), 16 km (10 mi.), 40 km (24.9 mi.), 60 km (37.3 mi.), and 80 km (50 mi.), and 16 directional sectors. The projected population estimates for Years 2010, 2020, 2030, and 2040 have been calculated with a formula adopted from the Weldon Cooper Center for Public Service (Reference 6) using the 1990 Census and 2000 Census data as the base.

2.1.3.1 Resident Population Within 10 Miles

Figure 2.1-2 shows the general locations of the municipalities and other features within 10 miles (16 kilometers) of the ESP site. According to the 2000 Census survey, Mineral, which has a population of 424 located within about 1 square mile (incorporated), is the largest community within 10 miles of the site (Reference 1). As reported in NAPS Updated Final Safety Analysis Report

(UFSAR) (Reference 3, Section 2.1.3.1), the population in 1990 was 452. Therefore, the population of Mineral has remained constant during the past decade.

The population distribution within 10 miles of the site has been computed by overlaying the 2000 Census block points data (the smallest unit of census data) (Reference 4) on the grid shown on Figure 2.1-2, and summing the population of the census block points falling in each of the polar sectors comprising the grid. The census block-point summation and allocation has been accomplished using the Landview 5 (LV5) software, operating directly on census data, and the MARPLOT mapping software (Reference 5). The system can display Census 2000 demographic data, jurisdictional entities and many statistical entities of the U.S. Census Bureau. It can also calculate Census 2000 population, racial distribution, census block count and housing unit count within a user-defined radius. Using MARPLOT, the grid system was created as shown on Figure 2.1-2. LV5 was designed to summarize the population distribution and other information, once the user selected an area of interest within the grid system. The entire grid system is evenly divided into sixteen directions, each direction consisting of 22.5 degrees.

The population distributions and related information were collected and the results tabulated in all distances of interest for all sixteen directions. The 10-mile population distribution for Year 2000 is shown on Figure 2.1-4. In order to generate more accurate counts, census block points were used in LV5 to calculate population distributions.

Population projections for the area within 10 miles of the ESP site for 10-year increments up to 40 years from the 2000 census are provided. Population projections for the year 2010, 2020, 2030 and 2040 are given in Figure 2.1-5 through Figure 2.1-8. The formula used for average annual growth (percentage of growth) is adopted from Reference 6. The Weldon Cooper Center for Public Service group has performed the 2001 provisional population estimates for the Commonwealth of Virginia.

$$\text{Annual Average Growth} = \frac{\text{Log}_{10}(\text{Population}_{2000} / \text{Population}_{1990})}{(2000 - 1990) \times 0.4342945}$$

The 1990 population distributions within each county and city considered in Virginia and Maryland were also obtained from the U.S. Census Bureau (Reference 4). The LV5 results show that the Year 2000 resident population within 6 miles (the low population zone (LPZ)) and 10 miles of the ESP site were 5890 and 15,511 persons, respectively.

2.1.3.2 Resident Population Between 10 and 50 Miles

The 50-mile (80-km) radius centered at the ESP site covers thirty counties and four cities in Virginia and one county in Maryland. The Town of Louisa is located approximately 12 miles to the west of the ESP site. The population of the town has increased from 1088 (Reference 12) to 1400 (Reference 2, Section 2.2.8.5) between 1990 and 2002. Estimates of the Year 2000 resident

population from within 10 miles to 50 miles from the ESP site were computed using the same methodology used to develop the 10-mile population distribution.

The population grid from 10 to 50 miles is shown on Figure 2.1-3 and the 50-mile population distribution for Year 2000 is shown on Figure 2.1-9.

Population projections for the area between 10 and 50 miles for the years 2010, 2020, 2030, and 2040 are based on the same methodology as the 10-mile projections. These population projections are given in Figure 2.1-10 through Figure 2.1-13, respectively.

Besides the thirty counties within Virginia, the 50-mile radius from the ESP site also encompasses Charles County, Maryland. The population distribution within that 50-mile radius for Charles County, which at its closest point is 37 miles northeast of the site, is 9270 based on the 2000 Census data.

2.1.3.3 Transient Population

2.1.3.3.1 Transient Population Within 10 miles

Information concerning transient population for the area has been collected from several sources, because this information is not available from the 2000 Census data. The area within 10 miles of the ESP site is predominantly rural and characterized by farmland and wooded tracts of land. Since there are no significant industrial or commercial facilities in the area, and none are anticipated (Reference 3, Section 2.1.3.3), the transient employment population is likely to move out of, rather than into, the area.

Recreational use of Lake Anna, including Lake Anna State Park, is the greatest contributor to transient population in the area. The usage of the lake has been estimated from a number of contributing factors including the number of boat ramps, wet slips, campsites, picnic areas, etc. These contributing factors are listed in Table 2.1-1.

An estimate of lake usage on a peak weekend day in the peak summer season has been developed based on representative use of recreational facilities (e.g., boating, picnicking, camping) provided by the Virginia Department of Conservation and Recreation (Reference 3, Section 2.1.3.3) and the Lake Anna facilities listed in Table 2.1-1. This estimate does not include lake use by local residents with their own docks. However, residents should be included in the census data. In addition, many residents without docks keep their boats in marina wet slips or use the boat ramps and are, therefore, included in the lake usage.

There are six marinas in the vicinity of the ESP site. The closest one is 1.4 miles north-northeast of the site. The remaining marinas are from 2 to 2.5 miles distant. A survey of several of the marina owners indicates that their actual boat launches per ramp range from 15 to 40 per ramp per peak day, which is significantly lower than the number of 80 per day provided by the Virginia Department of Conservation and Recreation as an upper limit for ramp usage. The usage per ramp has dropped as new ramps are added. This has been attributed to parking space limitations and the fact that the

lake usage by recreational boaters may be approaching saturation. A rate of 50 launches per ramp per day has been selected as being representative of Lake Anna conditions.

Based on 50 launches per ramp per day, these marinas and other boat ramps, including those at Lake Anna State Park, could provide access for up to 1450 pleasure crafts on the North Anna Reservoir. Peak day usage estimates of boats moored in wet slips have ranged from 30 to 50 percent. Assuming that all slips are rented, 150 additional boats would be added, bringing the total (excluding boats from private docks) to 1600. The resulting transient population at three persons per boat would be 4800 (Reference 3, Section 2.1.3.3).

The two commercial campgrounds, with a combined total of more than 200 campsites, are estimated by the Virginia Department of Conservation and Recreation to contribute about 650 persons to the transient population, assuming three persons per campsite. The number of picnickers has been estimated at 450. Since both campsites have boat ramps, significant double counting is likely (Reference 3, Section 2.1.3.3).

Lake Anna State Park, which provides facilities for picnicking, fishing, boat launching, swimming, and biking, has increased in popularity each year. The Park Manager has estimated a peak daily attendance at 4372 from June through August 2002, and an annual attendance of 187,302 between July 1, 2001 and June 30, 2002 based on traffic counters. Double counting is likely, as boaters are included in the traffic count.

The resulting estimated total peak daily transient population on Lake Anna (including the WHTF and Lake Anna State Park) is less than 11,270 (Table 2.1-2). Given these assumptions and the potential for double counting, this number is conservative.

Since use of the WHTF is limited to residents and their quests, there are no public boat ramps. The transient population, estimated at less than 1000, is based on one guest for each resident in the polar sectors encompassing the WHTF.

Annual transient population is uncertain because of the dramatic drop in boating on weekdays and non-summer months. Based on Lake Anna State Park data, assuming 180 days of operation, the average daily attendance is less than one quarter of the peak daily attendance. Conservatively assuming that the average attendance, excluding the park, is one half the peak daily figure, the total annual attendance would be about 807,300, based on a 180-day season.

Transient population within 10 miles of the ESP site when combined with the resident population in that same area for year 2000 and for projected years 2010, 2020, 2030, and 2040 are presented in Figure 2.1-4 through Figure 2.1-8.

2.1.3.3.2 Transient Population Between 10 and 50 Miles

It is difficult to provide an accurate count of the transient population between 10-mile and 50-mile concentric circles from the ESP site. There are colleges, schools and hospitals within the 50-mile

radius of the site. However, compared to the resident population within the same 50-mile radius area, transient population use of these facilities is expected to be insignificant.

Between 10 and 50 miles of the ESP site, Paramount's Kings Dominion Amusement Park is a major recreational facility that induces a significant amount of transient population. Paramount's Kings Dominion is located 35 miles southeast of the ESP site. The park opens from March to November and hosts about 2 to 2.5 million visitors annually. According to the park's public relations manager, the park could experience slow growth in the future until it reaches its current maximum capacity of 2.875 million visitors per year (i.e., an additional 15 percent above the current attendance). On average, the park opens to the public about 138 days per year (Reference 7). Using the maximum capacity of the park and the average number of days open, the average daily park visitor count is estimated to be 20,830.

There is no official count of visitors that come from areas outside the 50-mile radius from the ESP site. However, the majority of the park visitors are expected to come from the Richmond and Fredericksburg areas due to their proximity to the park. It is conservatively assumed that 40 percent of the daily park visitors come from areas outside the 50-mile radius. The 8350 park visitors from further than 50 miles are considered transient population and that number is included in the population distribution estimates.

Transient population between 10 and 50 miles of the ESP site when combined with the resident population in that area for year 2000 and for projected years 2010, 2020, 2030, and 2040 are presented in Figure 2.1-9 through Figure 2.1-13.

2.1.3.4 Low Population Zone

The LPZ for the ESP site is the same as the LPZ for the existing units. As shown in Figure 2.1-2, a 6-mile-radius circle centered at the Unit 1 containment building defines the LPZ. design basis accidents (DBAs) are evaluated in Chapter 15 to demonstrate that doses at the LPZ are within the dose limits of 10 CFR 100.11(a)(2). Exposure of individuals to radiation in the LPZ would be within the limits established in 10 CFR 20.

The resident population distribution within the LPZ is indicated in Figure 2.1-4 through Figure 2.1-8, based on the 2000 Census and projections every 10 years through Year 2040. These figures use an increment of 2 km for distances within a 10-km radius of the ESP site. The 6-mile radius LPZ falls within the 8-10 km (5-6.2 mi.) range. For reporting purposes, the LPZ population is represented by the population enclosed within the 10-km distance circle.

In summary, the LPZ population for 2000 and the projected population through 2040 are as follows:

Year	Population
2000	5890
2010	7910
2020	9940
2030	11,960
2040	13,980

The only school in the LPZ is Livingston Elementary, which is located in Spotsylvania County, 5.7 miles to the north-northeast of the ESP site. Schools within 10 miles of the ESP site are listed in Table 2.1-3 (Reference 8) (Reference 9).

As demonstrated in the previous section, the only significant source of transient population within 10 miles is recreational use of Lake Anna. Since most of the lake area falls within the LPZ, almost the entire estimated peak transient population within 10 miles could be in the LPZ.

Considering the available road network leading from the LPZ, together with the availability of private as well as public vehicles, there is reasonable assurance that these populations could be evacuated in a timely manner in the event of a design-basis accident.

2.1.3.5 Population Center

The nearest population center to the ESP site with more than 25,000 residents is the City of Charlottesville, with a population of 45,049 (Reference 4). The closest point of Charlottesville to the site is 36 miles west. The next closest population center is Fredericksburg, which is 22 miles northeast of the ESP site. Fredericksburg has a projected Year 2040 population of about 20,300. The distance to Fredericksburg is well in excess of the minimum population center distance required by 10 CFR 100.

2.1.3.6 Population Density

Given an approved ESP period of 20 years and an assumed ESP approval date of 2005, the startup date of new units is conservatively assumed to be 2025. Assuming an operational period of 40 years for new units, new unit operations could extend until 2065.

Figure 2.1-14 shows the actual cumulative populations in Year 2000 and projected cumulative population in Year 2040 as a function of 10-mile to 50-mile radial distances from the site. On the same figure, population density curves, spanning the same radial distances, are shown for 500 persons per square mile, and 1000 persons per square mile.

By inspection of the curves for actual population densities of Year 2000 and Year 2040 projections, it is concluded that at the time of initial site approval and within about 5 years thereafter, the

population densities, including weighted transient population, averaged over any radial distance out to 20 miles (cumulative population at a distance divided by the circular area at that distance), would not exceed 500 persons per square mile. The results conform to the guidance in RG 4.7, Regulatory Position C.4 (Reference 10).

Similarly, by inspection and projection of the same curves to account for trends over the lifetime of new units, it is concluded that the expected population densities, including weighted transient population, averaged over any radial distance out to 30 miles (cumulative population at a distance divided by the area at that distance), would not exceed: 1) 500 persons per square mile at the time of initial operation, and 2) 1000 persons per square mile over the lifetime of new units (Reference 11, Section 2.1-3).

Section 2.1 References

1. Town of Mineral, Website, www.louisa.net/mineral/, accessed October 14, 2002.
2. NUREG-1437, Generic Environmental Impact Statement for License Renewal of Nuclear Plants, Supplement 7, Regarding North Anna Power Station, Units 1 and 2, U.S. Nuclear Regulatory Commission, November 2002.
3. North Anna Updated Final Safety Analysis Report, Rev. 38, Dominion Virginia Power.
4. U.S. Department of Commerce, Bureau of the Census, 2000 Census of Population, Website, www.census.gov/main/www/cen2000.html, accessed October 1, 2002.
5. LandView 5, U.S. Census Bureau, U.S. Environmental Protection Agency, U.S. Geological Survey, National Oceanic and Atmospheric Administration, June 2002.
6. Weldon Cooper Center for Public Service, Website www.ccps.virginia.edu/demographics/estimates/city-co/2001estimates.pdf, accessed September 22, 2003.
7. Paramount's Kings Dominion, Website, www.kingsdominion.com/visit_calendar.jsp, accessed August 15, 2003.
8. Louisa County High School, Website, www.greatschools.net/modperl/browse_school/va/1016, accessed October 11, 2002.
9. Louisa County Middle School, Website, www.greatschools.net/modperl/browse_school/va/1018, accessed October 11, 2002.
10. Regulatory Guide 4.7, Rev. 2, General Site Suitability Criteria for Nuclear Power Plants, U.S. Nuclear Regulatory Commission, April 1998.

11. NRC Review Standard RS-002, Processing Applications of Early Site Permits: Draft for Interim Use and Public Comment, U.S. Nuclear Regulatory Commission, Office of Nuclear Reactor Regulation, December 23, 2003, as supplemented.
12. Town of Louisa, Virginia, louisatown.org/, accessed October 14, 2002.

Table 2.1-1 Lake Anna Recreational Facilities

Facility	Distance	Number of Wet Slips	Number of Ramps	Camp Sites
Marinas				
Anna Point	2.3 miles NNW	25	1	—
Dukes Creek	2.2 miles E	55	5	—
High Point	2.3 miles NNW	50	4	—
Lake Anna	1.4 miles NNE	160	2	—
Rocky Branch	2.3 miles NNE	None	4	—
Sturgeon Creek	2 miles N	36	5	—
Public Landings				
Christopher Run Campground	6 miles WNW	—	1	152
Hunters Landing	6.6 miles NW	—	1	—
Lake Anna Campground	2.5 miles NW	—	1	61
Lake Anna Landing	9 miles NW	—	1	—
Lake Anna State Park	4.3 miles NNW	—	2	—
Pleasants Landing	5.6 miles SE	—	1	—
Sullivan's Landing	8 miles NW	—	1	—
Total		326	29	213

Source: Reference 3, Table 2.1-1

Note: "—" means no data was reported in source

Table 2.1-2 Tourist Attractions, Parks and Recreational Areas

Facility	Location	Annual Usage	Peak Daily Usage *	Comments
Lake Anna Recreational Usage	1.4 mi, NNE	530,000	5900 **	Annual usage based on 180 days at 2950 people per day.
Waste Heat Treatment Facility	—	90,000	<1000	Peak daily usage based on doubling the resident population in cooling lagoon sectors (one guest per resident). Annual usage based on 180 days at 500 people per day.
Lake Anna State Park	2.8 mi, NNW	187,300	4370	Annual use was 187,300 between July 1, 2001 and June 2002. Park closed in winter. Use includes occupants of boats launched at the park.
Paramount's Kings Dominion Amusement Park	35 mi, SE	2,875,000	20,830	Annual use was 2 to 2.5 million between March and November. Add 15% to calculate maximum capacity. Park closed in winter.

* Peak daily usage is based on a peak weekend day during the summer.

** This number is based on an average of 3 persons per boat, campsite and picnic area.

Table 2.1-3 Schools Within 10 Miles of ESP Site

School	Number of Students (2002)	Distance (miles)	Direction from Plant
Louisa County			
Louisa County High School	1232 ^a	7	WSW
Louisa County Middle School	1.035 ^b	7	WSW
Spotsylvania County			
Livingston Elementary	477	6	NE

a. Source: Reference 8

b. Source: Reference 9

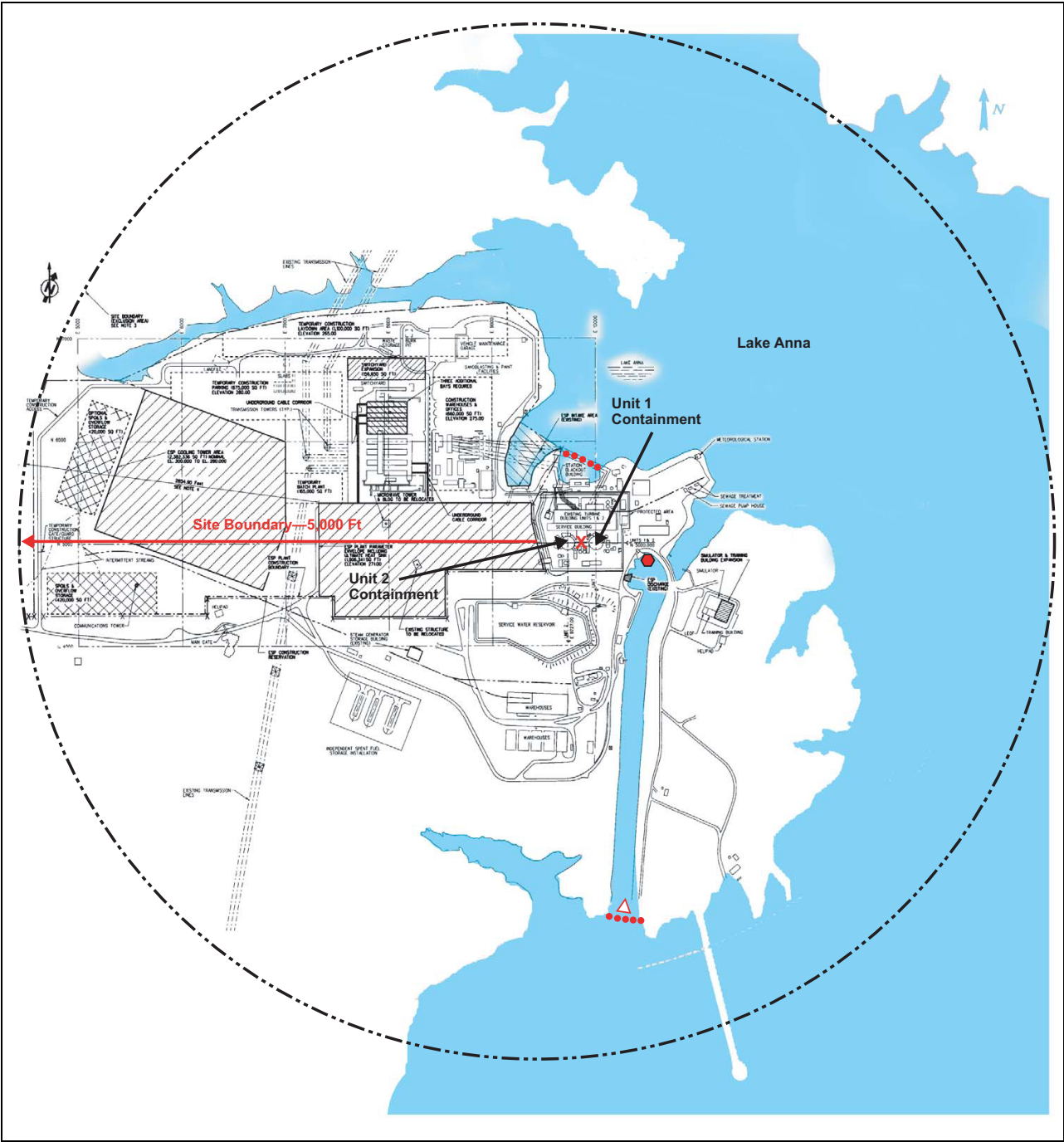


Figure 2.1-1 Site Boundary

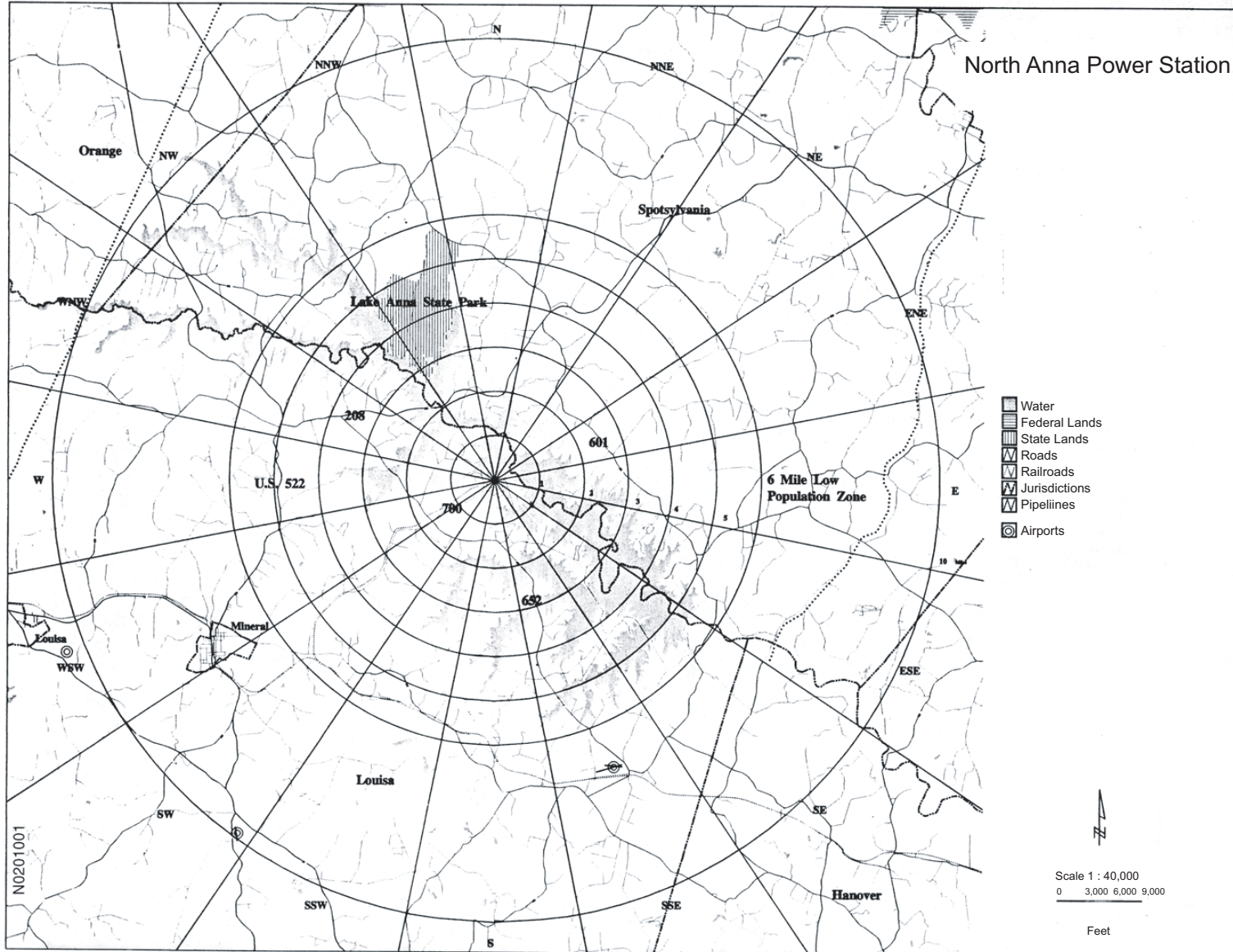


Figure 2.1-2 Ten-Mile Surrounding Area

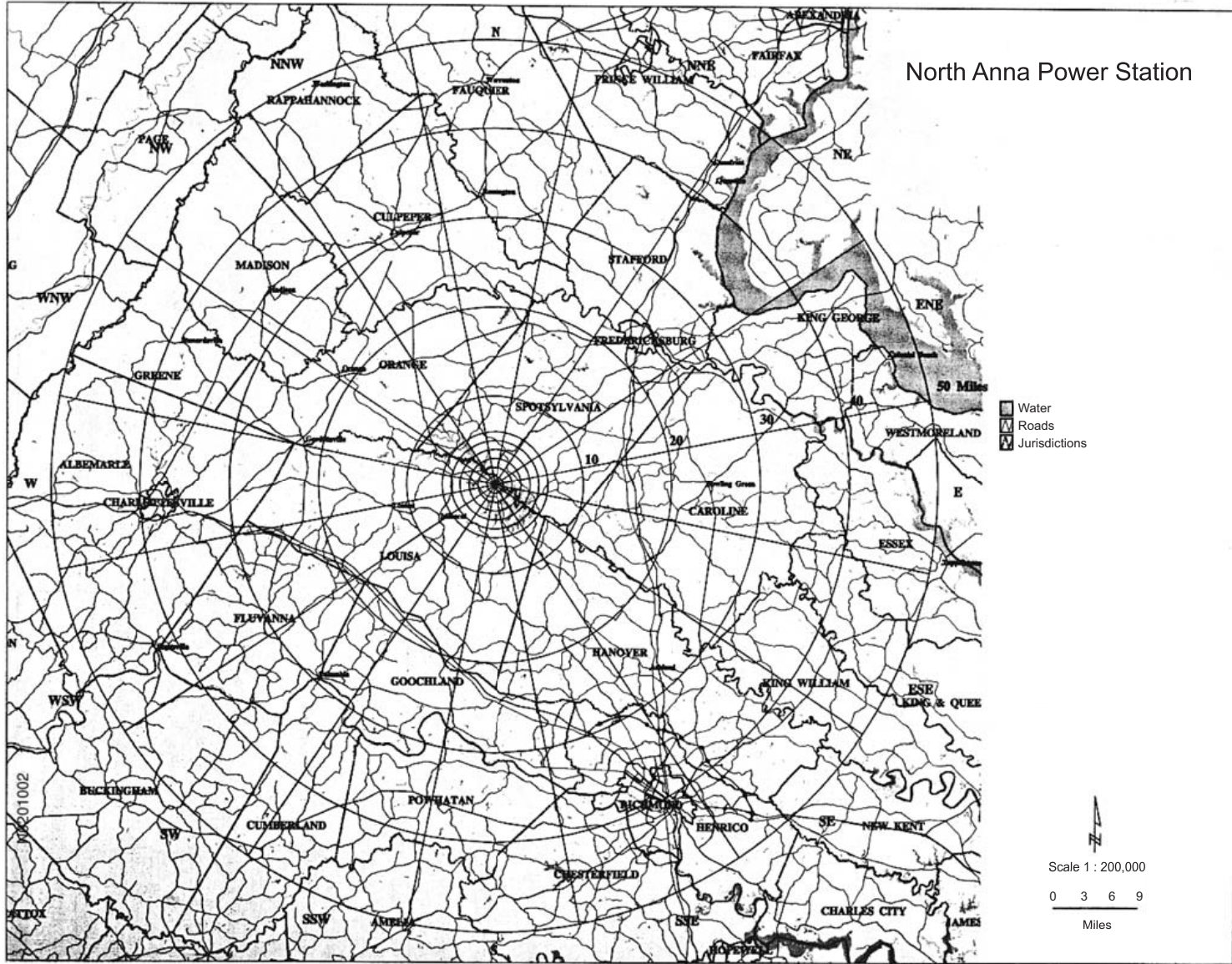


Figure 2.1-3 Fifty-Mile Surrounding Area

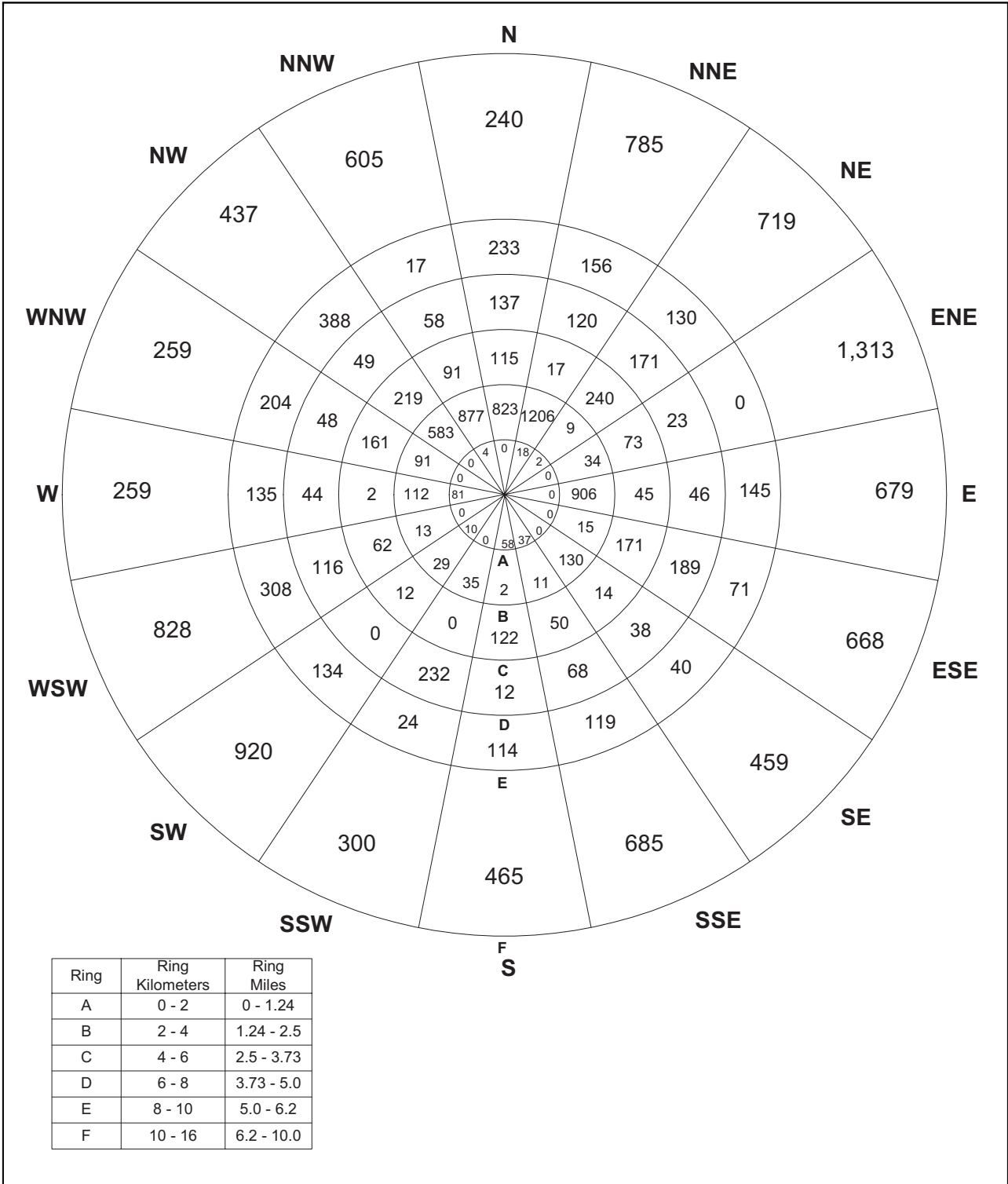


Figure 2.1-4 16-Kilometer (10-Mile) Resident and Transient Population Distribution—2000

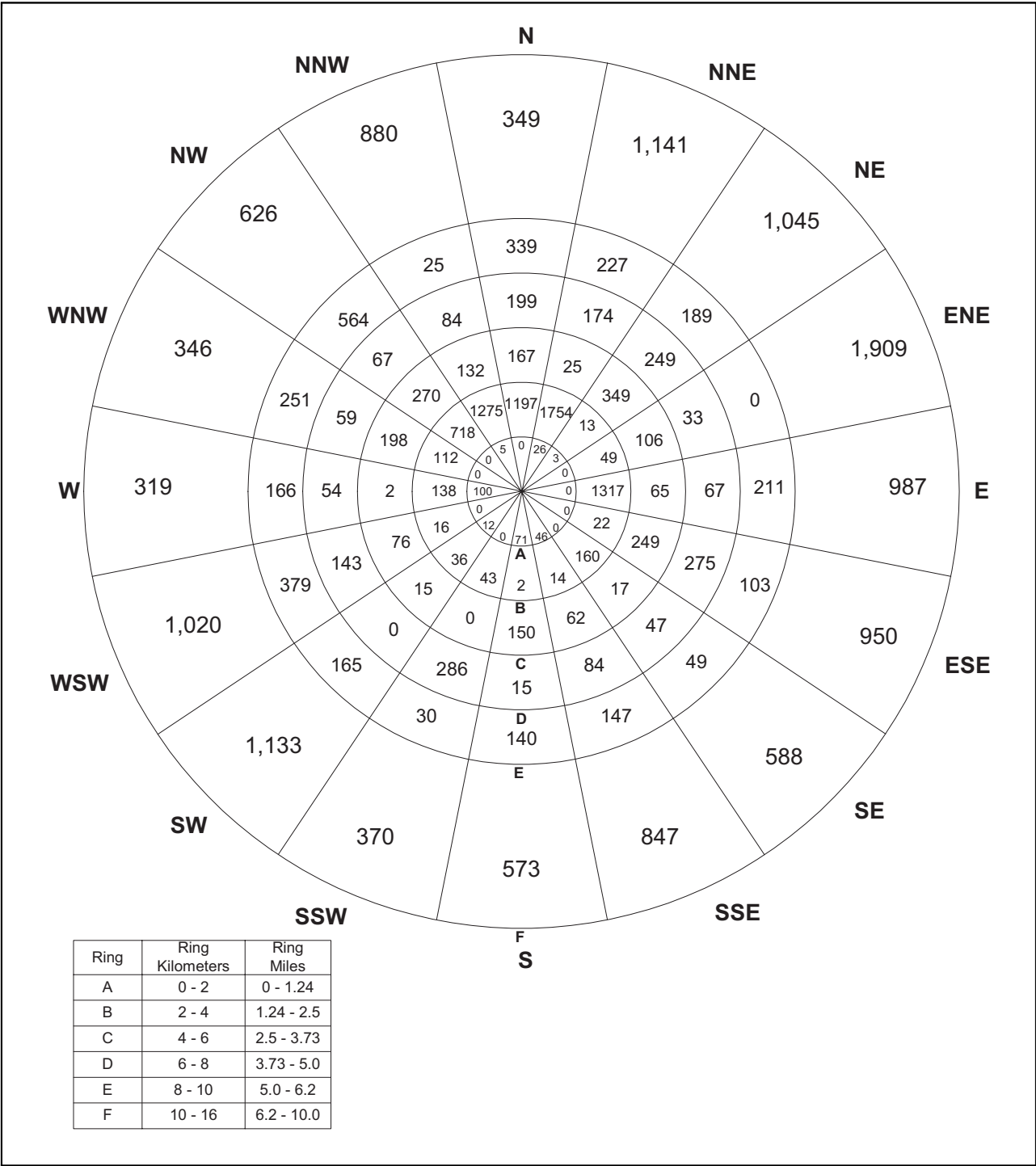


Figure 2.1-5 16-Kilometer (10-Mile) Resident and Transient Population Distribution—2010

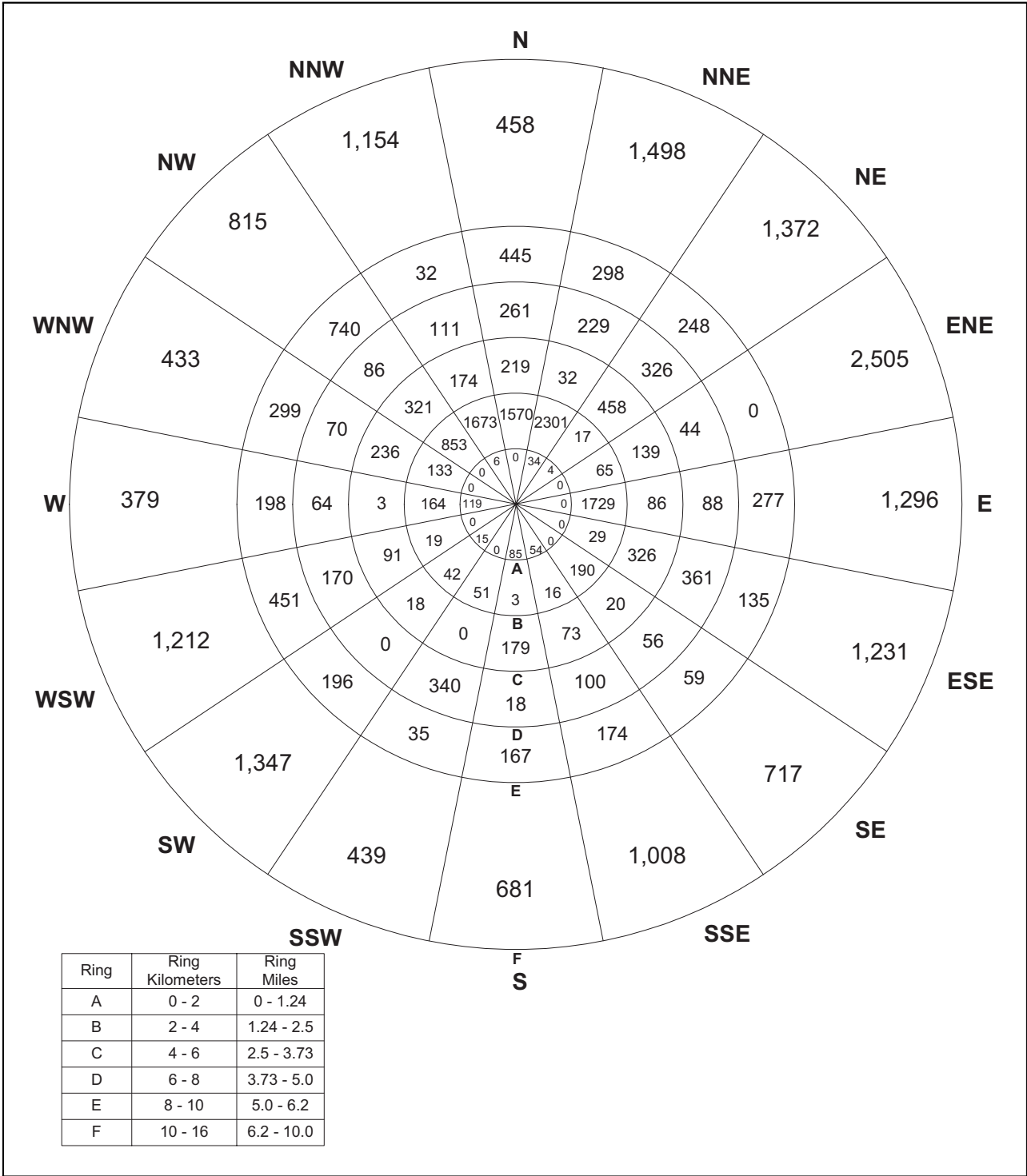


Figure 2.1-6 16-Kilometer (10-Mile) Resident and Transient Population Distribution—2020

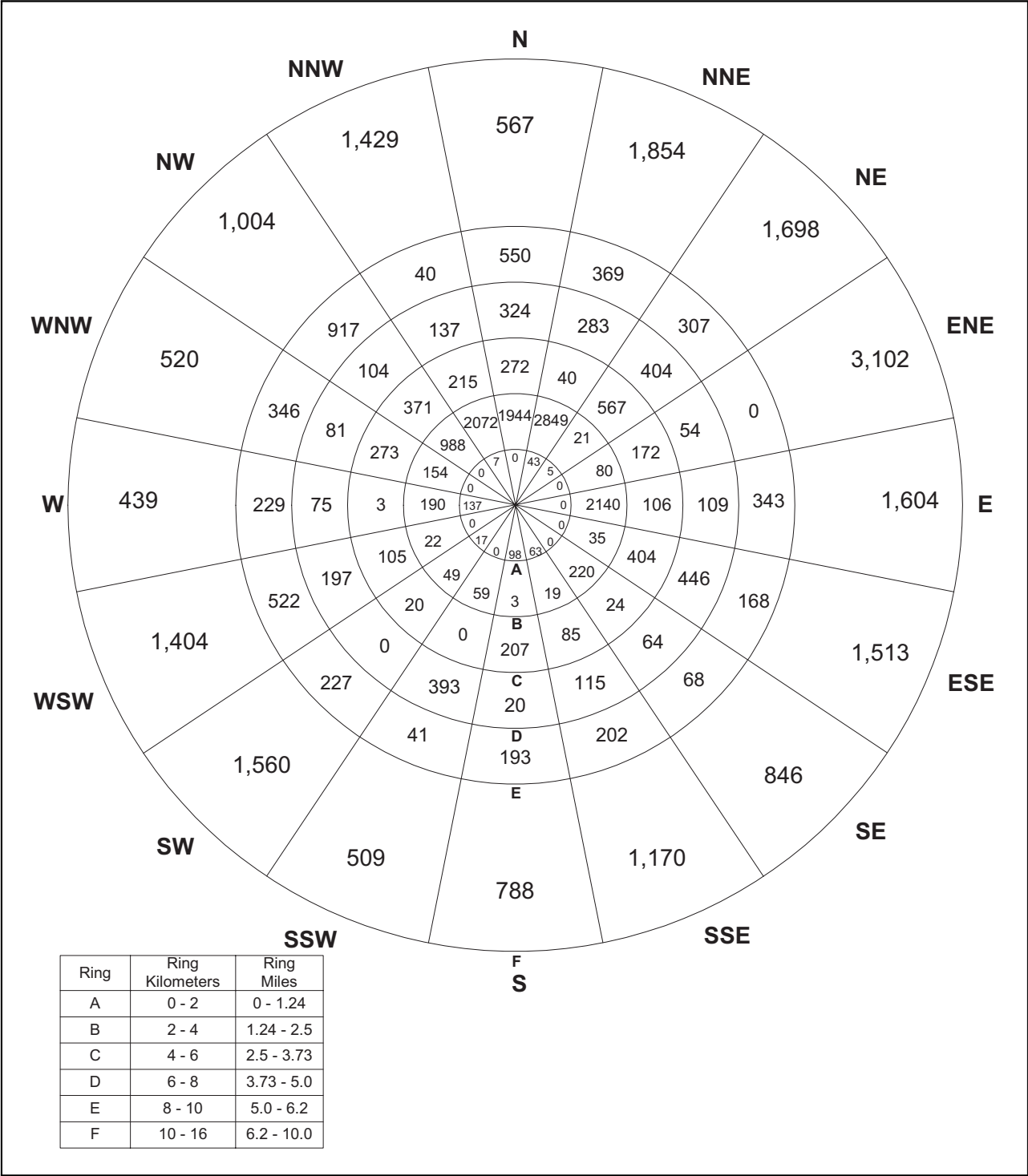


Figure 2.1-7 16-Kilometer (10-Mile) Resident and Transient Population Distribution—2030

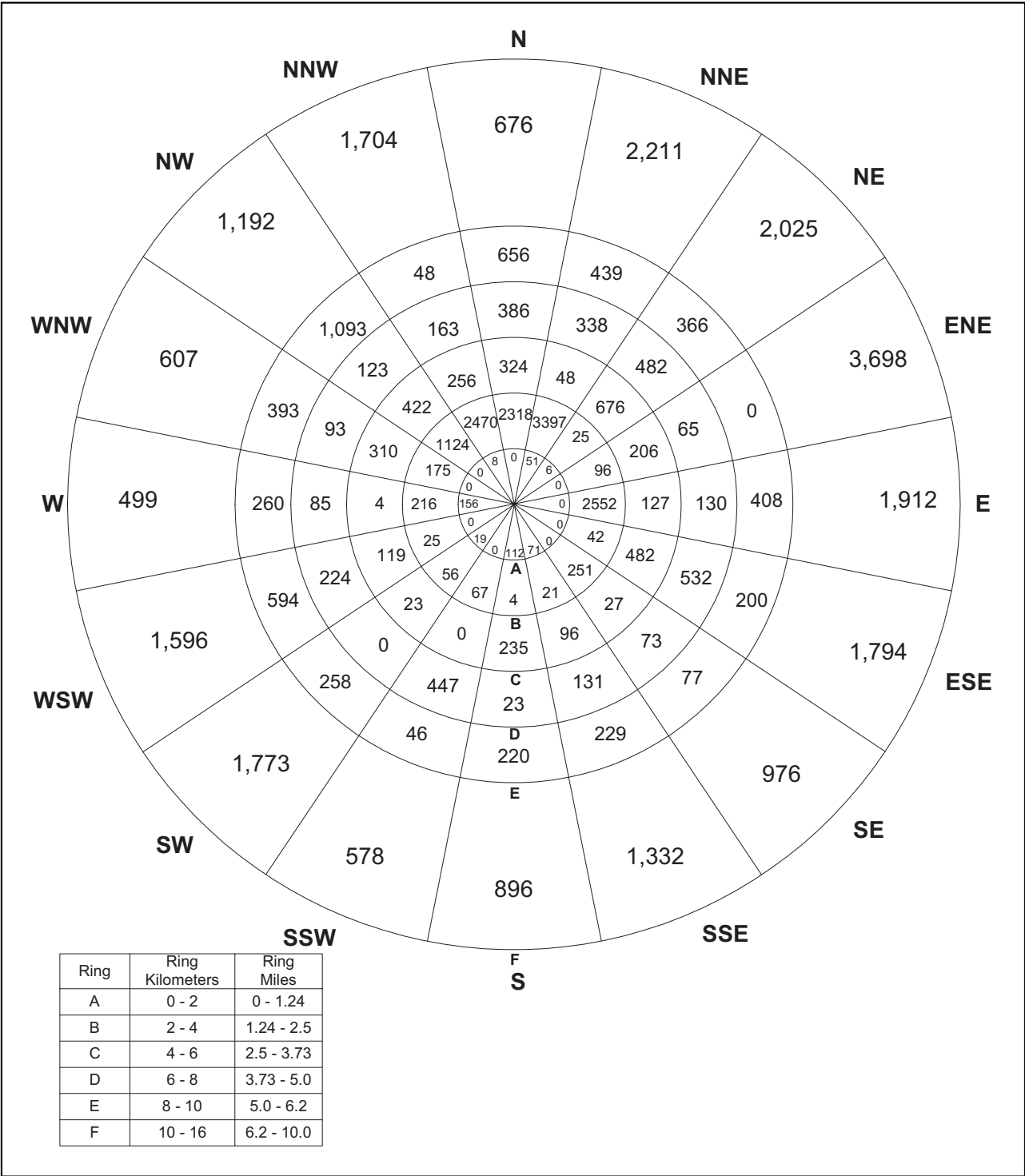


Figure 2.1-8 16-Kilometer (10-Mile) Resident and Transient Population Distribution—2040

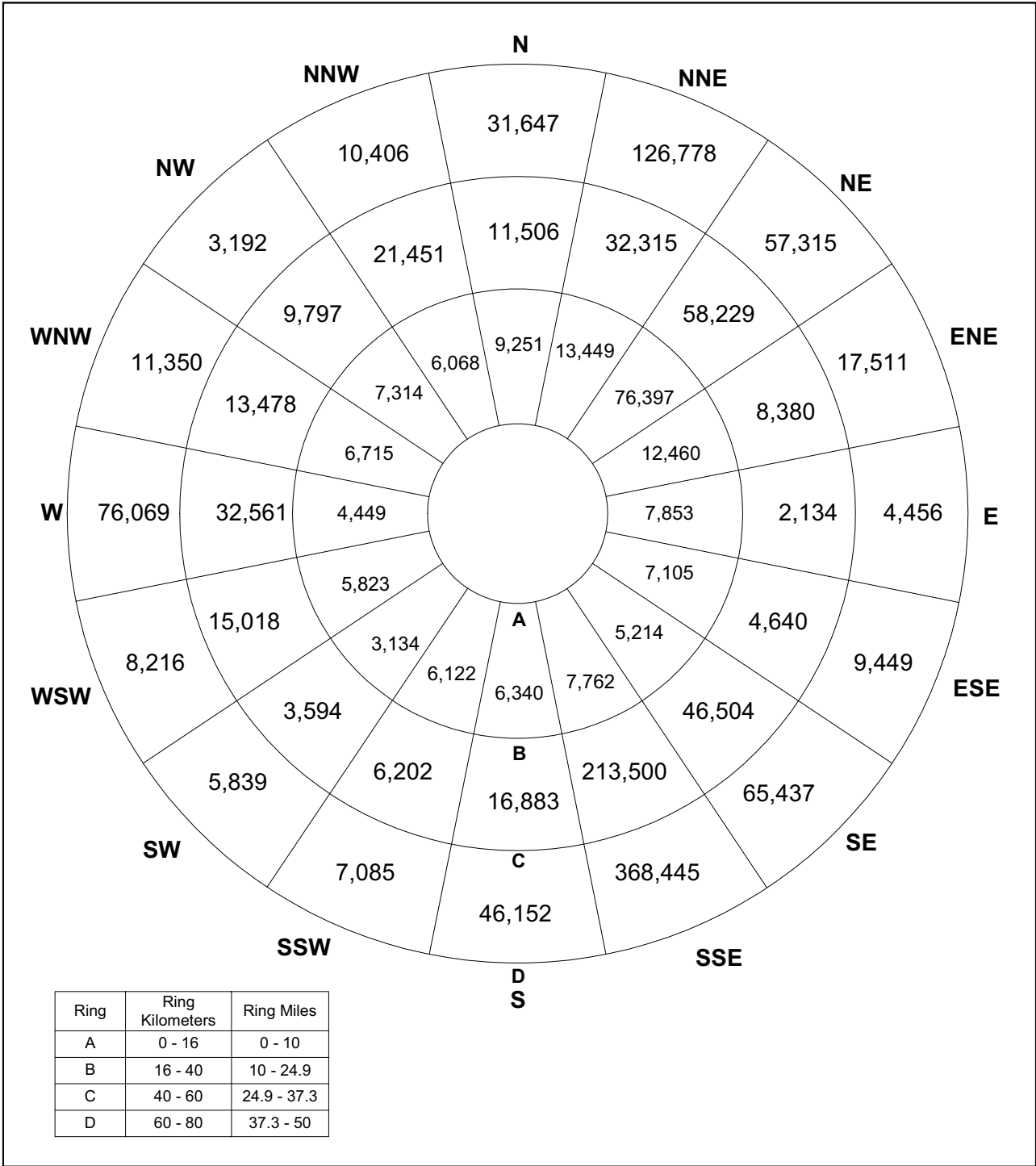


Figure 2.1-9 80-Kilometer (50-Mile) Resident and Transient Population Distribution—2000

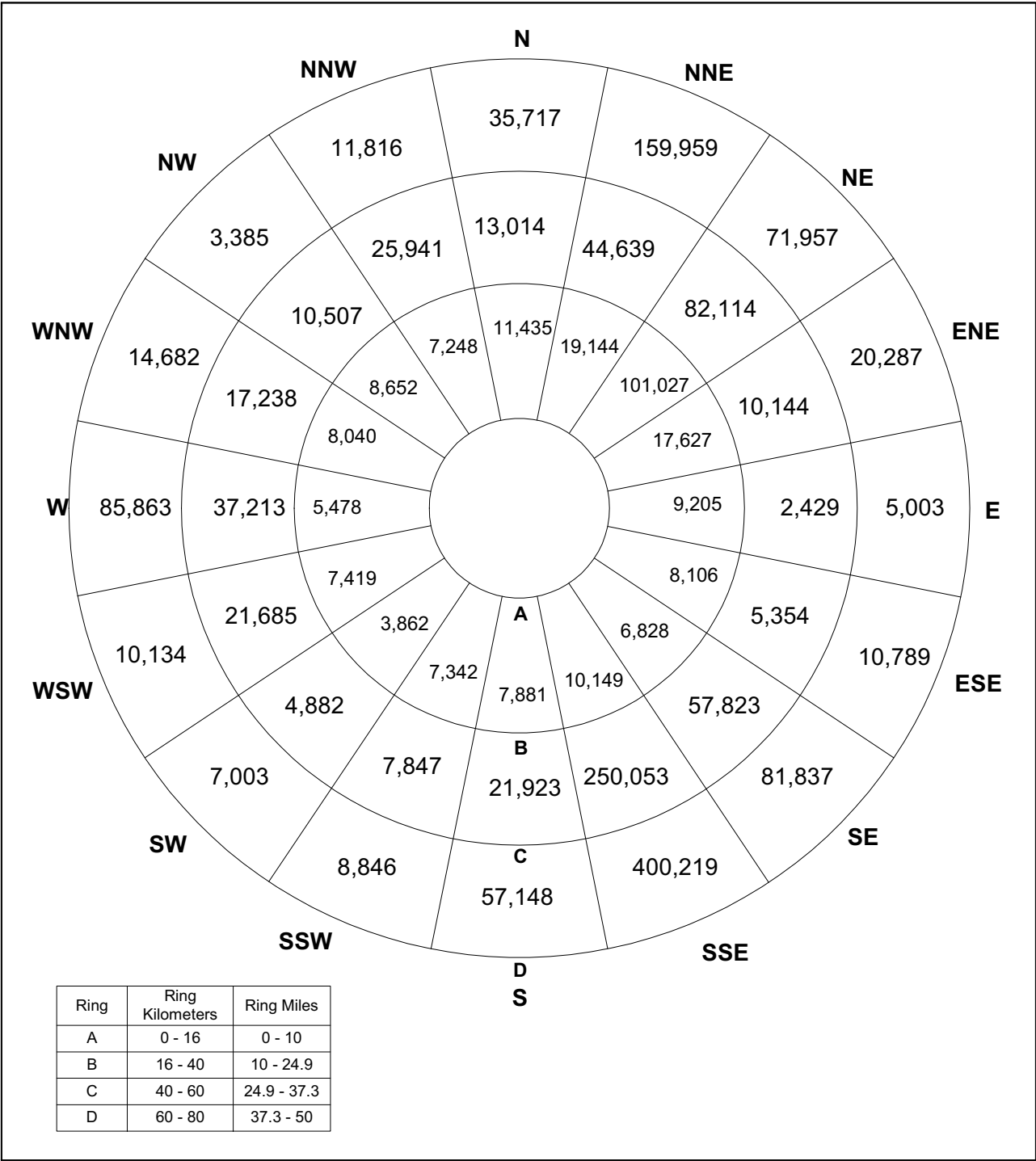


Figure 2.1-10 80-Kilometer (50-Mile) Resident and Transient Population Distribution—2010

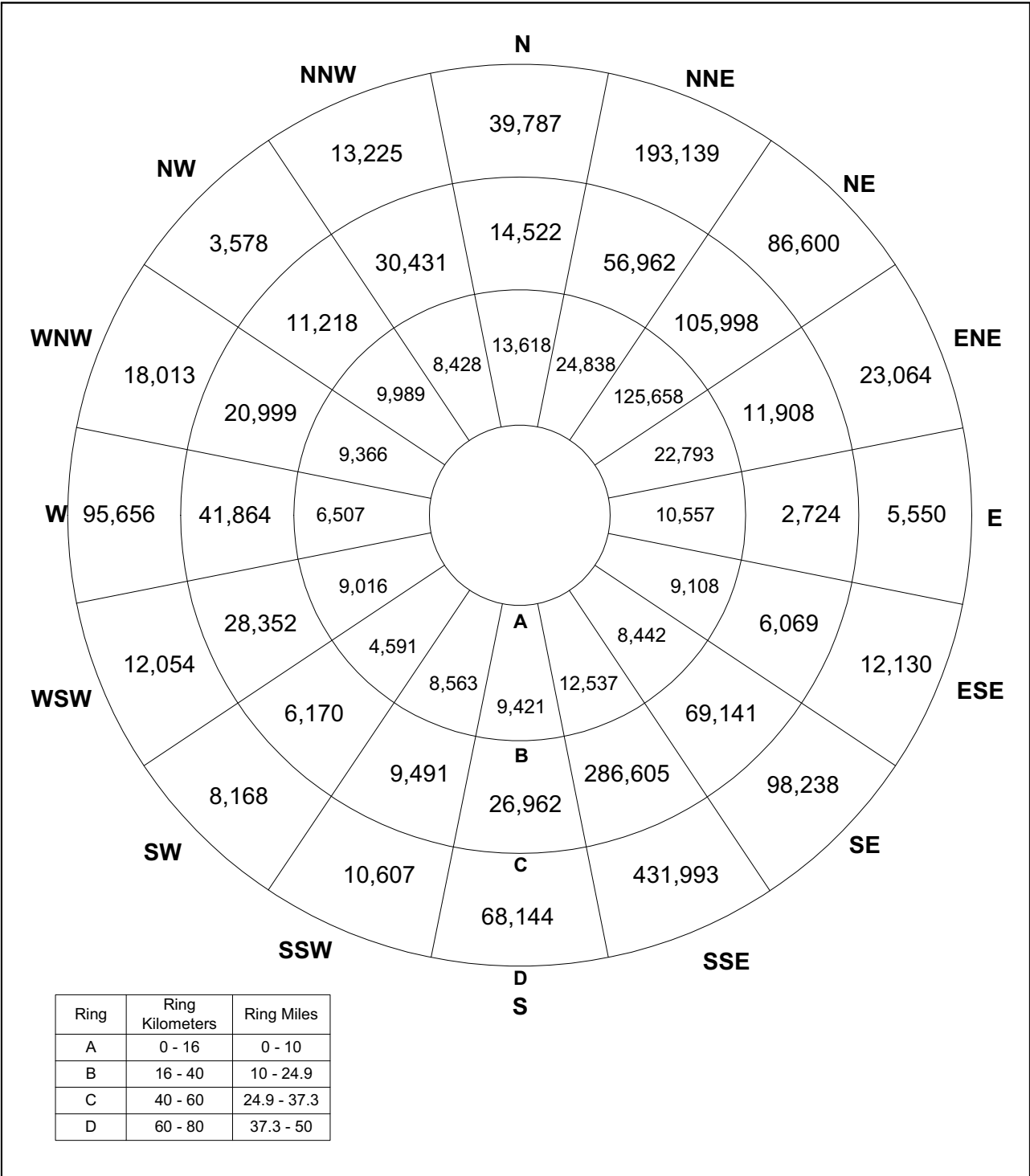


Figure 2.1-11 80-Kilometer (50-Mile) Resident and Transient Population Distribution—2020

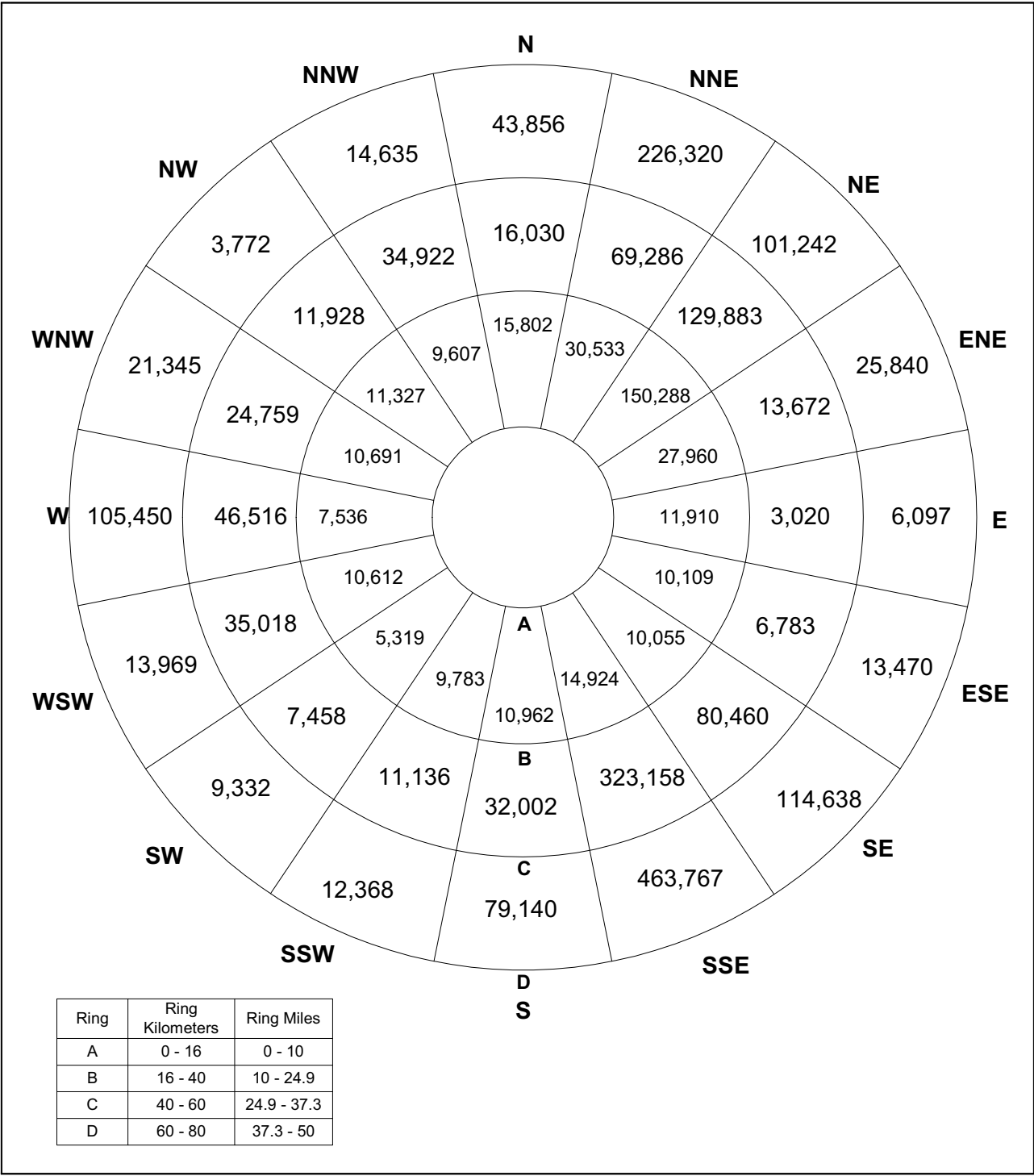


Figure 2.1-12 80-Kilometer (50-Mile) Resident and Transient Population Distribution—2030

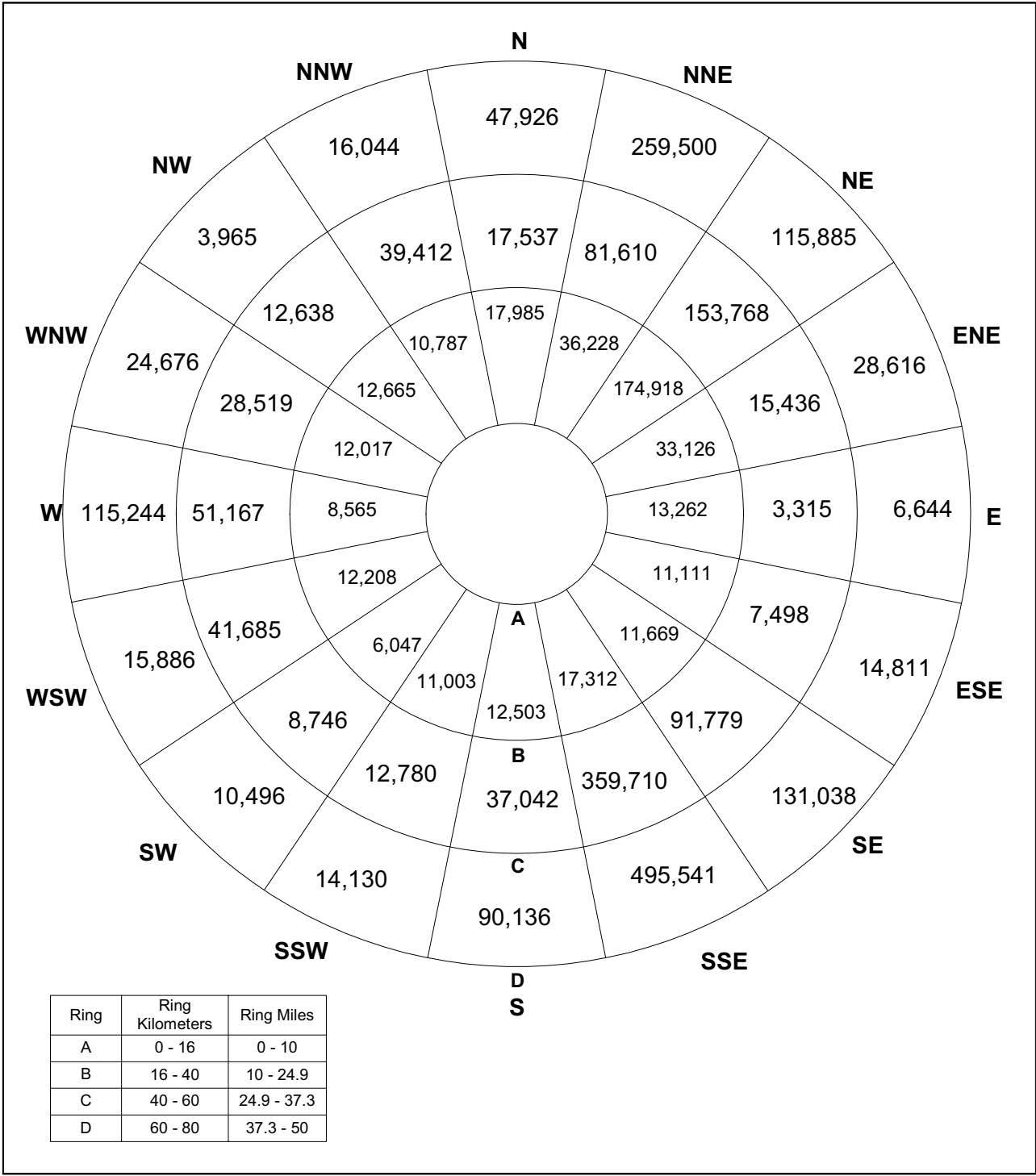


Figure 2.1-13 80-Kilometer (50-Mile) Resident and Transient Population Distribution—2040

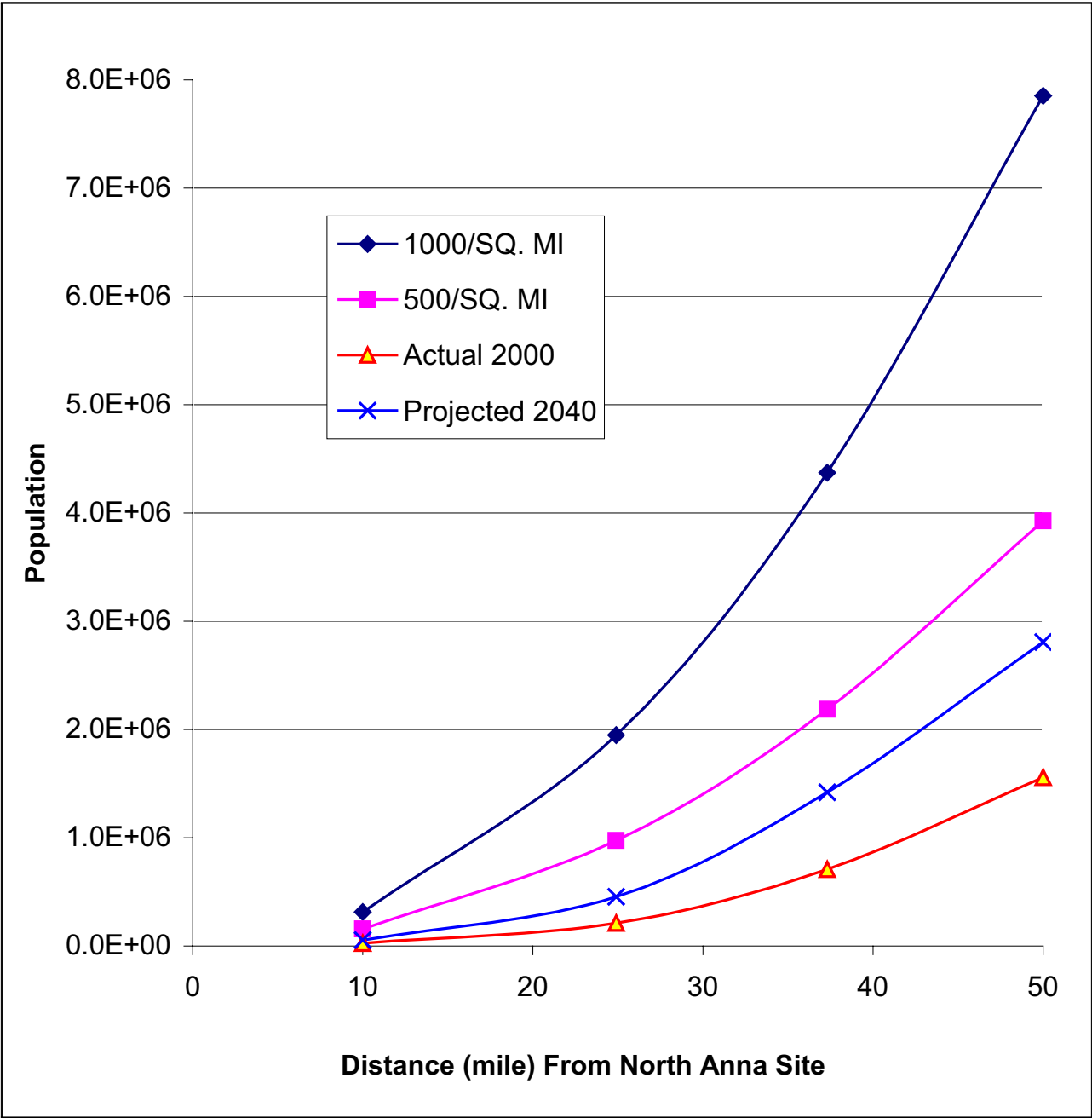


Figure 2.1-14 Population Density

2.2 Nearby Industrial, Transportation, and Military Facilities

2.2.1 Location and Routes

Based on the NAPS UFSAR, Section 2.2.1(Reference 1)), no military bases, missile sites, manufacturing plants, chemical plants, chemical or other storage facilities, airports, major railroad lines, major water transportation, or oil and gas pipelines are located within 5 miles of the ESP site.

Major highways, such as Interstates 95 and 64, are located more than 16 miles away from the site. Nearby U.S. Route 522, is located about 5 miles west of the site. The closest point of Virginia Route 652 is 1.5 miles to the south of the site. The only road that provides access to the site is State Route 700, coming from the southwest to within about half a mile of the site. No public or commercial highways, railroads, or waterways traverse the site.

2.2.2 Descriptions

2.2.2.1 Industrial Facilities

Louisa County is a rural and residential area. There are no substantial industrial activities within 5 miles of the ESP site. Any major industrial expansion in the area is subject to the approval from the local county planning commission. The Louisa County Board of Supervisors has approved a zoning ordinance allowing industrial development of approximately 620 acres near the site EAB. Within 10 miles of the site, there are several other areas zoned for industrial development, the largest one being 150 acres near Pendleton, Virginia. However, there are no plans for development in this area (Reference 1, Section 2.2.1.1).

Population projections provided in Section 2.1 indicate that among all the neighboring counties, Spotsylvania County is one of the largest and fastest growing counties in Virginia. The development in the county is concentrated in the City of Fredericksburg, 22 miles northeast of the ESP site, and along the I-95 corridor, which is about 16 miles away from the proposed site (Reference 2). In addition, nearly half of the county residents commute to the DC area or to Richmond. Therefore, future major industrial developments are more likely to be concentrated along the I-95 corridor rather than within 5 miles of the site.

2.2.2.2 Mining Activities

There are no mining activities within 5 miles of the ESP site.

2.2.2.3 Roads

The roads within 10 miles of the ESP site are shown in Figure 2.1-1. Virginia State Route 700 provides access to the site and State Routes 601 and 652, which run parallel to the Lake Anna shoreline, pass about 2.2 miles northeast and 1.5 miles south of the site, respectively. Primary State Route 208 crosses Lake Anna at a point about 2 miles northwest of the site and joins U.S. Route 522 about 5 miles west of the site.

2.2.2.4 Railroads

The closest railroad line to the ESP site is the main line of the Chesapeake and Ohio Railway, which runs from Newport News to Chicago. It passes through the towns of Louisa, Mineral, Fredericks Hall, and Bumpass; its closest approach to the site is about 5.5 miles southwest. A spur line connects the ESP site with this line.

2.2.2.5 Marine Transportation

There are six marinas in the vicinity of the ESP site (Reference 1, Table 2.1-1). These marinas, including wet slips and other boat ramps, provide access for up to 1600 pleasure craft on Lake Anna on a peak day. The closest marina is 1.4 miles north-northeast of the site. The remaining marinas are from 2 to 2.3 miles distant. The nearest marina stores gasoline in amounts up to about 4000 gallons. There are no large boats or barges on Lake Anna.

2.2.2.6 Airports and Airways

2.2.2.6.1 Airports

Airports within 15 miles of the ESP site as of 2002 are listed in Table 2.2-1; their locations are presented in Figure 2.2-1. None of the airports are expected to grow substantially in the foreseeable future (Reference 1, Section 2.2.1.6.1). Only two of the airports are within 10 miles of the site: Lake Anna Airport and Cub Field.

The Louisa County Airport (Freeman Field), located 11 miles west-southwest of the site, began operation in 1987 after NAPS was licensed. The airport has a 4300-foot east-west-oriented asphalt runway, and a shorter 2000-foot turf runway. Operations involve single-engine light aircraft, primarily. Thirty-two aircraft are based at this airport: 25 single-engine airplanes, 6 multi-engine airplanes, and one jet. It is a modern well-maintained facility with 120 aircraft operations per week. (Reference 3)

The Lake Anna Airport, near Bumpass, is 7 miles south-southeast of the site. The airport has limited facilities. A flight instructor at the Louisa County Airport stated that traffic at the Lake Anna Airport was very light and consisted primarily of practice landings (Reference 1, Section 2.2.1.6.1). Landing facilities consist of a 2560-foot asphalt runway. Only two single-engine airplanes are based at this airport, and on average there are about 70 landings per week (Reference 4).

Cub Field, a private landing strip with an unlighted 1400-foot turf runway, is 10 miles southwest of the site. It is not licensed and the reported volume of traffic is very light. No aircraft are based at this field. (Reference 1, Section 2.2.1.6.1)

Data on these airports are provided in Table 2.2-1.

2.2.2.6.2 Airways

One civil airway – V223 – and three military training routes – IR714, IR760, and VR1754 – pass near the ESP site as shown in Figure 2.2-1, which is extracted from the Washington Sectional Aeronautical Chart issued in 2003 (Reference 5). The centerline of V223 is 5.5 miles west of the ESP site, and the corridor width is 4 miles on either side of the centerline. No data are kept on traffic in this airway. The Federal Aviation Administration (FAA) stationed at Richmond International Airport has characterized the airway as “not heavily used” and estimates traffic at no more than 200 aircraft per day. (Reference 1, Section 2.2.1.6.2)

The centerlines of the military training routes, which are 10 miles across, lie within 1 mile south of the ESP site. The Oceana Naval Air Station in Virginia Beach, Virginia, which provided data on their use, controls these routes. Pilots are directed to avoid the NAPS site by flying at the edge of the air corridor. An officer at Oceana has stated that the aircraft pass no closer than 3 to 4 miles from the NAPS site. The combined number of flights using these three routes has remained fairly constant. Flights typically consist of 1 or 2 aircraft, rarely 4 aircraft in a flight. (Reference 1, Section 2.2.1.6.2)

2.2.2.7 Natural Gas or Petroleum Pipelines

There are no oil or gas pipelines within 5 miles of the ESP site.

2.2.2.8 Military Facilities

There are no military facilities within 5 miles of the ESP site.

2.2.3 Evaluation of Potential Accidents

2.2.3.1 Explosions and Flammable Vapor Clouds

The effects of explosion and formation of flammable vapor clouds from the nearby sources are evaluated below.

2.2.3.1.1 Truck Traffic

The largest explosive load routinely transported by truck on Virginia highways contains 8500 gallons of gasoline. The explosive force of this quantity of gasoline is estimated to be equivalent to 50,700 pounds of TNT, using a simple TNT-equivalent yield formula. (Reference 1, Section 2.2.2.1.1)

According to NRC RG 1.91 (Reference 6), if this amount of gasoline were to explode, a peak overpressure of 1 pound per square inch (psi) would be experienced as far as 1900 feet away from the point of explosion. The closest point of Virginia Route 652 to the ESP site is 1.5 miles (6420 feet). RG 1.91 cites 1 psi as a conservative value of peak positive incident overpressure, below which no significant damage would be expected. Thus, no significant damage would occur in the event of an explosion resulting from a gasoline truck traffic accident.

2.2.3.1.2 Pipelines

No natural gas pipeline or mining facilities are located within 10 miles of the ESP site. Therefore, the potential for explosions from these sources is minimal.

2.2.3.2 Aircraft Crashes

In accordance with NUREG-0800, Section 3.5.1.6 (Reference 8), a review of aircraft hazards was performed because the ESP site lies within 5 miles of the edge of a military route and within 2 miles of the edge of a federal airway.

2.2.3.2.1 Airports

None of the airports within 10 miles of the ESP site, as described in Section 2.2.2.6.1 and Table 2.2-1, supports operations in excess of the threshold criteria specified in RG 1.70 (Reference 7, Section 2.2.2.5).

2.2.3.2.2 Airways

The probabilities (P_{FA}) per year of an aircraft flying on the nearby airways crashing into a new unit at the ESP site were estimated using the following relationship, as specified in NUREG-0800 (Reference 8, Section 3.5.1.6).

$$P_{FA} = C \times N \times A/W$$

Where:

C = crash rate per mile of flight

N = number of flights per year

A = effective plant area in square miles

W = width of airway (plus twice the distance from the airway edge to the site when the site is outside the airway) in miles

The PPE indicates that the tallest reactor height is 234 feet above grade. Including consideration of the nearby safety-related structures (i.e., control building, service building, and auxiliary building) (Reference 9, Figures 1.2-13, 1.2-15, 1.2-17, 1.2-21, 1.2-23, 1.2-26, 1.2-28, 1.2-29, and 1.2-30), a total effective plant area of 0.013 square miles was conservatively used in the evaluation.

For Civil Airway V223:

$$C = 4 \times 10^{-10} \text{ (Reference 8)}$$

$$W = 8 + (2 \times 1.5) = 11 \text{ miles}$$

$$N = 200 \times 365 = 73,000 \text{ aircraft/year}$$

$$P_{FA} = 3.45 \times 10^{-8}$$

For the military routes:

$$C = 0.2 \times 10^{-8} \text{ (Reference 1, Section 2.2.2.2.2)}$$

$W = 10$ miles

$N = 3000$ flights/year \times 2 aircraft/flight = 6000 aircraft/year

$P_{FA} = 1.56 \times 10^{-8}$

These accident probabilities are within the NUREG-0800 guideline of less than 10^{-7} per year.

2.2.3.3 Toxic Chemicals

RG 1.78 (Reference 10) requires evaluation of control room habitability for a postulated release of chemicals stored within 5 miles of the control room. As described in Section 2.2.2, there are no manufacturing plants, chemical plants, storage facilities, major water transportation routes, and oil or gas pipelines within 5 miles of the ESP site. Therefore, as described in RG 1.78, only two scenarios were evaluated:

1. Chemicals transported on routes within a 5-mile radius of the site, at a frequency of 10 or more per year, and with weights outlined in the RG.
2. Chemicals stored within 0.3 miles of the control room in a quantity greater than 100 pounds.

Four roads (State Roads 652, 601, and 208, and U.S. Route 522) pass within 5 miles of the ESP site. U.S. Route 522 passes about 5 miles to the west-northwest; the other three routes pass the site at closer distances.

The NAPS UFSAR (Reference 1, Section 6.4.1.3.3) states that due to lack of chemicals and industrial facilities along these state routes, and considering the longer distance between Route 522 and the site, no chemicals are transported along these routes at a frequency and weight sufficient to require evaluation in accordance with the RG. Therefore, the UFSAR concludes that no significant control room habitability impact on the existing units is expected due to chemicals being shipped along these routes. Because of the close proximity of the new units to the existing units, no significant impact would be expected on those persons inhabiting future control rooms for the new units due to chemical accidents on these routes.

Reported toxic chemicals stored at the NAPS site, which could impact control room habitability for the existing units, are listed in Table 2.2-2. The list is comparable to that used for the toxic release evaluation reported in Reference 1, Section 6.4.1.3.3. These chemicals have been evaluated for the worst-case accidental release of each type of chemical. The results of the evaluation indicate that the worst-case concentration inside the control room of the existing units for each chemical analyzed is less than the toxicity limit that could cause a health hazard to the control room operators. (Reference 1, Section 6.4.1.3.3)

The locations and quantities of chemicals that would be stored for the new units at the ESP site have not been determined, and no detailed control room design parameters are available at this

time. The impact on the new units from chemicals stored onsite or nearby would be evaluated in the COL application.

Section 2.2 References

1. Updated Final Safety Analysis Report, North Anna Power Station, Revision 38.
2. Web Page: Spotsylvania County, Virginia, www.simplyfredericksburg.com/spotsylvania/spotsylvania.shtml, accessed June 27, 2003.
3. Web Page: Louisa County Airport/Freeman Field, Louisa, Virginia, www.airnav.com/airport/LKU/, accessed June 23, 2003.
4. Web Page: Lake Anna Airport, Bumpass, Virginia, www.airnav.com/airport/7W4, accessed June 23, 2003.
5. Washington Aeronautical Chart, 73rd Edition, published by the U.S. Department of Transportation, Federal Aviation Administration, National Aeronautical Chart Office, February 20, 2003.
6. Regulatory Guide 1.91, Evaluations of Explosions Postulated to Occur on Transportation Routes Near Nuclear Power Plants, Revision 1, U.S. Nuclear Regulatory Commission, February 1978.
7. Regulatory Guide 1.70, Standard Format and Content of Safety Analysis Reports for Nuclear Power Plants, LWR Edition, Revision 3, U.S. Nuclear Regulatory Commission, November 1978.
8. NUREG-0800, Standard Review Plan, U.S. Nuclear Regulatory Commission, July 1981.
9. AP1000 Design Control Document, Rev. 1, Tier 2 Material, Westinghouse Electric Company, 2002.
10. Regulatory Guide 1.78, Evaluating the Habitability of a Nuclear Power Plant Control Room During a Postulated Hazardous Chemical Release, Revision 1, U.S. Nuclear Regulatory Commission, December 2001.

Table 2.2-1 Airports Within 15 Miles of the ESP Site

Airport	Number of Flight Operations					Longest Runway			
	Type	Distance	Sector	Commercial	Total ^(a)	kd ² ^(b)	Orientation	Length	Comments
Lake Anna	Civil	6 miles	SSE	None	3640	12,500	WSW-ENE	2560 ft	Occasional use for practice landings. Planes based there.
Cub Field	Private	10 miles	WSW	None	Few	100,000	SSW-NNE	1400 ft	Unpaved strip, no facilities, no planes based there.
Louisa County	Civil	11 miles	WSW	None	6240	121,000	W-E	4300 ft	32 planes based there.

Source: Reference 1, Table 2.2-1.

a. Year 2002

b. RG 1.70: $d < 10$ miles, $k = 500$; $d > 10$ miles, $k = 1000$; where d is the distance in miles from the site, and k is a constant.

Table 2.2-2 Toxic Chemicals– Largest Single Container Stored at the NAPS Site

Chemical	Quantity
Ammonium Hydroxide	55 gallons
Carbon Dioxide	17 gallons
Hydrazine	300 gallons
Sodium Hydroxide	700 gallons

Source: Reference 1, Table 2.2-3.

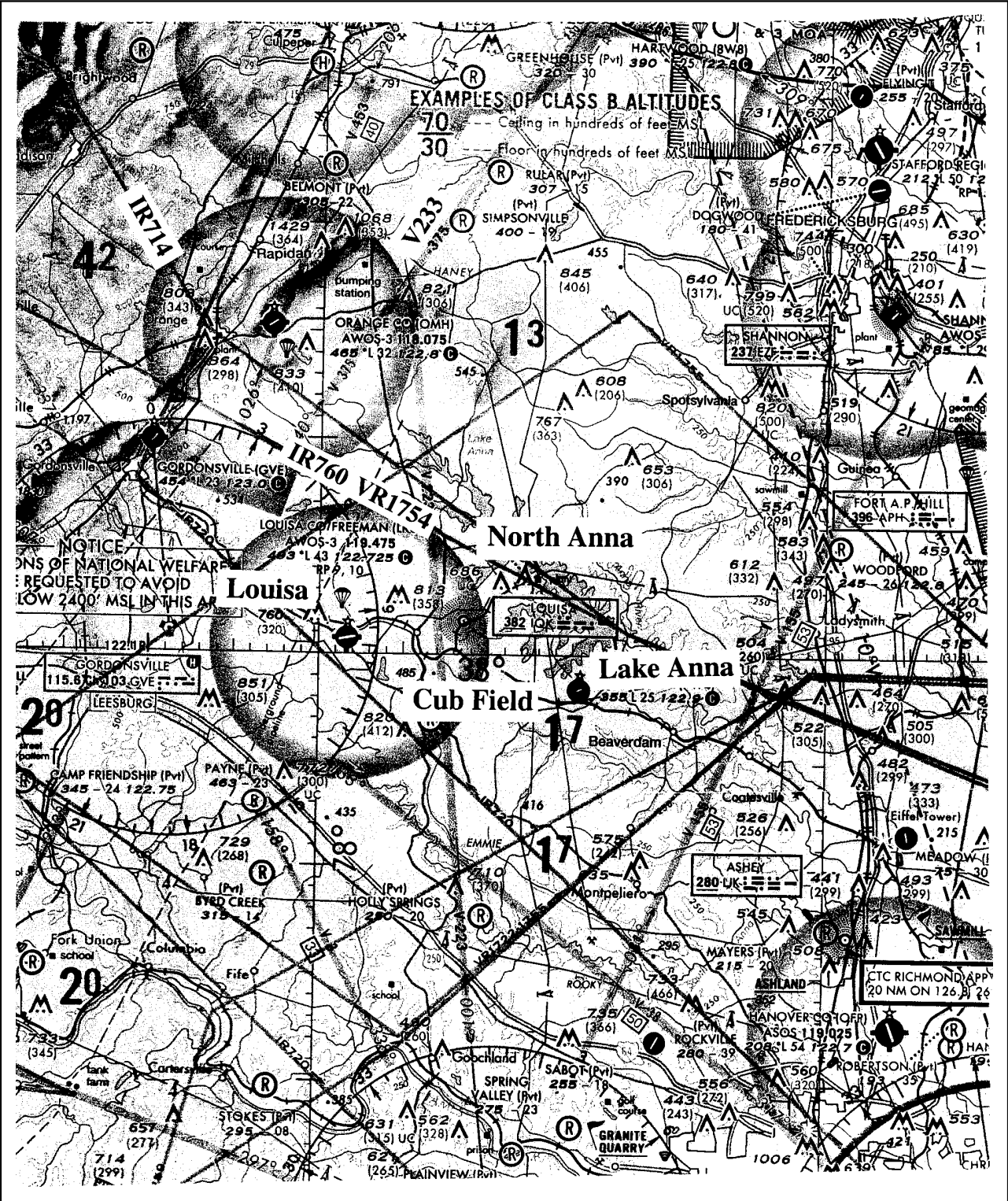


Figure 2.2-1 Location of Airports And Airways
Source: Reference 5

2.3 Meteorology

2.3.1 Regional Climatology

2.3.1.1 Data Sources

Data acquired by the National Weather Service (NWS) and summarized by the Environmental Data Service have been used to determine the regional climatology pertinent to the ESP site.

The 2001 Local Climatological Data (LCD), Annual Summary with Comparative Data (Reference 1) for Richmond, Virginia, prepared by the National Oceanic and Atmospheric Administration (NOAA) has been used to determine the climatological characteristics of the region.

Extreme wind data have been obtained from studies by Thom (Reference 2). Severe weather data have been obtained from a variety of sources. Severe storm, tornado, and hurricane data have been obtained from Storm Events for Virginia (Reference 3), Thom (Reference 4), Neumann (Reference 5), 1989 LCD for Richmond, Virginia (Reference 6), and Virginia Tropical Cyclone Climatology (Reference 7). Since the NWS changed the averaging interval for collecting the maximum wind speeds in 1990, the 1989 LCD (Reference 6) has been used to provide the fastest mile wind information on a long-term basis (1958-1989).

Data for meteorological extremes have been obtained from the 2001 LCD for Richmond (Reference 1). Temperature and precipitation extremes for other meteorological stations in the site region have been obtained from climatological summaries (Reference 8 through Reference 12) and from the NAPS UFSAR (Reference 13).

Storm events for Virginia (Reference 3) have been used for reporting the number of occurrences of hail and ice storms. Data for thunderstorms have been obtained from the 2001 Richmond LCD (Reference 1).

Climatological data for restrictive dilution conditions have been obtained from a variety of sources dealing with stagnating conditions in the United States (Reference 14) (Reference 15) (Reference 16).

2.3.1.2 General Climate

The climate in the Piedmont region of Virginia, where ESP site is located, is classified as modified continental. Summers are warm and humid, and winters are generally mild. The Blue Ridge Mountains to the west act as a partial barrier to outbreaks of cold, continental air in winter. The mountains also tend to channel winds along a general north-south orientation. Temperatures in the site region rarely exceed 100°F or fall below 0°F (Reference 1).

Based on 30 years of data (1971-2001), the area around the site receives an annual average rainfall of approximately 43.2 inches. Rainfall is fairly well distributed over the entire year, with the exception of July and August, when thunderstorm activity raises monthly totals to about 5.0 inches

(Reference 1). Extra-tropical storms can also contribute significantly to precipitation during September.

The 60-year climatological records show that monthly average snowfall of 4 inches or more occurs only in January. Snow usually remains on the ground only 1 or 2 days at a time. Richmond averages about 16.3 inches of snow a year (Reference 1).

2.3.1.2.1 Interaction Between Synoptic Scale Processes and Local Conditions

Synoptic scale processes are commonly examined with respect to the general circulation and general climatological characteristics of a region. Therefore, synoptic scale processes generally involve examination of gross meteorological conditions, such as prevailing wind patterns, temperature variability, precipitation patterns, and the occurrence of meteorological phenomena (e.g., fog, severe storms) in the site region. The analysis of the micrometeorology (local conditions) of a region usually encompasses the examination of the gross climatic characteristics of the region with respect to how local conditions can alter or influence a change in the general climatology of the region at a specific location. There are times when certain meteorological variables would deviate from the expected normal due to topographic effects or man-made interference.

In general, during light wind conditions, the local environmental conditions predominate, resulting in a channeling effect of winds such that the airflow patterns follow the contour lines of the region. Lake Anna has a moderating effect with respect to extreme temperatures in the immediate vicinity of the site region. For the most part, the general synoptic conditions predominate in regard to climatic characteristics of the site region; however, during periods of extreme temperatures or light wind conditions, the local conditions have an influence on the micrometeorology.

2.3.1.3 Severe Weather

2.3.1.3.1 Extreme Winds

According to Thom's latest compilation for characterizing extreme winds, the extreme 1-mile wind speed at 30 feet above the ground (100-year return period) is 80 MPH (Reference 2). The values for other occurrence intervals are listed in Table 2.3-4 (Reference 2). The fastest mile wind speed is defined as the 1-mile passage of wind with the highest speed for the day. The fastest mile wind recorded at Richmond during the 1958–1989 period of record, 68 MPH, occurred in October 1954 (Reference 6).

2.3.1.3.2 Tornadoes

During the period of January 1950 through June 2002, a total of 71 tornadoes were reported within a 50-mile radius of the ESP site (Reference 3). This averages 1.35 tornadoes per year within this 50-mile radius, which includes thirty counties in Virginia and one county (Charles County) in Maryland. Among those 71 tornadoes, 70 of them occurred in Virginia, and one occurred in Maryland.

According to statistical methods proposed by Thom, the probability of a tornado striking a point within a given area may be estimated as follows (Reference 4):

$$P = \frac{z \times t}{A}$$

Where

P = the mean probability per year

z = the mean path area of a tornado

t = the mean number of tornadoes per year

A = the area of concern

The Event Record Details provided in the Storm Events Report list path length and path width of a specific tornado (Reference 3). For tornado events with the 50-mile radius from the North Anna site, the calculated mean tornado path length is about two miles and the calculated mean path width is about 115 yards, according to the available recorded data. These values yield a z value of 0.131 square miles. Using a 50-mile radius as a basis for A and a value of 1.35 tornadoes per year yields an annual probability of 2.25×10^{-5} , or a recurrence interval of 44,400 years.

In 1988, the NRC developed an interim position (Reference 38) to replace the criteria for design basis tornadoes as specified in the 1974-issued RG 1.76 (Reference 17). Because a considerable quantity of tornado data is now available that was not available when RG 1.76 was developed, the Interim Position has concluded that regional maximum wind speed as reported in RG 1.76 were too conservative, and the contiguous United States is better represented by four tornado regions instead of three. The ESP site is located in Interim Position designated Region II, which has a maximum wind speed of 300 mph.

Tornado strength is measured by the Fujita-Pearson scale, ranking from F0 (gale) to F5 (incredible). During the 53-year period, no F3 or higher tornadoes were reported in Louisa or Spotsylvania counties. The wind speeds of an F3 tornado range from 158 mph to 206 mph (Reference 18).

The tornado maximum wind speed consists of two components, a rotational wind speed and a translational wind speed. Using methods provided in Reference 18 and an assumed radius of maximum rotational wind speed of 150 feet, other tornado parameters have been calculated and provided in Table 2.3-1. The radius of maximum rotational wind speed of 150 feet was suggested in Reference 18 for intense tornadoes.

Table 2.3-1 ESP Site Tornado Parameters

Criteria	Unit	Site Tornado
Max. Wind Speed	mph	206
Max. Rotational Velocity	mph	164.8
Max. Translation Velocity	mph	41.2
Radius of Max. Rotational Velocity	ft	150
Pressure Drop	psi	0.92
Rate of Pressure Drop	psi/s	0.37

2.3.1.3.3 Tropical Storms and Hurricanes

From January 1950 through June 2002, a total of 7 hurricanes and 2 tropical storms passed within 100 nautical miles of the ESP site (Reference 3). The last of these hurricanes was Hurricane Irene, which was a Category 1 (weak) hurricane at the time of closest approach to Wakefield, Virginia (80 miles southeast of the site), during the overnight hours of October 18, 1999. The storm brought heavy rain into southeast Virginia. The highest sustained wind speeds were 24 MPH at the Norfolk International Airport. The hurricane did not impact the site area any more than a heavy summer thunderstorm or a major winter storm.

The most recent tropical storm to affect the area was induced a month earlier by Hurricane Floyd on September 16, 1999. Rainfall reports for this tropical storm of over 3 inches were common, including a 5.97-inch measurement in Spotsylvania, Virginia (Reference 3). A maximum rainfall of 6.52 inches and a maximum 2-minute wind of 40 MPH were recorded in Richmond, Virginia, on that day (Reference 19).

Over the past 100-year period (1899–1998), a total of 164 Category 1 (weak) through 5 (devastating) hurricanes have crossed the U.S. coastline at one or more points. This frequency is equivalent to an average of five hurricanes every three years (Reference 5). On average, a tropical storm can be expected to impact Virginia annually, with hurricanes expected once every 2.3 years (Reference 7).

2.3.1.3.4 Precipitation Extremes

Table 2.3-5 lists some extremes of meteorological measurements in Richmond and Charlottesville. The maximum amount of precipitation recorded for a 24-hour period was 8.79 inches, which occurred in Richmond in August 1955. This rainfall occurred during the passage of several thunderstorms associated with a frontal passage. The maximum monthly snowfall measured in the region was 29.8 inches at Charlottesville in March 1960 (Reference 8). The maximum 24-hour snowfall observed in Richmond was 21.6 inches in January 1940 (Reference 1).

2.3.1.3.5 Hail, Snowstorms, and Ice Storms

Hail can occasionally occur at the ESP site (associated with well-developed thunderstorms). A review of data for the period between 1950 and 2002, indicates that there was a total of 65 reported hail storms in Louisa County, and in the immediately surrounding counties of Hanover, Caroline, Spotsylvania, and Orange (Reference 3). Among those hail storms, 17 occurred in Louisa County. There were four cases of 1.75-inch hailstones.

During the same 53-year period, there were 19 snowstorms in Louisa County, while the immediately surrounding counties had 19 to 22 snowstorms during the same period (Reference 3).

An examination of the same period indicates that there were 10 documented ice storms in Louisa County and in the immediately surrounding counties (Reference 3). Two of these storms occurred in Louisa County, and also impacted Hanover, and Caroline counties. One of the two storms affected Spotsylvania County also. Two other ice storms affected Orange and Spotsylvania Counties, within 8 hours of each other. The ice storms that occurred in Louisa County caused damage to trees and power lines in the nearby Hanover and Caroline Counties.

2.3.1.3.6 Thunderstorms

Based on 65 years of records, Richmond averages 36 days of thunderstorms per year, with July having the highest frequency of thunderstorms, 8.2 days (Reference 1).

2.3.1.3.7 Restrictive Dilution Conditions

In the ESP site region, the annual frequency of low-level inversions or isothermal layers based at or below a 500-foot elevation is approximately 30 percent according to Hosler (Reference 14). Seasonally, the greatest frequencies of inversions occur during the fall and winter (34 and 33 percent, respectively). Spring and summer have the lowest inversion frequencies (about 28 percent of the time for each season). Most of these inversions are nocturnal in nature generated through nighttime cooling.

The mean maximum mixing height depth (MMMD) is another indication of the restriction to atmospheric dilution at a site. The mixing depth is the distance above the ground to which relatively free vertical mixing occurs in the atmosphere (Reference 15). According to Holzworth, the annual afternoon MMMD value for the ESP site, is about 4900 feet (Reference 16). The seasonal afternoon MMMD values for fall and winter are about 4600 feet and 3300 feet, respectively. Shallow mixing depths have a greater frequency of occurrence during the fall and winter seasons: fall and winter have a higher frequency of inversions. The actual effect of the mixing height on pollutants emitted within the mixing depth is determined by the actual hourly mixing heights.

2.3.2 Local Meteorology

2.3.2.1 Data Sources

Data acquired from the National Climatic Data Center (in Asheville, NC) have been used to determine the norms, means, and extremes of temperature, precipitation, relative humidity, and fog applicable to the ESP site. The 2001 Richmond Local Climatological Data (Reference 1) provides detailed climatological data for this first-order station. Climatological summaries (Reference 8 through Reference 12) provide data for other stations in the area also provide supplemental information.

Direction and distance of the NWS stations closest to the ESP site are provided in Table 2.3-2.

Table 2.3-2 NWS Stations Near ESP Site

NWS Station	Distance (miles)	Direction
Richmond	44	Southeast
Fredericksburg	25	Northeast
Charlottesville	41	West
Gordonsville	25	West-Northwest
Louisa	14	West
Partlow	8	East

The closest station, Partlow, was closed on December 31, 1976 (Reference 20); therefore, recent data are not available from this station.

Besides using data from the nearby meteorological stations, data collected from the existing units meteorological monitoring system was also used to characterize local meteorological conditions. The onsite primary meteorological tower is located about 1750 feet east-northeast from the Unit 1 containment building (see Figure 2.3-23 and Figure 2.3-24). Based on proximity, the meteorological parameters (i.e., wind speed and wind direction) collected by this tower are representative of the ESP site. Consequently, they are appropriate for use in describing local meteorological conditions.

2.3.2.2 Normal and Extreme Values of Meteorological Parameters

2.3.2.2.1 Local Climatological Data

Climatological extremes for Richmond and Charlottesville are presented in Table 2.3-5. Normal and extremes of available temperature, precipitation, relative humidity, fog and other data are presented for Richmond in Table 2.3-6. Temperature and precipitation means for other applicable stations are presented in Table 2.3-7.

The closest available fog data for the ESP site area are from the NWS observations at Richmond International Airport in Richmond. The local climatological data for Richmond through 2001 (Reference 1) indicate an average of 27.1 days per year of heavy fog, based on 73 years of records. Heavy fog is defined by the NWS as fog that reduces visibility to one-quarter of a mile or less. The frequency of fog conditions at the ESP site would be expected to be somewhat different from Richmond. The ESP site is characterized by gentle rolling terrain that rises to an average height of 50 to 150 feet above Lake Anna's level. Low regions at the site and also in the vicinity of the lake would be expected to have a higher frequency of fog occurrences attributed to the accumulation of relatively cool surface air due to drainage flows from higher elevations when compared to the relatively flat region of the Richmond airport.

a. Average Wind Direction and Speed

The distribution of wind direction and speed is an important consideration when evaluating transport conditions relevant to site diffusion climatology. The topographic features of the site region and/or the general circulation to the atmosphere (i.e., movement of pressure systems and location of semi-permanent zones) are factors in influencing the wind direction within the site region. For the ESP site, the prevailing wind is from the south-southwest during the summer season and from the northwest and north during the winter season. These wind directions are due primarily to the location of the Bermuda High off the eastern coast of the United States during the summer season and the development of a cold high-pressure zone over the eastern portion of the United States during the winter season.

However, the topographic features of the ESP site region, in conjunction with the movement of pressure systems and the location of the semi-permanent pressure zones, have a definite influence on the wind direction distribution. The Blue Ridge Mountains, which are oriented in a south-southwest to north-northeast direction, are located approximately 40 to 50 miles northwest of the ESP site. Consequently, the prevailing winds during the summer season are from the south and south-southwest because of the channeling effect created by the presence of the Blue Ridge Mountains. Additionally, the Blue Ridge Mountains act as a barrier to the prevailing westerly winds at the surface; but even more so, they act as a barrier to the movement of low-pressure cells from the Gulf of Mexico region to the northeast portion of the United States. Consequently, low-pressure cells that are generated in the Gulf are frequently forced to move toward the east on the back (west) side of the Blue Ridge Mountains; therefore, resulting in a southerly flow of air in the ESP site region instead of a southeast or easterly wind.

Topographic features also influence the wind direction distribution during light winds. Usually, during episodes of near calm, the pressure gradient is weak and there is no organization in the general circulation. However, due to topographic effects such as the presence of Lake Anna, the airflow would typically follow the contour lines of the land. Air is channeled along Lake Anna and the North Anna River Valley during light wind conditions. If there is a sufficient

temperature gradient between the ambient air over the lake and surrounding land, a weak lake breeze could form. However, the lake breeze would affect only the area in the immediate vicinity of the lake (less than 1 mile) (Reference 13, Section 2.3.2.2.1.1).

The seasonal and annual average distributions of wind direction based on site data are presented in Figure 2.3-1 through Figure 2.3-10 for the lower (33 ft) and upper (159 ft) tower levels (Reference 13). Winds occur on an annual basis along a north-south orientation with a general westerly component. Wind direction distributions based on the lower level data are similar to those based on the upper level data. However, the upper level data indicate a more distinct north-south orientation of wind flows. Richmond wind data show a south-southwest/north orientation (Reference 1) that is similar to the general wind flow at the ESP site.

Wind direction distributions show seasonal variations. The frequencies of northerly and southerly winds are generally equivalent during the fall season. Winds from the northwest and south-southwest sectors characterize wind flows during the winter. During the spring season, the wind flow is predominantly from the northwest at the lower level. During the summer months, the predominant wind is from the south-southwest.

Atmospheric dilution is directly proportional to the wind speed (other factors remaining constant). The seasonal and annual median wind speeds at the ESP site are presented in Table 2.3-8. As indicated in the table, mean wind speeds show seasonal variations.

The mean annual wind speeds at the ESP site are 6.3 mph and 8.6 mph at the lower and upper tower level, respectively. The annual frequencies of calm are 0.37 and 0.75 percent for the lower and upper tower levels, respectively (Reference 13, Section 2.3.2.2.1.1).

b. Wind Direction Persistence

Wind persistence is important when considering potential effects of radiological release. It is defined as a continuous flow from a given direction or range of directions. Wind persistence roses for meteorological data collected at the NAPS site are presented in Figure 2.3-11 through Figure 2.3-20. The maximum 22.5-degree range direction persistence episodes recorded at NAPS during the period of record from the data for the lower level was a 26-hour wind from the north. The maximum persistence period at the upper level was 33 hours from the west-northwest. In general, extreme persistence periods (greater than 18 hours) at the ESP site are associated with moderately high winds and relatively low or moderate turbulence (Reference 13, Section 2.3.2.2.1.2).

c. Atmospheric Stability

Atmospheric stability, as applied in this report, is determined by the ΔT method as defined by the NRC (Reference 13, Section 2.3.3.2).

The seasonal and annual frequencies of stability classes and associated wind speeds for the ESP site are presented in Table 2.3-9. The vertical stability data, based on ΔT site measurements, indicate the predominance of neutral and slightly stable conditions (Reference 13, Section 2.3.2.2.1.1).

Extremely unstable conditions (A) are more frequent and extremely stable conditions (G) are less frequent during the summer than during the winter. This situation is attributed to the greater solar heating of the surface during the summer and the large-scale restrictive dilution conditions that generally occur during the winter. Also, ground snow cover is conducive to the formation of stable (or inversion) conditions.

Instrumentation is available in the main control room of the existing units by which personnel can identify atmospheric stability. This instrumentation is discussed in Section 2.3.3.1.5. From the temperature recorder discussed in Section 2.3.3.1.3, a ΔT can be ascertained. The existing units Emergency Plan Implementing Procedures identify station-specific instructions and appropriate temperature values for determining RG 1.23, Table 2 (Reference 21) atmospheric stability classifications. This stability classification method allows for the rapid assessment of pertinent meteorological parameters by control room personnel in the event of an accidental release of radioactive material to the atmosphere.

2.3.2.3 Potential Influence of the Plant and the Facilities on Local Meteorology

Lake Anna, comprising the North Anna Reservoir and the WHTF, has some effects on diffusion climatology, with those effects mainly confined to the immediate area of the lake. Slade (Reference 22) has documented that on average, a 50 percent reduction of horizontal wind direction fluctuation values and a 25 percent increase in wind speeds occurs after over-water trajectories of 7 miles. Because of the complex configuration of the lake, over-water trajectories would generally be less than 2.5 miles. Since the average water temperature in the reservoir is higher at the outfall and immediate surroundings within the WHTF than the average air temperature is, enhanced low-level atmospheric turbulent vertical mixing would occur. Although it is difficult to extrapolate Slade's results to other distances, the reduction of horizontal wind direction fluctuation values and the increase in wind speeds would be smaller than those reported by Slade due to the shorter over-water trajectories near the ESP site. Therefore, the offsite impact due to the effect of the lake on local diffusion climatology would be minimal.

2.3.2.4 Topographic Description

The ESP site and exclusion area (approximately 1803 acres) is located in the northeastern portion of Virginia in Louisa County along the North Anna River. The site region is characterized by gently rolling terrain that rises to an average height of 50 to 150 feet above Lake Anna's level and is divided by the North Anna River. The topography in the site region is characteristic of the Central Piedmont Plateau, which has a gently undulating surface that varies from 200 to 500 feet above

sea level. Figure 2.3-21 and Figure 2.3-22 present the topographic features of the site. Section 2.3.2.2.1 discusses how the topographic features of the site influence wind direction distribution.

Lake Anna, which extends approximately 17 miles along the old North Anna riverbed, was formed by damming up the North Anna River about 5 miles southeast of the site. The lake comprises the North Anna Reservoir and WHTF, which together cover a surface area of about 13,000 acres and contain approximately 100×10^9 gallons of water (Reference 13, Section 2.1.1.2).

Because of the gently rolling terrain, cold air drains into low-lying areas at night. Some wind channeling along Lake Anna is expected during low wind speed conditions. This same effect also occurred in the natural lowland area before the lake was developed.

2.3.3 Onsite Meteorological Measurements Program

2.3.3.1 Onsite Meteorological Measurements Program for Station Operation

The existing onsite meteorological monitoring program would be used for the ESP site. Detailed information about the existing program is described in Section 2.3 of the NAPS UFSAR (Reference 13). The existing program is ideally suited for the ESP-required onsite meteorological measurements, because the ESP site is within the existing NAPS site.

2.3.3.1.1 General Program Description

Based on the NAPS UFSAR (Reference 13), the existing onsite meteorological measurements program meets the requirements of 10 CFR 50.47 (Reference 23) and the criteria set forth in NUREG-0696 (Reference 24), NUREG-0737 (Reference 25), NUREG-0654, Appendix 2 (Reference 26), as well as the system accuracy presented in the Proposed Revision 1 to RG 1.23 (Reference 27).

The onsite meteorological program has three basic functions:

- Makes meteorological measurements
- Makes real-time predictions of atmospheric effluent transport and diffusion
- Enables remote interrogation of the atmospheric measurements and predictions by appropriate organizations

Meteorological measurements are available from both a primary and backup system, as required in 10 CFR 50, Appendix E (Reference 28). The backup system functions when the primary system is out of service, thus providing assurance that basic meteorological information is available during and immediately following an accidental airborne radioactivity release.

Because of the proximity of the new units to the existing units, meteorological parameters collected at the onsite primary and backup towers would be representative of the dispersion conditions at the ESP site.

The primary NAPS meteorological monitoring program consists of a Rohn Model 80, guyed, 160-foot tower located approximately 1900 feet east of the Unit 1 reactor containment building. Sensors are located at the 10-meter, 48.4-meter, and ground levels. Wind speed, wind direction, horizontal wind direction fluctuation, ambient temperature, one-half of differential temperature, and dew point temperature are measured at the 10-meter elevation. Wind speed, wind direction, horizontal wind direction fluctuation, and one-half of differential temperature are measured at the 48.4-meter elevation. Precipitation is monitored at the ground level. Signal cables are routed through conduit from each location into the instrument shelter at the base of the tower. Inside the shelter, the signals are routed to the appropriate signal-conditioning equipment whose outputs go to: 1) digital data recorders, and 2) an interface with the intelligent remote multiplex system.

The NAPS backup meteorological monitoring site consists of a Rohn Model 25, freestanding 10-meter tower. This tower is located approximately 1300 feet northeast of the Unit 1 containment building and serves as the backup meteorological monitoring site. A sensor at the top of the mast monitors wind speed, wind direction, and horizontal wind direction fluctuation. The signal path, instrument shelter, and data recording are identical to those described at the primary tower. All three parameters are interfaced to the intelligent remote multiplexing system equipment.

2.3.3.1.2 Location, Elevation, and Exposure of Instruments

The location of the primary meteorological tower is shown on Figure 2.3-23. Distances and bearings to ground features in the vicinity of the primary tower are shown on Figure 2.3-24. The nearest major structure is the training center building (completed in 1982) located 740 feet from the tower on a line of bearing of 205 degrees from true north. The minor structures, forming the recreational facility in the immediate vicinity of the tower have been evaluated as having no adverse effect on the measurements taken at the tower. Trees in the immediate vicinity of the tower have been topped to heights of 10–15 feet. The nearest contiguous tree line is more than 500 feet away from the tower and tree heights are 40 to 50 feet (Reference 13, Section 2.3.3.2.2).

The PPE shows that the highest structure at the ESP site would be about 234 feet above grade level. The primary tower is located about 2500 feet east of the proposed plant envelope. Since the primary tower is located more than 10 building heights away from the tallest structure within the plant envelope, the structure would not influence the meteorological measurements (Reference 27). The backup tower is located about 1800 feet to the closest ESP plant envelope boundary. However, the tallest structure (234 feet above grade) could be located about 650 feet west of the eastern edge plant envelope boundary. As a result, the backup tower would be located about 2400 feet away from the highest structure. Therefore, the structure would not influence the meteorological measurements taken at the backup either. These towers and the original satellite tower have the same relative proximity to Lake Anna.

Ground cover at the location is characteristically native grasses. Comparable cover is maintained at the base of the tower.

The primary tower is a guyed, triaxial, open-lattice structure. The lower level instrumentation is at 32.8 feet (10 m) above ground level. The upper instrumentation is at 158.9 feet above the finished plant grade of 271 ft mean sea level (msl).

The wind sensors are positioned so that the tower would not influence the prevailing south-southwest wind flow detected by the sensors. The wind speed, wind direction, and horizontal wind direction fluctuation sensors are mounted on booms longer than one times the tower face width.

Ambient temperature, differential temperature, and dew point temperature sensors are housed in motor-aspirated shields to insulate them from thermal radiation. These shields have a less than 0.2°F error at a maximum solar radiation of 1.6 gm-cal/cm²/min (Reference 13, Section 2.3.3.2.2).

At the primary meteorological monitoring site, a lithium chloride dew point sensor measures dew point temperature at the 32.8-foot (10-meter) level. The sensor signals are input into a dew point processor, which provides output signals proportional to the ambient dew point temperatures. The dew point levels are recorded to an accuracy of at least ±1.5°C (2.7°F), in accordance with (Reference 27). The backup tower does not collect dew point temperature.

At the primary meteorological monitoring site, precipitation is monitored at the ground level. The precipitation is measured with a recording rain gauge that has a resolution of 0.25 mm (0.01 in.). The accuracy is at least ±10 percent of the total accumulated catch, in accordance with Reference 27. The backup tower does not collect precipitation.

2.3.3.1.3 Meteorological Sensor Type and Performance Specifications

Wind speed, wind direction, and horizontal wind direction fluctuation are measured at both the lower and upper tower levels. Electro-mechanical instruments are used to measure wind speed and wind direction, and horizontal wind direction fluctuation is calculated by the digital data acquisition system.

Temperature is measured at the 32.8-foot level and differential temperature is measured between the 32.8-foot and 158.9-foot level. The sensors consist of one single-element, high-precision, platinum resistance temperature sensor located at the 158.9-foot level for measuring part of the differential temperature; and 1 single-element, precision, platinum resistance sensor located at 32.8-foot level for measuring ambient temperature and the other part of differential temperature. The sensors' signals are input into a temperature/delta temperature processor, which provides output signals proportional to an ambient and differential (ΔT) temperature.

A lithium chloride dew point sensor measures dew point temperature at the 32.8-foot level. The sensor signals are input into a dew point processor, which provides output signals proportional to the ambient dew point temperatures (Reference 13, Section 2.3.3.2.3).

2.3.3.1.4 Instrument Calibration and Maintenance

The meteorological monitoring installation is calibrated not less than semi-annually. Inspection, service, and maintenance are performed as required to ensure not less than 90 percent data recovery (Reference 27). Instrument technicians have the requisite expertise to service and, in the event of a system failure, repair the monitoring equipment. The on-site instrument group provides these technicians.

An inventory of spare sensors and parts are maintained for the replacement of major components in the event of a system outage. Redundant recording systems are incorporated into the program to further minimize data loss due to recorder failure. As an example, for this ESP application, the data recovery rates for more recent observations are presented. As shown in Table 2.3-10, the data recovery rates for meteorological parameters (wind direction, wind speed, and atmospheric stability class) used for the dispersion analyses discussed in Section 2.3.4 and Section 2.3.5 are very high and exceed the 90 percent requirement stated in Reference 27.

2.3.3.1.5 Data Recording Systems

a. Control Room Systems

Meteorological data collected from the primary and backup towers would be electronically sent to the designated control room and technical support center (TSC) to provide direct access to operators in the event of emergency. The required meteorological parameters are collected by the emergency response facility (ERF) data system, via the intelligent remote multiplex system (Reference 13). The parameters are also placed in the ERF database, thus making the site meteorological field data available for display in the local emergency operations facility (LEOF), the corporate emergency response center (CERC), and the central emergency operations facility (CEOF) located in the CERC.

Table 2.3-11 and Table 2.3-12 list each meteorological input parameter and its transmitted location for the primary tower and backup tower, respectively. Table 2.3-11 and Table 2.3-12 describe data that can be made available for remote interrogation at any time. During emergency conditions, selected meteorological parameters can be made available to the NRC through the emergency response data system (ERDS). Once activated, this meteorological data is transmitted from the ERF computer, via modem, to the NRC operations center (Reference 13, Section 2.3.3.2.5.1).

b. Tower Base Shelter Systems

A nominal 8 ft x 8 ft x 18 ft shelter is at the meteorological tower's base. The shelter is insulated, and thermostatically controlled heat and air conditioning maintain an interior temperature within a range appropriate for proper equipment operation. The enclosure is located so as to minimize any micrometeorological effects on the tower instrumentation. Equipment and circuitry for two separate data recording systems are housed in the enclosure.

Microprocessor-based data acquisition systems are the primary method of data acquisition. The sensor analog signals are collected, processed, and telemetered to a system computer. The data acquisition systems have a built-in battery, which maintains the time and date and initialized parameters. In addition to the power-up diagnostic checks, memory diagnostic tests are continually being performed to insure data integrity (Reference 13, Section 2.3.3.2.5.2).

The instruments and data acquisition systems detailed herein are consistent with the current level of technology for meteorological monitoring and the accuracy of the components ensures system accuracy consistent with proposed Revision 1 to RG 1.23 (Reference 27).

c. Meteorological Data Analysis Procedure

The collected data are used to generate a sequential file of 1-hour values for each parameter. The average values are calculated by the digital data collection system.

In addition to being transmitted real-time to the ERF system, the data are telemetered daily to a computer in the corporate office. Personnel in the air quality department check the data for representativeness and reasonability. The data are compared with those recorded from other offsite meteorological towers, as well as with the real-time data received at the corporate meteorological operations center. The current calendar month of data is maintained on a personal computer. At the end of each month, the data are transferred to the corporate mainframe computer for inclusion in the historical database.

This sequential file is used as the database for all subsequent data summaries and historical calculations. Routine data summaries are generated for each day, each calendar month, and each calendar year on certain meteorological parameters recorded on strip charts in the control room or the existing units. An annual summary is provided to health physics personnel by the air quality department. Other data summaries are prepared by the air quality department upon request.

The format of the onsite data summaries conforms to the recommended format found in RG 1.23, Table 1 (Reference 21). To facilitate comparison, the joint frequency distributions of wind speed and wind direction for each stability class, as defined by horizontal wind sigma and differential temperature, are displayed side by side. Joint frequency distributions for each wind sensor are presented (Reference 13, Section 2.3.3.2.5.2).

2.3.4 Short-Term (Accident) Diffusion Estimates

2.3.4.1 Basis

To evaluate potential health effects for DBAs, a hypothetical accident is postulated to predict upper-limit concentrations and dosages that might occur in the event of a radiological release. The NRC-sponsored PAVAN computer code (Reference 29) was used to estimate relative ground-level

air concentrations (χ/Qs) at the EAB and LPZ for potential accidental releases of radioactive material.

Recent readily available site meteorological data (1996–1998) were used for a quantitative evaluation of the hypothetical accident at the ESP site. Onsite data provide representative measurements of local dilution conditions appropriate to the ESP site, and are reasonably representative of long-term conditions. The use of the recent 3-year data for dispersion analysis involving accidental releases is consistent with the approach used in the license renewal application for the existing units (Reference 30), also satisfies the requirements of RG 4.7 (Reference 31).

According to 10 CFR 100 (Reference 32), it is necessary to consider the dosages for various time periods immediately following the onset of a postulated ground-level release at the exclusion distance and for the duration of exposure for the LPZ and population center distances. Therefore, relative air concentrations (χ/Qs) are estimated for various time periods ranging from 2-hours to 30 days.

Meteorological data were used to determine various hypothetical accident conditions as specified in RG 1.145 (Reference 33). Compared to an elevated release, a ground-level release usually results in higher ground-level concentrations at downwind receptors due to less dilution from shorter traveling distances. Because the ground level release scenario provides a bounding case, elevated releases were not evaluated.

The PAVAN program implements the guidance provided in RG 1.145 and performs the following calculation procedures. The code computes χ/Q values at the EAB and LPZ for each combination of wind speed and atmospheric stability for each of the 16 downwind direction sectors. The χ/Q values for each sector are then ranked in descending order, and an associated cumulative frequency distribution is derived based on the frequency distribution of wind speed and stabilities for that sector. The χ/Q value that is equaled or exceeded 0.5 percent of the total time becomes the maximum sector-dependent χ/Q value.

The χ/Q values are also ranked independent of wind direction into a cumulative frequency distribution for the entire site. The PAVAN Program then selects the χ/Q values that are equaled or exceeded 5 percent of the total time.

The larger of the two values, the maximum sector-dependent 0.5 percent χ/Q and the overall site 5 percent χ/Q value, is used to represent the χ/Q value for a 0–2 hour time period. To determine χ/Q values for longer time periods, the program calculates an annual average χ/Q value using the procedure described in RG 1.111 (Reference 34). The program then uses logarithmic interpolation between the 0-to-2-hour χ/Q values and the annual average χ/Q values to calculate the values for intermediate time periods (i.e., 8 hours, 16 hours, 72 hours, and 624 hours). As suggested in NUREG/CR-2858, each of the sector-specific 0–2-hour χ/Q values provided in the PAVAN output

file were examined for “reasonability” by comparing them with the ordered χ/Q values presented in the model output.

The PAVAN model was configured to calculate offsite χ/Q values assuming both wake-credit allowed and wake-credit not-allowed. As described in Section 2.1, the EAB is the perimeter of a 5000-foot-radius circle from the center of the abandoned Unit 3 containment. There are no residential areas in the EAB. The PPE indicates that the highest expected structure would be about 234 feet above grade level. Therefore, the closest EAB is more than 10 building heights away from the boundary of the plant envelope developed for the ESP site. As a result, the entire EAB is located beyond the wake influence zone that would be induced by a containment building. The LPZ is a 6-mile-radius circle centered at the Unit 1 containment building. Because it is located further away from the plant site than the EAB, the “wake-credit not allowed” scenario of the PAVAN results was used for the χ/Q analysis at the EAB and LPZ.

To be conservative, the shortest distances between the ESP plant envelope boundaries to the 5000-ft-radius circle for each downwind sector were entered as input to calculate the χ/Q values at the EAB. Similarly, the shortest distance from the ESP plant envelope area boundary to the LPZ was entered as input to calculate the χ/Q values at the LPZ. With respect to the ESP site, the shortest distance between the ESP plant envelope area and the LPZ is 8843 m (about 5.5 mi.) measured from the southwest of the plant envelope area.

The PAVAN model input data are presented below:

- Meteorological Data: Three-year (January 1, 1996 to December 31, 1998) combined onsite joint frequency distribution of wind speed, wind direction, and atmospheric stability.
- Type of Release: Ground level
- Wind Sensor Height: 33 ft
- Vertical Temperature Difference: 33 ft–158.9 ft
- Number of Wind Speed Categories: 7
- Release Height: 33 ft (default height)
- Distances From the Release Point to the EAB: See Table 2.3-13
- Distances From the Release Point to the LPZ: 8843 m (5.5 miles) for all downwind sectors

2.3.4.2 PAVAN Modeling Results

To calculate the maximum χ/Q values, the shortest distances from the plant envelope boundary to the EAB at each downwind sector were used. These distances are presented in Table 2.3-13. As presented in the table, the maximum 0–2 hours 0.5 percentile direction-dependent χ/Q value ($1.77 \times 10^{-4} \text{ sec/m}^3$) is greater than the corresponding 5 percentile overall site χ/Q value ($1.16 \times 10^{-4} \text{ sec/m}^3$) at the EAB. Therefore, the direction-dependent 0.5 percentile χ/Q values were used as the proper χ/Q values at EAB.

To be conservative, this shortest distance has been used as the LPZ distance for all downwind sectors in PAVAN modeling. Similarly, Table 2.3-14 shows the maximum 0–2 hours 0.5 percentile direction-dependent χ/Q value ($3.85 \times 10^{-5} \text{ sec/m}^3$) is greater than the corresponding 5 percentile overall site χ/Q value ($1.61 \times 10^{-5} \text{ sec/m}^3$) at the LPZ. Therefore, the direction-dependent 0.5 percentile χ/Q values were used at the LPZ.

The maximum χ/Q values presented in Table 2.3-13 and Table 2.3-14 for the EAB and LPZ, respectively, are summarized below.

Table 2.3-3 PAVAN Results (0.5% Limiting Case, 1996-98 Meteorological Data)

Source Location	Receptor Location	Downwind Dir/Dist (m)	0–2 hr	0–8 hr	8–24 hr	1–4 days	4–30 days	Annual
Plant Envelope	EAB	ESE/1420	1.77E-04	1.17E-04	9.53E-05	6.09E-05	3.21E-05	1.46E-05
Plant Envelope	LPZ	ESE/8843	3.85E-05*	1.73E-05	1.16E-05	4.89E-06	1.41E-06	3.08E-07

* The 0–2-hour χ/Q value is reported here for reference only. It is not required based on RG 1.145.

2.3.5 Long-Term (Routine) Diffusion Estimates

2.3.5.1 Basis

The NRC-sponsored XOQDOX computer code (Reference 35) was used to estimate χ/Q values due to routine releases. The XOQDOQ model implements assumptions outlined in RG 1.111 (Reference 34). A straight-line trajectory was assumed between the release point and all receptors by the XOQDOQ model. (Reference 35)

The primary function of the XOQDOQ computer code, obtained from RSICC (Reference 36), is to calculate annual χ/Q values and annual average relative deposition, D/Q values, at interested receptors (i.e., EAB, LPZ, nearest milk cow, residence, garden, meat animal, etc.). The χ/Q and D/Q values due to intermediate releases, which occur during routine operation, may also be evaluated using the XOQDOQ model. The program assumes that the material released to the atmosphere is a Gaussian distribution around the plume centerline. In estimating concentrations for longer time periods, the Gaussian distribution is assumed to be evenly distributed within the directional sector.

Input data and assumptions in the XOQDOQ modeling are presented below:

- Meteorological Data: Three-year combined (1996–1998) onsite joint frequency distribution of wind speed, wind direction and atmospheric stability.
- Type of Release: Ground level
- Wind Sensor Height: 33 ft

- Vertical Temperature Difference: 33 ft–158.9 ft
- Number of wind speed categories: 7
- Release Height: 33 ft (default height)
- Minimum Building Cross-Sectional Area: 2250 m²
- Distances from the release point to the nearest residence, nearest site boundary, milk cow, vegetable garden, milk goat, meat animal: See Table 2.3-15.

For dispersion analysis, a smaller cross-sectional area usually results in higher ground level concentrations. To be conservative, the minimum building cross-sectional area of 2250 m² was used to evaluate building downwash effect.

When compared to elevated releases, ground level releases usually produced higher pollutant concentrations for receptors located at ground level. Therefore, ground level releases were conservatively assumed in the χ/Q analysis. Distances from the Unit 1 containment building to various interested receptors (nearest residence, garden, meat animal and vegetable garden) for each directional sector are provided in Reference 37, Appendix C. However, because the plant envelope area proposed for the ESP site is an area (not a point), the shortest distances from any point of the plant envelope to the interested receptors were re-calculated for each directional sector. The results are presented in Table 2.3-15. The maximum annual χ/Q (no decay) at the EAB (0.88 mile to the ESE of the plant envelope) is 3.70×10^{-6} sec/m³. The maximum annual average χ/Q value calculated for the nearest residence (0.96 mile to the NNE of the plant envelope) is 2.4×10^{-6} sec/m³. The maximum annual χ/Q for the nearest vegetable garden (0.94 mile NE of the plant envelope) is 2.0×10^{-6} sec/m³. Finally, the maximum annual χ/Q for the nearest meat animal (1.37 miles to the SE of the plant envelope) is 1.4×10^{-6} sec/m³.

Table 2.3-16 summarizes the maximum χ/Q and D/Q values predicted by the XOQDOQ model for the sensitive receptors due to routine releases. Table 2.3-17 summarizes the annual average χ/Q values at distances between 0.25 mile to 50 miles and for various segment boundaries.

Section 2.3 References

1. *Richmond, Virginia, Local Climatological Data, Annual Summary with Comparative Data*, National Climatic Data Center, NOAA, 2001.
2. Thom, H. C. S. *New Distribution of Extreme Mile Winds in the United States*, ASCE Environmental Engineering Conference, Dallas, Texas, 1967.
3. *Storm Events for Virginia, 01/01/1950 Through 6/30/2002*, National Climatological Data Center, National Oceanic and Atmospheric Administration, Website, www4.ncdc.noaa.gov/cgi-win/wwcgl.dll?wwevent~storms, accessed December 2, 2002.

4. Thom, H. C. S. *Tornado Probabilities*, Monthly Weather Review, 1963, Vol. 91, Nos. 10-12, 730-736.
5. Neumann, C. J, B. R. Jarvinen, C. J. McAdie, and G. R. Hammer. *Tropical Cyclones of the North Atlantic Ocean, 1871-1998*, Historical Climatology Series 6-2, Fifth Revision, National Climatological Data Center, National Oceanic and Atmospheric Administration, 1999.
6. *Richmond, Virginia, Local Climatological Data, Annual Summary with Comparative Data*, National Climatic Data Center, National Oceanic and Atmospheric Administration, 1989.
7. Virginia Tropical Cyclone Climatology, Website, www.hpc.ncep.noaa.gov/research/roth/vaclimohur.htm, accessed December 12, 2002.
8. Charlottesville, Virginia, Climatological Summary, Period 1951-1980, Climatography of the United States, No. 20.
9. Fredericksburg, Virginia, Climatological Summary, Period 1951-1980, Climatography of the United States, No. 20.
10. Louisa, Virginia, Climatological Summary, Period 1951-1980, Climatography of the United States, No. 20.
11. *Piedmont Research Station, Virginia, Climatological Summary*, Period 1951-1980, Climatography of the United States, No. 20.
12. Partlow, Virginia, Climatological Summary, Period 1952-1971, Climatography of the United States, No. 20-44.
13. North Anna Updated Final Safety Analysis Report, Rev. 38, Dominion Virginia Power
14. Hosler, C. R. *Low-Level Inversion Frequency in the Contiguous United States*, Monthly Weather Review, 1961, Vol. 89, No. 9, 319-332.
15. *Guidelines for Air Quality Maintenance Planning and Analysis*, Vol. 10, EPA-450/4-77-001, U.S. Environmental Protection Agency, 1977.
16. Holzworth, G. C. *Mixing Heights, Wind Speeds, and Potential for Urban Air Pollution Throughout the Contiguous United States*, U.S. Environmental Protection Agency, 1971.
17. Regulatory Guide 1.76, Design Basis Tornado for Nuclear Power Plants, U.S. Nuclear Regulatory Commission, April 1974.
18. *Technical Basis for Interim Regional Tornado Criteria*, WASH-1300, U.S. Atomic Energy Commission, May 1974.

19. Richmond, Virginia, Local Climatological Data, Annual Summary with Comparative Data, National Climatic Data Center, NOAA, 1999.
20. *Virginia Climate Advisory 12/00*, Virginia State Climatology Office, Website, climate.virginia.edu/advisory/2000/ad00-12.htm, accessed March 24, 2003.
21. Regulatory Guide 1.23, Onsite Meteorological Program, U.S. Nuclear Regulatory Commission, 1972.
22. Slade, D. H. *Estimates of Dispersion from Pollutant Releases of a Few Seconds to 8 Hours in Duration*, Technical Note 39-ARL-3, Report No. 3, Environmental Science Services Administration, U.S. Department of Commerce, April 1966.
23. 10 CFR 50.47, *Emergency Plans*, January 19, 2001.
24. NUREG-0696, *Functional Criteria for Emergency Response Facilities*, Final Report, U.S. Nuclear Regulatory Commission, 1981.
25. NUREG-0737, *Clarification of TMI Plan Requirements*, U.S. Nuclear Regulatory Commission, 1980.
26. NUREG-0654, FEMA-REP-1, Rev. 1, *Criteria for Preparation and Evaluation of Radiological Emergency Response Plans and Preparedness in Support of Nuclear Power Plants*, U.S. Nuclear Regulatory Commission, 1996.
27. Regulatory Guide 1.23, *Meteorological Programs in Support of Nuclear Power Plants*, Second Proposed Revision 1, U.S. Nuclear Regulatory Commission, 1986.
28. 10 CFR 50, Appendix E, *Emergency Planning and Preparedness for Production and Utilization Facilities (Integrated)*, June 14, 1996.
29. NUREG/CR-2858, PAVAN: An Atmospheric Dispersion Program for Evaluating Design Basis Accidental Releases of Radioactive Materials from Nuclear Power Stations, PNL-4413, U.S. Nuclear Regulatory Commission, 1982.
30. NUREG-1437, Supplement 7, *Generic Environmental Impact Statement for License Renewal of Nuclear Plants Regarding North Anna Power Station, Units 1 and 2*, Final Report, U.S. Nuclear Regulatory Commission, November 2002.
31. Regulatory Guide 4.7, *General Site Suitability Criteria for Nuclear Power Stations*, Rev. 2, U.S. Nuclear Regulatory Commission, April 1998.
32. 10 CFR 100, *Reactor Site Criteria*, Code of Federal Regulations, December 4, 2002.

33. Regulatory Guide 1.145, Rev. 1, Atmospheric Dispersion Models for Potential Accident Consequence Assessments at Nuclear Power Plants, U.S. Nuclear Regulatory Commission, 1982.
34. Regulatory Guide 1.111, Methods for Estimating Atmospheric Transport and Dispersion of Gaseous Effluents in Routine Releases for Light-Water-Cooled Reactors, Rev. 1, U.S. Nuclear Regulatory Commission, 1977.
35. NUREG/CR-2919, XOQDOQ: Computer Program for the Meteorological Evaluation of Routine Effluent Releases at Nuclear Power Stations, Final Report, U.S. Nuclear Regulatory Commission, 1982.
36. NRCDOSE 2.3.2, CCC-684, Radiation Safety Information Computational Center, 2002.
37. Radiological Environmental Monitoring Program, 2001 Annual Report, Dominion Virginia Power, North Anna Power Station, Prepared by Dominion Virginia Power and Teledyne Brown Engineering Services.
38. Safety Evaluation by the Office of Nuclear Reactor Regulation of Recommended Modification to the RG. 1.76 Tornado Design Basis for the ALWR, U.S. Nuclear Regulatory Commission, 1988.

Table 2.3-4 Extreme 1-Mile Wind Passage at Richmond, Virginia

Probability	Speed (MPH)	Recurrence Interval (years)
0.5	48	2
0.1	60	10
0.04	68	25
0.02	72	50
0.01	80	100
0.001	105	1000

Source: Thom, H. C. S., New Distribution of Extreme Mile Winds in the United States, ASCE Environmental Engineering Conference, Dallas, Texas, 1967.

Table 2.3-5 Selected National Weather Service Stations for Meteorological Extremes in the ESP Site Region (Date of Occurrence)

Meteorological Extremes	Charlottesville		Richmond	
	Value	Date	Value	Date
Maximum Temperature	107°F	(9/54)	105°F	(7/77)
Minimum Temperature	-9°F	(1/85)	-12°F	(1/40)
Maximum Monthly Rainfall	16.96 in.	(10/44)	18.87 in.	(7/45)
Maximum Monthly Snowfall	29.8 in.	(3/60)	28.5 in.	(1/40)
Maximum 24-hr Rainfall	8.00 in.	(9/44)	8.79 in.	(8/55)
Maximum 24-hr Snowfall	N/A		21.6 in.	(1/40)
Fastest Mile Wind, Speed	N/A		68 mph	(10/54)
Fastest Mile Wind, Direction	N/A		SE	(10/54)

N/A – Data not available.

Source: NAPS, UFSAR, Revision 38.

Table 2.3-6 Richmond Climatological Data

NORMALS, MEANS, AND EXTREMES

RICHMOND, VA

LATITUDE:		LONGITUDE:		ELEVATION (FT):		TIME ZONE:						NBAN: 13740				
37° 30' 40" N		77° 19' 24" W		GRND: 164	BARO: 167	EASTERN (UTC + 5)										
ELEMENT		NO.	JAN	FEB	MAR	APR	MAY	JUN	JUL	AUG	SEP	OCT	NOV	DEC	YEAR	
TEMPERATURE °F	NORMAL DAILY MAXIMUM	30	45.7	49.2	59.5	70.0	77.8	85.1	88.4	87.1	80.9	70.7	61.3	50.2	68.8	
	MEAN DAILY MAXIMUM	81	47.4	50.3	58.9	69.3	77.6	85.1	88.3	86.5	80.8	70.6	60.4	50.0	68.8	
	HIGHEST DAILY MAXIMUM	72	80	83	93	96	100	104	105	102	103	99	86	81	105	
	YEAR OF OCCURRENCE		1950	1932	1938	1990	1941	1952	1977	1983	1954	1941	1993	1998	JUL 1977	
	MEAN OF EXTREME MAXS.	81	69.4	71.2	80.2	87.8	91.1	96.0	97.5	95.9	93.1	85.5	77.8	70.1	84.6	
	NORMAL DAILY MINIMUM	30	25.7	28.1	36.3	44.6	54.2	62.7	67.5	66.4	59.0	46.5	37.9	29.9	46.6	
	MEAN DAILY MINIMUM	81	28.4	30.0	36.6	45.4	54.7	63.5	68.0	66.6	60.1	47.8	38.4	30.9	47.5	
	LOWEST DAILY MINIMUM	72	-12	-10	11	23	31	40	51	46	35	21	10	-1	-12	
	YEAR OF OCCURRENCE		1940	1936	1960	1985	1956	1967	1965	1934	1974	1962	1933	1942	JAN 1940	
	MEAN OF EXTREME MINS.	81	10.2	14.2	21.6	30.9	41.0	51.1	57.8	55.6	45.4	32.4	22.7	14.6	33.1	
	NORMAL DRY BULB	30	35.7	38.7	48.0	57.3	66.0	73.9	78.0	76.8	70.0	58.6	49.6	40.1	57.7	
	MEAN DRY BULB	81	38.0	40.1	47.8	57.4	66.2	74.3	78.2	76.6	70.5	59.2	49.5	40.4	58.2	
	MEAN WET BULB	17	34.0	36.7	41.9	50.5	59.4	67.3	71.5	66.0	63.6	53.7	44.9	36.8	52.2	
	MEAN DEW POINT	17	27.0	29.1	33.9	43.0	54.3	63.2	68.1	63.1	59.9	48.7	38.6	30.0	46.6	
	NORMAL NO. DAYS WITH:															
	MAXIMUM ≥ 90°	30	0.0	0.0	0.1	0.0	2.3	8.7	13.8	11.0	4.1	0.3	0.0	0.0	41.1	
MAXIMUM ≤ 32°	30	4.3	1.7	0.1	0.0	0.0	0.0	0.0	0.0	0.0	0.0	0.0	1.5	7.6		
MINIMUM ≤ 32°	30	23.0	19.5	10.8	2.3	0.1	0.0	0.0	0.0	0.0	2.1	9.4	19.2	86.4		
MINIMUM ≤ 0°	30	0.3	0.1	0.0	0.0	0.0	0.0	0.0	0.0	0.0	0.0	0.0	0.0	0.4		
H/C	NORMAL HEATING DEG. DAYS	30	908	736	527	341	61	0	0	0	23	233	462	772	3963	
	NORMAL COOLING DEG. DAYS	30	0	0	0	10	92	270	403	366	173	34	0	0	1348	
RH	NORMAL (PERCENT)	30	68	66	63	61	70	72	75	77	77	74	69	69	70	
	HOUR 01 LST	30	75	73	72	73	83	86	88	90	90	86	79	76	81	
	HOUR 07 LST	30	79	78	78	76	81	83	86	90	90	89	84	80	83	
	HOUR 13 LST	30	56	53	49	45	52	54	57	58	57	52	51	55	53	
	HOUR 19 LST	30	65	62	57	53	63	66	69	74	77	75	68	68	66	
R	PERCENT POSSIBLE SUNSHINE	46	54	58	62	66	65	69	68	66	65	63	59	54	62	
W/O	MEAN NO. DAYS WITH: HEAVY FOG (VISIBY≤1/4 MI)	72	2.7	2.1	1.7	1.6	1.8	1.5	2.0	2.4	2.9	3.3	2.3	2.8	27.1	
	THUNDERSTORMS	65	0.2	0.4	1.6	2.4	5.3	6.6	8.2	6.2	2.9	1.0	0.6	0.2	35.6	
CLOUDINESS	MEAN: SUNRISE-SUNSET (OKTAS)	1			5.6		5.6	3.2								
	MIDNIGHT-MIDNIGHT (OKTAS)	1			5.6											
	MEAN NO. DAYS WITH: CLEAR	1	2.0	1.0	9.0		9.0	10.0								
	PARTLY CLOUDY	1		1.0	5.0		4.0	8.0								
CLOUDY	1	7.0	4.0	10.0		8.0	1.0									
PR	MEAN STATION PRESSURE (IN)	28	29.91	29.89	29.85	29.81	29.81	29.81	29.83	29.86	29.89	29.92	29.92	29.93	29.87	
	MEAN SEA-LEVEL PRESS. (IN)	17	30.12	30.11	30.05	29.99	30.00	29.99	30.01	30.04	30.08	30.12	30.14	30.14	30.07	
WINDS	MEAN SPEED (MPH)	43	8.3	8.7	9.3	9.2	7.9	7.5	7.1	6.6	7.0	7.2	7.7	7.9	7.9	
	PREVAIL. DIR (TENS OF DEGS)	26	01	01	36	19	19	20	19	19	36	36	19	36	19	
	MAXIMUM 2-MINUTE: SPEED (MPH)	6	38	39	37	46	41	45	33	44	40	37	36	40	46	
	DIR. (TENS OF DEGS)	6	31	23	22	33	30	26	29	36	01	10	16	15	33	
	YEAR OF OCCURRENCE		2000	1997	1996	1999	1997	2000	1999	1996	1999	1996	1999	1996	APR 1999	
	MAXIMUM 5-SECOND: SPEED (MPH)	6	48	49	49	56	60	55	44	59	53	46	46	48	60	
	DIR. (TENS OF DEGS)	6	31	26	22	25	28	27	29	32	08	10	16	16	28	
	YEAR OF OCCURRENCE		2000	1997	1996	1998	1996	2000	1999	2000	1996	1996	1999	1996	MAY 1996	
PRECIPITATION	NORMAL (IN)	30	3.24	3.16	3.61	2.96	3.84	3.62	5.03	4.40	3.34	3.53	3.17	3.26	43.16	
	MAXIMUM MONTHLY (IN)	64	7.97	5.97	8.65	7.33	8.87	9.24	18.07	14.10	16.60	9.39	7.64	7.07	18.07	
	YEAR OF OCCURRENCE		1978	1979	1984	1987	1972	1938	1945	1955	1999	1971	1959	1973	JUL 1945	
	MINIMUM MONTHLY (IN)	64	0.64	0.48	0.94	0.64	0.87	0.38	0.51	0.52	0.26	0.01	0.17	0.40	0.01	
	YEAR OF OCCURRENCE		1981	1978	1966	1963	1965	1980	1983	1943	1978	2000	2001	1980	OCT 2000	
	MAXIMUM IN 24 HOURS (IN)	64	3.31	2.67	3.43	2.97	3.08	4.61	5.73	8.79	6.52	6.50	4.07	3.16	8.79	
	YEAR OF OCCURRENCE		1962	1979	1992	1987	1981	1963	1969	1955	1999	1961	1956	1958	AUG 1955	
NORMAL NO. DAYS WITH: PRECIPITATION ≥ 0.01	30	10.4	9.4	10.2	9.0	10.7	9.6	10.4	9.5	7.6	7.0	8.0	9.1	110.9		
PRECIPITATION ≥ 1.00	30	0.8	0.7	0.8	0.6	1.0	0.9	1.4	1.3	1.0	1.2	0.8	0.7	11.2		
SNOWFALL	NORMAL (IN)	30	5.8	5.5	2.4	0.1	0.0	0.0	0.0	0.0	0.0	T	0.3	2.2	16.3	
	MAXIMUM MONTHLY (IN)	62	28.5	21.4	19.7	2.0	T	0.0	0.0	0.0	0.0	T	7.3	12.5	28.5	
	YEAR OF OCCURRENCE		1940	1983	1960	1940	1994						1979	1953	1958	JAN 1940
	MAXIMUM IN 24 HOURS (IN)	62	21.6	16.8	12.1	2.0	T	0.0	0.0	0.0	0.0	T	7.3	7.5	21.6	
	YEAR OF OCCURRENCE		1940	1983	1962	1940	1994						1979	1953	1966	JAN 1940
	MAXIMUM SNOW DEPTH (IN)	77	18	20	13	1	0	0	0	0	0	0	6	9	20	
	YEAR OF OCCURRENCE		1922	1922	1980	1964							1938	1958	FEB 1922	
NORMAL NO. DAYS WITH: SNOWFALL ≥ 1.0	30	1.5	1.4	0.6	0.*	0.0	0.0	0.0	0.0	0.0	0.0	0.1	0.7	4.3		

Source: Richmond, Virginia, Local Climatological Data, Annual Summary with Comparative Data 2001, NCDC, NOAA.

Table 2.3-7 Mean Annual Meteorological Data for Stations in the Site Region

Location	Mean Annual Temperature (°F)	Mean Annual Precipitation (in.)	Mean Annual Snowfall (in.)
Charlottesville	56.8	45.72	24.2
Fredericksburg	56.2	40.99	17.7
Louisa	56.3	41.62	19.9
Piedmont Research Station	55.9	38.68	22.0
Partlow	55.2	42.24	18.6

Source: Reference 8 through Reference 12.

Table 2.3-8 ESP Site Mean Wind Speeds (MPH) 1974-1987

Elevation	Spring (Mar, Apr, May)	Summer (Jun, Jul, Aug)	Fall (Sept, Oct, Nov)	Winter (Dec, Jan, Feb)	Annual
Upper Level	9.6	7.5	8.3	9.2	8.6
Lower Level	7.1	5.4	5.9	6.6	6.3

Source: Reference 13

Table 2.3-9 ESP Site Vertical Stability (ΔT) and Low Level Wind Speed Distribution 1974-1987

Period	Vertical Stability Categories						
	A	B	C	D	E	F	G
Spring							
Frequency (%)	20.04	5.41	4.86	29.87	24.18	7.92	7.71
Wind Speed (MPH)	(8.6)	(8.4)	(8.6)	(7.9)	(6.3)	(4.0)	(2.9)
Summer							
Frequency (%)	25.33	5.38	5.10	29.52	27.21	6.42	1.44
Wind Speed (MPH)	(6.1)	(6.2)	(6.2)	(5.7)	(4.3)	(3.2)	(2.9)
Fall							
Frequency (%)	21.28	4.16	4.25	28.71	25.57	10.26	6.14
Wind Speed (MPH)	(6.9)	(7.1)	(7.4)	(6.8)	(4.9)	(3.4)	(3.2)
Winter							
Frequency (%)	13.39	4.82	4.85	35.10	27.55	8.09	6.60
Wind Speed (MPH)	(7.6)	(7.8)	(8.2)	(7.4)	(5.6)	(3.5)	(2.8)
Annual							
Frequency (%)	20.00	4.91	4.74	30.69	26.08	8.22	5.46
Wind Speed (MPH)	(7.2)	(7.4)	(7.6)	(7.0)	(5.2)	(3.5)	(3.0)

Source: Reference 13

**Table 2.3-10 Meteorological Data Recovery Rates (percent)
(ESP Site, January 1, 1996 – December 31, 2001)**

Year	ΔT Included		ΔT not Included	
	33-ft Wind Data	150-ft Wind Data	33-ft Wind Data	150-ft Wind Data
1996	98.88	99.30	98.92	99.48
1997	98.96	90.09	99.36	99.20
1998	99.21	99.43	99.12	99.34
1999	98.91	98.90	99.45	99.44
2000	98.73	98.76	99.23	99.24
2001	98.88	91.78	99.76	92.59

Source: NAPS onsite meteorological monitoring program

Table 2.3-11 Primary Tower Parameters

Parameter	Transmitted Locations		
	ERF Data Base	Control Room	Remote Interrogation
Wind Direction (upper)	X	X	X
Wind Speed (upper)	X	X	X
Sigma theta (upper)			X
Wind Direction (lower)	X	X	X
Wind Speed (lower)	X	X	X
Sigma theta (lower)			X
Ambient Temperature (lower)	X	X	X
Dew point (lower)			X
Delta Ambient Temperature (upper-lower)	X	X	X
Precipitation			X

Note: All parameters going to the ERF database are available for printout in the existing TSC and EOF.
The Units 1 & 2 control room parameters are hardwired.

Source: Reference 13

Table 2.3-12 Backup Tower Parameters

Parameter	Transmitted Locations		
	ERF Data Base	Control Room	Remote Interrogation
Wind Speed	X	X	X
Wind Direction	X	X	X
Sigma Theta	X	X	X

Note: All parameters going to the ERF database are available for printout in the existing TSC and EOF.
The Units 1 & 2 control room parameters are hardwired.
Source: Reference 13

Table 2.3-13 PAVAN Results for %/Q Values at the EAB

/Plant Name: North Anna ESP
 Data Period: 1996-98 JFD
 Type of Release: Ground-Level Release
 Source of Data: Onsite

Meteorological Instrumentation
 Wind Sensors Height: 33 ft
 ΔT Heights: 33 ft–158.9 ft

Comments: Data period: 1/1/96 - 12/31/98

Program: PAVAN, 10/76, 8/79 Revision, Implementation of Regulatory Guide 1.145

0 Relative Concentration (%/Q) Values (sec/cubic meter) versus Averaging Time

Downwind Sector	Distance (Meters)	0-2 Hours	0-8 Hours	8-24 Hours	1-4 Days	4-30 Days	Annual Average	Hours Per Year Max 0-2 hr %/Q Is Exceeded in Sector	Downwind Sector
S	954.	8.96E-05	6.29E-05	5.27E-05	3.59E-05	2.07E-05	1.06E-05	8.3	S
SSW	894.	8.83E-05	6.09E-05	5.06E-05	3.39E-05	1.90E-05	9.37E-06	6.9	SSW
SW	872.	8.83E-05	6.03E-05	4.99E-05	3.30E-05	1.82E-05	8.79E-06	7.0	SW
WSW	876.	8.76E-05	5.92E-05	4.86E-05	3.18E-05	1.72E-05	8.16E-06	7.3	WSW
W	872.	1.03E-04	7.06E-05	5.83E-05	3.85E-05	2.12E-05	1.03E-05	13.0	W
WNW	902.	9.22E-05	6.20E-05	5.09E-05	3.31E-05	1.78E-05	8.36E-06	8.5	WNW
NW	988.	8.72E-05	5.79E-05	4.72E-05	3.03E-05	1.60E-05	7.34E-06	6.7	NW
NNW	1164.	7.06E-05	4.51E-05	3.61E-05	2.22E-05	1.11E-05	4.72E-06	2.7	NNW
N	1399.	7.85E-05	5.35E-05	4.42E-05	2.91E-05	1.60E-05	7.72E-06	2.6	N
NNE	1420.	8.96E-05	6.17E-05	5.12E-05	3.42E-05	1.92E-05	9.43E-06	3.9	NNE
NE	1454.	8.20E-05	5.50E-05	4.50E-05	2.92E-05	1.56E-05	7.29E-06	3.7	NE
ENE	1474.	8.11E-05	5.01E-05	3.94E-05	2.34E-05	1.11E-05	4.43E-06	3.8	ENE
E	1433.	1.21E-04	7.95E-05	6.44E-05	4.07E-05	2.10E-05	9.39E-06	13.5	E
ESE	1420.	1.77E-04	1.17E-04	9.53E-05	6.09E-05	3.21E-05	1.46E-05	43.7	ESE

Table 2.3-13 PAVAN Results for χ/Q Values at the EAB

/Plant Name: North Anna ESP
 Data Period: 1996-98 JFD
 Type of Release: Ground-Level Release
 Source of Data: Onsite

Meteorological Instrumentation
 Wind Sensors Height: 33 ft
 ΔT Heights: 33 ft–158.9 ft

Comments: Data period: 1/1/96 - 12/31/98

Program: PAVAN, 10/76, 8/79 Revision, Implementation of Regulatory Guide 1.145

0 Relative Concentration (χ/Q) Values (sec/cubic meter) versus Averaging Time

Downwind Sector	Distance (Meters)							Hours Per Year	Downwind Sector
		0-2 Hours	0-8 Hours	8-24 Hours	1-4 Days	4-30 Days	Annual Average	Max 0-2 hr χ/Q Is Exceeded in Sector	
SE	1338.	1.72E-04	1.10E-04	8.84E-05	5.47E-05	2.75E-05	1.18E-05	39.9	SE
SSE	1166.	1.03E-04	6.79E-05	5.51E-05	3.50E-05	1.82E-05	8.20E-06	14.4	SSE
Max χ/Q		1.77E-04						Total Hours Around Site: 185.8	
Site Limit		1.16E-05	8.20E-05	6.92E-05	4.77E-05	2.80E-05	1.46E-05		

00.5 Percent χ/Q to an Individual Is Limiting

Table 2.3-14 PAVAN Results for %/Q Values at the LPZ

1USNRC Computer Code-PAVAN, Version 2.0

/Plant Name: North Anna ESP
 Data Period: 1996-98 JFD
 Type of Release: Ground-Level Release
 Source of Data: Onsite

Meteorological Instrumentation
 Wind Sensors Height: 33 Ft
 ΔT Heights: 33 ft–158.9 ft

Comments: Data period: 1/1/96 - 12/31/98

Program: PAVAN, 10/76, 8/79 Revision, Implementation of Regulatory Guide 1.145

0 Relative Concentration (%/Q) Values (sec/cubic meter) versus Averaging Time

Downwind Sector	Distance (Meters)	0-2 Hours	0-8 Hours	8-24 Hours	1-4 Days	4-30 Days	Annual Average	Hours Per Year Max 0-2 hr %/Q Is Exceeded in Sector	Downwind Sector
S	8843.	7.27E-06	3.46E-06	2.39E-06	1.07E-06	3.36E-07	8.16E-08	2.6	S
SSW	8843.	6.26E-06	2.94E-06	2.02E-06	8.90E-07	2.75E-07	6.53E-08	128.8	SSW
SW	8843.	6.02E-06	2.80E-06	1.91E-06	8.34E-07	2.54E-07	5.91E-08	1.6	SW
WSW	8843.	6.11E-06	2.81E-06	1.90E-06	8.19E-07	2.44E-07	5.55E-08	1.7	WSW
W	8843.	8.25E-06	3.75E-06	2.53E-06	1.08E-06	3.16E-07	7.05E-08	3.3	W
WNW	8843.	7.35E-06	3.33E-06	2.24E-06	9.46E-07	2.75E-07	6.06E-08	2.2	WNW
NW	8843.	7.80E-06	3.53E-06	2.37E-06	1.00E-06	2.91E-07	6.40E-08	2.1	NW
NNW	8843.	7.96E-06	3.50E-06	2.32E-06	9.52E-07	2.65E-07	5.53E-08	.9	NNW
N	8843.	1.25E-05	5.93E-06	4.09E-06	1.83E-06	5.76E-07	1.40E-07	1.3	N
NNE	8843.	1.49E-05	7.16E-06	4.96E-06	2.24E-06	7.18E-07	1.78E-07	2.2	NNE
NE	8843.	1.38E-05	6.53E-06	4.48E-06	1.99E-06	6.16E-07	1.47E-07	2.6	NE
ENE	8843.	1.39E-05	6.11E-06	4.05E-06	1.66E-06	4.59E-07	9.54E-08	3.1	ENE
E	8843.	2.34E-05	1.06E-05	7.14E-06	3.03E-06	8.83E-07	1.96E-07	11.1	E

Table 2.3-14 PAVAN Results for χ/Q Values at the LPZ

1USNRC Computer Code-PAVAN, Version 2.0

/Plant Name: North Anna ESP
 Data Period: 1996-98 JFD
 Type of Release: Ground-Level Release
 Source of Data: Onsite

Meteorological Instrumentation
 Wind Sensors Height: 33 Ft
 ΔT Heights: 33 ft–158.9 ft

Comments: Data period: 1/1/96 - 12/31/98

Program: PAVAN, 10/76, 8/79 Revision, Implementation of Regulatory Guide 1.145

0 Relative Concentration (χ/Q) Values (sec/cubic meter) versus Averaging Time

Downwind Sector	Distance (Meters)	0-2 Hours	0-8 Hours	8-24 Hours	1-4 Days	4-30 Days	Annual Average	Hours Per Year Max 0-2 hr χ/Q Is Exceeded in Sector	Downwind Sector
ESE	8843.	3.85E-05	1.73E-05	1.16E-05	4.89E-06	1.41E-06	3.08E-07	43.7	ESE
SE	8843.	3.54E-05	1.52E-05	9.94E-06	3.96E-06	1.06E-06	2.11E-07	34.1	SE
SSE	8843.	1.40E-05	6.13E-06	4.06E-06	1.66E-06	4.61E-07	9.61E-08	8.4	SSE
Max χ/Q		3.85E-05						Total Hours Around Site: 249.9	
Site Limit		1.61E-05	8.37E-06	6.03E-06	2.97E-06	1.07E-06	3.08E-07		

00.5 Percent χ/Q to an Individual Is Limiting

Table 2.3-15 ESP Application Nearby Sensitive Receptors

Sector	Nearest Resident		Nearest Site Boundary		Milk* Cow	Meat Animal		Milk* Goat	Veg. Garden 500 ft ²	
	(mile)	(km)	(mile)	(km)		(mile)	(km)		(mile)	(km)
N	1.48	2.38	0.87	1.40		2.18	3.51		1.78	2.86
NNE	0.96	1.54	0.88	1.42		1.56	2.51		1.66	2.67
NE	0.94	1.51	0.90	1.45		1.44	2.32		0.94	1.51
ENE	2.18	3.51	0.91	1.47		2.58	4.15		2.18	3.51
E	1.38	2.22	0.89	1.43		3.58	5.76		1.38	2.22
ESE	1.77	2.85	0.88	1.42		None	None		3.57	5.74
SE	1.37	2.20	0.83	1.34		1.37	2.20		1.37	2.20
SSE	0.91	1.46	0.73	1.17		2.71	4.36		1.21	1.95
S	1.01	1.63	0.62	0.99		None	None		1.11	1.79
SSW	1.1	1.77	0.57	0.92		1.90	3.06		1.50	2.41
SW	2.78	4.47	0.54	0.87		None	None		2.78	4.47
WSW	1.22	1.96	0.55	0.88		1.22	1.96		1.52	2.45
W	1.30	2.09	0.54	0.87		4.20	6.76		4.80	7.72
WNW	0.98	1.58	0.56	0.90		3.98	6.40		None	None
NW	0.88	1.42	0.62	0.99		None	None		0.98	1.58
NNW	0.93	1.50	0.72	1.16		1.93	3.11		1.13	1.82

Note: No milk cow or goats within a 5-mile radius of the NAPS. Source: Reference 37.

Table 2.3-16 XOQDOQ Predicted Maximum χ/Q and D/Q Values at Specific Points of Interest

Type of Location	Direction from Site	Distance (miles)	χ/Q (No Decay)	χ/Q (2.26 Day Decay)	χ/Q (8 Day Decay)	D/Q
Residence	NNE	0.96	2.4E-06	2.4E-06	2.1E-06	7.2E-09
EAB	ESE	0.88	3.7E-06	3.7E-06	3.3E-06	1.2E-08 ^a
Meat Animal	SE	1.37	1.4E-06	1.4E-06	1.2E-06	3.1E-09 ^b
Veg. Garden	NE	0.94	2.0E-06	2.0E-06	1.8E-06	6.0E-09

Notes:

χ/Q – sec/m³

D/Q – 1/m²

a. direction = south

b. direction = north-northeast

Table 2.3-17 XOQDOQ Predicted Maximum Annual Averages (Ground-Level Release)

No Decay Undepleted

Distance in Miles From the Site											
ESE	0.25	0.50	0.75	1.00	1.50	2.00	2.50	3.00	3.50	4.00	4.50
χ/Q (s/m ³)	2.685E-5	8.740E-6	4.697E-6	3.103E-6	1.742E-6	1.163E-6	8.527E-7	6.634E-7	5.373E-7	4.482E-7	3.822E-7
Distance in Miles From the Site											
ESE	5.00	7.50	10.00	15.00	20.00	25.00	30.00	35.00	40.00	45.00	50.00
χ/Q (s/m ³)	3.317E-7	1.934E-7	1.325E-7	7.833E-8	5.418E-8	4.079E-8	3.239E-8	2.668E-9	2.257E-8	1.948E-8	1.709E-8
Segment Boundaries in Miles From the Site											
ESE	0.5 - 1	1 - 2	2 - 3	3 - 4	4 - 5	5 - 10	10 - 20	20 - 30	30 - 40	40 - 50	
χ/Q (s/m ³)	4.887E-6	1.787E-6	8.596E-7	5.394E-7	3.831E-7	1.971E-7	7.964E-8	4.100E-8	2.675E-8	1.951E-8	

2.26 Day Decay, Undepleted

Distance in Miles From the Site											
ESE	0.25	0.50	0.75	1.00	1.50	2.00	2.50	3.00	3.50	4.00	4.50
χ/Q (s/m ³)	2.681E-5	8.712E-6	4.674E-6	3.083E-6	1.725E-6	1.148E-6	8.388E-7	6.504E-7	5.251E-7	4.365E-7	3.711E-7
Distance in Miles From the Site											
ESE	5.00	7.50	10.00	15.00	20.00	25.00	30.00	35.00	40.00	45.00	50.00
χ/Q (s/m ³)	3.210E-7	1.841E-7	1.241E-7	7.095E-8	4.750E-8	3.462E-8	2.662E-8	2.124E-8	1.740E-8	1.455E-8	1.237E-8
Segment Boundaries in Miles From the Site											
ESE	0.5 - 1	1 - 2	2 - 3	3 - 4	4 - 5	5 - 10	10 - 20	20 - 30	30 - 40	40 - 50	
χ/Q (s/m ³)	4.864E-6	1.770E-6	8.458E-7	5.272E-7	3.719E-7	1.878E-7	7.233E-8	3.485E-8	2.131E-8	1.459E-8	

Table 2.3-17 XOQDOQ Predicted Maximum Annual Averages (Ground-Level Release)

8.0 Day Decay, Depleted

Distance in Miles From the Site											
ESE	0.25	0.50	0.75	1.00	1.50	2.00	2.50	3.00	3.50	4.00	4.50
χ/Q (s/m ³)	2.540E-5	7.974E-6	4.180E-6	2.711E-6	1.475E-6	9.592E-7	6.875E-7	5.240E-7	4.166E-7	3.415E-7	2.866E-7
Distance in Miles From the Site											
ESE	5.00	7.50	10.00	15.00	20.00	25.00	30.00	35.00	40.00	45.00	50.00
χ/Q (s/m ³)	2.450E-7	1.344E-7	8.739E-8	4.735E-8	3.047E-8	2.153E-8	1.614E-8	1.261E-8	1.015E-8	8.357E-9	7.007E-9
Segment Boundaries in Miles From the Site											
ESE	0.5 - 1	1 - 2	2 - 3	3 - 4	4 - 5	5 - 10	10 - 20	20 - 30	30 - 40	40 - 50	
χ/Q (s/m ³)	4.370E-6	1.521E-6	6.945E-7	4.187E-7	2.874E-7	1.381E-7	4.874E-8	2.176E-8	1.268E-8	8.388E-9	
Relative Deposition/Area											
Distance in Miles from Site											
NNE	0.25	0.50	0.75	1.00	1.50	2.00	2.50	3.00	3.50	4.00	4.50
D/Q (1/m ²)	6.2570E-8	2.116E-8	1.086E-8	6.671E-9	3.326E-9	2.017E-9	1.364E-9	9.882E-10	7.514E-10	5.920E-10	4.793E-10
Distance in Miles from Site											
NNE	5.00	7.50	10.00	15.00	20.00	25.00	30.00	35.00	40.00	45.00	50.00
D/Q (1/m ²)	3.964E-10	1.943E-10	1.219E-10	6.161E-11	3.729E-11	2.500E-11	1.792E-11	1.345E-11	1.046E-11	8.355E-12	6.820E-12
Segment Boundaries in Miles From the Site											
NNE	0.5 - 1	1 - 2	2 - 3	3 - 4	4 - 5	5 - 10	10 - 20	20 - 30	30 - 40	40 - 50	
D/Q (1/m ²)	1.129E-8	3.487E-9	1.388E-9	7.583E-10	4.820E-10	2.070E-10	6.420E-10	2.544E-11	1.359E-11	8.410E-12	

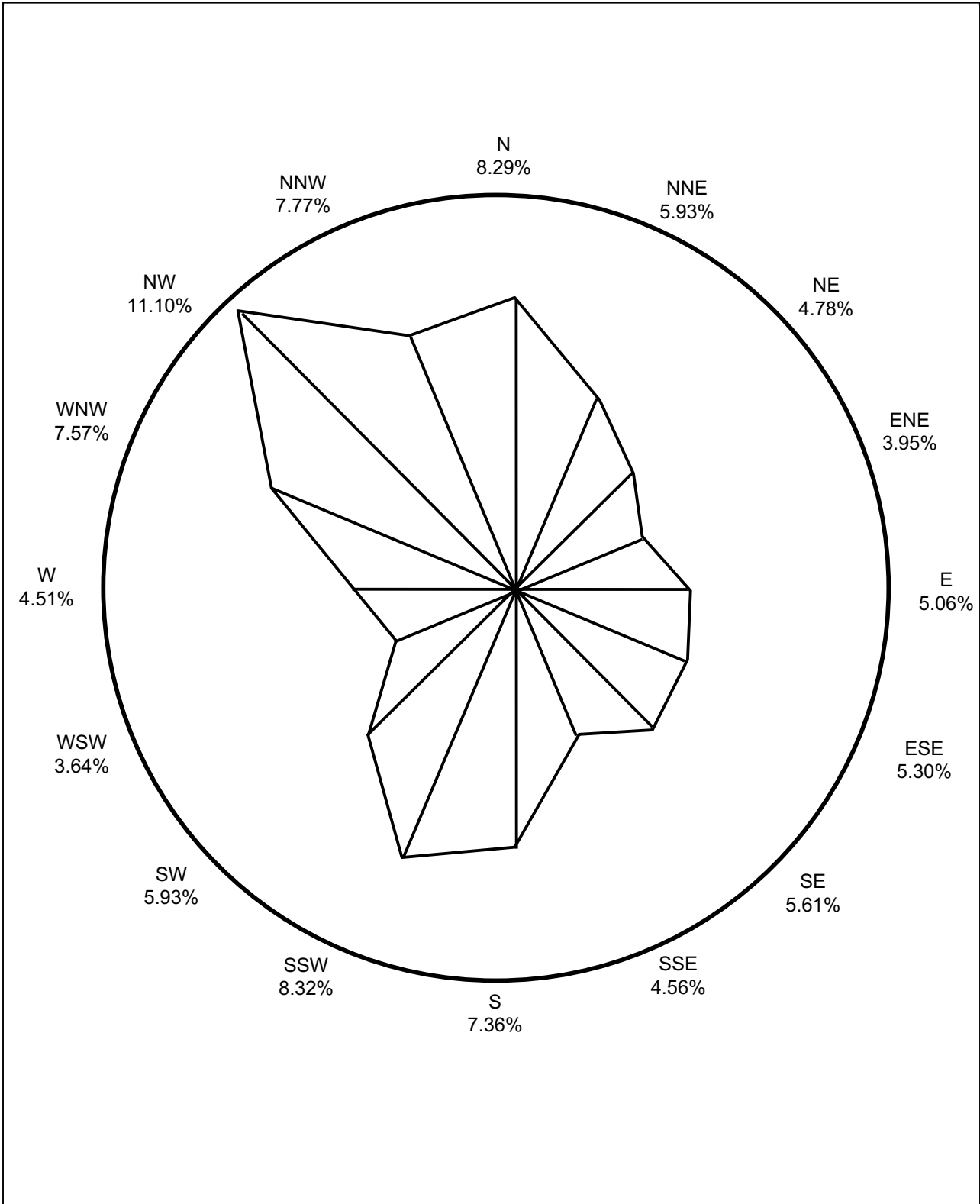


Figure 2.3-1 North Anna Seasonal Wind Direction Roses: Low-Level Winds: 1974-1987: Season = Spring

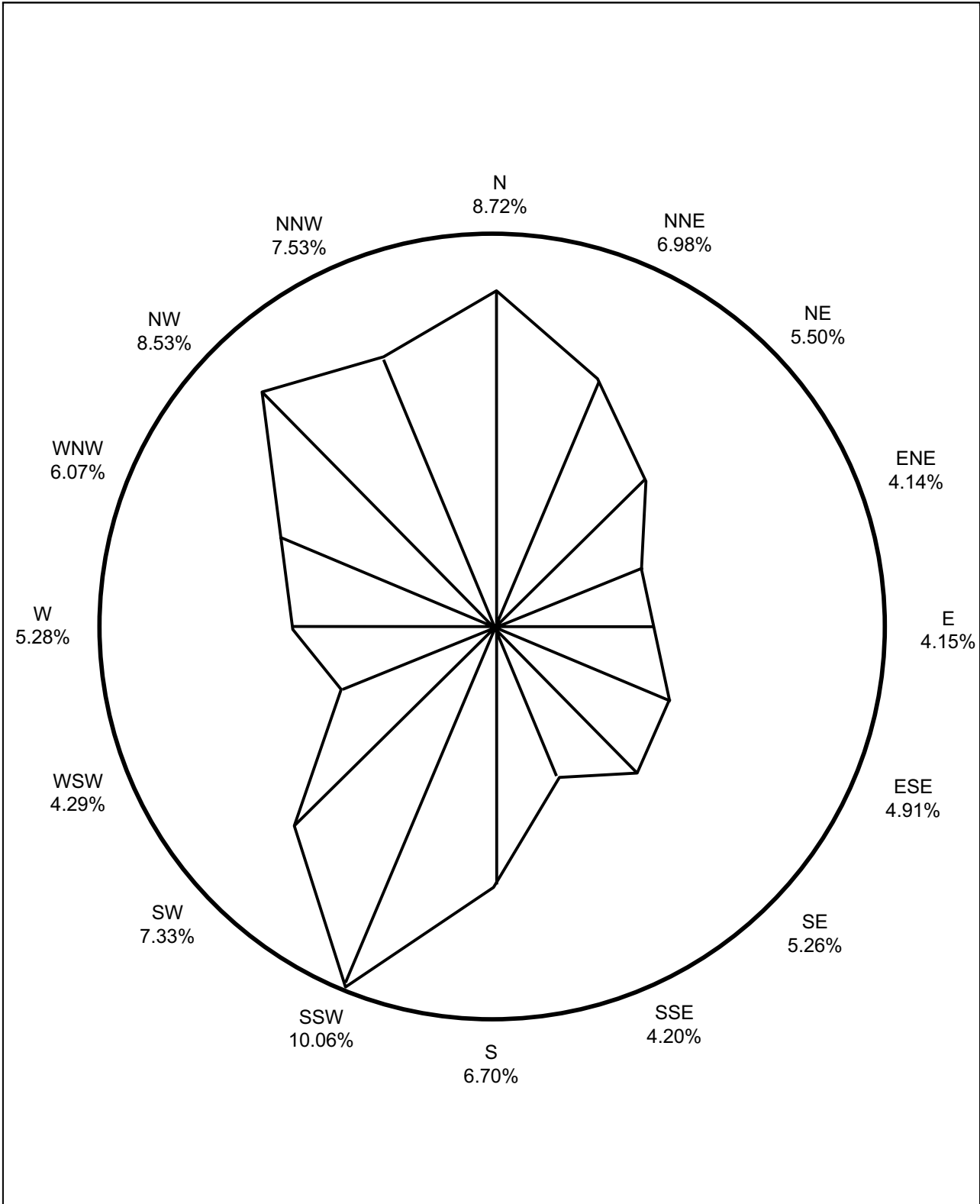


Figure 2.3-2 North Anna Seasonal Wind Direction Roses: High-Level Winds: 1974-1987: Season = Spring

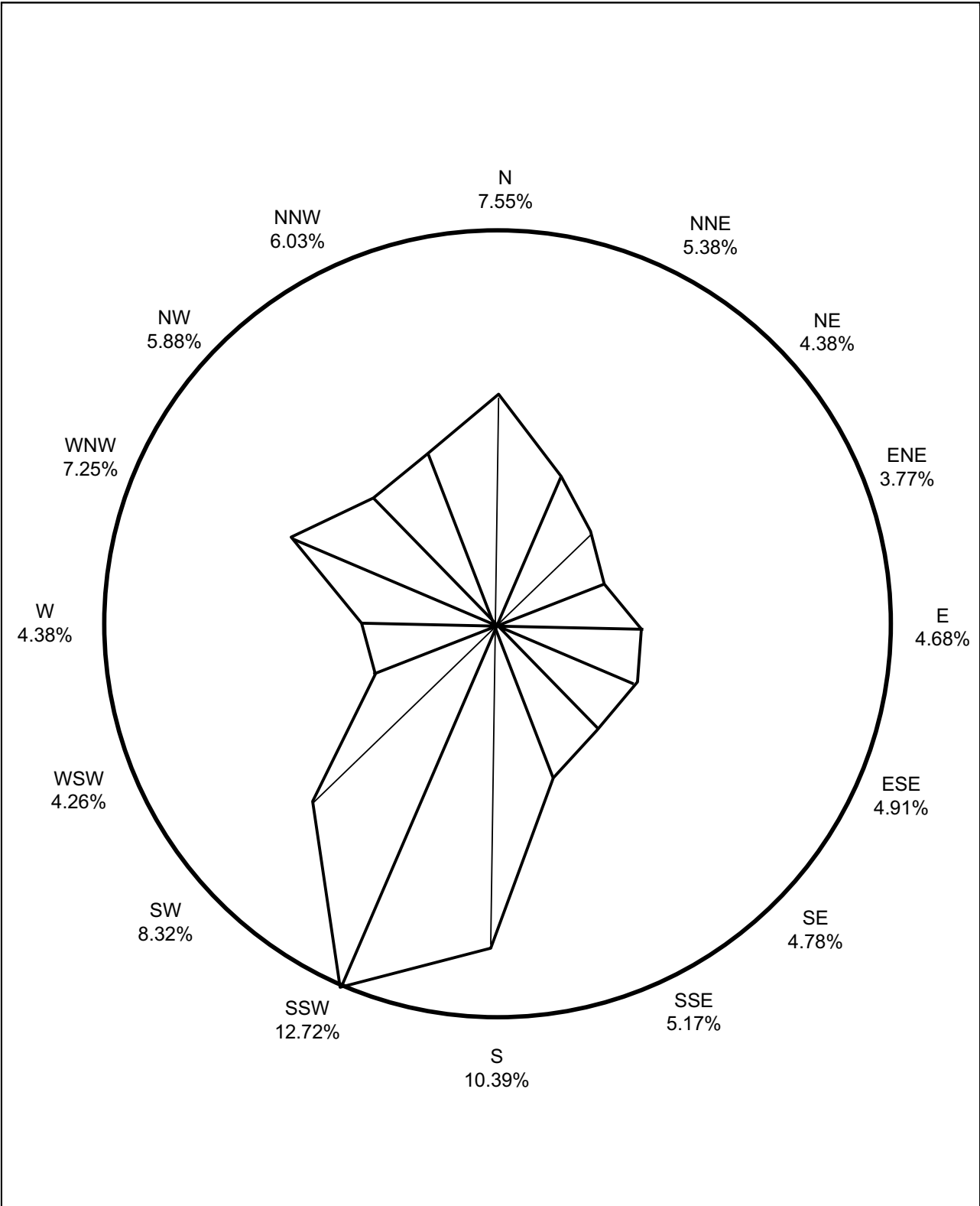


Figure 2.3-3 North Anna Seasonal Wind Direction Roses: Low-Level Winds: 1974-1987: Season = Summer

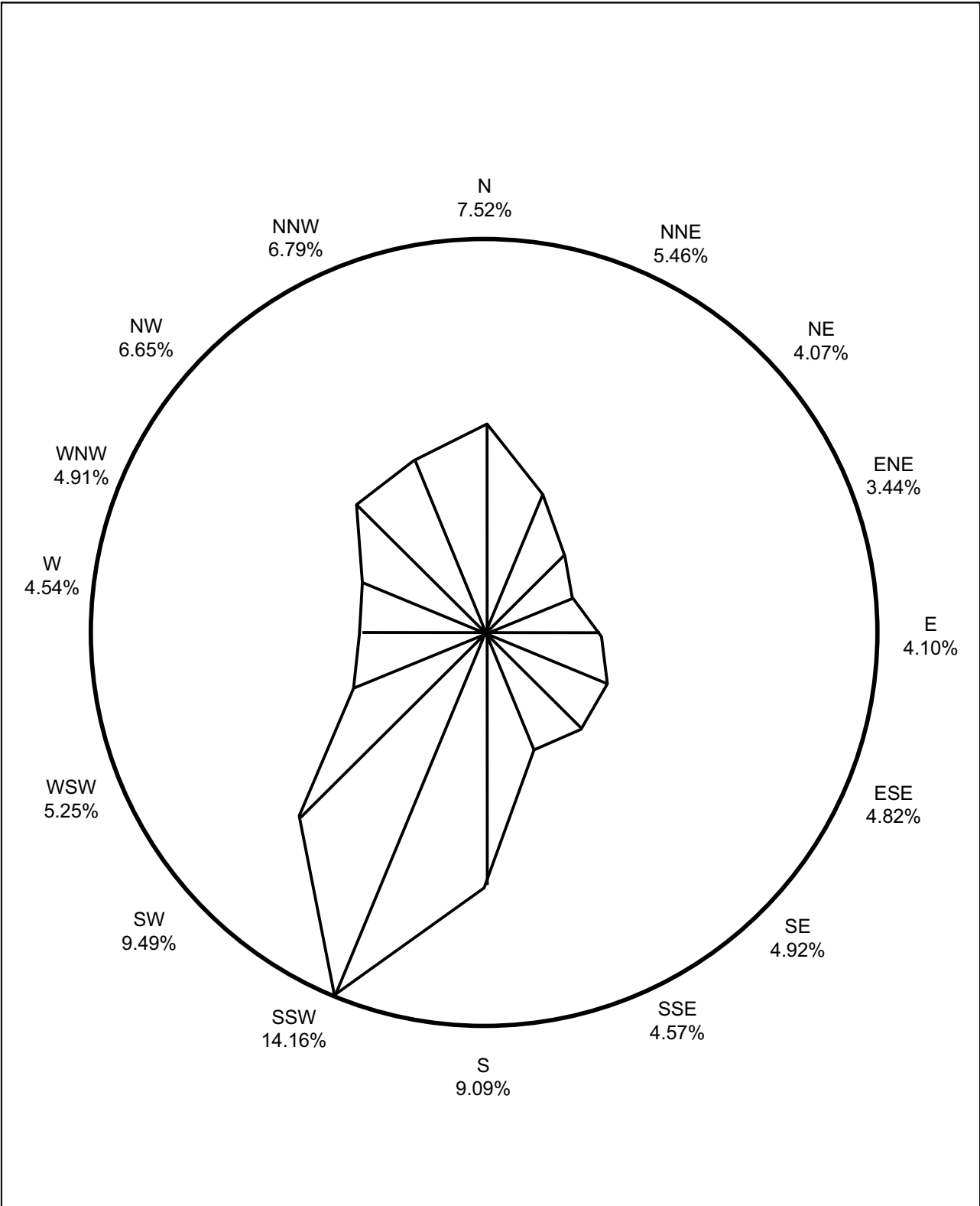


Figure 2.3-4 North Anna Seasonal Wind Direction Roses: High-Level Winds: 1974-1987: Season = Summer

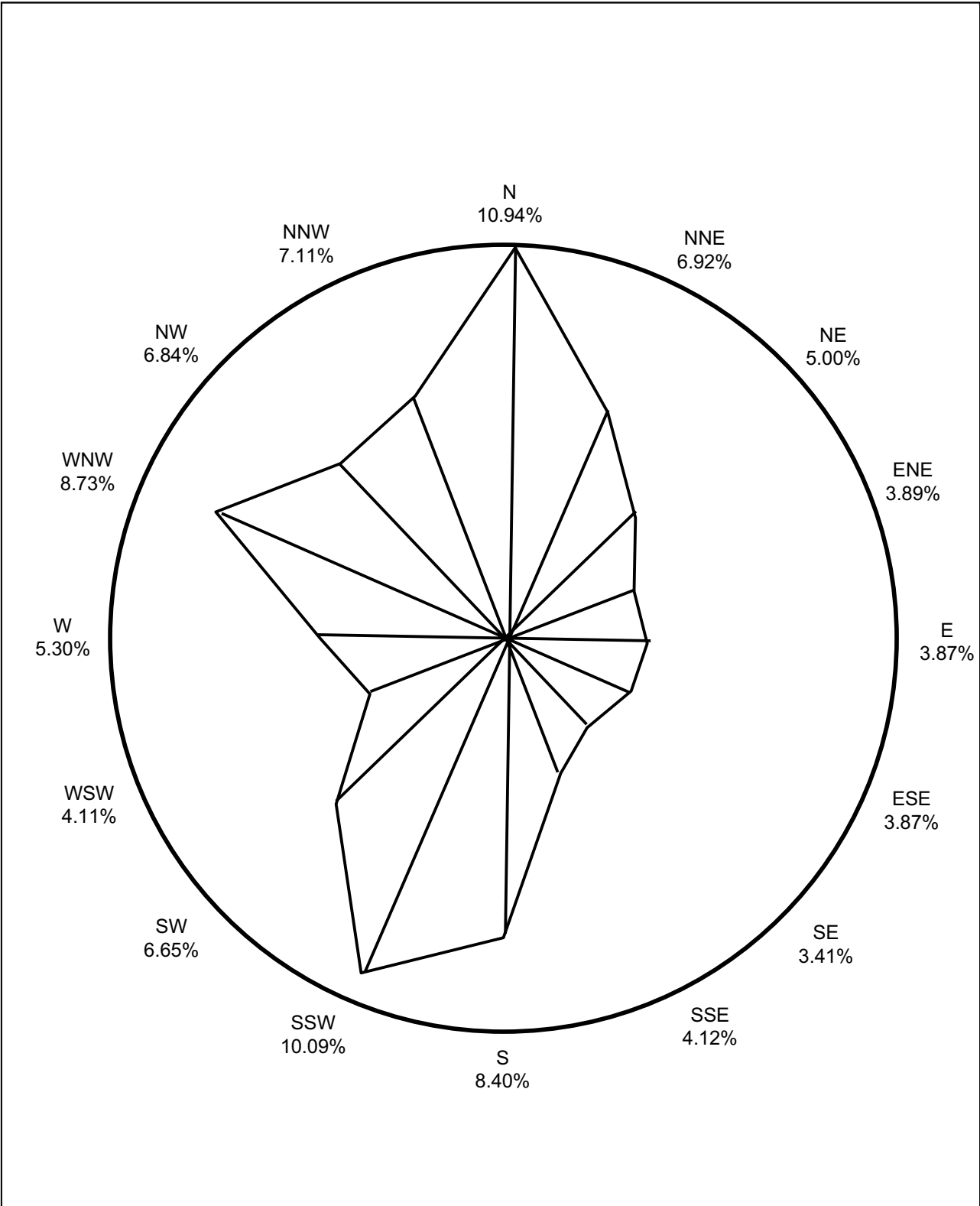


Figure 2.3-5 North Anna Seasonal Wind Direction Roses: Low-Level Winds: 1974-1987: Season = Fall

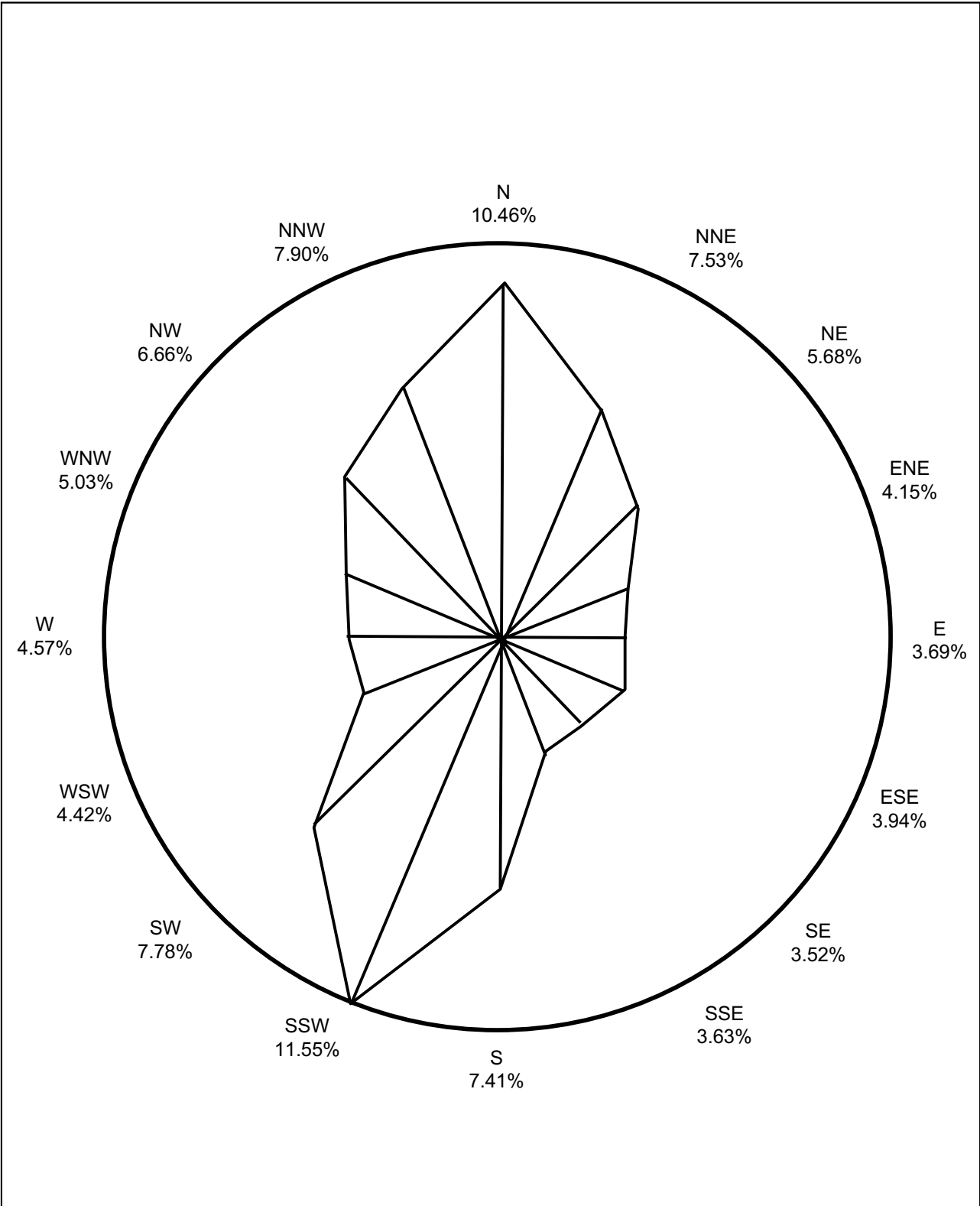


Figure 2.3-6 North Anna Seasonal Wind Direction Roses: High-Level Winds: 1974-1987: Season = Fall

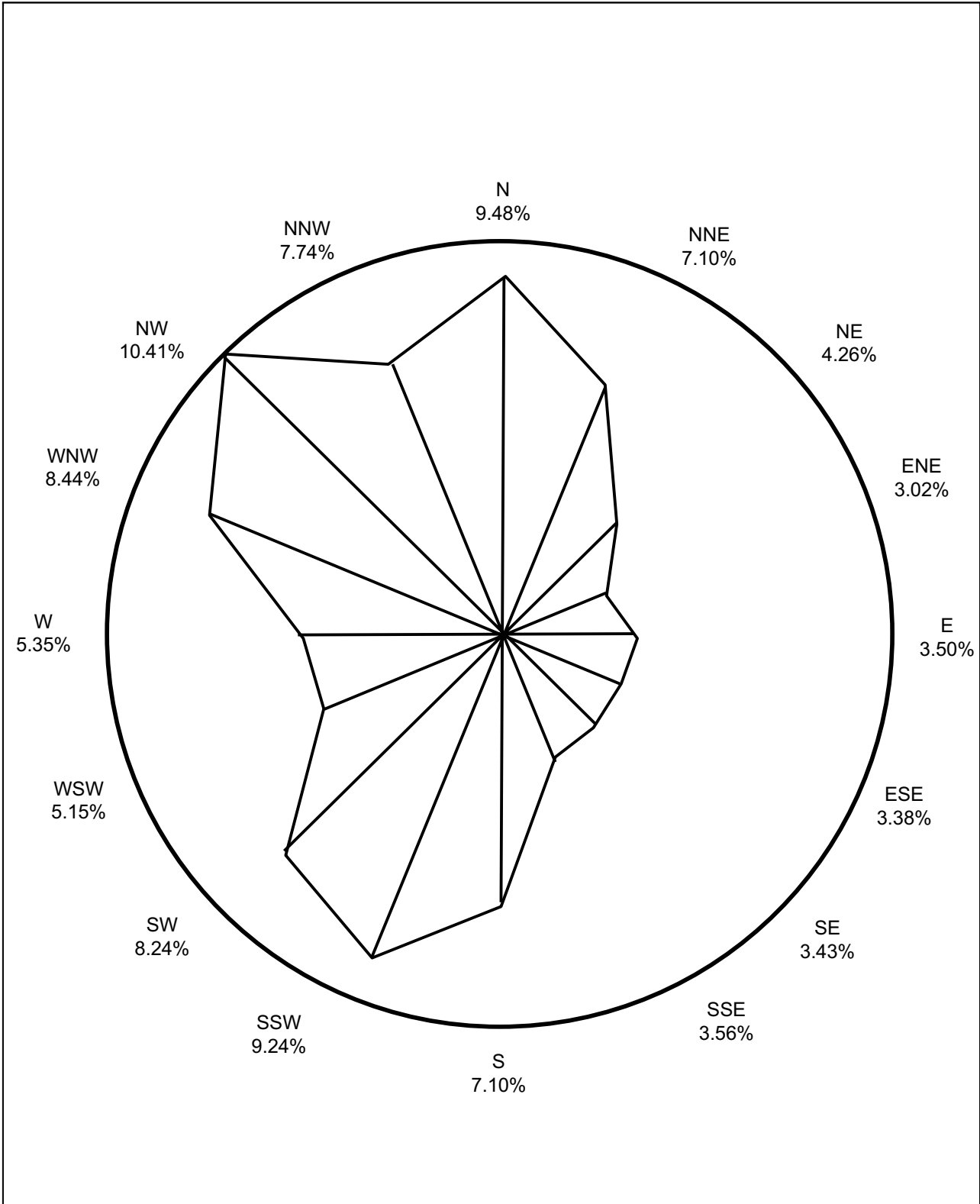


Figure 2.3-7 North Anna Seasonal Wind Direction Roses: Low-Level Winds: 1974-1987: Season = Winter

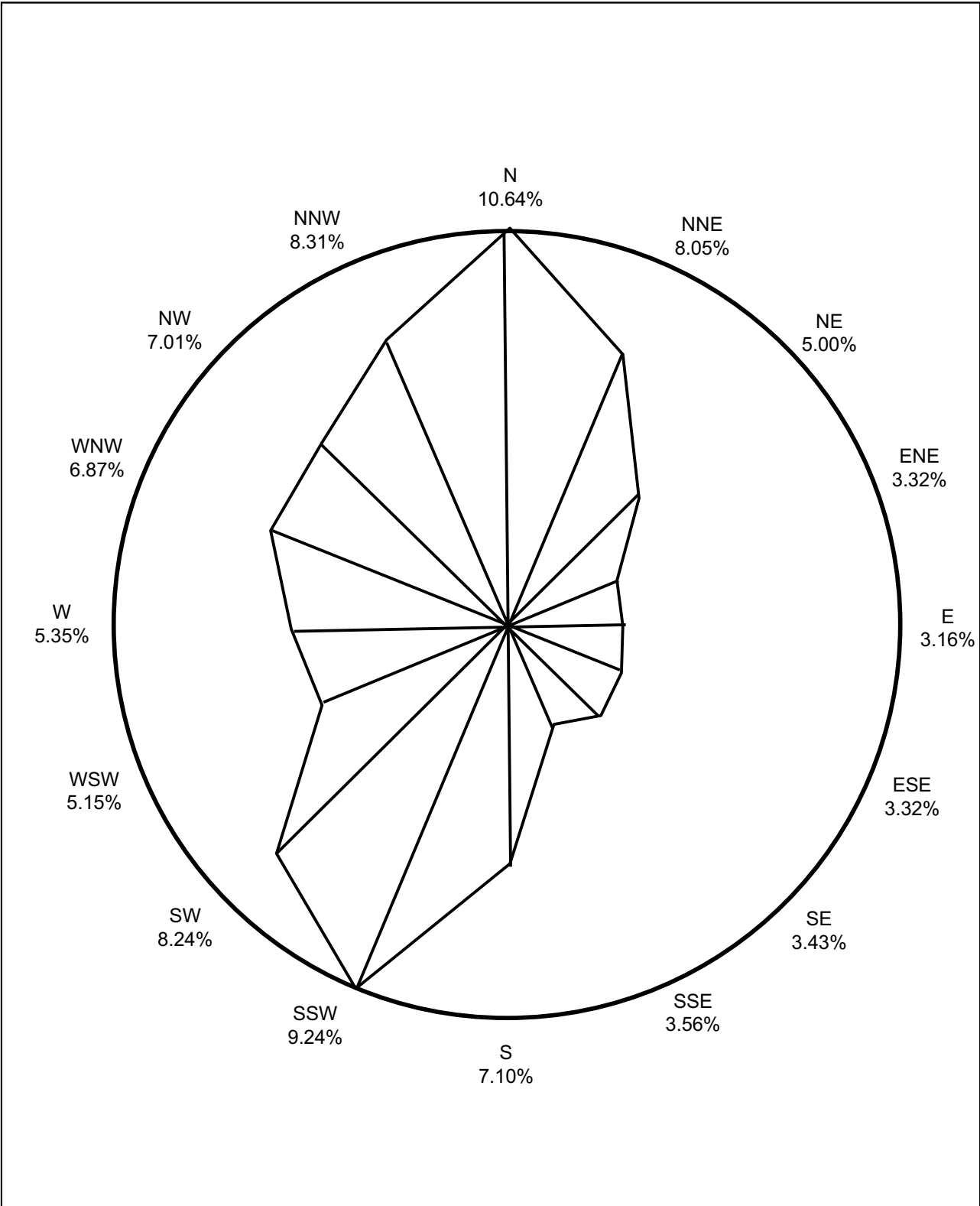
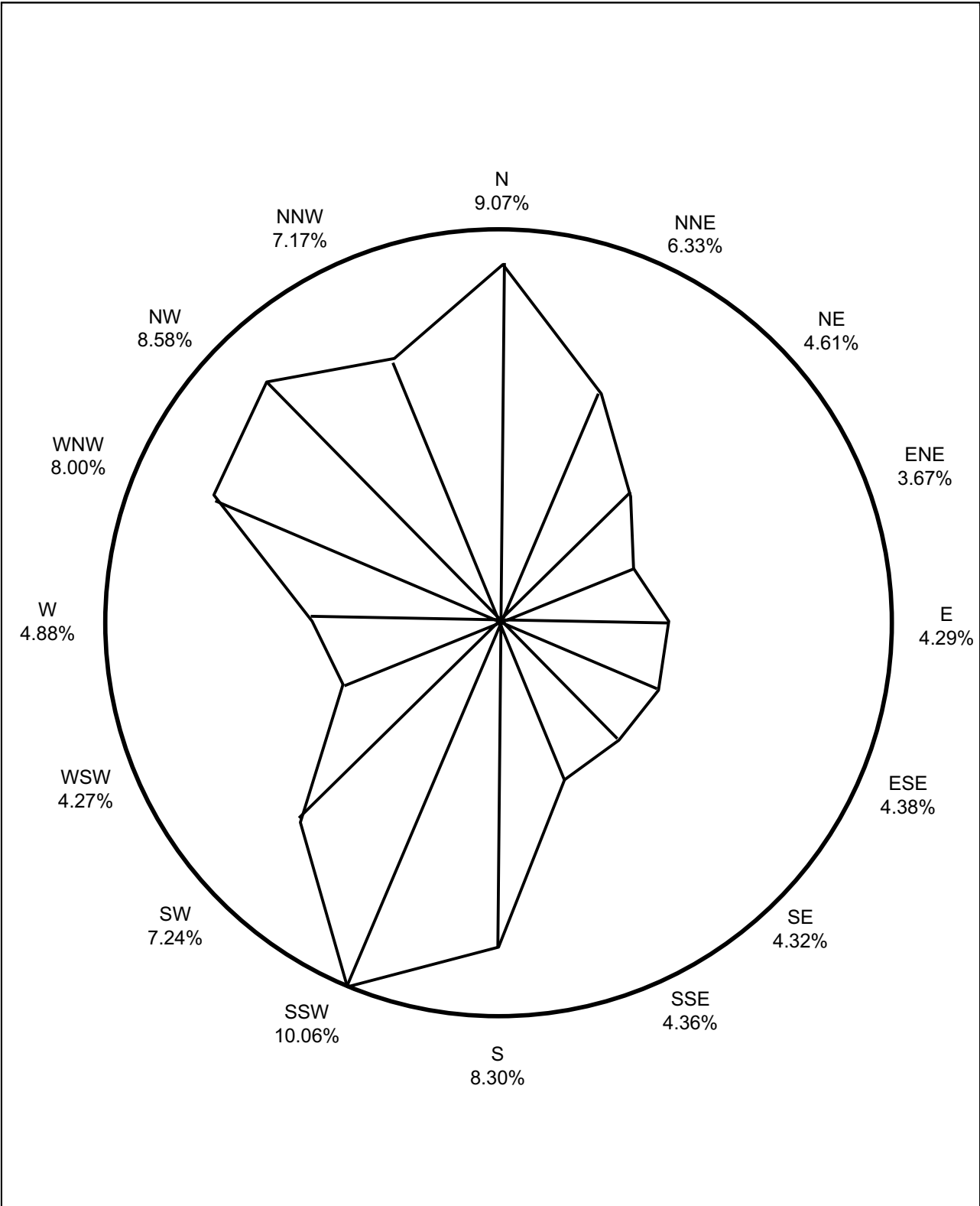


Figure 2.3-8 North Anna Seasonal Wind Direction Roses: High-Level Winds: 1974-1987: Season = Winter



**Figure 2.3-9 North Anna Seasonal Wind Direction Roses: Low-Level Winds:
1974-1987: Season = Overall**

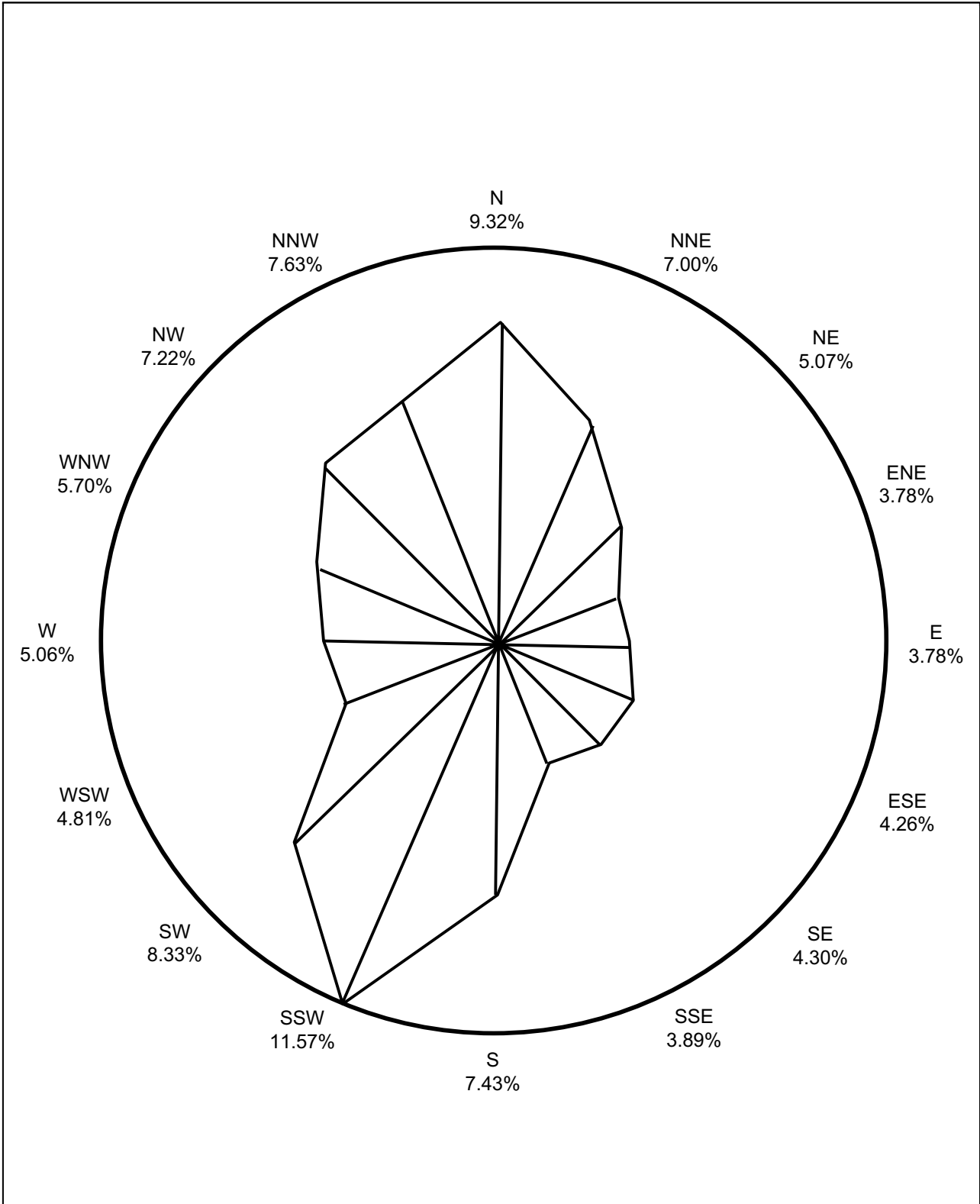


Figure 2.3-10 North Anna Seasonal Wind Direction Roses: High-Level Winds: 1974-1987: Season = Overall

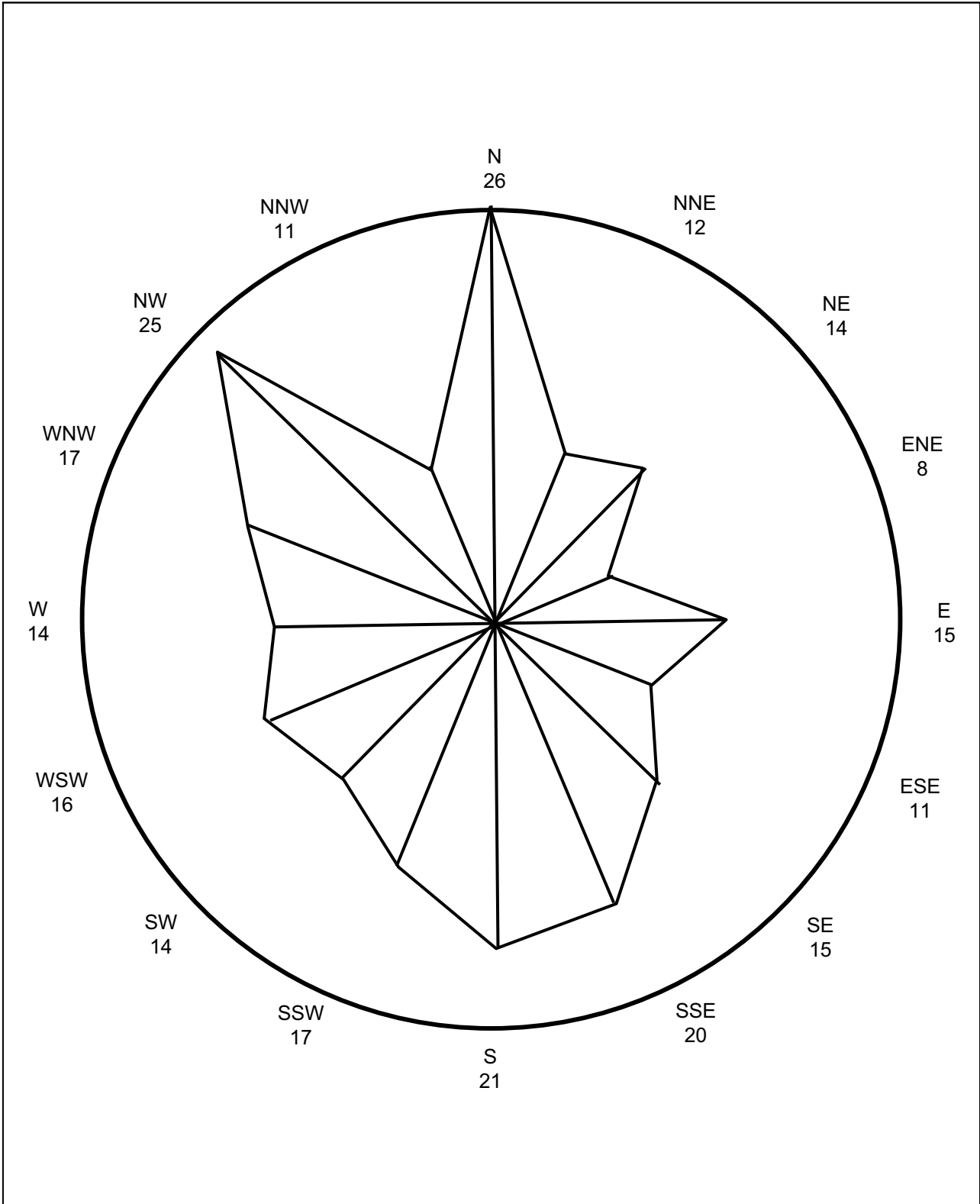


Figure 2.3-11 North Anna Seasonal Wind Persistence Roses: Low-Level Winds: 1974–1987: Season = Spring

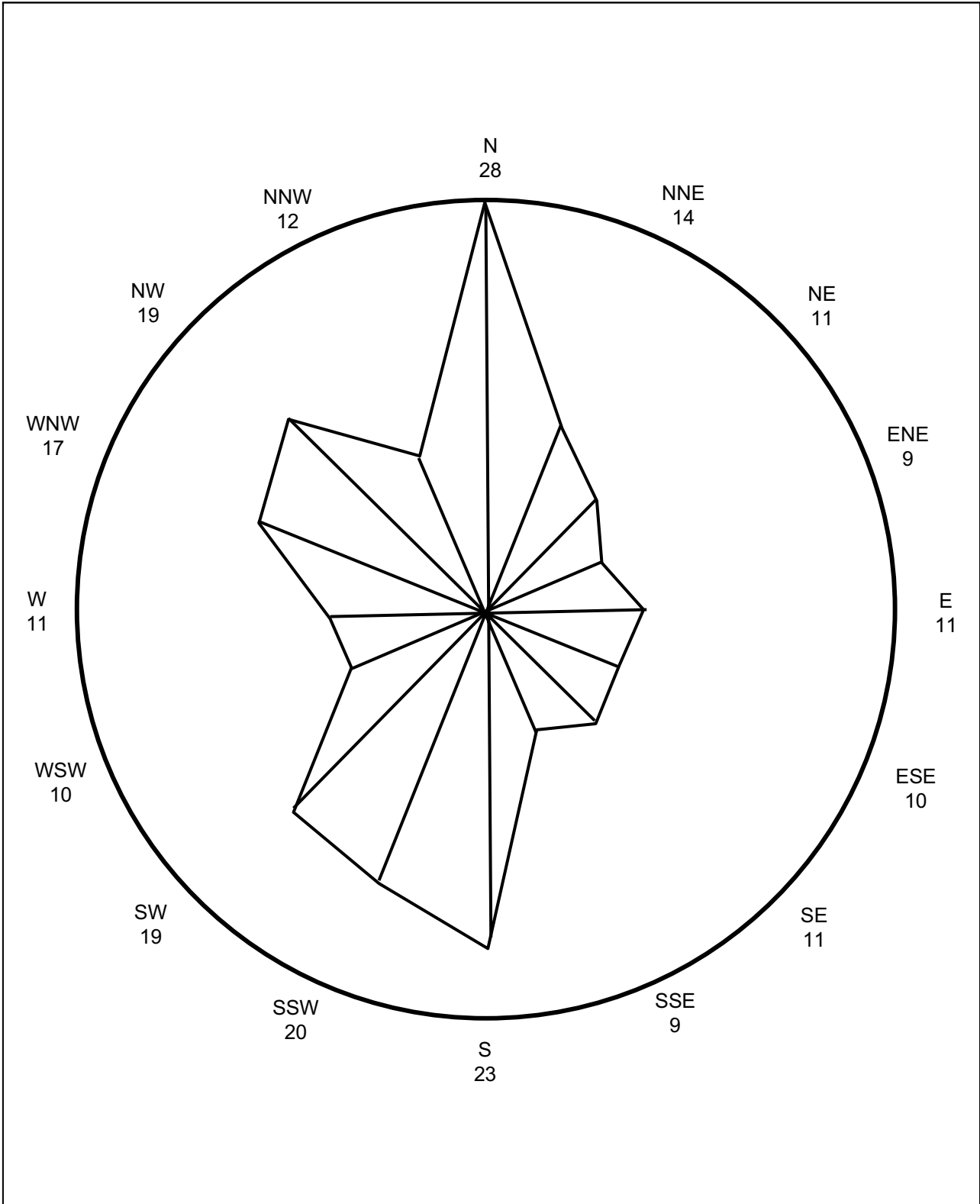


Figure 2.3-12 North Anna Seasonal Wind Persistence Roses: High-Level Winds: 1974-1987: Season = Spring

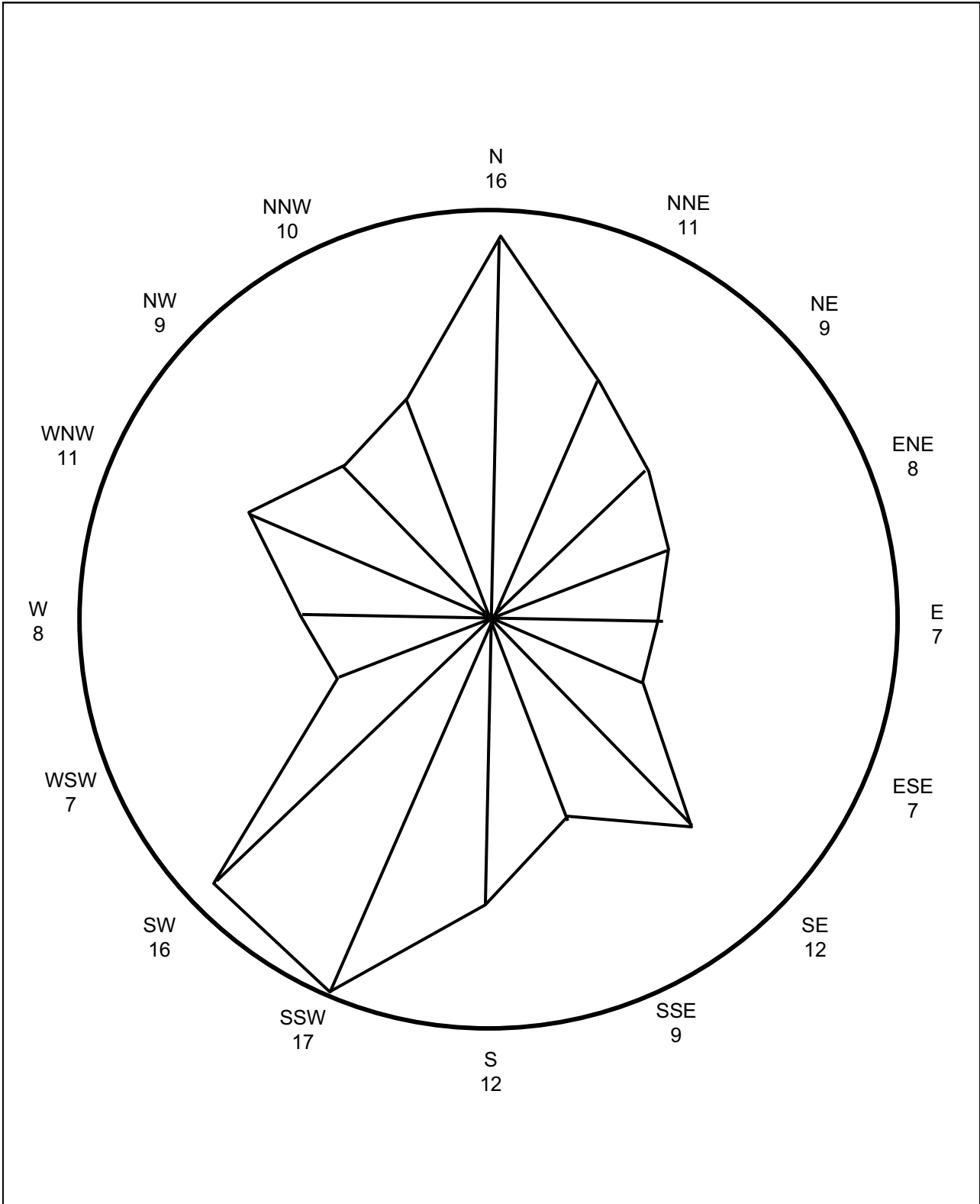


Figure 2.3-13 North Anna Seasonal Wind Persistence Roses: Low-Level Winds: 1974-1987: Season = Summer

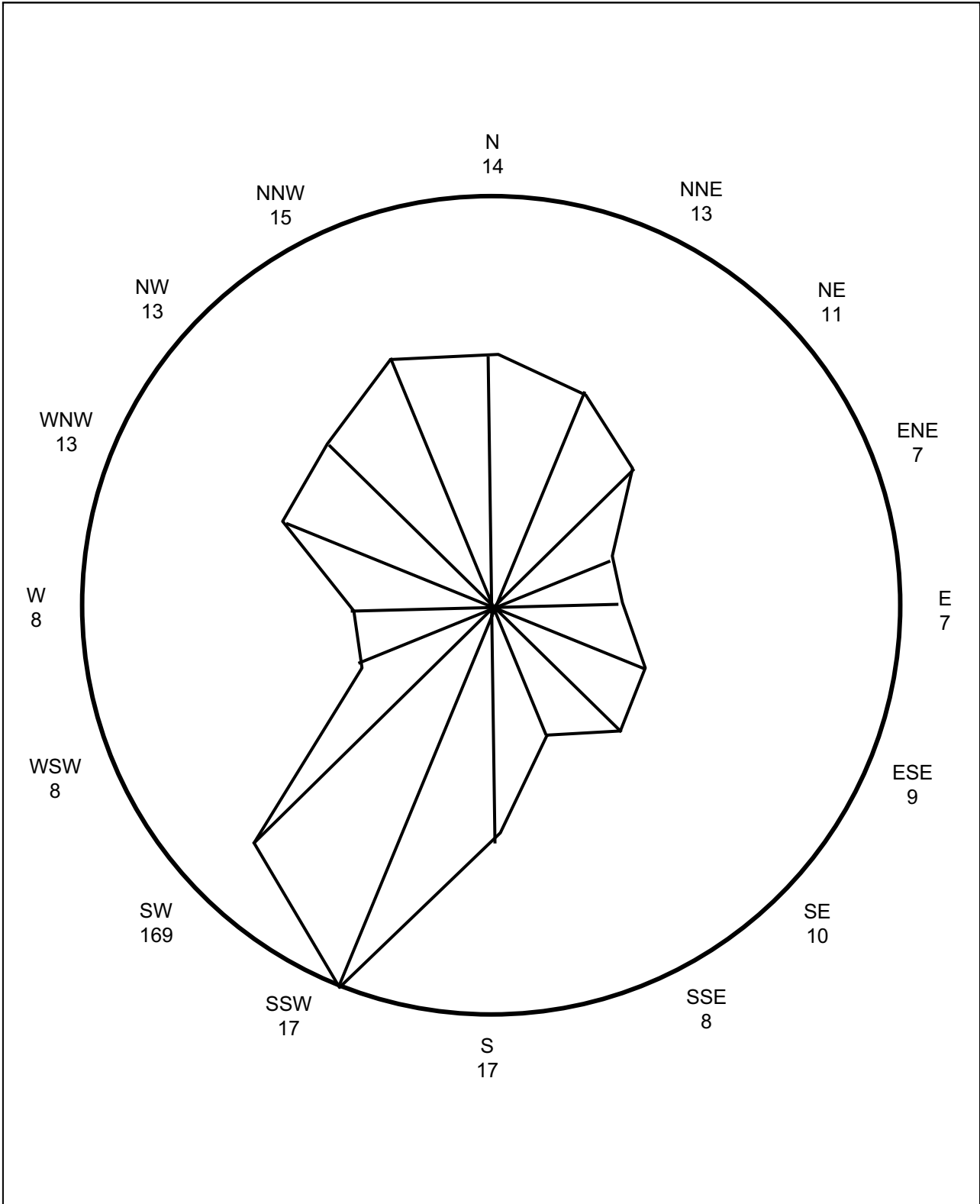


Figure 2.3-14 North Anna Seasonal Wind Persistence Roses: High-Level Winds: 1974-1987: Season = Summer

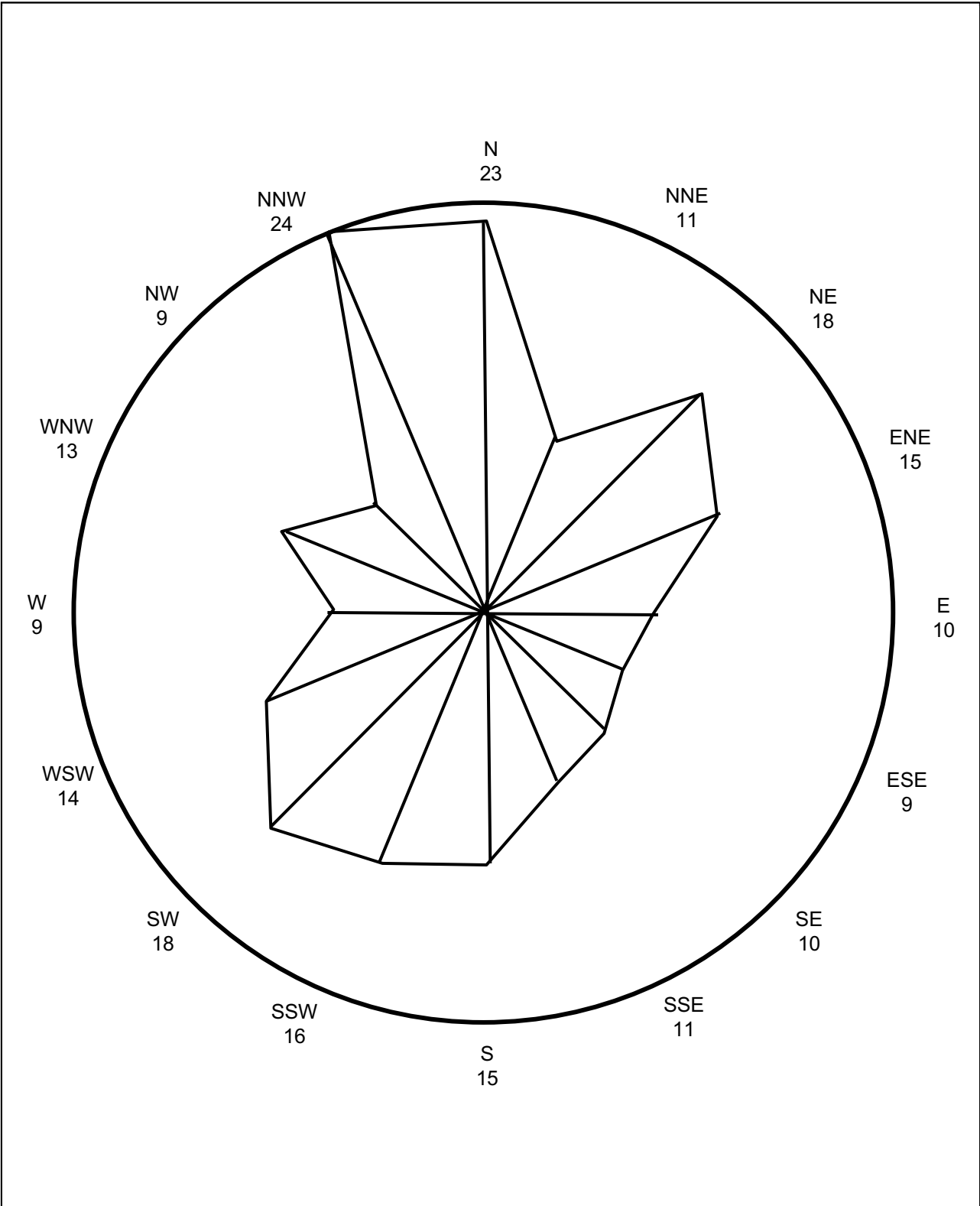


Figure 2.3-15 North Anna Seasonal Wind Persistence Roses: Low-Level Winds: 1974-1987: Season = Fall

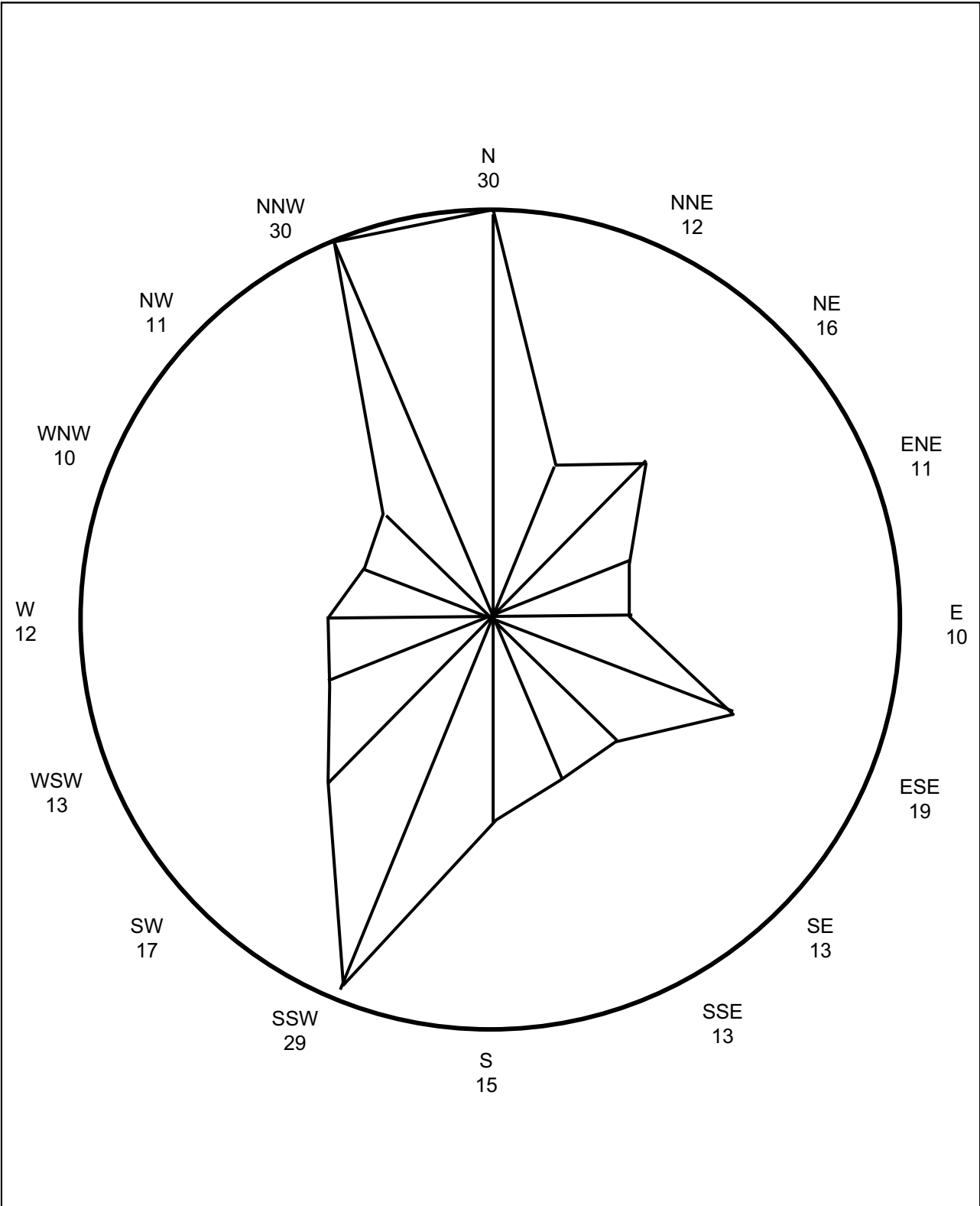


Figure 2.3-16 North Anna Seasonal Wind Persistence Roses: High-Level Winds: 1974-1987: Season = Fall

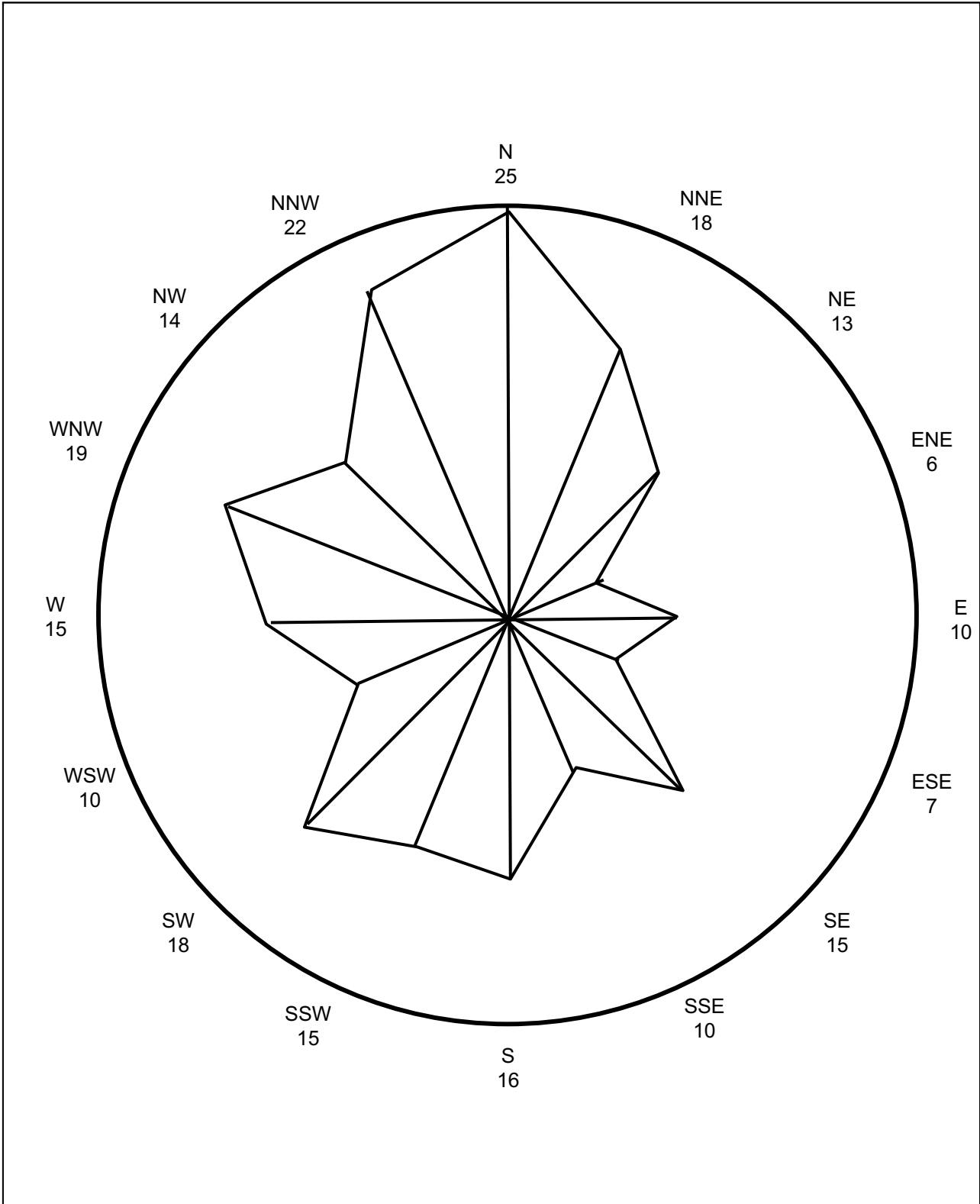


Figure 2.3-17 North Anna Seasonal Wind Persistence Roses: Low-Level Winds: 1974-1987: Season = Winter

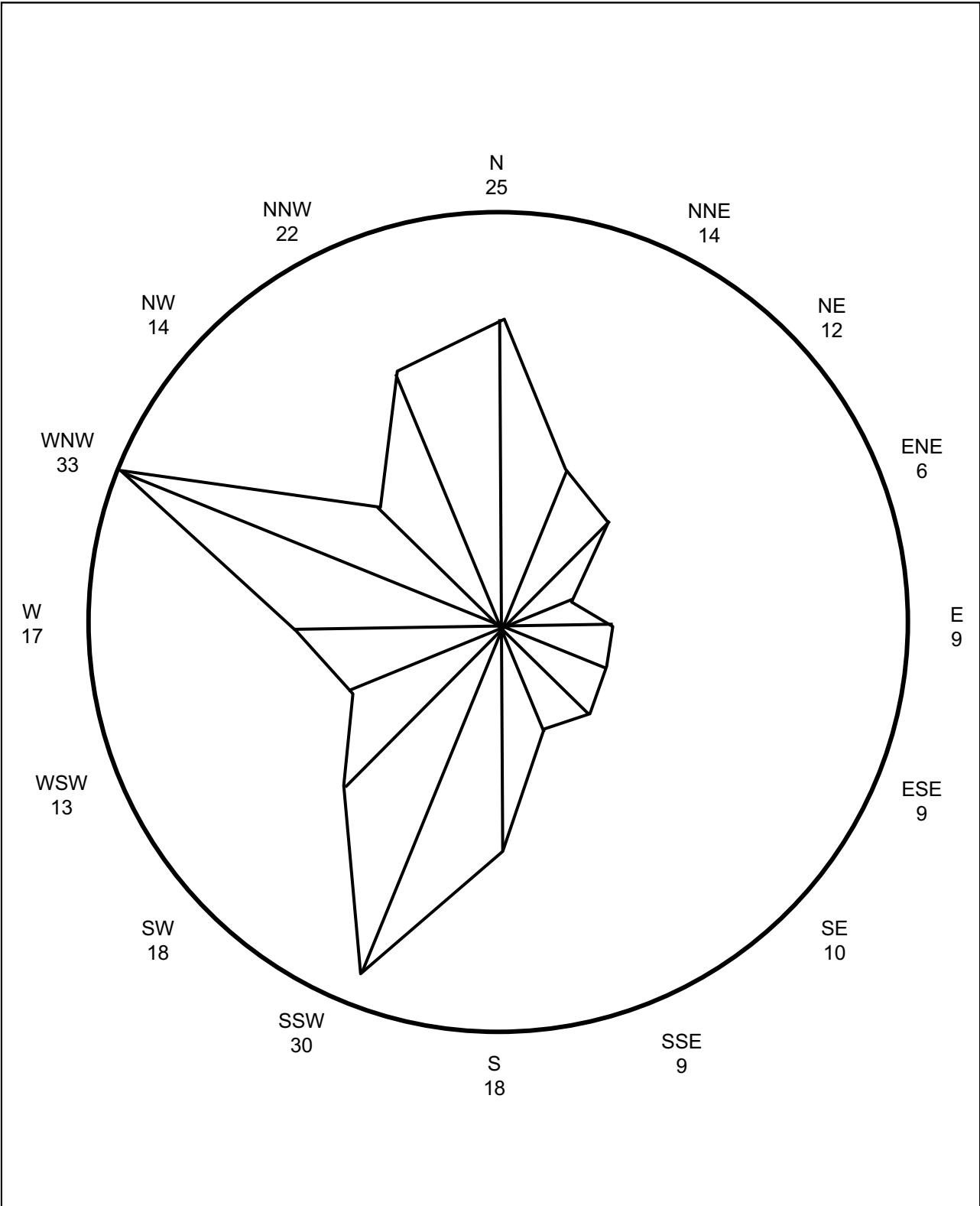


Figure 2.3-18 North Anna Seasonal Wind Persistence Roses: High-Level Winds: 1974–1987: Season = Winter

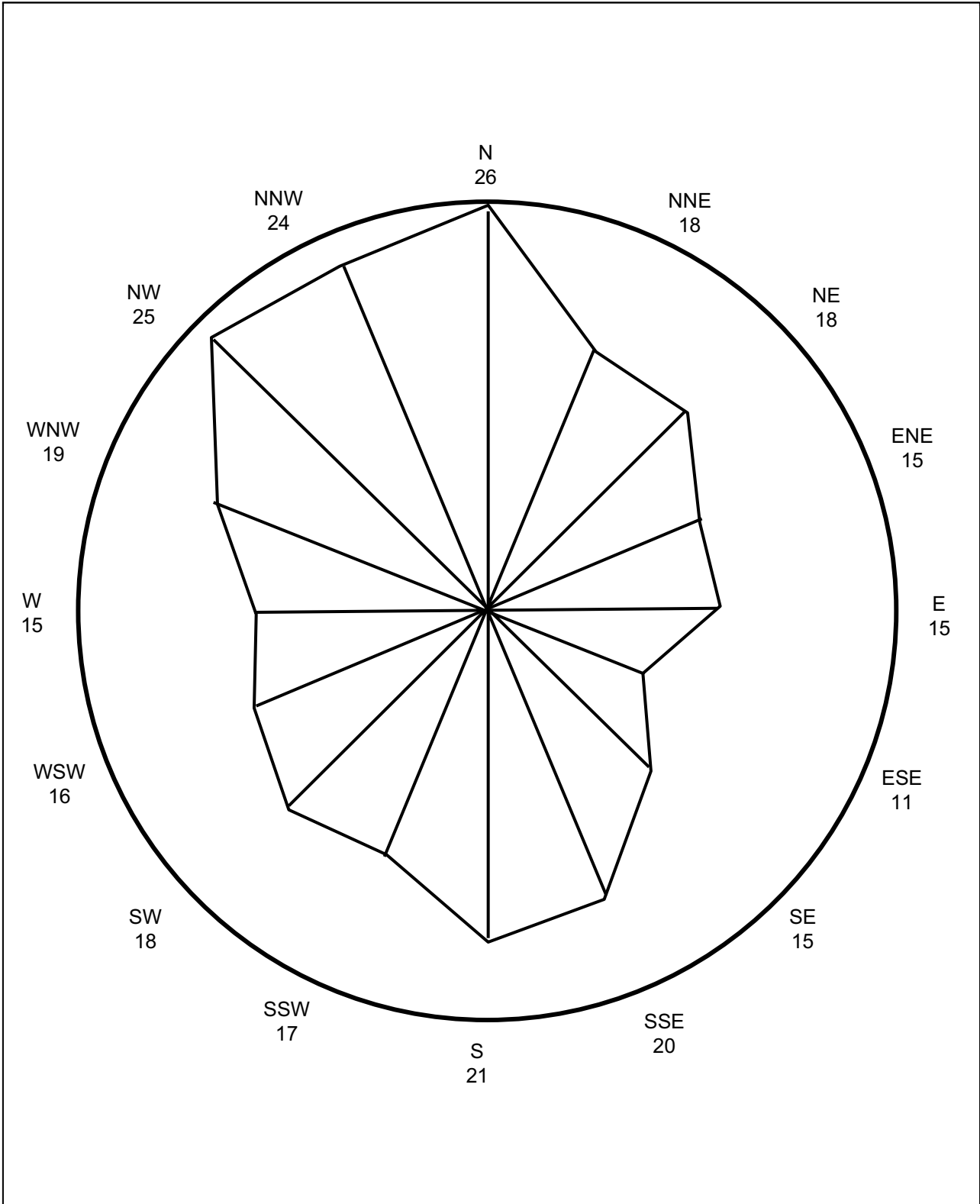


Figure 2.3-19 North Anna Seasonal Wind Persistence Roses: Low-Level Winds: 1974-1987: Season = Overall

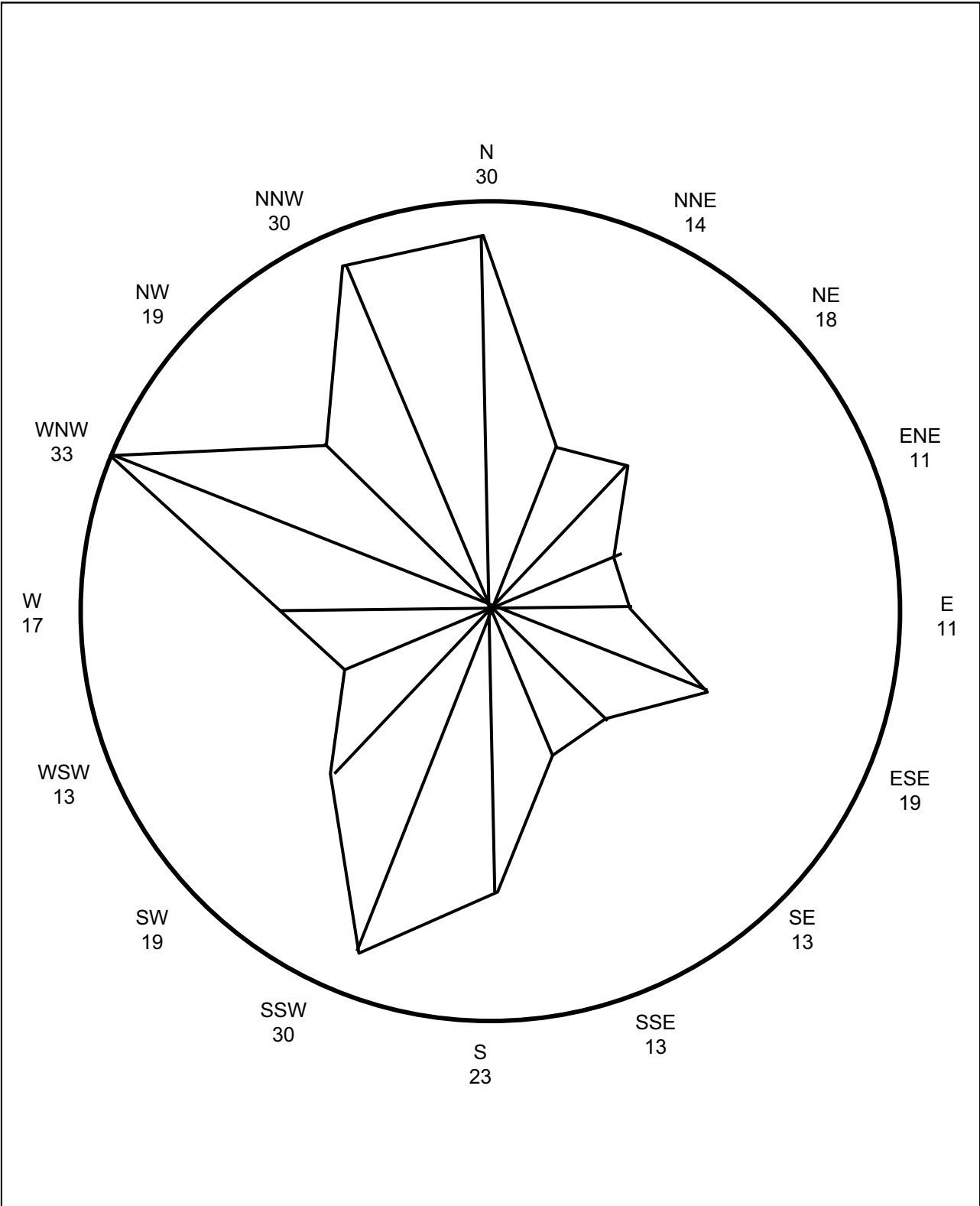


Figure 2.3-20 North Anna Seasonal Wind Persistence Roses: High-Level Winds: 1974–1987: Season = Overall

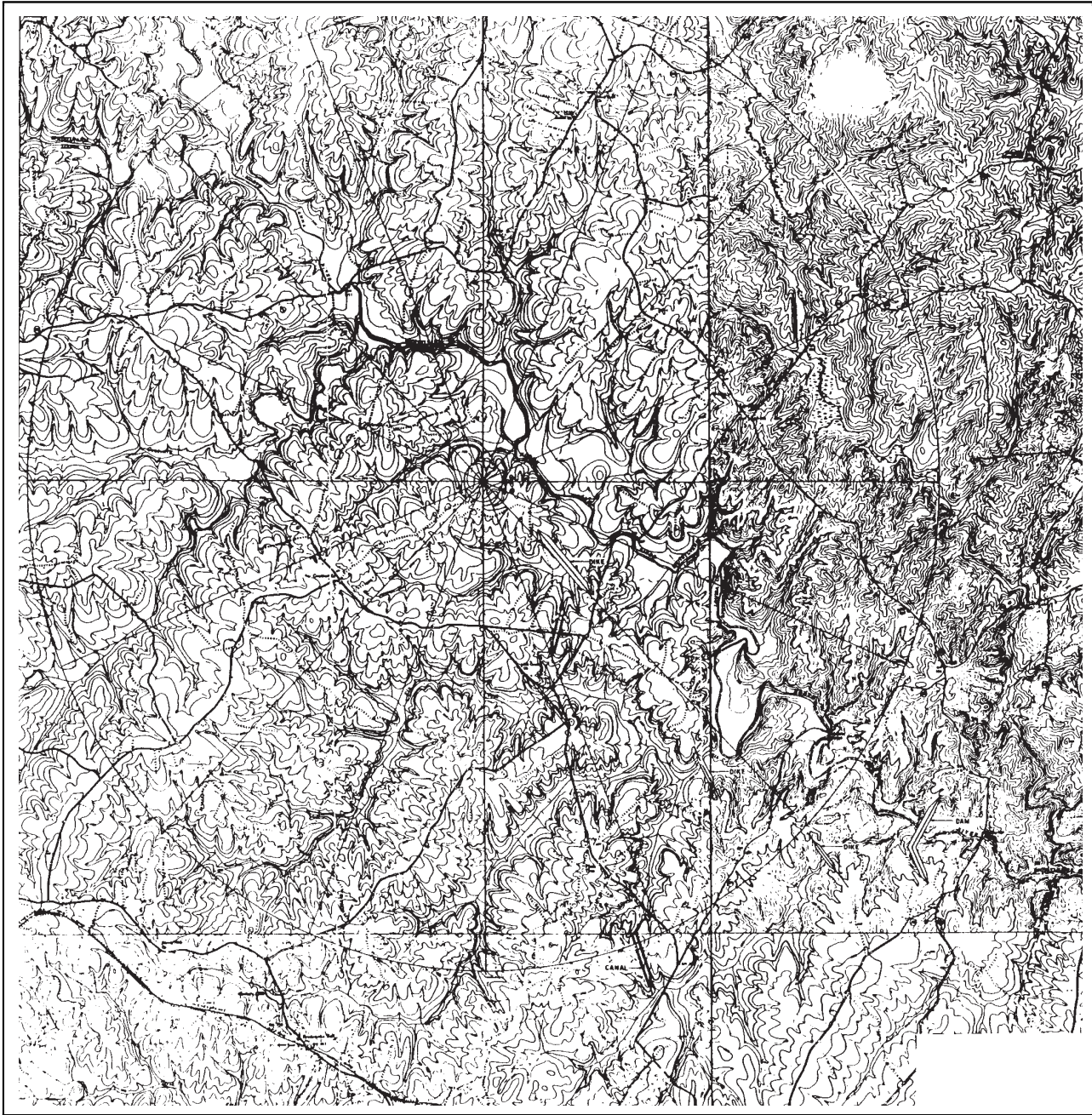


Figure 2.3-21 Topographic Map

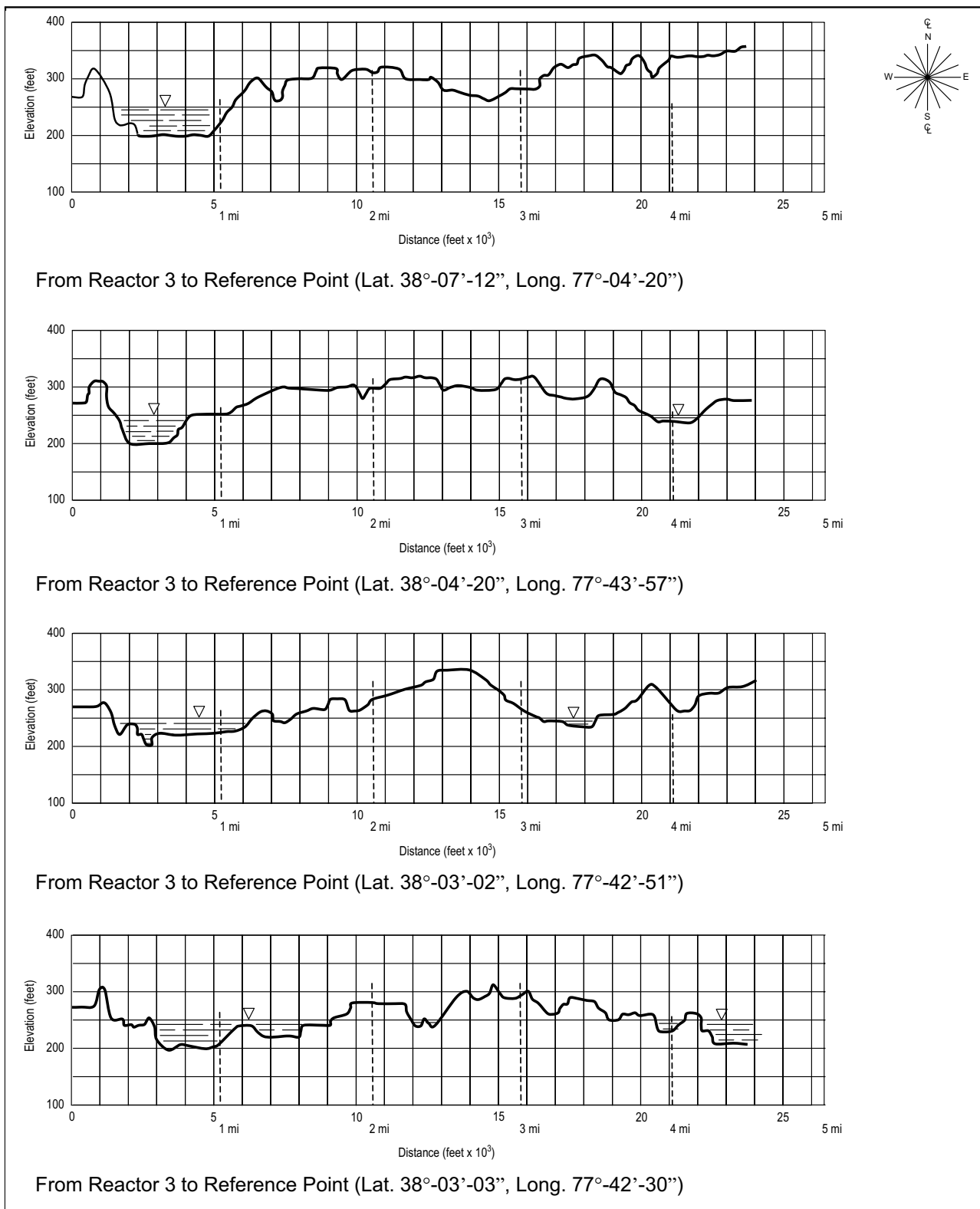


Figure 2.3-22 Vertical Profiles (Sheet 1 of 4)

Source: Reference 13

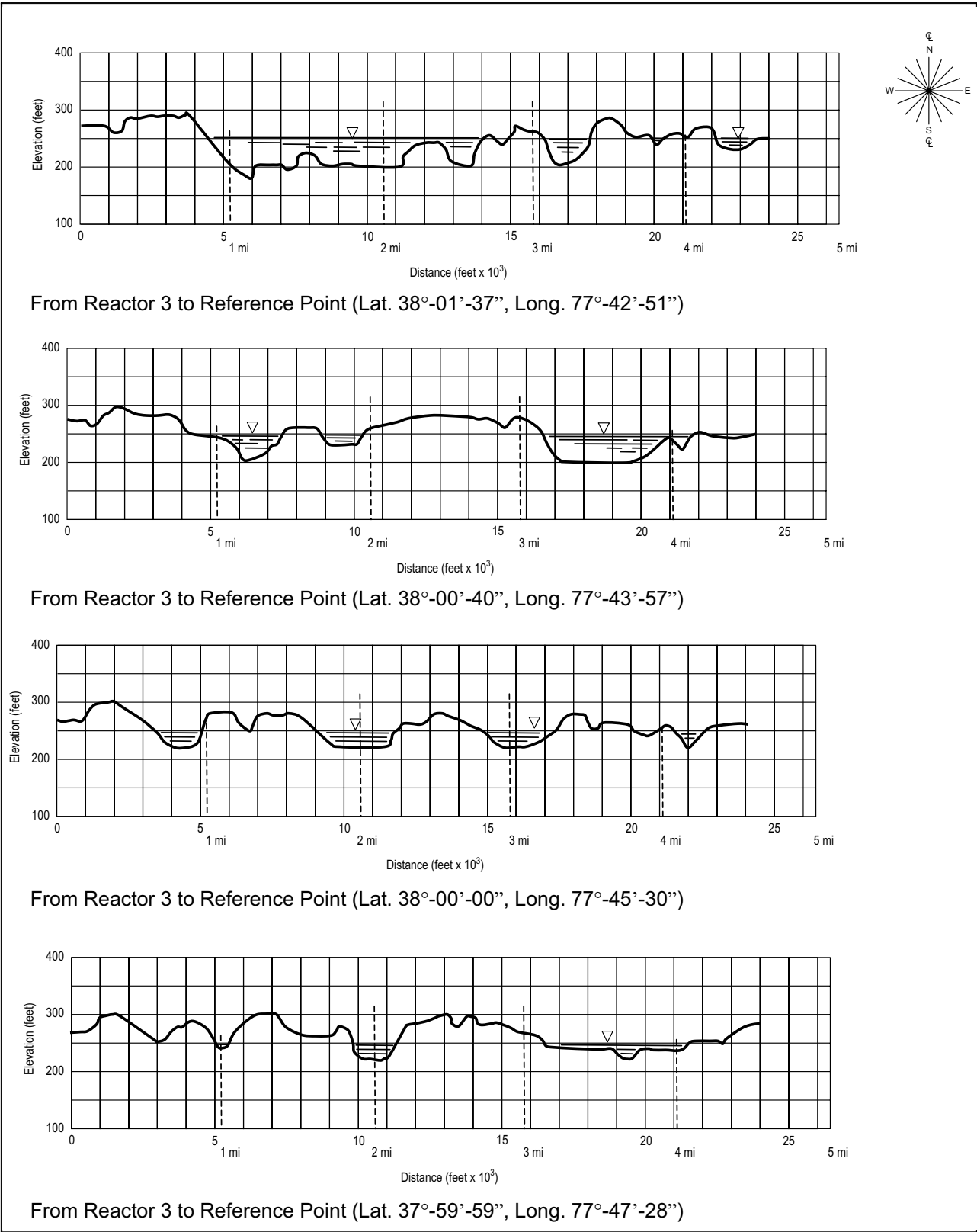


Figure 2.3-22 Vertical Profiles (Sheet 2 of 4)

Source: Reference 13

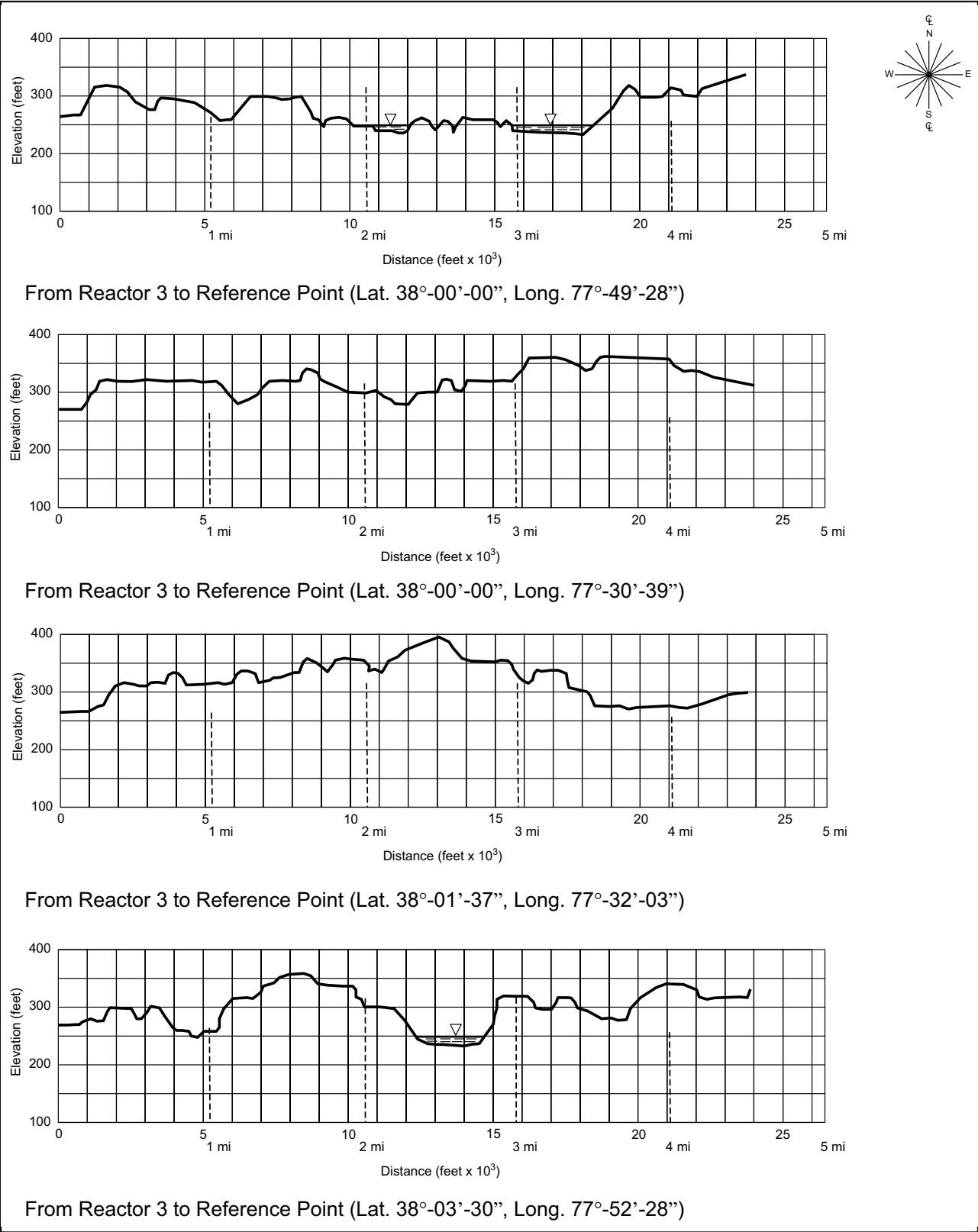


Figure 2.3-22 Vertical Profiles (Sheet 3 of 4)

Source: Reference 13

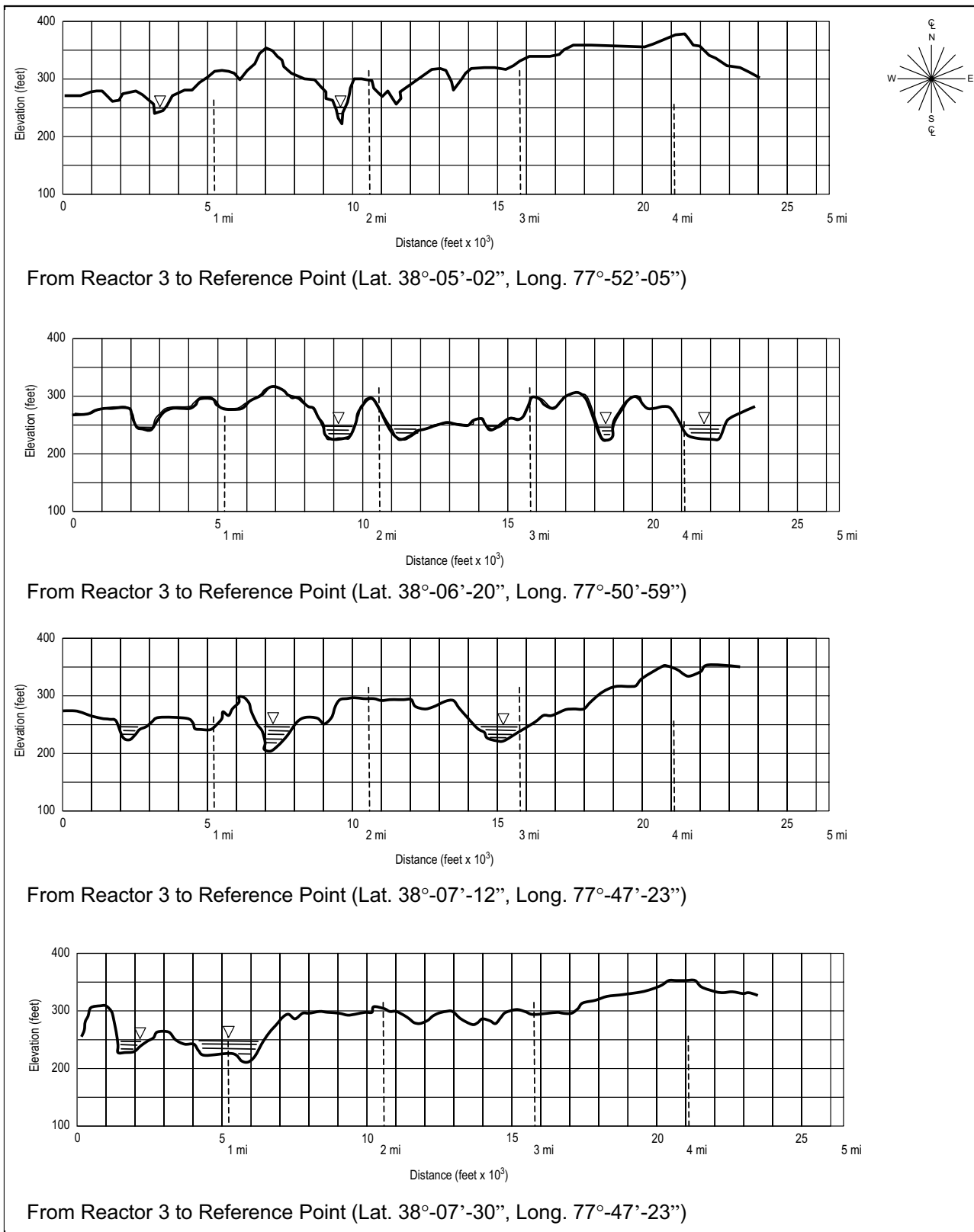


Figure 2.3-22 Vertical Profiles (Sheet 4 of 4)

Source: Reference 13

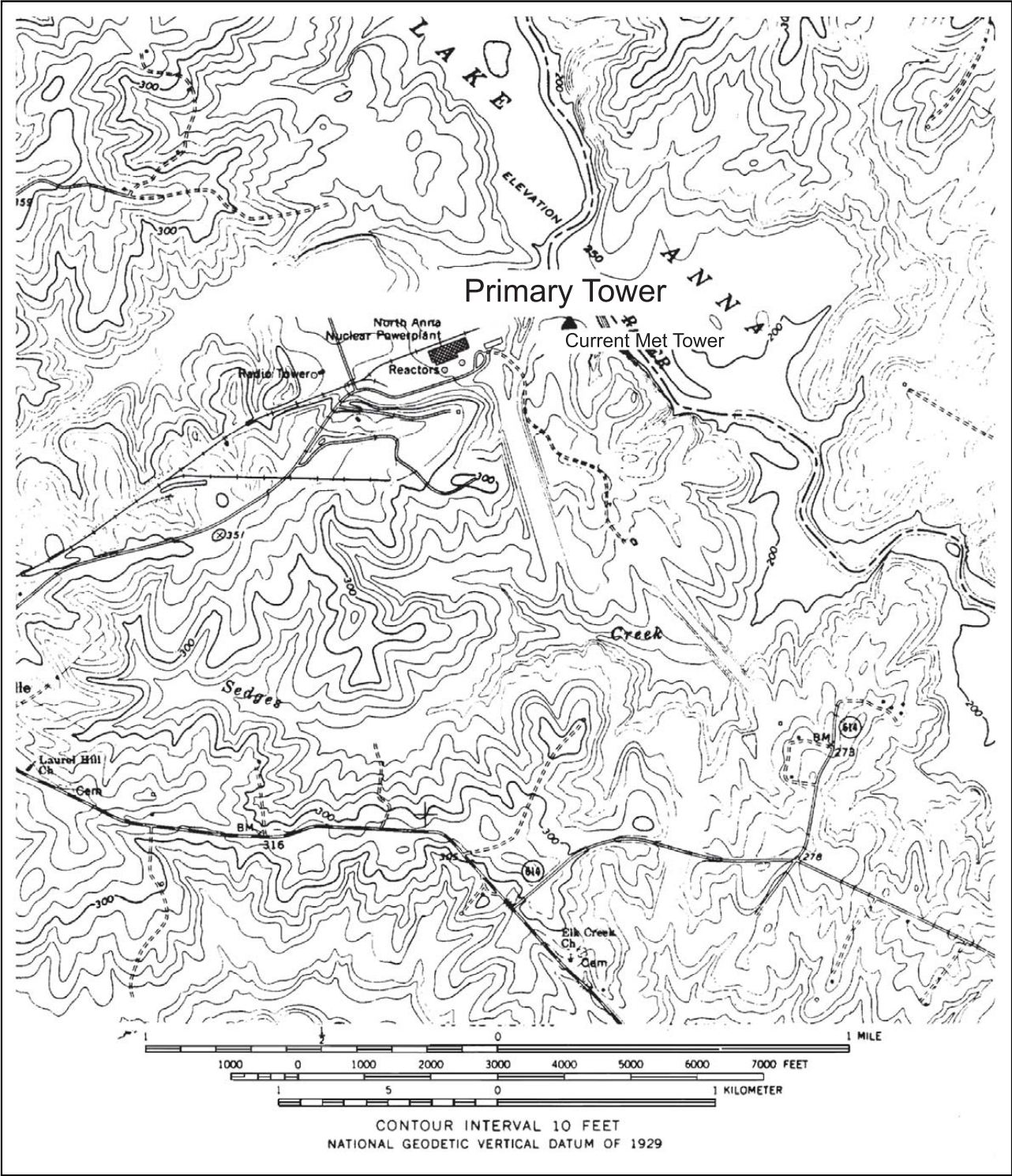


Figure 2.3-23 Location of Meteorological Tower

Source: Reference 13

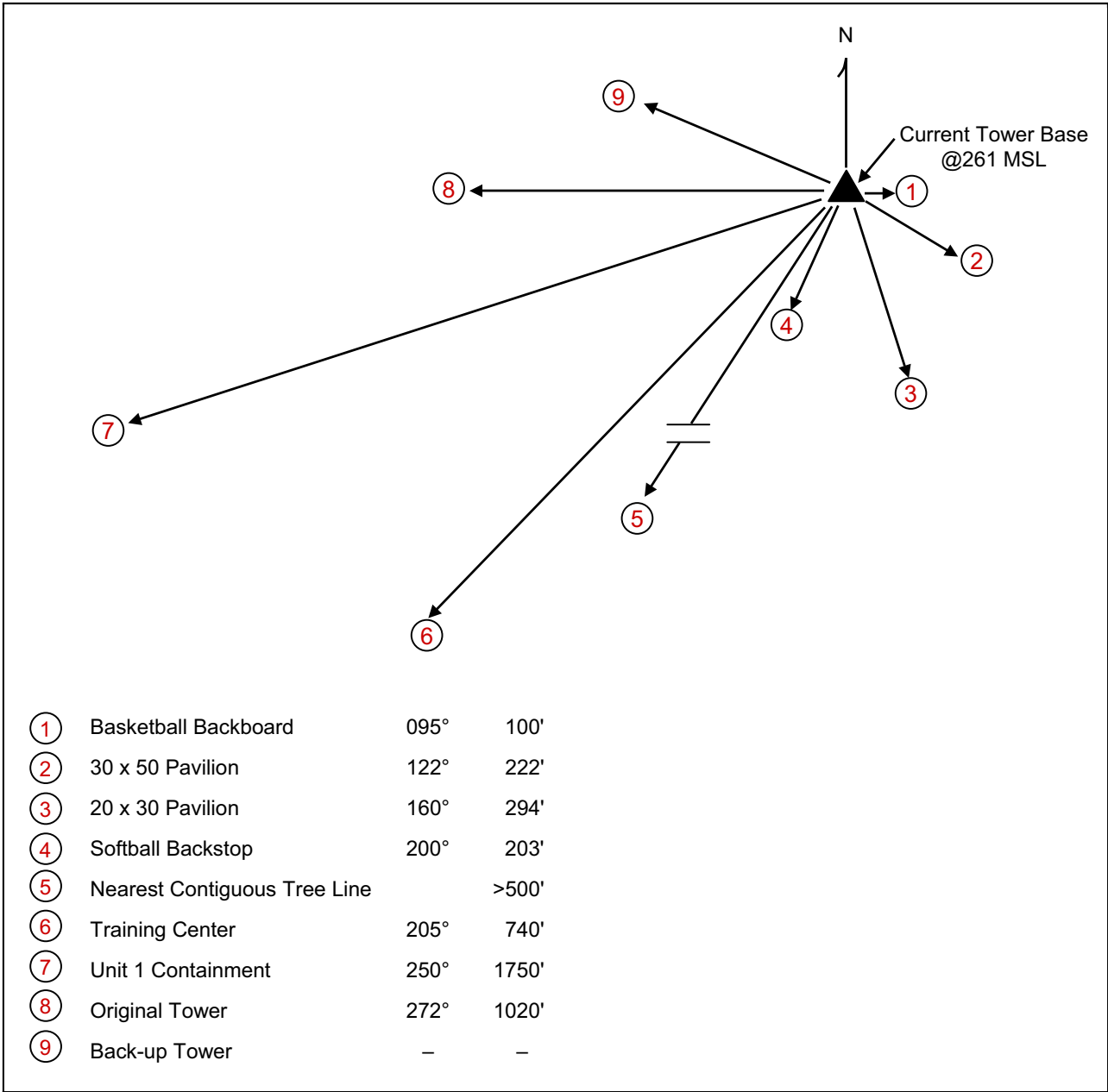


Figure 2.3-24 Location of Meteorological Tower Relative to Local Ground Features

Source: Reference 13

2.4 Hydrology

2.4.1 Hydrologic Description

This section identifies the interface of the new units with the hydrosphere, the hydrological causal mechanisms that may require special plant design bases or operating limitations with regard to floods and water supply requirements, and the surface water and groundwater uses that may be affected by operation of new units at the ESP site.

2.4.1.1 Site and Facilities

The water source for the new units on the ESP site is an impoundment of the North Anna River, referred to as Lake Anna. This impoundment was created by a dam constructed across the North Anna River as part of the overall development of the NAPS site. The North Anna Reservoir currently serves as the principal water source for the two existing units, which use once-through cooling systems to dissipate heat from the turbine condensers.

The ESP site is situated approximately 5 miles upstream from the main dam and adjacent to the existing units. The grade of the proposed site would have the same minimum elevation as the existing units, which is 271 ft msl (Reference 1). There are no natural drainage features that require changes to accommodate new units at the ESP site. Figure 1.2-4 shows the external structures and components, to the extent known, of the new units that might be constructed at the ESP site.

The new units would also use the North Anna Reservoir as the source of cooling water. New Unit 3 would use a once-through cooling system that would withdraw water at rate of about 2540 cubic feet per second (cfs) from the North Anna Reservoir, circulate it through the condensers, and return the water to the reservoir via the WHTF. New Unit 4 would use a closed-cycle cooling water system and mechanical or natural draft cooling towers for heat rejection. Approximately 44 cfs of water would be required for the Unit 4 cooling tower make-up. About 9 cfs would be discharged to the WHTF as blowdown from the Unit 4 cooling towers. Make-up water would be obtained from the North Anna Reservoir and supplemented by an external source during critical low flow periods to maintain acceptable lake levels. The external source of make-up water and the associated demands would be identified during detailed engineering and described in the COL application.

2.4.1.2 Hydrosphere

2.4.1.2.1 Hydrologic Characteristics of Streams, Lakes, and Groundwater

The North Anna River originates in the eastern slopes of the Southwestern Mountains in the Appalachian mountain range near Gordonsville, Virginia, and follows a southeasterly course to its confluence with the South Anna River 5 miles northeast of Ashland, Virginia, where the Pamunkey River is formed. The Pamunkey continues on a general southeasterly course to West Point, Virginia, where it is joined by the Mattaponi River to form the York River. The York River flows into the Chesapeake Bay about 15 miles north of Hampton, Virginia (Reference 1). The North Anna

River drains a watershed area of 343 square miles above the dam, which is located about 4 miles north of Bumpass, Virginia, and about a half mile upstream of Virginia Route 601.

As shown in Figure 2.4-1, Lake Anna is about 17 miles long and inundates several small tributaries; thereby, resulting in an irregular shape having a shoreline length of approximately 272 miles. To provide optimum thermal performance for the existing units, Lake Anna is separated into two segments by a series of dikes and canals. The larger segment of about 9600 acres is referred to as the North Anna Reservoir and functions as a storage impoundment to ensure adequate water supplies for condenser cooling. The smaller segment, called the WHTF, has an area of about 3400 acres and functions primarily as a heat exchanger for transferring most of the existing units heat rejection to the atmosphere. When both existing units are operating, eight circulating water pumps draw water from Lake Anna at a rate of 4246 cfs, circulate it through the condensers, and return it to the reservoir via the WHTF (Reference 1).

The principal tributaries of Lake Anna include the North Anna River, Pamunkey Creek, and Contrary Creek. Several smaller tributaries drain to the lake as well. Only two of the tributaries draining into Lake Anna are gauged: Pamunkey Creek at Lahore, Virginia (USGS 01670180), and Contrary Creek Near Mineral, Virginia (USGS 01670300). The Pamunkey Creek station gauges a drainage area of 40.5 square miles, while the daily streamflow record extends from August 1989 through July 1993 (Reference 2). The Contrary Creek station gauges a drainage area of 5.53 square miles. The daily streamflow record for this station extends from October 1975 through January 1987 (Reference 3). The remaining 297 square miles of the 343 square mile Lake Anna watershed are not gauged and cannot be characterized accurately for inflows to the impoundment. Inflows can be estimated, however, from records obtained from the North Anna River near Doswell, Virginia, which has a record that measures streamflow from April 1929 through September 1988. This gauging station is located approximately 15 miles downstream of the dam and gauges a drainage area of 441 square miles (Reference 4).

Using the portion of the Doswell, Virginia record preceding dam closure (i.e., April 1929 through December 1971), inflows to Lake Anna were estimated. The flows at Doswell are larger than the flows at the dam due to the larger contributing drainage area. Thus, these flows were adjusted by multiplying by the ratio of the drainage area at the dam to the drainage area at Doswell, Virginia. Table 2.4-2 summarizes the observed and estimated mean monthly inflows to Lake Anna estimated as described above.

Outflows from Lake Anna have been measured on the North Anna River near Partlow, Virginia, which is located just downstream of the dam at the Virginia Route 601 bridge. The drainage area at this stream gauge is 344 square miles. The daily streamflow record for this gauging station extends from October 1978 through September 1995. The discharge at this station reflects the regulated outflow from Lake Anna for the entire period of record since the dam was completed in 1972. (Reference 5) Table 2.4-2 summarizes the mean monthly outflows from the Lake Anna impoundment using streamflow data from the U.S. Geological Survey (USGS). Note that the period

of record for the estimated total inflow precedes the closure of the North Anna Dam whereas the period of record for the outflow occurs after dam closure. Mean monthly outflows may, therefore, exceed the mean monthly inflows for some months.

Lake Anna water levels have been recorded since the existing units began operating. The available record extends from August 1978 through March 2003. Mean monthly water levels were calculated from these data and are summarized in Table 2.4-2.

Section 2.4.12 describes the regional and local groundwater environments.

2.4.1.3 Existing and Proposed Water Control Structures

The North Anna Dam is the only existing water control structure on the North Anna River. The design basis of the North Anna Dam is described in the NAPS UFSAR (Reference 1).

The dam is an earth-filled structure about 5000 feet long, with a central concrete spillway about 200 feet long. The dam crest is at Elevation 265 ft msl and has a width of 30 feet. The dam has a maximum height above the streambed of about 90 feet and contains approximately 900,000 cubic yards of compacted earth materials. The concrete spillway section is founded on sound bedrock and the earthen section of the dam is founded partly on firm residual soils and partly on the bedrock. (Reference 1)

The earth dam section is constructed of local soils with a cross-section of a homogeneous-type compacted fill provided with vertical chimney and horizontal downstream foundation drains constructed of select pervious sand. An upstream impervious blanket is provided where it is necessary to lengthen the seepage path through residual foundation materials. Earth slopes are protected with riprap, and, where necessary, they are placed on suitable filters. Other earth slopes are seeded with grass. A service road is constructed on the dam crest. The stability of the earth dam is ensured through the use of conservative design procedures coupled with closely controlled construction techniques. The structure is designed with factors of safety that adequately resist all applied loads and forces, which is discussed in greater detail in the NAPS UFSAR (Reference 1).

The concrete spillway contains three radial crest gates, each 40 feet wide by 35 feet high, separated by 10-foot-wide concrete piers. The discharge capacity of each of the three main gates is shown in Figure 2.4-3. The crest of the spillway ogee is at Elevation 219 feet msl. Concrete gravity walls on each side of the spillway retain the earth portions of the dam.

A spillway bridge is provided at Elevation 265 feet msl for access to each of the individual electric motor-operated gate hoists. An auxiliary generator at the dam operates the spillway gate hoists if normal power supplies are interrupted. Two adjustable skimmer gates are provided for regulating small releases. The discharge capacity of each of the two skimmer gates, which measure 8.5 feet by 8.5 feet, is shown in Figure 2.4-4. A concrete apron downstream of the spillway provides energy dissipation for Lake Anna releases.

The North Anna Dam also incorporates at its base an 855-kW hydroelectric power plant that is owned and operated by Virginia Power. The hydroelectric facility consists of two separate generating units (Units 5A and 5B), each unit possessing a single state, open runner-type vertical turbine. Peak operational efficiency is at a flow of 40 cfs for Unit 5A and 133 cfs for Unit 5B. Water for the hydroelectric facility, which is withdrawn from near the surface of Lake Anna (depth of less than 7 feet), flows through a skimmer gate and associated sluice pipe that is connected to a 5-foot-diameter penstock. The water is then directed by a bifurcation piece through 24-inch and 48-inch conduits to Units 5A and 5B, respectively. After passing through the turbines, water is discharged into the North Anna River just downstream of the dam's spillway (Reference 6).

While Lake Anna was constructed for power generation purposes, it also provides the additional benefits of low streamflow augmentation, flood control, and recreation. The normal pool level is maintained at an elevation of 250 feet msl. The Commonwealth of Virginia requires a 40-cubic-feet-per-second minimum discharge of water from the North Anna Dam except under drought conditions. These minimum flow requirements are established to maintain in-stream flows and water quality in the North Anna River below the dam and in the Pamunkey and York Rivers, which are further downstream. Should drought conditions occur such that the Lake Anna water surface elevations fall below 248 feet msl, Virginia Power may reduce releases below 40 cfs, in accordance with the Lake Level Contingency Plan as stipulated in Part I.F of the Virginia Pollutant Discharge Elimination System (VPDES) Permit (Reference 7). A flood surcharge of 15 feet above the normal pool level is provided for flood storage. The total Lake Anna volume of 550,000 acre-feet is allocated as described in Table 2.4-1(Reference 1):

Table 2.4-1 Lake Anna Storage Allocation

Purpose	Volume (acre-feet)
Minimum recreational pool and inactive storage below 246 feet msl	255,000
Conservation and active storage, 246 to 250 feet msl	50,000
Flood control storage, 250 to 265 feet msl	245,000
Total storage	550,000

No additional water control structures are necessary or proposed for the new units on the ESP site.

2.4.1.4 Surface Water and Groundwater Users

Surface water users whose intakes could be adversely affected by the accidental release of contaminants were identified using the water use database maintained by the Virginia Department of Environmental Quality (VDEQ) (Reference 8). This database includes users whose average daily withdrawal in any single month exceeds 10,000 gallons per day (gpd). Users on Lake Anna are limited to the existing units which use the lake for cooling water. Data reported for the 1996-2001

period indicates an average annual use of 744,313 million gallons per year. Users on the North Anna River include the Bear Island Paper Co. and the Doswell Water Treatment Plant. The Bear Island Paper Co. is located at the confluence of the North Anna River and the Little River. Data given for the 1996-2001 period indicates an average annual use of 252.22 million gallons per year. The Doswell Water Treatment Plant obtains its water from the North Anna River and supplies water to major customers in the Doswell area, including the Bear Island Paper Co., the Doswell Limited Partnership electric generation facility, Paramount's Kings Dominion Amusement Park, and provides supplemental water to the Hanover County suburban service area. The plant is rated at 4.0 million gallons per day (mgpd). There are no other known users of either the North Anna River or the Pamunkey River into which it flows, until it reaches the York River some 60 miles downstream at West Point, Virginia, where the St. Laurent Paper Products plant is located. Although the St. Laurent Paper Products is included in the VDEQ water use database, they reported no withdrawals for the 1996-2001 period.

Section 2.4.12 identifies groundwater users that may be affected by operation of new units on the ESP site.

Table 2.4-2 Mean Monthly Hydrologic Statistics for Lake Anna

Month	Pamunkey Creek Inflow^a (cfs)	Contrary Creek Inflow^b (cfs)	Estimated Total Inflow^c (cfs)	Outflow^d (cfs)	Water Level^e (ft msl)
January	61.2	7.97	411	401	249.79
February	37.5	9.37	449	507	249.89
March	49.0	8.92	497	601	249.95
April	62.0	8.36	454	485	249.91
May	43.0	4.33	286	330	249.88
June	23.9	2.46	171	215	249.77
July	19.3	1.34	161	133	249.59
August	9.72	3.40	228	134	249.43
September	14.5	1.20	125	109	249.12
October	31.8	3.16	174	138	248.97
November	31.8	5.05	218	244	249.14
December	47.6	5.46	298	265	249.49

- a. USGS 01670180 Pamunkey Creek at Lahore, Virginia, September 1989 – April 1993 (Reference 2).
- b. USGS 01670300 Contrary Creek Near Mineral, Virginia, October 1975 – December 1986 (Reference 3).
- c. USGS 01671000 North Anna River Near Doswell, Virginia, January 1929 – December 1971 (Reference 4), scaled to Lake Anna drainage area.
- d. USGS 01670400 North Anna River Near Partlow, Virginia, October 1978 – September 1995 (Reference 5).
- e. August 1978 – March 2003.

2.4.2 Floods

2.4.2.1 Flood History

Annual peak discharges for flooding events that have occurred on the North Anna River and available annual peak North Anna Reservoir water levels, since completion of the dam, are presented in Table 2.4-14. The flood history information for the period of record was obtained from the North Anna UFSAR (Reference 1) and from USGS stream gage records (Reference 4) (Reference 5). The reservoir water level data presented for the period of record from 1979 to 1995 is obtained from Lake Anna water level data compiled by Virginia Power.

The largest flood of record on the North Anna River occurred in 1969, with a peak discharge of 24,800 cfs at the Doswell, Virginia USGS gaging station, approximately 15 miles downstream from the dam and 14 miles downstream of the Partlow, Virginia gaging station (Reference 4). The flood that occurred as a result of hurricane Agnes in 1972 nearly matched the flood of record with a peak discharge of 24,000 cfs at Doswell, VA. Although the North Anna Dam had been completed in December 1971, the reservoir was not yet filled, thus the water level in North Anna Reservoir during this event was well below the normal pool elevation of 250.00 ft, msl.

Since completion of the dam and subsequent filling of the reservoir, the largest flood of record occurred on two separate occasions, February 1979 and June 1995. For both of these events, the peak discharge at the Partlow gaging station was measured to be 11,700 cfs with a peak water level in Lake Anna of 252.0 ft, msl, measured at the dam.

2.4.2.2 Flood Design Considerations

The design basis flood for the ESP site was determined by considering a number of different flooding possibilities. The possibilities applicable to this site include the probable maximum flood (PMF) on streams and rivers, potential dam failures, probable maximum surge and seiche flooding, and ice effect flooding. Each of these flooding scenarios was investigated in conjunction with stream flooding on the North Anna River as per guidelines addressed in ANSI/ANS-2.8-1992 (Reference 9). Details of the individual scenarios are discussed in Section 2.4.3 through Section 2.4.7.

The highest water level from among the number of flooding possibilities is selected as the design basis flooding level. For the ESP site, the design basis flooding level was derived from the PMF on Lake Anna produced by the probable maximum precipitation (PMP) (Section 2.4.3.1) over the lake's watershed. The PMP was developed using Hydro-Meteorological Reports (HMR) 51 and 52, published by the NOAA (Reference 10) (Reference 11). Wind generated setup and runup elevations were also considered in conjunction with the maximum still water level on Lake Anna to produce a design basis flooding level of 267.39 ft, msl at the site. Details of the flooding level determination are discussed in Section 2.4.3.

Elevations for safety-related components and structures are not yet established for the new units. However, the grade elevation in the power block area of the ESP site has been established at Elevation 271.0 ft. msl, providing 3.61 ft of freeboard above the design basis flooding level. This is the same grade elevation as the existing units. Therefore, all above grade, safety-related structures, systems and components of the new units would be located above the Lake Anna design basis flooding level.

2.4.2.3 Effects of Local Intense Precipitation

The design basis for local intense precipitation at the ESP site is the PMP. The PMP values discussed and listed in Section 2.4.3.1 were developed for the 343 square-mile Lake Anna watershed. The drainage areas for storm water conveyance facilities around the ESP site would be less than one square mile. Additionally, the time of concentration for these facilities would also be much shorter than for the Lake Anna watershed. Thus, a different set of PMP values appropriate for smaller watersheds and storm durations of less than one hour and drainage areas one square mile or less were used for local intense precipitation at the site. These values were obtained from HMR 52 (Reference 11) and are listed in Table 2.4-3.

Table 2.4-3 North Anna Power Station Local Probable Maximum Precipitation Values

Duration	1-Hour Multiplier	PMP Depth (in)
6-hour	1.527	27.9
1-hour	1.0	18.3
30-minutes	0.749	13.7
15-minutes	0.522	9.6
5-minutes	0.333	6.1

(Values are for a 1-mi² drainage area.)

The site layout and facilities at the ESP site have not been finalized. Thus, the location and design of storm water conveyance facilities have not been determined. These tasks would be performed as part of detailed engineering and described in the COL application. The general design of the storm water conveyance facilities would be to discharge the runoff to Lake Anna. Using the PMP values listed in Table 2.4-3, storm water conveyance facilities would be designed such that the peak discharges from the PMP would not flood safety-related facilities of the new units or of the existing units. Drainage facilities used during the construction phase of the new units would also be designed such that safety-related facilities of the existing units would not be adversely affected by flood elevations as a result of the local PMP and construction of the new units. In addition, applicable federal, state, and local storm water management regulations would be followed in the design of storm water conveyance facilities.

2.4.3 Probable Maximum Flood on Streams and Rivers

Two previous Lake Anna PMF analyses have been performed. The first analysis was performed for the original Unit 1 and 2 NAPS Final Safety Analysis Report. The second analysis was performed in 1976 to update the runoff model unit hydrograph based on water level observations since the construction of North Anna Dam. The 1976 analysis is described in the current North Anna UFSAR (Reference 1). The PMP values used in the 1976 analysis were based on information contained in the NWS's Hydro-Meteorological Report (HMR) No. 33 (Reference 12). Since 1976, the NWS, now under the NOAA, has updated PMP estimates and published HMR Nos. 51, 52 and 53 to reflect the updated estimates (Reference 10) (Reference 11) (Reference 13). In general, the PMP estimates in the later HMRs are greater and of longer duration than those presented in HMR No. 33. Thus, for this section, the PMF analysis has been revised to incorporate the updated PMP information from HMR Nos. 51, 52, and 53.

The present analysis consisted of developing the PMP estimates from the current HMRs. The runoff unit hydrograph and precipitation losses used in the 1976 study were compared with observed results from storms that have occurred since 1976 and adjusted as necessary. Also, the flood inflow hydrograph and still water elevations in Lake Anna were computed using the U.S. Army Corps of Engineer's (USACE's) computer program, HEC-1 (Reference 14). The backwater effects along with appropriate wind-generated setup and wave run-up in accordance with ANS/ANSI-2.8-1992 (Reference 9) were added to the still water elevation to determine the final PMF elevation and design basis flooding level at the ESP site. Details of the analysis are presented in Section 2.4.3.1 through Section 2.4.3.6.

The results of the analysis indicate a design basis flooding elevation of 267.39 ft msl at the ESP site, which is 3.61 ft below the ESP site grade elevation of 271.0 ft msl. Since the ESP site grade elevation is above the design basis flooding level, all above-grade, safety-related structures, systems, and components of the new units would be located above the design basis flooding elevation.

2.4.3.1 Probable Maximum Precipitation

The PMP was developed according to procedures outlined in HMR Nos. 51, 52, and 53 (Reference 10) (Reference 11) (Reference 13). The values are presented in Table 2.4-4. They have been estimated based on the size and shape of the combined North Anna Reservoir and WHTF watershed drainage area in accordance with the procedures outlined in HMR No. 52 (Reference 11). The 343 square mile watershed drainage area is shown on Figure 2.4-5. The PMP isohyetal pattern was oriented over the watershed such that the maximum precipitation volume over the entire drainage area has been obtained. The 72-hour PMP storm was temporally distributed according to guidelines in HMR No. 52 and ANS/ANSI-2.8-1992 (Reference 11) (Reference 9) and is shown in Table 2.4-7.

Table 2.4-4 Maximum Precipitation Depths

6-hour Incremental Depths		Total PMP Depths	
6-Hour Increment	Incremental PMP Depth (in)	Storm Duration (hr)	Total PMP Depth (in)
1	17.71	6	17.71
2	3.67	12	21.38
3	2.24	24	24.89
4	1.27	48	29.09
5	1.27	72	30.65
6	1.07		
7	0.98		
8	0.88		
9	0.59		
10	0.39		
11	0.29		
12	0.29		

For the runoff analysis, an antecedent storm condition was assumed as indicated in ANS/ANSI-2.8-1992 (Reference 9). A rainstorm equivalent to 40 percent of the PMP was initially modeled, followed by three days with no precipitation, and then the full 72-hour PMP storm was applied. Based on the historical snowfall information for the NAPS region, snowmelt does not make a significant contribution to flooding situations (Reference 15). Therefore, antecedent snow-pack conditions were not considered in the PMF analysis.

2.4.3.2 Precipitation Losses

Precipitation losses for the 1976 study were determined by comparing the rainfall-runoff relationships for various storms. Precipitation losses were determined using historical storms and the HEC-1 loss rate parameter optimization (Reference 1).

In addition to the historical storms investigated for the 1976 study, three additional storms were investigated in the present study to determine precipitation losses, including the influence of recent data. The storms occurred in February 1979, March 1994, and June 1995, and were selected because they produced high water levels in the North Anna Reservoir. Hourly precipitation data for these storms were collected from various precipitation gaging stations near the watershed from the National Climatic Data Center (Reference 16). The Thiessen polygon method was used to

determine a watershed basin average precipitation for each storm (Reference 17). The precipitation weighting and basin average precipitation for each storm are shown in Table 2.4-8 through Table 2.4-10. For these three recent storms, the HEC-1 loss rate parameters were also optimized by comparing the North Anna Dam outflow HEC-1 results with North Anna Dam discharges calculated from observed Lake Anna water levels and gate openings. The precipitation loss rates from the recent storms were factored with the loss rates for the storms analyzed in the 1976 study, and loss rates were determined for the PMF runoff analysis. The loss rates for each of the actual storms and the loss rates for the 1976 and present PMF storms are shown in Table 2.4-11.

2.4.3.3 Runoff Model

The revised 1976 analysis used the unit hydrograph method to determine the PMF levels in Lake Anna. The unit hydrograph was developed using historical rainfall records from nearby precipitation stations and historical stage-discharge data for the dam. The procedure, as presented in the NAPS UFSAR, is outlined below:

1. An isohyetal map of total storm rainfall for each storm was plotted and a Thiessen's polygon was drawn on the isohyetal map to determine the distribution of basin rainfall.
2. Mass curves of rainfall were drawn to define the time distribution of rainfall.
3. The base flow was subtracted from the measured stream flow hydrograph to obtain the runoff hydrograph for each storm.
4. The basin infiltration was adjusted to balance rainfall excess with flood runoff.
5. Using the runoff hydrograph and the time distribution of rainfall excess for guidance, the unit hydrograph for each flood was determined.

From the individual unit hydrographs, a composite unit hydrograph for the combined WHTF and North Anna Reservoir watershed was developed. The composite unit hydrograph used in the 1976 HEC-1 runoff model for the combined watershed drainage area (322.7 square miles), excluding the reservoir and WHTF surface areas, is shown on Figure 2.4-6. A separate runoff hydrograph was developed for the drainage area comprising the reservoir and WHTF surface areas (20.3 square miles). This second hydrograph directly reflected the storm precipitation pattern. No infiltration losses were used for the runoff over the combined reservoir and WHTF surface areas.

For the current analysis, the precipitation data for each of the three recent storms discussed in Section 2.4.3.2 was applied to the 1976 watershed and lake unit hydrographs. The resulting runoff hydrographs were then combined and routed through Lake Anna using the computer program HEC-1 (Reference 14). The HEC-1 computed discharges from Lake Anna for each storm were then compared with Lake Anna discharges calculated based on gate opening data and water levels measured at the dam during the storms. Adjustments were made to both the base flow and the

precipitation loss (infiltration) coefficients. Comparisons of the HEC-1 computed Lake Anna discharges with the discharges based on measured water levels are shown on Figure 2.4-7 through Figure 2.4-9. The results indicated that the 1976 unit hydrograph produced inflow hydrographs that accurately represent the observed lake discharge hydrographs for recent storms. Thus, the same 1976 unit hydrographs were used for the present PMF runoff analysis.

Routing of flood flows through Lake Anna was accomplished using the level pool reservoir routing procedure in HEC-1. For modeling purposes, the reservoir and the WHTF were treated as a single storage facility, Lake Anna. Four dividing dikes, one of which allows limited flow exchange, separate the two facilities. The top crest elevation of the dikes is 260 ft msl. However, there is a 350-foot long saddle in Dike 3 at Elevation 253.5 ft msl, which functions as a spillway for the WHTF. Thus, once the water level in either storage facility rises above 253.5 ft msl, equalization of the water level between the two facilities occurs. In view of the fact that flow between the two facilities is restricted for elevations below 253.5 ft msl, the reservoir modeling used in HEC-1 conservatively assumed that all rainfall and runoff was routed only through the North Anna Reservoir until the water level reached Elevation 253.5 ft msl. This is equivalent to assuming that the WHTF was full to Elevation 253.5 ft msl at the beginning of the PMF. The Lake Anna stage-storage data provided to the HEC-1 model reflected the conservative modeling approach for the WHTF. For elevations below 253.5 ft msl, only the North Anna Reservoir's storage volume was input into the model and made available for runoff and rainfall storage. For elevations above 253.5 ft msl, the storage from both facilities was input into the model and made available. The stage-storage curve for the combined WHTF and North Anna Reservoir, reflecting the conservative approach described, is shown on Figure 2.4-10.

Two adjustable skimmer gates and three spillway radial gates provide control of the discharge from the North Anna Dam, as described in Section 2.4.1.2. The stage-discharge relationship used in the HEC-1 runoff model was based on the adopted spillway rule curve and is the same that was used in the previous 1976 PMF analysis. The skimmer gate and spillway discharge capacities are shown on Figure 2.4-3 and Figure 2.4-4.

The present PMF runoff analysis was performed by applying the PMP values in Section 2.4.3.1 to the watershed and lake surface area unit hydrographs, combining the two hydrographs, and routing the resultant inflow hydrograph through Lake Anna.

2.4.3.4 Probable Maximum Flood Flow

The computed PMF inflow hydrograph to the combined WHTF and North Anna Reservoir is shown in Figure 2.4-11. The peak PMF inflow discharge is about 302,100 cfs, and the peak discharge over the dam is about 141,000 cfs. The controlling PMF hydrograph shows a result of the runoff from a 72-hour storm with precipitation values equal to 40 percent of the PMP, followed by three days with no precipitation and then the 72-hour PMP storm.

There are no other dams in existence on the North Anna River, either upstream or downstream of the ESP site. The only impoundments in the Lake Anna drainage area are small farm ponds and two small recreational lakes, Lake Louisa and Lake Orange, whose failures would not produce any measurable effect on the Lake Anna water levels. Thus, these effects were not included in the PMF flow.

2.4.3.5 Water Level Determination

The PMF inflow hydrograph was routed through the combined reservoir using HEC-1 to determine the maximum still water level associated with the PMF. This routing resulted in a peak outflow of 141,000 cfs with a maximum water level at the dam of 264.07 ft msl. These values may be compared with the 1976 analysis that resulted in a peak outflow discharge of 142,000 cfs and a peak water level of 264.2 ft. msl.

For the 1976 analysis, included in the NAPS UFSAR, a backwater profile curve was developed for the peak discharge of 142,000 cfs, indicating the lake level at the NAPS site to be about 0.2 feet higher than the water level at the dam (Reference 1). Since the peak outflow discharge for the present analysis is slightly less than the previous discharge, the results of the previous backwater analysis have been conservatively applied to the elevation computed for this PMF analysis. By adding the backwater effect of 0.2 ft to the PMF still water elevation of 264.07 ft msl at the dam, the PMF still water elevation at the site is 264.27 ft msl.

2.4.3.6 Coincident Wind Wave Activity

In accordance with procedures outlined in ANS/ANSI-2.8-1992, the wave setup and run-up generated by a 2-year return period wind speed were added to the PMF still water elevation to determine the maximum PMF water level at the ESP site (Reference 9). The 2-year overland wind speed for the site was determined by investigating data presented in ANS/ANSI 2.8-1992 and NUREG/CR-2639 (Reference 9) (Reference 18). From these two references a fastest-mile 2-year wind speed of 50 mph, measured 30 feet above the ground over land, was selected. This translates to a fastest-mile 2-year wind speed over water of 56.0 mph (Reference 19). The fetch diagram used to determine an effective fetch length of 4700 ft with a maximum fetch of 10,600 ft is shown on Figure 2.4-12.

Using these values and procedures outlined in the U.S. Bureau of Reclamation publication, *Freeboard Criteria and Guidelines for Computing Freeboard Allowances for Storage Dams*, (Reference 19) and the USACE–*Shore Protection Manual* (Reference 20), a significant wave height of 2.15 ft and a maximum wave height of 3.60 ft were calculated. From these values a maximum wind set-up value of 0.09 ft and a wave run-up value of 3.03 ft were calculated. Adding the wind setup and wave run-up values to the PMF still-water elevation at the site resulted in a maximum PMF elevation at the site of 267.39 ft msl.

2.4.4 Potential Dam Failures

As indicated in Section 2.4.1.1, the ESP site is located adjacent to Lake Anna and approximately 5 miles upstream of the North Anna Dam. Lake Anna was created to supply water to the existing power station. Amendment 15 to the North Anna Unit 1 and 2 Preliminary Safety Analysis Report (PSAR) (Reference 21) demonstrates that the design of the North Anna Dam complies with the requirements associated with Seismic Class I structures. Thus, as described in the NAPS UFSAR, a seismically induced failure of the dam is not credible (Reference 1).

Lake Anna would serve as a cooling water source and the primary service water source for the new units. As described in Section 2.4.11.6, the ultimate heat sink (UHS) would consist of a mechanical draft cooling tower over a buried water storage basin or other passive water storage facility as required by the reactor design. The UHS facilities would provide a source of water for the service water system in the event that the primary source becomes unavailable. Therefore, adequate service water would be immediately available to maintain any new unit or units in a safe condition, even if Lake Anna were to be drained due to a dam failure. No safety-related structures or systems of any new units would be adversely affected by the loss of water in Lake Anna due to dam failure.

No other dams exist on the North Anna River, either upstream or downstream of the ESP site. The only impoundments in the area are small farm ponds and two small recreational lakes – Lake Louisa and Lake Orange – that are located on small tributaries to the North Anna River and whose failures would not produce any measurable effect on the Lake Anna, North Anna Dam, or any safety-related systems.

2.4.5 Probable Maximum Surge and Seiche Flooding

Since the ESP site is not located on an estuary or open coast, surge or seiche flooding would not produce maximum water levels at the site. The maximum surge and seiche flooding is to be considered using an antecedent water level corresponding to the 100-year maximum water level in the lake (Reference 22). The published Flood Insurance Study for Louisa County, Virginia, indicates only an approximate flood hazard area for Lake Anna (Reference 23). From the flood hazard shading, an approximate flood elevation of 255 ft msl was estimated. This elevation is 9.07 ft below the maximum still-water elevation of 264.07 ft msl, as discussed in Section 2.4.3.

Section 2.4.3 describes the analysis of wind setup (surge) and wave runup completed as part of the PMF evaluation. This analysis indicates that the maximum fetch length at the site is 10,600 ft, and the effective fetch length is 4700 feet. Given these relatively short lengths, the surges and waves produced from winds generated in a probable maximum hurricane or from the oscillatory waves generated by lake reflection or harbor resonance would not be sufficient to produce water levels greater than the still water level resulting from the PMP over the watershed.

2.4.6 Probable Maximum Tsunami Flooding

Since the site is at an inland location and not located on an estuary or open coast, tsunami flooding is not a design consideration.

2.4.7 Ice Effects

2.4.7.1 Ice Conditions

Ice at a nuclear power plant site can occur in any one of the following forms:

- Surface ice and its associated forces
- Anchor ice formation on components
- Frazil ice that could clog intake flow passages
- Ice jams that can affect flow path to the intake
- Ice accumulation on roofs of safety related structures and components.

Historical data quantifying ice and snow conditions at the NAPS site have been collected and evaluated and are presented in Section 2.4.7.3.

The following subsections describe the cooling water system for the existing units and the new units. A summary of the historic ice conditions at the NAPS site, as well as ice prediction and its effects on the design of the new units are included.

2.4.7.2 Description of the Cooling Water System

The existing units use a once-through cooling system that withdraws water from the North Anna Reservoir, circulates it through condensers, and returns the water to the reservoir via the WHTF, as is described in Section 2.4.1. The emergency cooling water and normal service water are provided from a service water reservoir (SWR) equipped with a spray system. This SWR is completely separated from the North Anna Reservoir and the WHTF. However, normal makeup water for the SWR is pumped from the plant intake structure on the North Anna Reservoir.

For the new units, Unit 3 would use a once-through cooling system using the North Anna Reservoir as the water source and discharging water to the WHTF. Unit 4 would use a closed-cooling water system and mechanical or natural draft cooling towers for heat dissipation. Cooling water make-up for Unit 4 would be obtained from the North Anna Reservoir and supplemented from outside sources, as necessary, to maintain acceptable lake levels. Normal service water for both new units would be provided from the reservoir through separate pumps located inside the pump intake structure. The emergency cooling water would be provided from a separate underground concrete storage basin covered by cooling towers to dissipate the rejected heat from the reactor during emergency conditions or from a passive water storage facility.

The cooling designs for Units 3 and 4 separate the normal cooling and the emergency cooling water systems. The discussion and analysis presented in this section demonstrates that the normal once-through (Unit 3) and closed-cycle (Unit 4) cooling water systems are reliable and would not be affected by the ice conditions in the lake. Furthermore, the section includes data analysis and discussion of the effect of combined snow and winter PMP on safety-related structures.

2.4.7.3 Historical Ice Formation

The climate at the ESP site is influenced throughout the year by the Chesapeake Bay climate. The long-term mean daily air temperature in Richmond ranges from about 38.0°F in January to 78.2°F in July, while the mean daily minimum air temperature for January is 28.4°F and for March is 36.6°F (Reference 24).

Snowfall in the region is infrequent and does not accumulate with debilitating impact. The maximum monthly snowfall in Richmond, Virginia occurred in January 1940 with a depth of 28.5 inches. The maximum monthly snowfall in recent years occurred in February 1983 with a depth of 21.4 inches. The maximum 24-hour snowfall in Richmond, Virginia occurred during January 1940 with a total snowfall of 21.6 inches (Reference 24). Charlottesville, Virginia snowfall data have also been examined. The maximum monthly snowfall observed in Charlottesville was 29.8 inches, which occurred in March 1960.

Assuming a snow density of 0.1, the estimated maximum monthly water equivalent for the snowfall at Richmond, Virginia is 2.85 inches in January to 1.97 inches in March. This depth is equivalent to a maximum load of 15 pounds per square foot. For the maximum 24-hour snowfall, the estimated water equivalent is 2.2 inches, which is equivalent to approximately 12 pounds per square foot on the ground. For the snowfall in Charlottesville, the equivalent water depth is approximately 3 inches, and approximately 16 pounds per square foot.

The combination of moderate air temperature and the relatively low winter precipitation does not lead to excessive snow and ice formation. Although, historically snowfall and ice have occurred at the site, accumulation has lasted for only short periods of a few days. Based on snow depth measurements recorded at the NAPS site, a maximum snow depth of 32 inches was observed on the roofs and on the ground in the winter of 1995–1996. The equivalent water depth for this snowfall is approximately 3.2 inches, which is equivalent to 17 pounds per square foot.

These historical monthly snow depths indicate that the maximum equivalent weight of water ranges from 15 to 17 pounds per square foot.

During the winter of 1977, after the construction of the dam and the filling of Lake Anna, and before the operation of the plant, an ice sheet was formed on the lake. However, since the beginning of the operation of the existing units, ice sheets have formed only on the upper reaches of Lake Anna, upstream of Route 208. This region is approximately 3 miles upstream of the cooling water intake the new units.

Ice formation has occurred on the transmission towers and switchyard at the ESP site during freezing rainfall. To date, events such as these have not affected the operation of the existing units. According to NAPS operation records, there have been no incidents of ice blockage of storm drains.

2.4.7.4 Frazil Ice

Research on the properties of frazil ice indicates that the nature and quantities of ice produced depends on the rate of cooling within a critical temperature range. Frazil ice forms when the water temperature is below 0°C (32°F), and the rate of super cooling is greater than 0.01°C (0.018°F) per hour in turbulent flows, and there is no surface ice sheet to prevent the cooling (Reference 25) (Reference 26). This type of ice, which is in the shape of discoids and spicules (Reference 25) typically forms in shallow flowing water, such as in rivers and lakes, when the flow velocity is approximately 2 feet per second (0.6 meters per second) (Reference 27).

If a submerged intake is located in shallow water where frazil ice is forming, ice may grow directly on metal surfaces such as the trash rack and/or traveling water screens. This type of frazil ice is called anchor ice (Reference 26).

At Lake Anna, formation of frazil ice is precluded due to the circulation of the Unit 1 and 2 condenser cooling water and current heat load. Historic water temperature data at the intake of North Anna Units 1 and 2 have shown that the minimum intake water temperature reached has been 1.2°C (34.2°F) with only one unit in operation.

The data presented in Table 2.4-12, obtained by Virginia Power as part of their thermal monitoring program, show the number of days during which the intake water temperature fell below 4°C (39.2°F). These data indicate that the water temperature at the intake during the winter months has historically been above freezing. In the presence of surface turbulence generated by winds, frazil ice would not form due to high surface temperature. With the operation of the new units, the additional waste heat discharged to the lake would further decrease the risk of frazil ice formation. Therefore, frazil ice would not be expected to form at the intakes of the new units.

If, for some reason, all of the units do not operate for a prolonged period in the winter, the lake water temperature would eventually decrease at a rate dependant on the prevailing air temperature and wind. Under these conditions super cooling could lead to the formation of frazil ice. However, for frazil ice to form, sufficient turbulence is required. Since the only pumps operating under this condition would be the service water pumps for Units 1 and 2, the low flow (about 2 cfs) (Reference 1), would result in a flow velocity much lower than the 2 feet per second. This low flow would not produce sufficient turbulence to generate frazil ice, based on criteria stated in Reference 27 and others. Turbulence also can be generated by strong and sustained wind over the lake during the same climatic conditions. Even though historical wind data at Richmond, Virginia (Reference 24) do not show the occurrence of such events, it is possible that such winds could develop over an open water body such as Lake Anna. If extreme events were to occur during a

period when no units are operating, it is possible that frazil ice could form in the intake area. In the event that it does, safety-related facilities would not be adversely affected. The UHS would provide a source of cooling and service water to maintain the plant in a safe mode should the North Anna Reservoir intake become inoperable due to frazil ice formation. Further information on the UHS is found in Section 2.4.11.

The formation of anchor ice on the trash racks and screens would be assessed during the design of the intake and described in the COL application.

2.4.7.5 **Surface Ice**

The formation of a surface ice sheet in a cooling water lake can exert forces on the contact structures due to ice expansion or to the drag force caused by wind acting on unrestrained ice sheets.

Shoreline intakes designed with approach channels can become obstructed by ice jams. This is possible at lake intakes where wind may drive the ice toward the shoreline. However, trash racks prevent the entry of large pieces of ice from broken ice sheets (Reference 28).

During the operation of the existing units, ice sheets have not formed in the area of the cooling lake between the discharge and the intake. The only area that has experienced the formation of ice sheets is upstream of Route 208. Since this area is far from the main circulation path of the cooling water, an ice sheet in this area would not impact operation of intakes for the new units.

However, if all of the existing and new units were off-line during a relatively sustained freezing weather period, the formation of surface ice is possible, based on examination of the mean daily air temperature for the 1961–1995 time period. The data show that there were several years in which the January and/or February mean daily temperature was below freezing for one to three weeks, as summarized in Table 2.4-13.

The maximum ice thickness that could have formed under historic low air temperatures with no units in service has been predicted. The meteorological data have been analyzed to determine the degree-days below freezing. In the 1977 January and February period, there were about 200 degree-days below freezing. Using this information and employing Assur's method as presented in Chow (Reference 29) (Reference 30), the calculated ice thickness is approximately 13.5 inches. This ice layer would not impact water flow upon restart due to the water depth at the new intakes (a minimum of approximately 24 feet). Instead, this surface ice layer would insulate and provide protection against the formation of frazil ice. However, the formation of surface ice can exert a high load on the intake structure wall in contact with the water. Ice forces would be accounted for in the design of the intake and described in the COL application. It should also be noted that the intakes and associated pumps for the new units would not be safety-related facilities. Emergency cooling and service water needed to maintain the new units in a safe mode would be supplied by a separate UHS. Therefore, no safety-related facilities would be affected by ice layer formation.

Upon restart of the units and the circulation of warm water, the ice would gradually melt and break. The velocity induced by the flow can cause some of the ice floes to be withdrawn or moved by the water (Reference 31). Although the design of the intake has not been developed to enable the determination of ice floe size that might be withdrawn, the presence of trash racks and traveling screens would prevent such ice from reaching the pumps. The accumulation of ice at the trash racks and traveling screens could clog them and reduce the flow capacity of the intake structure. However, since emergency cooling and service water would be provided by the UHS, no safety-related facilities would be affected by ice floe accumulation.

2.4.7.6 Ice and Snow Roof Loads on Safety Related Structures

Historic data indicate that since the existing units were put into operation, snowfall in Richmond and at the ESP site has been infrequent and without debilitating impacts when compared to other "snow" regions in the country, as discussed in Section 2.4.7.3. The presence of snow accumulation could cause blockage of roof drains. The design snow load presented in the PPE is 50 pounds per square foot, which is equivalent to a water depth of 9.6 inches. Because winter PMP depths in the region are greater than 9.6 inches (Reference 13), the design of roofs and roof scuppers for the new units would be evaluated as part of detailed engineering to demonstrate acceptable performance and the results described in the COL application.

2.4.7.7 Effect of Ice and Snow Accumulation on Site Drainage

Historic observations at the ESP site do not indicate the presence of ice and snow that would cause blockage of the storm drains. From the winter air temperature data summarized in Table 2.4-13, mean daily temperatures below freezing in the winter have historically lasted between 5 to 16 consecutive days. This introduces the possibility of blockage of small catch basins and drains. However, the design of on-site drainage facilities would assume that culverts, catch basins, and storm drains are blocked. With this assumption, the drainage facilities would be designed to pass the flows from the PMP without flooding any safety-related facility. Therefore, local flooding produced by PMP, coincident with ice and snow on the ground, would be precluded. Details of site drainage are discussed in Section 2.4.2.3.

2.4.8 Cooling Water Canals and Reservoirs

As described in Section 2.4.1, new Unit 3 would use a once-through cooling system for normal plant cooling. The cooling system would withdraw cooling water at a rate of about 2540 cfs, from a new intake structure located west of the intake structures for the existing units, pump it through the Unit 3 condensers and auxiliary heat exchangers, and discharge it to the WHTF for heat dissipation through a new outfall located adjacent to the existing units' outfall at the head of the discharge channel.

As described in Section 2.4.1, new Unit 4 would use a closed-cycle cooling system with dry- or wet-evaporative cooling towers to transfer the rejected heat to the atmosphere during normal plant

operation. Cooling tower make-up would come from the North Anna Reservoir or an external source, the design and requirements of which would be determined during detailed engineering and described in the COL application. Based on the characterization of the lake water quality at the ESP site, it is estimated that the closed-cycle wet cooling tower system for new Unit 4 would require approximately 44 cfs of make-up water and would discharge about 9 cfs of blowdown during normal plant operation. An equivalent dry cooling system would have minimal make-up water requirements, and no blowdown discharge. A separate screen well and pump house next to the Unit 3 intake structure would be used to supply make-up water to the plant, if necessary. Any blowdown would be discharged to the WHTF via the new outfall.

The UHS for the new units would consist of a mechanical draft cooling tower over a buried water storage basin or other passive water storage facility, as required by the reactor type. These UHS facilities would have their own source of water, independent of the lake, for safety-related cooling in the event that use of the UHS is required. Therefore, the North Anna Reservoir and the WHTF would not be safety-related facilities. The design basis for these existing non-safety-related cooling facilities is discussed in the following paragraphs.

As indicated in Section 2.4.1.2, a series of dikes and canals divide Lake Anna into two segments, the smaller segment forming the WHTF and the larger segment forming the North Anna Reservoir (Figure 2.4-1). Circulating water for the existing units is withdrawn from the North Anna Reservoir at the existing screen well and pump house near the power station and, from there, is pumped through the condenser and discharged through circulating water discharge tunnels into the circulating water discharge canal at the upstream end of the WHTF (Figure 2.4-13). The circulating water then flows through the ponds and interconnecting canals of the WHTF for heat dissipation, and reaches Dike 3 at the easternmost end of the WHTF. Dike 3 contains six submerged adjustable skimmer wall gates through which the circulating water is discharged to the North Anna Reservoir, as shown in Figure 2.4-14. About 40 percent of the rejected heat is lost to the atmosphere in the WHTF, mainly through evaporation. The remaining heat is dissipated in the main reservoir with only a small percentage of heat released from the North Anna Dam. (Reference 1)

Three dikes and two canals form and interconnect the three ponds of the WHTF. Hydraulic losses of circulating water as it flows through the canals and the Dike 3 skimmer wall structure cause the water level in the upstream end of the WHTF to be about 1.5 feet higher than the normal North Anna Reservoir pool level. (Reference 1)

The dikes used to create the WHTF consist of compacted earth materials, except for a 700-foot length of the easternmost dike, Dike 3, which is constructed of dumped rock fill. The submerged skimmer wall discharge structure is constructed within this rock fill section. The rock fill section serves as an emergency overflow for the WHTF. The crest of the rock fill section is at Elevation 253.5 ft msl, while the crest of the earth fill section for the remainder of the dikes is at Elevation 260 ft msl. Thus during high water conditions, when the water level in the WHTF exceeds Elevation 253.5 ft msl, the rock fill section would be overtopped, thereby allowing excess flood

waters to enter the main body of the reservoir without causing the differential level between the reservoir and the WHTF to exceed 2 feet. It is expected that the emergency overflow spillway would operate once in approximately 100 years. (Reference 1)

The earth dikes have a crest width of 26 feet and a side slope of 2.5 to 1 (horizontal to vertical). Each side slope has rip-rap erosion protection. Diversion pipes through the base of each dike, which were necessary for construction purposes, have been closed off with stop logs and left intact during the filling of Lake Anna. (Reference 1)

The discharge canal and the two interconnecting canals in the WHTF are each designed to convey approximately 8000 cfs (Reference 1). This capacity is in excess of the circulating water flow rate of 4246 cfs from the existing units plus the circulating water flow rate of 2540 cfs from the new Unit 3 cooling system and the blowdown discharge rate of 9 cfs from the new Unit 4 cooling system, the total being 6795 cfs. With the addition of Units 3 and 4, the normal design water level of Elevation 251.5 feet for the WHTF would not be affected, since total flow through the facility is less than the original 8000 cfs design capacity of the cooling water canals and discharge structure.

The canals are constructed through soil and bedrock and are unpaved. Erosion protection is provided by vegetation along all banks, except in the vicinity of the circulating water discharge structure at Dike 3, where riprap is provided (Reference 1).

The physical characteristics and design parameters for the North Anna Reservoir and the North Anna Dam are described in Section 2.4.1. Discussion of the PMF level in the North Anna Reservoir and its derivation is provided in Section 2.4.3. The effects of potential dam failures, probable maximum surge and seiche flooding, and ice effect flooding are addressed in Section 2.4.4, Section 2.4.5, and Section 2.4.7, respectively.

2.4.9 Channel Diversions

The possibility of an upstream diversion of the North Anna River is considered extremely remote. Historical information indicates that the river has not had a major change of course in recent history (Reference 1) (Reference 6). Localized ice jams would not create a low-flow period of sufficient duration to affect the cooling water supply.

2.4.10 Flooding Protection Requirements

The maximum design basis Lake Anna flood elevation, discussed in Section 2.4.2, is 267.39 ft msl. This elevation is below the site grade at Elevation 271.0 ft msl. Since the ESP site grade is above the maximum water level, including wind setup and wave runup, the possibility of flooding above-grade, safety-related structures, systems, and components of the new units at the ESP site is precluded. Rip-rap protection of the slope embankment at the circulating water intake location on Lake Anna would be provided to prevent wave activity from eroding the embankment near the on-shore intake structure. It should be noted that although protection would be provided for this structure, the intake is not a safety-related facility.

As mentioned in Section 2.4.2, the effects of intense local precipitation would be considered in the design of drainage facilities for the ESP site. These facilities would be designed such that the peak discharge from the local PMP would not produce flood elevations that would pose a flooding hazard to any safety-related structure, system, or component of the potential new generation units at the ESP site. Additionally, the design of the drainage facilities would incorporate measures to ensure that the existing units safety-related facilities would not be subject to flooding during the construction or operation of the new units. Applicable NRC, federal, state, and local storm water management regulations would be followed in the design of the drainage facilities.

2.4.11 Low Water Considerations

2.4.11.1 Low Flow in Streams

Prior to construction of the North Anna Dam, the average daily flow measured at Doswell, Virginia was 370 cfs (Reference 32). The lowest instantaneous flow recorded at Doswell, Virginia, was 1 cfs; however, the lowest recorded flow for a 24-hour period was 2 cfs. (Reference 1)

Since construction of the dam, minimum release requirements have maintained the low flows in the North Anna River downstream of the dam at flow rates higher than those listed above. For lake water elevations at or above Elevation 248 ft msl, a minimum release of 40 cfs is mandated. For water levels below 248 ft msl the release may be lowered in accordance with the criteria set forth in VPDES Permit Number VA0052451, which requires a minimum instantaneous release from the dam of no less than 20 cfs. (Reference 7) The minimum daily flows recorded at Partlow, Virginia (1978–1995) and Doswell, Virginia (1972–1988) since construction of the dam are 38 and 40 cfs, respectively (Reference 5) (Reference 4). Since 1995, Lake Anna water level and dam operation data compiled by Virginia Power, indicate that the minimum release from the dam during this period was 20 cfs (occurring during severe drought conditions).

Lake Anna, which was formed by the construction of the North Anna Dam on the North Anna River, provides cooling water for the existing units. Lake Anna would also provide cooling water for the new units, as described in Section 2.4.1. Currently, the lake is maintained at an operating water level of 250 ft msl. The existing units can continue to operate with lake water levels as low as Elevation 244.0 ft msl before shutdown of the units must occur in accordance with the plant's Technical Requirements Manual (Reference 33). Changes to the existing intake configuration may lower the shutdown elevation for the existing units to Elevation 242.0 ft msl. For the new units, the anticipated minimum lake level for operation is Elevation 242.0 ft msl. Dominion would work with Virginia Power to change the minimum operating level of the existing units to 242 ft msl. All intake elevations for cooling water and plant service water needs would be based on this elevation, with sufficient margin to ensure plant operation during low water events. The historic low water levels in Lake Anna are discussed in Section 2.4.11.3.

Although low water levels could conceivably require a shutdown of the existing units and the new units, no safety-related structures, systems or components at the existing units or the new units would be affected. Thus, low water levels do not pose a safety-related risk to either the existing or new units. The UHS for the new units would also be unaffected by low water levels in the lake. Details on the design basis for the UHS of the new units are addressed in Section 2.4.11.6.

2.4.11.2 Low Water Resulting from Surges, Seiches, or Tsunami

As discussed in Section 2.4.11.1, Lake Anna does not provide the cooling water to safety-related structures, systems, or components. In accordance with RG 1.70, low water resulting from surges, seiches, or tsunami need only be considered when such conditions could affect safety-related facilities. A low-water surge of 0.3 feet below the lake’s still water level during a probable maximum hurricane has been estimated in the UFSAR for the existing units (Reference 1). Low water conditions as a result of icing have also been considered and are described in Section 2.4.7.

2.4.11.3 Historical Low Water

Table 2.4-5 shows the annual minimum recorded water levels on Lake Anna since the commencement of plant operations in 1978. The lowest minimum recorded water level on the lake was Elevation 245.1 ft msl on October 10, 2002. This low water level followed the driest September to August period and the third driest October to September period in the 108-year record for Virginia state-wide precipitation (Reference 34) (Reference 35). Prior to this historic low, the lowest recorded water level was Elevation 247.4 ft msl in 2001. Since 1978, the water level has fallen below Elevation 248.0 ft msl on five occasions, and below Elevation 247.0 ft msl only once. Historic low water flows are discussed in Section 2.4.11.1.

Table 2.4-5 Lake Anna Annual Minimum Water Level

Year	Minimum Water Level ft msl	Year	Minimum Water Level ft msl	Year	Minimum Water Level ft msl
1978	249.03	1987	248.90	1996	249.80
1979	249.01	1988	248.40	1997	249.10
1980	248.38	1989	249.42	1998	247.60
1981	248.00	1990	249.51	1999	247.60
1982	249.02	1991	248.50	2000	249.20
1983	248.11	1992	249.30	2001	247.40
1984	248.87	1993	247.90	2002	245.10
1985	249.18	1994	249.40		
1986	248.16	1995	248.80		

During drought conditions, the water level in the lake is determined by a combination of the lake inflow, dam release, lake evaporation, and any consumptive uses of water. The heat load rejected from the existing units influences lake evaporation. With the addition of waste heat to the WHTF from the new Unit 3 via its once-through cooling system, lake evaporation would increase and reduce water levels during times of drought when inflow is insufficient to replace outflows from dam releases and evaporation. Unit 4, which would use a closed-cycle cooling system, may withdraw make-up water from the North Anna Reservoir to replace the water lost to evaporation from its cooling towers. During critical low flow periods, however, water from a source other than Lake Anna would be needed to supplement the make-up water supply to maintain acceptable lake levels. The effects of new units on the Lake Anna water levels are discussed in Section 2.4.11.4.

2.4.11.4 Future Controls

Other than the required releases from the North Anna Dam, the only other consumptive water user for Lake Anna is the existing units. To determine the impact of new units on Lake Anna water levels, a water budget analysis of the lake with the existing and future units was performed. This analysis can be found in Part 3: Section 5.2.2. The period analyzed extended from October 1979 to April 2003 with two different water use scenarios investigated, which are described below.

Existing The existing units running at a plant capacity factor of 93%, which is in excess of their historical operating experience.

Proposed The existing units and new Unit 3, all using once-through cooling systems withdrawing water from the North Anna Reservoir and discharging to the WHTF.

The minimum calculated Lake Anna water levels for the Existing and Proposed scenarios are 245.1 and 242.6 ft msl, respectively. The durations of low lake water levels from the analysis are shown in Table 2.4-6. While the type of cooling towers and source of make-up water for Unit 4 have not been determined, the impact on minimum lake level would be constrained to the minimum level required for operations. The impact evaluation would be described in the COL application.

2.4.11.5 Plant Requirements

Based on the calculated water levels and the cooling system selected for the new units, a minimum plant operating lake level would be established in the COL application. When the lake water level falls below this elevation, a plant shutdown sequence would be initiated. All sump inverts, pump levels, and submergence requirements would be based on the minimum plant operating lake level. Lake Anna would not directly supply cooling water to any safety-related facilities and would not serve as the UHS.

Table 2.4-6 Lake Anna Low Water Level Durations

Lake Level (ft, msl)	Percent of the Time Water Level Is Less Than Indicated Value	
	Existing	Proposed
248.0	5.2%	11.6%
246.0	1.1%	3.0%
244.0	0%	1.1%
242.0	0%	0%

Existing – Unit 1 and 2 using once-through cooling

Proposed – Units 1, 2 and 3 using once-through cooling

2.4.11.6 Heat Sink Dependability Requirements

The UHS concept used for the new units would depend on the reactor type selected. According to the PPE, certain reactor types (e.g., the AP-1000, IRIS, and PBMR reactors) do not require a conventional UHS to provide safety-related cooling during emergency shutdown. Some (e.g., the AP-1000 and IRIS reactors) make use of a passive cooling system and utilize water stored in onsite tanks. Others (e.g., the PBMR) provide for safety-related decay heat removal by the RCCS boil-off mode.

For the other three reactor types listed in the PPE and any other reactor requiring a UHS, the concept would consist of a mechanical-draft cooling tower separate from the condenser circulating water system. The UHS cooling tower would be located over a concrete basin water reservoir with sufficient water to maintain the plant in a safe shutdown mode for 30 days. Since the cooling tower basin for the UHS would contain its own 30-day water supply, water levels in Lake Anna would not affect the ability of the UHS to provide emergency cooling for safe shutdown. A detailed description of the UHS, if required by the reactor design selected, would be provided in the COL application.

2.4.12 Groundwater

2.4.12.1 Description and Onsite Use

2.4.12.1.1 Regional Hydrogeology

The region within a 200-mile radius around the ESP site encompasses parts of six physiographic provinces as described in Section 2.5.1.1.1. These include, from east to west, the Continental Shelf, Coastal Plain, Piedmont, Blue Ridge, Valley and Ridge, and Appalachian Plateau Physiographic Provinces. Groundwater occurrence is of significance to the ESP site only within the Piedmont Province. However, a brief discussion of groundwater within the other provinces, except the Continental Shelf off the east coast, is included below to provide a more complete picture of regional hydrogeologic conditions.

Unconsolidated to semiconsolidated deposits and bedrock throughout the region comprise the aquifers and intervening confining layers that determine the hydrogeologic characteristics of the subsurface materials. When two or more aquifers are grouped together they are considered to constitute an aquifer system. Within the site region, the aquifers and aquifer systems have generally been grouped into three categories based on the degree of consolidation of the materials comprising them. (Reference 36) Quaternary age deposits are generally unconsolidated; Cretaceous and Tertiary age materials are generally considered to be semiconsolidated; and Precambrian, Paleozoic, and early Mesozoic age materials are generally consolidated. In some areas, particularly the Piedmont Physiographic Province, unconsolidated materials overlying the bedrock are derived from in situ weathering of the consolidated rock strata. In other areas such as stream valleys, unconsolidated sediments of sand and gravel generally occur as alluvial deposits.

a. Coastal Plain Physiographic Province

Within the Coastal Plain Physiographic Province in the site region (200-mile radius), 6 regional aquifers, consisting primarily of semiconsolidated sands separated by clay confining layers, have been described as comprising the Northern Atlantic Coastal Plain aquifer system. These 6 aquifers, from youngest to oldest, are the: 1) Surficial aquifer, 2) Chesapeake aquifer, 3) Castle Hayne-Aquia aquifer, 4) Severn-Magothy aquifer, 5) Peedee-upper Cape Fear aquifer, and 6) Potomac aquifer. Local aquifers and confining units of limited areal extent and variable thickness comprise all or part of these regional aquifers on a site-specific basis. The Coastal Plain sediments are thin along the western boundary of the province, where they terminate at the contact with the Piedmont Province, and they thicken in an easterly to southeasterly direction. The sediments, ranging in age from Holocene to Early Cretaceous, overlie crystalline igneous and metamorphic rocks that are an eastward extension of the bedrock underlying the Piedmont Physiographic Province. (Reference 36) In Virginia, these sediments reach a thickness of over 3000 feet at the Atlantic Ocean shoreline.

Almost half of Virginia's groundwater use occurs in the Coastal Plain Province. Groundwater is withdrawn from the unconfined Surficial aquifer and from the deeper confined aquifers of the Northern Atlantic Coastal Plain aquifer system. These aquifers are recharged principally in their outcrop area along the western boundary of the province and, to a lesser degree, from leakage through the overlying strata. The thickness and areal extent of the aquifers results in a very large storage capacity for groundwater, more than that of aquifers in any other physiographic province in Virginia. The quality of the groundwater in the 6 regional aquifers is generally good, except where they approach the coastline and saltwater begins to intrude into them. (Reference 37)

The U.S. Environmental Protection Agency (EPA) has designated two aquifers within the Coastal Plain Physiographic Province of Virginia as Sole Source Aquifers. EPA defines a Sole Source Aquifer as:

“...one which supplies at least 50 percent of the drinking water consumed in the area overlying the aquifer. These areas can have no alternative drinking water source(s) that could physically, legally, and economically supply all those who depend upon the aquifer for drinking water.”

The designation protects an area's groundwater resource by requiring that the EPA review any proposed projects receiving federal financial assistance within the designated area. All such projects are subject to review to ensure that they do not substantially impact the groundwater source. The two Coastal Plain Sole Source Aquifers in Virginia are located at the southern end of the Delmarva Peninsula in Accomack and North Hampton Counties, about 120 miles southeast of the ESP site. The aquifers are the Columbia, correlative with the Surficial aquifer, and the Yorktown-Eastover aquifer, correlative with the upper portion of the Chesapeake aquifer. (Reference 38)

An area southeast of the site has been designated as the Eastern Virginia Ground Water Management Area by the VDEQ. Groundwater withdrawal in this area is permitted based on need and an evaluation by the VDEQ of the impacts of proposed withdrawals. The area, comprised of several counties or portions thereof in southeastern Virginia, lies entirely within the Coastal Plain Province. (Reference 39)

b. Piedmont Physiographic Province

In addition to the Surficial aquifer system in the unconsolidated deposits in the Piedmont Physiographic Province in the site region (200-mile radius), three types of aquifers are present within the consolidated rock strata. The consolidated aquifer types are comprised of crystalline and undifferentiated sedimentary rocks, carbonate rocks, and early Mesozoic age rift-basin sedimentary and igneous rocks. Although the crystalline rocks form the predominate aquifers in the Piedmont Province, the carbonate rocks, which are primarily found from Maryland northward in the Piedmont, form the most productive aquifers. (Reference 36) Development of significant water supplies generally occurs within a few hundred feet of the ground surface due to the presence of water-bearing fractures, which tend to decrease in size and number with depth. The potential for groundwater development in the Piedmont Province is much lower than for the Coastal Plain Province. Yields from wells in the Piedmont commonly range from 3 to 20 gallons per minute (gpm). Wells yielding in excess of 50 gpm are considered to be exceptional and are generally in areas of extensive fracture or fault systems that are often found along the western margin of the Piedmont Province at its boundary with the Blue Ridge Mountains. (Reference 37) No Sole Source Aquifers have been designated in the Piedmont Province of Virginia (Reference 38). A more complete description of groundwater conditions in the Piedmont Province in the vicinity of the ESP site is provided in Section 2.4.12.1.2.

c. Blue Ridge Physiographic Province

The Blue Ridge Physiographic Province lies along the western boundary of the Piedmont Province and consists of a relatively narrow band of mountains with the highest elevations in Virginia. Igneous and metamorphic rocks are generally found along the eastern flank of the Blue Ridge Province while sedimentary rocks are generally found on the western flank. Bedrock underlies a generally thin layer of soil and weathered rock. Beneath the weathered zone, the rock is relatively impervious, with groundwater generally occurring in fractures in the rock. (Reference 37)

Groundwater development is most likely achieved along the lower slopes of the mountains. However, well yields are generally low in the Blue Ridge Province (less than 50 gpm) and withdrawal is primarily used for domestic purposes. (Reference 37) (Reference 40) Groundwater emanating from springs is common and is often used as a source of domestic water supply.

d. Valley and Ridge Physiographic Province

The Valley and Ridge Physiographic Province lies about 50 miles west of the ESP site and is separated from the Piedmont Province by the Blue Ridge Province. Aquifers underlying the Valley and Ridge Province occur within Paleozoic age folded and faulted rock strata of sedimentary origin. The strata consist mostly of sandstone, shale, and limestone, with minor amounts of coal, dolomite and conglomerate. Locally, the rocks have been metamorphosed into quartzite, slate, and marble. (Reference 36)

Carbonate and sandstone layers form the principal aquifers in the Virginia through New Jersey portion of the Valley and Ridge Province. Carbonate rocks, primarily limestone, generally form most of the more productive aquifers and underlie valleys within the province. The folded rock strata and network of surface streams in the Valley and Ridge have resulted in the creation of a series of shallow, isolated, local groundwater flow systems. Recharge to these flow systems is generally a result of direct precipitation and the down-gradient movement of surface and subsurface water from the ridges to the valley floors. Groundwater flow paths are generally short, except where carbonate-rock aquifers consist of an extensive network of solution openings. Yields to wells in carbonate-rock strata of the Valley and Ridge Province in western Virginia can range from 150 to 1000 gpm, but may be less in rocks with fewer fractures or solution cavities. (Reference 36)

e. Appalachian Plateau Physiographic Province

The eastern boundary of the Appalachian Plateau Physiographic Province is over 100 miles west of the ESP site. Aquifers underlying the Province occur in Paleozoic age sedimentary rock strata. These strata are nearly flat-lying to gently folded and consist mainly of shale, sandstone, conglomerate, and carbonate rocks. Most of the aquifers are sandstone of Pennsylvanian and Mississippian age. Locally, carbonate rocks of Mississippian age are also

productive aquifers, and small volumes of water are obtained from conglomerate beds of Pennsylvanian age. (Reference 36)

Recharge to the bedrock aquifers in the Appalachian Plateau Province from precipitation is limited due to generally thin soil cover and the highly dissected nature of the land surface, resulting in slopes that facilitate runoff. Groundwater circulation is generally limited to local or intermediate-scale flow systems rather than large-scale regional flow. This results in a relatively shallow zone of fresh water, underlain by saline water or brine within close proximity to the ground surface. The limited circulation of fresh water can generally be attributed to one or more of the following factors:

- the flat-lying nature of the rock strata impeding the vertical movement of groundwater;
- less intense fracturing of the rock strata compared with that in the Valley and Ridge Province and a decrease in the number of fractures with depth; and
- a lack of solution-riddled carbonate rock units like those in the Valley and Ridge Province that facilitate the vigorous circulation of groundwater.

Yields to wells in southwestern Virginia are generally less than 12 gpm but may reach 50 gpm in carbonate rock strata. (Reference 36)

2.4.12.1.2 Local Hydrogeology

Recharge to aquifers in the Piedmont Physiographic Province occurs largely as infiltration of local precipitation in interstream areas. That portion of the precipitation that does not migrate laterally through the unconsolidated surficial materials for discharge to nearby streams or low areas percolates vertically downward to the bedrock, where it enters water-bearing openings in the rock. (Reference 36) The average recharge to aquifers from precipitation in the Piedmont Province of Virginia is estimated to be about 8 to 10 inches per year (Reference 41) (Reference 42). Although an intricate network of rivers and streams that follow a dendritic drainage pattern generally dissects the Piedmont Province, some of the drainage (or portions thereof) follow nearly straight courses that are controlled by joint or fault systems in the underlying bedrock. Those streams passing through the area from other geologic provinces provide a secondary source of recharge to the groundwater. The Piedmont Province of Virginia is estimated to have as much as 1.5 billion gallons of water per square mile held in storage in the consolidated and unconsolidated aquifers. This volume of water is considered suitable for domestic and other small supply requirements. (Reference 42)

In the area around the ESP site, the bedrock consists of Precambrian to Paleozoic age crystalline metamorphic and igneous rocks, while the overlying unconsolidated material is largely a weathering product (residual soil or saprolite) of the underlying bedrock. Groundwater in the crystalline rocks is stored and transmitted through joints and fractures in the rocks, while the main body of the rock between the joints and fractures is essentially impermeable. The number and extent of the

joints/fractures, and the width of the openings between their surfaces, generally decrease with depth, thus limiting the significance of the water-transmitting capability of the bedrock to its upper few hundred feet. (Reference 37)

Saprolite at the ESP site is generally exposed at the ground surface or underlies a thin layer of residual soil or fill. The saprolite extends to the top of the rock from which it was derived; however, the contact between the saprolite and sound rock may be gradational and not well defined (Reference 1). The saprolite is reported to range in thickness from about 2 to 125 feet and is of variable lithology, depending on the type of parent material from which it was derived (Reference 43). Borings drilled as part of the ESP subsurface investigation program penetrated saprolite to depths ranging from about 6 to 35 feet (Appendix 2.5.4B). The saprolite penetrated by these borings is classified as a micaceous, silty-clayey, fine to coarse sand or sandy silt, with occasional rock fragments.

Bedrock beneath the saprolite at the ESP site belongs to the Ta River Metamorphic Suite. In the site area, these rocks are predominantly biotite gneiss and schist with smaller amounts of amphibolite gneiss. (Reference 44) The results of borings at the ESP site indicate the main rock type to be a gneiss. The gneiss is generally described as quartz gneiss with some biotite quartz gneiss; and interbedded quartz gneiss, biotite quartz gneiss, and hornblende gneiss. The rock exhibits a variable weathering profile and joint/fracture presence. The degree of jointing and fracturing is the controlling factor for groundwater movement through the rock.

Groundwater at the ESP site occurs in unconfined conditions in both the saprolite and underlying bedrock. The results of previous investigations at the site indicate that a hydrologic connection exists between the saprolite and the bedrock. (Reference 45) This condition has been confirmed as part of the ESP subsurface investigation program (Appendix 2.5.4B) by the presence of nearly equal water level elevations recorded in two observation wells (OW-845 and OW-846, Table 2.4-15) installed adjacent to each other and sealed in the bedrock and saprolite, respectively. At the ESP site, the water table is considered to be a subdued reflection of the ground surface and, therefore, the direction of groundwater movement is toward areas of lower elevations (Reference 45). Measurements made between December 2002 and June 2003 in observation wells at the site exhibit water level elevations ranging from about Elevation 241 ft msl to Elevation 311 ft msl, with corresponding ground surface elevations of about Elevation 283 and Elevation 335 ft msl, respectively (Table 2.4-15). The measurements shown in Table 2.4-15 represent three quarterly rounds of groundwater level measurements taken at the ESP site to characterize seasonal variability in the water levels. Figure 2.4-15 presents hydrographs based on the water levels provided in this table for the nine observation wells (OW-841 through OW-849) installed as part of the ESP subsurface investigation program. The other wells that were monitored (P- and WP-) were installed previously for NAPS groundwater monitoring purposes around the SWR and the ISFSI, respectively.

A piezometric head contour map (Figure 2.4-16), prepared using the water levels measured in March 2003 (Table 2.4-15), indicates that groundwater flow is generally to the north and east, toward Lake Anna. Freshwater Creek and Elk Creek, both of which flow to Lake Anna, form hydrologic boundaries to the west and south of the site, respectively (Reference 46). Because the water levels in the observation wells are generally above the top of the well screen, the water level elevation represents the piezometric head. An evaluation of the piezometric head contours shown on Figure 2.4-16 indicates a hydraulic gradient toward Lake Anna of about 3 feet per 100 feet. This gradient compares with an initial hydraulic gradient estimated for the site before the filling of Lake Anna of 8 feet per 100 feet. At that time, groundwater flow was toward the North Anna River or its tributaries. (Reference 43) Prior to the filling of Lake Anna, it was estimated that a gradient of 6 feet per 100 feet would develop following filling of the lake (Reference 1).

Prior to construction of the existing units, it was predicted that the filling of Lake Anna would raise the base level of groundwater discharge about 50 feet. It was estimated that this would result in a small rise in the water table where it intersects the surface of the impoundment area. Beyond this zone of intersection, however, it was estimated that the filling of the lake would have only a minor effect on the water table, and that the water table in the area of the existing units would essentially remain unchanged. (Reference 43)

The nine groundwater observation wells installed at the site as part of the ESP subsurface investigation program were tested using the slug test method to determine hydraulic conductivity values for the saprolite and underlying shallow bedrock (Appendix 2.5.4B). Hydraulic conductivities calculated for the saprolite, based on tests in eight of the wells, range from 0.2 to 3.4 ft/day, with a geometric mean value of 1.3 ft/day. The hydraulic conductivity of the shallow bedrock, as determined from two tests in one of the wells, is estimated to be about 2 to 3 ft/day, although the results of the test are of limited value due to the short duration of stable water level recovery measurements. Table 2.4-16 summarizes the available hydraulic conductivity data.

Laboratory tests performed on samples of saprolite from the site indicate a bulk density for this material of 125 to 130 pounds per cubic foot (pcf). Bulk densities for the bedrock range from 145 pcf for highly to moderately weathered rock to 163 pcf for moderately weathered to fresh rock. Laboratory tests to determine moisture contents of saprolite samples indicate an average moisture content of about 26 percent, while the moisture content in the vadose zone ranges from about 11 to 40 percent with an average of about 22 percent. Using the average moisture content of 26 percent and a value of 2.68 for the specific gravity of the saprolite (Reference 1), the void ratio of the saprolite is estimated to be about 0.7. A total porosity of about 41 percent is estimated from this void ratio and an effective porosity of about 33 percent is estimated based on 80 percent of the total porosity. The specific yield of the saprolite at the ESP site was not determined; however, an estimate of this value taken from published literature for materials of similar composition indicates that it may be in the range of 0.30 to 0.33 (Reference 47).

Based on the estimated hydraulic gradient, hydraulic conductivity, and effective porosity indicated above, groundwater beneath the ESP site is expected to flow toward Lake Anna at a rate of about 0.12 ft/day. Using a distance of approximately 1800 feet from the center of the overall plant footprint for the new units to the closest point along the shoreline of Lake Anna, the groundwater travel time from the ESP site to Lake Anna is estimated to be about 40 years.

2.4.12.1.3 Plant Groundwater Use

Groundwater withdrawal for use by the existing units is accomplished from 4 water supply wells permitted for public use by the Virginia Department of Health (VDH). These 4 wells (Nos. 2, 3A, 4 [new], and 6) comprise a single water supply system at the site. A 5th well (No. 4 [old]) was originally part of this system but is no longer used and is considered to be available for emergency purposes only. A separately permitted (NANIC) well provides the water supply for the North Anna Nuclear Information Center. A new well was constructed at the site in 2003 to support an increase in water demand at the security training building. The proposed location of this well was evaluated by the VDH prior to its construction. The locations of these wells are shown on Figure 2.4-17 and the wells are described in Table 2.4-17. Four small wells not requiring permits at the NAPS site provide minor additional water for plant use (Reference 6). The locations of these 4 wells are not well documented. One of the wells is likely to be the well used to supply the Metrology laboratory and its location is shown on Figure 2.4-17. A second well is located at the Security Training Building in the vicinity of the newly constructed well described above.

The four active wells comprising the primary groundwater supply system for the existing units have individual capacities ranging from 9 to 55 gpm and a total capacity of 160 gpm. However, these four wells are permitted for a total design capacity of only 53,040 gpd or about 37 gpm. This capacity is currently dictated by the available storage tank capacity at the site. The NANIC well has a measured capacity of 74 gpm but a design capacity of 19,600 gpd or only about 14 gpm. (Reference 48) (Reference 49)

As a condition of the well permits, Virginia Power is required to submit an annual report of water withdrawals for the previous year to the VDEQ by January 31 of each year. Table 2.4-18 shows the monthly withdrawal quantities that were reported for the year ending December 31, 2002. It can be determined from this table that the four combined primary wells withdrew a combined average of almost 14 gpm for the year, and that the NANIC well withdrew an average of a little over 1 gpm. The highest total monthly withdrawal in 2002 for the five wells averaged almost 38 gpm in January. This is less than the highest previously reported monthly withdrawal average of 41 gpm in March 1994 (Reference 6). The four wells not requiring permitting are also not required to report their withdrawals, but based on their small size and limited use they are not expected to add more than 1 or 2 gpm to the average withdrawal by the permitted wells (Reference 6).

Any groundwater supply required by the new units would likely come from an increase in the storage capacity for the existing wells or from drilling additional wells. In either event, additional

groundwater withdrawal by the new units is not expected to impact any offsite wells due to: 1) their distance from the site, 2) the direction of the hydraulic gradient toward Lake Anna and the lake's recharge effect, and 3) the existence of hydrologic divides between the ESP site and the offsite wells.

2.4.12.2 Groundwater Sources and Use

Groundwater for use in the vicinity of the ESP site is obtained from springs and wells in either the saprolite or underlying crystalline bedrock. Most wells completed in the saprolite have been excavated either by hand digging or augering. These wells are susceptible to becoming dry due to seasonal fluctuations in the water table. Drilled wells generally extend through the saprolite to depths of up to several hundred feet in the underlying bedrock. These wells are cased from the ground surface to the top of bedrock. (Reference 50) The production of groundwater in the vicinity of the ESP site is generally not sufficient to satisfy large water demands because of the relatively low yield of the aquifers, as discussed in Section 2.4.12.1.2. The majority of groundwater development in the area is for domestic and agricultural use, with some public, light industrial and commercial use (Reference 45).

There are no known users of large quantities of groundwater within 25 miles of the ESP site (Reference 1). The vast majority of wells in the area yield less than 50 gpm (Reference 50). Based on the presence of Lake Anna and the hydrologic boundary it presents to groundwater movement north and east of the ESP site, further discussion of groundwater use in the vicinity of the site is limited to Louisa County.

Every 5 years, the USGS compiles national water-use estimates and publishes a report containing the results of this effort. Data from the latest available report, for the year 1995, are provided on the USGS website for Virginia, by county or independent city (Reference 51). The following groundwater withdrawal estimates for Louisa County, in millions of gallons per day (mgpd), are provided by withdrawal category:

- Public water supply = 0.18 mgpd
- Domestic water supply = 1.45 mgpd
- Commercial/Industrial water supply = 0.10 mgpd
- Thermoelectric power water supply = 0.02 mgpd
- Agricultural water supply = 0.05 mgpd

The VDEQ requires that any groundwater user in Virginia whose average daily withdrawal during any single month exceeds 10,000 gpd provide a report by January 31 of each year containing water withdrawal and use data for the previous year. The only exceptions to this regulation are agricultural users who have slightly modified requirements based on their location, withdrawal or withdrawal facility. (Reference 8) For the year 2001, no withdrawals were reported for Louisa County that meet or exceed this threshold.

A study previously performed for Louisa County included the compilation and evaluation of records of wells permitted by the Louisa County Health Department (Reference 50). These records addressed 2155 drilled wells and 1743 dug or augered (bored) wells. The majority of the drilled wells serve single-family residences. The locations of the wells are currently referenced only to county tax maps.

The average yield of all wells in Louisa County is estimated to be about 14.5 gpm. However, the average yield of public wells is estimated to be about 42 gpm. The public water supply wells have an average depth of nearly 300 feet, and almost all are less than about 400 feet deep. The residential wells are generally only 100 to 200 feet deep. The Louisa County and previous studies in the Piedmont Province suggest that yields from individual wells in this area can vary greatly over distances as small as 100 feet. (Reference 50)

Recent evidence for a connection between well yield and Lake Anna is contained in the Lake Anna Special Area Plan (Reference 52). This plan indicates that average well yields are higher in areas adjacent to Lake Anna than in other areas of the Lake Anna watershed, which are, in turn, slightly higher than in other areas of Louisa County. It has been concluded that these higher yields are likely due to the presence of Lake Anna, which enhances groundwater recharge.

There are 29 public water supplies in Louisa County that obtain their water from springs or wells. Data describing these public water supplies are presented in Table 2.4-19. The public supplies closest to the existing units are Lake Anna Plaza, about 2.6 miles to the northwest, and Jerdone Island, about 4.3 miles to the south-southeast. Based on their distance from the ESP site and the presence of one or more arms of Lake Anna between the site and these public water supplies, any impact the new units may have on the aquifers beneath the site is not expected to affect these supplies. Likewise, withdrawal by these public supplies would not affect the ability of the new units to withdraw groundwater for potable water needs.

Private water wells provide about 80 percent of the domestic water supply to residents of Louisa County (Reference 53). The residential water supply well nearest the existing units is located about one mile to the south-southeast in Lot 32 of the Aspen Hill subdivision. Based on its distance from the ESP site and the presence of Sedges Creek between the ESP site and this well, any impact the new units may have on the aquifers beneath the site would not affect the domestic water supply provided by this well. Likewise, withdrawal by the well would not affect the ability of the new units to withdraw groundwater for potable water needs.

Population growth projections for Louisa County by the year 2015 range from about 32,000 to 46,000. Such growth would result in an estimated public water supply demand of between 2.8 and 4.1 mgd for an average day and between 4.5 and 6.6 mgd on a peak day. This water supply demand is expected to be satisfied largely by the use of surface water sources such as Northeast Creek Reservoir and Lake Gordonsville. However, these sources are expected to be supplemented by groundwater supply where available. To meet projected water demands beyond the year 2015, a

large groundwater supply may need to be considered in conjunction with the development of alternative surface water sources. (Reference 50)

2.4.12.3 **Monitoring or Safeguard Requirements**

Groundwater monitoring for the ESP site takes place through programs implemented for both the existing units and as part of Dominion's ESP effort. Current groundwater monitoring programs for the existing units are addressed in Station Administrative Procedure Number VPAP-2103N (Reference 54), and NAPS Engineering Periodic Test Procedure Number 0-PT-75.7 (Reference 55). The results of these programs are reported to the NRC on a yearly or as-required basis.

Station Administrative Procedure Number VPAP-2103N, the Offsite Dose Calculation Manual (ODCM) for the existing units, establishes the requirements for the Radiological Environmental Monitoring Program and specifies the conduct of the program. Groundwater samples are collected and tested in accordance with the directions provided in the ODCM.

Engineering Periodic Test Procedure Number 0-PT-75.7 provides instructions for measuring and evaluating groundwater levels beneath the SWR with respect to seepage through the embankment. Seven open-tube standpipe piezometers (P-10, P-14, and P-18 through 22) are currently monitored in accordance with the test procedure, along with two additional piezometers (P-23 and P-24) that are monitored for information purposes only Figure 2.4-16.

A third groundwater monitoring effort at the site consists of three monitoring wells located around the ISFSI. These wells, shown as WP-1 through WP-3 in the ISFSI SAR, Figure 2-11 (Reference 46), are sampled yearly and the samples are tested for radiological constituents in accordance with a request from the Louisa County Board of Supervisors.

Because the existing units groundwater monitoring wells were not considered to be of sufficient areal extent to determine groundwater levels beneath the ESP site, 9 additional observation wells were installed as part of the ESP subsurface investigation program. Water levels in these 9 wells and 10 of the existing units' monitoring wells are being measured quarterly for one year to provide data on groundwater flow direction, gradient, and seasonal groundwater level fluctuations at the site.

As part of detailed engineering, an evaluation of the existing NAPS groundwater monitoring programs, with respect to placement of the new units, would be performed to determine if any additional sampling of existing wells or construction of new monitoring wells would be required to adequately monitor for impacts on groundwater. This evaluation would include a review of the observation wells installed for the ESP application to determine if they can be used as part of any longer-term groundwater monitoring program. The results would be described in the COL application.

Safeguards would be used to minimize the potential for adverse impacts to the groundwater by construction and operation of the new units. These safeguards may include the use of lined containment structures around storage tanks and hazardous materials storage areas, emergency cleanup procedures to capture and remove surface contaminants, or other measures deemed necessary to prevent or minimize adverse impacts to the groundwater beneath the ESP site.

2.4.12.4 Design Bases for Subsurface Hydrostatic Loading

The existing units plant grade is at Elevation 271 feet. The containment (reactor) building and associated structures for new units on the ESP site would be constructed at the same plant grade elevation. Previous studies conducted for NAPS resulted in a prediction that maximum groundwater elevations beneath the site in the plant area could reach as high as Elevation 265 to 270 feet (Reference 1). This estimate was based on a simplified water table profile sloping uniformly from Elevation 271 feet at the toe of the slope south of abandoned Units 3 and 4 (north of the SWR) to Elevation 250 feet at Lake Anna.

One groundwater observation well (OW-844) was constructed at the existing plant grade as part of the ESP subsurface investigation program (Appendix 2.5.4B). The well is located near the toe of the slope north of the SWR (Figure 2.4-16). A second well (OW-841) was constructed in the partially backfilled excavation for abandoned Units 3 and 4. The top of this well is about 20 feet below the plant grade. Maximum measured groundwater level elevations in these wells ranged from about Elevation 250 feet in OW-841 to Elevation 267 feet in OW-844 between December 2002 and June 2003 (Table 2.4-15). Considering the general conformance of the location of OW-844 with the water table profile discussed above, these groundwater levels and the piezometric head contours shown on Figure 2.4-16 appear to support the design groundwater level determined for the existing units as described above.

Based on the preceding information, a design groundwater level ranging from Elevation 265 to 270 feet in the plant area of the ESP site appears to be reasonable. For other structures that may be constructed at higher elevations in support of new units on the ESP site, a higher design groundwater level may be justified.

2.4.13 Accidental Releases of Liquid Effluents to Ground and Surface Waters

The PPE approach adopted in this ESP application allows for the possibility of different reactor designs at the ESP site. The locations, volumes, and radionuclide inventories of any above- or below-ground tanks that might be associated with these designs are currently unknown. Therefore, appropriate source term values would be developed and the consequences of accidental releases of liquid effluents to ground and surface waters would be evaluated in the COL application. The results of these analyses would be provided in the COL application and reviewed against the applicable 10 CFR 20 effluent limits.

Section 2.4 References

1. Updated Final Safety Analysis Report, Rev. 38, North Anna Power Station, Virginia Power.
2. USGS 01670180 Pamunkey Creek at Lahore, VA, U. S. Geological Survey, 2003. Available at waterdata.usgs.gov/nwis/nwisman/?site_no=01670180&agency_cd=USGS. Accessed February 3, 2003.
3. USGS 01670300 Contrary Creek Near Mineral, VA, U. S. Geological Survey, 2003. Available at waterdata.usgs.gov/nwis/nwisman/?site_no=01670300&agency_cd=USGS. Accessed February 3, 2003.
4. USGS 01671000 North Anna River Near Doswell, VA, U. S. Geological Survey, 2003. Available at waterdata.usgs.gov/nwis/nwisman/?site_no=01671000&agency_cd=USGS. Accessed January 28, 2003.
5. USGS 01670400, North Anna River Near Partlow, VA., U. S. Geological Survey, 2003. Available at waterdata.usgs.gov/nwis/nwisman/?site_no=01670400&agency_cd=USGS. Accessed January 28, 2003.
6. North Anna Power Station Units 1 and 2, Appendix E – Applicant’s Environmental Report, Operating License Renewal Stage, Dominion, May 2001.
7. Permit No. VA0052451. Authorization to Discharge Under the Virginia Pollutant Discharge Elimination System and the Virginia State Water Control Law, Virginia Electric & Power Company, North Anna Nuclear Power Station, Commonwealth of Virginia, Department of Environmental Quality, 2001.
8. Virginia DEQ Water Programs, Water Withdrawal Reporting, Virginia Department of Environmental Quality, October 18, 2002. Available at www.deq.state.va.us/water/waterwith.html,
9. ANSI/ANS-2.8-1992, Determining Design Basis Flooding at Power Reactor Sites, American National Standard, American Nuclear Society, July 1992.
10. Hydrometeorological Report No. 51, Probable Maximum Precipitation Estimates, United States East of the 105th Meridian, Office of Hydrology, National Weather Service, National Oceanic and Atmospheric Administration, June 1978.
11. Hydrometeorological Report No. 52, Application of Probable Maximum Precipitation Estimates - United States East of the 105th Meridian, Office of Hydrology, National Weather Service, National Oceanic and Atmospheric Administration, August 1982.

12. Hydrometeorological Report No. 33, Seasonal Variation of the Probable Maximum Precipitation East of the 105th Meridian for Areas from 10 to 1000 Square Miles and Durations of 6, 12, 24, and 48 Hours, U.S. Weather Bureau, 1956.
13. Hydrometeorological Report No. 53, Seasonal Variation of 10-Square-Mile Probable Maximum Precipitation Estimates – United States East of the 105th Meridian, Office of Hydrology, National Weather Service, National Oceanic and Atmospheric Administration, April 1980.
14. Computer Program 723-X6-L2010, HEC-1 Flood Hydrograph Package. (MAP193), Version 4.0, Computer Program and User's Manual, Hydrologic Engineering Center, U.S. Army Corps of Engineers, September 1990.
15. Local Climatological Data, Annual Summaries for 1999, Part 1 Eastern Region, National Climatic Data Center, National Oceanic and Atmospheric Administration, 2000.
16. TD3240, U.S. Hourly Precipitation Data, Volumes 1 and 2, CD ROM Data Set, Forecast Systems Laboratory and National Climatic Data Center, National Oceanic and Atmospheric Administration, July 1998.
17. Linsley, Ray K., Jr., Max A. Kohler, Joseph L. H. Paulhus. Hydrology for Engineers, Third Edition, McGraw-Hill Book Company, 1982.
18. NUREG/CR-2639, Historical Extreme Winds for the United States – Atlantic and Gulf of Mexico Coastlines, U.S. Nuclear Regulatory Commission, May 1982.
19. ACER Technical Memorandum No. 2, Freeboard Criteria and Guidelines for Computing Freeboard Allowances for Storage Dams, Assistant Commissioner – Engineering Research, U.S. Bureau of Reclamation, December 1981.
20. Shore Protection Manual, Volumes 1 and 2, Fourth Edition, Coastal Engineering Research Center, Waterways Experiment Station, U.S. Army Corps of Engineers, 1984.
21. *Report on Design and Stability of North Anna Dam for Virginia Electric and Power Company, Amendment 15 to the North Anna 1 and 2 Preliminary Safety Analysis Report (PSAR).* Virginia Electric and Power Company, May 7, 1971.
22. Regulatory Guide 1.70, *Standard form and Content of Safety Analysis Reports for Nuclear Power Plants*, LWR Edition, Revision 3, office of Standards Development, U.S. Nuclear Regulatory Commission, November 1978.
23. *Flood Insurance Rate Map, Louisa County, VA and Incorporated Areas*, Federal Emergency Management Agency, U.S. Department of Interior, November 1997.

24. Local Climatological Data Annual Summary and Comparative Data, National Climatic Data Center, 2001.
25. Daly, Steven F. *Frazil Ice Blockage of Intake Trash Racks*, U.S. Army COE CRREL, Technical Digest No. 91-1, March 1991.
26. Griffen, A. V. *The Occurrence and Prevention of Frazil Ice at Water supply Intakes*, Research Branch Pub No. W43, Ministry of the Environment, Toronto, Ontario, 1973.
27. Carstens, T. *Heat Exchange and Frazil Formation*, IAHR, ICE Symposium, Reykjavik, 1970.
28. Carey, L. Kevin. *Ice Blockage of Water Intakes*, U.S. Army COE, CRREL, NUREG/CR-0548, Hanover, NH, March 1979.
29. Chow, Ven. T. *Handbook of Applied Hydrology*, McGraw Hill Inc., 1964.
30. *Engineering and Design Prediction and Calculation of Incremental Ice Thickening*, Engineering Technical Letter, Personal Communication, U.S. Army COE, June 1981.
31. Uzuner, S. M., and John F. Kennedy. *Stability of Floating Ice Blocks*, ASCE Jour of the HYD Division, HY 12, December 1972.
32. *Surface Water Supply of the United States, 1966-70, Part 1, North Atlantic Basins, Volume 3. Basins from Maryland to York River*, Geological Survey Water-Supply Paper 2103, U.S. Department of Interior, Geologic Survey, 1976
33. *Technical Requirements Manual for North Anna Units 1 & 2*. Revision 28, Dominion, August 1, 2002.
34. *Climate of 2002 – August Virginia Drought*, National Oceanic And Atmospheric Administration, National Climatic Data Center, accessed online at lwf.ncdc.noaa.gov/oa/climate/research/2002/aug/st044dv00pcp200208.html, accessed April 22, 2003.
35. *Climate of 2002 – September Virginia Drought*, National Oceanic And Atmospheric Administration, National Climatic Data Center, accessed online at lwf.ncdc.noaa.gov/oa/climate/research/2002/sep/st044dv00pcp200209.html, accessed April 23, 2003.
36. Trapp, H., Jr., and M. A. Horn. *Ground Water Atlas of the United States, Segment 11, Delaware, Maryland, New Jersey, North Carolina, Pennsylvania, Virginia, West Virginia*, U.S. Geological Survey, Hydrologic Investigations Atlas 730-L, 1997.

37. Poff, J. A., *A Guide to Virginia's Ground Water*, Virginia Water Resources Research Center, Virginia Polytechnic Institute and State University, Blacksburg, Virginia, www.vwrrc.vt.edu/publications/publicat.htm, 1999.
38. *Source Water Protection, Designated Sole Source Aquifers in EPA Region III, District of Columbia, Delaware, Maryland, Pennsylvania, Virginia, West Virginia*, U.S. Environmental Protection Agency, Region 3, Water Protection Division, www.epa.gov/OGWDW/swp/ssa/reg3.html, November 26, 2002.
39. *Status of Virginia's Water Resources, A Report on Virginia's Water Supply Planning Activities*, A Report to the Honorable James S. Gilmore III, Governor, and the General Assembly of Virginia, Virginia Department of Environmental Quality, available at www.deq.state.va.us/pdf/gareports/waterresources2001.pdf, October 2001.
40. Sinnott, A., and E. M. Cushing. *Summary Appraisals of the Nations's Ground-Water Resources – Mid-Atlantic Region*, U.S. Geological Survey, Professional Paper 813-I, 1978.
41. van der Leeden, F., *Water Atlas of Virginia*, Tennyson Press, Lexington, Virginia, 1993.
42. Powell, J. D., and J. M. Abe. *Availability and Quality of Ground Water in the Piedmont Province of Virginia*, U.S. Geological Survey, Water Resources Investigations Report 85-4235, 1985.
43. *Report, Site Environmental Studies, Proposed North Anna Power Station, Louisa County, Virginia*, (included in Units 1 and 2 PSAR as Appendix A), Dames & Moore, January 13, 1969.
44. Mixon, R. B., L. Pavlides, D. S. Powars, A. J. Froelich, R. E. Weems, J. S. Schindler, W. L. Newell, L. E. Edwards, and L. W. Ward. *Geologic Map of the Fredericksburg 30' x 60' Quadrangle, Virginia and Maryland*, U.S. Geological Survey, Geologic Investigations Series Map I-2607, 2000.
45. *Report, Site Environmental Studies, North Anna Nuclear Power Station, Proposed Units 3 and 4, Louisa County, Virginia*, Dames & Moore, August 18, 1971.
46. *Independent Spent Fuel Storage Installation Safety Analysis Report, North Anna Power Station, Units 1 and 2*, Revision 3, Virginia Electric and Power Company, June 2002.
47. McWhorter, D. B., and D. K. Sunada. *Ground-Water Hydrology and Hydraulics*, Water Resources Publications, Littleton, Colorado, 1977.
48. *Water Description Sheet*, Virginia Health Department, January 15, 1998.
49. *Engineering Description Sheet*, Virginia Health Department, June 17, 1991.

50. *County of Louisa, Water Quality Management Plan and Groundwater Study*, Thomas Jefferson Planning District Commission, Virginia Division of Mineral Resources, Louisa County Planning Department, Louisa County Water Authority, Draper Aden Associates, January 1998.
51. *Total Water Withdrawals for Virginia, 1995*, U.S. Geological Survey, va.water.usgs.gov/w_use/wu_index.htm, January 2, 2003.
52. *Lake Anna Special Area Plan*, Lake Anna Special Area Plan Committee, March 2000.
53. NUREG-1437, *Generic Environmental Impact Statement for License Renewal of Nuclear Plants, Supplement 7, Regarding North Anna Power Station, Units 1 and 2*, U.S. Nuclear Regulatory Commission, Office of Nuclear Reactor Regulation, Division of Regulatory Improvement Programs, November 2002.
54. VPAP-2103N, *Offsite Dose Calculation Manual (North Anna)*, Rev. 4, Station Administrative Procedure, Dominion.
55. 0-PT-75.7, *Service Water Reservoir – Ground Water Level*, Engineering Periodic Test, Rev. 7, Dominion, December 2002.
56. *Report of Installation of Standpipe Piezometers Along the Toe of the Service Water Reservoir, North Anna Power Station Units 1 and 2*, Virginia Geotechnical Services, P.C., July 21, 1998.
57. *Annual Report of Water Withdrawals, North Anna Nuclear Power Plant, January 1, 2002 to December 31, 2002*, submitted to Virginia Department of Environmental Quality by Dominion, January 31, 2003.
58. *Safe Drinking Water Information System (SDWIS), Virginia, Louisa County*, U.S. Environmental Protection Agency, www.epa.gov/enviro/html/sdwis/sdwis_query.html, April 16, 2003.
59. *Engineering Description Sheet*, Virginia Health Department, July 24, 1991.
60. *Engineering Description Sheet*, Virginia Department of Health, February 28, 2003.

Table 2.4-7 Probable Maximum Precipitation Temporal Distribution

Time (hours)	Time Increment	Incremental PMP Depth (in)
0 to 6	12	0.29
6 to 12	11	0.29
12 to 18	10	0.39
18 to 24	9	0.59
24 to 30	4	1.27
30 to 36	2	3.67
36 to 42	1	17.71
42 to 48	3	2.24
48 to 54	5	1.27
54 to 60	6	1.07
60 to 66	7	0.98
66 to 72	8	0.88

Table 2.4-8 February 1979 Rainfall Data

Date	Time	Station Measured Precipitation (in.)			
		Columbia #44192900 (3 mi ²)	Piedmont #44671200 (307 mi ²)	Elkwood #44272900 (34 mi ²)	Basin Weighted Average
24 Feb	6am – 9am	0	0	0	0.00
	9am – 12pm	0.6	0.4	0.3	0.39
	12pm – 3pm	0.3	0.5	0.6	0.51
	3pm – 6pm	0.5	0.3	0.3	0.30
	6pm – 9pm	0.8	0.5	0.3	0.48
	9pm – 12am	0.1	0.1	0.1	0.10
	25 Feb	12am – 3am	0	0	0.1
3am – 6am		0	0	0	0.00
6am – 9am		0.1	0	0	0.00
9am – 12pm		0	0	0	0.00
12pm – 3pm		0.3	0.1	0	0.09
3pm – 6pm		0.6	0.6	0.7	0.61
6pm – 9pm		0.2	0.3	0.4	0.31
9pm – 12am		0.1	0.1	0.4	0.13
Total		3.6	2.9	3.2	2.94

Table 2.4-9 March 1994 Rainfall Data

Date	Time	Station Measured Precipitation (in.)			
		Bremo Bluff #440399302 (0 mi ²)	Culpeper #44215904 (343 mi ²)	Richmond #44720102 (0 mi ²)	Basin Weighted Average
27 Mar	12am – 3am	0	0	0	0.00
	3am – 6am	0.2	0.4	0.01	0.40
	6am – 9am	0.7	0.7	0.43	0.70
	9am – 12pm	0	0.1	0.46	0.10
	12pm – 3pm	0	0	0	0.00
	3pm – 6pm	0	0	0	0.00
	6pm – 9pm	0.3	0.2	0	0.20
	9pm – 12am	0.2	0.5	0.44	0.50
28-Mar	12am – 3am	0.5	0.7	0.01	0.70
	3am – 6am	0.4	0.3	0	0.30
	6am – 9am	0.3	0.1	0.12	0.10
	9am – 12pm	0.2	0	0.32	0.00
	12pm – 3pm	0	0	0.04	0.00
	3pm – 6pm	0.1	0.1	0.1	0.10
	6pm – 9pm	0.1	0.3	0.05	0.30
	9pm – 12am	0.2	0.2	0.15	0.20
29 Mar	12am – 3am	0.3	0.2	0.2	0.20
	3am – 6am	0.2	0.19*	0.17	0.19
	6am – 9am	0.1	0.06*	0.02	0.06
	9am – 12pm	0	0.04*	0.07	0.04
	Total	3.8	4.1	2.59	4.09

* Due to missing data at the station, the value is estimated from data at Richmond and Bremo Bluff.

Table 2.4-10 June 1995 Rainfall Data

Date	Time	Station Measured Precipitation (in)		
		Piedmont #44671204 (343 mi ²)	Richmond #44720102 (0 mi ²)	Basin Weighted Average
27 Jun	12am – 3am	0.7	0.0	0.7
	3am – 6am	1.7	0.0	1.7
	6am – 9am	3.4	0.0	3.4
	9am – 12pm	0.1	0.0	0.1
	12pm – 3pm	0.0	0.0	0.00
	3pm – 6pm	0.0	0.02	0.00
	6pm – 9pm	0.0	0.0	0.00
	9pm – 12am	0.0	0.0	0.00
	Total	5.9	0.02	5.90

Table 2.4-11 Lake Anna Watershed HEC-1 Precipitation Loss Rates

Storm	HEC-1 Precipitation Loss Coefficients			
	DKLTR	ERAIN	RTIOL	STRKR
June 1972*	4.02	0.55	3.86	0.44
April 1973*	1.93	0.34	22.07	0.14
March 1975*	0.00	0.52	10.39	0.12
1976 PMF Storm	2.00	0.47	12.11	0.233
February 1979	0.00	0.60	12.11	0.01
March 1994	0.80	0.55	12.11	0.10
June 1995	5.20	0.50	12.11	0.15
2003 PMF Storm	1.37	0.54	12.11	0.10

* Storms investigated in 1976 PMF analysis

ERAIN - Exponent of precipitation for loss rate function
 RTIOL – Loss coefficient recession constant
 STRKR – Initial value of loss coefficient (in/hr)
 DKLTRR – Initial accumulated rain loss during which the loss coefficient is increased (in)

Table 2.4-12 Historic Minimum Intake Water Temperature of Less Than 4°C (39.2°F) During The Operation of North Anna Units 1 and 2 from 1978 to 2001

Date	Temperature Range °C (°F)	Remarks
Feb 7, 1979–Feb 24, 1979	1.2–3.7 (34.2–38.7)	Only Unit 1 was in Operation
Feb 2–Feb 21, 1980	2.8–3.9 (37–39)	Only Unit 1 was in Operation
Jan 14–Feb 5, 1982	2.1–3.8 (35.8–38.8)	Unit 2 was put into operation in Fall 1980
Feb 1–Feb 7, 1985	3.0–3.9 (37.4–39)	Units 1 and 2 in operation
Dec 24, 1989–Jan 4, 1990	2.9–3.6 (37.2–38.5)	Units 1 and 2 in operation
Jan 19–28, 1994	2.1–3.9 (35.8–39 F)	Units 1 and 2 in operation
Feb 3–10, 1996	3.1–3.8 (37.6–38.8)	Units 1 and 2 in operation
Jan 26–29, 2001	3.6–3.8 (38.5–38.8)	Units 1 and 2 in operation

Table 2.4-13 Historic Winter Minimum and Mean Low Daily Temperature with Durations Equal to or Exceeding 5 Days in Richmond, Virginia, for the Period of 1961 to 1995 (Reference 24)

Year	Month	Number of Consecutive Days	Temperature °C (°F)	
			Minimum	Mean
1964	Jan	7	-8.2 (17.2)	-4.2 (24.4)
1966	Jan/Feb	14	-10.8 (12.5)	-4.9 (23.1)
1968	Jan	8	-7.8 (18)	-4.9 (23.2)
1970	Jan	7 & 6	~-14 & ~-11 (~7 & ~13)	-7.9 & -6.6 (17.7 & 20.2)
1970/71	Dec/Jan	9	-3.7 (25.4)	-1.7 (29)

Table 2.4-13 Historic Winter Minimum and Mean Low Daily Temperature with Durations Equal to or Exceeding 5 Days in Richmond, Virginia, for the Period of 1961 to 1995 (Reference 24)

Year	Month	Number of Consecutive Days	Temperature °C (°F)	
			Minimum	Mean
1973	Feb	5	-4.8 (23.4)	-2.8 (27)
1977	Jan & Feb	24**, 5 & 3	-13.16, -6.45, & -5.54 (8.34, 19.49 & 22.03)	-4.82, -3.66, & -5.03 (23.32, 25.42, & 22.95)
1978	Feb	11	-6.39 (20.5)	-3.8 (25.2)
1979	Feb	16	-12.7 (9.2)	-5.8 (21.6)
1980	Jan/Feb	9	-4.9 (23.2)	-2.6 (27.3)
1984	Jan	13*	-9.2 (15.4)	-3.6 (25.6)
1988	Jan	8	-8.2 (17.3)	-2.6 (27.4)
1989	Dec	10	-10.2 (13.7)	-5.9 (21.3)
1994	Jan	8	-14.6 (5.8)	-7.1 (19.2)

* One day with T=0.03°C (32.06°F) is included.

** Two non-consecutive days with temperature greater than 0°C (32°F)

Table 2.4-14 Annual Peak Discharges On the North Anna River

Water Year	Date ^a	Peak Flow at Doswell (cfs) ^b	Peak Flow at Partlow (cfs) ^c	Peak North Anna Reservoir Water Level at Dam (ft, msl)
1972	Jun. 22, 1972	23,300	- ^d	239.0 ^e
1973	Apr. 28, 1973	7100	-	-
1974	Sep. 7, 1974	6180	-	-
1975	Sep. 26, 1975	11,600	-	-
1976	Jan. 1, 1976	6520	-	-
1977	Oct. 21, 1976	4160	-	-
1978	Jan 26, 1978	9730	-	-
1979	Feb. 26, 1979	13,900 ^f	11,700	252.00
1980	Oct. 2, 1979	7700 ^f	6050	251.10
1981	Feb. 11, 1981	-	87	248.95
1982	Feb. 4, 1982	4750	4080	250.90
1983	Apr. 25, 1983	5990	5200	250.97
1984	Mar. 30, 1984	11,700	9030	251.72
1985	Feb 2., 1985	4650 ^g	2240	250.34
1986	Nov. 5, 1985	10,700 ^f	8690	251.51
1987	Apr. 17, 1987	-	6660	251.16
1988	Nov. 30, 1987	-	4810	250.80
1989	May 6, 1989	-	6680	251.25
1990	May 29, 1990	-	5230	250.89
1991	Jan. 12, 1991	-	4620	250.74
1992	Feb. 26, 1992	-	1970	250.20
1993	Mar. 5, 1993	-	8230	251.80
1994	Nov. 28, 1993	-	8690	251.60
1995	Jun. 27, 1995	-	11,700	252.00

- a. Date shown corresponds to peak flow shown at Parlow and peak North Anna Reservoir water level.
- b. Gage # 01671000, Drainage Area: 441 square miles.
- c. Gage # 01670400, Drainage Area: 344 square miles.
- d. Blank cells (-) represent dates outside the period of data record or missing data.
- e. Lake Anna Reservoir was not yet completely filled.
- f. The peak discharge at Doswell occurred one day later than indicated at Partlow.
- g. The peak discharge at Doswell occurred on Aug. 19, 1985.

Table 2.4-15 Quarterly Groundwater Level Elevations

Observation Well No.	Well Depth* (ft)	Reference Point Elev. (ft)	Reference Point Stickup** (ft)	Top of Well Screen Elev. (ft)	Well Screen Length (ft)	Groundwater Level Elevations		
						12/17/02	03/17/03	06/17/03
OW-841	34.3	251.6	1.5	228.1	9.7	248.9	249.6	249.6
OW-842	49.6	336.7	1.5	297.8	9.6	307.5	308.9	310.8
OW-843	49.2	320.6	1.5	282.1	9.7	285.1	288.1	290.8
OW-844	24.6	273.5	1.5	257.6	9.6	265.5	266.7	267.3
OW-845	55.0	297.3	1.5	253.0	9.7	272.7	274.9	277.4
OW-846	32.7	297.3	1.5	273.5	9.8	272.5	274.8	277.1
OW-847	49.8	319.7	1.5	280.6	9.6	285.4	287.0	289.5
OW-848	47.3	284.5	1.5	240.8	5.0	241.7	242.9	243.6
OW-849	49.8	298.5	1.5	259.4	9.7	265.5	269.5	271.7
P-10	22.5	286.4	2.4	267.0	5	274.4	274.8	275.2
P-14		327.1				271.6	272.2	272.8
P-18		329.0				285.7	286.5	287.5
P-19	58.5	322.3			5	284.3	285.2	286.3
P-20	61.0	320.6			5	274.9	275.4	275.8
P-21	58.5	319.2			5	Dry	261.2	262.0
P-22	60.0	320.5			5	276.8	277.8	278.6
P-23	41.2	296.4	1.9	258.7	5	261.1	262.6	263.3
P-24	25.0	293.4	2.3	271.3	5	276.4	277.1	278.4
WP-3		317.9(?)		266.5	5	299.7	301.0	302.8
Lake Anna Water Level Elevation						248.1	250.1	250.4
Service Water Reservoir Water Level Elevation						314.6	313.3	314.6

OW- wells installed in December 2002 as part of ESP Subsurface Investigation Program.

P- wells installed previously to monitor NAPS Units 1 and 2 Service Water Reservoir.

WP- well installed previously as part of Interim Spent Fuel Storage Installation monitoring program.

* Below ground surface at time of installation.

** Above ground surface at time of installation.

Note: Blank entries indicate data not available.

Table 2.4-16 Hydraulic Conductivity Values

Observation Well No.	Depth Interval Tested (ft)	Elevation	Material	Hydraulic Conductivity	
				cm/sec	ft/day
PT-1 ^(a)	Near-surface	Unknown	Saprolite	2.8×10^{-5}	0.08
PT-2 ^(a)	Near-surface	Unknown	Saprolite	1.4×10^{-5}	0.04
P-10 ^(b)	14.5 - 22.5	269.5 - 261.5	Saprolite	6.1×10^{-4} to 6.1×10^{-5}	1.7 to 0.17
P-24 ^(b)	16.8 - 25.0	274.3 - 266.1	Saprolite	2.9×10^{-4} to 6.6×10^{-6}	0.8 to 0.02
P-23 ^(b)	33.7 - 41.2	260.7 - 253.2	Saprolite	6.6×10^{-5}	0.19
OW-844 ^(c)	12.7 - 24.6	259.3 - 247.4	Saprolite	9.9 to 8.9×10^{-5}	0.28 to 0.25
OW-841 ^(c)	20.1 - 34.3	230.0 - 215.8	Saprolite	8.2 to 7.8×10^{-4}	2.3 to 2.2
OW-846 ^(c)	20.3 - 32.7	275.5 - 263.1	Saprolite	1.2×10^{-3} to 6.8×10^{-4}	3.4 to 1.9
OW-847 ^(c)	35.0 - 49.8	283.2 - 268.4	Saprolite	2.3 to 2.1×10^{-4}	0.66 to 0.58
OW-842 ^(c)	35.3 - 49.6	299.9 - 285.6	Saprolite	3.3×10^{-4}	0.93
OW-849 ^(c)	35.6 - 49.8	261.4 - 247.2	Saprolite	1.1×10^{-3} to 7.0×10^{-4}	3.2 to 2.0
OW-843 ^(c)	36.4 - 49.2	282.7 - 269.9	Saprolite	4.9 to 4.5×10^{-4}	1.4 to 1.3
OW-848 ^(c)	39.1 - 47.3	243.9 - 235.7	Saprolite	1.2×10^{-3} to 9.9×10^{-4} ^(d)	3.4 to 2.8 ^(d)
OW-845 ^(c)	39.7 - 55.0	256.1 - 240.8	Quartz Gneiss	1.1×10^{-3} to 6.3×10^{-4} ^(e)	3.1 to 1.8 ^(e)

Laboratory Test Results

B-48 ^a	3.5	290.5	Sandy silt	1×10^{-6}	0.003
B-8 ^a	5.5	293.5	Fine sand, tr. silt	1×10^{-6}	0.003
B-2 ^a	15.5	269.5	Fine to med. sand, w/clayey silt	4×10^{-5}	0.11
B-15 ^a	36	281	Silty fine sand	1.3×10^{-5}	0.04

a. Reference 43

b. Reference 56

c. Appendix 2.5.4B

d. Results may not be accurate due to static water level approximately 0.5 ft below top of well screen.

e. Results may not be accurate due to short duration of stable water level recovery measurements.

Table 2.4-17 North Anna Power Station Water Supply Wells

Well	Depth (ft)	Measured Yield (gpd)	Design Yield (gpd)	Water Treatment
No. 2 (a,b)	385	12,960	53,040	Chlorination (normally not in use)
No. 3A (a,b)	185	74,880		
No. 4 (new) (a,b)	305	63,360		
No. 6 (a,b)	375	79,200		
No. 4 (old) (a,b) (not used)	200	77,760	NA	NA
NANIC (a,c)	260	106,560	19,600	Calcite filtration
Security Training Building	Unknown	Unknown	Unknown	Unknown

a. Reference 50

b. Reference 48

c. Reference 49

**Table 2.4-18 North Anna Power Station Groundwater Use^a
January 1, 2002 to December 31, 2002 (Millions of Gallons)**

Month	Well #2	Well #3A	Well #4	Well #6	NANIC
January	0.0032	0.4268	0.4519	0.7444	0.0485
February	0.0032	0.1395	0.4010	0.5095	0.0467
March	0.0025	0.0263	0.1050	0.1642	0.0555
April	0.0046	0.0368	0.1253	0.1459	0.0474
May	0.0076	0.0376	0.2565	0.1041	0.0690
June	0.0021	0.0531	0.2524	0.1458	0.0502
July	0.0018	0.0511	0.3585	0.0189	0.0525
August	0.0077	0.0611	0.3434	0.0526	0.0656
September	0.0071	0.1020	0.4018	0.1655	0.0474
October	0.0062	0.0874	0.2118	0.1574	0.0651
November	0.0148	0.0694	0.2126	0.1846	0.0586
December	0.0037	0.2005	0.0648	0.2070	0.0482
Total	0.0645	1.2916	3.1850	2.5999	0.6547
Monthly Average	0.0054	0.1076	0.2654	0.2167	0.0546

a. Reference 57

Table 2.4-19 Public Groundwater Supplies In Louisa County

Installation	Type^(a)	Water Source	Depth (ft)	Measured Yield (gpd)	Design Yield (gpd)	Population Served^(a)
Town of Louisa ^(b) (primary source is surface water)	Community	spring	NA	38,880		1950
		3 wells	200–405	43,200–53,280		
Town of Mineral ^(b)	Community	2 springs	NA	57,600		670
		4 wells	200–600	14,400–165,600		
Acorn West Trailer Park ^(b)	Community	well	120	8640		70
Blue Ridge Shores ^(b)	Community	4 wells	163–405	288,000	160,000	1380
Bumpass Park/Lake Anna Rescue ^(a)	Non-Community					250
Burger King Zion Crossroads ^(a)	Non-Community					250
Christopher Run Campground ^(a)	Non-Community					608
Crescent Inn Restaurant ^(a)	Non-Community					200
Crossing Point (VA Oil Co) ^(b)	Non-Community	2 wells	305	21,600–28,800	10,400	45
East End Elementary School ^(b)		well	345	61,920	31,200	
Expressions Learning Center ^(b)	Non-Community	well	205	17,280		45
Jerdone Island ^(b,c)	Community	well	200	83,520	19,600	49
Jouette Elementary School ^(b)	Non-Community	well	345	61,920	19,600	741
Klockner Barrier Films ^(b)		well	305	53,280	22,000	
Klockner-Pentaplast ^(b)	Non-Community	2 wells	205 - 280	21,600 - 57,600	44,000	526
Lake Anna Family Campground ^(a)	Non-Community					240
Lake Anna Plaza ^(d)	Community	2 wells	335 - 230	11,520 - 86,400	41,200	
Louisa County Zion Crossroads ^(a)	Non-Community					30
Louisa Water Authority ^(b)		well	550	34,560		

Table 2.4-19 Public Groundwater Supplies In Louisa County

Installation	Type ^(a)	Water Source	Depth (ft)	Measured Yield (gpd)	Design Yield (gpd)	Population Served ^(a)
Prospect Hill ^(a)	Non-Community					50
Shenandoah Crossing ^(b)	Non-Community	2 wells	280 - 300	123,840 - 97,920	98,400	850
Siebert's Amoco & Dairy Queen ^(a)	Non-Community					25
Six-o-Five Village ^(b)	Community	2 wells	310 - 365	64,800 - 10,800	10,700	201
Small Country Campground ^(a)	Non-Community					112
Tavern on the Rail ^(a)	Non-Community					150
Trevillians Elementary School ^(b)	Non-Community	well	204	57,600	19,600	676
Trevilians Square Apartments ^(a)	Community					61
Twin Oaks Community ^(b)	Community	well	250 ^(e)	7200		75
West End Elementary School ^(b)		well	204	57,600	20,000	

Note: Blank entries indicate data not provided in cited reference.

- a. Reference 59
- b. Reference 50
- c. Reference 59
- d. Reference 60
- e. Reference 1

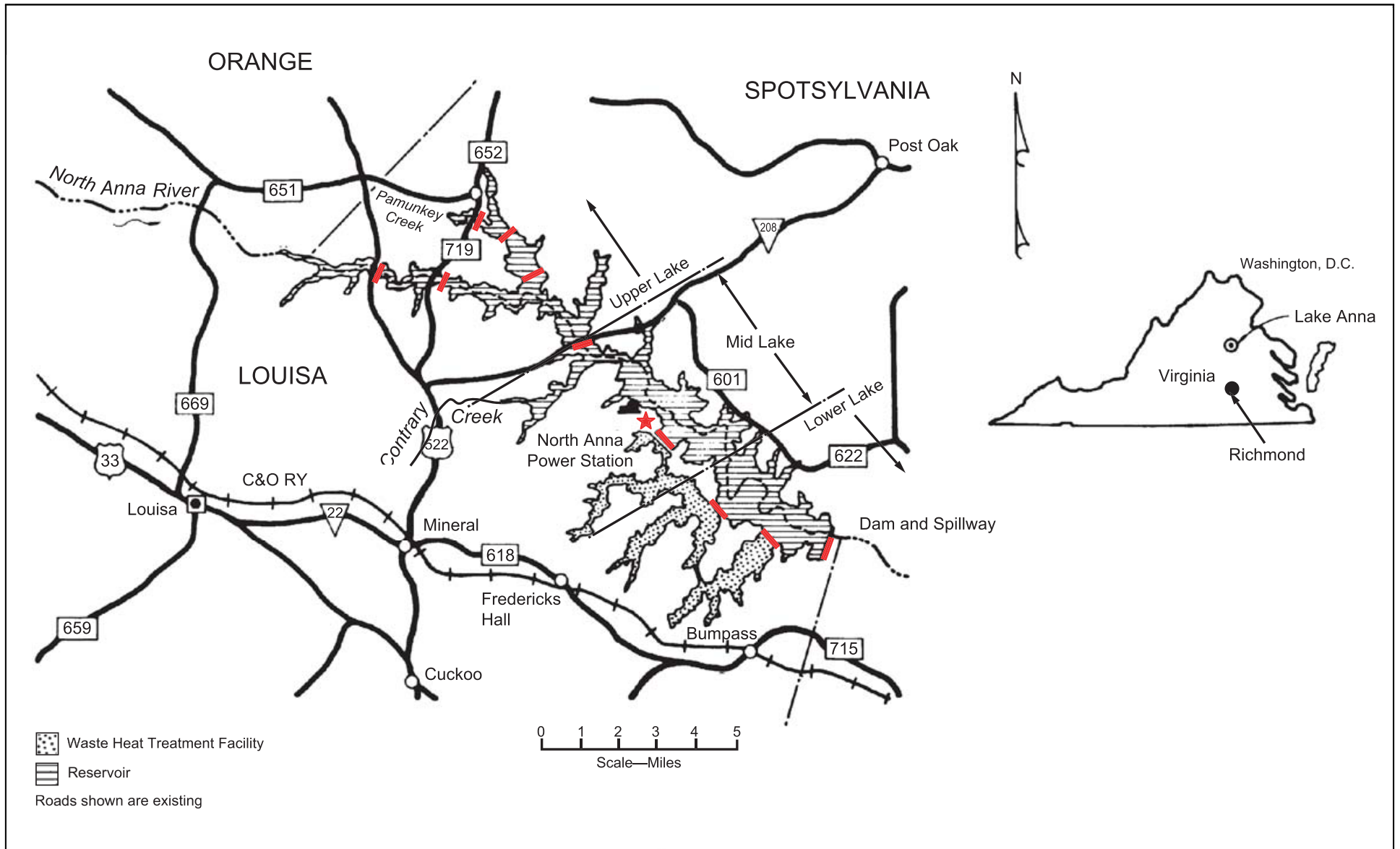


Figure 2.4-1 Lake Anna Hydrologic Features

Figure 2.4-2 Deleted

|

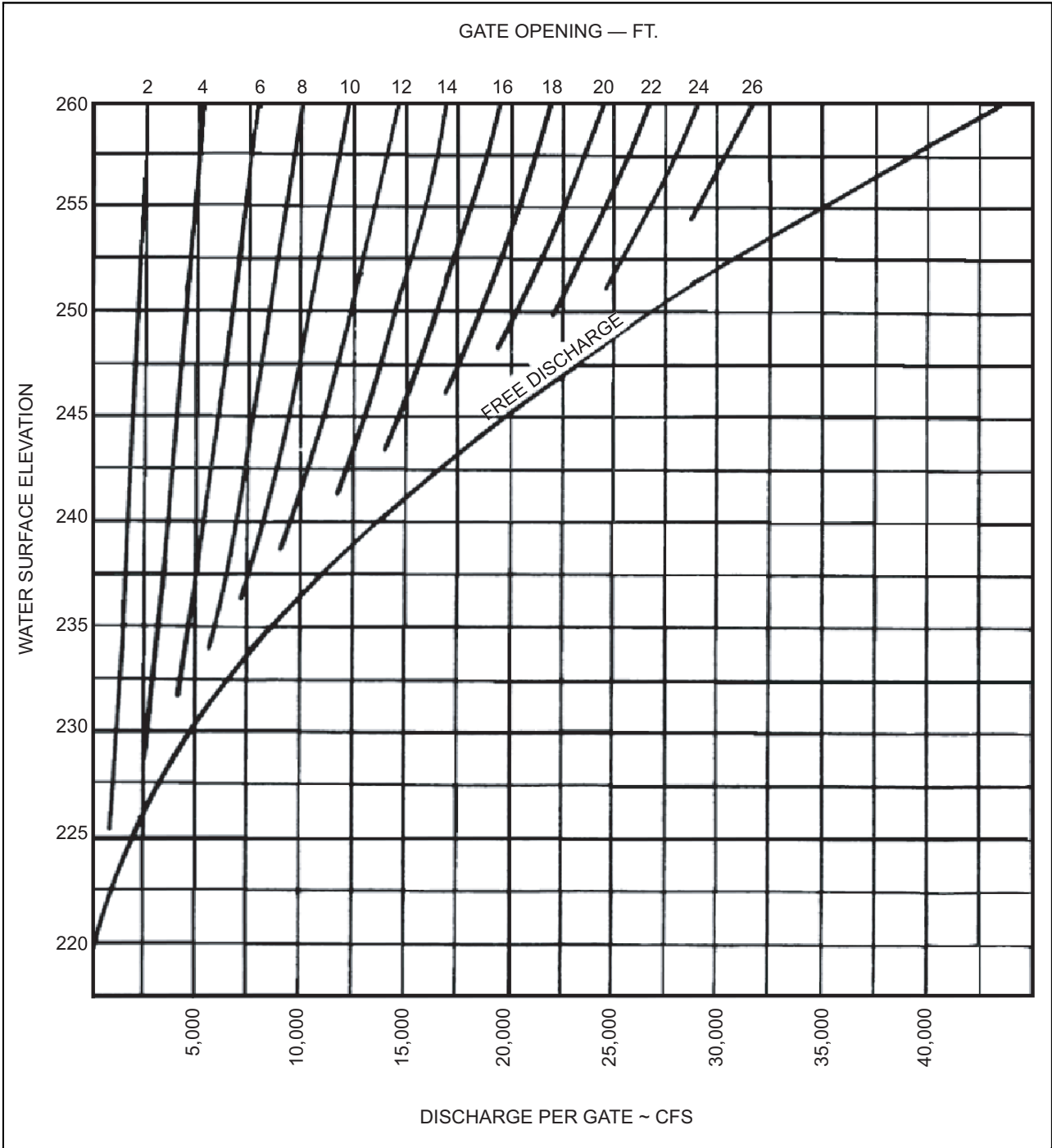


Figure 2.4-3 Spillway and Discharge Capacity (One Gate of Three) North Anna Dam

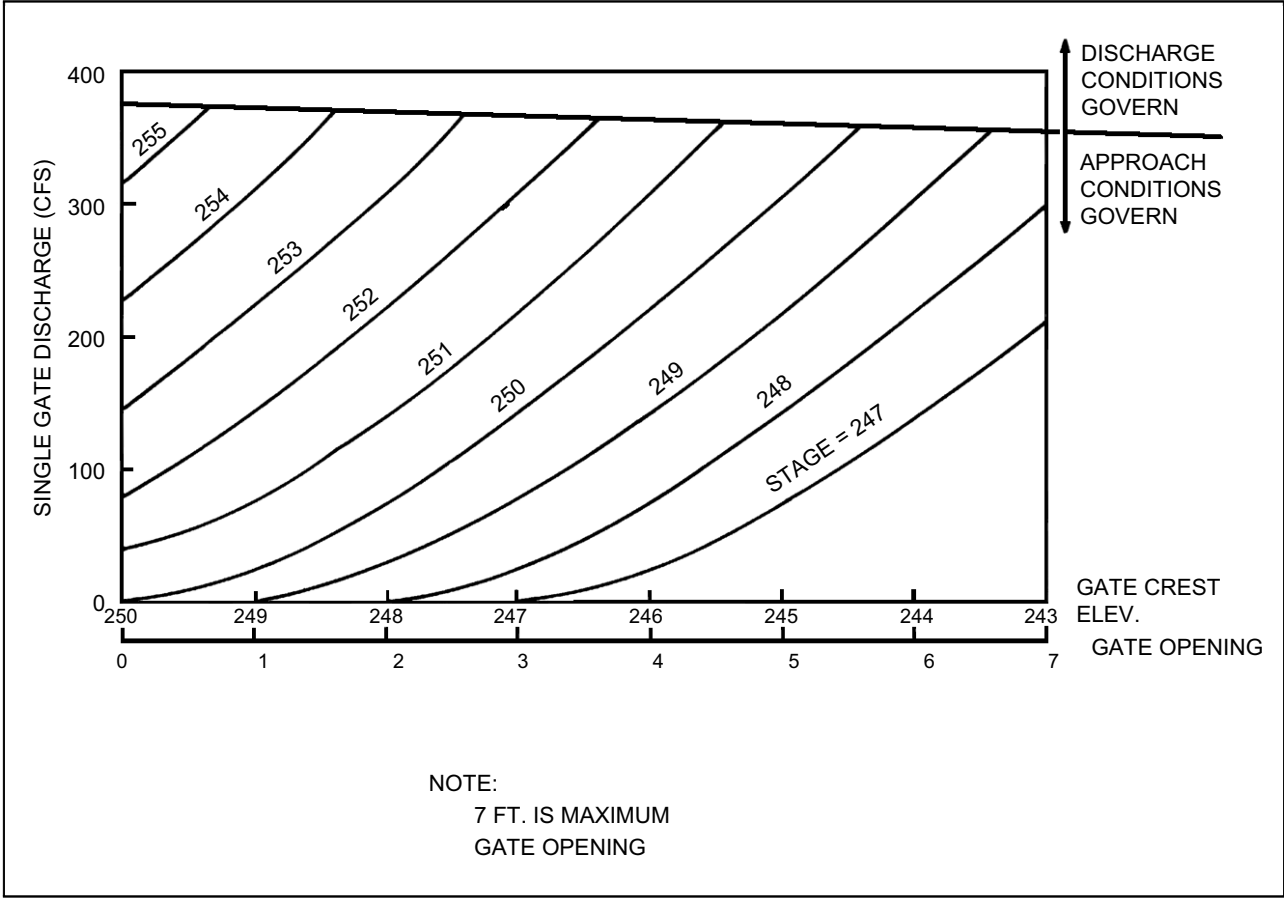


Figure 2.4-4 Skimmer Gate Discharge Capacity North Anna Dam

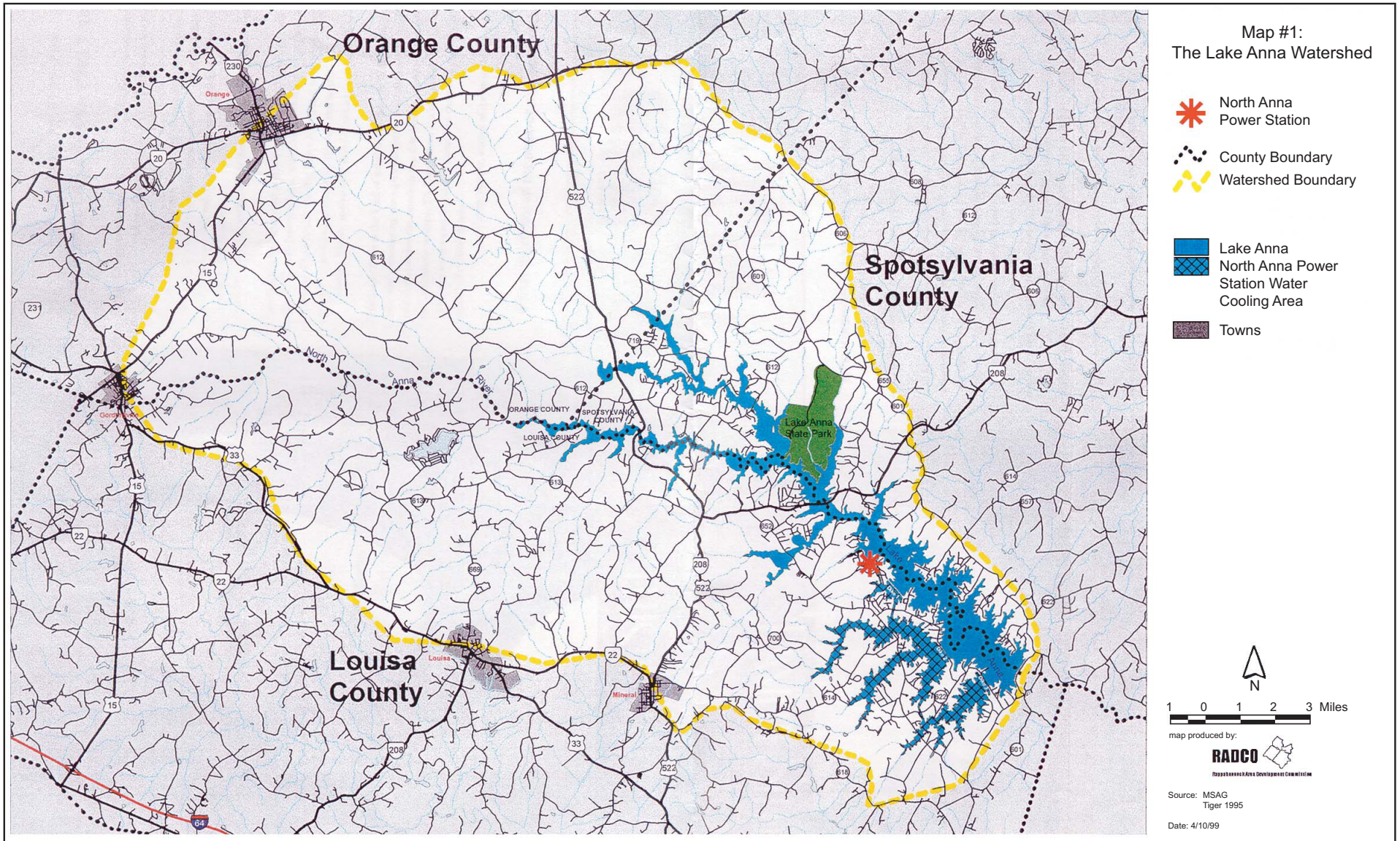


Figure 2.4-5 Combined Lake Anna and WHTF Drainage Area

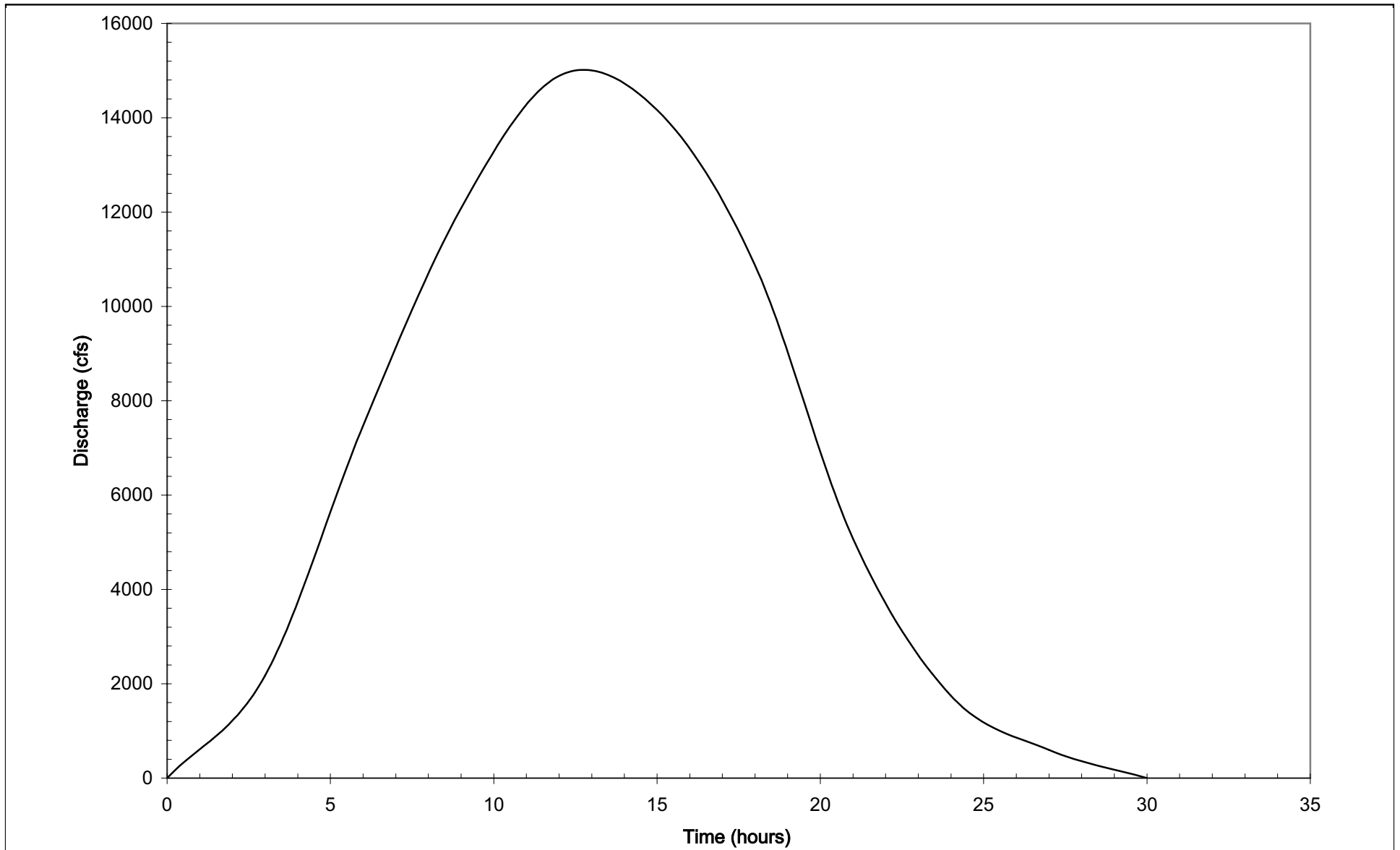


Figure 2.4-6 Combined North Anna Reservoir and WHTF Watershed: 3-Hour Unit Hydrograph

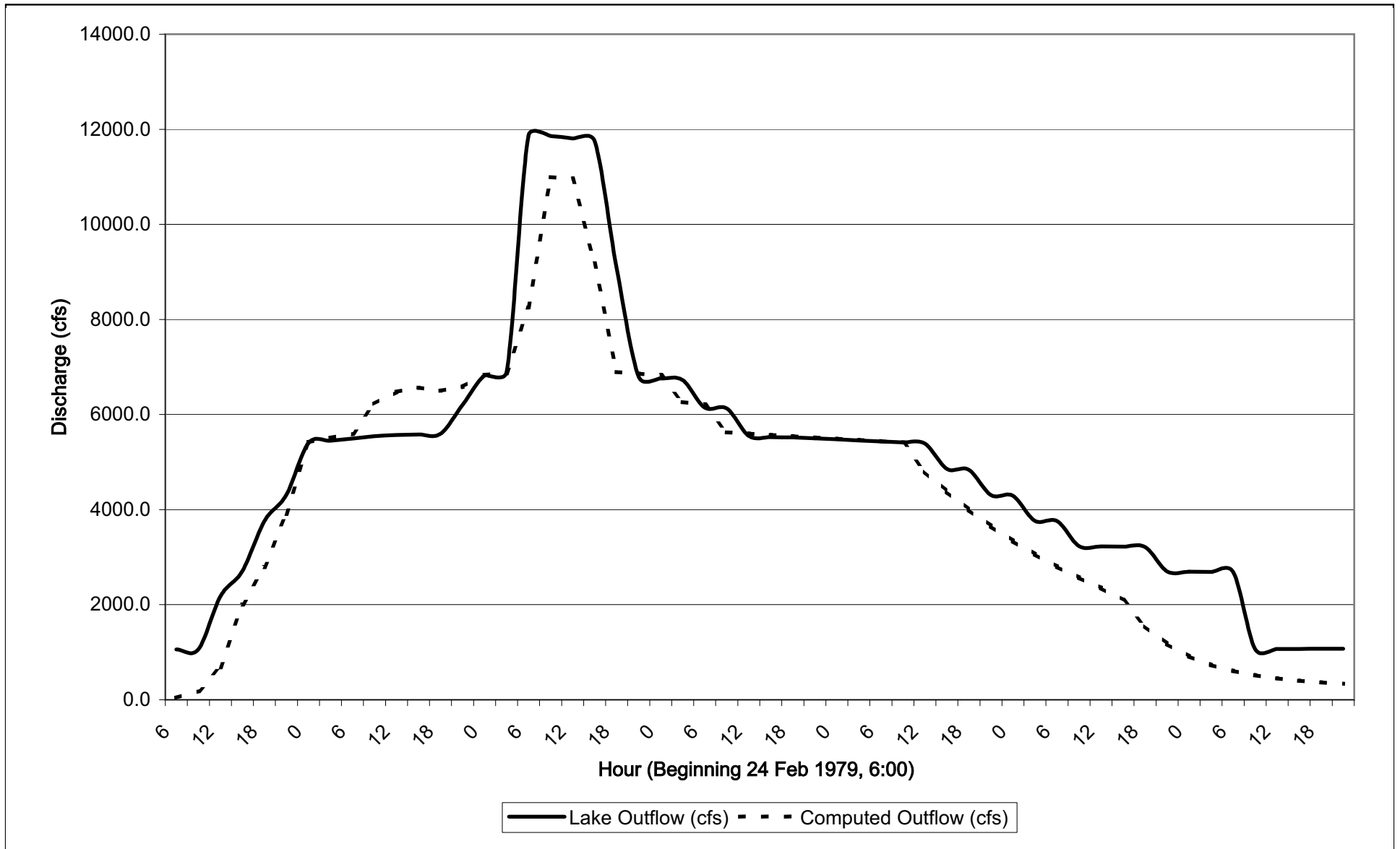


Figure 2.4-7 1979 Storm Outflow Hydrograph Comparison

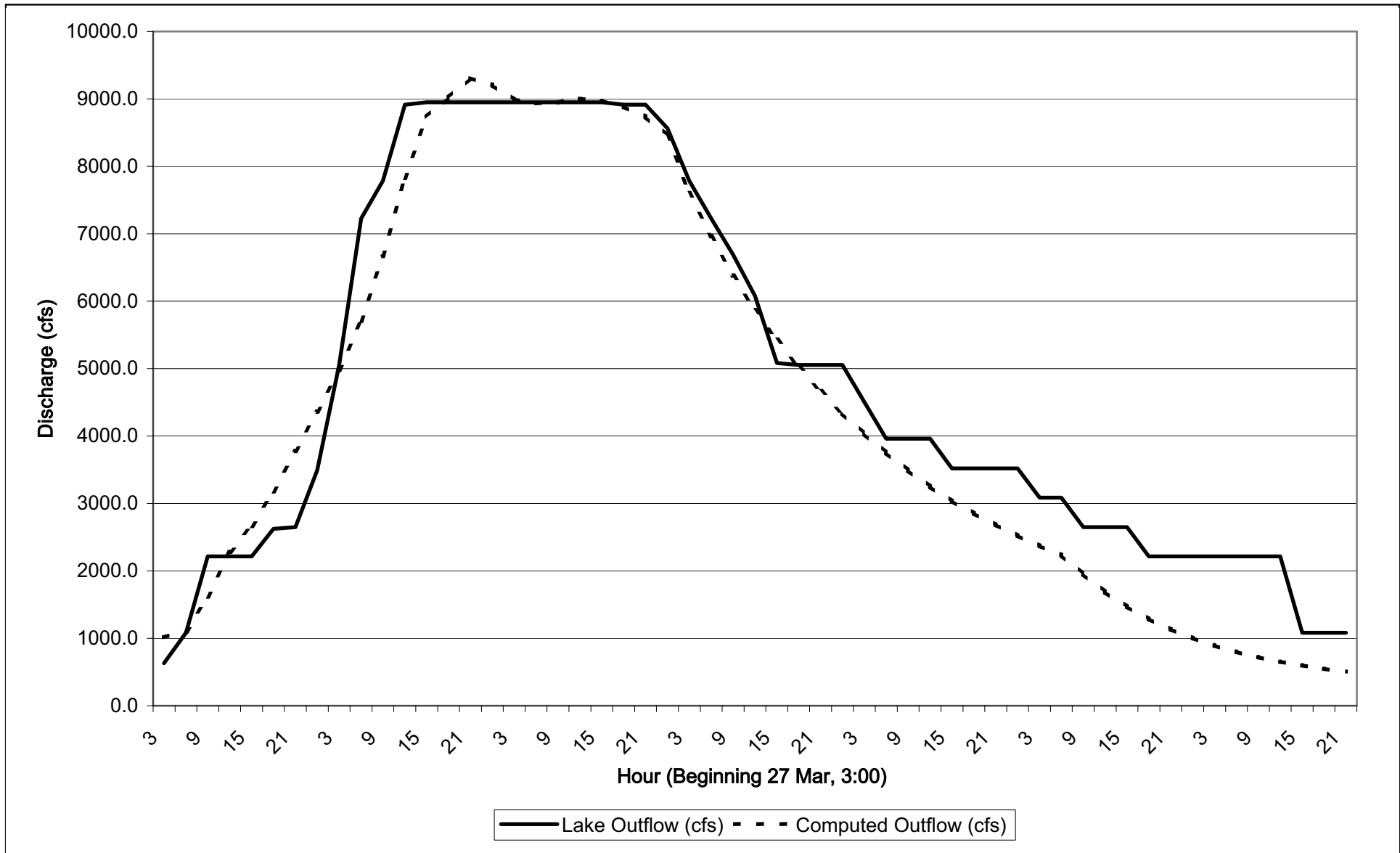


Figure 2.4-8 1994 Storm Outflow Hydrograph Comparison

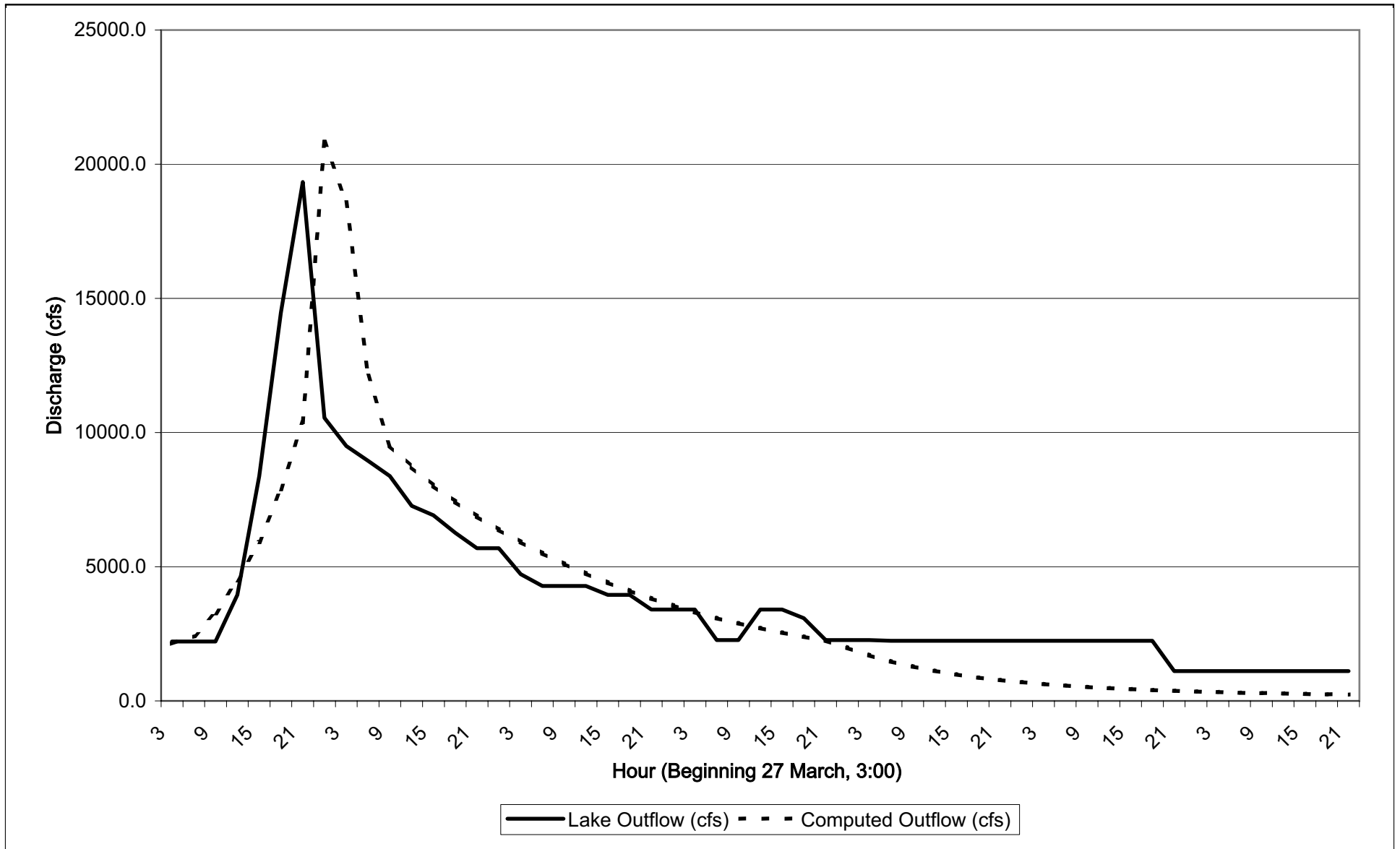


Figure 2.4-9 1995 Storm Outflow Hydrograph Comparison

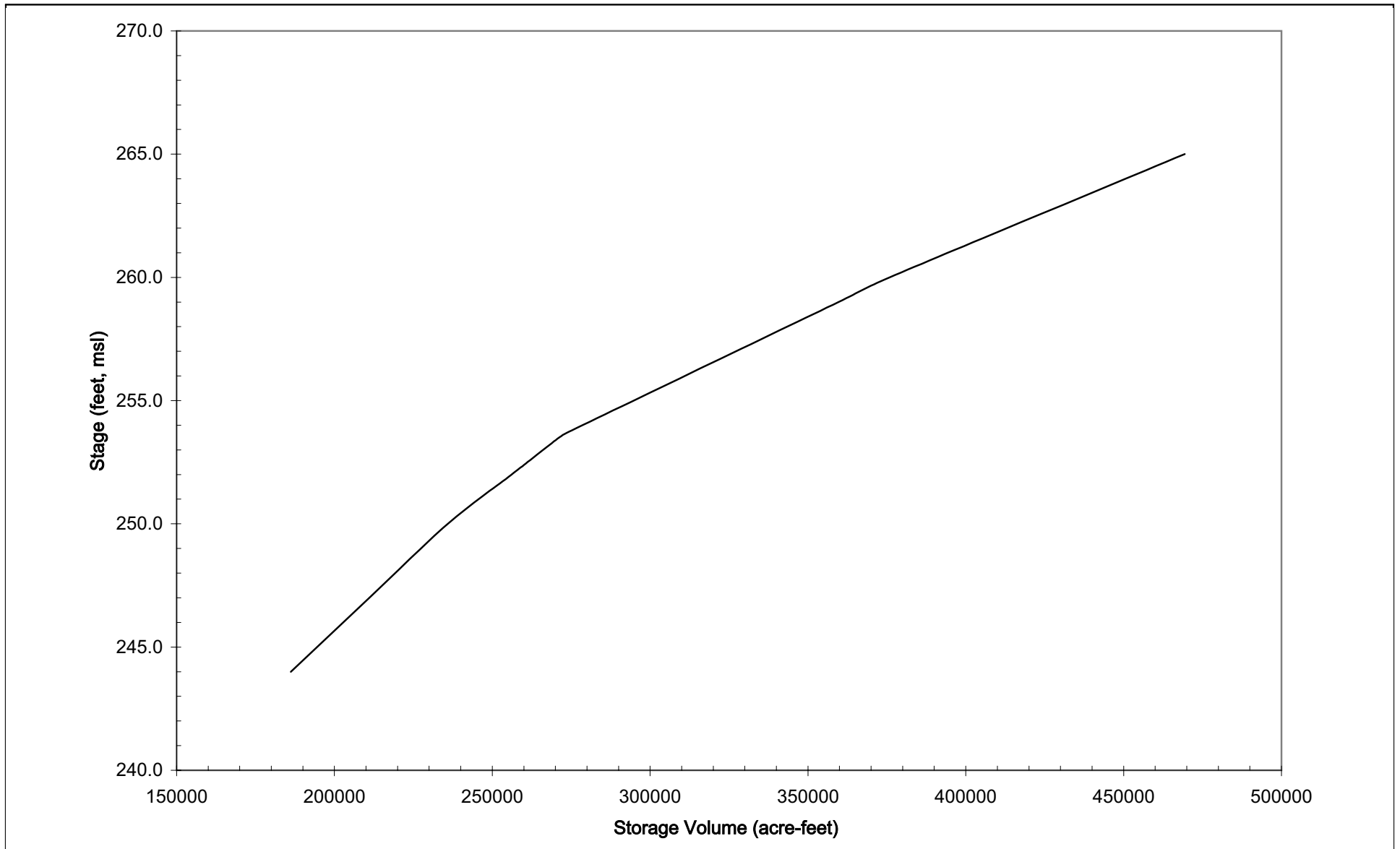


Figure 2.4-10 North Anna Reservoir & WHTF Combined Stage-Storage

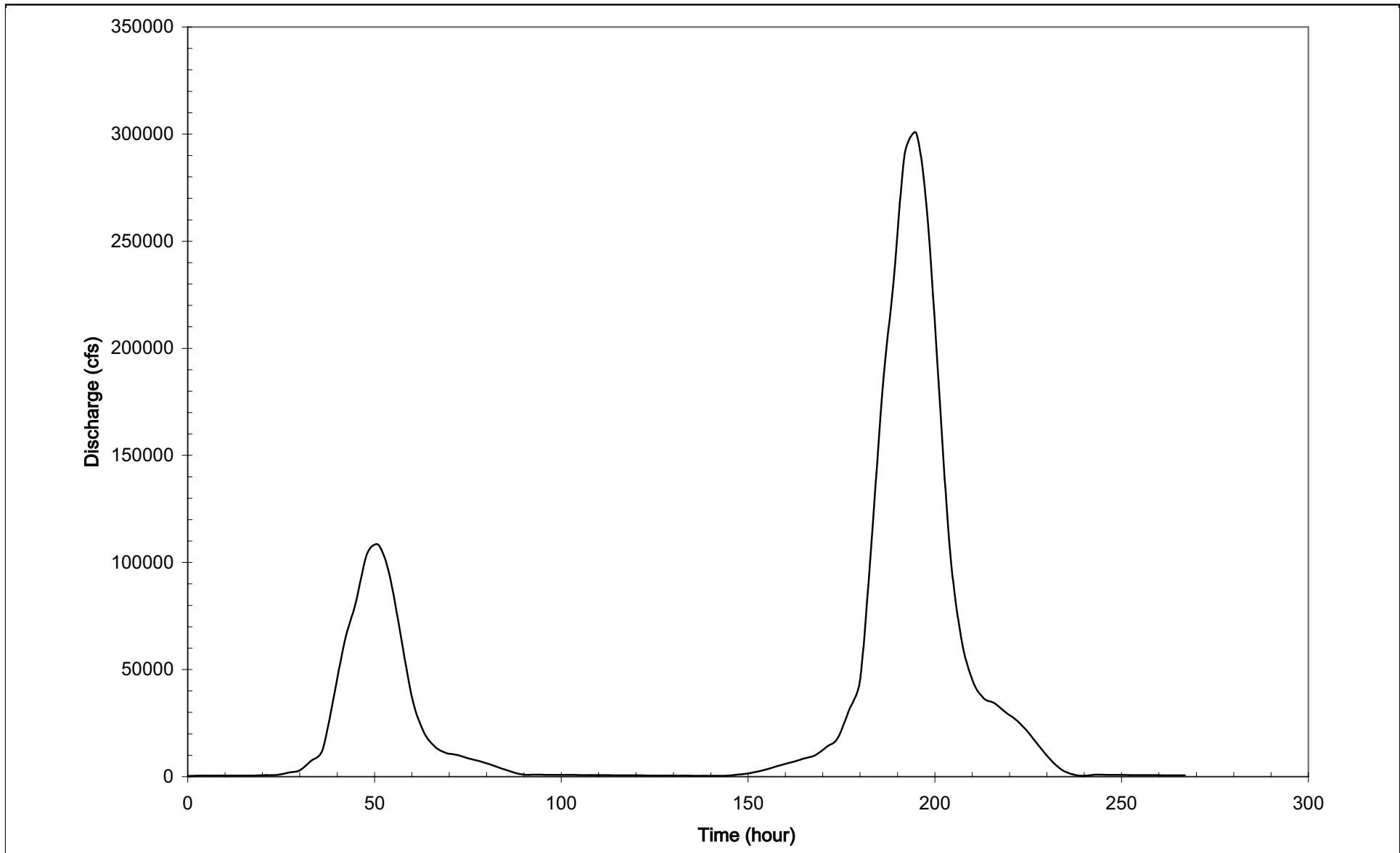


Figure 2.4-11 Combined North Anna Reservoir & WHTF PMF Inflow Hydrograph

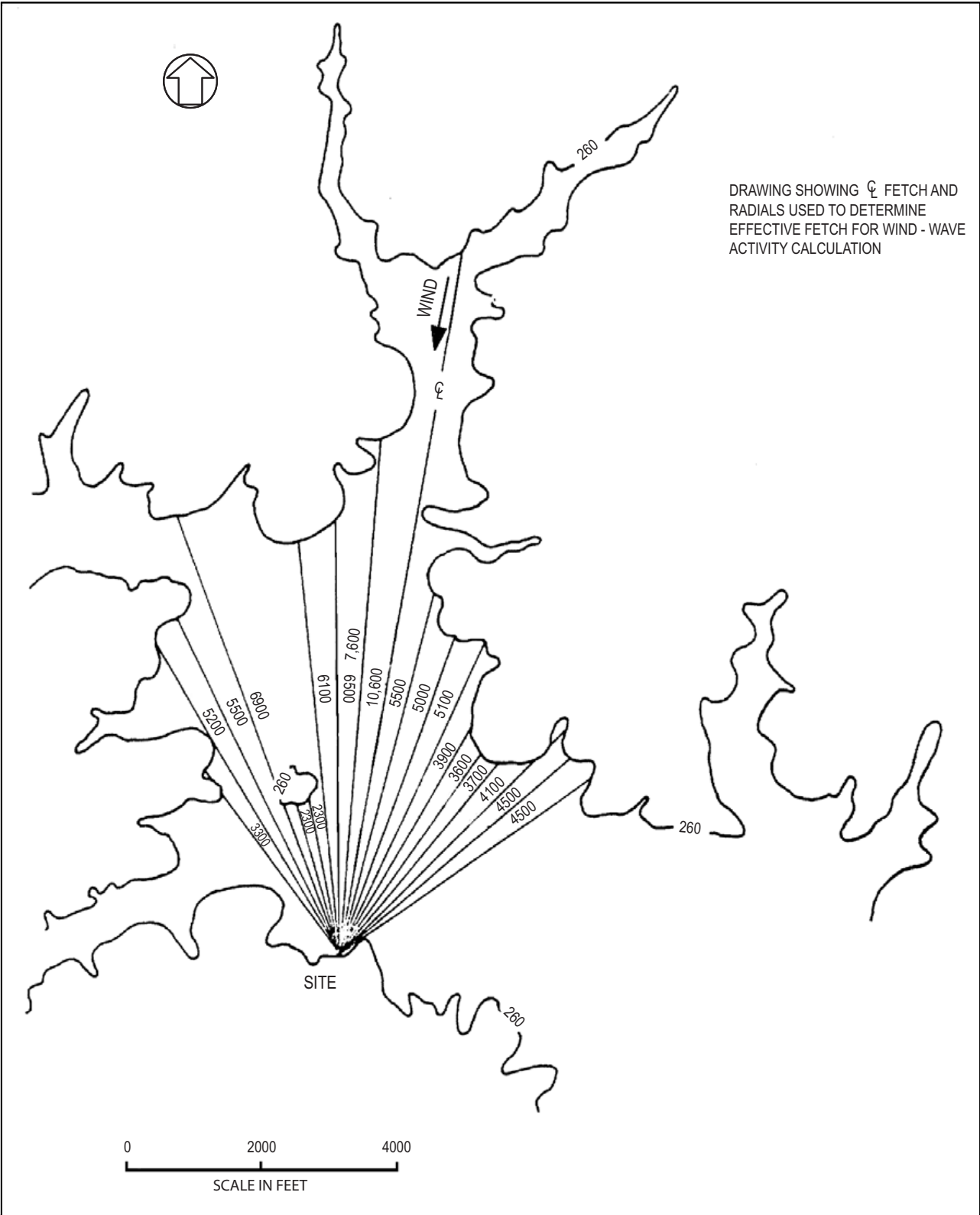


Figure 2.4-12 North Anna Site - Fetch Diagram

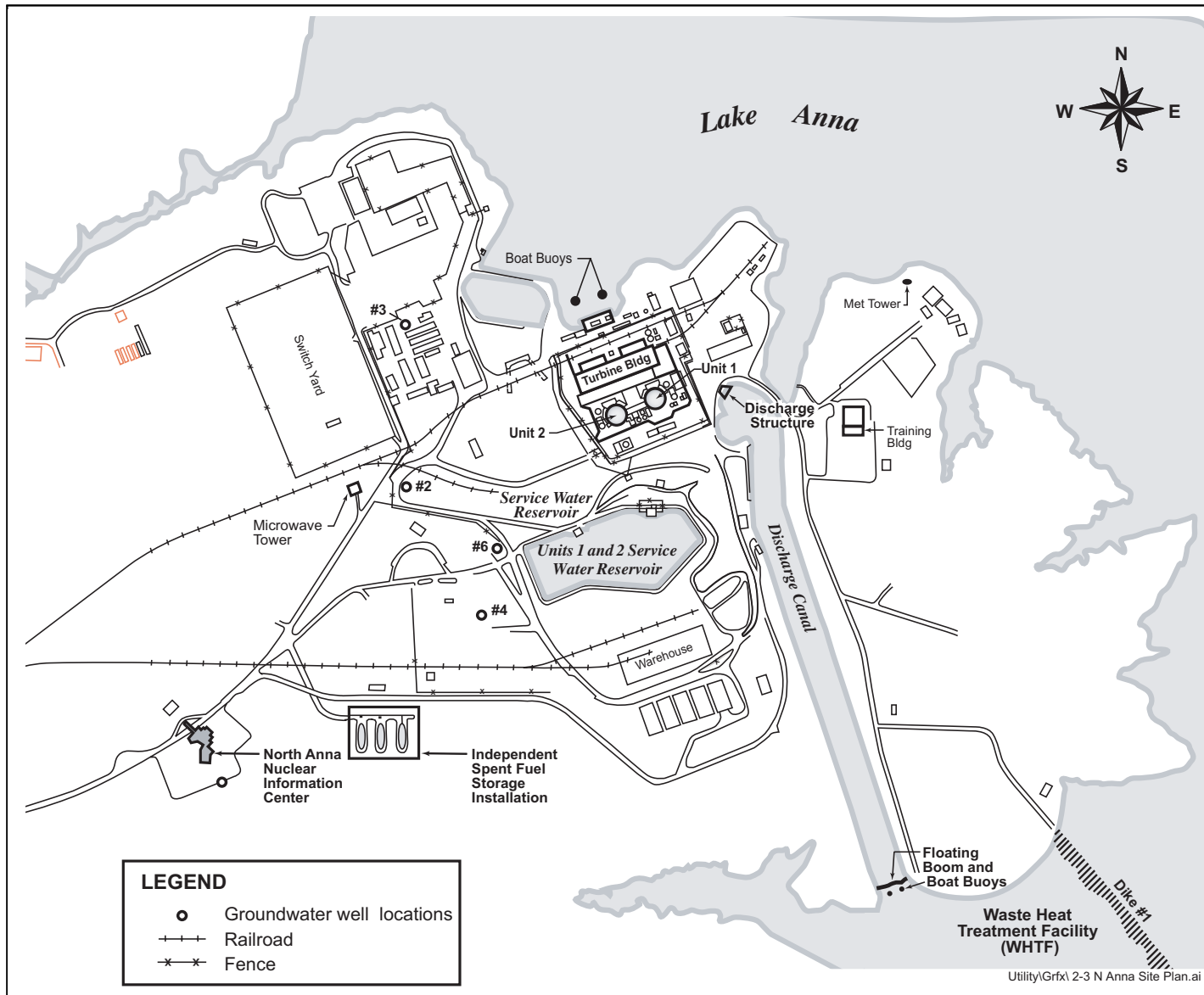


Figure 2.4-13 Existing Cooling Water Canals and Reservoirs

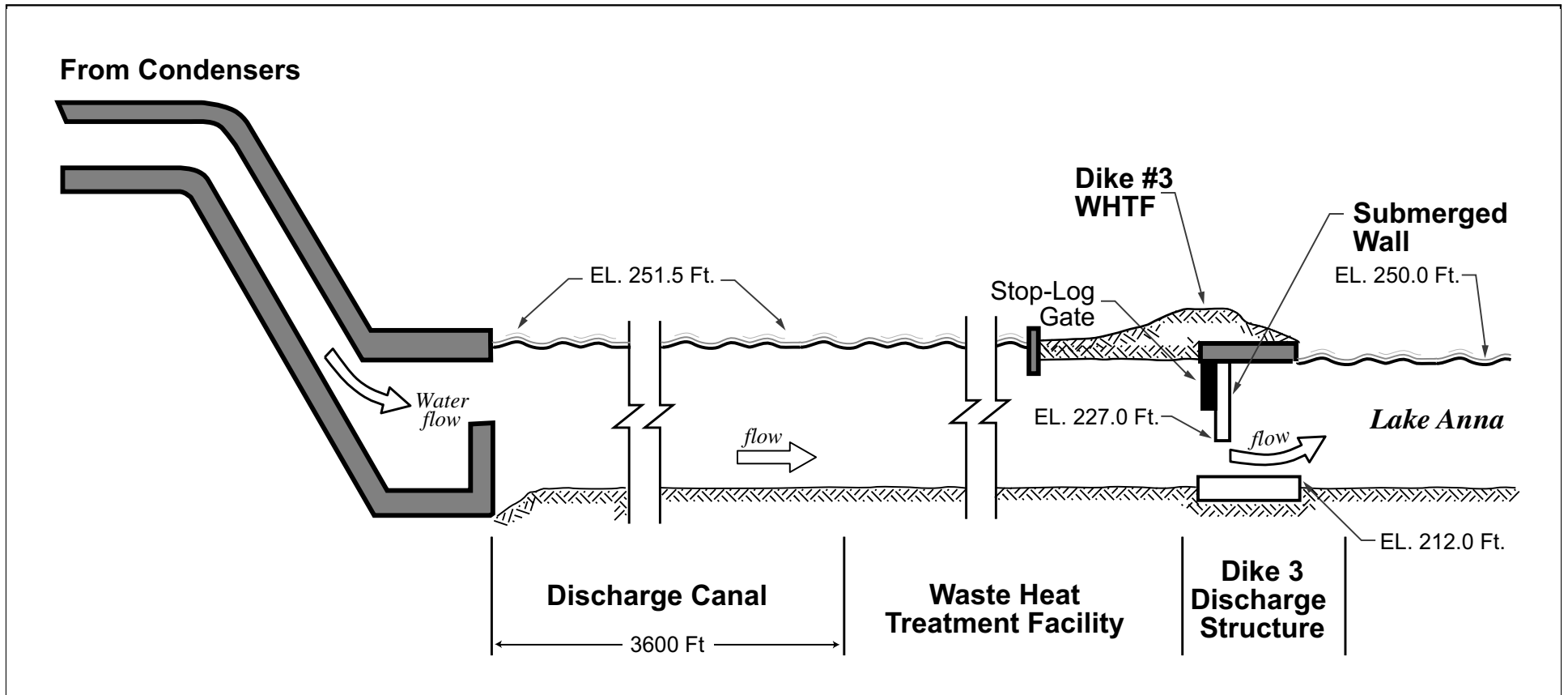


Figure 2.4-14 Schematic Cross-Sectional Diagram of Water Discharge System at Dike 3 WHTF

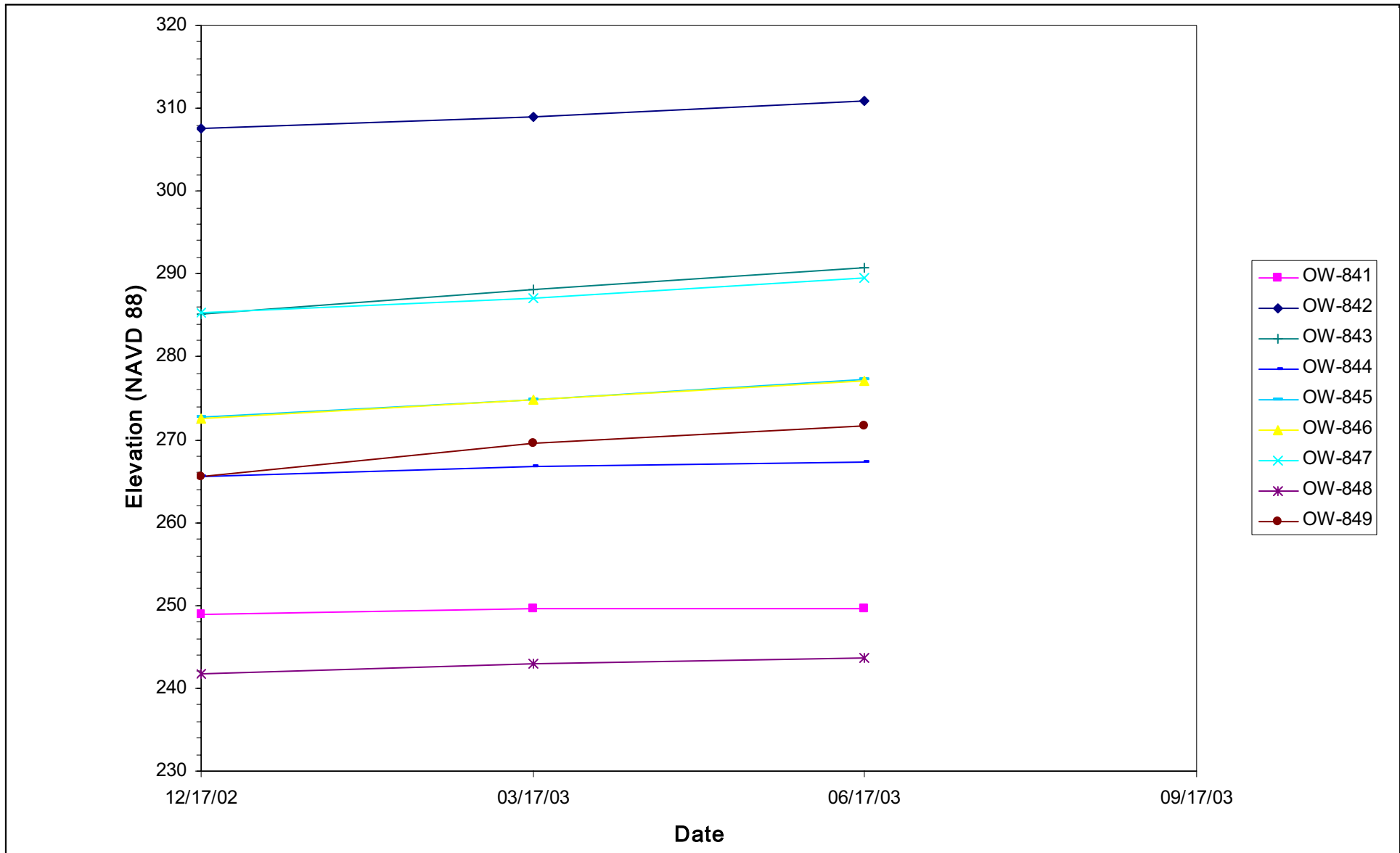


Figure 2.4-15 Groundwater Level Hydrographs

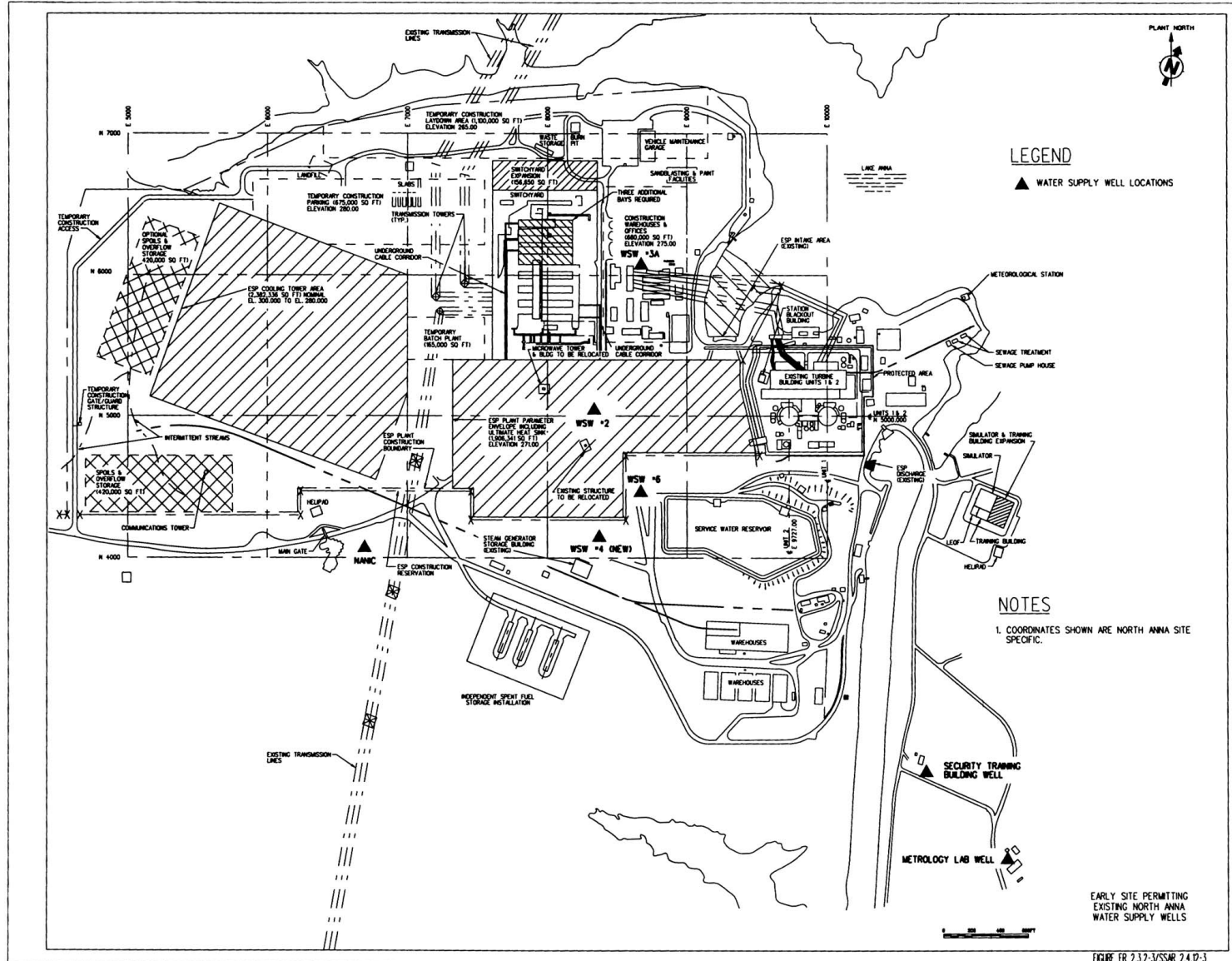


Figure 2.4-17 Existing North Anna Water Supply Wells

2.5 Geology, Seismology, and Geotechnical Engineering

This section presents information on the geological, seismological and geotechnical engineering properties of the ESP site. Section 2.5.1 describes basic geological and seismologic data, focusing on those data developed since publication of the Electric Power Research Institute (EPRI) 1986 seismic source model (Reference 1) for the Central and Eastern United States. Section 2.5.2 describes the vibratory ground motion at the site, including an updated seismicity catalog, description of seismic sources, and development of the Safe Shutdown Earthquake (SSE) and Operating Basis Earthquake (OBE) design ground motions. Section 2.5.3 describes the potential for surface faulting in the site area, and Section 2.5.4, Section 2.5.5 and Section 2.5.6 describe the stability of surface materials and foundations at the site.

RG 1.165, Appendix D, "Geological, Seismological and Geophysical Investigations to Characterize Seismic Sources" (Reference 2), provides guidance for the level of investigation recommended at different distances from a proposed site for a nuclear facility. The site region is that area within 200 miles (320 km) of the site location. The site vicinity is that area within 25 miles (40 km) of the site location. The site area is that area within 5 miles (8 km) of the site location. The site is that area within 0.6 mile (1 km) of the site location. These terms, site region, site vicinity, site area, and site, are used in Section 2.5.1 through Section 2.5.3 to describe these specific areas of investigation. These terms are not applicable to other sections of the SSAR.

2.5.1 Basic Geologic and Seismic Information

This section presents information on the geological and seismological characteristics of the ESP site region and area. The information is divided into two parts. Section 2.5.1.1 describes the geologic and tectonic setting of the site region and Section 2.5.1.2 describes the geology and structural geology of the site area. The geological and seismological information was developed in accordance with the guidance presented in RG 1.70, Section 2.5.1, "Basic Geologic and Seismic Information" (Reference 3), and RG 1.165, "Identification and Characterization of Seismic Sources and Determination of Safe Shutdown Earthquake Ground Motion," and is intended to satisfy the requirements of 10 CFR 100, "Reactor Site Criteria," Section 100.23, "Geologic and Seismic Siting Criteria," paragraph (c) "Geological, Seismological and Engineering Characteristics" (Reference 4). The geological and seismological information presented in this section are used as a basis for evaluating the geologic, seismic, and man-made hazards at the site.

RG 1.165 states that the vibratory design ground motion for a new nuclear power plant may be developed using either the EPRI or Lawrence Livermore National Laboratory (LLNL) probabilistic seismic hazard methodology. As described in Section 2.5.2, the EPRI methodology has been used to develop the SSE and OBE design ground motions for the ESP site. RG 1.165 further requires that the geological, seismological, and geophysical database be updated and any new data be evaluated to determine whether revisions to the 1986 EPRI seismic source model would be required (discussed in Section 2.5.2). This section, therefore, provides an update of the geological,

seismological, and geophysical database for the ESP site, focusing on whether any data published since 1986 would indicate a significant change to the 1986 EPRI seismic source model. In addition, the geotechnical properties of the ESP site location are described to evaluate the ground motion site response characteristics of the site and other non-tectonic geologic and man-made hazards at the site (discussed in Section 2.5.4).

The geological and seismological information presented in this section was developed from a review of previous reports prepared for the existing units and abandoned Units 3 and 4, published geologic literature, interpretation of aerial photography, and a subsurface investigation and field and aerial reconnaissance conducted in preparation of this ESP application. Previous site-specific reports reviewed include the UFSAR (Reference 5) and the ISFSI Safety Analysis Report (Reference 6). Reports prepared by Dames and Moore for design and construction of the existing units (Reference 7) and the abandoned Units 3 and 4 (Reference 8) (Reference 9) were also reviewed. A review of published geologic literature was used to supplement and update the existing geological and seismological information. This literature was identified using the GeoRef database (American Geological Institute) and the USGS library catalogue. In addition, relevant unpublished geologic literature, studies and projects were identified by contacting the USGS and State geological surveys and universities. A list of the references used to compile the geological and seismological information presented in the following sections is provided at the end of Section 2.5.

2.5.1.1 Regional Geology

This section discusses the physiography, geologic history, stratigraphy, and tectonic setting within a 200-mile radius of the ESP site. Summaries of these aspects of regional geology are presented to provide the framework for evaluation of the geologic and seismologic hazards discussed in the succeeding sections.

2.5.1.1.1 Regional Physiography and Geomorphology

The ESP site lies within the Piedmont Physiographic Province (Figure 2.5-1). The area within a 200-mile radius of the site (site region) encompasses parts of five other physiographic provinces. These are: the Coastal Plain Physiographic Province and the Continental Shelf Physiographic Province, which are located successively east of the Piedmont Province and the Blue Ridge Physiographic Province, the Valley and Ridge Physiographic Province, and the Appalachian Plateau Physiographic Province, which are located successively west and northwest of the Piedmont Province (Reference 10).

Each of the physiographic provinces present within the site region is discussed in the following sections. The physiographic provinces in the site region are shown on Figure 2.5-1.

a. Piedmont Physiographic Province

The Piedmont Physiographic Province is a rolling to hilly area that extends from the Fall Line on the east to the foot of the Blue Ridge Mountains on the west (Figure 2.5-1). The Fall Line is

a low east-facing scarp that separates crystalline rocks of the Piedmont Province to the west from less resistant sedimentary rocks of the Coastal Plain Province to the east (Reference 11). The Piedmont Province is about 40 miles wide in northern Virginia and broadens southwards to about 165 miles along the Virginia-North Carolina border. Elevations range from about 800 to 1500 feet along the western border of the province and slope eastward to elevations of about 200 feet at the Fall Line (Reference 12).

The Piedmont Province is divided into the Piedmont Upland section to the east and the Piedmont Lowland section to the west (section is referred to as subprovince in some publications) (Figure 2.5-1). The Piedmont Upland section is underlain by metamorphosed sedimentary and crystalline rocks of Precambrian to Paleozoic age. These lithologies are relatively resistant and their erosion has resulted in a moderately irregular surface. Topographically higher terrain is underlain by Cambrian quartzites and Precambrian crystalline rocks (Reference 13). The Piedmont Lowland section is a less rugged terrain containing fault-bounded basins filled with sedimentary and igneous rocks of Triassic and Early Jurassic age. Valleys are developed on sandstone and shale strata and trend northeast-southwest, parallel to the strike of the bedrock. Higher and more rugged terrain is underlain by intrusive and extrusive rocks consisting predominantly of diabase and basalt (Reference 13).

The Piedmont Province is characterized by deeply weathered bedrock and a relative paucity of solid rock outcrop (Reference 14). Saprolites that cover the bedrock may reach thicknesses of up to 300 feet. In the hillslope areas, the saprolite is capped locally by colluvium (Reference 15).

b. Coastal Plain Physiographic Province

The Coastal Plain Physiographic Province extends eastward from the Fall Line to the coastline (Figure 2.5-1). The Coastal Plain Province is a low-lying, gently rolling terrain developed on a wedge-shaped mass of Cretaceous, Tertiary and Quaternary age non-metamorphosed sedimentary rocks that thicken toward the coast. The thickness of the sediments at the New Jersey coastline is about 4000 feet, but the sediments attain thicknesses of as much as 8000 feet along the coast of Maryland and about 10,000 feet along the coast of North Carolina (Reference 16). Topographic relief is generally less than 200 feet and the topographic gradient is usually less than 5 feet per mile (Reference 13).

Northeast of the Chesapeake Bay, the Coastal Plain consists of extensive areas of nearly level plain, less than 100 feet above sea level. This morphology resulted from deposition and erosion associated with the rise and fall of sea level during Pleistocene time. Southwest of the Chesapeake Bay, marine and fluvial terraces developed during the Pliocene and Pleistocene. As a result of post-Pleistocene sea level rise, the outline of the present day coastline is controlled by the configuration of drowned valleys, typified by the deeply recessed

Chesapeake and Delaware Bays. Exposed headlands and shorelines have been modified by the development of barrier islands and extensive lagoons (Reference 13).

c. Continental Shelf Physiographic Province

The Continental Shelf Physiographic Province is the submerged continuation of the Coastal Plain Province and extends from the shoreline to the continental slope (Figure 2.5-1). The shelf is characterized by a shallow gradient and many shallow water features that are relicts of lower sea levels (Reference 13). The shelf extends eastward for about 75 to 80 , where sediments reach a maximum thickness of about 40,000 feet (Reference 17).

The Continental Shelf can effectively be separated into two geomorphic regions based on the 100 m bathymetric contour. Southeast of the 100 m bathymetric contour, the contours essentially follow the morphology of the shelf edge. Northwest of the 100 m bathymetric contour, the majority of the shelf is characterized by linear, low relief features, more closely aligned with the present shoreline (Reference 13).

d. Blue Ridge Physiographic Province

The Blue Ridge Physiographic Province is bounded on the east by the Piedmont Province and on the west by the Valley and Ridge Province (Figure 2.5-1). The Blue Ridge Province, aligned in a northeast-southwest direction, is a deeply dissected mountainous area, divided into two distinctly different parts by the Roanoke River, which flows to the southeast (Reference 12).

North of the Roanoke River a single ridge dominates the topography. The ridge is about 10 miles wide and summit elevations range from 2000 to over 3500 feet (Reference 18). Much of the mountain range is underlain by a pervasively faulted anticlinorium, a large composite anticline composed of lesser folds (Reference 19) that is strongly asymmetrical. South of the Roanoke River, the province becomes broader, reaching a width of more than 50 miles along the North Carolina border, with higher elevations than exhibited by the northern ridge. South of the border it becomes a mountainous upland with elevations typically ranging from 2400 to 3000 feet and a few peaks rising to elevations of over 5000 feet (Reference 20). The Blue Ridge is composed chiefly of granite, greenstone and other crystalline rocks along the crest and eastern slopes of the anticlinorium. On the steeper western slope, it is underlain by sandstones and shales (Reference 12).

e. Valley and Ridge Physiographic Province

The Valley and Ridge Physiographic Province lies west of the Blue Ridge Province and east of the Appalachian Plateau Province (Figure 2.5-1). It is aligned in a northeast-southwest direction and is between 25 and 50 miles wide. The Great Valley portion of the province, to the east, is divided into many distinct lowlands by ridges or knobs, the largest lowland being the Shenandoah Valley. Elevations within the Shenandoah Valley typically range between 500 and 1200 feet. The Valley and Ridges (Appalachian Mountains) portion of the province, to the west, is characterized by a series of roughly parallel ridges and valleys, some of which are

long and narrow (Reference 12). Elevations within the Valley and Ridges range from about 1000 to 4500 feet (Reference 20). The Great Valley typically is underlain by long belts of limestone and shale, while the rocks of the Valley and Ridges consist of more resistant sandstone and other quartz-rich rocks (Reference 12).

f. Appalachian Plateau Physiographic Province

The Appalachian Plateau Physiographic Province lies west of the Valley and Ridge Province (Figure 2.5-1). The Allegheny Front is the topographic and structural boundary between the Appalachian Plateau on the west and the Valley and Ridge Province on the east (Reference 15). It is a bold, high escarpment, underlain primarily by clastic sedimentary rocks capped by sandstone and conglomerates. In eastern West Virginia, elevations along this escarpment reach 4790 feet (Reference 21). The rocks of the Appalachian Plateau to the west lie flat or are gently folded and consist of sandstone, shale and coal. In southwest Virginia, the Appalachian Plateau has an average elevation of about 2000 feet. It is deeply dissected by streams into a maze of deep, narrow valleys and high narrow ridges (Reference 12).

2.5.1.1.2 Regional Geologic History

The geologic and tectonic setting of the ESP site region is the product of a long, complex history of continental and island arc collisions and rifting, spanning a period of over 1 billion years. This history of deformation imparts a pre-existing structural grain in the crust that is important for understanding the current seismotectonic setting of the region. Episodes of continental collisions have produced a series of accreted terranes separated, in part, by low angle detachment faults. Sources of modern day seismicity may occur in the overlying exposed or buried terranes or may occur along structures within the North American basement buried beneath the accreted terranes. That is, regional seismicity may not be related to any known surface structure. Intervening episodes of continental rifting have produced high angle normal or transtensional faults that either sole downward into detachment faults or penetrate entirely through the accreted terranes. Understanding the history of evolution and geometry of these pre-existing crustal faults, therefore, is important for identifying potentially active faults and evaluating the distribution of historical seismicity within the tectonic context of the site region.

Major tectonic events in the site region include five compressional orogenies and two extensional episodes (Reference 22). Currently the site region is located on the passive, divergent trailing margin of the North American plate following the last episode of continental extension and rifting. Each of these episodes of deformation is described in the following sections.

a. Grenville Orogeny

The first of the compressional orogenies was the Grenville orogeny that occurred during Middle to Late Precambrian time as a result of the convergence of the ancestral North American and African tectonic plates. During this orogeny, various terranes were accreted onto the edge of the ancestral North American plate, forming the Grenville Mountains

(Reference 22), which were likely the size of the present day Himalayas (Reference 23). The Grenville orogeny was followed by several hundred million years of tectonic quiescence, during which time the Grenville Mountains were eroded and their basement rocks exposed. In Virginia, the Grenville basement rocks are exposed in the Blue Ridge Province and portions of the Piedmont Province (Reference 23).

b. Late Precambrian Extensional Episode

Following the Grenville orogeny, crustal extension and rifting began during Late Precambrian time, which caused the separation of the North America and African plates and created the proto-Atlantic Ocean (Iapetus Ocean). Rifting is interpreted to have occurred over a relatively large area, sub-parallel to the present day Appalachian mountain range (Reference 22). During rifting, the newly formed continental margin began to subside and accumulate sediment. Initial sedimentation resulted in an eastward thickening wedge of clastic sediments consisting of graywackes, arkoses, and shales deposited unconformably on the Grenville basement rocks. These rocks are presently exposed on the eastern side of the Blue Ridge Anticlinorium (Reference 13). Subsequent sedimentation included a transgressive sequence of additional clastic sediments followed by a thick and extensive sequence of carbonate sediments. Remnants of the rocks formed from these sediments can be found within the Valley and Ridge and Piedmont Provinces (Reference 23). Accumulation of this eastward thickening wedge of clastic and carbonate sediments is thought to have occurred from the Middle to Late Cambrian into Ordovician time (Reference 13).

c. Penobscot Orogeny

During Late Cambrian time, as the now tectonically stable continental margin continued to subside, micro-continents and volcanic arcs, characteristic of an intra-oceanic island-arc terrane, began to develop in the proto-Atlantic Ocean as a result of east-directed oceanic subduction and initial closing of the proto-Atlantic. The Penobscot orogeny, the earliest known Paleozoic orogeny in the Appalachian region, is thought to have been caused by crustal convergence and accretion of these volcanic arcs thrust over micro-continents along the North American plate margin (Figure 2.5-2). This orogeny is considered to represent the beginning of the convergent phase in the closing of the proto-Atlantic Ocean (Reference 22). Subsequent convergent phases in the closing of the proto-Atlantic include the Taconic and Acadian orogenies and the Allegheny orogeny that finally closed the proto-Atlantic in the Permian.

d. Taconic Orogeny

The Taconic orogeny occurred during Middle to Late Ordovician time and was caused by continued collision of micro-continents and volcanic arcs with eastern North America along an eastward dipping subduction zone during progressive closure of the proto-Atlantic Ocean (Figure 2.5-2). Taconic terranes are preserved today in the Piedmont in a series of belts

representing island-arcs and micro-continents. They include the Chopawamsic belt, the Carolina Slate belt, the Eastern Slate belt and the Goochland-Raleigh belt. These Taconic terranes are considered to have collided with and accreted to eastern North America at different times during the orogeny (Reference 23).

Accretion of the island-arcs and micro-continents to the eastern margin of North America created a mountain system, the Taconic Mountains, that became a major barrier between the proto-Atlantic to the east and the carbonate platform to the west. The growth of this barrier transformed the area underlain by carbonate sediments to the west into a vast, elongate sedimentary basin, the Appalachian Basin. The present day Appalachian Basin extends from the Canadian Shield in southern Quebec and Ontario Provinces, Canada, southwestward to central Alabama, approximately parallel to the Atlantic coastline (Reference 24). The formation of the Appalachian Basin is one of the most significant consequences of the Taconic orogeny in the region defined by the Valley and Ridge and Appalachian Plateau Provinces. The Taconic mountain system was the source of most of the siliclastic sediment that accumulated in the Appalachian Basin during Late Ordovician and Early Silurian time. A continent-wide transgression in Early Silurian time brought marine shales and carbonate sedimentation eastward over much of the basin, and a series of transgressions and regressions thereafter repeatedly shifted the shoreline and shallow marine facies. Carbonate deposition continued in the eastern part of the basin into Early Devonian time (Reference 25).

e. Acadian Orogeny

The Acadian orogeny occurred during the Middle to Late Devonian Period and was caused by the collision of the micro-continent Avalon (formerly Armorica) with eastern North America. At its peak, the orogeny produced a continuous chain of mountains along the east coast of North America and brought with it associated volcanism and metamorphism. Remnants of the Avalon terrane (the Acadian Mountains) can be found in the Piedmont Province within the pre-existing Taconic Goochland belt, Carolina Slate belt and the Chopawamsic belt (Reference 23). The Acadian orogeny ended the largely quiescent environment that dominated the Appalachian Basin during the Silurian, as vast amounts of terrigenous sediment from the Acadian Mountains were introduced into the basin and formed the Catskill clastic wedge. Thick accumulations of clastic sediments belonging to the Catskill Formation are spread throughout the Valley and Ridge Province (Reference 25). During the Mississippian Period, the Acadian Mountains were completely eroded and the basement rocks of the Avalon terrane were exposed (Reference 23).

f. Allegheny Orogeny

The Allegheny orogeny occurred during the Late Carboniferous Period and extended into the Permian Period. The orogeny represents the final convergent phase in the closing of the proto-Atlantic Ocean in the Paleozoic. Metamorphism and magmatism were significant events

during the early part of the Allegheny orogeny. The Allegheny orogeny was caused by the collision of the North American and African plates and produced the Allegheny Mountains. As the African continent thrust westward over North America, the Taconic and Acadian terranes were detached and also were thrust westward over Grenville basement rocks (Reference 23). The northwest movement of the displaced rock mass above the thrust was progressively converted into deformation of the rock mass, primarily in the form of thrust faults and fold-and-thrust structures, as seen in the Blue Ridge and Piedmont Provinces. The youngest manifestation of the Allegheny orogeny was northeast-trending strike-slip faults and shear zones in the Piedmont Province. The extensive thick and undeformed Appalachian Basin and its underlying sequence of carbonate sediments were deformed and a fold-and-thrust array of structures, long considered the classic Appalachian structure, was impressed upon the basin. The tectonism produced the Allegheny Mountains and a vast alluvial plain to the northwest. The Allegheny Front in the Appalachian Plateau Province is thought to represent the westernmost extent of the Allegheny orogeny. Rocks throughout the Valley and Ridge Province are thrust faulted and folded up to this front, whereupon they become relatively flat and only slightly folded west of the Allegheny Front (Reference 26).

g. Early Mesozoic Extensional Episode

Crustal extension during Early Mesozoic time (Late Triassic and Early Jurassic) marked the opening of the Atlantic Ocean. This extensional episode produced numerous local, closed basins ("Triassic basins") along eastern North America (Reference 26). The elongate basins generally trend northeast, parallel to the pre-existing Paleozoic structures. The basins range in length from less than 20 miles to over 100 miles and in width from less than 5 miles to over 50 miles. Generally, the basins are asymmetric half-grabens with the principal faults located along the western margin of the basins. Triassic and Jurassic age rocks that fill the basins primarily consist of clastic sediments interbedded with basaltic volcanics.

h. Cenozoic History

The Early Mesozoic extensional episode gave rise to the Cenozoic Mid-Atlantic spreading center. The Atlantic seaboard presently represents the trailing passive margin related to the spreading at the Mid-Atlantic ridge. Ridge push forces resulting from the Mid-Atlantic spreading center are believed to be responsible for the NE-SW directed horizontal compressive stress presently observed along the Atlantic seaboard.

During Cenozoic time, as the Atlantic Ocean opened, the newly formed continental margin cooled and subsided, leading to the present day passive trailing divergent continental margin. As the continental margin developed, continued erosion of the Appalachian Mountains produced extensive sedimentation within the Coastal Plain. The Cenozoic history of the Atlantic continental margin, therefore, is preserved in the sediments of the Coastal Plain Province, and under water along the continental shelf. The sedimentary record is of a gently

east-dipping, seaward-thickening wedge of sediments, caused by both subsidence of the continental margin and fluctuations in sea level. Sediments of the Coastal Plain Province cover igneous and metamorphic basement rocks and part or all of some of the Triassic basin rift deposits (Reference 13).

During the Quaternary Period much of the northern United States experienced multiple glaciations interspersed with warm interglacial episodes. The last (Wisconsinian) Laurentide ice sheet advanced over much of North America during the Pleistocene. The southern limit of glaciation extended into parts of northern Pennsylvania and New Jersey, but did not cover the ESP site vicinity. South of the ice sheet, periglacial environments persisted throughout the site region (Reference 27). Present-day Holocene landscapes therefore, are partially the result of geomorphic processes responding to isostatic uplift, eustatic sea level change, and alternating periglacial and humid to temperate climatic conditions (Reference 28).

2.5.1.1.3 Regional Stratigraphy

The regional stratigraphy within each of the physiographic provinces is discussed below. The generalized stratigraphy within a 200-mile radius of the ESP site is shown on Figure 2.5-3. The stratigraphy shown on Figure 2.5-3 is from a portion of The Geologic Map of the United States (Reference 29). The classification of the rock units shown on Figure 2.5-3 is illustrated by the legend that accompanies the figure. The rock units are essentially classified based on age and type. Rocks of approximately the same age are shown at the same horizontal level in the legend. Successive vertical columns show different rock types and facies.

a. Piedmont Physiographic Province

There are two distinct divisions to the rocks of the Piedmont Physiographic Province. The first is a set of Late Precambrian and Paleozoic age crystalline rocks and the second is a set of Early Mesozoic (Triassic) age sedimentary rocks deposited locally in down-faulted basins within the crystalline rocks (Reference 30) (Figure 2.5-3). The rocks are overlain by residual soils derived from weathering of the crystalline rocks, and by Quaternary age alluvium and colluvium.

1. Crystalline Rocks (Late Precambrian and Paleozoic)

Crystalline rocks of the Piedmont Province primarily occur within the Piedmont Upland section. The crystalline rocks consist of deformed and metamorphosed meta-sedimentary, meta-igneous, and meta-volcanic rocks intruded by mafic dikes and granitic plutons (Reference 31). The rocks belong to a number of northeast-trending belts that are defined on the basis of rock type, structure and metamorphic grade (Reference 32) and are interpreted to have formed along and offshore of ancestral North America (Reference 33). From east to west the main lithotectonic belts are: the Goochland-Raleigh belt; the Carolina and Eastern slate belts; the Charlotte, Milton, and Chopawamsic belts; and the

Western Piedmont belt (Reference 32) (Figure 2.5-4). These lithotectonic belts are discussed in the following paragraphs.

Goochland-Raleigh Belt

The Goochland-Raleigh belt stretches southward from Fredericksburg, Virginia, to the North Carolina State line east of the Spotsylvania fault (discussed in Section 2.5.1.1.4) (Reference 34) (Figure 2.5-4). The Goochland belt (Virginia) is composed predominantly of granulite facies (high grade) metamorphic rocks and the Raleigh belt (North Carolina) is composed of sillimanite (very high grade) metamorphic rocks (Reference 30). The Goochland-Raleigh belt is interpreted to be a micro-continent that was accreted to ancestral North America during the Taconic orogeny. Some geologists believe that the micro-continent was rifted from ancestral North America during the proto-Atlantic rifting while others believe that it formed outboard of ancestral North America (exotic or suspect terrane). Rocks of the Goochland-Raleigh belt are considered to be the oldest rocks of the Piedmont Province and bear many similarities to the Grenville age rocks of the Blue Ridge Province (Reference 35).

The Po River Metamorphic Suite and the Goochland terrane, that lie southeast of the Spotsylvania fault, make up the easternmost part of the Goochland-Raleigh belt. The Po River Metamorphic Suite was named after the Po River in the Fredericksburg area and comprises amphibolite grade (high grade) metamorphic rocks, predominantly biotite gneiss and lesser amounts of hornblende gneiss and amphibolite (Reference 36). The age of this unit is uncertain, but it has been assigned a provisional age of Precambrian to Early Paleozoic (Reference 37). The Goochland terrane was first studied along the James River west of Richmond, Virginia, and contains the only dated Precambrian rocks east of the Spotsylvania fault. It is a Precambrian granulite facies (very high grade) metamorphic terrane comprised of, from the base up, the State Farm Gneiss, the Sabot Amphibolite, and the Maidens Gneiss. The Maidens Gneiss, which is the most widespread unit, is lithologically similar to the Po River Metamorphic Suite and is co-extensive with it. It is a heterogeneous formation and dominant layered lithologies include garnet-biotite-quartz plagioclase gneiss, biotite-quartz-plagioclase-potassium feldspar-augen gneiss, and biotite granitic gneiss (Reference 36).

Carolina Slate and Eastern Slate Belts

The Carolina Slate belt extends southward from southern Virginia to central Georgia, while the Eastern Slate belt is located predominantly in North Carolina, east of the Goochland-Raleigh belt (Figure 2.5-4). Both the Carolina and Eastern Slate belts are composed of greenschist facies (low grade) metamorphic rocks (Reference 30), including meta-graywacke, tuffaceous argillites, quartzites, and meta-siltstones (Reference 32). The Carolina and Eastern Slate belts are interpreted to be island-arcs that were accreted to ancestral North America during the Taconic orogeny. The island-arcs are interpreted to

have been transported from somewhere in the proto-Atlantic Ocean, and are therefore considered to be exotic or suspect terranes. Rocks of the Carolina and Eastern Slate belts generally are considered to be Early Paleozoic in age. Granitic and gabbro-rich plutons that intrude the belts generally are considered to be Middle to Late Paleozoic in age (Reference 32).

Charlotte, Milton, and Chopawamsic Belts

The Charlotte, Milton and Chopawamsic belts comprise a broad central part of the Piedmont Province from Virginia to Georgia (Figure 2.5-4). The belts are interpreted to be part of an island-arc and consist predominantly of meta-sedimentary and meta-volcanic rocks.

The Charlotte belt extends southward from northern North Carolina to Georgia (Figure 2.5-4). Meta-sedimentary rocks within this belt consist of epidote-bearing gneiss and migmatite. The Milton belt extends southward from southern Virginia to northern North Carolina (Figure 2.5-4) and is characterized by strongly foliated gneiss and schist (Reference 32). The Chopawamsic belt extends southward from northern to central Virginia (Figure 2.5-4). The ESP site is located within the Chopawamsic belt.

The Chopawamsic belt, also referred to as the “Chopawamsic Volcanic Belt” (Reference 38) and the “Central Virginia Volcanic-Plutonic Belt (Reference 39), takes its name from exposures along Chopawamsic Creek in northern Virginia. The belt trends northeastward from the North Carolina state line, crosses the James River between Richmond and Charlottesville and continues northeastward to south of Washington D.C., where it is covered by Coastal Plain deposits. The Chopawamsic belt is bounded on the west by the Chopawamsic fault and on the east by the Spotsylvania fault. The Chopawamsic belt is interpreted to be an island-arc that was accreted to ancestral North America during the Taconic orogeny. The Chopawamsic belt is regarded as an exotic or suspect terrain. Rocks in the Chopawamsic belt have long been known to be Early Paleozoic in age. Recent U-Pb studies consistently yield Ordovician ages for Chopawamsic volcanic rocks and Rb-Sr and U-Pb dating of granite rocks give late Ordovician ages (Reference 35).

The Chopawamsic belt is comprised of the Chopawamsic Formation and the Ta River Metamorphic Suite. The Chopawamsic Formation and the Ta River Metamorphic Suite are interpreted to have formed as an island-arc. The Chopawamsic Formation is interpreted to have formed as the continent-ward side of the island-arc and the Ta River Metamorphic Suite as the ocean-ward side (Reference 40). The Chopawamsic Formation consists of a sequence of felsic, intermediate and mafic meta-volcanic rocks with subordinate meta-sedimentary rocks. The Ta River Metamorphic Suite consists of a sequence of amphibolites and amphibole-bearing gneisses with subordinate ferruginous

quartzites and biotite gneiss. Rocks of the Ta River Metamorphic Suite are generally thought to be more mafic and to have experienced higher-grade regional metamorphism than the rocks of the Chopawamsic Formation (Reference 35).

The Chopawamsic Formation and Ta River Metamorphic Suite are unconformably overlain by the Quantico and Arvonias Formations. The Quantico and Arvonias Formations consist of meta-sedimentary rocks including slates, phyllites, schists, and quartzites. These meta-sedimentary rocks are considered to have been deposited in successor basins after the subjacent terranes were eroded and formed depositional troughs. Rocks of the Arvonias Formation are exposed in the Arvonias and Long Island synclines, while rocks of the Quantico Formation are exposed in the Quantico syncline (Figure 2.5-5). Rocks of the Arvonias, Long Island, and Quantico synclines form three belts across the central Virginia Piedmont, the Quantico synclines to the southeast and the Arvonias and Long Island synclines to the north (Reference 35).

The Chopawamsic Formation and the Ta River Metamorphic Suite are intruded by a number of granite plutons. The number of plutons and their relation to one another, however, remains uncertain (Reference 35). Rocks of the Falmouth Intrusive Suite intrude the Ta River Metamorphic Suite and Quantico Formation in the form of dikes, sills, and small irregular intrusions (Reference 37).

Western/Inner Piedmont Belt

The Western Piedmont belt, referred to as the Inner Piedmont belt in some publications, extends southward from Virginia through North Carolina and into Georgia (Figure 2.5-4). It is composed of greenschist facies (low grade) and amphibolite facies (high grade) meta-sedimentary rocks. These meta-sedimentary rocks enclose blocks of meta-basalt, ultramafic rocks, granite and other quasi-exotic lithologies and are called *mélanges* (Reference 40). These *mélanges* are interpreted to have formed in a Cambrian-Ordovician back-arc or marginal basin that lay on the continent-ward side of an island-arc terrane (Reference 36).

Two distinct types of *mélange* deposits occur within a collage of thrust slices in the Western Piedmont belt. The first type is a block-in-phyllite *mélange* that constitutes the Mine Run Complex of Virginia. It consists of a variety of meta-plutonic, meta-volcanic, mafic, and ultramafic blocks enclosed within a matrix of phyllite or schist and meta-sandstones of feldspathic or quartz meta-graywacke. The Mine Run complex is interpreted to consist of four imbricated thrust slices (numbered I through IV), each with its own distinctive exotic block content (Reference 36).

The second *mélange* type within the Western Piedmont belt is a meta-diamictite and contains a less extensive variety of exotic blocks, the most common being mafic and ultramafic blocks. The exotic blocks are enclosed in a micaceous quartzofeldspathic

matrix, which has contemporaneously deposited schist and quartz-lump fragments as its characterizing features. Several varieties of meta-diamictite have been recognized in Virginia and described as the Lunga Reservoir and Purcell Branch Formations (Reference 36).

The mélanges of the Western Piedmont are overlain unconformably by Ordovician age meta-sedimentary rocks and are intruded by Ordovician age and Late Ordovician or Early Silurian age felsic plutons, such as the Lahore and Ellisville plutons (Reference 36).

2. Sedimentary Rocks (Early Mesozoic)

Mesozoic sedimentary rocks of the Piedmont Province occur primarily within the Piedmont Lowland section. The sediments were deposited in a series of northeast-trending down-faulted basins faulted into crystalline rocks. Structurally, the basins are half-grabens with a main fault on the western side only (Reference 30). Sediments filling the basins include intermontane fanglomerates, fresh-water limestone, mudstones, siltstones and sandstones, and basic igneous and volcanic rocks (Reference 31). The Lower Mesozoic sediments deposited in these basins usually are referred to as Triassic basin deposits, although the basins are now known to also contain Lower Jurassic rocks. The Culpepper basin in the Piedmont Lowland section of Virginia is the largest basin, but numerous smaller basins include the Richmond, Farmville, and Danville, which are scattered throughout the Piedmont Lowland section (Reference 30).

3. Surficial Sediments (Cenozoic)

Surficial sediments in the Piedmont Province consist of residual and transported material. The residual soils have developed in place from weathering of the underlying rocks, while the transported material – alluvium and colluvium – has been moved by water or gravity and laid down as unconsolidated deposits of clay, silt, sand, gravel and rock fragments (Reference 41). Surficial sediments in the Piedmont Upland section are interpreted to be the product of Cenozoic weathering, Quaternary periglacial erosion and deposition, and recent anthropogenic activity (Reference 42).

Residual soil in the Piedmont Province consists of completely decomposed rock and saprolite. Residual soils occur almost everywhere, except where erosion has exposed the bedrock on ridges and in valley bottoms. Soils produced by the weathering of rock but which retain the basic visual structure of the original rock are called saprolites. Saprolite comprises the bulk of residual soil in the Piedmont Province and is defined as an earthy material in which the major rock-forming minerals (other than quartz) have been altered to clay but the material retains most of the textural and structural characteristics of the parent rock. The saprolite forms by chemical weathering, its thickness and mineralogy being dependent on topography, parent rock lithology and the presence of surface and/or groundwater (Reference 28).

Relief affects the formation of soils by causing differences in internal drainage, runoff, soil temperatures, and geologic erosion. In steep areas where there is rapid runoff, little percolation of water through the soil and little movement of clay, erosion is severe and removes soil as rapidly as it forms. Gently sloping areas, on the other hand, are well drained and geologic erosion in these areas is generally slight. The characteristics of the underlying rock strongly influence the kind of changes that take place during weathering. Because of differences in these characteristics, the rate of weathering varies for different rock types. The igneous, metamorphic and sedimentary rocks of the Piedmont Province are all sources of parent material for the soils. Gabbro, an igneous rock that is fairly resistant to weathering, produces soils that are between about 3 and 5 feet thick. Granite gneiss, however, weathers deeply and produces soils that range in thickness from about 6 to 20 feet (Reference 41).

Colluvium in the Piedmont Province occurs discontinuously on hilltops and side slopes, while thicker colluvium occurs in small valleys lacking perennial streams. Alluvium is present in all valleys with perennial streams (Reference 42).

b. Coastal Plain Physiographic Province

The Coastal Plain Physiographic Province is underlain by Mesozoic and Cenozoic age fluvial and marine, predominantly clastic, sedimentary materials that dip gently to the east and southeast (Reference 31). The Mesozoic and Cenozoic stratigraphic units that have been mapped on the surface and in the subsurface of the Coastal Plain comprise a lower sequence of Jurassic and Early Cretaceous age terrestrial sediments and an overlying sequence of well defined marine stratigraphic units, primarily Late Cretaceous and Tertiary in age. Quaternary deposits that overlie the Tertiary age sediments are found predominantly as valley fill, caps on upland ridges and hills, and as a relatively thin blanket in the coastal areas (Figure 2.5-3). The Quaternary age strata are generally not thicker than 50 feet (Reference 13).

c. Blue Ridge Physiographic Province

The Blue Ridge Physiographic Province is underlain by a broad, northeast-trending, structurally complex metamorphic terrane (Reference 43). In its widest place, the Blue Ridge is over 20 miles wide and can be traced southward from south-central Maryland through Virginia into North Carolina (Reference 44). The Blue Ridge terrain consists of stratified meta-sedimentary rocks and meta-basalts of Early Paleozoic and Late Precambrian age and an underlying gneissic and granitic basement-rock complex of Middle to Late Precambrian age (Figure 2.5-3).

d. Valley and Ridge Physiographic Province

The Valley and Ridge Physiographic Province is underlain primarily by layered sedimentary rock that has been intensely folded and locally thrust faulted. The sedimentary rocks range in age from Cambrian to Pennsylvanian. The valley areas within the Great Valley are underlain

predominantly by thick sequences of limestone, dolomite and shale. The upland areas of the Valley and Ridges (Appalachian Mountains) to the west are underlain predominantly by resistant sandstones and conglomerates, while the lowland areas are underlain predominantly by less resistant shale, siltstone, sandstone and limestone (Reference 16) (Reference 24) (Figure 2.5-3).

e. Appalachian Plateau Physiographic Province

The Appalachian Plateau Physiographic Province is underlain by rocks that are continuous with those of the Valley and Ridge Province, but in the Appalachian Plateau the layered rocks are nearly flat-lying or gently tilted and warped, rather than being intensely folded and faulted (Reference 16). Rocks of the Allegheny Front along the eastern margin of the province consist of thick sequences of sandstone and conglomerate, interbedded with shale, ranging in age from Devonian to Pennsylvanian. Rocks of the Appalachian Plateau west of the Allegheny Front are less resistant and consist of Permian age sandstone, shale and coal (Reference 12) (Reference 21) (Figure 2.5-3).

2.5.1.1.4 Regional Tectonic Setting

In 1986, the Electric Power Research Institute (EPRI) developed a seismic source model for the Central and Eastern United States (CEUS), which included the ESP site region (Reference 1). The EPRI source model included the independent interpretations of six Earth Science Teams and reflected the general state of knowledge of the geoscience community as of 1986. The seismic source models developed by each of the six teams were based on the tectonic setting and the occurrence, rates, and distribution of historical seismicity. The original seismic sources identified by EPRI (Reference 1) are thoroughly described in the EPRI 1986 reports and are summarized in Section 2.5.2.2.

Since 1986, additional geological, seismological, and geophysical research has been completed in the ESP site region. The focus of this section is to summarize the current state of knowledge on the tectonic setting and tectonic structures in the site region and to highlight new information acquired since 1986 that is relevant to the assessment of seismic sources. The following sections describe the site region in terms of plate tectonic evolution, origin and orientation of tectonic stress, and primary tectonic features and seismic sources. Historical seismicity occurring in the site region is described in Section 2.5.2.1.

a. Plate Tectonic Evolution of the Appalachian Orogenic Belt at the Latitude of the Site Region

The ESP site lies within the central Appalachians region of Virginia, which is part of the northeast-trending Appalachian orogenic belt, that extends nearly the entire length of the eastern United States. The Appalachian orogenic belt formed during the Paleozoic Era by a series of compressional tectonic events along the Precambrian continental margin of eastern North America. The geologic history of the region surrounding the site was discussed in Section 2.5.1.1.2.

The Appalachian orogenic belt has been subdivided in different ways by geologists studying the region. These subdivisions include provinces (physiographic and geologic), belts, and terranes. Provinces, which are generally more regional in extent, have been defined based on both physiography (landforms) and geology. As described in Section 2.5.1.1.1, six Physiographic Provinces have been defined across Virginia. From west to east these are the Appalachian Plateau, Valley and Ridge, Blue Ridge, Piedmont, Coastal Plain, and Continental Shelf Physiographic Provinces. Provinces of the Appalachian orogen, such as the Piedmont Province, have been subdivided into different lithotectonic belts of similar rock type and tectonic origin (Figure 2.5-4). Some of the belts have been further subdivided by some researchers (Reference 45) (Reference 46) into individual terranes. The two terms, belt and terrane, are used interchangeably in this section to represent fault-bounded blocks of crust that are internally homogeneous in terms of stratigraphy and tectonic history.

Figure 2.5-6 is a simplified tectonic map showing the five onshore physiographic provinces of Virginia and the belts and terranes within the Blue Ridge and Piedmont Provinces, as delineated by Hatcher (Reference 45) and Horton and others (Reference 46) since publication of the 1986 EPRI study. As described by these authors the following is a brief discussion of the major subdivisions of the Virginia Appalachian orogenic belt and the rock protoliths of these regions from west to east (excluding the Appalachian Plateau Province). The Valley and Ridge Province is a belt of sedimentary rocks originally deposited on North American crust and deformed by folds and thrust faults. The Blue Ridge Province is a thrust-bounded sheet of crystalline rocks with overlying sedimentary strata. The Jefferson terrane is the easternmost terrane within this province and is composed of sedimentary and volcanic rocks. The Western Piedmont, Chopawamsic, Carolina Slate, and Goochland belts belong to the Piedmont Province. The southern terrane of the Western Piedmont belt in Virginia is the Smith River terrane (Reference 45), and like the Jefferson terrane of the Blue Ridge Province, is composed of sedimentary and volcanic rocks. The Chopawamsic and Carolina Slate belts both consist of volcanic and intrusive rocks, whereas the Goochland terrane is composed of intrusive rocks interpreted by some to be continental crust. The Coastal Plain Province is composed of a sequence of predominantly Cretaceous and Tertiary marine sediments overlying crystalline rocks.

There is general agreement that folded strata in the Valley and Ridge Province and the crystalline rocks in the Blue Ridge Province are native to North America (Reference 40) (Reference 45) (Reference 47) and that these units have been transported westward from their original position along Paleozoic east-dipping, west-verging thrust faults. Interpretations differ primarily over the origin and emplacement of belts and terranes in the Piedmont Province.

Modern plate tectonic reconstructions of the southern and central Appalachian orogenic belt published since the 1986 EPRI study interpret that at least some of the major regional

Paleozoic deformation events (e.g., the Taconic, Acadian and Allegheny orogenies) are associated with collisions of exotic or suspect terranes with ancestral North America (Reference 40) (Reference 45) (Reference 47) (Reference 48). Major differences between plate tectonic models arise from varying interpretations of which belts/terranes represent exotic or suspect terranes (allochthons) and the location of primary tectonic boundaries or sutures that juxtapose such exotic terranes against North American crust. The most important of these differences are described in the following paragraphs as they relate to the age and geometry of tectonic sutures and accreted terranes along the eastern North American margin.

In a reconstruction by Hatcher (Reference 45), bedrock east of the Blue Ridge was accreted to North America during the Taconic and Acadian orogenies. These orogenies are interpreted to be the result of collisions of two distinct terranes with North America at the latitude of central Virginia (Figure 2.5-2). The Taconic orogeny is attributed to collision and suturing of a volcanic island arc, which is interpreted to have formed in the Iapetus Ocean east of North America during the Paleozoic, above an east-dipping subduction zone. In this model, the Smith River and Jefferson terranes (Figure 2.5-6) are interpreted to be remnants of the accretionary complex that formed above the subduction zone on the west side of the island arc, and the Chopawamsic volcanics are interpreted to be the remnants of the arc itself (Figure 2.5-2). The Taconic suture between North America and the accreted units is interpreted to be the thrust fault underlying the Smith River and Jefferson terranes (Figure 2.5-6 and Figure 2.5-2). During Taconic accretion, an east-dipping thrust fault west of the Chopawamsic terrane is interpreted to have detached a slice of North American continental basement and displaced it westward to form the Blue Ridge nappe (Figure 2.5-2).

In the Hatcher (Reference 45) model, accretion of the Carolina Slate belt occurred during the Acadian orogeny, although others interpret that the Carolina Slate belt was accreted during the Taconic orogeny. Later strike-slip displacement along the continental margin during the subsequent transpressional Allegheny orogeny in early Mississippian to Permian time juxtaposed the Goochland terrane against the Chopawamsic terrane and Carolina Slate belt along the Spotsylvania thrust fault (Figure 2.5-6 and Figure 2.5-2). Final closure of the Iapetus Ocean and collision of Africa with North America occurred during the Allegheny orogeny (Reference 45).

An alternative model proposed by Glover and others (Reference 47) in 1995, which incorporates detailed geologic and geophysical investigations across the Appalachian belt in central Virginia, interprets fewer exotic terranes in the amalgam of Paleozoic belts and terranes, and infers a different geometry for the major Paleozoic sutures (Figure 2.5-7). This model represents the only significant alternative interpretation of the origin and affinity of the crust east of the Spotsylvania thrust fault in the region of the ESP site published since the 1986 EPRI study. Glover and others attribute the Taconic orogeny to collision of an exotic Chopawamsic volcanic arc, but interpret most of the sedimentary and volcanic rocks of the

Smith River and Jefferson terranes to have originally been deposited on the passive margin of North America, rather than accreted with the arc. Accordingly, Glover and others place the Taconic suture in the central Piedmont east of the location proposed by Hatcher (Reference 45) (Figure 2.5-8).

Glover and others correlate the Chopawamsic volcanics with the rocks of the Carolina Slate belt, concluding that all of these rocks were part of a single island arc terrane (Carolina terrane) that collided with ancestral North America during the Taconic orogeny. If this is correct, then the western fault boundary of the Carolina Slate belt is a Taconic suture, not an Acadian suture, as proposed by Hatcher (Reference 45). Glover and others propose that the Acadian orogeny is associated with dextral transpressional deformation as the Iapetus Ocean progressively closed and Africa began to impinge on North America, and thus is not associated with a collisional suture at the latitude of Virginia. They interpret the Allegheny orogeny to be the final collision and suturing of Africa to North America.

Based in part on analysis of seismic reflection data (Figure 2.5-8), Glover and others interpret the Goochland terrane not to be exotic to North America, but rather a deep slice of North American basement that was detached during the Allegheny orogeny and thrust westward along the Spotsylvania thrust fault, similar to the initial formation of the Blue Ridge Mountains during the Taconic orogeny (Figure 2.5-2). The Spotsylvania thrust fault, in the site vicinity, is interpreted to cut across Taconic units in the Piedmont, leaving them as isolated klippe. The Taconic suture is interpreted to be offset and repeated by the Spotsylvania thrust fault, and present beneath the deposits of the Coastal Plain Province as well as in the Piedmont Province (Figure 2.5-8).

Despite varying interpretations of the origin and emplacement of fault-bounded belts and terranes, there is good agreement among tectonic models regarding first-order structural features of the Appalachian orogenic belt. In Virginia, the North American basement of the Iapetan passive margin underlies the Valley and Ridge, Blue Ridge, and Western Piedmont Provinces. Deformed rocks in these provinces west of the Spotsylvania thrust fault lie above a basal decollement (thrust), which is at a depth of about 3 to 6 miles below the ground surface in the site vicinity (Figure 2.5-8). The basal decollement is a low angle thrust fault that dips gently southeast and separates the overlying Appalachian crust from the underlying North American basement. Given the shallow depth to the decollement, it is unlikely that the Paleozoic thrust faults within these provinces have rupture widths sufficient to generate large earthquakes. Although potential seismogenic sources may be present within the North American basement below the decollement (Reference 49), the location, dimensions and geometry of these deeper sources is not necessarily expressed in the exposed fold-thrust structures above the detachment. Tectonic models generally agree that major Paleozoic faults east of the Chopawamsic terrane, such as the Spotsylvania thrust fault, are not detached at

shallow levels and penetrate deep into the crust, possibly extending to the base of the crust (Reference 47) (Figure 2.5-8).

Wheeler (Reference 49) noted that many earthquakes in the eastern part of the Piedmont Province and beneath the Coastal Plain Province are associated spatially with faults related to rifting that occurred during the Mesozoic Era. Normal faults in this region that bound Triassic basins may be listric into the Paleozoic detachment faults or may penetrate through the crust as high angle faults. If active in the modern tectonic setting, Triassic normal faults east of the Chopawamsic terrane have greater potential for generating large earthquakes by virtue of their larger potential rupture dimensions.

b. Tectonic Stress in the Mid-Continent Region

Expert teams that participated in the 1986 EPRI evaluation of intra-plate stress found that tectonic stress in the CEUS region is primarily characterized by NE-SW-directed horizontal compression. In general, the expert teams concluded that the most likely source of tectonic stress in the mid-continent region was ridge-push force associated with the Mid-Atlantic ridge, transmitted to the interior of the North American plate by the elastic strength of the lithosphere. Other potential forces acting on the North American plate were judged to be less significant in contributing to the magnitude and orientation of the maximum compressive principal stress. Some of the expert teams noted that deviations from the regional NE-SW trend of principal stress may be present along the east coast of North America and in the New Madrid region. They assessed the quality of stress indicator data and discussed various hypotheses to account for what were interpreted as variations in the regional stress trajectories.

Since 1986, an international effort to collate and evaluate stress indicator data has resulted in publication of a new World Stress Map (Reference 50) (Reference 51). Data for this map are ranked in terms of quality, and plate-scale trends in the orientations of principal stresses are assessed qualitatively based on analysis of high-quality data (Reference 52). Subsequent statistical analyses of stress indicators confirmed that the trajectory of the maximum compressive principal stress is uniform across broad continental regions at a high level of statistical confidence. In particular, the NE-SW orientation of principal stress in the CEUS inferred by the EPRI experts is statistically robust, and is consistent with the theoretical trend of compressive forces acting on the North American plate from the mid-Atlantic ridge (Reference 53).

The more recent assessments of lithospheric stress do not support inferences by some EPRI expert teams that the orientation of the principal stress may be locally perturbed in the New England area, along the east coast of the United States, or in the New Madrid region. Zoback and Zoback (Reference 50) summarized a variety of data, including well-bore breakouts, results of hydraulic fracturing studies, and newly calculated focal mechanisms, which indicate that the New England and eastern seaboard regions of the U.S. are characterized by

horizontal NE-SW to E-W compression. Similar trends are present in the expanded set of stress indicators for the New Madrid region. Zoback and Zoback grouped all of these regions, along with a large area of eastern Canada, with the CEUS in an expanded "Mid-Plate" stress province characterized by NE-SW directed horizontal compression.

In addition to better documenting the orientation of stress, research conducted since 1986 has addressed quantitatively the relative contributions of various forces that may be acting on the North American plate to the total stress within the plate. Richardson and Reding (Reference 54) performed numerical modeling of stress in the continental U.S. interior, and considered the contribution to total tectonic stress to be from three classes of forces:

- Horizontal stresses that arise from gravitational body forces acting on lateral variations in lithospheric density. These forces commonly are called buoyancy forces. Richardson and Reding emphasize that what is commonly called ridge-push force is an example of this class of force. Rather than a line-force that acts outwardly from the axis of a spreading ridge, ridge-push arises from the pressure exerted by positively buoyant, young oceanic lithosphere near the ridge against older, cooler, denser, less buoyant lithosphere in the deeper ocean basins (Reference 55). The force is an integrated effect over oceanic lithosphere ranging in age from about 0 to 100 million years (Reference 56). The ridge-push force is transmitted as stress to the interior of continents by the elastic strength of the lithosphere.
- Shear and compressive stresses transmitted across major plate boundaries (strike-slip faults and subduction zones).
- Shear tractions acting on the base of the lithosphere from relative flow of the underlying asthenospheric mantle.

Richardson and Reding concluded that the observed NE-SW trend of principal stress in the CEUS dominantly reflects "ridge-push" body forces. They estimated the magnitude of these forces to be about 2 to 3×10^{12} N/m (i.e., the total vertically integrated force acting on a column of lithosphere 1 m (3.28 ft) wide), which corresponds to average equivalent stresses of about 40 to 60 MPa distributed across a 30-mile thick elastic plate. Richardson and Reding found that the fit of the model stress trajectories to data was improved by the addition of compressive stress (about 5 to 10 MPa) acting on the San Andreas fault and Caribbean plate boundary structures. The fit of the model stresses to data further indicated that shear stresses acting on these plate boundary structures must also be in the range of 5 to 10 MPa.

Richardson and Reding noted that the general NE-SW orientation of principal stress in the CEUS also could be reproduced in numerical models that assume a shear stress, or "drag," acting on the base of the North American plate. Richardson and Reding (Reference 54) and Zoback and Zoback (Reference 50) do not favor this as a significant contributor to total stress in the mid-continent region, however, because it predicts or requires that the horizontal

compressive stress in the lithosphere increases by an order of magnitude moving east to west, from the eastern seaboard to the Great Plains. Zoback and Zoback noted that the state of stress in the southern Great Plains is characterized by NNE-SSW extension, which is contrary to this prediction. They further observed that the level of background seismic activity is generally higher in the eastern United States than in the Great Plains, which is not consistent with the prediction of the basal drag model that compressive stresses (and presumably rates of seismic activity) should be higher in the middle parts of the continent than along the eastern margin.

Analyses of regional tectonic stress in the CEUS since the 1986 EPRI studies have not significantly altered the characterization of the NE-SW orientation of the maximum compressive principal stress. The orientation of a planar tectonic structure relative to the principal stress direction determines the magnitude of shear stress resolved onto the structure. Given that the current interpretation of the orientation of principal stress is similar to that adopted in the 1986 EPRI studies, a new evaluation of the seismic potential of tectonic features based on a favorable or unfavorable orientation to the stress field would yield similar results. Thus, there is no significant change in the understanding of the static stress in the CEUS since the publication of the EPRI source models in 1986, and there are no significant implications for existing characterizations of potential activity of tectonic structures.

c. Principal Tectonic Structures

Principal tectonic structures within the 200-mile ESP site region can be divided into four categories based on their age of formation or reactivation. These categories include structures that were most recently active during Paleozoic, Mesozoic, Tertiary, or Quaternary time. Most of the Paleozoic and Mesozoic structures are regional scale, and geologically and geophysically recognizable. The Mesozoic rift basins and bounding faults show a high degree of parallelism with the structural grain of the Appalachian orogenic belt, which generally reflects reactivation of pre-existing Paleozoic structures. Tertiary and Quaternary structures are generally more localized and may be related to reactivation of portions of older bedrock structures.

1. Paleozoic Tectonic Structures

The central and western portions of the ESP site region encompass portions of the Piedmont, Blue Ridge, Valley and Ridge, and Appalachian Plateau Physiographic Provinces. Rocks and structures within these provinces are associated with thrust sheets that formed during convergent Appalachian orogenic events of the Paleozoic Era. Tectonic structures of this affinity also exist beneath the sedimentary cover of the Coastal Plain Province. These types of structures include the following: 1) sutures juxtaposing allochthonous (tectonically transported) rocks with North American crust, 2) regionally extensive Appalachian thrust faults and oblique-slip shear zones, and 3) a multitude of

smaller structures that accommodated Paleozoic deformation within individual blocks or terranes (Figure 2.5-8). The majority of these structures dip eastward and shallow into a low angle, basal Appalachian decollement. The Appalachian orogenic crust is relatively thin across the Valley and Ridge Province, Blue Ridge Province, and western part of the Piedmont Province, and thickens eastward beneath the eastern part of the Piedmont Province and the Coastal Plain Province (Figure 2.5-8). Below the decollement are rocks that form the North American basement complex. The basement rocks contain northeast-striking Iapetan normal faults that formed during the Late Precambrian to Cambrian rifting of the Iapetus Ocean.

Researchers have observed that much of the sparse seismicity in eastern North America occurs within the North American basement below the basal decollement. Therefore, seismicity within the Appalachians may be unrelated to the abundant, shallow thrust sheets mapped at the surface (Reference 49). For example, seismicity in the Giles County seismic zone, located in the Valley and Ridge Province, is occurring at depths ranging from 3 to 16 miles (5 to 25 km) (Figure 2.5-8) (Reference 57), which is generally below the Appalachian thrust sheets and basal decollement (Reference 58).

Paleozoic faults within 200 miles of the site are shown on Figure 2.5-3 and Figure 2.5-9. No seismicity is attributed to these faults and published literature does not indicate that any of these faults offset late Cenozoic deposits or exhibit geomorphic expression indicative of Quaternary deformation. Crone and Wheeler (Reference 59) do not show any of these faults to be potentially active Quaternary faults. Therefore, these Paleozoic structures in the site region are not considered to be capable tectonic sources, as defined in RG 1.165, Appendix A.

Major Paleozoic tectonic structures within the 25-mile ESP site vicinity include the Hylas shear zone, Spotsylvania thrust fault, Long Branch thrust fault, Chopawamsic thrust fault, Lake of the Woods thrust fault, and the Mountain Run fault zone (Figure 2.5-10). The Spotsylvania, Chopawamsic, and Long Branch thrust faults extend to within 5 miles of the ESP site. Four smaller faults also extend to within 5 miles of the site (Figure 2.5-11). Additional smaller Paleozoic faults are present within 25 miles of the site and are typically associated with larger Paleozoic structures and accommodate internal deformation within the intervening structural blocks. None of the faults located within 25 miles of the site are considered to be capable tectonic sources, as defined in RG 1.165, Appendix A.

Between 5 and 25 miles from the site, the Hylas shear zone, Mountain Run fault zone, and Lake of the Woods thrust fault are prominent structural features. These structures exhibit mylonitic textures, indicative of the ductile conditions in which they formed during the Paleozoic Era. The Hylas shear zone, for example, comprises a 1.5-mile wide zone of ductile shear fabric and mylonites, and was active between 330 and 220 million years ago based on the presence of mylonitized and unmylonitized intrusive rocks across the fault

zone (Reference 60). The Hylas shear zone and Mountain Run fault zone also locally border Mesozoic basins and appear to have been locally reactivated during Mesozoic extension to accommodate growth of the basins. The Mountain Run fault zone exhibits geomorphic expression suggestive of potential Tertiary or Quaternary reactivation. There is no geomorphic expression, historical seismicity, or Quaternary deformation along either the Hylas shear zone or Lake of the Woods thrust fault (Reference 59). These structures are not considered to be capable tectonic sources.

No new information has been published since 1986 on any Paleozoic fault in the site region that would cause a significant change in the EPRI seismic source model.

2. Mesozoic Tectonic Structures

Mesozoic basins have long been considered potential sources for earthquakes along the eastern seaboard and were considered by most of the EPRI teams in their definition of seismic sources (Reference 1). A series of elongate rift basins of early Mesozoic age are exposed in a belt extending from Nova Scotia to South Carolina. These rift basins, also commonly referred to as Triassic basins, exhibit a high degree of parallelism with the surrounding structural grain of the Appalachian orogenic belt. The rift basins formed during extension and thinning of the crust as Africa and North America rifted apart to form the modern Atlantic Ocean.

Generally, the exposed rift basins are asymmetric half-grabens (Figure 2.5-8) with the primary rift-bounding faults on the western margin of the half-grabens. Typically, in a rift basin, strata dip toward the western border fault zone, and so basin deposits are thickest along this margin. Ratcliffe and others (Reference 61) interpret most Mesozoic basins appear to have formed as a result of extensional reactivation of east-dipping, low-angle Paleozoic thrust fault. At depth, the faults are believed to merge with the low angle thrust faults that formed during the compressional tectonics that characterize the Paleozoic orogenies (Figure 2.5-8). As a result, the rift-bounding normal faults are listric at depth and merge into the low angle basal decollement (Reference 62). Others interpret that the rift-bounding faults penetrate the Paleozoic Appalachian thrust faults (Reference 49). The Triassic basins, therefore, are relatively shallow crustal features and rocks of Triassic and Jurassic age that fill the basins are generally comprised of a sequence of continental clastic sediments interbedded with basaltic volcanics (Reference 63).

There are numerous Triassic basins within a 200-mile radius of the ESP site (Figure 2.5-9). Basins exposed in the Piedmont and Blue Ridge Provinces include the Culpeper, Newark, Gettysburg, Taylorsville, Richmond, Scottsville, Farmville, Danville, and the Deep River basins. Five of these basins are located within 50 miles of the site. These are the Culpeper, Taylorsville, Richmond, Scottsville, and Farmville basins. Two of these basins (Culpeper and Taylorsville) are within 25 miles of the site. There are also

several basins buried beneath the Atlantic Coastal Plain and Continental Shelf (Figure 2.5-9).

The Culpeper basin is located about 20 miles northwest of the site. The Taylorsville basin is located about 22 miles southeast of the site and the Richmond basin is about 30 miles southeast of the site. The smaller Scottsville and Farmville basins are located about 40 miles southwest of the site (Figure 2.5-9 and Figure 2.5-10). All five of these structures are asymmetric basins, with the major basin-forming fault located along the western margin of the basin. The Culpeper basin, unlike the other basins, also has a complex of faults along its eastern margin. One such fault along the eastern margin of the basin is the Mountain Run fault zone.

Given the acquisition of additional offshore seismic profiles since the 1986 EPRI study, more buried Mesozoic basins are recognized today than were known during the EPRI study. However, all of the exposed major basins closest to the site were known to exist during the 1980s and several were incorporated into seismic sources by the different EPRI teams. No new data have been developed to demonstrate that any of the Mesozoic basins are currently active, and Crone and Wheeler (Reference 59) do not recognize any basin-margin faults that have been reactivated during the Quaternary in the site region. Therefore, all of the information on timing of displacement was available and incorporated into the EPRI seismic source models in 1986. No Mesozoic basin in the site region is associated with a known capable tectonic source, and no new information has been developed since 1986 that would require a significant revision to the EPRI seismic source model. Seismicity potentially associated with reactivation of faults bordering or beneath the Mesozoic basins is captured in the existing EPRI seismic source model. There is no new published information on rate or size of earthquakes potentially associated with the Mesozoic Basins that would cause a significant change in the 1986 EPRI source parameters.

3. Tertiary Tectonic Structures

Within a 200-mile radius of the ESP site, only a few faults have been active during the Tertiary Period. These faults generally occur in the Coastal Plain Province where Tertiary strata have exhibited deformation during this period (Figure 2.5-9). These faults include the Brandywine fault system in Maryland, the National Zoo faults in Washington, D.C., the Dutch Gap fault in Virginia, and several other small, unnamed faults that displace Tertiary strata (Reference 64). Within 25 miles of the site, the only fault zone with well-documented Tertiary displacement is the Stafford fault system, which is discussed in the following paragraphs.

Stafford Fault System

The Stafford fault system approaches to within 16.5 miles of the site to the northeast (Figure 2.5-10). The 42-mile long fault system was identified and described by Newell and others (Reference 65) and consists of a series of northeast-striking, northwest-dipping, high-angle reverse faults including, from north to south, the Dumfries, Fall Hill, Hazel Run, and Brooke faults. These individual faults are 10 to 25 miles long and are separated from one another by 1.2- to 2.5-mile wide en echelon left step-overs. The left-stepping pattern and horizontal slickensides found on the Dumfries fault suggest a component of dextral shear on the fault system (Reference 66).

Locally, the Stafford fault system coincides with the Fall Line and a northeast-trending portion of the Potomac River. Mixon and Newell (Reference 67) suggest that the Fall Line and river deflection may be tectonically controlled. Following discovery of the fault system by Newell and others (Reference 65), Dames & Moore (Reference 9) performed an investigation of the origin and age of the fault system. Detailed drilling, trenching, and mapping in the Fredericksburg region showed that the youngest identifiable fault movement on any of the four primary faults comprising the Stafford fault system was pre-middle Miocene in age (more than 10 million years ago).

Subsequent studies performed along the Stafford fault system, however, better document the timing and origin of the fault system. Slip during the Mesozoic and Tertiary is documented by displacement of Ordovician bedrock over lower Cretaceous bedrock along the Dumfries fault and abrupt thinning of the Paleocene Aquia Formation across multiple strands of the fault system (Reference 66). Minor late Tertiary activity of the fault system is documented by an 11-inch displacement of a Pliocene terrace along the Rappahannock River by the Fall Hill fault (Reference 68) (Reference 69) and an 18-inch displacement of upland gravels of Miocene or Pliocene age on the Hazel Run fault (Reference 68). These latter displacements indicate post middle to late Pliocene activity along the Stafford fault system.

All of the information on timing of displacement was available and incorporated into the EPRI seismic source models in 1986. No new significant information has been developed since 1986 regarding the activity of the Stafford fault system. Field and aerial reconnaissance performed for this ESP application also did not reveal any geologic or geomorphic features indicative of potential Quaternary activity along the fault system. Similarly, Crone and Wheeler (Reference 59) do not show the Stafford fault system as a Quaternary structure in their compilation of active tectonic features in the CEUS. The Stafford fault system, therefore, is not a capable tectonic source and there is no new information developed since 1986 that would require a significant revision to the EPRI seismic source model.

4. Quaternary Tectonic Features

In an effort to provide a comprehensive database of Quaternary features, Crone and Wheeler (Reference 59) compiled geological information on Quaternary faults, liquefaction features, and possible tectonic features in the CEUS. They evaluated and classified these features into one of four categories (Classes A, B, C, D) based on geological evidence of Quaternary faulting or deformation. The definitions of the Crone and Wheeler classes are provided in Table 2.5-1. Within a 200-mile radius of the ESP site, 11 potential Quaternary features were identified (Figure 2.5-12, Table 2.5-2). Based on their evaluation, Crone and Wheeler (Reference 59) characterized only the Central Virginia seismic zone as having geologic evidence demonstrating the existence of a Quaternary fault of tectonic origin (Class A). The small set of faults at Pembroke in Giles County, Virginia, were assigned to Class B and the remaining nine features were assigned to Class C. The paleo-liquefaction features within the Central Virginia seismic zone demonstrate the presence of a Holocene active seismogenic source. None of the other features identified by Crone and Wheeler (Reference 59) have demonstrated evidence of Quaternary activity that would imply recurrent activity in the past 500,000 years.

Within approximately 25 of the site, Crone and Wheeler (Reference 59) found only two features described in the literature that exhibited potential evidence for Quaternary activity (Figure 2.5-12, Table 2.5-2). These two features are the paleo-liquefaction features within the Central Virginia seismic zone, and the Mountain Run fault zone. Both of these features are described below. The Central Virginia seismic zone does not represent a tectonic fault, and therefore, is not considered a capable tectonic source. Similarly, the Mountain Run fault, which was categorized as a Class C feature in the Crone and Wheeler (Reference 59) evaluation, does not exhibit evidence of Quaternary slip and, therefore, is not a capable tectonic source.

In 1998, Weems defined and named seven fall lines across the Piedmont and Blue Ridge Provinces of North Carolina and Virginia. These fall lines are based on the alignment of short stream segments with anomalously steep gradients. Weems (Reference 70) explores possible ages and origins (rock hardness, climatic, and tectonic) of the fall lines and “based on limited available evidence favors a neo-tectonic origin” for these geomorphic features during the Quaternary. This work has not been confirmed by detailed studies and Crone and Wheeler (Reference 59) does not include these fall lines as possible Quaternary features in their compilation. Therefore, these features do not represent capable tectonic sources.

Paleo-Liquefaction Features within the Central Virginia Seismic Zone

The Central Virginia seismic zone is an area defined primarily by historical seismicity. Crone and Wheeler (Reference 59) report that two Holocene paleo-liquefaction features have been identified by Obermeier and McNulty (Reference 71) within the seismic zone.

The presence of these paleo-liquefaction features on the James and Rivanna Rivers, about 25–30 miles from the site, shows that the Central Virginia seismic zone reflects both an area of paleo-seismicity as well as observed historical seismicity. Based on the absence of widespread paleo-liquefaction, however, Obermeier and McNulty (Reference 71) conclude that an earthquake of Magnitude 7 or larger has not occurred within the seismic zone in the last 2000–3000 years, or in the eastern portion of the seismic zone for the last 5000 years. They also conclude that the geologic record of one or more magnitude 6 or 7 earthquakes might be concealed between streams, but that such events could not have been abundant in the seismic zone. In addition, these isolated locations of paleo-liquefaction may have been produced by local shallow moderate magnitude earthquakes of **M** 5 to 6. Thus, the presence of these liquefaction features do not indicate a change in the minimum magnitude level assigned to the Central Virginia seismic zone in the 1986 EPRI study. Because the causative faults remain unidentified, the Central Virginia seismic zone is best characterized as a seismogenic source and not a capable tectonic source, as defined by RG 1.165.

Mountain Run Fault Zone

The Mountain Run fault zone is located along the eastern margin of the Culpeper basin and lies approximately 18 miles northwest of the site (Figure 2.5-9 and Figure 2.5-5). The 75-mile long fault zone is mapped from the eastern margin of the Triassic Culpeper basin near the Rappahannock River southwestward to near Charlottesville, Virginia (Reference 72). The fault zone is a broad zone of sheared rocks, mylonites, breccias, and phyllites of variable width.

The Mountain Run fault zone is interpreted to have formed initially as a thrust fault upon which back-arc basin rocks (mélange deposits) of the Mine Run Complex were accreted onto ancestral North America at the end of the Ordovician (Reference 36). This suture separates the Blue Ridge and Piedmont terranes (Reference 73). Subsequent reactivation of the fault during the Paleozoic and/or Mesozoic produced strike-slip and dip-slip movements. Horizontal slickensides found in boreholes at several places near the foot of the Mountain Run scarp suggest strike-slip movement and small-scale folds in the uplands near the scarp suggest a dextral sense of slip (Reference 40). The timing of the reverse and strike-slip histories of the fault zone, and associated mylonitization and brecciation, is constrained to be pre-Early Jurassic, based on the presence of undeformed Early Jurassic diabase dikes that cut rocks of the Mountain Run fault zone (Reference 40).

The northeast-striking Mountain Run fault zone is one of the most clearly recognizable faults in the region (Reference 40). Two pronounced northwest-facing scarps occur along the fault zone, including the 1-mile long Kelly's Ford scarp located directly northeast of the Rappahannock River and the 7-mile long Mountain Run scarp located along the southeast margin of the linear Mountain Run drainage (Figure 2.5-5). Conspicuous bedrock scarps

in the Piedmont, an area characterized by deep weathering and subdued topography, has led some experts to suggest that the fault has experienced a Late Cenozoic phase of movement (Reference 40) (Reference 73).

Near Everona, Virginia, a small reverse fault, found in an excavation, vertically displaces "probable Late Tertiary" gravels by 5 feet (Reference 73). Others have estimated that the offset colluvial gravels are Pleistocene age (Reference 62). This Everona fault, which has no geomorphic expression, is located about 1/2 mile west of the Mountain Run fault zone. Due to their proximity, these two features are considered to be part of the same zone of faults (Everona fault-Mountain Run fault zone) (Reference 59). Crone and Wheeler (Reference 59) assessed that the faulting at Everona is likely to be of Quaternary age, but because the likelihood has not been tested by detailed paleo-seismological or other investigations, this feature has been assigned to Class C.

Field and aerial reconnaissance performed for this ESP application did not reveal any geologic or geomorphic features indicative of potential Quaternary activity along the Mountain Run fault zone. A review of 1:24,000 scale topographic maps revealed that the steeper portions of the Mountain Run scarp correlate with the areas where the Mountain Run (stream) is impinging on the scarp. In addition, the northwest side of the narrow Mountain Run valley is steepest where the stream is impinging on that side of the valley. These observations suggest that the scarp most likely formed due to erosion, as southeastward-migrating streams impinge against the more resistant rocks of the Mountain Run fault zone.

All of the information on timing of displacement of the Mountain Run fault zone and associated faults was available and incorporated into the EPRI seismic source models in 1986. No significant new information has been developed since 1986 regarding the activity of the Mountain Run fault zone. Similarly, Crone and Wheeler (Reference 59) do not show the Mountain Run fault zone as a known Quaternary structure in their compilation of active tectonic features in the CEUS, having assigned it to Class C. It is concluded that the Mountain Run fault zone is not a capable tectonic source and that no new information has been developed since 1986 that would require a significant revision to the EPRI seismic source model.

East Coast Fault System

The postulated East Coast fault system (ECFS) is located approximately 70 miles southeast of the site (Figure 2.5-3). The 370-mile long fault system, which was identified and described by Marple and Talwani (Reference 74), consists of three, 125-mile-long segments extending from the Charleston area in South Carolina northeastward to near the James River in Virginia (Figure 2.5-13). The three segments were initially referred to as the southern, central, and northern zones of river anomalies (ZRA-S, ZRA-C, ZRA-N) and

are herein referred to as the southern, central and northern segments of the ECFS. The southern segment is located in South Carolina, the central segment is located primarily in North Carolina, and the northern segment extends from northeast North Carolina to southeast Virginia, and is located about 70 miles southeast of the ESP site. Marple and Talwani (Reference 74) have mapped the northern terminus of the fault system between the Blackwater River and James River, southeast of Richmond. Identification of the fault system is based on the alignment of geomorphic features along Coastal Plain rivers, areas of uplift, and local faulting (Reference 74).

The southern segment of the fault system, first identified by Marple and Talwani (Reference 75) as an approximately 125-mile long and 6-9-mile wide zone of river anomalies, has been attributed to the presence of a buried fault zone. The southern end of this segment is associated with the Woodstock fault, a structure defined by fault-plane solutions of micro-earthquakes and thought to be the causative source of the 1886 Charleston earthquake (Reference 74). The southern segment is geomorphically the most well defined segment of the fault system and is associated with micro-seismicity at its southern end. This segment was included as an alternative geometry to the areal source for the 1886 Charleston earthquake in the 2002 USGS hazard model (discussed in more detail in Section 2.5.2) for the National Seismic Hazard Mapping Project (Reference 76).

The central and northern segments of the fault system were not included in the 2002 USGS model, nor were they considered in the workshops to develop the USGS model (Reference 77). The segments also were not presented in workshops or included in models for the Trial Implementation Project (TIP), a study that characterized seismic sources and ground motion attenuation models at two nuclear power plant sites in the southeastern United States (Reference 78).

The ECFS represents, in part, a new tectonic feature that was not known to the EPRI Earth Science Teams in 1986. The 1986 EPRI models include areal sources to model the Charleston seismic source; therefore, the southern segment of the East Coast fault system is in essence covered by the different Charleston sources zone geometries. However, the central and northern segments represent a new tectonic feature in the Coastal Plain that postdates the EPRI studies. The closest approach of the northern segment to the site is approximately 70 miles as described above.

Although the postulated ECFS represents a potentially new tectonic feature in the Coastal Plain of Virginia and North Carolina (Reference 74), current interpretations of the feature and current existing data indicate that the fault zone probably does not exist and, if it exists, is not a capable tectonic source. For example, Crone and Wheeler (Reference 59) do not include the northern and central segments of the fault in their compilation of potentially active Quaternary faults. In addition, workshops convened for the 2002 USGS seismic hazard model (Reference 77) and for the TIP project (Reference 78) do not

identify the northern and central segments of the fault system as a Quaternary active fault. As a member of both the USGS and TIP workshops, Talwani did not propose the northern and central segments of the fault system for consideration as a potential source of seismic activity. In addition, the northern and central segments of the fault system are not associated with any seismicity and are not associated with any gravity or magnetic anomaly.

In summary, the northern segment of the ECFS, as postulated by Marple And Talwani (Reference 74), is located approximately 70 miles southeast of the site. Marple and Talwani (Reference 74) further suggest that the southern segment of the fault system may be the source of the 1886 Charleston earthquake, implying that the northern and central segments may produce earthquakes of similar size. Although current interpretations and aerial reconnaissance performed for this ESP application indicate that the northern segment of the fault zone probably does not exist or has a very low probability of activity if it does exist, given the proximity of the fault to the site and uncertainty regarding the existence and activity of the fault, a sensitivity analysis was performed to evaluate the faults potential contribution to hazard at the ESP site. The results of this sensitivity analysis are described in Section 2.2.2.6.2.

d. Seismic Sources Defined by Regional Seismicity

Within 200 miles of the ESP site, two seismic sources are defined by a concentration of small to moderate earthquakes. These two sources have produced the two largest historical earthquakes in the state of Virginia and have been identified as seismogenic sources in the 1986 EPRI studies as well as more recent seismic hazard models (Reference 57) (Reference 79). These two seismic sources are the Central Virginia and Giles County seismic zones (Figure 2.5-14).

1. Central Virginia Seismic Zone

The Central Virginia seismic zone is an area of persistent, low-level seismicity in the Piedmont Province (Figure 2.5-14). The zone extends about 75 miles in a north-south direction and about 90 miles in an east-west direction from Richmond to Lynchburg (Reference 80). The ESP site is located near the northern boundary of the Central Virginia seismic zone. The largest historical earthquake to occur in the Central Virginia seismic zone was the body-wave magnitude (m_b) 5.0 Goochland County event on December 23, 1875 (Reference 80). The maximum intensity estimated for this event was Modified Mercalli Intensity (MMI) VII in the epicentral region. Isoseismals indicate that the ESP site experienced shaking of Intensity V (Reference 81).

Seismicity in the Central Virginia seismic zone ranges in depth from about 2 to 11 miles (Reference 82). Coruh and others (Reference 83) suggest that seismicity in the central and western parts of the zone may be associated with west-dipping reflectors that form the

roof of a detached antiform, while seismicity in the eastern part of the zone near Richmond may be related to a near-vertical diabase dike swarm of Mesozoic age. However, given the depth distribution of 2 to 11 miles (Reference 82) and broad spatial distribution, it is difficult to uniquely attribute the seismicity to any known geologic structure and it appears that the seismicity extends both above and below the Appalachian detachment.

No capable tectonic sources have been identified within the Central Virginia seismic zone, but two paleo-liquefaction sites, as discussed previously, have been identified within the seismic zone (Reference 59) (Reference 71). The paleo-liquefaction sites reflect pre-historical occurrences of seismicity within the Central Virginia seismic zone, and do not indicate the presence of a capable tectonic source.

The 1986 EPRI source model includes various source geometries and parameters to capture the seismicity of the Central Virginia seismic zone. Subsequent hazard studies have used maximum magnitude (M_{max}) values that are within the range of maximum magnitudes used by the six EPRI models. Collectively, upper-bound maximum values of M_{max} used by the EPRI teams range from m_b 6.6 to 7.2 (discussed in Section 2.5.2.2). More recently, Bollinger (Reference 79) has estimated an M_{max} of m_b 6.4 for the Central Virginia seismic source. Chapman and Krimgold (Reference 57) have used an M_{max} of m_b 7.25 for the Central Virginia seismic source and most other sources in their seismic hazard analysis of Virginia. This more recent estimate of M_{max} is similar to the M_{max} values used in the 1986 EPRI studies. Similarly, the distribution and rate of seismicity in the Central Virginia seismic source have not changed since the 1986 EPRI study (discussed in Section 2.5.2.2.8). Thus, there is no change to the source geometry or rate of seismicity. Therefore, the conclusion is that no new information has been developed since 1986 that would require a significant revision to the EPRI seismic source model.

2. Giles County Seismic Zone

The Giles County seismic zone is located in Giles County, southwestern Virginia, near the border with West Virginia. The largest known earthquake to occur in Virginia and the second largest earthquake in the entire southeastern United States is the 1897 m_b 5.8 Giles County event. The earthquake would have produced an MMI VIII in the epicentral area (Reference 84) and Intensity V at the ESP site (Reference 81).

Earthquakes in the Giles County seismic zone occur at depths between 3 and 16 miles and appear to define a 25-mile long tabular zone striking N44E and dipping steeply southeast beneath the Valley and Ridge thrust sheets (Reference 57) (Reference 58). The lack of seismicity in the shallow Appalachian thrust sheets, estimated to be about 2 to 3.5 miles thick, implies that the seismogenic structures in the Giles County seismic zone are unrelated to the surface geology of the Appalachian orogen (Reference 58). Potential structures most likely responsible for the seismicity in Giles County are Iapetan normal

faults within the Iapetan passive margin of the North American basement beneath the Appalachian thrust sheets (Reference 49) (Reference 58).

No capable tectonic sources have been identified within the Giles County seismic zone, but a zone of small Late Pliocene to Early Quaternary age faults have been identified within the Giles County seismic zone, near Pembroke, Virginia (Reference 59). The Pembroke zone is a set of extensional faults exposed in terrace deposits overlying limestone bedrock along the New River (Reference 85) (Reference 86). These faults were rated by Crone and Wheeler as Class B (Reference 59) (Table 2.5-1 and Table 2.5-2) because it has not yet been determined whether the faults are tectonic or the result of solution collapse. The shallow Pembroke faults do not appear to be related to the seismicity within the Giles County seismic zone, which is occurring beneath the Appalachian basal decollement in the North American basement.

The EPRI source model includes various source geometries and parameters to represent the seismicity of the Giles County seismic zone. Subsequent hazard studies have used M_{max} values that were within the range of maximum magnitudes used by the six EPRI models. Collectively, upper-bound maximum values of M_{max} used by the EPRI teams ranged from m_b 6.6 to 7.2 (discussed in Section 2.5.2.2). More recently, Bollinger (Reference 79) estimated an M_{max} of m_b 6.3 for the Giles County seismic source using three different methods. Chapman and Krimgold (Reference 57) used an M_{max} of m_b 7.25 for the Giles County zone and most other sources in their seismic hazard analysis of Virginia. Both of these more recent estimates of M_{max} are similar to the range of M_{max} values used in the 1986 EPRI studies. Therefore, no new information has been developed since 1986 that would require a significant revision to the EPRI seismic source model.

3. Selected Seismogenic and Capable Tectonic Sources Beyond the Site Region

Because of the potential for distant, large earthquakes in the CEUS contributing to the long period ground motion hazard, a discussion of three additional seismic sources based on seismicity is provided in the following paragraphs. These sources include the Eastern Tennessee, New Madrid and Charleston seismic sources, which produced the largest historical earthquakes in the CEUS (Figure 2.5-14).

Eastern Tennessee Seismic Zone

The ESP site is located over 300 miles east of the Eastern Tennessee seismic zone, which is a pronounced seismic source in the central and southeastern United States (Figure 2.5-14). The zone, located in the Valley and Ridge Province of eastern Tennessee, is about 185-miles long and 30-miles wide and has not produced a damaging earthquake in historical time (Reference 87). However, this zone has produced the second highest release of seismic strain energy in the CEUS during the 1980s, when normalized by crustal area (Reference 87).

Earthquakes in the Eastern Tennessee seismic zone are occurring at depths between 3 and 16 miles but none have exceeded a moment magnitude (**M**) of 4.6 (Reference 88). The mean focal depth within the seismic zone is 9 miles, which is well below the Appalachian basal decollement's maximum depth of 3 miles. The lack of seismicity in the shallow Appalachian thrust sheets implies that the seismogenic structures in the Eastern Tennessee zone are unrelated to the surface geology of the Appalachian orogen. Potential structures most likely responsible for the seismicity in Eastern Tennessee are reactivated lapetan normal faults within the lapetan passive margin beneath the Appalachian thrust sheets (Reference 49) (Reference 58).

The majority of earthquake focal mechanisms show right-lateral slip on northerly-trending planes or left-lateral slip on easterly-trending planes (Reference 88). Statistical analyses of focal mechanisms and epicenter locations suggest that seismicity is occurring on a series of northeast-trending en echelon basement faults, intersected by several east-west-trending faults (Reference 88).

Earthquakes within the Eastern Tennessee seismic zone cannot be attributed to known faults (Reference 87) and no capable tectonic sources have been identified within the seismic zone. However, the seismicity is spatially associated with major geophysical lineaments. The large majority of seismicity lies between the New York-Alabama lineament on the west and the Clingman and Ococee lineaments on the east (Reference 89).

The EPRI source model includes various source geometries and parameters to represent the seismicity of the Eastern Tennessee seismic zone. Subsequent hazard studies have used M_{max} values that were within the range of maximum magnitudes used by the six EPRI models. Collectively, upper-bound maximum values of M_{max} used by the EPRI teams ranged from m_b 6.6 to 7.4. Using three different methods specific to the Eastern Tennessee seismic source, Bollinger (Reference 79) estimated an M_{max} of m_b 6.45. Chapman and Krimgold (Reference 57) used a M_{max} of m_b 7.25 for the Eastern Tennessee zone and most other sources in their seismic hazard analysis of Virginia. Both of these more recent estimates of M_{max} are similar to the range of M_{max} values used in the 1986 EPRI studies. Therefore, it is concluded that no new information has been developed since 1986 that would require a significant revision to the EPRI seismic source model.

Charleston Seismic Zone

The Charleston seismic source lies about 375 miles south of the ESP site. The August 31, 1886, Charleston, South Carolina, earthquake is the largest historical event to occur in the eastern United States. The event produced MMI X shaking in the epicentral area and was felt strongly as far away as Chicago (MMI V) (Reference 90). As a result of

this earthquake, considerable effort has gone into identifying the source of the earthquake and recurrence history of large magnitude events in the region (Reference 74) (Reference 91).

The 1886 Charleston earthquake produced no identifiable primary tectonic surface deformation, and, therefore, the source of the earthquake has been inferred based on the geology, geomorphology, and instrumental seismicity of the region. Talwani (Reference 92) infers that the 1886 event was produced by the north-northeast-striking Woodstock fault (inferred from seismicity) near its intersection with the northwest-striking Ashley River fault (also inferred from seismicity). Marple and Talwani (Reference 74) have more recently suggested that a northeast-trending zone of river anomalies, referred to as the East Coast fault system, represents the causative fault for the 1886 Charleston event. The southern segment of the East Coast fault system coincides with a linear zone of micro-seismicity that defines the northeast-trending Woodstock fault of Talwani (Reference 92) and the isoseismal zone from the 1886 earthquake.

Johnston (Reference 90) estimated a magnitude of $M 7.3 \pm 0.26$ for the 1886 Charleston event. More recently, Bakun and Hopper (Reference 93) estimated a smaller magnitude of $M 6.8$ with a 95 percent confidence level corresponding to a range of $M 6.4$ to 7.1 . Both of these more recent estimates of M_{max} are similar to the upper-bound maximum range of M_{max} values used in the 1986 EPRI studies (m_b 6.8 to 7.5). Therefore, no new information has been developed since 1986 that would require a significant revision to the EPRI seismic source model in terms of magnitude.

Because there is very little surface expression of faults within the Charleston seismic zone, earthquake recurrence estimates are based largely on dates of paleo-liquefaction events. The most recent summary of paleo-liquefaction data (Reference 91) suggests a mean recurrence time of 550 years for Charleston, which was used in the 2002 USGS model (Reference 76). This recurrence interval is less than the 650 year recurrence interval used in the 1996 USGS hazard model, and is roughly an order of magnitude less than the seismicity-based recurrence estimates used in the 1986 EPRI studies.

Therefore, the most significant update of source parameters in the Charleston seismic zone since the 1986 EPRI study is the reduction of the recurrence interval from several thousand years based on seismicity data to the characteristic recurrence of 550 years based on paleoseismic observations. This new information was incorporated into a sensitivity analysis to evaluate its significance to hazard at the ESP site. This sensitivity analysis is described in Section 2.5.2.

New Madrid Seismic Zone

The New Madrid seismic zone extends from southeastern Missouri to southwestern Tennessee and is over 620 miles west of the ESP site. The New Madrid seismic zone lies

within the Reelfoot Rift and is defined by post-Eocene to Quaternary faulting and historical seismicity. Given the significant distance between the site and the seismic zone, the New Madrid seismic zone did not contribute to 99 percent of the hazard at the NAPS site in the 1986 EPRI study. However, it is described in this section because several recent studies provide significant new information regarding magnitude and recurrence interval for the seismic zone.

The New Madrid seismic zone is approximately 125-miles long and 25-miles wide. Research conducted since 1986 has identified three distinct fault segments embedded within the seismic zone. These three fault segments include a southern northeast-trending dextral slip fault, a middle northwest-trending reverse fault, and a northern northeast-trending dextral strike-slip fault (Reference 94). In the current east-northeast to west-southwest directed regional stress field, Precambrian and Late Cretaceous age extensional structures of the Reelfoot Rift appear to have been reactivated as right-lateral strike-slip and reverse faults.

The New Madrid seismic zone historically has produced three large magnitude earthquakes between December 1811 and February 1812 (Reference 95). The December 16, 1811 earthquake is associated with strike-slip fault displacement along the southern portion of the New Madrid seismic zone. Johnston (Reference 90) estimated a magnitude of **M** 8.1 \pm 0.31 for the December 16, 1811 event. However, Hough and others (Reference 95) have re-evaluated the isoseismal data for the region and concluded that the December 16 event had a magnitude of **M** 7.2 to 7.3. Bakun and Hopper (Reference 93) have similarly concluded this event had a magnitude of **M** 7.2.

The February 7, 1812, New Madrid earthquake is associated with reverse fault displacement along the middle part of the New Madrid seismic zone (Reference 96). This earthquake most likely occurred along the northwest-trending Reelfoot Fault that extends approximately 43 miles from northwestern Tennessee to southeastern Missouri. The Reelfoot Fault is a northwest-trending southwest-vergent reverse fault. The Reelfoot Fault forms a topographic scarp developed as a result of fault-propagation folding (Reference 97) (Reference 98) (Reference 99) (Reference 100). Johnston (Reference 90) estimated a magnitude of **M** 8.0 \pm 0.33 for the February 7, 1812 event. However, Hough and others (Reference 95) have re-evaluated the isoseismal data for the region and concluded that the February 7 event had a magnitude of **M** 7.4 to 7.5. More recently, Bakun and Hopper (Reference 93) estimated a similar magnitude of **M** 7.4.

The January 23, 1812, earthquake is associated with strike-slip fault displacement on the East Prairie Fault along the northern portion of the New Madrid seismic zone. Johnston (Reference 90) estimated a magnitude of **M** 7.8 \pm 0.33 for the January 23, 1812, event; however, Hough and others (Reference 95) have re-evaluated the isoseismal data for the

region and have concluded that the January 23 event had a magnitude of **M** 7.1. More recently, Bakun and Hopper (Reference 93) have estimated a similar magnitude of **M** 7.1.

Because there is very little surface expression of faults within the New Madrid seismic zone, earthquake recurrence estimates are based largely on dates of paleo-liquefaction and offset geological features. The most recent summary of paleo-liquefaction data (Reference 101) suggests a mean recurrence time of 500 years, which was used in the 2002 USGS model (Reference 76). This recurrence interval is half of the 1000-year recurrence interval used in the 1996 USGS hazard model, and an order of magnitude less than the seismicity-based recurrence estimates used in the 1986 EPRI studies.

The upper-bound maximum values of M_{\max} used in the 1986 EPRI study range from m_b 7.2 to 7.9. Since the EPRI study, estimates of M_{\max} have generally been within the range of maximum magnitudes used by the six EPRI models. The most significant update of source parameters in the New Madrid seismic zone since the 1986 EPRI study is the reduction of the recurrence interval to 500 years. This new information on recurrence interval for the New Madrid Seismic zone is addressed for the probabilistic seismic hazards analysis (PSHA) at the ESP site in Section 2.5.2.6.2.

2.5.1.1.5 Regional Gravity and Magnetic Data

Regional maps of the gravity and magnetic fields in North America were published by the Geological Society of America (GSA) in 1987 as part of the Society's Decade of North American Geology (DNAG) project. The maps present the potential field data at 1:5,000,000-scale, and thus are useful for identifying and assessing gravity and magnetic anomalies with wavelengths on the order of tens of kilometers or greater. More recent gravity and magnetic data have been incorporated in studies of crustal-scale structure of the Appalachian orogen in Virginia (Reference 102). These studies combine geologic map data and reflection seismic data to evaluate the down-dip geometry of major Appalachian tectonic units. Comparison of the crustal structure with potential field data facilitates geologic interpretation of gravity and magnetic anomalies visible on the regional maps. All of this information was published following the 1986 EPRI study.

a. Gravity Data

Gravity data compiled at 1:5,000,000 scale for the DNAG project provide additional documentation of previous observations that the gravity field in the eastern United States at the latitude of Virginia is characterized by a long-wavelength, east-to-west gradient (Reference 103). Bouguer gravity values increase eastward from about -80 mgal in the Valley and Ridge Province of western Virginia to about $+10$ mgal in the Coastal Plain Province (Reference 104), corresponding to an approximately 90 mgal regional anomaly across the width of the state. This regional gradient is called the "Piedmont gravity gradient" (Reference 103), and is interpreted to reflect the eastward thinning of the North American

continental crust and the associated positive relief on the Moho discontinuity with proximity to the Atlantic margin.

The Piedmont gravity gradient is punctuated by several smaller positive anomalies with wavelengths ranging from about 15 to 30 miles, and amplitudes of about 10 to 20 mgal. Most of these anomalies are associated with accreted Taconic terranes such as the Chopawamsic terrane. Collectively, they form a gravity high superimposed on the regional Piedmont gradient that can be traced NE-SW on the 1:5,000,000 DNAG map relatively continuously along the trend of the Appalachian orogenic belt through North Carolina, Virginia, and Maryland. The continuity of this positive anomaly diminishes to the southwest in South Carolina, and the trend of the anomaly is deflected eastward in Maryland, Pennsylvania, and Delaware (Reference 104).

The short-wavelength anomalies and possible associations with upper crustal structure are illustrated by combining gravity profiles with seismic reflection data and geologic data (Reference 102) (Reference 103). In some cases, short-wavelength positive anomalies are associated with antiformal culminations in Appalachian thrust sheets. For example, there is a positive anomaly associated with the anticline at the western edge of the Blue Ridge nappe along the Interstate I-64 transect of Harris and others (Reference 103). The anomaly is presumably due to the presence of denser rocks transported from depth and thickened by antiformal folding in the hanging wall of the thrust. In other cases, positive anomalies are directly associated with east-dipping, thrust-bounded bodies of relatively denser rock. For example, Glover and Klitgord (Reference 102) show that a local positive gravity anomaly is associated with an east-dipping body of meta-volcanic rock near the boundary between the eastern Piedmont and Coastal Plain Provinces in central Virginia; they interpret that this body of meta-volcanic rocks is the preserved Taconic suture at this latitude.

In general, expression of Triassic basins as local gravity lows at the 1:5,000,000 scale of the DNAG map is modest to non-existent. There is a discernible, low-amplitude negative gravity anomaly associated with the Richmond Basin, but no obvious or pronounced gravity low associated with the Culpeper Basin (Reference 104).

Gravity data published since the mid-1980s confirm and provide additional documentation of previous observations of a gradual "piedmont gravity gradient" across the Blue Ridge and Piedmont Provinces of Virginia. Harris and others (Reference 103) depict this gradient as an 80 mgal increase from west to east over a distance of about 85 miles. The presence of the "Piedmont Gravity Anomaly" was known at the time of the 1986 EPRI study. This anomaly is a first-order feature of the gravity field and is interpreted to reflect eastward thinning of the North American crust and lithosphere. Second-order features in the regional field primarily reflect density variations in the upper crust associated with the boundaries and geometries of Appalachian thrust sheets and accreted terranes. Negative anomalies in Virginia associated with Triassic basins are third-order features of the regional gravity field.

b. Magnetic Data

Magnetic data compiled for the DNAG project reveal numerous NE-SW-trending magnetic anomalies, generally parallel to the structural features of the Appalachian orogenic belt (Reference 104). Unlike the gravity field, the magnetic field is not characterized by a regional, long-wavelength gradient that spans the east-west extent of the state. A magnetic profile along Interstate I-64 published to accompany a seismic reflection profile (Reference 103) shows an approximately constant 11-gamma background field punctuated by anomalies with wavelengths of about 6 to 30 miles. Harris and others (Reference 103) concluded that anomalies in the magnetic field primarily are associated with upper-crustal variations in magnetic susceptibility and, unlike the gravity data, do not provide information on crustal-scale features in the lithosphere.

The most prominent magnetic anomalies in Virginia lie in a NE-SW-trending band across the central part of the state (Reference 104). These anomalies are associated with accreted Taconic units such as the Smith River, Jefferson, and Chopawamsic terranes. The high magnetic intensities of these units probably are due to the presence of island-arc-related mafic and ultramafic rocks. Lower intensities are associated with the Goochland terrane and related eastern Piedmont units, which primarily represent thrust-bounded slices of autochthonous (in place) North American basement. Discrete magnetic lows associated with the Richmond and Culpeper basins are discernible at the 1:5,000,000 scale of the DNAG map (Reference 104). The low magnetic intensities presumably arise because the basin fill deposits are derived from a provenance region that contains fewer mafic and ultramafic rocks than the underlying bedrock terranes.

A magnetic profile along an approximately WNW-ESE transect through central Pennsylvania (Reference 102) indicates that paired high and low magnetic anomalies are associated with the western margins of crustal units truncated by thrust faults. Many of these anomalies have very high amplitudes and short wavelengths. For example, there is a 400-600 nT anomaly associated with the western margin of the Blue Ridge thrust nappe. Similarly, there is a 1500-2000 nT anomaly associated with the western edge of the Jefferson and Smith River terranes, and an 800 nT anomaly associated with a body of meta-volcanic rocks within the Goochland terrane that Glover and Klitgord (Reference 102) interpret as the Taconic suture.

Magnetic data published since the mid-1980s provide additional information on the geometry and extent of anomalies associated with fault-bounded upper crustal units, primarily in the Blue Ridge and Piedmont Provinces. The magnetic data provide additional characterization of the geophysical properties of upper crustal rocks, as well as supporting evidence for interpretation of seismic reflection data (Reference 102) (Reference 103). The magnetic data published since 1986 does not reveal any new anomalies related to geologic structures that were not previously identified prior to the 1986 EPRI study.

2.5.1.2 **Site Area Geology**

The following sections present a summary of geologic conditions of the ESP site and site area (5-mile radius). They provide information concerning the physiography, stratigraphy, geologic history, geologic structure, engineering geology and groundwater conditions relative to the ESP site. The information presented in these sections is based on a review of previous NAPS reports, geologic literature, and the results of recent geotechnical and geologic field reconnaissance investigations conducted at and in the vicinity of the ESP site.

2.5.1.2.1 **Site Area Physiography and Geomorphology**

The ESP site is located within the Piedmont Upland section of the Piedmont Physiographic Province. It is situated approximately 15 miles west of the Fall Line boundary between the Piedmont and Coastal Plain Physiographic Provinces.

The site is bordered by Lake Anna to the north and east, and to the south and west by forest and brushwood-covered land interspersed with an occasional farm (Reference 6). The area is well dissected by streams; the inter-stream divides being generally fairly wide and sloping or rolling. Some of the divides become steeper along the lower tributaries of the larger streams, and along these tributaries entrenchment has been rapid (Reference 41) (Figure 2.5-15).

The topography in the site region is characteristic of the Piedmont Upland section, with a gently undulating surface varying in elevation from about 200 to 500 feet (Reference 5). The slopes in the region typically range from 2 to 5 percent, with steeper slopes along the lower tributaries of some of the larger streams ranging from 7 to 10 percent (Figure 2.5-15).

Site grade for the existing units is at an approximate elevation of 271 feet. The ground surface generally rises to the west and south to elevations of over 300 feet (Figure 2.5-16).

2.5.1.2.2 **Site Area Geologic History**

Since Early Paleozoic time, rocks of the Piedmont Physiographic Province have undergone extensive tectonic activity, primarily from three compressional orogenies (Taconic, Acadian, and Allegheny) during the Paleozoic Era and one extensional episode during the Mesozoic Era (as discussed in Section 2.5.1.1.2). These orogenies produced a very complex regional pattern of folding and faulting. The texture, mineralogy, and structure of rocks in the Piedmont Province, with the exception of Triassic age rocks, generally reflect the effects of these major episodes of tectonic activity. The rocks exhibit varying degrees of metamorphism, depending on their location in relation to the axis of major stress, which generally trends northeast-southwest (Reference 8).

The ESP site is located within the previously described Chopawamsic lithotectonic belt (Section 2.5.1.1.3). Within a 5-mile radius of the site are the Western Piedmont and the Goochland-Raleigh belts, approximately 4.5 miles west and east of the site, respectively (Figure 2.5-11). The rocks within these belts are believed to be derived from sediments deposited in an intra-oceanic island-arc subduction zone, situated eastward of ancestral North America. Rocks

of the Mine Run Complex within the Western Piedmont belt are interpreted to have formed in a back-arc marginal sea between ancestral North America and an offshore island-arc. Rocks of the Chopawamsic Formation and Ta River Metamorphic Suite, within the Chopawamsic belt, are interpreted to have formed this island-arc. East of the island-arc, rocks of the Po River Metamorphic Suite, within the Goochland-Raleigh belt, are interpreted to have formed as a micro-continent. Successive thrusting and deformation of rocks within each of these belts in a general northwest direction during Paleozoic time has produced the present day bedrock conditions at and in the vicinity of the ESP site (Figure 2.5-17).

During the Penobscot orogeny westward and northward thrusting of the island-arc terrain was initiated. Sediment was shed from the Chopawamsic island-arc (Figure 2.5-5) into the eastern parts of the back-arc basin, where sediments of the Mine Run Complex were accumulating (Reference 40).

During the subsequent Taconic orogeny, which occurred during Middle to Late Ordovician, the Chopawamsic island-arc terrane and back-arc basin deposits continued to be thrust westward and were accreted to the eastern margin of ancestral North America. The rocks were episodically folded and faulted and plutonism occurred. Granitoids were emplaced in the back-arc terrane and tonalites were emplaced in the island-arc terrane (Reference 33). This period of deformation and metamorphism was followed by an interval of uplift and erosion during the Late Ordovician and Early Silurian. To the east, sand and pelitic sediments were unconformably deposited on the volcanic and plutonic rocks of the foundered and eroded island-arc rocks. These sediments now constitute the meta-sedimentary Quantico Formation (Reference 33). The Quantico Formation outcrops approximately 2 miles west of the ESP site. At about the same time as the sediments of the Quantico Formation were being deposited, the Ellisville pluton intruded rocks of the back-arc basin terrane. The Ellisville pluton outcrops approximately 5 miles west of the ESP site.

During the Acadian orogeny the micro-continent that had formed eastward of the island-arc terrane, comprised of rocks of the Po River Metamorphic Suite, was thrust westward onto the island-arc terrane. By Devonian time, the back-arc basin and island-arc terranes and the micro-continent were all believed to have been accreted over the continental crust (Reference 40).

During the Allegheny orogeny that followed in the Late Carboniferous Period, the generally undeformed Quantico Formation and the subjacent Ta River Metamorphic Suite were folded into structurally conformable upright isoclinal folds. The unconformity between the Chopawamsic and Quantico Formations became a decollement along which the Long Branch thrust fault developed (discussed in Section 2.5.1.2.4). The upright isoclinal folding is inferred to be related to the westward thrusting of rocks of the Po River Metamorphic Suite along the developing Spotsylvania thrust fault. With continuing deformation, the upright isoclinal folds to the east of the Quantico synclinorium became westward-verging recumbent folds (Reference 40). The Po River Metamorphic Suite was metamorphosed to amphibolite grade and polydeformed. It is thought that much of the deformation and metamorphism occurred before westward thrusting along the Long

Branch and related faults and the juxtaposition, probably toward the end of the Allegheny orogeny, of the eastern, higher grade metamorphic terranes with the greenschist facies rocks of the Chopawamsic Formation. The granitoids of the Falmouth Intrusive Suite generally intruded rocks within the Chopawamsic belt prior to final thrusting along the Long Branch fault (Reference 40). Rocks of the Falmouth Intrusive Suite lie approximately 2 miles southwest and 3.5 northeast of the ESP site (Figure 2.5-11).

During the Mesozoic extensional episode a series of northeast-trending grabens and half-grabens formed in the Piedmont Province, predominantly along the boundaries of the Western Piedmont belt. Within the ESP site area no such basins exist. The closest basin to the site, the Culpeper Basin, lies about 20 miles northwest of the site.

During Cenozoic time, the area surrounding the ESP site was subject to erosion along the passive continental margin. Erosion continued during the Pleistocene glacial and interglacial periods. Periglacial environments persisted in the area of the ESP site during this time. Weathering processes characteristic of periglacial environments include frost-shattering, freeze-thaw cycles, accelerated wind erosion and accelerated solifluction. These weathering processes in conjunction with down-cutting of streams and rivers during Cenozoic time have produced the residual soils that cover bedrock at the ESP site.

2.5.1.2.3 Site Area Stratigraphy

The ESP site is underlain by rocks of the Ta River Metamorphic Suite, which are in turn underlain by rocks of the Chopawamsic Formation and the Mine Run Complex. The Ta River Metamorphic Suite is juxtaposed against the Quantico Formation west of the site and is juxtaposed against the Po River Metamorphic Suite east of the site along north-northwest trending faults (Figure 2.5-11). The Ta River Metamorphic Suite is intruded by rocks of the Falmouth Intrusive Suite to the southwest and northeast of the site. Rocks of the Mine Run Complex and Chopawamsic Formation are intruded by the Ellisville pluton west of the site. Surficial sediments at the site are comprised predominantly of residual soil and saprolite, which mantles most of the site. Alluvium in the vicinity of the site is generally found along stream channels, and marine and fluvial sands and gravels are found locally capping the tops of hills and hill slopes.

Extensive geological and geotechnical data for the ESP site are available as a result of investigations completed for the existing units and for the abandoned Units 3 and 4. Sixty borings were completed to depths ranging between 20 and 150 feet during the investigation for the existing units (Reference 7). Forty-seven borings were completed to depths ranging between 40 and 175 feet for the abandoned Units 3 and 4 (Reference 8). Additional borings were completed in the areas of the SWR (Reference 5) and the ISFSI (Reference 6). The results of the borings are discussed in detail Section 2.5.4.

In addition to the existing geological and geotechnical data for the existing units, 7 new borings, 8 cone penetrometer tests (CPTs), 2 seismic cone penetrometer tests, and cross-hole and down-hole

seismic tests were performed as part of the ESP application subsurface investigation program. The borings and geotechnical testing are discussed in detail in Section 2.5.4. The data developed are presented in Appendix 2.5.4B.

The sequence and configuration of the stratigraphic units within a 5-mile radius of the site are shown in Table 2.5-3 and on Figure 2.5-11 and Figure 2.5-17, respectively. The configuration of the stratigraphic units within a 0.6-mile radius of the site is shown on Figure 2.5-18.

a. Po River Metamorphic Suite (Late Precambrian to Early Paleozoic)

The Po River Metamorphic Suite is juxtaposed along the Spotsylvania thrust fault against the Ta River Metamorphic Suite, east and southeast of the site (Figure 2.5-11 and Figure 2.5-17). The Po River Metamorphic Suite belongs to the Goochland-Raleigh lithotectonic belt of the Piedmont Upland section. A provisional age of Late Precambrian to Early Paleozoic has been assigned to the rocks of the Po River Metamorphic Suite (Reference 66).

Rocks of the Po River Metamorphic Suite are within the amphibolite facies (high grade) of regional metamorphism (Reference 40) and consist of predominantly of biotite gneiss and schist. Characteristically, the gneiss is a dark colored, layered and foliated rock with micaceous minerals and quartz and feldspar typically concentrated in dark and light layers. Feldspar also occurs as large augen-shaped grains. Hornblende-bearing gneiss is found within the Po River, but in subordinate amounts compared to the biotite gneiss. It resembles the biotite gneiss in color and texture but contains varying amounts of hornblende as well as biotite. Garnetiferous mica schist is also found locally within the Po River and has a foliation conformable with the adjacent gneisses (Reference 66).

Many foliated gneissic granitoid rocks, including pegmatoids, exist in tabular bodies as well as non-tabular masses in the Po River. The tabular granitoid and pegmatoid bodies form concordant sill-like layers that range from less than 2.5 centimeters (cm) to as much as 7.6 m thick. Locally, granitoid layers about 0.5 to 1.0 cm thick are conformable with the foliation in the gneiss. The non-tabular, irregularly shaped granitoid bodies generally form relatively large masses that may be parts of plugs or plutons of various sizes (Reference 66).

b. Ta River Metamorphic Suite (Cambrian and/or Ordovician)

The Ta River Metamorphic Suite underlying the site is bounded on the east by the Spotsylvania thrust fault and on the west is juxtaposed against the Quantico Formation by a series of unnamed faults (Figure 2.5-11). Two thrust-fault-bounded slivers of the Ta River Metamorphic Suite are located west of the Quantico Formation (Figure 2.5-11 and Figure 2.5-17). The Ta River Metamorphic Suite belongs to the northeast-trending Chopawamsic lithotectonic belt of the Piedmont Upland section. Rocks of the Ta River Metamorphic Suite are thought to be Cambrian and/or Ordovician in age (Reference 35).

The Ta River Metamorphic Suite is intruded by plutonic rocks to the southwest (Elk Creek pluton) and northeast (Northeast Creek pluton) of the site (Figure 2.5-11). The rocks are correlative with the Falmouth Intrusive Suite.

The Ta River Metamorphic Suite is thousands of feet thick (Reference 105) and the rocks within the suite are within the amphibolite facies (high grade) of regional metamorphism (Reference 40). The rocks are dark-gray to black gneisses, which range from amphibolite through various types of amphibolite gneiss to biotite gneiss. In the site area, the rocks are predominantly biotite gneiss and schist with smaller amounts of amphibolite gneiss. Regional metamorphism is considered to be of a higher grade in this area than to the north (Reference 66). Descriptions of the amphibolitic gneisses have ranged from well-foliated and rarely layered (Reference 66) to poorly to well lineated and massive to well layered. Layers of biotite gneiss, ferruginous quartz and minor felsic meta-volcanic rocks are common and quartz-epidote lenses and veins often occur in the amphibole-bearing rocks (Reference 105).

Borings completed during previous subsurface investigations (Reference 7) (Reference 8) and borings completed as part of the recent ESP application subsurface investigation program (discussed in Section 2.5.4) encountered rocks of the Ta River Metamorphic Suite at the ESP site. The main rock types at the site are shown on Figure 2.5-18 and consist of gray to dark gray:

- quartz gneiss with some biotite quartz gneiss,
- hornblende gneiss, biotite quartz gneiss, and quartz gneiss, and
- quartz mica schist.

Residual soil and saprolite at the ESP site have been categorized as Zone I and II respectively, while bedrock has been categorized as Zone III, III-IV and IV, based on the degree of weathering of the rock (Reference 7) (Reference 8). Zone III rocks are generally highly to moderately weathered; Zone III-IV rocks are slightly to moderately weathered; and Zone IV rocks are slightly weathered to fresh.

Borings B-801 to B-805 encountered moderately to highly weathered rock (Zone III) at depths ranging between about 6 feet (Elevation 266) and 31 feet (Elevation 261) below the ground surface. This Zone III rock ranges in thickness from about 1-foot to 18 feet, and is comprised of brown, orange, tan, and gray, biotite quartz gneiss and quartz gneiss, with traces of clay, iron oxide staining, epidote, chlorite, pyrite and magnetite. Slightly weathered to moderately weathered rock (Zone III-IV) was encountered in the borings at depths ranging between about 8 feet (Elevation 263) and 39 feet (Elevation 232) below the ground surface. The Zone III-IV rock ranges in thickness from about 2 feet to 37 feet and is comprised of gray to dark gray, quartz gneiss and biotite quartz gneiss. The top of the slightly weathered to fresh rock (Zone IV) was encountered in the borings at depths ranging between about 20 feet

(Elevation 229) and 76 feet (Elevation 195) below the ground surface and is comprised of dark gray, quartz gneiss and biotite quartz gneiss.

In boring B-806, alternating zones of moderately to highly weathered rock (Zone III) and slightly weathered to moderately weathered rock (Zone III-IV) were encountered throughout much of the boring. The Zone III rock was encountered at depths of about 8 feet (Elevation 292), 15 feet (Elevation 284), 26 feet (Elevation 273), and 56 feet (Elevation 243) below the ground surface. The alternating Zone III-IV rock was encountered at depths of about 11 feet (Elevation 288), 21 feet (Elevation 278), 33 feet (Elevation 266) and 60 feet (Elevation 239) below the ground surface. The boring was terminated at a depth of 65 feet below the ground surface, approximately 1 foot into slightly weathered to fresh rock (Zone IV).

In boring B-807, alternating zones of moderately to highly weathered rock (Zone III) and residual soils were encountered throughout the full depth of the boring. The Zone III rock was initially encountered at a depth of about 35 feet (Elevation 276) below the ground surface and was 14 feet thick. A second zone of this rock was encountered at a depth of about 56 feet (Elevation 255) below the ground surface and extended for 16 feet, whereupon the boring was terminated.

The borings drilled as part of the ESP application subsurface investigation program (discussed in Section 2.5.4) revealed severely weathered, fractured and jointed intervals in the Zone III-IV and Zone IV rock. Severely weathered fracture zones were encountered in Zone III-IV rock at varying depths, ranging from about 11 feet (Elevation 260) to 81 feet (Elevation 211) below the ground surface. These fracture zones were encountered in four of the borings (B-802, B-803, B-805, and B-806) and ranged in thickness from about 0.5 to 1-foot thick. Characteristically they exhibit clay filling, iron oxide staining, and quartz. Significant water loss during drilling occurred in two of the fracture zones in boring B-803. Joints (typically sets of 3 to 10 joints) in the slightly weathered to fresh (Zone IV) rock typically exhibit clay filling, iron oxide staining, quartz, mica, and traces of chlorite and manganese oxide.

Several quartz, potassium feldspar and mica bands were encountered during the drilling of boring B-803. The bands were encountered in the slightly weathered to fresh (Zone IV) rock at depths ranging between about 115 feet (Elevation 177) and 147 feet (Elevation 145) below the ground surface. Quartz bands were also encountered in several of the borings. Borings performed as part of the previous subsurface investigation programs (Reference 7) (Reference 8) also encountered occasional quartz seams, in addition to bands containing abundant mica and hornblende, and occasional chlorite, epidote and pyrite.

Petrographic analyses of thin sections prepared from the quartz gneiss at the ESP site have revealed the predominant minerals to be quartz and feldspar (alkali and plagioclase). According to these analyses, quartz makes up between 34 and 40 percent of the total volume of the rock; alkali feldspar makes up between about 21 and 37 percent of the total volume of

the rock, and plagioclase feldspar makes up between 23 and 33 percent of the total volume of the rock. Biotite is the only major ferromagnesian mineral. Accessory minerals include muscovite, vermiculite, magnetite and hematite. Minor accessory minerals include sphene, zircon, cordierite, apatite and epidote (Reference 106).

c. Chopawamsic Formation (Cambrian and/or Ordovician)

The Ta River Metamorphic Suite is underlain by the Chopawamsic Formation (Figure 2.5-17). The formation crops out west and northwest of the site and is bounded on the east by the Long Branch thrust fault and on the west by the Chopawamsic thrust fault (Figure 2.5-11). The Chopawamsic Formation belongs to the Chopawamsic lithotectonic belt of the Piedmont Upland section. Rocks of the Chopawamsic Formation are thought to be Cambrian and/or Ordovician in age (Reference 35).

The Chopawamsic Formation is several thousand feet thick (Reference 105). Rocks within the formation are typically within the greenschist facies (low grade) of regional metamorphism and characteristically contain an albite-chlorite-epidote mineral assemblage (Reference 40). The Chopawamsic Formation consists of laterally discontinuous lenses and tongues of meta-volcanic and meta-sedimentary rocks. The meta-volcanic rocks include silic, intermediate, and mafic varieties, some of which are interpreted to be flows as indicated by their highly vesicular character. Fragmental rocks within the formation are mainly breccia and tuff. Fine-grained feldspathic schist and phyllite of the formation are mineralogically and chemically similar to the more distinctive volcanic rocks and may be tuffaceous. Schist, meta-arenite, and, locally, amphibole-free gneiss of probable sedimentary origin are interlayered with the meta-volcanic rocks; the proportion of meta-sedimentary rocks varies from place to place along the formation. Silic meta-volcanic rock typically is light gray; some varieties have small phenocrysts of quartz and/or feldspar. Some felsic meta-volcanic rocks contain albitic plagioclase and quartz in a finer grained, quartzofeldspathic groundmass and have been classified as keratophyres. Intermediate meta-volcanic rocks are dark to light green and commonly have a nematoblastic groundmass texture formed by aligned prismatic amphibole intergrown with fine-grained quartz and feldspar. Mafic rocks of the Chopawamsic Formation include amphibolite greenstone, and various dark schists (Reference 66).

The Chopawamsic Formation lies close to the Ellisville pluton, which intruded the Mine Run Complex west of the site (Figure 2.5-11 and Figure 2.5-17). The enclosing rocks of the pluton show recognizable contact metamorphism. The phyllitic country rocks near the intrusive contact have been metamorphosed to schists and gneissic rocks, and megacrystic muscovite and biotite are common in addition to kyanite and staurolite. On the eastern side of the pluton within the Chopawamsic Formation, kyanite is present in fine-grained sulfidic schist, which is interlayered with meta-felsite and with chloritoid-bearing phyllite and schist. Minerals found in the Chopawamsic Formation within the thermal aureole of the Ellisville pluton include gahnite, margarite, tourmaline, allanite-clinozoisite, and chlorite (Reference 40).

d. Mine Run Complex (Cambrian to Ordovician)

The Chopawamsic Formation is underlain by mélanges of the Mine Run Complex (Figure 2.5-17). Mélange Zone II of the Mine Run Complex outcrops west and northwest of the site and is bounded on the east by the Chopawamsic thrust fault and on the west by the Lake of the Woods thrust fault (Figure 2.5-11). Mélange Zones III and IV outcrop successively northwest of Mélange Zone II. The Mine Run Complex belongs to the Western Piedmont lithotectonic belt of the Piedmont Upland section. The mélanges of the Mine Run Complex are estimated to be Cambrian to Ordovician in age (Reference 36).

The Mine Run Complex is hundreds of feet thick (Reference 105). The mélanges of the complex are typically within the greenschist facies (low grade) of regional metamorphism and are characterized by chlorite-muscovite or chlorite-muscovite-garnet assemblages (Reference 40). Mélange Zone II contains felsic and mafic meta-volcanic blocks and granitoid blocks of altered tonalite and granodiorite in a schist and phyllite mélange matrix. The exotic blocks of the mélange are petrographically similar to rocks within the Chopawamsic Formation and are interpreted as fragments of the Chopawamsic Formation (Reference 66). Mélange Zone III contains metamorphosed mafic and ultramafic blocks, while Mélange Zone IV contains mafic and ultramafic blocks.

The mélanges of the Mine Run Complex are intruded by the Ellisville pluton. The phyllitic country rocks near the intrusive contact have been metamorphosed to schists and gneissic rocks and megacrystic muscovite and biotite are common in addition to kyanite and staurolite. Chlorite also occurs within the thermal aureole of the pluton (Reference 40).

e. Quantico Formation (Ordovician)

The Quantico Formation is faulted against the Ta River Metamorphic Suite and the Chopawamsic Formation west of the site (Figure 2.5-11 and Figure 2.5-17). It is bounded on the west by the Long Branch thrust fault and on the east by a series of smaller thrust faults. The Quantico Formation formed within the northeast-southwest trending Quantico synclinorium. The Quantico formation belongs to the Chopawamsic lithotectonic belt of the Piedmont Upland section. Fossils contained in the formation indicate a Late Ordovician age (Reference 35).

Within the Quantico synclinorium, the Quantico Formation is at garnet-staurolite grade (high grade) metamorphism. The Quantico Formation is comprised of dark-gray phyllite and micaceous, fine- to medium-grained staurolite schist and biotite-muscovite garnetiferous schist that locally contains kyanite. Calc-silicate layers are also present and quartzite forms discontinuous lenses within the formation and locally at its base (Reference 66). The formation thickness has been estimated at 300 feet (Reference 105).

f. Ellisville Pluton (Silurian)

The Ellisville pluton intrudes the Mine Run Complex west of the site (Figure 2.5-11 and Figure 2.5-17). The pluton is interpreted to have formed along the continental margin of ancestral North America after accretion of the back-arc basin and island-arc terrane. It is interpreted to have formed from a crustal source, as opposed to a mantle source. It is considered to have intruded and thermally metamorphosed the surrounding country rock during the Silurian Period (Reference 40). A general depth of emplacement of about 11 to 8 miles is estimated for the Ellisville pluton with a temperature of emplacement of about 760°C. Gravity data suggests that the Ellisville pluton may have an appreciable subsurface extension to the northeast from its surface exposure (Reference 33).

The Ellisville pluton is composed almost entirely of coarse- to medium-grained biotite granodiorite that is commonly mesocratic, equigranular to porphyritic in texture, and massive to strongly foliated. It contains granitoid intrusions or inclusions of Cambrian and Silurian age and a Late Precambrian to Cambrian age amphibolitic xenolith (Reference 66).

g. Falmouth Intrusive Suite (Carboniferous)

Two small irregularly shaped plutons containing rocks of the Falmouth Intrusive Suite intrude the Ta River Metamorphic Suite (Figure 2.5-11). The Elk Creek and Northeast Creek plutons intrude the Ta River suite southwest and northeast of the site, respectively. Rocks of the Falmouth Intrusive Suite are the youngest felsic rocks in the area and have been isotopically dated as Carboniferous in age (Reference 40).

The Falmouth Intrusive Suite is composed of fine-grained monzogranite and pegmatitic granite, fine-grained granodiorite and, less commonly tonalite. The granitoids are strongly to weakly foliated and are marked by the exceptional development of myrmekite (Reference 66).

h. Residual Soil and Saprolite (Cenozoic)

Residual Soil

The ESP site and surrounding area is generally mantled by residual soil derived from the weathering of the underlying metamorphic rocks. Weathering has destroyed all parent geologic structure in the residual soils to an average depth of 4 to 5 feet. The residual soil generally consists of clay, silt, and sand-sized particles with minor rock fragments (Reference 5).

Residual soil was encountered in only one of the borings drilled at the site as part of the ESP subsurface investigation (B-804). It extends from the ground surface to a depth of 1.5 feet below the ground surface in this boring. The soil consists of red and brown, slightly gravelly sandy clay.

Saprolite

Saprolite is encountered at the ground surface or underlies residual soil at the ESP site and in the surrounding area. The saprolite is derived from weathering of the underlying metamorphic rock, but retains many of the structural and mineralogical features of the rock. The saprolite extends to the top of the rock from which it was derived, although the contact between the saprolite and underlying rock may be gradational and poorly defined (Reference 5).

At the ESP site, the saprolite has been categorized based on its general composition and grain-size (discussed in Section 2.5.4). Zone IIA saprolite is divided into coarse-grained saprolite, comprised of sand-size particles, and fine-grained saprolite, comprised of clay-and/or silt-size particles. Zone IIA saprolite typically contains less than 10 percent rock fragments. Zone IIB saprolite consists predominantly of sand-size particles and contains between 10 and 50 percent rock fragments.

Borings drilled as part of the ESP subsurface investigation program (Section 2.5.4) encountered Zone IIA saprolite from the ground surface or just below the ground surface to depths of between 6 feet (Elevation 265.5) and 35 feet (Elevation 261.4). The saprolite consists of orange, brown, tan, and gray, micaceous, silty, clayey, fine to coarse sand, and sandy silt with occasional rock fragments. Zone IIB saprolite was encountered at depths of between 21 feet (Elevation 289.6) and 49 feet (Elevation 261.6) below the ground surface and ranges in thickness from 7 to 14 feet. It consists of brown, orange, tan and gray, micaceous silty, slightly clayey, fine to coarse sand with some to many rock fragments.

Results of mineralogical tests performed on samples of saprolite derived from the quartz gneiss at the ESP site indicate that the saprolite consists of quartz, kaolin, mica and feldspar. X-ray diffraction tests further indicate that the portion of the sample less than 2 microns in diameter consists of 85 percent kaolinite and 15 percent mixed-layer minerals (Reference 7). In fact, additional studies conducted on the clay mineralogy of the saprolite indicate that the major clay mineral is halloysite, which is a hydrated form of kaolinite. Lesser amounts of the clay minerals illite and montmorillonite are also found in the saprolite (Reference 5).

i. Sand and Gravel (Miocene)

Miocene age sand and gravel commonly cap interfluvial areas and constitute the thin Coastal Plain outliers capping the higher hills where deposits directly overlie the crystalline rocks (Figure 2.5-11). The sand and gravel unit reaches a thickness of up to 33 feet (Reference 66).

The sand and gravel unit consists of gray to light yellowish gray, fine-to-coarse gravelly sand, sandy gravel, silt and kaolinitic clay. The sand and gravel are commonly oxidized to yellowish orange and yellowish and reddish brown. Pebbles and cobbles in the unit are mainly quartz, quartzite, and crystalline rocks and are commonly well rounded, deeply etched, and crumbly in part (Reference 66).

j. Alluvium (Quaternary)

Alluvium in the site area has been deposited mainly in the stream channels and along their flood plains (Figure 2.5-11). Along the steeper valley walls at the margins of the deposits, they grade into colluvium. The alluvium is mainly Holocene in age, but may include low-lying Pleistocene terrace deposits. The thickness of the alluvium along the major streams is as much as 49 feet (Reference 66).

The alluvium consists of light-to-medium gray and yellowish gray, fine-to-coarse gravelly sand and sandy gravel, silt, and clay. Clasts in the alluvium consist mainly of vein quartz, quartzite, and other metamorphic rocks (Reference 66).

k. Artificial Material

Artificial material (fill) is present at the ESP site in areas associated with construction of the existing units and abandoned Units 3 and 4. Borings performed as part of the ESP application subsurface investigation program encountered fill to depths of between 2.5 and 19 feet below the ground surface. The fill consists of a mixture of orange, brown, and tan sand, silt and clay. The maximum thickness of fill (19 feet) was encountered in boring B-801 in the excavated and partially backfilled powerblock area for abandoned Units 3 and 4.

2.5.1.2.4 Site Area Structural Geology

The local structural geology of the ESP site described in this section is based primarily on a summary of published geologic mapping (Reference 66) (Reference 105) and results of earlier investigations performed at the NAPS site (Reference 7) (Reference 9) (Reference 107). Structural features at and within a 5-mile radius of the ESP site consist of a series of northeast-striking faults and folds (anticlines and synclines) within the metamorphic bedrock.

Seven bedrock faults have been identified within a 5-mile radius of the ESP site (Figure 2.5-11):

- Spotsylvania thrust
- Chopawamsic thrust
- Long Branch thrust
- Sturgeon Creek fault
- Unnamed fault ("a") traversing the NAPS site
- Unnamed fault ("b") separating the Ta River Metamorphic Suite from the Quantico Formation
- Unnamed fault ("c") separating the Northeast Creek pluton from the Quantico Formation

The faults are described in detail in Section 2.5.3. None of these faults are considered capable tectonic sources, as defined in RG 1.165, Appendix A. One of the faults traverses the NAPS site (unnamed fault "a") and was the subject of intensive studies following its exposure within the excavations for abandoned Units 3 and 4 (Reference 9). This fault is briefly described within this

section of the report, but a more comprehensive summary of the fault and investigations is provided in Section 2.5.3.

The Spotsylvania, Chopawamsic, and Long Branch thrust faults are northeast striking, east-dipping Paleozoic structures that can be mapped for tens of miles within the Piedmont Province (Reference 66). The Spotsylvania and Chopawamsic thrust faults bound the eastern and western margins of the Chopawamsic belt, respectively, and therefore represent the largest surficial tectonic structures within the site area.

The Sturgeon Creek fault and the three unnamed faults (“a”, “b”, and “c” on Figure 2.5-11) also strike northeast; however, they are smaller structures than the other three thrust faults. The fault closest to the ESP site is the unnamed fault (“a”) that traverses the site. This fault has been given a length of about 3000 feet through the site by Dames & Moore (Reference 9) (Figure 2.5-18) based on geologic mapping of excavations and trenches. The fault consists of 4 individual shear zones and chlorite seams and generally strikes N65°E and dips between 45 degrees and 50 degrees to the northwest (Reference 108). Dames & Moore (Reference 9) concluded that the fault was not capable and the AEC (Reference 108) agreed stating:

“The North Anna fault zone is neither genetically nor structurally related to any known, capable fault. Thus the staff concludes that the faults are not “capable,” as defined by Appendix A of 10 CFR Part 100.”

(Refer to Section 2.5.3 for additional discussion.)

The three largest folds within a 5-mile radius of the ESP site include, from west to east, the Quantico synclinorium, the Rappahannock anticlinorium, and the Matta nappe (Figure 2.5-5). These structures exhibit multiple phases of metamorphism and deformation of Paleozoic age (Reference 40). The Quantico synclinorium and Rappahannock anticlinorium are located within the Chopawamsic belt, which is bounded on the west by the Chopawamsic thrust fault and on the east by the Spotsylvania thrust fault (Figure 2.5-11). East of the Chopawamsic belt, lies the Matta nappe, a west-verging, recumbently folded sheet of Po River Metamorphic Suite rocks that was thrust westward over the island-arc terrane by the Spotsylvania thrust fault (Figure 2.5-5). Because the nappe contains northeast-trending, generally upright folds parallel to compositional layering, the Matta nappe is considered a large-scale recumbent foliation fold (Reference 40).

The Rappahannock anticlinorium, which is bounded by the Long Branch and Spotsylvania faults, extends southwest from Stafford, Virginia, to the James River and beyond (Reference 36). Most of the folds along the Rappahannock anticlinorium are foliation folds formed by the folding of an earlier schistosity (Reference 40). In the site area, foliation folds within the Ta River Metamorphic Suite are upright, northeast plunging or doubly plunging (Figure 2.5-11). The youngest set of folds within the Rappahannock anticlinorium and Matta nappe refold the earlier foliation folds (Reference 40).

West of the Rappahannock anticlinorium lies the Quantico synclinorium, a large upright foliation fold that is mapped over 20 miles parallel to the Long Branch thrust fault. Near the southern end of the

fold, the Sturgeon Creek fault curves to the southwest into the axis of the Quantico synclinorium (Reference 40).

The ESP site lies within the complexly folded Ta River Metamorphic Suite of the Rappahannock anticlinorium. On Figure 2.5-11, 3 anticlines and 2 synclines, trending northeast and ranging in length from 1.5 to 5 miles, are mapped within the Rappahannock anticlinorium near the site. The folds are closely spaced with axes approximately 0.1 to 0.2 miles apart. Foliations in the metamorphic rocks range in dip from 40 degrees to vertical (Figure 2.5-11).

The most detailed mapping at the site was performed by Dames & Moore in a series of reports in the early 1970s as part of the site-specific studies for the existing NAPS site (Reference 7) (Reference 8) (Reference 9). Field mapping was supplemented with geotechnical borings, bedrock exposures in excavations, and geophysical surveys. The mapping delineated different compositional layering within the gneisses and schists. These rocks, which were later classified as the Ta River Metamorphic Suite, were split into three main rock types at the site and consist of gray to dark gray quartz gneiss with biotite, interbedded with a biotite quartz gneiss; and interbedded quartz gneiss, biotite quartz gneiss and hornblende gneiss. The distribution of these bedrock units illustrates the folding at the site (Figure 2.5-18).

The most prominent folds at the site are the northerly plunging syncline/anticline pair located in the western portion of the site (Figure 2.5-18). The axis of the syncline passes near an area of exposed bedrock (quarry area shown on Figure 2.5-18) and foliations near the axis of the fold dip steeply (65–90 degrees).

In the deeply weathered Piedmont Province, the presence of a thick saprolite limits the quantity and quality of structural observations and measurements in competent bedrock materials. However, because the ESP site contains deep excavations and abundant subsurface explorations, a much greater amount of structural data is available for the site than the surrounding region. Exposures of bedrock, and therefore structural observations within the site, are concentrated in the excavations for the existing units and abandoned Units 3 and 4, foundation excavations for other structures, and cuts for roads and railroad spurs (Figure 2.5-18). There are still large portions of the site where detailed structural measurements (orientations of foliations, joints, and fractures) are sparse.

Foliation in the metamorphic bedrock is generally oriented northeasterly across much of the site. However, due to the deformed and folded nature of the metamorphic rocks, the strikes and dips are highly variable. Dips of the foliation in the metamorphic rocks at the site range from as low as ≈15 degrees to as steep as 90 degrees. The majority of dips measured at the site are typically steeper than 45 degrees.

The existing units and abandoned Units 3 and 4 are located in an area of northeast-striking, northwest-dipping bedrock foliations, which may represent the northwest flank of an anticline (Figure 2.5-11 and Figure 2.5-5). Bedrock foliations generally strike about N45°E and dip

moderately to the northwest in this portion of the site. Specifically, foliation orientations within excavations for abandoned Units 3 and 4 strike N55-75°E and dip 40-60°NW (Reference 107).

The mapping of joints and fractures from rock outcrops and rock cores recovered from borings drilled during previous site investigations (Reference 7) reveal that the bedrock is extensively jointed. The joint pattern was characterized by Dames & Moore (Reference 7) from field outcrops and test pits excavated into the saprolite, prior to mapping exposures in the large foundation excavations at the site. Several joint sets were identified by the initial studies.

- Release joints are one of the most abundant sets of joints in the gneiss. They strike slightly east of north, dip steeply to the west, are usually tight and smooth and rarely show any shear movement or contain any clay fill.
- Bedding plane joints are also abundant. They form parallel to schistosity, are generally smooth, tight, and rarely contain clay fill.
- Several sets of cross joints strike east-west, dip steeply to the north, are smooth and contain some clay fill, while other sets are essentially horizontal, rough and generally highly weathered with as much as 2 inches of clay fill. These joints are limited in areal extent.
- Two sets of diagonal joints in the gneiss strike northeast and northwest, are usually smooth, contain some clay fill, and are slickensided in places. These joints are characterized as extensive and widely spaced.
- A set of joints that strike northeast and dip moderately to the southeast commonly exhibit reverse shear movements. These discontinuities are more common near the hornblende gneiss contact and are believed to be the result of minor adjustments of the rock mass during folding. They are clay-filled, smooth, and show displacements of up to 1.5 feet.

Detailed mapping of excavation walls for the abandoned Unit 3 and 4 reactor containment structures revealed a less weathered, more intact rock mass than was available in earlier studies of the site by Dames & Moore (Reference 7). The deep excavations revealed three major joint sets and less prominent sets similar to the joint pattern observed near the ground surface. The orientation, properties, and spacing of major joint sets in excavations for abandoned Units 3 and 4 were characterized by Stone & Webster Engineering Corporation (Reference 107) as follows:

- Strike N20E, dip 70-90°NW – tightly closed, clean with occasional iron staining, smooth, and spaced at 8- to 24-inch intervals.
- Strike N55-75E, dip 40-60°NW (foliation plane joints) – tightly closed, variably iron stained, smooth, and spaced at 6- to 36-inch intervals.
- Strike N50-80E, dip 20-55°SE (cross foliation joints) – closed, iron stained to moderately weathered, rough, discontinuous, and spaced at irregular intervals.

In the excavation for abandoned Unit 3, a minor joint set exhibits strike of N20-60W and dip of 40-65°SW and is spaced at irregular intervals. In the abandoned Unit 4 excavation, a minor joint set

was found to strike N40E and dip 60-85°NW. This set is tightly closed and spaced at 8- to 24-inch intervals.

2.5.1.2.5 Site Area Geologic Hazard Evaluation

The only geologic hazard determined to be associated with the ESP site is earthquake activity with its resulting vibratory ground motion effects and potential for surface faulting. A detailed discussion of earthquakes and their effects on the ESP site is provided in Section 2.5.2 and Section 2.5.3.

2.5.1.2.6 Site Engineering Geology Evaluation

Evaluation of engineering geology conditions at the ESP site has been performed based on a review of existing site-specific reports, geologic and geotechnical investigations, and geologic literature. The results of the geotechnical investigations are discussed in detail in Section 2.5.4.

a. Engineering Behavior of Soil and Rock

Soil

The saprolite at the ESP site is comprised of micaceous silty, clayey sand and sandy silt/clay with occasional-to-many relict rock fragments. Depending on the degree of weathering, the saprolite more or less retains the fabric or structure of the parent bedrock. Weathering tends to decrease with increasing depth, resulting in a boundary between the saprolite and weathered bedrock that is generally not well defined. While the saprolite has the relict structure of the parent bedrock, its engineering properties typically resemble those of a soil. It exhibits certain aspects that are characteristic of both cohesive and cohesionless soils.

The saprolite at the site has been categorized into Zone IIA and Zone IIB saprolite, based on its general composition and grain size (Section 2.5.4). Zone IIA saprolite has been classified as silty sand (SM), clayey sand (SC), and high and low plasticity silt and clay (MH, ML, CH, and CL). Zone IIB saprolite has been classified as silty sand (SM). Zone IIA saprolite is the more weathered of the two saprolites and contains less than 10 percent relict rock fragments. An average SPT N-value of 20 blows per foot (bpf) for this saprolite indicates medium dense conditions. Zone IIB saprolite contains between 10 and 50 percent relict rock fragments, and an average SPT N-value of 100 bpf. Section 2.5.4 provides an extensive discussion of the geotechnical properties of the saprolite at the ESP site.

The presence of mica in the saprolite is likely to reduce its maximum compacted density and increase its compressibility. The SWR pump house for the existing units was constructed on about 65 feet of Zone IIA saprolite, consisting mainly of sandy silt, with frequent layers of micaceous sandy silt. For about two years after its construction, the pumphouse structure underwent relatively high settlement that declined significantly thereafter. The settlement was caused by the weight of the SWR dike fill built up around the pumphouse. The micaceous nature of the material is considered to have played a major role in the settlement. High

compressibilities and low maximum densities of the saprolite, therefore, preclude using it as engineered fill at the ESP site.

The geotechnical engineering design properties of the saprolite are presented and discussed in Section 2.5.4. The behavior of the saprolite with respect to liquefaction and slope stability is discussed in Section 2.5.4 and Section 2.5.5, respectively.

Rock

Bedrock at the ESP site is comprised predominantly of gray to dark gray quartz gneiss with biotite, interbedded with a biotite quartz gneiss; and interbedded quartz gneiss, biotite quartz gneiss and hornblende gneiss of the Ta River Metamorphic Suite. The gneiss is a hard, foliated rock, which exhibits various degrees of weathering. It is the degree of weathering of the rock that affects its engineering behavior and properties.

The gneiss at the site has been categorized into Zone III, Zone III-IV, and Zone IV based on its degree of weathering. Zone III is the uppermost weathered part of the bedrock. It is highly to moderately weathered and fractured and contains traces of clay and iron oxide. Based on the results of the borings drilled for the ESP investigation (Appendix 2.5.4B) and previous geotechnical investigations (Reference 7) (Reference 8), the average percentage of rock core recovered by borings in Zone III is 60 percent and the average rock quality designation (RQD) value is 20 percent. An RQD of 20 percent is indicative of poor quality rock (Reference 109). These results indicate that Zone III is not a suitable bearing surface for the safety-related plant structures.

Zones III-IV and IV are considerably less weathered, the degree of weathering typically decreasing with increasing depth. Zone III-IV is slightly to moderately weathered and Zone IV is slightly weathered to fresh. Based on the results of the borings drilled for the ESP investigation (Appendix 2.5.4B) and previous geotechnical investigations (Reference 7) (Reference 8), the average percentage of rock core recovered from Zones III-IV and IV are 90 percent and 100 percent, respectively. The average RQD values for Zones III-IV and IV are 50 percent and 95 percent, respectively. RQD values of between 50 and 90 percent are indicative of fair to excellent quality rock (Reference 109). Therefore, the boring results indicate that Zones III-IV and IV are suitable bearing surfaces on which to found the Category I plant structures. The joints and fractures present in both zones are not considered to be of sufficient density or areal extent to affect the engineering behavior of the rock with respect to its foundation bearing capacity or integrity.

Geologic mapping of foundation rock performed during excavation for the abandoned Units 3 and 4 (Reference 107) revealed primarily fresh and sound gneiss, with weathering generally limited to the joints and shear zones. Major joint sets were reported as generally tightly closed and clean with some iron staining. While not evenly distributed throughout the rock mass, minor joint sets were reported to yield rhombic blocks of intact gneiss with side dimensions of

about 1 foot to 2 feet. Minor overbreak and the development of rock wedges, caused by jointing in the rock, were reported during excavation.

The slipping of rock wedges and the “popping” of rock blocks would be likely to occur during excavation at the site can be caused not only by the interception and condition of joints in the rock mass but also by stress relief in the rock. The gneiss has been tectonically stressed and so residual stress in the rock is likely to be relieved by slippage along foliations and joints, the “popping” of rock blocks, and the opening of joints. These adjustments to stress are likely to be minor and any unstable rock wedges or blocks would either be removed or adequately supported; open joints would be filled with cement grout.

The geotechnical engineering design properties of the bedrock are presented and discussed in Section 2.5.4. The behavior of the bedrock with respect to slope stability is discussed in Section 2.5.5.

b. Zones of Alteration, Weathering and Structural Weakness

Borings drilled as part of the ESP investigation (Appendix 2.5.4B) and previous geotechnical investigations (Reference 7) (Reference 8), and excavations for construction of the existing units and abandoned Units 3 and 4 (Reference 107) indicate that the gneiss at the ESP site is moderately to intensely jointed. Several joint sets have been identified at the site, namely foliation plane joints and cross foliation joints. They are typically of limited extent, slightly rough to smooth, and contain iron oxide and some clay fill indicative of minor shear movement. Those joints that are continuous over a larger area of the site are generally tight, smooth, and seldom show any shear movement or clay fill.

Micro-shear zones and zones of severely weathered and fractured rock have also been identified in the gneiss at the site. The micro-shear zones have developed within the foliation, and are discontinuous. They reflect minor adjustment to stress during regional deformation.

Several zones of severely weathered and fractured rock were encountered in the borings drilled as part of the ESP investigation (Appendix 2.5.4B). The zones were typically found in slightly weathered to moderately weathered gneiss at depths ranging between 11 feet (Elevation 260) and 81 feet (Elevation 211) below the ground surface. The zones are typically 0.5 to 1-foot thick and contain quartz, clay and iron oxides.

Because of the tendency for zones of severely weathered and fractured rock to weather further upon exposure, they would be removed and replaced with cement grout where encountered in excavations for the new units. This would ensure adequate bearing capacity of the foundation rock mass.

c. Deformational Zones

A shear zone was found in the Ta River Metamorphic Suite during the excavation for abandoned Units 3 and 4. The shear zone was investigated by Dames and Moore

(Reference 9) and the results presented to the U.S. Atomic Energy Commission (Reference 105). The results of the investigation concluded that movement occurred along the shear zone approximately 200 million years ago, and that movement has not occurred since, or at least not within the last one million years, given the relatively undisturbed thickness of residual soil that overlies the shear zone. The results of the investigation also concluded that the shear zone is of limited extent, and while it was traced through the existing units foundation area, no evidence of movement was observed along this section of the shear zone.

The U.S. Atomic Energy Commission, following a review of the results of the above mentioned investigation, concluded that the shear zone at the site is not “capable”, within the meaning of Section III(g) of 10 CFR 100, Appendix A (Reference 108).

d. Prior Earthquake Effects

There is no physical evidence of any fissuring, liquefaction, landsliding, lurching, or caving of banks to indicate that past earthquake ground shaking has disturbed either the surficial sediments or bedrock beneath the ESP site. Given the relatively low intensity of historic ground shaking at the site, it is not expected that these types of features would have formed during the historical period. Given the lack of seismically-induced features in the geologic record, there is no evidence of any prior earthquake effects at the site.

The maximum earthquake intensity the site has experienced historically is MMI V. The site experienced this level of shaking in both the 1897 Giles County and 1875 Goochland County earthquakes, the two largest earthquakes to occur in the State of Virginia. The m_b 5.8 Giles County earthquake occurred on May 31, 1897 and produced MMI VII-VIII shaking in the epicentral area of Pearisburg in southwestern Virginia. Isoseismal maps of this event show that the ESP site experienced MMI V (Reference 58). The earlier m_b 5.0 event centered in Goochland County occurred on December 23, 1875 and is the largest earthquake to occur in the Central Virginia seismic zone. The maximum intensity estimated for this event is MMI VII in the epicentral region (Reference 80). The ESP site is located within the Central Virginia seismic zone, which is an area of persistent, low-level seismicity in the Piedmont Province (as discussed in Section 2.5.1.1.4).

e. Effects of Human Activities

Mineral Extraction

Massive sulfide and gold deposits have been mined from meta-sedimentary and meta-volcanic rocks of the Chopawamsic belt in the vicinity of the ESP site from the 1700s to 1974. The deposits have been mined predominantly in and around the town of Mineral, approximately 7 miles west of the site. Deposits within a 5-mile radius of the site have been designated the Allah Cooper, Sulfur, Cofer, and Old Dominion. The Allah Cooper deposit is about 3 miles northwest of the site, while the Sulfur, Cofer and Old Dominion deposits are

approximately 5 miles southwest of the site (Reference 110) (Reference 111) (Reference 112) (Reference 113).

Based on published documentation of these mining activities and their proximity to the site, the ESP site has not been affected, nor would it be affected, by these mining activities.

Groundwater Withdrawal

Regional groundwater (discussed in Section 2.4.12) withdrawal from the surficial sediments and bedrock around the ESP site is not an issue due to the low withdrawal quantities and limited areal extent of the withdrawals. Withdrawals at the site have included temporary dewatering for foundation construction of the existing units and abandoned Units 3 and 4. No adverse affects from this dewatering are reported to have occurred. Current site groundwater withdrawal is generally limited to water supply wells for plant drinking and process water purposes. No adverse affects as a result of these water supply withdrawals have been documented.

f. Construction Groundwater Control

Groundwater at the ESP site generally occurs at depths ranging from about 6 to 58 feet below the present day ground surface. The exception to this is the area of the abandoned Unit 3 and 4 excavation, which was partially backfilled and where groundwater is within about 2 feet of the ground surface. Groundwater levels at the site would likely result in the need for temporary dewatering of foundation excavations extending below the water table. Dewatering would be performed in a manner that would minimize drawdown effects on the surrounding environment. Drawdown effects would be expected to be limited to the ESP site and no offsite users would be anticipated to be affected.

g. Unforeseen Geologic Features

Future excavations for safety-related structures would be geologically mapped. Unforeseen geologic features that are encountered would be evaluated. The NRC would be notified when any excavations for safety-related structures are open for their examination and evaluation.

2.5.1.2.7 Site Groundwater Conditions

Groundwater is present in unconfined conditions in both the surficial sediments and underlying bedrock at the ESP site. Between December 2002 and June 2003, nine observation wells installed at the site as part of the subsurface investigation program have exhibited groundwater level elevations ranging from about Elevation 241 to Elevation 311. Hydraulic conductivity values for the saprolite in which eight of the wells were screened, based on the results of slug tests in the wells, range from about 0.2 to 3.4 ft/day. The hydraulic conductivity of the shallow bedrock in which one of the wells was screened is estimated to be about 2 to 3 ft/day. Groundwater movement at the site is generally to the north and east, toward Lake Anna.

A detailed discussion of the site groundwater conditions is provided in Section 2.4.12.

2.5.2 Vibratory Ground Motion

The purpose of Section 2.5.2 is to determine ground motions at the ESP site from possible earthquakes that might occur in the NAPS site region and beyond. The information provided in this section complies with NUREG-0800, Section 2.5.2, Revision 3 (Reference 114). The procedure described in RG 1.165 (Reference 2) has been used with certain exceptions as discussed below, and has its basis in the seismic hazard calculations published by the Electric Power Research Institute (EPRI) (Reference 115). As recommended in the RG, the following general steps were followed:

- Review and update EPRI seismic source models
- Review and update EPRI ground motion models
- Perform sensitivity studies or updated probabilistic seismic hazard analyses to determine whether any new seismic source or ground motion models significantly increase the published EPRI results
- Derive safe shutdown earthquake (SSE) ground motions from the original or updated seismic hazard results

Section 2.5.2.1 through Section 2.5.2.4 document the review and update of the available EPRI seismic source and ground motion models. Section 2.5.2.5 summarizes basic information about the seismic wave transmission characteristics of the ESP site with reference to more detailed discussion of all engineering aspects of the shallow subsurface in Section 2.5.4.

Section 2.5.2.6 describes development of the SSE ground motion for the ESP site. This development begins with implementation of the provisions of RG 1.165, specifically Regulatory Position 2 and Appendix E. As discussed in Section 2.5.2.6.5, the combined effect of new seismic source/seismicity information is small, leading to an increase of only several percent in the longer period (1 Hz) 10^{-5} median seismic hazard at the ESP site and no significant increase in the higher-frequency (10 Hz) motion. The effect of the new EPRI recommended ground motion models (Reference 116) is complex, depending on interplay between details of both the median ground motion relations and their aleatory uncertainties, and the impact varies for different ground motion spectral frequencies and specified seismic hazard levels. At the highest-frequency (10 Hz) ground motion and seismic hazard level (10^{-5} median seismic hazard) specified under RG 1.165 guidance, increased aleatory uncertainty in the new EPRI-recommended ground motion models results in spectral accelerations over 55 percent higher than the previous EPRI model. Therefore, the change in ground motion models would likely result in significant changes in hazard predictions for the selected plant sites used to estimate the reference probability as shown in RG 1.165, Table B.1. If general revisions to PSHA methods or data bases result in significant changes in hazard predictions for the selected plant sites in Table B.1 of RG 1.165, Appendix B, the RG provides the methodology that should be used to determine a revised reference probability. The procedure specified in RG 1.165, Appendix B to establish a reference probability requires a three-step

calculation of the seismic hazard results for the 29 sites of Table B.1. First, the seismic hazard must be determined at each site for spectral responses at 5 and 10 Hz. Second, the composite annual probability of exceeding each site's licensing-basis SSE must be determined for spectral responses at 5 and 10 Hz using median hazard estimates. Finally, a reference probability is determined by finding the median of the distribution of probabilities for the 29 plants in Table B.1. Any revised calculation of the reference probability, therefore, would require a new seismic analysis for the remaining 28 sites of Table B.1.

As an alternative to performance of a complete new 29-site reference probability analysis, the ESP site seismic hazard analysis was performed with a methodology adopted from three recent studies that recommend seismic design levels for nuclear facilities in the United States. These studies are DOE 1020 (Reference 117), a draft ASCE standard (Reference 118), and NUREG/CR-6728 (Reference 119). This approach develops a "performance-based-spectrum" that has a mean annual frequency of 10^{-5} of unacceptable performance of nuclear structures, systems, and components as a result of seismically initiated events. The performance-based spectrum is achieved by starting from a ground motion spectrum with a mean 10^{-4} annual frequency of exceedance, and modifying this spectrum by a scale factor that is based on the slope of the mean seismic hazard curve between 10^{-4} and 10^{-5} . Although based on a different statistic (10^{-4} mean rather than the 10^{-5} median ground motion of RG 1.165), the same source and ground motion models may be used in both cases and only seismic hazard curves at the ESP site need be used to develop the SSE.

Section 2.5.2.6 documents the calculations and derivation of the selected SSE ground motions for the ESP site using this alternative approach. Definition of the OBE, as a simple multiple of the SSE, is given in Section 2.5.2.7.

2.5.2.1 Seismicity

The seismic hazard analysis conducted by EPRI (Reference 115) relied on an analysis of historical seismicity in the Central and Eastern United States (CEUS) to estimate seismicity parameters (rates of activity and Richter b-values) for individual seismic sources. The historical earthquake catalog used in the EPRI analysis was complete through 1984. To evaluate the potential significance of any re-interpretation of past earthquakes of more recent seismicity, the EPRI earthquake catalog was reviewed and updated for the ESP site region for the time period from 1985 through 2001.

2.5.2.1.1 Regional Seismicity Catalog Used for 1989 EPRI Study

Many seismic networks record earthquakes in the CEUS. A large effort was made during the EPRI study to combine available data on historical earthquakes, and to develop a homogeneous earthquake catalog that contained all recorded earthquakes for the region. "Homogeneous" means that estimates of body-wave magnitude m_b for all earthquakes are consistent, that duplicate earthquakes have been eliminated, that non-earthquakes (e.g., mine blasts and sonic booms) have

been eliminated, and that significant events in the historical record have not been missed. Thus, the EPRI catalog forms a strong basis on which to estimate seismicity parameters.

2.5.2.1.2 Updated Seismicity Data

The EPRI catalog includes earthquakes in the CEUS through 1984. To extend the catalog, several more recent sources of data were examined. The region within 200 miles of the ESP site was used to guide the selection of catalogs and events, to concentrate on the area that has the most significance to seismic hazard at the ESP site. This region is bounded by the latitude-longitude window 35° – 41° N and 74° – 82° W. Regarding magnitude scales for this region, a variety of body-wave magnitudes or their equivalents have been used in the CEUS, including m_b , m_{bLg} , m_N , and m_{Lg} . For the purpose of this section, these magnitudes are considered equal.

The most complete regional catalog for recent times is considered to be that published by the Virginia Polytechnic Institute and State University (VT) and maintained by Martin Chapman of VT. This catalog is available through 2001 for the states of Virginia, Maryland, Delaware (south of 40° N), West Virginia (south of 40° N), North Carolina, South Carolina, Georgia, Florida, Alabama, Tennessee (east of 88° W), and Kentucky (east of 88° W). This catalog is considered the authoritative catalog for the southeastern US by the Advanced National Seismic System (ANSS) website (quake.geo.berkeley.edu/anss). It is considered complete since 1985 down to $m_b = 3.0$ for the states surrounding the ESP site.

North of the southern border of Pennsylvania (approximately 39.7° N) the VT catalog is not complete. To supplement the catalog of earthquakes within 200 miles of the site but north of 39.7° N, the catalog from ANSS was used. This catalog is considered complete through May 15, 2003 for $m_b \geq 3$.

The VT catalog and the ANSS catalog were merged, using the VT catalog for latitudes below 39.7° N and using the ANSS catalog for latitudes of 39.7° N and higher, and retaining only earthquakes with $m_b \geq 3.0$. This gave 97 earthquakes from the VT catalog (1985 through 2001) and 45 earthquakes from the ANSS catalog (1985 through May 15, 2003), 8 of which occurred in 2002 and 2003. Most of the VT catalog events had m_b magnitude values assigned instrumentally, with coda and intensity-based magnitudes also assigned in some cases. (One earthquake from the VT catalog north of 39.7° N with coda magnitude = 3.0 was retained because it was not included in the ANSS catalog). For conservatism the largest of the magnitude assignments was used in later analysis. Some of the ANSS catalog events (north of 39.7° N) indicated ML (local magnitude), **M** (moment magnitude), or unknown magnitude values. These were taken to be equivalent to m_{Lg} . This approximation for these low-magnitude earthquakes was considered acceptable because the region where the ANSS catalog was used (north of 39.7° N) does not include the Central Virginia seismic zone, the dominant source of seismic hazard at the ESP site, as discussed in Section 2.5.2.6.1. Further, only 6 ANSS earthquakes occurred within 200 miles of the ESP site, i.e., at latitudes less than 41° N.

The result of the above process was a catalog of 30 earthquakes (24 from the VT catalog, 1985 through 2001, and 6 from the ANSS catalog, 1985 through May 15, 2003) within the region bounded by 35°–41°N and 74°–82°W, again, which defines a region including everything within 200 miles of the ESP site. These earthquakes are listed in Table 2.5-4.

For the purpose of mapping updated regional seismicity along with the EPRI 1989 (Reference 115) seismic source model beyond 200 miles of the ESP site—specifically, outside the area bounded by 35°–41°N and 74°–82°W—the ANSS catalog alone was used to supplement the seismicity catalog update discussed above for events from 1985 onward, retaining the EPRI catalog for events through 1984. As with the update of the seismicity within 200 miles of the ESP site, the largest of the magnitude assignments in the ANSS catalog was used.

2.5.2.2 Geologic Structures and EPRI Seismic Source Model for the Site Region

As described in Section 2.5.1, a comprehensive review of available geological, seismological, and geophysical data has been performed for the ESP site region and adjoining areas. The following sections summarize in some detail seismic source interpretations from the 1989 EPRI study and the interpretations of new sources based on more recent data.

Based on evaluation of this information, no new information was found that would suggest potentially significant modifications to the EPRI seismic source model with the following three exceptions:

- The East Coast Fault System (ECFS) represents a new postulated seismic source along the Atlantic Seaboard, as described in Section 2.5.1. The northern segment comes within 70 miles of the ESP site.
- The average recurrence interval for large magnitude earthquakes in the Charleston seismic source zone currently is believed to be 550 years based on paleoliquefaction data, rather than several thousand years based on seismicity used in the EPRI seismic source model, and the Charleston source geometry has been modified to include the possibility that the Charleston earthquake occurred on the southern segment of the ECFS.
- The average recurrence interval for large magnitude earthquakes in the New Madrid seismic zone currently is believed to be 500 years based on paleoliquefaction data, rather than several thousand years based on seismicity used in the EPRI seismic source model.

Sensitivity analyses were performed to evaluate the potential significance of the ECFS and of the new reference model for a characteristic Charleston-type earthquake to seismic hazard at the ESP site, as described in Section 2.5.2.6.3. Based on the results of these analyses it is shown that the effect of the current model for recurrence of large New Madrid-type earthquakes is not significant.

2.5.2.2.1 Summary of EPRI Seismic Sources

This section summarizes the seismic sources and parameters used in the 1989 EPRI project (Reference 115). The description of seismic sources is limited to those sources within 200 miles of the ESP site (the “site region”) and those at distances greater than 200 miles that may impact the hazard at the ESP site.

In the EPRI project, six independent Earth Science Teams (ESTs) evaluated geologic, geophysical, and seismological data to develop seismic sources in the CEUS. These sources were used to model the occurrence of future earthquakes and evaluate earthquake hazards at nuclear power plant sites across the CEUS. The six ESTs involved in the EPRI project were the Bechtel Group, Dames & Moore, Law Engineering, Rondout Associates, Weston Geophysical Corporation, and Woodward-Clyde Consultants. Each team produced a report (Volumes 5 through 10 of Reference 120) providing detailed descriptions of how they identified and defined seismic sources. The results were implemented into a probabilistic seismic hazard analysis (PSHA) reported in Reference 115. For the computation of hazard in the 1989 study, a few of the seismic source parameters were modified or simplified from the original parameters determined by the six ESTs. The parameters used in final PSHA calculations are summarized in Reference 121, which is the primary source for the seismicity parameters used in this study. Each of the six ESTs provided more detailed descriptions of the philosophy and methodology used in evaluating tectonic features and establishing the seismic sources (refer to Volumes 5 through 10 of Reference 120).

The seismic source models developed for each of the six EPRI teams are shown on Figure 2.5-19 through Figure 2.5-24. Within each figure, the sources that contributed 99 percent of the North Anna site hazard are shown in color and are labeled. For the 1989 EPRI seismic hazard calculations, a screening criterion was implemented so that all sources whose combined hazard was less than 1 percent of the total hazard were excluded from the analysis (Reference 115, Section 2). Earthquakes with body-wave magnitude $m_b \geq 3.0$ are also shown on Figure 2.5-19 through Figure 2.5-24 to show the spatial relationship between seismicity and seismic sources. Earthquake epicenters include events from the EPRI earthquake catalog for the period between 1627 and 1984, updated with seismicity in the CEUS for the period between 1985 and 2001 as described in Section 2.5.2.1.2.

The maximum magnitude, closest distance, and probability of activity of each team’s seismic sources are summarized in Table 2.5-5 through Table 2.5-10. These tables present the parameters assigned to each source and specify whether or not the source contributed to 99 percent of the site hazard in the original EPRI seismic hazard analyses. The tables also indicate whether new information has been identified that would lead to a revision of the source’s geometry, maximum earthquake magnitude, or recurrence parameters. The seismicity recurrence parameters (a- and b-values) used in the EPRI seismic hazard study were computed for each 1-degree latitude and longitude cell that intersects any portion of a seismic source.

The nomenclature used by each team to describe the various seismic sources in the CEUS varies from team to team. That is, a number of different names may have been used by the EPRI teams to describe the same or similar tectonic features or sources, or one team may describe seismic sources that another team does not. For example, the Woodward-Clyde team identified their source that covers the seismicity of central Virginia as the “State Farm Complex” source, whereas most of the other teams named their source as the Central Virginia seismic zone. Each team’s source names, data, and rationale are included in their team-specific documentation (Volumes 5 through 10 of Reference 120).

The EPRI seismic hazard study expressed maximum magnitude (M_{max}) values in terms of body-wave magnitude (m_b), whereas most modern seismic hazard analyses describe M_{max} in terms of moment magnitude (M). To provide a consistent comparison between magnitude scales, the current study uses an average of three individual magnitude conversion relations (Reference 122) (Reference 123) (Reference 124) to convert m_b to M and vice-versa. Throughout this section, the largest assigned values of M_{max} distributions assigned by the ESTs to seismic sources are presented for both magnitude scales, to give perspective on the maximum earthquakes that were considered possible in each source. For example, EPRI m_b values of M_{max} are followed by the equivalent M value.

The following sections describe the most significant EPRI sources for each of the six ESTs, with respect to the ESP site. For each team, the listed sources contributed to 99 percent of the total seismic hazard for that team at the ESP site. The assessment of these and other EPRI sources within the site region has found that the EPRI source parameters (maximum magnitude, geometry, recurrence) are sufficient to capture the current understanding of the seismic hazard in the site region.

Except for the three specific cases described earlier, no new seismological, geological, or geophysical information in the literature published since the publication of the 1986 EPRI source model (Reference 120) suggests that these sources should be modified. The three cases where new information requires modification of the EPRI source characterizations is the addition of the northern segment of the East Coast Fault System (ECFS-N) as a new potential seismic source, the new recurrence and geometry parameters for the existing Charleston source (modeled after the southern segment of the East Coast Fault System (ECFS-S)), and the new recurrence parameters for the New Madrid source. These cases are discussed in Section 2.5.2.6.3, and sensitivity analyses are performed for the new ECFS and the modified Charleston source in Section 2.5.2.6.5.

2.5.2.2.2 Sources Used for EPRI PSHA – Bechtel Group

Bechtel Group identified and characterized four seismic sources that contributed to 99 percent of the hazard at the ESP site. All four of these sources are within the site region and are the:

- Central Virginia (E)
- Southern Appalachians Region (BZ5)

- Bristol Block (24)
- Atlantic Coastal Region (BZ4)

Also identified within the site region were seven other seismic sources that did not contribute to 99 percent of the hazard at the site. These sources included the:

- Stafford Fault
- Eastern Mesozoic Basins
- New York-Alabama Lineament
- Lebanon Trend
- Giles County
- SE Craton Region
- SE Appalachians

Seismic sources identified by the Bechtel Group team within the site region are listed in Table 2.5-5. A map showing the locations and geometries of the Bechtel seismic sources is provided in Figure 2.5-19. Seismic sources identified by the Bechtel Group that contribute most to the site hazard are the Central Virginia Seismic Zone and Southern Appalachians Region sources. Following is a brief discussion of each of the seismic sources that contributed to 99 percent of the site hazard.

a. **Central Virginia (E)**

The ESP site is located within the Central Virginia seismic zone (E) approximately 15 miles south of its northern boundary. The source was defined exclusively on the basis of seismicity in the central Virginia region. No tectonic features were identified within the source. The largest maximum earthquake magnitude (M_{max}) that the Bechtel Group assigned to this zone was body-wave magnitude (m_b) 6.6 (**M 6.5**).

b. **Southern Appalachians Region (BZ5)**

The ESP site is located within the Southern Appalachians Region background source (BZ5). It is a large background source that extends from New York to Georgia and encompasses a majority of the site region. The largest M_{max} assigned by the Bechtel Group to this zone was m_b 6.6 (**M 6.5**).

c. **Bristol Trends (24)**

The Bristol Trends source (24) is about 38 miles northwest of the ESP site. This source was defined based on series of magnetic and gravity lows bordered on the west by the New York-Alabama lineament and on the east by the Clingman lineament. The largest M_{max} assigned by the Bechtel Group to this zone was m_b 6.6 (**M 6.5**).

d. Atlantic Coastal Region (BZ4)

The Atlantic Coastal Region background source (BZ4) is located about 90 miles southeast and east of the ESP site. This source is a large background zone that extends from offshore New England to Georgia and encompasses the easternmost portion of the site region. The largest M_{\max} assigned by the Bechtel Group to this zone was m_b 7.4 (**M 7.9**).

2.5.2.2.3 Sources Used for EPRI PSHA – Dames & Moore

Dames & Moore identified and characterized 7 seismic sources that contributed to 99 percent of the hazard at the ESP site. All 7 of these sources are within the site region and include:

- Central Virginia Seismic Zone (40)
- Southern Cratonic Margin (41)
- Southern Appalachian Mobile Belt (53)
- Newark-Gettysburg Basin (42)
- Connecticut Basin (47)
- Appalachian Fold Belts (4)
- Kink in Fold Belt (4B)

Also identified within the site region were 12 other seismic sources that did not contribute to 99 percent of the hazard. These less significant sources include the Stafford Fault Zone, Hopewell Fault Zone, several Triassic basins, and two combination zones.

Seismic sources identified by Dames & Moore within the site region are listed in Table 2.5-6. A map showing the locations and geometries of these seismic sources is provided in Figure 2.5-20. The seismic source identified by Dames & Moore that contributes the most to the North Anna site hazard is the Central Virginia seismic zone. Following is a discussion of each of the seismic sources that contribute to 99 percent of the hazard at the ESP site.

a. Central Virginia (40)

The Central Virginia seismic zone (40) is about 15 miles south of the ESP site. This source was defined based on the pattern of clustered seismicity in the central Virginia area. No known tectonic features were associated with this seismic activity. The largest M_{\max} assigned by the Dames & Moore team to this zone was m_b 7.2 (**M 7.5**).

b. Southern Cratonic Margin (41)

The ESP site is located within the Southern Cratonic Margin default zone (41), a large background source. This large default zone is located between the Appalachian Fold Belt (4) and the Southern Appalachian Mobile Belt (53) and includes the region of continental margin deformed during Mesozoic rifting. Located within this default zone are many Triassic basins

and border faults. The largest M_{\max} assigned by the Dames & Moore team to this zone was m_b 7.2 (**M 7.5**).

c. **Southern Appalachians Mobile Belt (53)**

The Southern Appalachians Mobile Belt default zone (53) is about four miles east of the ESP site. This default source comprises crustal rocks that have undergone several periods of divergence and convergence. The source is bounded on the east by the East Coast magnetic anomaly and on the west by the westernmost boundary of the Appalachian gravity gradient. The largest M_{\max} assigned by the Dames & Moore team to this zone was m_b 7.2 (**M 7.5**).

d. **Newark-Gettysburg Basin (42)**

The Newark-Gettysburg Basin source (42) is about 20 miles northwest of the ESP site. This source incorporates the Newark, Gettysburg, and Culpeper Triassic basins that formed during Mesozoic rifting. The largest M_{\max} assigned by the Dames & Moore team to this zone was m_b 7.2 (**M 7.5**).

e. **Connecticut Basin (47)**

The Connecticut Basin (47) source is about 25 miles east of the ESP site. Similar to the Newark-Gettysburg Basin (42), this source was defined based on the presence of a Triassic basin and the assumption that the bounding Mesozoic rift structures could be reactivated. The largest earthquake maximum magnitude value assigned by the Dames & Moore team to this zone was m_b 7.2 (**M 7.5**).

f. **Appalachian Fold Belts (4)**

The Appalachian Fold Belts source (4) is about 46 miles west of the ESP site. This source extends from New York to Alabama and consists of the Appalachian folded mountain belt of Paleozoic age. The largest M_{\max} assigned by the Dames & Moore team to this zone was m_b 7.2 (**M 7.5**).

g. **Kink in Fold Belt (4B)**

The Kink in Fold Belt source (4B) is about 90 miles west of the ESP site. Kinks in Paleozoic fold belts were defined based on bends of the fold belts and areas of greater seismicity. Kink (4B) includes the zone of seismicity in the Giles County area and was thought to contain the arm of a failed rift. The largest M_{\max} assigned by the Dames & Moore team to this zone was m_b 7.2 (**M 7.5**).

2.5.2.2.4 Sources Used for EPRI PSHA – Law Engineering

Law Engineering identified and characterized 14 seismic sources that contributed to 99 percent of the hazard at the ESP site. These sources include:

- Eastern Basement (17)
- seven individual mafic plutons (M19, M20, M21, M22, M23, M24, M27)

- Eastern Basement Background (217)
- Eastern Piedmont (107)
- Reactivated Eastern Seaboard Normal (22)
- Mesozoic Basins (C09)
- two combination sources (C10 and C11)

Law Engineering also identified 15 other seismic sources within the site region that did not contribute to 99 percent of the hazard. The majority of these 15 are mafic pluton seismic sources.

Seismic sources identified by Law Engineering within the site region are listed in Table 2.5-7. A map showing the locations and geometries of the Law Engineering seismic sources is provided in Figure 2.5-21. Seismic sources identified by the Law Engineering team that contribute most to the North Anna site hazard are the Eastern Basement (17) and local mafic pluton source (M22). Following is a brief discussion of each of the seismic sources that contributed to 99 percent of the site hazard.

a. **Eastern Basement (17)**

The ESP site is located within the Eastern Basement source (17) approximately 5 miles from its eastern boundary. This source was defined as an area containing pre-Cambrian and Cambrian normal faults, developed during the opening of the Iapetus Ocean, in the basement rocks beneath the Appalachian decollement. The Giles County and eastern Tennessee zones of seismicity are included in this source. The largest M_{max} assigned by the Law Engineering team to this zone was m_b 6.8 (**M 6.8**).

b. **Mafic Plutons (M19, M20, M21, M22, M23, M24, M27)**

The seven most significant mafic pluton sources (M19, M20, M21, M22, M23, M24, M27) are located between 23 and 159 miles from the ESP site. Mafic pluton M22 is located 23 miles west of the site and represents one of the two most significant sources to the site. Law Engineering considered pre- and post-metamorphic plutons in the Appalachians to be stress concentrators, and therefore, earthquake sources. Law Engineering did not define a seismic source in central Virginia, but the plutons, of small areal extent, capture a majority of the seismicity of central Virginia, due to the method in which 70 percent of the seismicity from the surrounding 1 degree square area (111 km x 111 km) was assigned to each pluton. A single M_{max} of m_b 6.8 (**M 6.8**) was assigned by the Law Engineering team to all mafic pluton sources.

c. **Eastern Basement Background (217)**

The ESP site is located within the Eastern Basement Background source (217) approximately five miles west of its eastern boundary. This source was characterized as a seismotectonic region having a negative Bouguer gravity field (Appalachian gravity low) and a pattern of long wavelength magnetic anomalies. The western boundary is the New York-Alabama lineament

and the eastern boundary is the Appalachian gravity gradient. The largest M_{\max} assigned by the Law Engineering team to this zone was m_b 5.7 (**M 5.3**).

d. **Eastern Piedmont (107)**

The Eastern Piedmont (107) is about four miles east of the ESP site. This source was characterized as a seismotectonic region having a positive Bouger gravity field and a pattern of short wavelength magnetic anomalies. Law Engineering interpreted this source to represent a crustal block underlain by mafic or transitional crust east of the relict North American continental margin. The largest M_{\max} assigned by the Law Engineering team to this zone was m_b 5.7 (**M 5.3**).

e. **Reactivated Eastern Seaboard Normal (22)**

The Reactivated Eastern Seaboard Normal (22) source is about four miles east of the ESP site. This source was characterized as a region along the eastern seaboard in which Mesozoic normal faults are reactivated as high-angle reverse faults. A single M_{\max} of m_b 6.8 (**M 6.8**) was assigned by the Law Engineering team to this zone.

f. **Mesozoic Basins (C09)**

The Mesozoic basins (C09) source includes eight bridged basins, the closest of which is about 18 miles from the ESP site. This source was defined based on northeast-trending, sediment-filled troughs in basement rock bounded by normal faults. The largest M_{\max} assigned by the Law Engineering team to this zone was m_b 7.4 (**M 7.9**).

g. **Combination sources (GC11, C10)**

The two combination sources (C10 and C11) represent Mesozoic Basins excluding the Charleston region, and the Reactivated Eastern Seaboard zone excluding the Charleston region. The largest M_{\max} assigned by the Law Engineering team to both combination sources was m_b 6.8 (**M 6.8**).

2.5.2.2.5 Sources Used for EPRI PSHA – Rondout Associates

Rondout identified and characterized three seismic sources that contributed to 99 percent of the hazard at the ESP site. All three sources are within the site region and include:

- Central Virginia (29)
- Giles County (30)
- Shenandoah (28)

Rondout also identified eight other seismic sources within the site region that did not contribute to 99 percent of the hazard at the site. These sources include:

- Quakers
- Norfolk Fracture Zone

- Appalachian
- Grenville
- Four combination zones

Seismic sources identified by Rondout within the site region are listed in Table 2.5-8. A map showing the locations and geometries of the Rondout seismic sources is shown in Figure 2.5-22. The seismic source identified by Rondout that contributes the most to the ESP site hazard is the Central Virginia seismic zone. Following is a discussion of each of the seismic sources that contribute to 99 percent of the hazard at the North Anna site.

a. **Central Virginia (29)**

The ESP site is on the northern boundary of the Rondout's Central Virginia source. This source was defined based on seismicity and the possible intersection of the extension of the Norfolk fault zone and the northeast-trending linear zone defined by aeromagnetic, gravity, and volcanic-plutonic rocks. The largest M_{\max} assigned by Rondout to this source was m_b 7.0 (**M 7.2**).

b. **Shenandoah (30)**

The ESP site is on the southern boundary of the Shenandoah source. The site lies essentially on the border of the adjacent Shenandoah and central Virginia sources (Figure 2.5-22). This Shenandoah source was defined based on geophysical and geologic features. The source includes the intersection of the Pittsburg-Washington lineament and the strong gravity gradient associated with the edge of the ancient Paleozoic craton. It also includes both the post-Cretaceous Brandywine and Stafford fault zones. Rondout assigned an M_{\max} of m_b 6.5 (**M 6.3**) to this source.

c. **Giles County (28)**

The Giles County source (28) is located about 117 miles west of the ESP site. This source was defined based on historical seismicity, most notably the 1897 m_b 5.8 Giles County earthquake. The largest M_{\max} assigned by Rondout to this source was m_b 7.0 (**M 7.2**).

2.5.2.2.6 Sources Used for EPRI PSHA – Weston Geophysical

Weston Geophysical identified and characterized seven seismic sources that contributed to 99 percent of the hazard at the ESP site. All seven of these sources are within the site region and include:

- Central Virginia Seismic Zone (22)
- Six combination zones (C21, C22, C34, C35, C23, C19)

Weston also identified 30 seismic sources within the site region that did not contribute to 99 percent of the hazard at the site. The majority of these sources are combination zones.

Seismic sources identified by Weston within the site region are listed in Table 2.5-9. A map showing the locations and geometries of the Weston seismic sources is provided in Figure 2.5-24. The seismic source identified by Weston that contributes the most to the site hazard is the Central Virginia Seismic Zone. Following is a discussion of each of the seismic sources that contribute to 99 percent of the hazard at the site.

a. **Central Virginia Seismic Zone (22)**

The ESP site is located within the Central Virginia Seismic Zone (22) about 10 miles south of the northern boundary. This source is defined based on a northwest trending alignment of seismicity that extends from Richmond to Waynesboro, Virginia. The largest M_{\max} value assigned by Weston to this zone was m_b 6.6 (**M 6.5**).

b. **Source Combinations (C21, C19, C22, C23, C34, C35)**

The ESP site is located within four different combination sources (C21, C22, C34, C35) defined by the Weston team. Two additional combination sources, C23 and C19, are located 10 and 27 miles from the site. Five of the combination sources represent the combination of different seismic sources within a large South Coastal Plain Background zone (104). The other sources within this background zone include the Central Virginia seismic zone (22), the Charleston seismic zone (25), the South Carolina seismic zone (26), and Mesozoic basins (28B, C, D, and E). The largest M_{\max} assigned by the Weston team to each of these six combination sources was m_b 6.6 (**M 6.5**).

2.5.2.2.7 **Sources Used for EPRI PSHA – Woodward-Clyde Consultants**

Woodward-Clyde identified and characterized five seismic sources that contributed to 99 percent of the hazard at the ESP site. Three of these sources are within the site region and are:

- State Farm Complex (27)
- Central Virginia Gravity Saddle (26)
- North Anna Background (B22)

The two seismic sources outside the site region are the South Carolina Gravity Saddle (29) and South Carolina Gravity Saddle No. 2 (29A).

Woodward-Clyde also identified eight seismic sources within the site region that did not contribute to 99 percent of the hazard at the site. These sources include:

- Richmond Basin
- Newark Basin
- Tyrone-Mt. Union Lineament
- Pittsburg-Washington Lineament
- New Jersey Isostatic Gravity Saddle

- Three combination zones

Seismic sources identified by Woodward-Clyde within the site region are listed in Table 2.5-10. A map showing the locations and geometries of the Woodward-Clyde seismic sources is provided in Figure 2.5-23. Seismic sources identified by the Woodward-Clyde team that contribute most to the ESP site hazard are the Central Virginia Gravity Saddle, State Farm Complex, and the North Anna Background zones. Following is a brief discussion of each of the seismic sources that contributed to 99 percent of the site hazard.

a. **State Farm Complex (27)**

The State Farm Complex source is about 3 miles south of the ESP site. This source was defined based on pre-Cambrian gneissic terrain located in central Virginia and bounded on the east by the Richmond Basin and on the west by Goochland fault. There is a strong concentration of seismicity on either side of the feature, which is centered in the Central Virginia seismic zone. The largest M_{\max} assigned by Woodward-Clyde to this source was m_b 6.9 (**M 7.0**).

b. **Central Virginia Gravity Saddle (26)**

The Central Virginia Gravity Saddle source is about 3 miles southwest of the ESP site. This source was defined based on a saddle in the northeast-trending gravity high associated with the Appalachians. Central Virginia seismicity is located along the south and southwest of the gravity saddle. This source is an alternative interpretation of the seismicity in the central Virginia area. The largest M_{\max} assigned by Woodward-Clyde to this zone was m_b 7.0 (**M 7.2**).

c. **North Anna Background (B22)**

The ESP site is located within the Woodward-Clyde North Anna Background source, a large rectangular background source that is centered on the site. The largest M_{\max} assigned by Woodward-Clyde to this zone was m_b 6.6 (**M 6.5**).

d. **South Carolina Gravity Saddle (29 and 29A)**

The South Carolina Gravity Saddle (29) and the South Carolina Gravity Saddle No. 2 (29A) are about 259 and 264 miles from the site, respectively. The largest M_{\max} assigned to both of these sources was m_b 7.4 (**M 7.9**).

2.5.2.2.8 **Characterization of the Central Virginia Seismic Zone**

In the 1989 EPRI seismic hazard study (Reference 115), the Central Virginia seismic zone represented the most significant seismic source for the North Anna site (see Section 2.5.2.6.1 below). The EPRI study was designed to elicit multiple expert opinions in an effort to capture the epistemic uncertainty related to lack of knowledge regarding seismic sources in the CEUS. The six ESTs characterized the Central Virginia seismic zone differently, as shown on Figure 2.5-25 and listed in Table 2.5-11. In spite of these different interpretations, the central portion of each source represents the densest cluster of earthquake activity in the region. The largest M_{\max} for these

different characterizations of the Central Virginia seismic zone range from m_b 6.6 to 7.2 (**M** 6.5 to 7.5), as listed in Table 2.5-11.

All ESTs, with the exception of Law Engineering, identified a source representing the Central Virginia seismic zone. Law Engineering instead identified multiple mafic plutons in the region. The seismicity parameters for these mafic plutons were calculated from a large region surrounding each pluton, which effectively captures the majority of seismicity in central Virginia. The mafic plutons, therefore, indirectly represent a local seismic source for Law Engineering (see Reference 120, Volume 7).

Since the EPRI study, two paleoliquefaction features have been found within the Central Virginia seismic zone, as described in Section 2.5.1.1.4. These new observations are consistent with the M_{max} values assigned by the EPRI teams. The near-total lack of widespread paleoliquefaction features in the 300 km of stream exposures searched within the Piedmont, has led some researchers (Reference 71) to conclude that it is unlikely that any earthquakes have occurred in central Virginia in excess of **M** ~7.

2.5.2.2.9 Post-EPRI Source Characterization Studies

Since the EPRI seismic hazard project (Reference 115), studies have been performed to characterize seismic sources within the North Anna site region for probabilistic seismic hazard analyses. These studies include:

- Sources and parameters for the Savannah River nuclear site (Reference 125),
- Seismic hazard of Virginia (Reference 126), and
- The USGS's National Seismic Hazard Mapping Project (Reference 123) (Reference 127).

These references are reviewed in the following paragraphs.

Bollinger (Reference 125) specified sources, recurrence rates, focal depths, and maximum magnitudes for earthquake sources in the southeastern United States to be used in probabilistic seismic hazard analyses at the Savannah River nuclear site in South Carolina (Table 2.5-12). Bollinger's approach to seismic zonation in the Eastern United States was based primarily on the historical record of earthquake activity. Maximum magnitudes were derived from a combination of three different estimates based on the 1000-year earthquake, the maximum historical earthquake plus one magnitude unit, and the calculated values from various published relationships between magnitude and fault rupture area. Bollinger identified three seismic sources within the North Anna site region (200-mile radius). These sources were the Central Virginia seismic zone, the Giles County seismic zone, and a complementary background zone (Table 2.5-12).

The Central Virginia seismic zone was defined by Bollinger as a rectangular zone centered on the majority of the seismicity in the central Virginia area. The maximum magnitude earthquake value estimated for this source was m_b 6.4 (Reference 125). For the Giles County and complimentary background zone, M_{max} values of m_b 6.3 and m_b 5.75 were used, respectively. The M_{max} values for

the Central Virginia, Giles County, and complementary background sources in the Bollinger (Reference 125) study are lower than the largest M_{max} values assigned by most of the EPRI teams.

In 1994, a seismic hazard assessment of Virginia was performed to examine the seismic hazard within Virginia on a county-by-county basis (Reference 126). Seismic sources and earthquake frequency-magnitude recurrence relationships were defined using the results of network monitoring by the Seismological Observatory at Virginia Polytechnic Institute and State University and using published geologic and geophysical investigations. The study defined a total of 10 seismic sources (Table 2.5-13). Within the North Anna site region, Chapman and Krimgold (Reference 126) defined seven contiguous, non-overlapping sources based primarily on patterns of seismicity. The two most prominent areas of historical seismicity within the site region were defined as the Central Virginia and Giles County seismic zones. An M_{max} value of **M** 7.53 (converted to m_b 7.25) was assigned to all sources in their model, with the exception of New Madrid. Chapman and Krimgold assumed that a Charleston-size event was capable of occurring in any of the sources within the North Anna site region. Subsequent to the Chapman and Krimgold study, Johnston (Reference 90) reduced his magnitude estimate of the Charleston earthquake to **M** 7.3 from the prior estimate of **M** 7.53 (as cited in (Reference 126)). Using the magnitude conversion described in Section 2.5.2.2.1, **M** = 7.3 converts to m_b =7.1, which is within the range of largest M_{max} values (m_b 6.6 to 7.2) assigned by the EPRI teams to both the Central Virginia and Giles County seismic zones. Thus these later studies are consistent with the interpretations of the EPRI teams.

In 2002, the USGS produced updated seismic hazard maps for the coterminous United States based on new seismological, geophysical, and geological information (Reference 127). The 2002 maps reflect changes to the source model used to construct the previous version of the national seismic hazard maps made in 1996 (Reference 123). The most significant changes to the CEUS portion of the source model included changes in the recurrence and geometry of the Charleston source; and changes in the recurrence, M_{max} , and geometry of the New Madrid sources. Unlike the EPRI models that incorporated many local sources, the USGS source model in the CEUS includes only a small number of sources. The hazard is largely based on historical seismicity and the variation of that seismicity within large background or "maximum magnitude" zones. Within the ESP site region, the USGS model has only defined a single seismic source (the Extended Margin Background zone), which covers nearly the entire eastern and southeastern United States. The USGS assigned a single M_{max} value of **M** 7.5 (m_b 7.2) to this zone (Table 2.5-14). This magnitude exceeds many of the individual EPRI team estimates of M_{max} for sources defined within the area covered by the USGS Extended Margin Background zone. However, because all Dames & Moore sources were assigned M_{max} values up to m_b 7.2 and selected sources from other teams were assigned M_{max} values up to m_b 7.4, the USGS **M** 7.5 (m_b 7.2) magnitude does not represent an inconsistency with the range of values assigned by EPRI teams.

The most significant impact of the 2002 USGS model (Reference 127) on seismic hazard for the ESP site is the updated Charleston source parameters. Modifications of the recurrence and

geometry of the fault were the most significant changes to this South Carolina source. The USGS (Reference 127) also revised estimates of M_{max} . These new estimates of Charleston source parameters have been incorporated into the seismic hazard calculations conducted here for the ESP site, as described in Section 2.5.2.6.3, Section 2.5.2.6.6 and Section 2.5.2.6.7.

2.5.2.3 Correlation of Seismicity with Geologic Structures and EPRI Sources

The final part of the review and update of the 1989 EPRI seismic source model was a correlation of updated seismicity with the 1989 model source. The EPRI seismicity catalog covers earthquakes in the CEUS for the time period from 1627 to 1984. This catalog has been updated for this ESP study for the time period from 1985 to 2001 as described in Section 2.5.2.1. Figure 2.5-19 through Figure 2.5-25 show the distribution of earthquake epicenters from both the EPRI (pre-1985) and updated (post-1984) earthquake catalogs in comparison to the seismic sources identified by each of the ESTs.

Comparison of the updated earthquake catalog to the EPRI earthquake catalog yields the following conclusions:

- The updated catalog does not show any earthquakes within the site region that can be associated with a known geologic structure. As described in Section 2.5.1, the majority of seismicity in the ESP site region appears to be occurring at depth within the basement beneath the Appalachian decollement.
- The updated catalog does not show a unique cluster of seismicity that would suggest a new seismic source outside of the EPRI seismic source model.
- The updated catalog does not show a pattern of seismicity that would require significant revision to the EPRI seismic source geometry.
- The updated catalog does not show or suggest any increase in M_{max} for any of the EPRI seismic sources.
- The updated catalog does not show any increase in seismicity parameters (rate of activity, b value) for any of the EPRI seismic sources (see Section 2.5.2.6.5).

2.5.2.4 1989 EPRI Probabilistic Seismic Hazard Analysis, Deaggregation, and 1 Hz, 2.5 Hz, 5 Hz, and 10 Hz Spectral Velocities

A probabilistic seismic hazard analysis (PSHA) was conducted for the NAPS site during the 1989 EPRI study ((Reference 115). The procedure used by EPRI to calculate the 1989 results is consistent with RG 1.165, Regulatory Position 3. This section reviews and replicates the 1989 EPRI PSHA for the NAPS site. RG 1.165 Regulatory Position 4 and Appendices C and F describe how to use PSHA results to determine the controlling earthquake(s) (defined by a magnitude(s) and distance(s) and the SSE design response spectrum. The procedure uses 1 Hz, 2.5 Hz, 5 Hz, and

10 Hz 10^{-5} median spectral velocity values. The controlling earthquake(s) and spectral velocities for these frequencies are also presented in this section.

The 1989 EPRI study developed seismic source interpretations based on inputs from six ESTs, as described in Section 2.5.2.2. For ground motion estimation, the 1989 EPRI study used three ground motion models, as described below. The 1989 EPRI study used these source interpretations and ground motion models to calculate seismic hazard for peak ground acceleration (PGA) and for 5 spectral frequencies (1, 2.5, 5, 10, and 25 Hz). Results were published for 57 nuclear plant sites in the CEUS (Reference 115) in the form of seismic hazard curves for PGA and uniform hazard spectra.

Three ground motion models were used in the 1989 EPRI PSHA study (see Reference 115, Table 4-1) for peak ground acceleration (PGA) and for spectral response at the five spectral frequencies. These are summarized in Table 2.5-15.

For all models and all frequencies, an aleatory uncertainty (sigma [natural log ground motion]) of 0.5 was used. These ground motion models were used without any correction for soil conditions, because, for purposes of the 1989 EPRI study, the North Anna site was considered a rock site.

For the ESP seismic hazard evaluation, the 1989 EPRI PSHA was reproduced using the 1989 seismic sources and 1989 ground motion models. Risk Engineering Inc.'s proprietary software FRISK88 was used for these calculations. The main results used in this replication were the PGA results (see Table 2.5-16) available for North Anna (see Reference 115, Appendix E, Table 3-61). Seismic hazard curves are available in digital form only for PGA in Reference 115. Selected results were checked for 1 Hz, 2.5 Hz, 5 Hz, and 10 Hz (see Table 2.5-17) based on spectral results for specific exceedance probabilities in Reference 115.

Seismic sources used to represent the seismic hazard for each of the six ESTs that participated in the 1989 EPRI study are listed in Table 2.5-18. These sources were used for the North Anna site in the original 1989 study, as documented in EPRI's computer input files.

The first step consisted of conducting a seismic hazard calculation for PGA for the ESP site. Results of this calculation are compared to the 1989 results in Table 2.5-16.

As listed in Table 2.5-16, the 1989 EPRI results are available only to 2 digits accuracy, which could lead to ± 5 percent apparent difference: $1.049\text{E-}3$ would be represented in 1989 as $1.0\text{E-}3$ and in 2003 as $1.05\text{E-}3$, leading to +5 percent apparent difference. On average over the nine seismic hazards compared, the average difference in annual probability of exceedance was +1.1 percent. The difference in ground motion for a given hazard would be even less, because seismic hazard H is related to ground motion amplitude a by:

$$H = C a^{-K} \qquad \text{Equation 2.5.2-1}$$

(see Equation 3 of Kennedy and Short (1994) (Reference 128)) where C is a constant and K is the slope of the hazard-vs-amplitude curve on log-log scale. From Reference 128, K typically ranges from 3.3 to 1.66. Equation 2.5.2-1 can be rewritten as:

$$a = C^{1/K} H^{-1/K} \qquad \text{Equation 2.5.2-2}$$

With K from 3.3 to 1.66, Equation 2.5.2-2 means that a 1.1 percent change in hazard corresponds to 0.3 percent to 0.7 percent change in ground motion amplitude. This difference is much less than the total uncertainty in seismic hazard and results from differences in numerical integration techniques in the FRISK88 code versus the EPRI code. This comparison confirms that the EPRI 1989 seismic sources and ground motion equations are being modeled correctly by the current application of the FRISK88 code.

The second step consisted of calculating seismic hazard for 1, 2.5, 5, and 10 Hz spectral velocity. FRISK88 was run at these four spectral frequencies to calculate seismic hazard and determine the median 10^{-5} hazard. These were compared to the 1989 EPRI seismic hazard results, as listed in Table 2.5-17. The apparent difference in values of spectral velocity in Table 2.5-17 is small, as it was for PGA, and results from numerical differences in how FRISK88 calculates seismic hazard compared to the software used in the EPRI study.

The third step was to apply the magnitude-distance deaggregation procedure described in RG 1.165 (Reference 2), using these PSHA results. In summary, this procedure requires deaggregating the seismic hazard at the median 10^{-5} ground motion at 1 Hz, 2.5 Hz, 5 Hz, and 10 Hz, combining the 1 and 2.5 Hz deaggregations, combining the 5 and 10 Hz deaggregations, and computing magnitudes and distances of controlling earthquakes for each combination.

Deaggregation plots following this procedure are shown in Figure 2.5-26 and Figure 2.5-27. The body-wave magnitude m_b and epicentral distance r_{epi} of controlling earthquakes were determined and are shown in Table 2.5-23. (For purposes of discussion in Section 2.5.2.6, equivalent moment magnitude **M** and closest distance, r_{CD} , values are also given in Table 2.5-20)

2.5.2.5 Seismic Wave Transmission Characteristics of the Site

The subsurface materials at the ESP site are described in detail in Section 2.5.4. The material characterization is summarized below. The foundation materials are divided into Zones I through IV:

- I Residual clays and clay silts – all structures of parent rock are lost
- IIA Saprolite – core stone less than 10 percent of volume of overall mass
- IIB Saprolite – core stone 10 to 50 percent of soil mass
- III Weathered rock – core stone more than 50 percent of volume of mass
- IV Parent rock – slightly weathered to fresh rock below zone of isolated core stones

In addition to these five categories, a sixth category termed Zone III-IV, representing a slightly to moderately weathered rock, was added to further describe the soil and rock with regard to engineering properties.

The containment (reactor) building and primary supporting safety-related structures would be founded on sound bedrock, either Zone IV or Zone III-IV. However, other safety-related structures (possibly the diesel generator building and certain tanks) may be founded on the Zone III weathered rock or the Zone II saprolitic soils.

The seismic wave transmission characteristics of the site materials are described in detail in Section 2.5.4.7. The description includes the shear wave velocity profile for the site, and the variation of shear modulus and damping with strain. Section 2.5.4.7 also includes a description of a site-specific acceleration-time history, and provides and discusses the results of soil column amplification/attenuation analyses.

2.5.2.6 Safe Shutdown Earthquake Ground Motion

RG 1.165 Regulatory Position 2 and Appendix E specify how to develop a safe shutdown earthquake (SSE) ground motion by updating the 1989 EPRI PSHA to include more recent information on seismic sources and ground motion. The following sections describe the information that was used to update the 1989 EPRI study.

2.5.2.6.1 New Regional Earthquake Catalog

Section 2.5.2.1.2 discusses updated seismicity information that was used to extend the 1989 EPRI seismic data to 2001. The effect of this additional data was examined to determine if it would have an impact on seismic hazard. This was accomplished by examining the effect of recent seismicity (1985 to 2001) on the seismic sources that dominate the seismic hazard at the ESP site.

As background for these calculations, the 1989 EPRI study (Reference 115) identified all seismic sources within 200 km of each site and included them in screening calculations. The 1989 study also included the New Madrid, Charleston, and La Malbaie sources in screening calculations for a site if they were within 500 km of that site. The screening included all sources for a given EST that contributed to 99 percent of the seismic hazard at one peak ground acceleration amplitude and one 1-sec spectral velocity amplitude (meaning that the composite contribution of all sources that were eliminated contributed less than 1 percent of the seismic hazard at those amplitudes). See Reference 115, Page 2-16, for further details of this screening process. The sources included for the North Anna site following screening during the 1989 study were used as the starting point for the current calculations.

Seismic hazard was calculated for PGA and 1 Hz spectral response, for each of the EPRI ESTs and for each seismic source used in the 1989 EPRI calculations. Figure 2.5-28 through Figure 2.5-33 show the mean hazards by source for each team for 1 Hz. This spectral frequency increases the relative contribution of more distant sources compared to PGA.

The significant seismic sources, i.e., the sources that contribute most of the hazard at the mean 10^{-5} level, are summarized in Table 2.5-19. This table indicates that representations of the Central Virginia seismic zone dominate the hazard at the ESP site. This is not surprising, since the Central Virginia seismic zone is the closest seismic source to the site. There are other contributing sources (such as the local background source for the Bechtel and Woodward-Clyde teams) representing regional sources that are active under scenarios when the source representing central Virginia seismicity is not active. Also, local smoothing of seismicity parameters by the EPRI teams means that these background sources are representing the higher seismicity in the central Virginia area. Local smoothing in the context of the EPRI study means that historical seismicity in the local area was used to estimate the activity rate in each degree cell within a large source; the historical seismicity was not smoothed over a very broad region. Thus regions such as the Central Virginia seismic zone that have had higher-than-average seismicity in the past would have that higher activity represented by the background source.

The local mafic pluton sources specified by the Law Engineering team had seismicity parameters calculated from historical seismicity in the 111 x 111 km area surrounding each mafic pluton, assigning 70 percent of this seismicity to the mafic pluton (see Reference 120, Volume 7, pages 6-7 to 6-8). This in effect assigned 70 percent of the central Virginia seismicity to mafic pluton sources in central Virginia. The conclusion is that various representations of seismicity for the central Virginia area and for the local background seismicity generally dominate the seismic hazard at the ESP site.

Table 2.5-19 identifies sources representing the Central Virginia seismic zone as dominating the seismic hazard at the site. The fundamental question to be addressed is whether seismicity recorded since 1984 indicates that the seismic activity rates used in the 1989 EPRI study (Reference 115) are inadequate or not sufficiently conservative for assessment of the seismic hazard at the ESP site. This question is addressed in Section 2.5.2.6.5.

2.5.2.6.2 New Maximum Magnitude Information

Geological and seismological data published since the 1986 EPRI seismic source model are presented in Section 2.5.1 and Section 2.5.2.1. Based on a review of these data, there are no significant changes in the EPRI maximum magnitude (M_{max}) parameters, with the exception of the Charleston seismic source. The review of M_{max} for each EPRI EST is provided in Table 2.5-5 through Table 2.5-10.

For the Charleston seismic source, a new geologic structure has been identified as the possible source of the 1886 Charleston earthquake, the southern segment of the East Coast Fault System (ECFS-S) (Reference 74). This new source is described further in Section 2.5.2.6.3.

For sensitivity analysis, the ECFS-S is treated as an alternative geometry for the Charleston seismic source with a characteristic M_{max} . For the M_{max} values, the 2002 USGS values and weights are used (Reference 127). These characteristic M_{max} values range from **M** 6.8 to 7.5,

meaning that the large magnitude earthquake occurs with a specified mean recurrence interval. By contrast, the six EPRI ESTs designated exponential magnitude distributions for sources representing the Charleston region and estimated the following maximum magnitudes for those sources (Reference 121):

Team	Charleston M_{max} range
Bechtel	m_b 6.8 to 7.4 (M 6.8 to 7.9)
Dames & Moore	m_b 6.6 to 7.2 (M 6.5 to 7.5)
Law Engineering	m_b 6.8 (M 6.8)
Rondout	m_b 6.6 to 7.0 (M 6.5 to 7.2)
Weston Geophysical	m_b 6.6 to 7.2 (M 6.5 to 7.5)
Woodward-Clyde Consultants	m_b 6.7 to 7.5 (M 6.7 to 8.0)

For some teams (e.g., the Law Engineering team), the 1989 EPRI interpretations are at the low end of current interpretations (see below). This difference and the shorter recurrence interval prompted a reevaluation of seismic hazard with the current interpretation of maximum magnitude for the Charleston seismic zone, as discussed in Section 2.5.2.2.9.

2.5.2.6.3 New Seismic Source Characterizations

Review of the updated geological, seismological and geophysical data base relative to the 1986 EPRI seismic source model generally shows that there are no significant changes to the EPRI source model with three exceptions as identified in Section 2.5.2.2.

- Identification of the postulated East Coast Fault System along the Atlantic seaboard
- Revision to the recurrence interval and source geometry of the Charleston seismic source
- Revision to the recurrence interval of the New Madrid seismic source

A sensitivity analysis was performed for the East Coast Fault System and the revised Charleston seismic source to evaluate the significance of these sources to hazard at the ESP site. Both of these sources are treated as active in addition to the sources designated by the EPRI ESTs in the sensitivity analysis. This sensitivity analysis is presented in Section 2.5.2.6.5.

a. East Coast Fault System

The East Coast Fault System (ECFS) is modeled as being located along the Atlantic seaboard and consists of three segments: the northern (ECFS-N), central (ECFS-C), and southern (ECFS-S) (Reference 74; Figure 2.5-13), as described in Section 2.5.1.1.4. The northern segment is located approximately 70 miles southeast of the ESP site. The southern segment extends through the Charleston meizoseismal zone and is postulated to be the source of the

1886 Charleston earthquake, implying that similar large magnitude earthquakes can occur on the northern and central segments of the ECFS.

Given the proximity of the northern segment to the ESP site, a sensitivity analysis was performed to evaluate the fault's potential contribution to hazard at the ESP site. The southern segment of the ECFS constitutes a possible alternative source geometry for the Charleston source zone, and is described further below.

Source parameters for the northern segment of the ECFS are shown on Figure 2.5-34. This logic tree shows four parameters: 1) probability of existence, 2) probability of activity, 3) maximum magnitude, and 4) recurrence interval.

For the ECFS-N segment, the fault was assumed to have a probability of existence of 0.1 and a probability of activity (given existence) of 0.1. M_{max} parameters and weights used in the USGS national seismic hazard map (Reference 127) for the Charleston source were adopted for the northern segment of the ECFS. Recurrence values and weights were selected to be 550 years [0.1], 25,000 years [0.5], and 50,000 years [0.4], respectively.

The probability of existence and probability of activity are assigned low weights (0.1) because the existence of the fault is not well documented and is highly uncertain, and because there is no direct geologic, geomorphic, or seismologic evidence that the fault exists as a tectonic feature or is active, if it does exist (described in Section 2.5.1.1.4).

b. Charleston Seismic Source

New data published since the 1986 EPRI study suggest revisions to the recurrence interval and source geometry to the Charleston seismic source. For the sensitivity analysis in Section 2.5.2.6.5, the USGS source parameters (Reference 127) were adopted, as shown on Figure 2.5-35. The magnitudes (**M**) and weights used in the USGS model also were adopted for the sensitivity analysis, although the range in magnitudes falls within the EPRI seismic source model characterization of the Charleston source. A recurrence interval of 550 years was used based on recent paleoliquefaction studies. This recurrence interval implies much more frequent events than the seismicity-based recurrence interval modeled by the EPRI ESTs of several thousand years. The southern segment of the ECFS was used as an alternative source geometry for the sensitivity analysis. In this approach, the southern segment was assumed to be active with a characteristic magnitude with mean recurrence interval of 550 years. This approach is conservative in that the mean recurrence interval may not be directly associated with earthquakes as large as the assumed maximum magnitudes.

c. New Madrid Seismic Source

The New Madrid seismic source is located over 600 miles west of the ESP site. Therefore, the results of revising the recurrence parameters of the Charleston seismic source approximately 300 miles south of the ESP site are used to evaluate whether the revised recurrence

parameters for the New Madrid seismic source would significantly increase hazard at the ESP site.

2.5.2.6.4 **New Ground Motion Models**

The ground motion models developed by the 2003 EPRI-sponsored study (Reference 116) were used to examine the effects on seismic hazard of current estimates of seismic shaking as a function of earthquake magnitude and distance. For general area sources, nine estimates of median ground motion are combined with four estimates of aleatory uncertainty, giving 36 combinations. For fault sources in rifted regions, which applies to the ECFS fault segments, 12 estimates of median ground motion are combined with four estimates of aleatory uncertainty, giving 48 combinations. When both area sources and faults are active, a specific correlation of area source models and fault source models is used to represent ground motion models that might apply together. These families of models (36 for area sources, 48 for fault sources) represent the epistemic uncertainty in ground motion, and contribute to the epistemic uncertainty in seismic hazard.

2.5.2.6.5 **Sensitivity Studies of New Geoscience Information**

The effect of new geoscience information (new seismic sources, new magnitudes, new recurrence parameters, and new ground motion models) was addressed by examining the effect of this new information on median seismic hazard at levels of 10^{-5} per year. The baseline for comparison purposes was the seismic hazard calculated using the 1989 EPRI seismic sources and ground motion models (see Section 2.5.2.4).

a. **Effect of New Earthquake Catalog on 1989 EPRI Seismic Hazard Results**

In Section 2.5.2.6.1, the Central Virginia seismic zone was identified as the zone that dominates the seismic hazard at the ESP site. To examine the effect of additional seismicity data from 1985 to 2001, we chose the representations of the Central Virginia seismic zone by the Bechtel and Rondout teams as representative. Figure 2.5-36 indicates the geometry of the Central Virginia seismic zone as modeled by these teams. These represent two alternative interpretations; in the Bechtel team source, the ESP site is encompassed by the Central Virginia seismic zone, and for the Rondout team source, the ESP site lies on the northern boundary of the source. Figure 2.5-36 also indicates locations of earthquakes identified in Table 2.5-4 as occurring in the region between 1985 and 2001. Five earthquakes have occurred during this time period, and all five fall within the Central Virginia seismic zone as modeled by both the Bechtel and Rondout teams.

In addition, a seismic source consisting of a polygon with an approximate 200-mile radius was selected for investigation. This source encompasses the entire region that contributed to the seismic hazard at North Anna from the 1989 EPRI study, both for high and low frequencies (see Figure 2.5-26 and Figure 2.5-27).

The seismicity in these three sources was investigated by running program EQPARAM (from the EPRI EQHAZARD package) first for the original EPRI catalog, to replicate the results obtained in the 1989 study (Reference 115). This confirmed that the proper parameters from the 1989 study were being used. Then an equivalent analysis was run using the augmented earthquake catalog (through 2001). Full smoothing of a- and b-values was selected for the comparison, because this was a common choice of many ESTs in the 1989 EPRI study. Further, if comparisons were to be made on an individual degree-cell basis, the rates in some cells might increase and in others might decrease, and for a source such as the Central Virginia seismic zone, a composite rate would have to be used to compare seismic rates using the earthquake catalog through 1984, to those using the earthquake catalog through 2001. The choice of full smoothing achieves this composite rate directly and automatically, since it is a composite rate for the entire source.

From the a- and b-values calculated with EQPARAM, recurrence rates for difference magnitudes were calculated. Figure 2.5-37, Figure 2.5-38, and Figure 2.5-39 compare the annual recurrence rates for the three sources for seismicity through 1984 and seismicity through 2001. For all three sources, the augmented catalog indicates that seismicity rates have decreased.

The conclusion is that the seismicity recorded from 1985 to 2001 does not indicate that seismic activity rates have increased in those sources contributing most to the hazard at the ESP site under the assumptions of the 1989 EPRI study. For this reason, the seismic activity rates as derived in the 1989 EPRI study (Reference 115) were used to calculate seismic hazard at the ESP site with the EPRI seismic sources.

b. Effect of New Maximum Magnitude Information

As discussed in Section 2.5.2.6.2, recent characterization of the Charleston Source indicates that **M** 6.8 to 7.5 earthquakes are possible on structures in the Charleston area and on the southern segment of the ECFS. The effect of these large magnitude earthquakes (which fall within the range of 1989 EPRI values) is considered in conjunction with the seismic sources themselves and their recurrence rates (see Section 2.5.2.6.5).

No other information was identified that would cause estimates of the magnitudes in the 1989 EPRI seismic sources to increase.

c. Effect of New Seismic Source Characterization

The effects of the ECFS-N (northern) and ECFS-S (southern) fault segments were examined by calculating seismic hazard from these two fault segments and comparing this seismic hazard to that from the 1989 EPRI seismic sources. It was appropriate to use the latest ground motion interpretations in this comparison, so that the effect for example of distant sources was properly assessed. Thus for these comparisons the 2003 EPRI ground motion models (described in Section 2.5.2.6.4) were used.

Figure 2.5-40 and Figure 2.5-41 show 1 Hz spectral acceleration seismic hazard curves (median and mean, respectively) at the ESP site for the original 1989 EPRI seismic sources, for the ECFS-N and ECFS-S faults individually, and for the combined hazard of the 1989 seismic sources and the ECFS-N and ECFS-S faults. The ECFS-N fault hazard does not show on Figure 2.5-40 for median hazard, because this fault has only a 1 percent probability of existing and being active (see Section 2.5.2.6.3). The median hazard from this fault alone is therefore zero. Figure 2.5-40 and Figure 2.5-41 indicate that the ECFS-S fault increases the total median and mean hazard by several percent at the 10^{-5} hazard level. This fault should therefore be included in seismic hazard calculations for the ESP site. The ECFS-N fault, however, results in much lower hazard than from the 1989 EPRI seismic sources, so this fault need not be included in calculations.

Figure 2.5-42 and Figure 2.5-43 show a similar comparison for 10 Hz spectral acceleration. In this case neither the ECFS-S or ECFS-N faults indicates much increase in seismic hazard. The reason is that 10 Hz ground motion is dominated by closer sources than 1 Hz ground motion, so the distant ECFS-S and ECFS-N faults have little effect on seismic hazard.

d. Effect of New Ground Motion Models

The effect of the 2003 EPRI ground motion models was determined by calculating seismic hazard using these models and the 1989 EPRI seismic sources, and comparing hazard to that using the 1989 EPRI ground motion (see Section 2.5.2.6.5).

Figure 2.5-44 shows a comparison of 10 Hz seismic hazard for the 1989 ground motion models and the 2003 ground motion models. At annual frequencies of 10^{-5} there is a significant increase for both the median and mean hazard. At annual frequencies around 10^{-3} and less, the 2003 ground motion models indicate less hazard for both the median and mean.

Figure 2.5-45 shows a similar comparison for 1 Hz. For this spectral frequency the 1989 and 2003 models indicate about the same median hazard at all annual frequency levels, but the 2003 mean hazard is significantly lower than the 1989 mean hazard.

A major difference between the 1989 and 2003 ground motion models is that the estimates of aleatory uncertainty are larger in the 2003 study. In 1989, a standard deviation of natural log(ground motion) of 0.5 was used for all frequencies, whereas in 2003, values of 0.6 and 0.7 are common (they vary depending on magnitude, distance, and frequency). At annual frequencies of 10^{-5} , which are sensitive to the tails of the ground motion aleatory distribution, this difference in standard deviation increases seismic hazard. This would likely be true for any CEUS location. A compensating factor at 1 Hz is the use of ground motion models that reflect a two-corner source, which acts to reduce 1 Hz ground motion estimates from those used in 1989. Thus the median 1 Hz seismic is about the same for both models. The mean amplitudes using the 2003 ground motion models are closer to the median amplitudes than is the case for the 1989 models, reflecting convergence on what are reasonable models to use for ground

motion estimation in the eastern US. In 1989, the ground motion models were quite diverse, with one model developed by estimating peak ground acceleration and velocity, then using spectral amplification factors to estimate spectral amplitudes. In 2003, the available models estimate spectral amplitudes directly.

2.5.2.6.6 Updated EPRI Probabilistic Seismic Hazard Analysis, Deaggregation, and 1 Hz, 2.5 Hz, 5 Hz, and 10 Hz Spectral Accelerations Incorporating Significant Increases Based on the Above Sensitivity Studies

The PSHA was recomputed for the ESP site incorporating the 2003 EPRI ground motion models and adding the ECFS-S fault. The latter fault was added to each of the six Earth Science Team's interpretations, since the occurrence of a large (M 6.8 to 7.5) earthquake with a mean recurrence interval of 550 years at Charleston was not modeled by the EPRI teams.

The results of the updated seismic hazard calculations are summarized in Table 2.5-22, compared to the results from the 1989 models (from Table 2.5-21). The largest difference is at 10 Hz, where the updated models indicate higher amplitudes for both the 10^{-5} median and mean by 47 percent to 55 percent. At 1 Hz, 2.5 Hz, and 5 Hz, the updated models indicate a higher median 10^{-5} hazard but a lower mean 10^{-5} hazard. At 1 Hz, the updated models and 1989 models indicate only a 6 percent increase in the median 10° amplitude.

The seismic hazard results were deaggregated using the procedure described in RG 1.165. Deaggregation plots are shown in Figure 2.5-46 and Figure 2.5-47. The body-wave magnitude m_b and epicentral distance r_{epi} of controlling earthquakes were calculated and are listed in Table 2.5-23.

The difference in the magnitudes and distances of the updated model compared with the 1989 model is that the magnitudes are slightly lower and the distances slightly smaller.

2.5.2.6.7 Selected SSE Ground Motion

The above analysis shows that the information developed since the 1989 EPRI results leads to a significant increase in the 1×10^{-5} median estimate of seismic hazard at the ESP site and that the dominant cause of this increase is the new ground motion models developed by EPRI in 2003 (Reference 116), particularly, aleatory uncertainty. As noted above, the increase in aleatory uncertainty would likely result in increased probabilistic seismic hazard results for 1×10^{-5} annual median frequencies for any location in the CEUS. The new ground motion would, therefore, be expected to increase the hazard at the other selected plant sites used to estimate the reference probability of RG 1.165. This would result in a different and higher reference probability. Because any 29-site calculation of reference probability was thought to be best performed only after consultation with the NRC on appropriate methodology and assumptions and because a 29-site analysis was judged not to be within the scope of an evaluation for a single site, an alternative approach was adopted and is described below to select the SSE ground motion spectrum for the ESP site.

The selected SSE ground motion spectrum was developed using the concept of a “performance-based spectrum” that has, as its goal, achieving a mean annual frequency of 10^{-5} of unacceptable performance of nuclear structures, systems, and components as a result of seismically initiated events. This goal is recommended by three studies undertaken in recent years to recommend seismic design levels for nuclear facilities in the United States, as described below. This performance goal approach establishes an absolute risk level (annual frequency of unacceptable performance) for all structural frequencies that does not depend directly on calibration of new designs to the hazard implied by existing plant designs.

The “base-case” assumptions used here regarding seismic sources and ground motion models are those described in previous sections as being the most relevant and up-to-date for the ESP site. For seismic sources, the 1989 EPRI seismic sources (Reference 115) were used with the addition of the ECFS-S fault representing an alternative geometry and more frequent occurrence of large earthquakes in the Charleston, South Carolina area. For ground motion, the 2003 EPRI ground motion model (Reference 116) was used, consisting of estimated spectral accelerations at 7 structural frequencies at 5 percent of critical damping, and including a quantification of aleatory and epistemic uncertainties.

The performance-based spectrum is achieved by starting from a ground motion spectrum with a mean 10^{-4} annual frequency of exceedance, and modifying this spectrum by a scale factor that is based on the slope of the mean seismic hazard curve between 10^{-4} and 10^{-5} . The scale factor SF is defined as:

$$SF = \max(1.0, 0.6 \times A_R^{0.8}) \quad \text{Equation 2.5.2-3}$$

where A_R is the multiplicative increase in ground motion corresponding to a decrease in seismic hazard from mean 10^{-4} to mean 10^{-5} . A_R and SF are determined on a frequency-by-frequency basis. The amplitude $A(f)$ defining the performance-based SSE ground motion spectrum at each frequency f is then calculated as:

$$A(f) = SA_4 \times SF \quad \text{Equation 2.5.2-4}$$

where SA_4 is the spectral acceleration corresponding to 10^{-4} mean annual frequency of exceedance. For sites and conditions in which the seismic hazard curve is very steep (i.e. A_R is 1.89 or less), $SF = 1$, and $A(f) = SA_4$. For most sites and frequencies in the CEUS at mean annual frequencies of 10^{-4} , A_R is in the range 2 to 4 (Reference 117, page C-9), and the 1×10^{-4} mean annual frequency of exceedance spectrum (SA_4) will be increased by a scale factor SF of 1.04 (for $A_R=2$) to 1.82 (for $A_R=4$) to achieve a mean 1×10^{-5} annual frequency of unacceptable performance.

This approach to recommending design levels based on scaling the 1×10^{-4} mean annual frequency of exceedance spectrum to achieve a 1×10^{-5} mean annual frequency of unacceptable performance has received substantial interest in recent years. The DOE (Reference 117) uses a scale factor on the 1×10^{-4} hazard spectrum for performance-category 4 structures, systems, and components (the most critical) to specify a design level that will have less than 10 percent probability of unacceptable performance, given the occurrence of the 1×10^{-4} ground motion. A scale factor dependent on the slope of the seismic hazard curve is discussed in Reference 117, Appendix C, and is illustrated graphically in Reference 128, upon which Reference 117 is based. Equation 2.5.2-3 above is taken from Reference 128, Equations 15a and 15b, with the coefficients given in Reference 128, Table 2-5.

Under research sponsored by the NRC (Reference 119), Risk Engineering, Inc. recommended a scale factor to convert a uniform hazard spectrum to a “uniform reliability spectrum” that achieves an approximately constant annual frequency of nuclear plant component failure that is a factor of 10 less than that of the uniform hazard spectrum. The scale factor recommended in Reference 119 also depends on the slope of the hazard curve between the mean 1×10^{-4} hazard and the mean 1×10^{-5} hazard.

A subcommittee of the American Society of Civil Engineers developed seismic design criteria for nuclear facilities (Reference 118) that are based on seismic hazard results. Scaling the mean 1×10^{-4} ground motion by a slope-dependent scale factor is shown to achieve a performance goal that is 0.1 times the 1×10^{-4} mean annual frequency. This subcommittee also recommended the scale factor used in Equation 2.5.2-3.

Table 2.5-24 shows the ground motion amplitudes corresponding to mean 10^{-4} and mean 10^{-5} seismic hazard levels, the calculated values of A_R , the calculated values of the scale factor SF, and the resulting performance-based spectral amplitudes $A(f)$. These results were calculated using the base-case assumptions discussed above. Table 2.5-24 shows that scale factor SF increases the mean 10^{-4} spectrum by a factor of 1.40 to 1.64 across the frequency range 0.5 Hz to 100 Hz.

The performance-based spectrum calculations were made for the seven frequencies shown in Table 2.5-24. These are the frequencies available from the 2003 EPRI ground motion model: 0.5, 1, 2.5, 5, 10, 25, and 100 Hz (the last being equivalent to PGA). Figure 2.5-48 shows the resulting spectrum. For frequencies above 10 Hz, spectral scaling was used for intermediate frequencies, scaling spectral shapes to the amplitudes shown in Table 2.5-24 at 10 Hz, 25 Hz, and 100 Hz (PGA) and using, for each intermediate frequency, a weighted amplitude based on the two closest calculated frequencies (10, 25, or 100 Hz). The weighting was based on the inverse logarithmic distance between the intermediate frequency and the calculated frequencies. This gives a realistic spectral shape at high frequencies. The spectral shape recommendations in Reference 119 were used to develop these spectral shapes, adopting a representative magnitude (**M**) of 5.5 and distance of 20 km (see the sensitivity studies described in the next section for perspective on this magnitude and distance), and giving equal weight to the one- and two-corner source models.

The spectrum shown in Figure 2.5-48 represents a scaled free-field rock ground motion spectrum for 5 percent of critical damping without any effects such as structure, embedment, or incoherence of seismic waves due to base mat size. Such effects would have to be determined on a design-specific basis, and their effect would be to modify the spectrum shown in Figure 2.5-48 for appropriate design levels of structures, systems, and components of that specific design.

2.5.2.6.8 Additional Sensitivity Studies

In evaluating the selected SSE ground motion spectrum, it is useful to understand how sensitive the spectrum is to the assumptions underlying its calculation. This gives perspective on the selected SSE spectrum as an appropriate ground motion to adopt for seismic design at the site. For these additional sensitivity studies the base-case assumptions on seismic sources and ground motion models were also used. Applications were made using different assumptions on the appropriate reference probability and on seismicity and ground motion parameters as discussed in the following subsections. These different assumptions gave alternative seismic hazard results that are compared to the base-case spectrum.

a. Spectrum based on new reference probability

One option in RG 1.165 is to establish a new reference probability (RP) on which design-basis ground motions should be calculated. In fact, RG 1.165 Appendix B states that a new RP should be calculated:

“...if general revisions to PSHA methods or data bases result in significant changes in hazard predictions for the selected plant sites in Table B.1.”

The revised EPRI recommended ground motion models (Reference 116) are a general revision to PSHA methods that would result in significant changes in hazard predictions. These new EPRI models would likely change estimates of seismic hazard for the sites listed in RG 1.165, Table B.1. An additional general revision to data bases is that the estimate of the mean recurrence interval for large earthquakes in the New Madrid, Missouri region and in the Charleston, South Carolina region has decreased since the EPRI (Reference 115) and LLNL (Reference 129) studies based on tectonic interpretations in the CEUS in the 1980s. At that time, mean recurrence intervals for major earthquakes were thought to be several thousand years or longer, but current estimates indicate recurrence intervals on the order of 500 years (see Section 2.5.2.6.1). These shorter mean recurrence intervals would increase the seismic hazard at sites affected by large earthquakes in these regions. Therefore, the sites listed in Table B.1 of RG 1.165 that are relatively close to New Madrid or Charleston would potentially have a greater seismic hazard than was used in deriving the RP in RG 1.165.

To examine the sensitivity of seismic design to changes in the RP, an RP corresponding to a mean 5×10^{-5} annual frequency of exceedance was chosen. This RP is a representative value that might be calculated from a detailed study of existing designs for the 29 plants listed in RG 1.165, Table B.1, and from a revised calculation of seismic hazard at those plants. The

mean annual frequency is chosen, rather than the median, because Reference 117, Reference 118, and Reference 119 recommend establishing design criteria based on the mean rather than the median, and use of the mean is consistent with the objective of meeting mean safety goals at nuclear facilities.

Table 2.5-25 shows the spectral accelerations calculated for a mean annual frequency of 5×10^{-5} , for 1 Hz, 2.5 Hz, 5 Hz, and 10 Hz. The seismic hazard at these frequencies and spectral accelerations were deaggregated. Figure 2.5-49 and Figure 2.5-50 show deaggregation plots for the combined magnitude-distance deaggregation at low frequencies (1 and 2.5 Hz) and high frequencies (5 and 10 Hz), respectively.

The controlling magnitudes and distances were calculated according to the procedure in RG 1.165, Appendix C, applied however to the mean 5×10^{-5} amplitudes rather than the median 1×10^{-5} amplitudes. The resulting controlling magnitudes and distances are shown in Table 2.5-26. These were calculated in terms of body-wave magnitude m_b and epicentral distance r_{epi} , and were converted to moment magnitude M and closest distance r_{CD} for purposes of scaling spectra according to Reference 119, which uses M and r_{CD} . These values support the $M = 5.5$, $r_{CD} = 20$ km values used in the previous section to develop a representative spectral shape at high frequencies.

Figure 2.5-51 shows a plot of the scaled spectra calculated using an RP of mean 5×10^{-5} , deaggregated at 1, 2.5, 5, and 10 Hz, and using the scaled spectra of Reference 119. The deaggregations by magnitude and distance in Figure 2.5-49 and Figure 2.5-50 are similar, indicating that the hazard at low and high frequencies is coming from the same earthquakes: $m_b \sim 5.5$ to 6 at a distance of about 20 to 25 km, which is consistent with an earthquake in the Central Virginia seismic zone. As a result, the scaled low- and high-frequency spectra in Figure 2.5-51 have a similar shape and almost overlie each other. This reinforces the method adopted in deriving the selected ground motion spectrum based on a uniform hazard spectrum, since different earthquakes do not dominate the low- and high-frequency portions of the ground motion spectrum.

Figure 2.5-51 also shows the selected performance-based SSE spectrum described in the previous section. The shapes and amplitudes of the spectra are similar, and this reinforces the concept of the performance-based spectrum. If a revised reference probability were to be derived according to RG 1.165, and this reference probability were applied to the ESP site, the resulting spectrum would be very similar to the selected performance-based spectrum.

b. Spectrum based on alternative minimum magnitude

Standard practice for seismic hazard investigations in the central and eastern U.S. has been to use a minimum body-wave magnitude of $m_b = 5$ for calculations. For example, the EPRI and LLNL seismic hazard studies (Reference 115) (Reference 129) referenced in RG 1.165 use a lower-bound magnitude of $m_b = 5.0$. This m_b value corresponds to approximately moment

magnitude $M = 4.6$ using the magnitude conversion method described in Section 2.5.2.2.1. There is abundant evidence that earthquakes with M less than 5 do not cause damage to nuclear plant structures and equipment. Reference 130 studied the lower-bound magnitude issue specifically as it affects seismic hazard calculations for nuclear plants in the U.S. and concluded:

“A magnitude of M 5.0 is a threshold for which there is a reasonable engineering assurance that ground motions associated with smaller events will not damage NPP components.” (Reference 130, page 8-9).

Thus, it is appropriate to calculate seismic hazard on the basis of lower-bound $M = 5.0$, which is approximately $m_b=5.4$.

To examine this sensitivity, the base-case models were adopted except that the lower-bound magnitude m_b was set to 5.4, and the seismic hazard analysis for the ESP site was recalculated with this change. These calculations were made for the seven frequencies available from the 2003 EPRI ground motion model: 0.5, 1, 2.5, 5, 10, 25, and 100 Hz (the last being equivalent to PGA). The mean 1×10^{-4} and mean 1×10^{-5} spectral amplitudes were calculated at these 7 frequencies, and the scale factors described in Equation 2.5.2-3 and Equation 2.5.2-4 were applied to calculate scaled values of spectral acceleration.

Table 2.5-27 shows the ground motion amplitudes corresponding to mean 10^{-4} and mean 10^{-5} seismic hazard levels, the calculated values of A_R , the calculated values of the scale factor SF, and the resulting scaled spectral amplitudes $A(f)$. Table 2.5-27 shows lower spectral accelerations than for the base case (Table 2.5-24), as would be expected for an increased lower-bound magnitude. The hazard curve slopes and scale factors are similar, however.

Figure 2.5-52 shows the resulting scaled hazard spectrum. For frequencies above 10 Hz, spectral scaling was used for intermediate frequencies, scaling spectral shapes in a manner identical to that used for the selected SSE spectrum (see Section 2.5.2). These shapes were scaled to the amplitudes shown in Table 2.5-27 at 10 Hz, 25 Hz, and 100 Hz (PGA) and using, for each intermediate frequency, a weighted amplitude based on the two closest calculated frequencies (10, 25, or 100 Hz). The weighting was based on the inverse logarithmic distance between the intermediate frequency and the calculated frequencies. This gives a realistic spectral shape at high frequencies. The spectral shape recommendations in Reference 119 were used to develop these spectral shapes, adopting a representative magnitude (M) of 5.5 and distance of 20 km.

Figure 2.5-52 shows that the assumption of a more realistic lower-bound $M = 5.0$ would lower the recommended ground motion spectrum by a substantial factor (by about 1% at 1 Hz, 16% at 10 Hz, and up to 20% for higher frequencies). Another way to state this is that there is substantial conservatism in the recommended ground motion spectrum.

c. Spectrum based on revised aleatory uncertainties in ground motion

The base-case ground motion model (Reference 116) has aleatory uncertainties that are higher than those reported based on empirical studies of ground motions recorded in California. This is illustrated in Figure 2.5-53, which compares aleatory standard deviations (of log spectral acceleration) vs. frequency for $M = 5.5$ and $r_{CD}=20$ km for the 2003 EPRI model and for four empirical studies that used recorded California strong-motion data. The values labeled “EPRI” are weighted-average values of four models of aleatory uncertainties recommended in the EPRI study (Reference 116). The EPRI model uncertainties lie above those reported for California, particularly for frequencies of 5 Hz and higher. The standard deviation of log spectral acceleration is an important parameter in the seismic hazard calculations, and increasing it by 0.1 (from 0.65 to 0.75, for example) can cause a large increase in calculated seismic hazard. In Figure 2.5-53, “AS97” represents the Abrahamson-Silva model (Reference 131), “SEA97” represents the Sadigh et al. model (Reference 132), “C97” represents the Campbell model (Reference 133), and “BJF97” represents the Boore-Joyner-Fumal model (Reference 134).

Certainly empirical uncertainties in the ground motions for the CEUS should be higher than those in California, because of the lack of strong-motion data in the former region with which to verify models. This difference is taken into account explicitly in the EPRI study. But there is no immediately apparent reason why aleatory uncertainties should be higher for ground motions in the eastern U.S. than in California. To gain additional perspective on the seismic hazard at the ESP site, it is useful and appropriate to examine the seismic hazard using aleatory uncertainties in ground motion that are typical of what is observed in California data.

To accomplish this, the Abrahamson-Silva model of aleatory uncertainty (Reference 131) was chosen. This model is similar to that of Reference 132 (labeled “SEA97” in Figure 2.5-53). The other two references did not report a significant change in aleatory uncertainty with magnitude (Reference 134) or frequency (Reference 133), both of which are important considerations in this sensitivity study. The Abrahamson-Silva model of sigma was substituted for the aleatory uncertainty model reported in the EPRI 2003 study, to determine the potential effect of using an empirically based estimate of this uncertainty.

The same procedure was used as for the recommended spectrum, that is, seismic hazard using the above described changes to the base-case model was calculated, and scaled to the mean 1×10^{-4} uniform hazard spectrum based on the slope of the hazard curves from 1×10^{-4} to 1×10^{-5} , using Equation 2.5.2-3 and Equation 2.5.2-4. Table 2.5-28 summarizes the hazard values, slopes, scale factors, and scaled spectral amplitudes.

Spectra were drawn, scaling high-frequency amplitudes to obtain a realistic spectral shape using a procedure identical to that used for the selected SSE spectrum, as described in Section 2.5.2.6.7. Figure 2.5-54 shows the resulting spectrum compared to the selected SSE spectrum and to a RG 1.60 spectrum anchored to 0.3g.

Figure 2.5-54 shows that a significant decrease in the selected spectrum would occur if empirically based aleatory ground motion uncertainties were used in place of those reported in the 2003 EPRI ground motion study (by about 11% at 1 Hz, 9% at 10 Hz, and up to 11% for higher frequencies). Stated another way, this sensitivity study shows considerable conservatism in the selected SSE spectrum.

d. **Summary**

These additional sensitivity studies have shown considerable conservatism in the selected spectrum for the ESP site, particularly for frequencies above 10 Hz. If either or both of the assumptions related to lower-bound magnitude or aleatory ground motion uncertainties were adopted, the selected spectrum based on scaling the mean 1×10^{-4} amplitudes would decrease. If a re-evaluation of the 29 sites used in developing RG 1.165 were undertaken, this would likely lead to a revised reference probability around 5×10^{-5} mean, and the resulting spectrum at the site would be consistent with the selected SSE spectrum. This gives considerable credibility to the selected SSE spectrum.

It must be emphasized that the selected SSE spectrum shown in Figure 2.5-48 represents a scaled spectrum of free-field rock ground motion spectrum for 5 percent of critical damping without any effects such as structure, embedment, or incoherence of seismic waves due to base mat size. Such effects must be determined on a design-specific basis, and their effect would be to modify the spectrum shown in Figure 2.5-48 for appropriate design levels of structures, systems, and components of that specific design.

2.5.2.6.9 Additional Modification of the Selected Spectrum

The selected SSE ground motion spectrum discussed in Section 2.5.2.6.7 could be termed the Seismological Design Spectrum (SDS). This is the ground motion with a mean 10^{-4} annual frequency of exceedance before modification by a design factor as described in Section 2.5.2.6. The SDS represents the maximum elastic responses of a number of damped, single frequency oscillators mounted on small, light pads on the free ground surface. Such small oscillators would not have sufficient mass to cause the modification of the input motion and would probably experience the high accelerations predicted by the SDS.

However, studies have shown that large structures will modify the ground motion and therefore the shaking experienced by these structures would be different than those predicted by the SDS. These studies have also shown that the ground response spectrum obtained from purely seismological considerations (i.e., SDS) have produced ground motions with significant high frequency content in the CEUS. Comparison of spectra obtained from the recorded motions on the basemat of large structures with input motions having high-frequency energy similar to the SDS shows substantial differences (Reference 135); the accelerations calculated from the recorded motions being far less than those of the input motion, particularly in the high frequency range. The reason for this difference is that the ground motions input to the basemat are actually modified by the presence of

large structures and the modifications become significant at higher frequencies, especially above 10 Hz.

Based on these studies, it was concluded that the SDS is an unrealistic input for the analysis and design of structures (Reference 136). In order to obtain a realistic design spectrum, the Engineering Design Spectrum (EDS), factors must be considered that affect the shape of the spectrum experienced by structures with large base mats, such as those typical of nuclear power plants.

Factors that affect the ground motion of the EDS compared to the ground motion of the SDS include the following:

- Horizontal spatial variation and incoherence of the ground motion,
- Vertical spatial variation of the ground motion, scattering effects, and soil-structure interaction.

The first factor is more prominent for structures with large plan dimensions and would reduce the input into the structure at high frequencies. This effect is more pronounced at rock sites. The vertical spatial variation is more prominent at soil sites and again would reduce the amplitude of high frequency motions (Reference 136). Incoherence has been recognized in the national standard for seismic analysis of safety-related structures and significant reductions in the SDS have been recommended (Reference 137).

In addition to the spatial variations of the ground motions, field observations after strong ground motions indicate that the high-frequency accelerations are less damaging to well-engineered structures (Reference 136). This is attributed to the fact that responses to high frequency motions are associated with small displacements and well-engineered structures have ample capacity to dissipate the corresponding limited energy without significant damage. Structures suffer severe damage only when the story drifts are relatively large, as observed during earthquake damage inspections. Large story drifts occur when the energy content of the input motion is high between about 1 and 10 Hz. Above 10 Hz, the energy content is low and the story drifts are small. As a result, the response to high-frequency input motion is essentially elastic and no visible damage occurs. Modification of this nature to the uniform hazard spectrum would be based on the principle of equal risk (i.e., equal factor of safety) across the entire frequency range.

The reduction in spectral accelerations in the high frequency range is also justified considering the responses of the sub-systems. It is known that high frequency content of the ground motion will be visible in the in-structure response spectra, if response analyses are performed with appropriate time steps and refined models. However, these high spectral accelerations are accompanied by small displacements and most sub-systems have adequate energy dissipation capability to accommodate such small displacements without failure. Nonlinear time history analyses demonstrate that these high-frequency motions are less damaging compared to low-frequency motions (Reference 136). Based on these studies, methodology for the reduction of spectral accelerations in the high frequency range have been developed (Reference 136).

Consideration of both the spatial variations of the ground motion and the non-damaging nature of the high frequency content lead to the conclusion that the SDS is only the first step in determining the design spectra for the analysis and design of typical nuclear power plant structures and equipment. The SDS must be modified considering the above factors to obtain the EDS. The EDS represents the proper input into the large nuclear power plant structures.

Another aspect of the high frequency content of the ground motion is the difficulty of capturing these effects as the motions propagate through the structure. Use of the SDS without modification would make it difficult to obtain realistic structural responses, as the analytical methods would have to be much more refined. In addition, structural response is unlikely to be significantly influenced by the high frequency content of the ground motion because of the filtering due to the presence of low natural frequency modes with high participation factors, which is typical for nuclear plant structures. Therefore, a method that will maintain a sufficient degree of accuracy in the predicted seismic responses while obviating the need for such refined modeling would be more practical.

2.5.2.6.10 Approach to Develop the EDS

The selected SSE design response spectrum based on the SDS with a mean 10^{-4} annual frequency of exceedence (and modified by a design factor as discussed in Section 2.5.2.6.7), has, as expected, high spectral accelerations in the high frequency range. The traditional spectra used in the design of nuclear power plants, such as RG 1.60 spectra that were developed from a small set of empirical western U.S. earthquake time histories from generally large earthquakes at generally large distances, have the amplified region between 1 and 10 Hz that is the area of greatest engineering concern for structures. However, the SDS peak for the ESP site occurs around 30 Hz. As discussed above, the high spectral accelerations in the high frequency range are not realistic design bases for the structures, systems and components (SSCs) of nuclear power plants.

The issues discussed above can be effectively addressed by developing an EDS that would take into account plant-specific structural characteristics and site soil conditions as well as the SDS. Because a specific reactor design has not yet been selected, development of the EDS is not included in this ESP application. As part of the COL application, the following information would be provided to develop the EDS:

- Studies on spatial variation of the ground motion would be performed to determine its effects on the spectral accelerations at the site. Such studies would consider the variability in soil data. Both horizontal and vertical spatial variation and incoherence effects would be examined.
- Using the conceptual design data for the safety-related structures of a specific reactor design, the energy dissipation characteristics of these structures, subject to high-frequency ground motions, would be determined. In these evaluations, available experimental and observational data would be used to calibrate the predicted analytical results. The end product would be a frequency-dependent factor that would be applied to the SDS that would produce a uniform factor of safety against failure under seismic loads, across the entire frequency range.

- The Engineering Design Spectrum combining the data from the preceding steps would be developed.

Thus, the EDS would be determined from a synthesis of the site-specific seismic parameters submitted in the ESP application and the plant-specific parameters that would be described in the COL application. The final outcome would be a realistic EDS that would be the input for seismic analysis and design of a specific plant design's SSCs.

2.5.2.7 Operating Basis Earthquake

A detailed analysis was not undertaken to establish the operating basis earthquake (OBE) ground motion. Rather, the simple decision was used to establish the OBE spectrum as one-third of the SSE spectrum in accordance with 10 CFR 50, Appendix S. Figure 2.5-55 plots the OBE spectrum and repeats the plot of the SSE spectrum presented in Figure 2.5-48. These spectra are based on 5 percent of critical damping, as are all other spectra presented in Section 2.5.2.

2.5.3 Surface Faulting

There is no potential for tectonic fault rupture and there are no capable tectonic sources within the 5-mile radius of the ESP site. A capable tectonic source is a tectonic structure that can generate both vibratory ground motion and tectonic surface deformation, such as faulting or folding at or near the earth's surface in the present seismotectonic regime (Reference 2). The following sections provide the data, observations, and references to support this conclusion. Information contained in these sections was developed in accordance with RG 1.165 (Reference 2), and is intended to satisfy 10 CFR 100.23, "Geologic and Seismic Siting Criteria" (Reference 4).

2.5.3.1 Geological, Seismological, and Geophysical Investigations

The following investigations were performed to assess the potential for surface fault rupture at and within a 5-mile radius of the ESP site:

- Compilation and review of existing data
- Interpretation of aerial photography
- Field reconnaissance
- Aerial reconnaissance
- Review of seismicity
- Discussions with current researchers in the area

An extensive body of existing information is available for the ESP site. This information is contained in three principal sources:

1. Work performed for the existing units (Reference 5) (Reference 7); abandoned Units 3 and 4 (Reference 9); and the ISFSI (Reference 6). These studies and their results were reviewed and accepted by the NRC (AEC) as part of previous licensing efforts for these facilities.
2. Published and unpublished geologic mapping performed primarily by the USGS and the Virginia Division of Mineral Resources.
3. Seismicity data compiled and analyzed in published journal articles and, more recently, as part of this ESP application (discussed in Section 2.5.2.1).

The existing information was supplemented by aerial and field reconnaissance efforts within the 25-mile radius ESP site vicinity and interpretation of aerial photography along all known faults within the 5-mile radius ESP site area. These studies were performed to verify, where possible, the existence of mapped bedrock faults in the site area and to assess the presence or absence of geomorphic features indicative of potential Quaternary fault activity along the mapped faults.

2.5.3.1.1 Previous Site Investigations

Previous site investigations performed for the existing units are summarized in the UFSAR (Reference 5). As cited in the UFSAR, these previous investigations provide the following results documenting the absence of Quaternary faults at and within the area of the ESP site:

1. Interpretation of air photos and topographic maps. This interpretation revealed no evidence of surface rupture, surface warping, or the offset of geomorphic features indicative of active faulting.
2. Seismicity analysis. This analysis showed that no macroseismic activity has occurred in the site area; the closest epicentral location is about 30 miles (50 km) away.
3. Detailed geologic mapping and inspection of excavations during construction. This mapping revealed no evidence of geologically recent or active faulting.
4. Borings drilled at the site. Borehole data has provided evidence of the continuity of strata across the site and the inspection of soil samples and rock core has revealed no adverse effects indicative of geologically recent active faulting.

Subsequent to the initial site investigations performed for the existing units and abandoned Units 3 and 4, a minor bedrock fault associated with a chlorite seam was encountered during foundation excavations for the abandoned Units 3 and 4. This prompted a comprehensive trenching, mapping, and soil stratigraphic study to evaluate the recency of movement of the fault. This study documented the absence of Quaternary deformation along the minor bedrock fault (Reference 9), demonstrating that the fault is not capable in accordance with 10 CFR 100, Appendix A, criteria at that time. The results and conclusions of this study were reviewed and accepted by the NRC (AEC) (Reference 108).

At the time of the original studies for NAPS in 1973 (Reference 9), there were no published maps showing bedrock faults within a 5-mile radius of the site. The closest significant bedrock faults mapped prior to 1973 were the border faults of the Triassic Culpeper Basin approximately 20 miles (32 km) west-northwest of the site (Reference 7).

Since 1973, extensive mapping of the Virginia Piedmont Province, principally by Louis Pavlides of the USGS, has greatly improved knowledge of the bedrock stratigraphy and structure within the area of the ESP site. The Piedmont mapping by Pavlides is incorporated in the Fredericksburg 1:100,000 scale map by Mixon and others (Reference 66), a portion of which comprises Figure 2.5-11. This mapping provides the principal basis for the recognition of bedrock faults within the site area.

In addition, the USGS recently completed a compilation of all Quaternary faults, liquefaction features, and possible tectonic features in the eastern United States (Reference 59). This compilation does not show any Quaternary faults within a 5-mile radius of the site. The nearest

Quaternary features summarized by Crone and Wheeler (Reference 59) are two paleo-liquefaction sites documented by Obermeier and McNulty (Reference 71) on the James and Rivanna Rivers within the Central Virginia seismic zone (discussed in Section 2.5.2.2.8). Both of these sites are located over 25 miles from the ESP site.

2.5.3.2 **Geological Evidence, or Absence of Evidence, for Surface Deformation**

As shown on Figure 2.5-11, seven bedrock faults are mapped within pre-Cambrian and Paleozoic rocks within 5 miles of the ESP site (Reference 66) (Reference 105). These seven bedrock faults are:

- Chopawamsic fault
- Spotsylvania thrust fault
- Unnamed fault traversing the North Anna site (fault “a”)
- Sturgeon Creek fault
- Long Branch thrust fault
- Unnamed fault separating the Ta River Metamorphic Suite from the Quantico Formation (fault “b”)
- Unnamed fault separating the Northeast Creek pluton from the Quantico Formation (fault “c”)

No deformation or geomorphic features indicative of potential Quaternary activity have been reported in the literature for these faults, and none were identified during aerial and field reconnaissance and air photo interpretation undertaken for the current ESP study. Several of the faults may have been locally reactivated during the Triassic episode of continental rifting (discussed in Section 2.5.1.1.4); although, none of these faults border Triassic basins, indicating that Triassic reactivation, if any, was not significant enough to produce a Triassic basin or depocenter.

The unnamed bedrock fault (“a”) that traverses the North Anna site was exposed during foundation excavations for abandoned Units 3 and 4. Detailed investigations of this fault (Reference 9) provide direct evidence for the absence of Quaternary faulting (discussed in Section 2.5.3.2.2). Thus, this fault is not a capable tectonic source, a position supported by the NRC (AEC) (Reference 108).

2.5.3.2.1 **Chopawamsic and Spotsylvania Thrust Faults**

The Chopawamsic and Spotsylvania thrust faults bound the eastern and western margins of the Chopawamsic belt, respectively. These two faults are regional Appalachian structures that have been mapped for tens of miles within the Piedmont Province (Reference 66). The Chopawamsic belt is interpreted to be an island-arc accreted to the North American continent during the Paleozoic age Taconic orogeny (discussed in Section 2.5.2.1.1).

The Chopawamsic thrust fault is located about 4.5 miles (7 km) northwest of the site and strikes north to northeast (Figure 2.5-11). It is interpreted to be a thrust fault that transported the island-arc

Chopawamsic belt westward onto the Mine Run Complex (discussed in Section 2.5.1.1.2) (Reference 40). Due to the fault's minimal exposure, there is little direct evidence for the continuity of the fault (Reference 66). However, interpretations of a thrust fault within a seismic reflection profile that was run along Interstate I-64 (Reference 103) indicate that this structure may extend for a distance of over 45 miles (70 km) (Reference 40).

The Spotsylvania thrust fault is located about 4.5 miles (7 km) southeast of the site (Figure 2.5-11). This northeast-striking fault is well documented by aeromagnetic and aero-radiometric data (Reference 138) (Reference 37). The fault juxtaposes rocks of the Ta River Metamorphic Suite (Chopawamsic belt) on the west against rocks of the Po River Metamorphic Suite (Goochland belt) on the east, but is not exposed at the surface within the Fredericksburg 1:100,000 quadrangle (Reference 66). The fault is defined by a 1.5-mile wide zone of faulting rather than a single fault (Reference 105) (Reference 37). The Spotsylvania thrust fault was first recognized as an aeromagnetic and aero-radiometric lineament (Reference 138), and initially was referred to as Neuschel's Lineament. Specific studies of this feature by Dames & Moore (Reference 139) demonstrate that the Spotsylvania thrust fault exhibits negligible vertical deformation of a pre- to early-Cretaceous erosion surface and is not related to Tertiary faulting along the younger Stafford fault zone (discussed in Section 2.5.1.1.4). The fault was determined by the NRC (AEC) to be not capable within the definition of 10 CFR 100, Appendix A (Reference 140). The Spotsylvania fault is also referred to as the Spotsylvania high-strain zone, which may connect southwest to the Hyco and Central Piedmont shear zones as a major structural boundary for a total length of over 300 miles (480 km) in the southern Appalachians (Reference 35).

The Chopawamsic and Spotsylvania thrust faults are not associated with seismicity and do not exhibit geomorphic evidence of potential Quaternary activity. In their recent compilation of Quaternary faults in the eastern United States, Crone and Wheeler (Reference 59) do not show either fault as a Quaternary feature. Therefore, it is concluded that these faults are not capable tectonic sources within the area of the ESP site.

2.5.3.2.2 Unnamed Fault Traversing the North Anna Site

As previously indicated, an unnamed fault (fault "a") was discovered in the foundation excavations for the abandoned Units 3 and 4 (Figure 2.5-11). A comprehensive study was performed by Dames & Moore (Reference 9) to evaluate the fault's location, geometry, and age. This study included detailed mapping of the excavation exposures, three fault trenches, interpretation of aerial photography, and a detailed soil profile analysis. Based on geologic mapping and trenching, the fault was mapped for a distance of about 3000 feet (Figure 2.5-18) (Plate 3 of Reference 9). Dames & Moore (Reference 9) concluded that the fault was not capable, in accordance with 10 CFR 100, Appendix A criteria, based on the following conditions:

- Direct evidence of no displacement of saprolitic soils in excess of 1 million years old
- Absence of geomorphic expression

- Potassium/argon (K/Ar) dating of chlorite infilling along the fault ranging from 214 to 303 million years old

In 1974, the NRC (AEC) issued Supplement No. 3 to the Safety Evaluation for Units 3 and 4, accepting the conclusion that the fault is not capable (Reference 106). Specifically, the NRC (AEC) made the following statement:

Regarding the age and most recent movement on the fault zone: The most recent movement on the fault zone occurred at least one to two million years ago according to dating of overlying saprolites and probably more that 200,000,000 years ago during the last significant tectonism in the Virginia Piedmont Province, which occurred in the Triassic Period. The major events associated with this tectonism were the emplacement of diabase dikes and the formation of down-faulted sedimentary basins. Earthquakes in the Piedmont Province do not correlate with known tectonic structures. No historic earthquake in this province has been known to cause faulting at or near the surface. The North Anna fault zone is neither genetically nor structurally related to any known, capable fault. Thus the staff concludes that the faults are not "capable" as defined by Appendix A of 10 CFR Part 100.

Subsequent to the Dames & Moore (Reference 9) site investigation, Pavlides (Reference 36) (Reference 141) extended this fault farther north and south of the North Anna site, for a total length of about 7 miles (11 km) (Figure 2.5-11). Aerial reconnaissance, field reconnaissance and air photo interpretation carried out for this ESP application, however, did not reveal any evidence for the existence of the fault as mapped by Pavlides. Bedrock exposures are poor to non-existent along the entire length of the fault, and there is no geomorphic expression of the fault trace. Since 1973, no new information has been published that would suggest potential Quaternary activity of the fault at the site. The absence of geomorphic expression along the entire fault length, as mapped by Pavlides (Reference 36), combined with the original Dames & Moore study (Reference 9) and investigations carried out for this ESP, support the interpretation that the fault traversing the North Anna site is not a capable tectonic source and that the position previously expressed by the NRC (AEC) (Reference 106) remains valid.

2.5.3.2.3 **Sturgeon Creek Fault**

The Sturgeon Creek fault is located about 1.2 miles (2 km) northwest of the site (Figure 2.5-11). The fault has a strike of about N70°E in the vicinity of Sturgeon Creek, but changes to a more southerly strike of N30-40°E south of the North Anna River, where it becomes coincident with the axial region of the Quantico synclinorium along Freshwater Creek (Reference 66). The fault, which has a mapped length of 10.5 miles (17 km), sinistrally displaces the faulted contact between the Quantico Formation and Ta River Metamorphic Suite by about 1.4 miles (2 km). More recent mapping to the south does not extend the Sturgeon Creek fault into the adjacent Richmond 1:100,000 scale map sheet (Reference 105) (Figure 2.5-11).

Field and aerial reconnaissance and interpretation of aerial photography carried out for this ESP application shows that there are no geomorphic features indicative of potential Quaternary activity along the fault and that the fault does not appear to offset any Quaternary surficial deposits. A linear reach of Freshwater Creek is present locally along the fault, but this appears likely to be a result of straightening by man, perhaps related to earlier mining operations. Based on the absence of geomorphic expression, absence of seismicity, and absence of offset of Quaternary surficial deposits it is concluded that the Sturgeon Creek fault is not a capable tectonic source.

2.5.3.2.4 Other Faults Within the Chopawamsic Terrane

Three other bedrock faults are mapped within the Chopawamsic terrane within 5 miles of the ESP site. These are the Long Branch thrust fault and two unnamed faults: one that juxtaposes the Quantico Formation against the Ta River Metamorphic Suite (fault "b"), and another that juxtaposes the Quantico Formation against the Northeast Creek pluton (fault "c") (Figure 2.5-11).

The Long Branch thrust fault, which borders the Quantico Formation on the northwest side, has a mapped length of over 45 miles (70 km) across the Fredericksburg and Richmond map sheets (Reference 66) (Reference 105). The fault is located about 2.2 miles (3.5 km) west of the site and strikes about N30°E. It is thought that the westward thrusting of the Long Branch fault began near the end of the Allegheny orogeny after much of the regional Allegheny amphibolite grade metamorphism had occurred (Reference 40). The Long Branch thrust fault is locally dextrally displaced by other minor bedrock faults within the Chopawamsic belt at distances beyond the 5-mile radius from the site area (Reference 66).

The two unnamed faults ("b" and "c") are located east of the Long Branch thrust fault, approximately 1 and 4 miles (1.5 and 6.5 km) west and north of the site, respectively (Figure 2.5-11). The longer of the two faults (fault "b") juxtaposes the Quantico Formation on the west with rocks of the Ta River Metamorphic Suite and the Elk Creek and Northeast Creek plutons on the east. This fault is mapped for a total distance of about 16 miles (26 km), is offset by the Sturgeon Creek fault, and is truncated at its northern end by unnamed fault "c" (Reference 66) (Reference 105). Unnamed fault "c" has a mapped length of 3.4 miles (5.5 km) and juxtaposes the Northeast Creek pluton against the Quantico Formation (Figure 2.5-11).

None of the faults described above are associated with any gravity or magnetic anomaly, or any seismicity, nor do they exhibit any geomorphic or Quaternary stratigraphic evidence of recent activity. Therefore, it is concluded that the Long Branch thrust fault and the two unnamed faults are related to the Paleozoic tectonic regime and are not capable tectonic sources.

2.5.3.3 Correlation of Earthquakes with Capable Tectonic Sources

No reported historical earthquake epicenters have been associated with bedrock faults within the 25-mile radius of the ESP site vicinity (Figure 2.5-56). Micro-earthquake monitoring for NAPS was initially conducted over a 2.5-year period from January 21, 1974, to August 1, 1976, and was

subsequently extended an additional year to August 1, 1977 (Reference 142). The purpose of the monitoring program was to determine if seismic activity could be associated with faults in the site area or if Lake Anna was producing reservoir-induced seismicity. Micro-earthquakes detected in the 3.5 years of monitoring could not be associated either with faults in the site area or with the impoundment of Lake Anna (Reference 5) (Reference 143) (Reference 144).

Four stations of the original 17-station network were incorporated into Virginia Polytechnic Institute and State University's Central Virginia Monitoring Network for the specific purpose of monitoring any changes in seismicity in the region of NAPS. To date, no changes in local earthquake occurrence have been observed that would alter the conclusions reached in 1977 regarding the lack of association of micro-earthquakes with the presence of Lake Anna or with faults in the site area. Micro-earthquakes observed in the site area appear to be part of, or are occurring at, a level no greater than the spatially varying background activity found in the Central Virginia seismic zone.

2.5.3.4 Ages of Most Recent Deformations

As discussed in Section 2.5.3.2, none of the seven faults within 5 miles of the ESP site exhibit evidence of Quaternary activity. All of the faults formed during the Paleozoic Era as part of the regional Taconic orogeny, and locally they may have been reactivated during the later Paleozoic Acadian and Allegheny orogenies or during Triassic continental rifting (discussed in Section 2.5.1.1.4). Based on a review of the available literature, no studies have been published that suggest or document post-Triassic activity on any of these structures. Therefore, the seven bedrock faults mapped within 5 miles of the site are considered to be old structures that formed during the Paleozoic age Appalachian orogenies or early Mesozoic age rifting.

2.5.3.5 Relationship of Tectonic Structures in the Site Area to Regional Tectonic Structures

The seven faults identified in the site area are located within the Chopawamsic belt, which is interpreted to be an island-arc that was accreted to North America during the Middle to Late Ordovician Taconic orogeny. Following accretion, rocks of the Chopawamsic belt and other rocks of the Piedmont Province were deformed and thrust westward during the Acadian and Allegheny orogenies that occurred from Devonian to Permian time. Locally, these rocks may also have been affected by extensional tectonics during Triassic rifting (discussed in Section 2.5.1.1.4).

As described in Section 2.5.3.2, the Chopawamsic, Spotsylvania, and Long Branch thrust faults are regional easterly-dipping faults that extend northeast and southwest of the site for tens of miles. The four other faults within the site area are much shorter in length and are located within the Appalachian thrust sheets and, therefore, do not represent structures that penetrate deep into the crust (discussed in Section 2.5.1.1.4).

2.5.3.6 Characterization of Capable Tectonic Sources

Based on previous discussions, there are no capable tectonic sources within 5 miles of the ESP site.

2.5.3.7 Designation of Zones of Quaternary Deformation Requiring Detailed Fault Investigation

There are no zones of Quaternary deformation requiring detailed investigation within the site area. A zone of minor faulting associated with chlorite seams (fault "a") was encountered in the foundation excavation for abandoned Units 3 and 4. Investigation of this minor fault showed that the zone of faulting is not capable (Reference 9) (Reference 108), in accordance with 10 CFR 100, Appendix A. Subsequent air photo interpretation, aerial reconnaissance, and field reconnaissance of the fault trace carried out for this ESP application confirms the conclusion reached by Dames & Moore (Reference 9), and no further investigation of this fault is considered necessary.

2.5.3.8 Potential for Tectonic or Non-Tectonic Deformation at the Site

The potential for tectonic deformation at the site is negligible. Since the original site studies in the early 1970s, no new information has been reported to suggest the existence of any Quaternary surface faults or capable tectonic sources within the site area. In addition, there is no evidence of non-tectonic deformation at the site, such as glacially induced faulting, collapse structures, growth faults, salt migration, or volcanic intrusion.

2.5.4 Stability of Subsurface Materials and Foundations

This section presents information on the stability of subsurface materials and foundations at the ESP site. The information has been developed in accordance with Review Standard RS-002, "Processing Applications for Early Site Permits" (Reference 145), following the guidance presented in RG 1.70, Section 2.5.4 (Reference 3), and the regulatory guides referenced in the subsections that follow. This geological, geophysical, geotechnical and seismological information is used as a basis to evaluate the stability of subsurface materials and foundations at the site.

Information presented in this section was developed from a review of reports prepared for the existing units and abandoned Units 3 and 4, geotechnical literature, and a subsurface investigation conducted for preparation of this ESP. Reports reviewed include the UFSAR (Reference 5) and the ISFSI Safety Analysis Report (Reference 6). Reports prepared by Dames and Moore for design and construction of the existing units (Reference 146) and the abandoned Units 3 and 4 (Reference 8) (Reference 9) were also reviewed.

The additional field and laboratory investigations performed for the ESP were intended to confirm the already large volume of geotechnical data developed for the existing units and the abandoned Units 3 and 4 within the ESP site area. Additional structure-specific exploration and testing would be performed during detailed engineering and would be described in the COL application.

2.5.4.1 Geologic Features

Section 2.5.1.1 describes the regional geology, including regional physiography and geomorphology, regional geologic history, regional stratigraphy, and the regional tectonic setting. Section 2.5.1.2 addresses site-specific geology and structural geology, including site physiography and geomorphology, site geologic history, site stratigraphy, site structural geology, and a site geologic hazard evaluation.

2.5.4.2 Properties of Subsurface Materials

2.5.4.2.1 Introduction

This section describes the static and dynamic engineering properties of the ESP site subsurface materials. An overview of the subsurface profile and materials is given in Section 2.5.4.2.2. The field investigations, described in Section 2.5.4.3, are summarized in Section 2.5.4.2.3. The saprolitic soils were studied in the investigation for the existing units. However, a more intensive investigation of these materials was undertaken during construction of the existing units when larger-than-expected settlements were recorded at the SWR pump house. Many undisturbed samples were recovered during these investigations, and laboratory testing included extensive dynamic as well as static testing. These tests and their results are summarized in Section 2.5.4.2.4, along with laboratory testing performed recently for the ESP investigation. The engineering properties of the subsurface materials are presented in Section 2.5.4.2.5.

2.5.4.2.2 Description of Subsurface Materials

Dames and Moore (Reference 146) (Reference 8) divided the site soils into five zone categories:

- I Residual clays and clay silts – all structures of parent rock are lost
- IIA Saprolite – core stone less than 10 percent of volume of overall mass
- IIB Saprolite – core stone 10 to 50 percent of volume of the overall mass
- III Weathered rock – core stone more than 50 percent of volume of the overall mass
- V Parent rock – slightly weathered to fresh rock below zone of isolated core stones

These zones have worked as a successful means for classifying the soil and rock with regard to engineering properties. This zone system was used in the UFSAR for the existing units and is also used in this ESP SSAR.

The materials overlying the parent Zone IV rock represent a continuously more pronounced form of in-place weathering. Both Dames and Moore and the UFSAR adopted an additional zone, termed Zone III-IV, to represent this slightly to moderately weathered rock. The Zone III-IV terminology is also used in this ESP application.

The following is a brief description of the subsurface materials, giving the soil and rock constituents, and their range of thickness encountered at the site. The information was taken from the 140 borings made to date at the site (outlined in Section 2.5.4.3.1). For reference, the existing site elevations in the areas explored range from about Elevation 250 to 330 feet, with a median of about Elevation 290 feet. The plant grade of the existing units is Elevation 271 feet. This is the powerblock elevation used for the new units. The engineering properties are provided in Section 2.5.4.2.5.

a. Zone IV Bedrock

The Zone IV bedrock is fresh to slightly weathered gneiss bedrock. Gneiss is a metamorphic rock that exhibits a banded texture (foliation) in which light and dark bands alternate. It is composed of feldspar, quartz, and one or more other minerals such as mica and hornblende. The recently completed ESP investigation (Reference 147, reproduced as Appendix 2.5.4B) describes the bedrock as a quartz gneiss with biotite (a dark mica) in the majority of cores, but also references biotite quartz gneiss and occasionally biotite gneiss. A detailed description of the bedrock is contained in Section 2.5.1.2.3.

The top of Zone IV (including Zone III-IV) bedrock encountered in the borings made at the ESP site range from Elevation 188 feet to 298 feet. Typical depths are illustrated on the subsurface profiles on Figure 2.5-57 and Figure 2.5-58. The locations of these profiles are shown on Figure 2.5-61.

b. Zone III Weathered Rock

The weathered rock has the same constituents as the parent rock. It is described as moderately to highly weathered rock, sometimes with unweathered seams and sometimes with high fracture frequency. It is defined as having at least 50 percent core stone.

The top of Zone III bedrock encountered in the borings made at the site range from Elevation 205 feet to 298 feet. The maximum thickness measured is 67 feet. Typical depths are illustrated on the subsurface profiles on Figure 2.5-57 and Figure 2.5-58.

c. Zone IIA and IIB Saprolites

Saprolites are a further stage of weathering beyond weathered rock. Saprolites have been produced by the disintegration and decomposition of the bedrock in place and have not been transported. Saprolites are classified as soils but still contain the relict structure of the parent rock, and they typically still contain some core stone of the parent rock. The ESP site saprolites in many instances maintain the foliation characteristics of the parent rock. They are classified primarily as silty sands, although there are also sands, clayey sands, sandy silts, clayey silts and clays, depending very much on their degree of weathering. The fabric is anisotropic. The texture shows angular geometrically interlocking grains with a lack of void network, very unlike the well-pronounced voids found in marine or alluvial sands and silts.

The distribution of the Zone IIA and IIB saprolites varies throughout the site. On average, the Zone IIB saprolites represent about 20 percent of the saprolites on site and are typically very dense silty sands with from 10 to 50 percent core stone. These soils were even rock-cored in some of the borings during the earlier investigations (Reference 8). The thickest Zone IIB deposit encountered in the borings was 37 feet.

The overlying Zone IIA saprolites comprise, on average, about 80 percent of the saprolitic materials on site. About 75 percent of the Zone IIA saprolites are classified as coarse grained (sands, silty sands), while the remainder are fine grained (clayey sands, sandy and clayey silts, and clays). A detailed breakdown of these percentages is given in Table 2.5-29. The saprolites typically become finer toward the ground surface. The thickest Zone IIA deposit encountered in the borings was 101 feet.

d. Zone I and Fill

There is typically very little of the Zone I residual soil onsite—on average, less than 1 percent of the soil is Zone I. The Zone I soils are either at the surface or are immediately below fill placed during construction of the earlier units. This fill is generally made up of Zone IIA soils. For any future foundations, Zone I soils and existing fills would be excavated. Thus, they are not considered further here.

e. Subsurface Profiles

Figure 2.5-57 and Figure 2.5-58 illustrate typical subsurface profiles across the powerblock area proposed for the ESP. The locations of these profiles are shown in Figure 2.5-61. These profiles are discussed with respect to excavation for the new units in Section 2.5.4.5 and for bearing capacity considerations in Section 2.5.4.10.

2.5.4.2.3 Field Investigations

The exploration programs performed previously for the existing units and abandoned Units 3 and 4, the SWR, and the ISFSI, and new investigations for the ESP site are described in Section 2.5.4.3. The borings from previous explorations are summarized in Table 2.5-30 through Table 2.5-37. The borings, observation wells, and cone penetrometer tests from the ESP site exploration program are summarized in Table 2.5-38 and Table 2.5-39. The soil sampling and rock coring results are summarized in Table 2.5-40 and Table 2.5-41. Previous geophysical surveys and new surveys for the ESP are described in Section 2.5.4.4.

2.5.4.2.4 Laboratory Testing

As with the field exploration, numerous laboratory tests of soil and rock samples were performed previously for the existing units and new tests have been performed for the ESP site investigation. The types and numbers of these tests are shown in Table 2.5-42. Note that the large majority of the tests on the Zone IIA saprolitic soils were performed for the various SWR investigations. The following paragraphs focus on these SWR tests and on the tests performed recently for the ESP site subsurface investigation.

a. Laboratory Tests for SWR

The laboratory testing of the SWR soils focused on the strength, compressibility and liquefaction potential of the Zone IIA saprolites. A large number of undisturbed thin-walled tube samples were taken. Thin sections were made from five undisturbed samples to assess the fabric, texture, and mineralogy of the saprolite. One of the boreholes was angled in an attempt to obtain undisturbed samples for unconsolidated-undrained (UU) triaxial tests perpendicular to the foliation of the saprolite. The laboratory tests are summarized in the following paragraphs.

1. Cyclic Triaxial Tests

Between November 1975 and June 1976, Geotechnical Engineers, Inc. (GEI) of Winchester, Massachusetts, performed 18 stress-controlled consolidated-undrained cyclic triaxial tests on undisturbed samples from 11 borings located on or adjacent to the SWR dike. Three tests were aborted due to testing/equipment failure. The 15 remaining tests were run primarily to provide input for liquefaction analysis of the soils beneath the SWR dike.

It should be noted that these tests were conducted by one of the country's premier geotechnical firms during the period when cyclic triaxial testing was at its zenith. This type of testing declined appreciably during the 1980s when field test results became the accepted input into liquefaction analysis. By the 1990s it was difficult to find a testing laboratory with the equipment or experience to perform these tests. In short, it would be difficult to obtain the quality of these GEI cyclic triaxial test results today.

Appendix 2.5.4A contains the details and results of the testing. This portion of the appendix is made up from parts of UFSAR Appendix E, Attachments 1 through 4. It contains the following information for each of the 15 tests:

- A summary table of the details and results of each test
- A plot of octahedral shear stress ratio versus number of cycles to reach 5 percent maximum compressive strain
- A plot of octahedral shear stress ratio versus consolidation stress
- Detailed visual descriptions of each of the samples
- Grain size curves of each of the test samples
- Plots of cyclic axial strain (compression, double amplitude and extension) versus cycle number for each of the tests

2. Static Triaxial Tests

Eight consolidated-undrained triaxial compression tests with pore pressure measurements were performed on undisturbed samples from SWR borings. The results of these tests are tabulated in Appendix 2.5.4A. Five of the tests were run on the in-situ Zone IIA saprolite, while three were conducted on compacted dike fill. Three of the in-situ saprolite samples failed along foliation planes.

Eighty undisturbed thin-walled tube samples were later obtained from borings on or close to the SWR dike. Sixty-two unconsolidated-undrained triaxial tests were performed on samples from these tubes. Details and results of these tests are tabulated in Appendix 2.5.4A. The table includes the mode of failure of each sample.

This portion of the appendix is made up of parts of Appendix E and UFSAR Appendix E, Attachment 4.

3. Consolidation Tests

Fifteen one-dimensional consolidation tests were performed on undisturbed samples from SWR borings. Tests were run at both constant rate of strain and by incremental loading. Non-plastic samples (which included most of the samples) were tested in sections cut from the thin-walled sampling tubes. Details and results of these tests are tabulated in

Appendix 2.5.4A. This portion of the appendix is made up from parts of UFSAR Appendix E.

4. Thin Sections

Twenty-seven thin sections from undisturbed samples from five borings were examined under plane and polarized light at magnifications up to 400X, to determine in a qualitative manner the fabric, texture, and mineralogy of the saprolite beneath the SWR dike.

The descriptions of the fabric, texture, and mineralogy of the Zone IIA saprolite contained in the UFSAR Appendix 3E, Attachment 4, are included in Appendix 2.5.4A.

b. Laboratory Tests for ESP

The laboratory testing for the ESP investigation was performed in accordance with the guidance presented in RG 1.138 (Reference 148), including Draft RG DG-1109 (Reference 149). The laboratory work was performed under an approved quality program with work procedures developed specifically for the ESP project. Soil and rock samples were shipped under chain-of-custody protection from the storage area (described in Section 2.5.4.3.2) to the testing laboratory. If required, samples were further divided and/or shipped to the appropriate testing laboratory under chain-of-custody rules. Laboratory testing was performed at the MACTEC laboratories in Raleigh, North Carolina (all soil testing except chemical analysis), and Atlanta, Georgia (all rock testing), and at Severn Trent Laboratory in Savannah, Georgia (chemical analysis).

The types and numbers of laboratory tests performed on the soil samples and rock cores from the ESP exploration program are included on Table 2.5-42. The numbers of tests were purposely limited in light of the large number of tests performed for previous investigations. The ESP tests focused primarily on the following tasks:

- Verifying the basic properties of the Zone IIA saprolite (e.g., grain size)
- Obtaining chemical test results on the Zone IIA saprolite (for corrosiveness toward buried steel and aggressiveness toward buried concrete)
- Obtaining additional strength and elastic modulus data for the bedrock on which the main safety-related structures would be founded

The details and results of the laboratory testing are included in Appendix 2.5.4B. Appendix 2.5.4B includes references to the industry standards used for each specific laboratory test. The results of the tests on soil samples are shown on Table 2.5-43. All of the samples tested are in-situ Zone IIA saprolite, except the three samples from B-801 (fill), and the bottom two samples from B-807 (Zone IIB saprolite). Table 2.5-44 summarizes the results of the unconfined compression tests on the rock cores. The ESP laboratory test results were similar to those obtained in the previous testing.

2.5.4.2.5 Engineering Properties

The engineering properties for Zones IIA, IIB, III, III-IV, and IV, derived from the previous studies and from ESP field exploration and laboratory testing programs, are provided in Table 2.5-45. The engineering properties obtained from the ESP field exploration and laboratory testing program were similar to those obtained from the previous field and laboratory testing programs.

The following paragraphs briefly describe the sources and/or methods used to develop the selected properties shown in Table 2.5-45.

a. Rock Properties

The Recovery and Rock Quality Designations (RQD) are based on the results provided in Table 2.5-41. The unconfined compressive strength is based on the ESP rock strength results shown in Table 2.5-44 and the rock strengths from the investigations for the existing units (Reference 146). The unit weight is based on the values measured in the ESP rock strength tests (Appendix 2.5.4B).

The elastic modulus values are based on the values shown in Table 2.5-44. These values agree well with those derived from the geophysical tests performed for the ESP exploration program as described in Section 2.5.4.4.2. The shear modulus values are derived from the elastic modulus values using the Poisson's ratio values tabulated in Table 2.5-45, which are based on the values provided in Table 2.5-44. Low and high strain modulus values are essentially the same for high strength rock that is, for the Zone IV rock. Similarly, no strain softening is assumed for the Zone III-IV rock. Some strain softening has been allowed for the Zone III rock. Low strain is defined here as 10^{-4} percent while high strain is taken as 0.25 to 0.5 percent, the amount of strain frequently associated with settlement of structures on soil.

The shear and compression wave velocities are based on the cross-hole and down-hole seismic tests performed as part of the ESP exploration program (Appendix 2.5.4B). These results are in agreement with the results of the geophysical tests performed for the existing units (Reference 146), and are summarized in Section 2.5.4.4.2.

b. Soil Properties

Grain size curves from 13 sieve analyses of Zone IIA silty sand samples from the ESP laboratory testing program (Appendix 2.5.4B) fit within the envelope of the 12 sieve analyses of Zone IIA silty sands sampled from borings near the SWR pump house (Reference 5, Figure 3.8-51). The range of fines in Table 2.5-45 for the coarse-grained Zone IIA soil is from these curves.

The natural moisture content of the fine-grained Zone IIA saprolite is the median value of 108 moisture content tests performed on fine-grained Zone IIA saprolites for the existing units, SWR, ISFSI, and ESP investigations. The range of moisture content in these tests was 14 to 56 percent.

The undrained shear strength of the fine-grained Zone IIA saprolite is estimated from SPT N-values and CPT results, as well as from the results of 18 unconsolidated-undrained triaxial compression tests and three unconfined compression tests. The effective strength parameters for the fine-grained saprolite are based on the results of consolidated-undrained triaxial tests on fine-grained saprolite run for the ISFSI and SWR investigations.

The effective angle of internal friction of the medium dense coarse-grained saprolite (N = 20 blows/foot) would typically be taken as around 35 degrees (Reference 150). However, the high silt content and the presence of low plasticity clay minerals reduce this angle. Consolidated-undrained triaxial tests reported in UFSAR Appendices 2C and 3E produced internal friction angles ranging from 23 to 33 degrees, with a median of 30.8 degrees. Thus, an angle of 30 degrees was selected. The average effective cohesive component from the Appendix 2C tests was 0.275 kps per square foot (ksf). A value of 0.25 ksf was selected for the cohesive component.

A large amount of testing was performed after low unit weights were measured in the Zone IIA saprolites in the SWR area (Reference 5, Appendix 3E, Attachment 4). It is concluded that there are isolated lower densities, but these are not typical. UFSAR Table 3.8-13 identifies 125 pounds per cubic foot (pcf) as a design total unit weight. The 130 pcf used in Table 2.5-45 for the Zone IIB saprolites reflects the high relative density of that material.

The SPT design N-value of 20 blows/foot for the Zone IIA saprolite is conservatively based on the results reported in Table 2.5-40. Those results show median N-values for the ESP and ISFSI investigations of 21 blows/foot, with the median N-values for the existing units, abandoned Units 3 and 4, and SWR investigations, ranging from 25 to 52 blows/foot.

The shear wave velocities measured in the ESP cross-hole seismic tests (Appendix 2.5.4B) in the Zone IIA sandy silt from 7.5 to 27 feet depth range from 650 to 1350 fps, with an average of 998 fps. The CPT seismic results are somewhat higher. The UFSAR has a value of 950 fps for the Zone IIA saprolite. The 950 fps average value has been selected for the Zone IIA saprolite in Table 2.5-45. This is discussed in more detail in Section 2.5.4.7.1.

For the Zone IIB saprolite, the shear wave velocity derived from the low strain value of shear modulus is in good agreement with the results from the CPT seismic tests, at around 1600 fps. The profile of shear wave velocity versus depth for the saprolite is given in Section 2.5.4.7.

The high strain (i.e., in the range of 0.25 to 0.5 percent) elastic modulus values for the coarse-grained Zone IIA saprolite and the Zone IIB saprolite have been derived using the relationship with SPT N-value given in Davie and Lewis (Reference 151). The high strain elastic modulus for the fine-grained Zone IIA saprolite has been derived using the relationship with undrained shear strength given in Davie and Lewis (Reference 151). The Zone IIA coarse and fine-grained values have been adjusted slightly to obtain a common value. The shear

modulus values have been obtained from the elastic modulus values using the relationship between elastic modulus, shear modulus and Poisson's ratio (Reference 150).

The low strain (i.e., 10^{-4} percent) shear modulus for the Zone IIA saprolite has been derived from the shear wave velocity of 950 fps. The low strain shear modulus of the Zone IIB saprolite has been derived from the shear wave velocity of 1600 fps. The elastic modulus values have been obtained from the shear modulus values using the relationship between elastic modulus, shear modulus, and Poisson's ratio (Reference 150).

The recompression ratio and the coefficient of secondary compression are the values derived from the settlement studies performed for the SWR pump house, as detailed in UFSAR Appendix 3E.

The values of unit coefficient of subgrade reaction are based on values for medium dense sand (Zone IIA saprolite) and very dense sand (Zone IIB saprolite) provided by Terzaghi (Reference 152).

The earth pressure coefficients are Rankine values, assuming level backfill and a zero friction angle between the soil and the wall.

c. Chemical Properties

Chemical tests were performed on selected Zone IIA samples. In addition to the tests performed for the ESP investigation (results shown in Table 2.5-43), chemical tests were previously performed on two samples from the subsurface investigation for the existing units (Reference 146). The six pH test results ranged from 5.7 to 6.9, in the mildly corrosive to neutral range. The six sulfate test results ranged from about 1 to 28 parts per million (ppm), which indicates no aggressiveness toward concrete. Three of the chloride test results ranged from 100 to 170 milligrams per kilogram (mg/kg), indicating little corrosive potential toward buried steel. The fourth chloride test produced 920 mg/kg, indicating potential corrosiveness toward buried steel.

2.5.4.3 Exploration

Section 2.5.4.3.1 summarizes previous subsurface investigations performed at the NAPS site, while Section 2.5.4.3.2 summarizes the ESP exploration program.

2.5.4.3.1 Previous Subsurface Investigation Programs

The locations of these borings and their depth ranges are shown on Figure 2.5-59.

a. Existing Units Borings

Sixty borings were performed from August through October 1968, with boring depths ranging from 20 to 150 feet, averaging 93 feet (Reference 146). Borings used standard penetration test sampling, Dames and Moore soil samplers, and NX-size double-tube core barrels for rock coring. Boring locations, depths, etc. are summarized in Table 2.5-30 and Table 2.5-31. Test

pits and trenches were also dug. Geophysical surveys conducted during this investigation are summarized in Section 2.5.4.4.1.

b. Abandoned Units 3 & 4 Borings

Forty-seven borings were performed during June and July 1971, with boring depths ranging from 40 to 175 feet, averaging 74 feet (Reference 8). Borings used standard penetration test sampling, Dames and Moore soil samplers, Denison thin-walled tube samplers, and NX-size double-tube core barrels for rock coring. Boring locations, depths, etc. are summarized in Table 2.5-32 and Table 2.5-33. Test pits and trenches were also dug.

c. SWR Borings

Twenty-two borings were performed during September 1975 (UFSAR Appendix 3E), and May 1976 (UFSAR Appendix 3E, Attachment 4) to address NRC concerns raised during licensing of the existing units. Boring depths ranged from 27 to 105 feet, and averaged 70 feet. Borings used standard penetration test sampling and thin-walled tube samplers. Boring locations, depths, etc., are summarized in Table 2.5-34 and Table 2.5-35.

d. ISFSI Borings

Nine borings were performed in April and July 1994 with boring depths ranging from 59 to 115 feet, averaging 81 feet (ISFSI SAR). Borings used standard penetration test sampling, thin-walled tube samplers, and NX-size double-tube core barrels for rock coring. Boring locations, depths, etc., are summarized in Table 2.5-36 and Table 2.5-37.

2.5.4.3.2 ESP Subsurface Investigation Program

The subsurface investigation for the ESP application was performed in November and December 2002 over a substantial portion of the ESP site to cover the area enveloped for the new units as well as cooling towers for the new units (Reference 147, Appendix 2.5.4B). This investigation consisted of relatively few exploration points, and was designed primarily to confirm the results obtained from the previous extensive investigations.

Additional structure-specific exploration and testing would be performed during detailed engineering and would be described in the COL application. The ESP exploration point locations are shown in Figure 2.5-60. The exploration points from the ESP investigation are combined with the boring locations from all of the previous investigations in Figure 2.5-61.

The scope of work and the special methods used to collect data are listed below:

- Seven exploratory borings (MACTEC Engineering and Consulting, Raleigh, North Carolina)
- Nine observation wells (MACTEC Engineering and Consulting, Raleigh, North Carolina)
- Eight cone penetrometer tests (CPT) plus 2 down-hole seismic cone tests and 2 pore pressure dissipation tests (Applied Research Associates, South Royalton, Vermont)

- Two sets of cross-hole seismic tests and 1 down-hole seismic test (Grumman Exploration, Columbus, Ohio)
- Survey of all exploration points (Stantec Consulting, Richmond, Virginia)
- Laboratory testing of borehole samples and cores (MACTEC, Raleigh, North Carolina, and Atlanta, Georgia, laboratories, and Severn Trent Laboratory of Savannah, Georgia)

The exploration program was performed using RG 1.132 (Reference 153), including Draft RG DG-1101 (Reference 154). The fieldwork was performed under an audited and approved quality program and work procedures developed specifically for the ESP project. The subsurface investigation and sample/core collection were directed by the MACTEC site manager who was on site at all times during the field operations. A Bechtel geotechnical engineer or geologist, along with a Dominion representative, were also on site continuously during these operations. MACTEC's QA/QC expert was on site part of the time. The draft boring and well logs were prepared in the field by MACTEC geologists.

Dominion personnel used electromagnetic and ground penetrating radar methods to check each planned exploration location for the presence of underground utilities. Some planned locations were adjusted to provide the necessary utility clearances. A digging, drilling and cutting permit for each exploration location was obtained before any drilling or CPT work was performed.

An on-site storage facility for soil samples and rock cores was established before the fieldwork began. This facility is within the limited access and climate controlled A Level area of the existing units' warehouse facility. Samples and cores were stored within a secured 6-foot high chain link enclosure erected in the A Level area. Each sample and core was logged into an inventory system. Samples removed from the facility were noted in the sample inventory logbook. A chain-of-custody form was also completed for all samples removed from the facility.

Details and results of the exploration program are contained in Appendix 2.5.4B. The borings, observation wells, and CPTs are summarized below. The laboratory tests are summarized and the results discussed in Section 2.5.4.2. The geophysical tests are summarized and the results discussed in Section 2.5.4.4.

a. Borings and Samples/Cores

The seven borings drilled ranged from 50 to 170 feet in depth, averaging 85 feet. The 170-foot deep boring was 30 feet deeper than the deepest reactor design being considered for the ESP. The borings were advanced in soil using rotary wash drilling techniques until standard penetration test (SPT) refusal occurred. Steel casing was then set into the rock, and the holes were advanced using wireline rock coring equipment consisting of a 5-foot long "NQ" core barrel with a split inner barrel.

The soil was sampled using an SPT sampler at 2.5-foot intervals to about 15 feet depth and at 5-foot intervals below 15 feet. The SPT was performed with rope and cathead, and was

conducted in general accordance with ASTM D 1586 (Reference 155). The recovered soil samples were visually described and classified by the onsite geologist. A selected portion of the soil sample was placed in a glass sample jar with a moisture proof lid. The sample jars were labeled, placed in boxes, and transported to the on-site storage area.

Rock coring was performed in general accordance with ASTM D 2113 (Reference 156). After removal from the split inner barrel, the recovered rock was carefully placed in wooden core boxes. The onsite geologist visually described the core, noting the presence of joints and fractures, and distinguishing natural breaks from mechanical breaks. The geologist also computed the percentage recovery and the rock quality designation (RQD). Filled core boxes were transported to the on-site sample storage facility, where a photograph of each core was taken.

The boring logs and the photographs of the rock cores are in Appendix 2.5.4B. Borehole locations, depths, etc. are summarized in Table 2.5-38 and Table 2.5-39. The soil and rock materials encountered in the ESP borings were similar to those found in the previous sets of borings conducted at the NAPS site.

b. Observation Wells

Eight of the observation wells were screened in soil and/or weathered rock and had depths ranging from about 25 to 50 feet. Boreholes for these wells were advanced with hollow stem augers. Samples were obtained at 5-foot intervals to provide information on an appropriate depth to set the slotted screen. The ninth well (OW-845) was screened in rock. This 55-foot-deep well was advanced using a rotary air-percussion drill rig without samples being taken. After the designated depth of each well was reached, and the PVC screen and casing set, the sand pack and bentonite seal were placed, and then a grout plug was placed from the top of the bentonite seal to the ground surface. Each well was capped with a locked steel cap and surrounded with a concrete pad.

Each well was developed by pumping. The well was considered developed when the pH and conductivity stabilized and the pumped water was reasonably free of suspended sediment. Permeability tests were then performed in each well in general accordance with ASTM D 4044, Section 8 (Reference 157), using a procedure that is commonly termed the slug test method. Slug testing involves establishing a static water level, lowering a solid cylinder (slug) into the well to cause an increase in water level in the well, and monitoring the time rate for the well water to return to the pre-test static level. The slug is then rapidly removed to lower the water level in the well, and the time rate for the water to recover to the pre-test static level is again measured. Electronic transducers and data loggers were used to measure the water levels and times during the test.

Appendix 2.5.4B contains the boring logs for the observation wells, the well installation records, the well development records, and the well permeability test results. Observation well locations, depths, etc. are summarized in Table 2.5-38 and Table 2.5-39.

c. Cone Penetrometer Tests

The cone penetrometer tests (CPTs) were advanced using a 30-ton self-contained truck rig. Each CPT was advanced to refusal, to depths ranging from 4 to 58 feet. The piezocone tests were performed in general accordance with ASTM D 5778 (Reference 158). The pore pressure filter was located immediately behind the cone tip. Down-hole seismic testing was performed in two of the CPTs (CPT-822 and CPT-825, see Section 2.5.4.4). Pore pressure dissipation tests were performed at a 27 feet depth in CPT-823, and at a 32.5 feet depth in CPT-827.

The CPT logs, shear wave time of arrival records, and pore pressure versus time plots are contained in Appendix 2.5.4B. CPT locations, depths, etc., are summarized in Table 2.5-38 and Table 2.5-39.

2.5.4.4 Geophysical Surveys

Section 2.5.4.4.1 summarizes previous geophysical investigations performed at the NAPS site, while Section 2.5.4.4.2 summarizes the ESP site geophysical program.

2.5.4.4.1 Previous Geophysical Survey Programs

Several geophysical studies were performed for the investigation for the existing units.

A seismic refraction survey was performed throughout the NAPS property between May and November 1968 (Reference 159). The seismic (compression wave) velocities measured in the “relatively unweathered rock” (Stratum IV) ranged from 13,000 to 16,000 fps. Seismic (compression wave) velocities measured in weathered rock were around 5000 fps. In-hole geophysical measurements were taken in two of the Dames and Moore sample bore holes and one well using a Birdwell 3-D velocity recorder and a Birdwell density recorder (Reference 146). Shear and compression wave velocities and in-situ densities obtained from the velocity and density recorders are summarized in Dames and Moore (Reference 146). Shear wave velocities in the Zone IV rock ranged from about 4000 to 8000 fps. The corresponding compression wave velocities were about 8000 to 16,000 fps. Unit weights ranged from about 140 to 170 pcf.

Weston Geophysical performed seismic cross-hole tests for 40 feet below Elevation 246.6 feet between the Unit 1 and 2 reactors (Reference 160) to provide data pertaining to the rock condition between the two reactor units prior to blasting below that elevation. They obtained shear wave velocities in the Zone IV rock between 5000 and 6000 fps.

The UFSAR gives cross-hole seismic survey shear wave velocities in the dam site area ranging from 800 to 850 fps for the near-surface soils. The shear wave velocity given for the saprolite (Stratum IIA) is 950 fps.

Dames and Moore (Reference 8) indicate that no additional geophysical testing was performed for abandoned Units 3 and 4. Data from the existing units were considered in the site evaluation for the abandoned Units 3 and 4. No separate geophysical investigations were performed for the SWR area or the ISFSI.

2.5.4.4.2 **ESP Geophysical Surveys**

Two cross-hole seismic tests, one down-hole seismic test in a borehole, and two down-hole seismic tests using a cone penetrometer were performed during the ESP site investigation.

a. **Cross-Hole Seismic Tests**

Cross-hole seismic tests were performed immediately adjacent to borings B-802 and B-805 (see Figure 2.5-60). The B-802 location was used to obtain readings in rock while the B-805 location was used to obtain readings in soil. The tests were performed in accordance with ASTM D 4428/D 4428M (Reference 161).

At the B-802 location, an air percussion drill was used to advance borings B-802A, B and C for the cross-hole tests. These holes were in-line, nominally 10 feet apart. The borings were 90 feet deep with about 70 feet in rock. Incliner casing was grouted into each hole to enable a deviation survey to be performed. Distances between holes 802B and 802C ranged from 10.18 feet at the top to 13.33 feet at the bottom. The distances measured in the deviation survey at each test depth were used in the seismic velocity computations.

At the B-805 location, rotary wash drilling with one of the geotechnical drill rigs was used to advance boreholes B-805A, B and C to 30 feet depth. These holes were in-line, nominally 10 feet apart. As with the deeper B-802 holes, inclinometer casing was grouted into each hole to enable a deviation survey to be performed. Distances between holes 805A and 805B ranged from 9.91 feet at the top to 9.11 feet at the bottom. The distances measured in the deviation survey at each test depth were used in the seismic velocity computations.

Details of the equipment used to create the seismic compression and shear waves, and to measure the seismic wave velocities are given in Appendix 2.5.4B, which also contains a detailed description of the results. These results are summarized below.

Tests in borings B-802A, B, and C were performed at 5-foot intervals in rock from 27 to 90 feet depth. However, only shear wave velocity results were obtained from 27 to 45 feet depth. Severe high frequency noise appeared to have degraded the results in general, but particularly below 45 feet depth. All of the compression wave forms were obscured by high-frequency noise. The shear wave velocities in rock between 27 and 45 feet depth ranged from 4500 to 6000 fps.

Tests in borings B-805A, B, and C were performed at 2.5 to 5-foot intervals in soil from near the surface to 27 feet depth. The seismic waveforms were reasonably clear, except for the bottom interval, close to the rock interface. The shear wave velocities ranged from about 610 to 1380 fps, the compression wave velocities ranged from about 1240 to 6550 fps, and the computed dynamic Poisson's ratio ranged from 0.27 to 0.49.

b. Down-Hole Seismic Tests in a Bore Hole

Since the cross-hole tests in borings B-802A, B, and C yielded no compression wave results and gave no shear wave velocity results below 45 feet depth, down-hole seismic testing was conducted in boring B-802B. Details of the equipment used to create the seismic compression and shear waves and to measure the seismic wave velocities are given in Appendix 2.5.4B, which also contains a detailed description of the results and the method used to compute the results. These results are summarized below.

The shear wave was reasonably well defined to 45 feet depth, less well defined from 45 to 65 feet depth, and not defined below 65 feet depth. Between 22.5 and 65 feet depth, shear wave velocities ranged from about 3400 fps to 6380 fps. Reasonable data were obtained for the compression wave. Between 22.5 and 87 feet depth, compression wave velocities ranged from about 10,000 fps to 16,600 fps. The computed dynamic Poisson's ratio ranged from 0.38 to 0.45.

c. Down-Hole Seismic Tests with Cone Penetrometer

The tests were performed at 5-foot intervals in CPT-822 and CPT-825 (see Figure 2.5-60). Only shear waves were generated. The wave arrival was recorded by a geophone attached near the bottom of the cone string.

The shear wave arrival time versus depth are plotted in Appendix 2.5.4B. In CPT-822, the computed shear wave velocity between 10 and 22 feet depth was about 1275 fps. In CPT-825, the computed shear wave velocity between 6 and 30 feet depth was 1175 fps. Between 30 and 45 feet depth the computed velocity was about 1660 fps, and between 45 and 52 feet depth the computed velocity was about 2438 fps.

d. Discussion and Interpretation of Results

Recommended design values of shear and compression wave velocities for each zone are provided in Section 2.5.4.2. The profile of shear wave velocity versus depth for the saprolite is given in Section 2.5.4.7.

2.5.4.5 Excavation and Backfill

This section describes the following topics:

- The extent (horizontally and vertically) of anticipated safety-related excavations, fills and slopes
- Excavation methods and stability

- Backfill sources and quality control
- Construction dewatering impacts

2.5.4.5.1 **Extent of Excavations, Fills and Slopes**

Within the ESP site envelope (Figure 2.5-61) that would contain safety-related structures, including the UHS, the existing elevation ranges from about Elevation 250 to 340 feet. (The Elevation 250 feet area is the backfilled excavation for the abandoned Units 3 and 4.) The subsurface profiles in Figure 2.5-57 and Figure 2.5-58 provide an impression of the grade elevation range across the ESP site. Plant grade for the new units would be at Elevation 271 feet. The base of the containment (reactor) building foundations for the new units would range from Elevation 238.25 to Elevation 131 feet, depending on the reactor design selected.

Construction of the new units would require a substantial amount of excavation. The excavation would be both in soil and in rock. Filling would consist almost entirely of backfilling around structures back up to plant grade. The only new permanent slope that may be created would be to the west of the SWR to accommodate the buried UHSs if required by the selected design. The amount (if any) of this cut depends on the type of design selected. The top of the slope would be at least 200 feet from the top of the SWR embankment, the same distance as for the existing slope to the north of the SWR. Thus, the slope would not impact the SWR. This slope is discussed in Section 2.5.5. The slopes discussed in the following sections would be temporary slopes for construction purposes.

2.5.4.5.2 **Excavation Methods and Stability**

a. **Excavation in Soil**

Excavation in the soils (Zones IIA and IIB) and any existing fills would be achieved with conventional excavating equipment. Excavation would adhere to OSHA regulations (Reference 162). Where space permits, the excavation would be open-cut, with slopes no steeper than 1.5-H to 1-V. Since the saprolitic soils can be highly erosive, even temporary slopes cut into the saprolite would be sealed and protected. Where there is insufficient space for open-cut slopes, vertical cuts would be supported with sheet pile or soldier pile and lagging walls. For the excavations envisaged for the new containment (reactor) buildings, UHS, etc., support for these walls would be provided by tiebacks, angled down and anchored into the bedrock, where possible.

b. **Excavation in Rock**

Excavation in the Zone III moderately to severely weathered rock would be achieved using conventional earthmoving equipment. Tied-back sheet piles or soldier piles and lagging would be used to support the excavation.

Excavation made for the abandoned Units 3 and 4 in the slightly to moderately weathered rock (Zone III-IV) and fresh to slightly weathered rock (Zone IV) is documented in Stone and

Webster (Reference 163). Techniques employed were similar to those used for the existing units (Reference 164) but with “lessons learned” applied. The proposed methods of rock excavation outlined below are based, in part, on the methods that worked successfully for the existing units and the abandoned Units 3 and 4.

- Controlled blasting techniques, including cushion blasting, pre-splitting and line drilling may be used, with appropriately dimensioned bench lifts. The blasted faces would be vertical except where the foliation dip is into the excavation. There, the excavation would be parallel to the foliation dip (typically about 1-H to 1-V).
- Any blasting would be strictly controlled to preserve the integrity of the rock outside the excavations and to prevent damage to existing structures, equipment, and freshly poured concrete. Peak particle velocity would be measured and kept within specified limits that would be a function of distance from the blast.
- The rock would be reinforced to ensure adequate support and safety. Reinforcing would include, installation of rock bolts in finished rock faces (typically at around 5-foot centers), and the use of welded wire mesh.
- The excavation would be mapped and photographed by experienced geologists. Necessary measures would be taken, if weathered or fractured zones were encountered. Instrumentation such as slope indicators and extensometers would be installed to monitor rock movements, especially on the foliation dip slopes.

Alternatives to blasting for the excavation of rock at the ESP site would be reviewed and considered prior to selection of the final excavation method. The alternative excavation methods to be considered may include one or more of the following:

- Thermal lance – A long pipe with a high temperature, enhanced oxygen flame. Used to cut slots in rock, or in boreholes to cause thermal expansion and splitting between adjacent holes.
- Plasma gun – Creates an electric arc at a spark gap. The device is inserted into boreholes filled with water and a spark is initiated, creating an explosion that breaks a cone of rock toward the free face of the excavation.
- Pile driver and expanding metal slug – An aluminum cylinder is inserted to the full depth of a close-fitting borehole. The cylinder is impacted by a pile driver with a rod-type mandrel that causes the aluminum cylinder to expand radially, fracturing the rock outwards from the borehole.
- Drilling and expansive grout – Holes are drilled into the rock and a grout mix is poured into them. As the grout begins to set, it expands, cracking the rock mass between adjacent boreholes.

- Hydraulic splitter – A bar consisting of two overlapping wedges is inserted into a pre-drilled hole. A hydraulic piston moves one of the wedges in an axial direction relative to the other wedge, causing the wedges to lock tightly in the hole. Further movement of the wedges causes the rock to split laterally outward from the borehole.
- Hoe ram – A percussion hammer is mounted on a backhoe and used to break the rock by chipping.
- Diamond wire saw – A steel cable with diamond-impregnated beads along its length is joined into a continuous loop. The cable is driven in a circular fashion while cutting angles and directions are controlled using pulleys.
- Trenching machine – A heavy-duty chain-type trench excavator using carbide cutting teeth to excavate rock.
- Water jet – High-pressure water jets that cut slots in rock with or without the use of an abrasive.

In addition to cost and schedule, other items to be considered in the evaluation of excavation methods would include vibration effects, hardness of the rock, and rock fabric. Almost all of the methods would generate some vibration that would be evaluated with respect to its effect on the existing units. The hardness of the rock would be considered with respect to the ability of each method to penetrate a potentially significant thickness of rock in a relatively confined area. The rock fabric refers to natural partings in the rock that can be taken advantage of with respect to breakage and removal of the rock in manageable size blocks.

2.5.4.5.3 **Backfill Sources and Quality Control**

Although a large amount of saprolitic soil would be excavated for the new units, this material would not be used as structural fill to support or back fill structures.

Structural fill would be either lean concrete or a sound, well-graded granular material, either a sandy gravel or a gravelly sand, with less than 10 percent passing the No. 200 sieve. This material does not exist naturally on site. However, given the large amount of rock that would need to be excavated for the new units, it could be economical to set up a crushing and blending plant onsite to produce crushed aggregate to the required gradation specifications for use as structural fill. The soundness of the aggregate would be confirmed using sulfate soundness and Los Angeles abrasion tests. This structural fill would be compacted to at least 95 percent of the maximum dry density as determined by ASTM D 1557 (Reference 165). The fill would be compacted to within 3 percent of its optimum moisture content. As an alternative or supplement to the onsite crushed rock, dense graded aggregate can be used as structural fill material. Dense Graded Aggregate such as Size 21A or 21B as specified by the Virginia Department of Transportation Road and Bridge Specifications (Reference 166) are suitable materials.

An onsite soils testing laboratory would be established to control the quality of the fill materials and the degree of compaction and to ensure the fill conforms to the requirements of the earthwork specification. The soil-testing firm would be independent of the earthwork contractor and would have an approved quality program. Sufficient laboratory compaction (modified Proctor) and grain size distribution tests would be performed to ensure that variations in the fill material are accounted for. Field density tests would be performed a minimum of one per 10,000 square feet of fill placed.

2.5.4.5.4 Control of Groundwater During Excavation

Construction dewatering is discussed in Section 2.5.4.6.2. Since the saprolitic soils can be highly erosive, sumps and ditches constructed for dewatering would be lined. The tops of excavations would be sloped back to prevent runoff down the excavated slopes during heavy rainfall.

2.5.4.6 Groundwater Conditions

2.5.4.6.1 Groundwater Measurements and Elevations

Groundwater is present in unconfined conditions in both the surficial sediments and underlying bedrock at the ESP site. The groundwater generally occurs at depths ranging from about 6 to 58 feet below the present day ground surface. The exception to this is the area of the abandoned Units 3 and 4 excavation that was partially backfilled, where groundwater is within about 2 feet of the ground surface.

Nine observation wells installed at the site as part of the ESP subsurface investigation program have exhibited groundwater levels ranging from about Elevation 241 to Elevation 311 feet between December 2002 and June 2003. The logs and details of these wells, and tests in the wells, are given in Appendix 2.5.4B. Hydraulic conductivity values for the saprolite in which eight of the wells were screened, based on the results of the slug tests in the wells, range from 0.2 to 3.4 feet/day. The hydraulic conductivity of the shallow bedrock in which one of the wells was screened is estimated to be about 2 to 3 feet/day. Groundwater movement at the site is generally to the north and east, toward Lake Anna. A detailed description of groundwater conditions is provided in Section 2.4.12.

Groundwater levels at the site may require temporary dewatering of foundation excavations extending below the water table during construction of the new units. Dewatering would be performed in a manner that would minimize drawdown effects on the surrounding environment. Drawdown effects are expected to be limited to the NAPS site. The relatively low permeability of the saprolite and underlying rock means that sumps and pumps should be sufficient for successful construction dewatering, as discussed in Section 2.5.4.6.2.

The design ground water level for the new units ranges from Elevation 265 to 270 feet. Derivation of this level is discussed in Section 2.4.12.

2.5.4.6.2 Construction Dewatering

Dewatering for all major excavations could be achieved by gravity-type systems.

a. Soils

Due to the relatively impermeable nature of even the coarse-grained saprolite, sump-pumping of ditches would be adequate to dewater the soil. These ditches would be advanced below the progressing excavation grade.

During the construction of the existing units, plant excavation and dewatering appeared to have been significant in causing local groundwater levels to decline. However, the extent of the area of influence of the dewatering was estimated to be less than 500 feet due to the low permeability of the materials being dewatered (Reference 164).

b. Rock

Sump-pumping would be used to collect water from relief drains that would be installed in the major rock excavation walls to prevent hydrostatic pressure buildup behind the walls. Such relief wells were spaced on 20-foot centers around the perimeters of the abandoned Units 3 and 4 containment excavations.

Although an approximately 40-foot head existed between excavation grade and the North Anna Reservoir during the final stages of excavation for the abandoned Units 3 and 4, no dewatering difficulties were encountered, due to the tight nature of the joints in the rock below Elevation 241 feet.

2.5.4.7 Response of Soil and Rock to Dynamic Loading

The containment (reactor) buildings for the new units would be founded on Zone III-IV or Zone IV bedrock. However, other safety-related structures may be founded on the Zone III weathered bedrock, the Zone IIB very dense saprolitic sand, and/or the Zone IIA saprolitic sand. The seismic acceleration at the sound bedrock level would be amplified or attenuated up through the weathered rock and soil column. To estimate this amplification or attenuation, the following data are required.

- Shear wave velocity profile of the weathered rock and overlying soil
- Variation with strain of the shear modulus and damping values of the weathered rock and soil
- Site-specific seismic acceleration-time history

2.5.4.7.1 Shear Wave Velocity Profile

Various measurements were made at the ESP site to obtain estimates of the shear wave velocity in the soil and rock. These are summarized in Section 2.5.4.4. Since the Zone IV bedrock is considered as the base rock at 70 feet depth in the amplification/attenuation analysis, its shear wave velocity value (6300 fps in Table 2.5-45) is not used. The materials of interest here are the Zone IIA and Zone IIB saprolitic soils, the Zone III weathered rock, and the Zone III-IV slightly to moderately weathered rock.

In some locations, the top of Zone III-IV or Zone IV bedrock is found close to or even above planned plant grade. (This applies to most locations along the east-west subsurface profile in Figure 2.5-57.) In such cases, safety-related structures would be founded on bedrock or on a thin layer of lean concrete or compacted structural fill on the bedrock. In other locations, sound bedrock is relatively deep. (This applies to the northern and southern portions of the north-south subsurface profile in Figure 2.5-58.) In this case, some safety-related structures (excluding the reactors) may be founded on the Zone III weathered rock, Zone IIB saprolite, or Zone IIA saprolite. The shear wave velocity profiles shown on Figure 2.5-62 focus on this latter situation.

Figure 2.5-62, Profile (a), shows the shear wave velocity values measured in Zone IIA saprolite for the ESP subsurface exploration program using cross-hole seismic and CPT down-hole seismic testing. The cross-hole seismic profile is the profile interpreted in Appendix 2.5.4B (Reference 147) from the cross-hole test measurements. Also shown is the shear wave velocity of 950 fps given in the UFSAR for the saprolite. This is the same average design value given in Table 2.5-45 for the Zone IIA saprolite for the ESP evaluation. The design shear wave velocity versus depth profile shown on Figure 2.5-62, Profile (a), is anchored about the design value of 950 fps for the Zone IIA saprolite but reflects the expected increasing values with depth demonstrated in the cross-hole and down-hole seismic tests.

As noted in Section 2.5.4.10.2, any Zone IIA saprolites supporting safety-related structures would be improved to reduce potential settlement. To compute the response of the improved Zone IIA saprolite to dynamic loading, the shear wave velocity through the improved soil is required. As noted in Section 2.5.4.12, vibro-stone columns would be a suitable ground improvement method for the Zone IIA saprolites. The stone column diameter and spacing would be designed to improve the overall stiffness of the saprolite by a factor of about 3. The shear wave velocities of the improved Zone IIA saprolite were computed based on this increase in stiffness. These computed shear wave velocities and the unimproved Zone IIA shear wave velocities are shown on Figure 2.5-62, Profile (b).

Figure 2.5-62, Profile (b), also shows the shear wave velocity values interpreted in Appendix 2.5.4B from the CPT-825 down-hole seismic tests taken to refusal at 52-foot depth during the ESP subsurface exploration program. The subsurface materials below 30 feet depth are interpreted in the CPT log as a silty sand and sandy silt mix. These could be either Zone IIB saprolitic sands or Zone III weathered rock (or both). From 30 to 40 feet depth, the design profile uses the shear wave velocity for the Zone IIB saprolite from Table 2.5-45 (1600 fps), which is very close to the 1650 fps measured in the CPT-825 down-hole seismic test. From 40 to 55 feet depth, the design profile uses the shear wave velocity for the Zone III weathered rock from Table 2.5-45 (2000 fps). This is close to the mean of the two CPT-825 down-hole seismic velocities measured in this zone, as shown in Figure 2.5-62, Profile (b).

Zone III-IV is assumed to extend from 55 to 70 feet depth. Shear wave velocity for this rock is 3300 fps, derived from several values measured in the down-hole seismic test performed adjacent

to boring B-802, and from elastic modulus values from unconfined compression tests (Section 2.5.4.2.5).

The shear wave velocity design profiles shown in Figure 2.5-57, Profile (b), plus the shear wave velocity of the Zone III-IV rock from 55 to 70 feet depth is used in the seismic amplification/attenuation analysis. Four soil profiles are used:

1. Profile from 0 to 70 feet, with 30 feet of unimproved Zone IIA saprolite, 10 feet of Zone IIB saprolite, 15 feet of Zone III rock, and 15 feet of Zone III-IV rock.
2. Profile from 30 to 70 feet depth for foundation sitting on 10 feet of Zone IIB saprolite, 15 feet of Zone III weathered rock, and 15 feet of Zone III-IV rock.
3. Profile from 40 to 70 feet depth for foundation sitting on 15 feet of Zone III weathered rock and 15 feet of Zone III-IV rock.
4. Profile from 0 to 70 feet, with 30 feet of improved Zone IIA saprolite, 10 feet of Zone IIB saprolite, 15 feet of Zone III weathered rock, and 15 feet of Zone III-IV rock.

2.5.4.7.2 Variation of Shear Modulus and Damping with Strain

a. Shear Modulus

The variation of soil shear modulus values of sands, gravels and clays with shear strain is well-documented by researchers such as Seed and Idriss (Reference 167), Seed, Wong, Idriss and Tokimatsu (Reference 168), and Sun, Golesorkhi and Seed (Reference 169). This research along with additional work has been summarized by EPRI (Reference 170). Normalized shear modulus reduction curves are shown in Figure 2.5-63.

Curve 1 in Figure 2.5-63 is for the Zone IIA saprolite (both unimproved and improved). This modulus reduction curve is the average of: 1) the Seed and Idriss (Reference 167) average curve for sand, and 2) five curves from Reference 170 that take into account several factors including reference strain and effective vertical stress. One of the five Reference 170 curves is a low plasticity clay curve to account for the cohesive component of the Zone IIA saprolite.

Curve 2 in Figure 2.5-63 is for the Zone IIB saprolite. This is the modulus reduction curve recommended by Reference 168 for gravels, based on tests of four different gravels and crushed stone samples. The Zone IIB saprolite contains the relict structure of the parent rock, and, with up to 50 percent of core rock remaining in the saprolite, would behave more like a gravel or crushed stone than a sand.

Solid rock does not exhibit the strain softening characteristics of soil. Like steel and concrete, sound rock has essentially the same modulus (shear and elastic) throughout the strain range. The elastic modulus values computed from the stress-strain measurements (relatively high strain) on samples of sound rock core, obtained during the ESP subsurface investigation, are

similar to those calculated from the ultra low strain cross-hole seismic tests. Thus the Zone III-IV rock has no modulus reduction curve. However, at some stage of weathering, rock becomes sufficiently decomposed to exhibit modulus reduction. The Zone III moderately to severely weathered rock is considered to fall into this sufficiently weathered state. Unlike soils, relatively little research has been performed on weathered rock. Curve 3 in Figure 2.5-63 (Reference 169) has been developed for mudstone (a soft rock) with a shear wave velocity of 1500 fps. Section 2.5.4.7.1 shows that Zone III has a shear wave velocity of 2000 fps. Mudstone Curve 3 is used for shear modulus input in the soil/rock column amplification/attenuation analysis for the Zone III weathered rock. As would be expected the shear modulus attenuation is significantly less than exhibited by the sand and gravel curves.

When the specific locations of safety-related structures are determined, if structures such as the diesel generator building and/or certain tanks are founded on saprolite or weathered rock, samples of foundation soils from those locations would be tested to determine location-specific shear modulus degradation relationships.

b. Damping

The publications cited above address the variation of soil damping with cyclic shear strain as well as the variation of shear modulus with shear strain. Figure 2.5-64 plots the variation of the equivalent damping ratio of saprolite and weathered rock as a function of cyclic shear strain.

Curve 1 in Figure 2.5-64 is for the Zone IIA saprolite (both unimproved and improved). This damping ratio versus cyclic shear strain curve is the average of: 1) the Seed and Idriss (Reference 167) average curve for sand, and 2) seven curves from Reference 170 that take into account several factors including reference strain and effective vertical stress. One of the seven Reference 170 curves is a low plasticity clay curve to account for the cohesive component of the Zone IIA saprolite.

Curve 2 in Figure 2.5-64 is for the Zone IIB saprolite. This is the Seed, et al. (Reference 168) curve for gravels. Curve 3 in Figure 2.5-64 is for the Zone III weathered rock. This curve was derived by comparing Curve 3 in Figure 2.5-63 with Curves 1 and 2 in Figure 2.5-63, and applying the differences proportionally to Figure 2.5-64.

There is no variation of damping ratio of the Zone III-IV rock with cyclic shear strain. However, this rock has some intrinsic damping properties. A value of damping ratio of 2 percent was selected.

2.5.4.7.3 Site Specific Acceleration-Time Histories

A spectral compatible acceleration-time history was developed for use in the soil column amplification/attenuation analysis described in Section 2.5.4.7.4. This acceleration-time history was chosen based on the probabilistic seismic hazard deaggregation information described in Section 2.5.2.

The development of the single horizontal component spectrum compatible time history was based on the mean 10^{-4} uniform hazard target spectrum described in Section 2.5.2. The spectral matching criteria given in NUREG CR-6728 (Reference 171) was followed from the development of the spectrum compatible time history for the frequency range of 100 Hz to 0.5 Hz.

2.5.4.7.4 Soil Column Amplification/Attenuation Analysis

The SHAKE2000 computer program was used to compute the site dynamic responses for the soil and rock profiles described in Section 2.5.4.7.1. The computation was performed in the frequency domain using the complex response method. The analysis used the acceleration-time history described in Section 2.5.4.7.3. Based on Section 2.5.2, an earthquake with moment magnitude of 5.5 and an acceleration at bedrock level of 0.22g was used in the SHAKE2000 analysis. The top of bedrock was at 70 feet depth.

SHAKE2000 uses an equivalent linear procedure to account for the non-linearity of the soil and weathered rock by employing an iterative procedure to obtain values for shear modulus and damping that are compatible with the equivalent uniform strain induced in each sublayer. At the outset of the analysis, a set of properties (based on the values of shear modulus and damping presented in Section 2.5.4.7.1, and total unit weight) was assigned to each sublayer of the soil and rock profile. The analysis was conducted using these properties and the shear strain induced in each sublayer was calculated. The shear modulus and damping ratio for each sublayer was then modified based on the shear modulus and damping ratio versus strain relationships presented in Section 2.5.4.7.2. The analysis was repeated until strain-compatible modulus and damping values were achieved.

The zero period acceleration (ZPA) results for the SHAKE2000 analysis for the four soil profiles listed at the end of Section 2.5.4.7.1 are shown in Table 2.5-46. The amplified accelerations were applied in Section 2.5.4.8 and Section 2.5.5.

2.5.4.8 Liquefaction Potential

Soil liquefaction is a process by which loose, saturated, granular deposits lose a significant portion of their shear strength due to pore pressure buildup resulting from cyclic loading, such as that caused by an earthquake. Soil liquefaction can occur, leading to foundation bearing failures and excessive settlements, when all of the following criteria are met.

1. Design ground acceleration is high.
2. Soil is saturated (i.e., close to or below the water table).
3. Site soils are sands or silty sands in a loose or medium dense condition.

The first criterion is met for the ESP site, and the second criterion applies in many areas of the NAPS site. However, the third criterion, involving the type and density of the soil, is much less

clearly applicable. The Zone IIB soils are extremely dense and the Zone III weathered rock has over 50 percent core stone and has typically been sampled by rock coring. Neither of these materials meets the loose or medium dense criterion, and neither has liquefaction potential. Any structural fill required would be a well compacted, well graded crushed stone that is not liquefiable. The only material discussed here regarding liquefaction is the Zone IIA saprolitic soil.

For the ESP site, most safety-related structures would be founded on sound bedrock. However, some safety-related supporting structures (diesel generator, certain pump structures, tanks, etc.) may be founded close to plant grade, and, depending on their location within the ESP site, could be underlain by Zone IIA saprolitic soil.

There has been no historical evidence of the Zone IIA saprolitic soils undergoing liquefaction at the ESP site. UFSAR Appendix 3E, Attachment 4, indicates that examination of the structure and fabric of the material “leads to the conclusion that the saprolite is not susceptible to liquefaction.” UFSAR Section 2.5 does not even mention liquefaction potential. The structure and fabric of the saprolite and their impact on liquefaction potential is discussed in Section 2.5.4.8.1.

As discussed in Section 2.5.4.10, the Zone IIA saprolite has relatively high resistance to bearing failure but can produce excessive settlements under certain conditions. Where this soil forms the foundation material for safety-related structures, it would be improved (as discussed in Section 2.5.4.12) to decrease potential settlement to acceptable values. This improvement would further decrease any potential for liquefaction.

Despite its apparent low potential for liquefaction, the Zone IIA saprolite at the NAPS site has been the subject of several liquefaction analyses. These analyses are examined in Section 2.5.4.8.2 in light of the accelerations being assumed for the ESP. In addition, state-of-the-art liquefaction analysis is performed on potentially liquefiable samples obtained from the recent ESP exploration program, and is presented in Section 2.5.4.8.2.

In Section 2.5.4.8.1 and Section 2.5.4.8.2, Draft RG DG-1105 (Reference 172), is used as a guide.

2.5.4.8.1 Effect of Soil Structure and Fabric on Liquefaction Potential

The following is a summary of the description in UFSAR Appendix 3E, Attachment 4, based on the results of examination of the 27 thin-sections of the Zone IIA silty sands noted in Section 2.5.4.2.4. The full description is contained in Appendix 2.5.4A.

As would be expected with these residual soils, the fabric is that of the parent rock, a biotitic quartz gneiss. There is strong foliation in the saprolite, dipping at angles of about 50 degrees to the horizontal. The fabric is strongly anisotropic. The texture shows angular geometrically interlocking grains with a lack of void network. The mineralogy also reflects the parent rock, with 30–40 percent quartz, 20 to 30 percent microcline, 25 to 40 percent clay minerals, and 5 to 20 percent biotite (mica). The major clay mineral is halloysite (a hydrated form of kaolinite) with lesser amounts of illite and montmorillonite. Much of the halloysite is in the form of aggregates that are larger than

2 micrometers (μm) and, therefore, would be classified as silt, allowing the sand to be classified as non-plastic.

The fabric of the saprolite contrasts strongly with that of an alluvial or marine deposited sand. Sand shows no foliation and no interlocking of grains, even though the grains can be quite angular. The thin sand section also shows a well-developed void network unlike that of saprolite. The fabric of saprolite is, therefore, not one of a transported soil but one of the parent rock material. The fabric is anisotropic, i.e., it has strongly directional properties.

The most striking feature of the saprolite is the angularity and interlocking nature of the grains. The geometric interlocking of the grains and the lack of a void network that would allow re-orientation of grains indicates that the saprolite could not liquefy.

2.5.4.8.2 Acceptable Factor of Safety Against Liquefaction

DG-1105 (Reference 172) suggests that factors of safety (FS) ≤ 1.1 against liquefaction are considered low, FS ≈ 1.1 to 1.4 are considered moderate, and FS ≥ 1.4 are considered high. The Committee on Earthquake Engineering (Reference 173) states, "There is no general agreement on the appropriate margin (factor) of safety, primarily because the degree of conservatism thought desirable at this point depends upon the extent of the conservatism already introduced in assigning the design earthquake. If the design earthquake ground motion is regarded as reasonable, a safety factor of 1.33 to 1.35...is suggested as adequate. However, when the design ground motion is excessively conservative, engineers are content with a safety factor only slightly in excess of unity."

The safe shutdown earthquake (SSE) at rock for the existing units has a maximum acceleration of 0.12g. This was amplified to 0.18g in the soil. The seismic margin maximum acceleration in soil (Reference 174) was 0.30g. The maximum ESP acceleration at hard bedrock rock is 0.22g, amplified at the unimproved soil surface to 0.59g (Table 2.5-46).

Based on the above facts, a FS ≥ 1.1 is considered adequate for the Zone IIA soils at the ESP site.

2.5.4.8.3 Previous Liquefaction Analyses

In December 1994, a detailed liquefaction analysis of the NAPS site soils was performed for a seismic margin assessment (Reference 174). A maximum acceleration of 0.30g, magnitude of 6.8, and the following three approaches to liquefaction assessment were employed.

- For the main plant area, a version of the Seed and Idriss (Reference 175), Simplified Procedure based on SPTs was used. The procedure was modified to account for the age of the saprolite because it is much older than the Holocene deposits on which the Seed and Idriss approach is based. Pavich et al. (Reference 176) estimate the saprolite to be 0.8 and 1.6 million years old, while Virginia Power (Reference 164) suggests an age between 0.66 and 2.3 million years. The Geotechnics (Reference 174) analysis also took some credit for the over-consolidated nature of the saprolites. The analysis did not take into account the structure and fabric of the saprolite. A

magnitude scaling factor of 1.60 was used in the analysis for the magnitude 6.8 earthquake. The liquefaction analysis in the main plant gave FS values against liquefaction ranging from 1.54 to 3.51.

- For the main plant area, a threshold shear strain analysis (Reference 177) was applied. The analysis used an average shear wave velocity in the saprolite of 950 fps (same as the ESP average value). The FS against liquefaction was just under 3.0 for a magnitude 6.5 earthquake.
- For the SWR, the results of the 15 stress-controlled cyclic triaxial tests described in Section 2.5.4.2.4 were used as the basis of the analysis. The FS values against liquefaction ranged from 1.51 to 1.99 for the SWR facilities (pump house, valve house, tie-in vault, service water lines). Analysis of the SWR embankment gave FS values ranging from 0.91 to 3.61, with an average of more than 1.5. The few FS values less than 1 occurred in localized zones. Geotechnics (Reference 174) concluded that overall factors of safety across the embankment are well within acceptable limits, and there is no consistent pattern of low safety factors across the foundation that would indicate that significant movements of the embankment would occur.

2.5.4.8.4 Liquefaction Analyses Performed for ESP

a. Magnitude and Acceleration Values for ESP Liquefaction Analyses

Based on Section 2.5.2, an earthquake with moment magnitude of 5.5 and an acceleration at bedrock level of 0.22g was used in the liquefaction analysis.

Table 2.5-46 shows the zero period acceleration values for the 4 soil/rock profiles described in Section 2.5.4.7.1. Since the Zone IIB saprolite and the Zone III weathered rock are non-liquefiable, Profiles 2 and 3 in Table 2.5-46 were not considered in the liquefaction analysis. In Profile 1, the Zone IIA saprolite (upper 30 feet) is not improved. In Profile 4, the Zone IIA saprolite is improved, i.e., this would be the profile for any safety-related structures founded on the Zone IIA saprolite. Examination of Profiles 1 and 4 shows that, except for the soil above 7.5 feet depth in Profile 1, the maximum acceleration is 0.41g. In the following analyses, the factors of safety against liquefaction of the Zone IIA saprolites were computed for a peak acceleration of 0.41g.

The top 7.5 feet of soils were also analyzed using the higher accelerations in the top 7.5 feet. In this analysis, the maximum acceleration was assumed to be the 0.55g value at 2.5 feet depth in Profile 1, since the soil at the surface is above the water table, and would be removed or recompacted in all situations.

b. Updated Seismic Margin Assessment

The seismic margin assessment described in Section 2.5.4.8.3 for the main plant area was modified in the ESP evaluation, maintaining the same assumptions as used in the original study but substituting the ESP design acceleration in soil of 0.41g and a moment magnitude of

5.5. A magnitude scaling factor of 2.5 was used in the analysis for the moment magnitude 5.5 earthquake. The resulting FS values ranged from 1.76 to 4.01.

Using 0.55g peak ground acceleration for the main plant structure gives FS values ranging from 1.32 to 3.0.

c. Analysis of ESP Samples and CPT Results

Liquefaction analysis of each sample of Stratum IIA saprolite obtained by SPT sampling during the ESP subsurface investigation was performed to determine the FS against liquefaction. The CPT results were also analyzed. The analysis conservatively ignored the age, overconsolidation, and mineralogy/fabric effects of the saprolite. Cohesive samples and/or samples above the groundwater table were considered non-susceptible to liquefaction.

The analysis followed the method proposed by Youd, et al. (Reference 178). This state-of-the-art liquefaction methodology is based on the evolution of the Seed and Idriss "Simplified Procedure" over the past 25 years and updates DG-1105 (Reference 172). A magnitude scaling factor of 2.5 was used in the analysis for the moment magnitude 5.5 earthquake. The K_{σ} factor for high overburden pressure was incorporated into the analysis, using a relative density of 60 percent.

Using a peak ground acceleration of 0.41g, the analysis of the SPT results gave FS values against liquefaction of 2.36 to 3.56 for those samples that were liquefiable. The analysis of the CPT results gave FS values against liquefaction ranging from 1.16 to 3.64, with most of the values greater than 2.0, for soils that were liquefiable. Using 0.55g peak ground acceleration for soils in the top 7.5 feet, one SPT result gave a FS less than 1.1; all the CPT results had FS values greater than 1.1.

d. Liquefaction Analysis Using Shear Wave Velocity Criteria

The design values of shear wave velocity shown in Figure 2.5-62 and tabulated on Table 2.5-46 were corrected for overburden pressure using the method outlined in Youd, et al. (Reference 178). The resulting values all fell into the "No Liquefaction" zone on Figure 9 of Reference 178.

e. Dynamic Settlement

Using the method outlined in Tokimatsu and Seed (Reference 179), the maximum estimated dynamic settlement of the Zone IIA saprolite due to earthquake shaking was less than 1 inch.

2.5.4.8.5 Conclusions about Liquefaction

The conclusions from the foregoing sections on the analysis of liquefaction potential are as follows:

- No historical signs of liquefaction have been observed at the North Anna Site.
- Only the Zone IIA saprolites fall into the gradation and relative density categories where liquefaction would be considered possible.

- The structure, fabric, and mineralogy of these saprolites lower the potential for liquefaction very substantially.
- For a conventional liquefaction analysis, a $FS \geq 1.1$ is adequate, based on the conservative estimate of the ESP design seismic acceleration.
- A seismic margin liquefaction analysis of the main plant area that was modified to use the ESP seismic parameters (M = 5.5 with 0.41g peak ground acceleration), and ignored structure, fabric, and mineralogy effects, gave adequate FS values.
- A state-of-the-art liquefaction analysis of the ESP SPT samples using the ESP seismic parameters (M = 5.5 with 0.41g peak ground acceleration) gave adequate FS values for each SPT result analyzed.
- A state-of-the-art liquefaction analysis of the ESP CPT measurements using the ESP seismic parameters (M = 5.5 with 0.41g peak ground acceleration) gave adequate FS values for each CPT result analyzed.
- A state-of-the-art liquefaction analysis of the shear wave velocity profile using shear wave velocity values corrected for overburden pressure indicated no liquefaction.
- When the peak ground acceleration is assumed to be 0.55g in the top 7.5 feet depth, the liquefaction analyses indicate the possibility of isolated zones of liquefaction in unimproved soils.
- Estimated dynamic settlements due to earthquake shaking are less than 1 inch.

Based on the above analysis results, it can be concluded that there would be no liquefaction of the Zone IIA saprolitic soils below 7.5 feet depth due to the ESP seismic acceleration value. Above 7.5 feet depth, the liquefaction analyses indicate the possibility of isolated zones of liquefaction in unimproved soils. If safety-related structures are founded on the Zone II saprolitic soils, these soils would be improved to reduce potential settlements to within acceptable tolerances, as outlined in Section 2.5.4.10 and Section 2.5.4.12. This would further reduce any liquefaction potential beneath safety-related structures.

2.5.4.9 Earthquake Design Basis

The safe shutdown earthquake (SSE) is derived, and discussed in detail, in Section 2.5.2.6.

The operating basis earthquake (OBE) is derived and discussed in Section 2.5.2.7.

2.5.4.10 Static Stability

As with the existing units and the abandoned Units 3 and 4, the containment (reactor) buildings at the ESP site would be founded on Zone III-IV or Zone IV bedrock. Depending on the location of the containment (reactor) buildings within the ESP site, the top of this bedrock could be below the level of the shallower reactor designs (PBMR and AP-1000 in particular). See the subsurface profiles in

Figure 2.5-57 and Figure 2.5-58. In such cases, excavation would be made to sound bedrock, and then lean concrete would be poured up to the bottom of the reactor foundation.

In some locations, the top of Zone III-IV or Zone IV bedrock is found close to or even above planned plant grade. (This applies to most locations along the east-west subsurface profile in Figure 2.5-57.) In such cases, safety-related structures would be founded on bedrock or on a thin layer of lean concrete or compacted structural fill on the bedrock. In other locations, sound bedrock is relatively deep. (This applies to the northern and southern portions of the north-south subsurface profile in Figure 2.5-58.) In this case, safety-related structures (excluding the reactors) may be founded on the Zone III weathered rock, Zone IIB saprolite, or Zone IIA saprolite. The following sections on bearing capacity and settlement focus on this latter situation. (As noted in Section 2.5.4.10.2, any Zone IIA saprolites supporting safety-related structures would be improved to reduce potential settlement.)

2.5.4.10.1 **Bearing Capacity**

The allowable bearing capacity values for each zone are given in Table 2.5-47.

The Zone IIA allowable bearing capacity value of 4 ksf is based on Terzaghi's bearing capacity equations modified by Vesic (Reference 180). The analysis includes consideration of the effective strength parameters for the coarse-grained material, and both the undrained and effective strength parameters for the fine-grained material given in Table 2.5-45. As discussed in Section 2.5.4.10.2, settlement considerations usually dominate when this material is used for supporting foundations, and the actual allowable bearing capacity may be less than 4 ksf, especially for larger foundations, if the soils are not improved.

The Zone IIB allowable bearing capacity value of 8 ksf is based on Terzaghi's bearing capacity equations modified by Vesic (Reference 180), using the effective angle of friction given in Table 2.5-45. Since the Zone IIB soil is usually found beneath the groundwater table, the effective unit weight of the soil has been used in computing the 8 ksf value.

The Zone III allowable bearing capacity of 16 ksf is based on the value of 20 percent of the ultimate crushing strength given in several building codes (Reference 181). The ultimate crushing strength is given as 0.6 kips per square inch (ksi) (86 ksf) in Table 2.5-45. The 16 ksf value is slightly lower than the 20 ksf given for weathered rock in Table 2.5-2 of the UFSAR. It should be noted that although the 16 ksf allowable bearing capacity is greater than the maximum bearing pressures from any of the reactor designs being considered in this ESP, the containment (reactor) buildings would not be founded on the Zone III weathered rock.

The Zone III-IV and Zone IV bedrock have design unconfined compressive strengths of 4 ksi (576 ksf) and 12 ksi (1728 ksf), respectively (Table 2.5-45). Allowable bearing capacities of these materials are much higher than any applied structure bearing pressure. If excavation during construction reveals any weathered or fractured zones at foundation level, such zones would be overexcavated and replaced with lean concrete. The allowable values of the bearing capacity of

80 ksf and 160 ksf for Zone III-IV and Zone IV rock, respectively, are presumptive values based on various building codes for moderately weathered to fresh foliated rock (Reference 181).

2.5.4.10.2 Settlement Analysis

For the large mat foundations that support the major power plant structures, general considerations based on geotechnical experience indicate that settlement should be limited to 2 inches, while differential settlement limit should be limited to 3/4 inch (Reference 182). For footings that support smaller plant components, the total settlement should be limited to 1 inch, while the differential settlement limit should be limited to 1/2 inch (Reference 182).

Settlement at the ESP site is only a consideration for structures that would be founded directly on the Zone IIA saprolite. The underlying materials consist of either extremely dense saprolitic sand (Zone IIB), weathered rock (Zone III) or sound rock (Zones III-IV and IV), and produce negligible settlement, as discussed next.

a. Settlement of Zones IIB, III, III-IV and IV

Any settlement of these materials is essentially elastic. A foundation has been analyzed for settlement assuming a conservative profile of 20 feet of Zone IIB underlain by 30 feet of Zone III, 50 feet of Zone III-IV, and 400 feet of Zone IV. The stiffness values used are the high-strain elastic modulus values given in Table 2.5-45. The foundation, a large one with an assumed size of 150 feet by 300 feet, has an average bearing pressure of 6 ksf (e.g., a turbine building). The computed total settlement of this structure was less than 1/2 inch.

b. Settlement of Zone IIA

As noted earlier, larger than expected settlements were recorded beneath the existing units' SWR pump house. The 4.6 inches of settlement were due to the weight of the pump house itself and the 30 feet of embankment fill that was built up around it, and occurred over a 30-month period. The in-situ soil that settled beneath the pump house consisted of about 65 feet thickness of Zone IIA mainly micaceous sandy silt. The primary cause of this fairly large settlement appears to be the 5 to 20 percent mica content of these saprolites, along with a significant portion of low plasticity clay minerals.

The settlement of the SWR pump house is an extreme case, due to the fact that 65 feet of mainly micaceous sandy silt underlying the pump house is thicker than is typically found on site, (the SWR pump house is at a higher elevation than the rest of the site, at about Elevation 300 feet). Also, the saprolite is commonly a more granular silty sand (Table 2.5-29). Nevertheless, the potential for excessive settlement of the Zone IIA saprolite makes the material unsuitable for support of any safety-related structure without ground improvement. Ground improvement is discussed in Section 2.5.4.12.

2.5.4.11 **Design Criteria**

Applicable design criteria are covered in various sections. The criteria summarized below are geotechnical criteria. Other geotechnical-related criteria that pertain to structural design (such as wall rotation, sliding, overturning) are not included.

Section 2.5.4.8 specifies that the acceptable factor of safety against liquefaction of site soils should be ≥ 1.1 .

Bearing capacity and settlement criteria are presented in Section 2.5.4.10. Table 2.5-47 provides allowable bearing capacity values for the site subsurface materials. Generally acceptable total and differential settlements are limited to 2 inches and 3/4 inch, respectively, for mat foundations, and 1 inch and 1/2 inch, respectively, for footings.

Section 2.5.5.2 specifies that the minimum acceptable long-term static factor of safety against slope stability failure is 1.5. Section 2.5.5.3 specifies that the minimum acceptable long-term seismic factor of safety against slope stability failure is 1.1.

2.5.4.12 **Techniques to Improve Subsurface Conditions**

As noted in Section 2.5.4.10.2, before the Zone IIA saprolitic soils can be used to support safety-related foundations, they would have to be improved to eliminate potential excessive settlements. Among the many choices for ground improvement that are available, the vibro-stone column is one of the most suitable techniques for reducing the settlement potential of the Zone IIA saprolitic soils. Vibro-stone columns have several advantages, including reduction of settlement, improvement of bearing capacity, and reduction of liquefaction potential, in addition to providing better resistance than piles or piers to seismic lateral forces.

Vibro-stone columns construction is accomplished by down-hole vibratory methods. A vibratory probe, typically about 18 inches in diameter, penetrates the ground under its own weight, aided by water jets or compressed air, and is advanced to the base of the stratum requiring improvement. Crushed stone is poured into the annulus and is densified by the vibrator. The end product is a series of highly compacted stone columns, typically about 3 feet in diameter, spaced on about 5- to 8-foot centers. For sites with loose to medium dense alluvial or marine sands, the sands themselves are densified by the technique. For sites with cohesive soils, or with soils that do not densify appreciably from vibratory energy (e.g., the Zone IIA saprolite), the ground improvement is predominantly due to the increased stiffness of the stone column. In soils that experience pore pressure buildup during seismic events, the stone columns can provide partial pressure relief from this buildup.

The stone column spacing defines the degree of soil improvement that is accomplished. The settlement improvement ratio (SIR) is defined as the ratio of foundation settlement for original ground conditions to foundation settlement for improved ground conditions. For the North Anna Zone IIA saprolite, the desired SIR would be between 2 and 3. The appropriate stone column

spacing can be computed from published empirical correlations based on SIR (Reference 193). Full-scale load tests involving several stone columns are performed on the improved and unimproved soil to confirm degree of improvement (Reference 194).

**APPENDIX 2.5.4A
TRIAxIAL AND CONSOLIDATION TESTS
OF SOILS AT SWR**

This appendix contains the details and results of the cycle triaxial testing performed in 1975 and 1976 on locations on and around the existing units SWR. This information resides in the North Anna Units 1 and 2 UFSAR. For convenience, the appendix replicates portions of the North Anna UFSAR, Appendix E, Attachments 1 through 4. It contains the following information for each of the tests:

- A summary table of the details and results of each test.
- A plot of octahedral shear stress ratio versus number of cycles to reach 5 percent maximum compressive strain.
- A plot of octahedral shear stress ratio versus consolidation stress.
- Detailed visual descriptions of each of the samples.
- Grain size curves of each of the test samples.
- Plots of cyclic axial strain (compression, double amplitude and extension) versus cycle number for each of the tests.

Contents

Triaxial Cyclic Load Tests	2.5.4 A-4
Summary of Cyclic Triaxial Tests	2.5.4 A-4
Description of Undisturbed Samples for Cyclic Tests	2.5.4 A-6
Preliminary Visual Descriptions of Cyclic Triaxial Test Samples	2.5.4 A-13
Grain Size Curves for Cyclic Test Samples	2.5.4 A-14
Plots of Cyclic Load Tests	2.5.4 A-29
Summary Plots of Cyclic Test Results	2.5.4 A-43
Consolidation and Static Triaxial Load Tests	2.5.4 A-45
Summary of Consolidation Tests	2.5.4 A-45
Summary of C-U Triaxial Compression Tests	2.5.4 A-46
Summary of U-U Triaxial Compression Tests	2.5.4 A-47
Composition of Saprolites	2.5.4 A-62
Description of Fabric, Texture and Mineralogy	2.5.4 A-62
Data for Samples Thin Sectioned	2.5.4 A-65
Micrographs of Soil Samples	2.5.4 A-66

Table 8
SUMMARY OF CYCLIC TRIAXIAL TESTS

Test No.	Boring No.	Sample No.	Depth ft.	Initial Water Content %	Dry Ujnit Weight (s)			Eff. Confining Press.	Consol. Stress Ration	Cyclic Deviator Stress	Cyclic Stress Ratio	Octa-hedral Shear Stress Ratio	Number of Cycle to Reach Maximum Compressive Strain equal to (s)			% Finer than #200 Sieve %	
					In the Tube (6) γ d pcf	Triaxial Specimen											
						Initial γ di pct	After Consol. γ dc pct										
CR-1	SWR7	ST5	42.5-43.1	26.1	94	93	95	1.0	2.0	1.47	0.74	0.52	-	2(3)	5	8	44
CR-2	SWR9	ST2	22.5-23.1	23.7	89	88	91	0.7	2.0	0.76	0.54	0.39	-	5(3)	13	30	21
CR-3	P11	ST3	37.3-37.9	20.2	99	96	100	1.0	2.0	1.14	0.57	0.40	-	32	95	152	29
CR-4	P12	ST2	17.5-18.1	18.4	106	103	105	0.4	3.0	0.80	1.00	0.56	-	41	119	213	32
CR-5	SWR3	ST3	42.6-44.2	18.7	108	105	108	1.5	1.5	1.05	0.35	0.28	-	24	39	65	22
CR-6	SWR5	ST5	57.2-58.9	27.1	94	90	94	1.5	1.5	1.24	0.41	0.33	-	73	120	122	23
CR-7	SWR9	ST1	17.1-18.5	32.6	83	80	83	1.0	1.5	1.01	0.50	0.41	-	34(4)	126	194	31
CR-8	P15	ST24	66.0-68.0	24.2	102.4	101.1	-	-	-	-(9)	-	-	-	-	-	-	-
CR-9	P16	ST7	37.5-39.5	17.8	(7)	104.1	107.2	2.5	-	-(10)	-	-	-	-	-	-	-
CR-10	P15	ST24	66.0-68.0	21.7	107.3	106.4	111.1	2.5	1.0	1.94	0.39	0.37	-	1	1	5	(11)
CR-11	P17	ST9	47.5-49.5	33.9	87.6	86.3	90.9	2.5	1.0	1.46	0.29	0.28	-	2	7	16	(11)
CR-12	P16	ST7	37.5-39.5	21.2	(7)	92.1	95.3	2.5	1.0	-(8)	-	-	-	-	-	-	-
CR-13	P17	ST9	47.5-49.5	28.0	93.7	92.8	97.6	2.5	1.0	1.20	0.24	0.23	-	14	23	37	(11)
CR-14	SWR11	ST1	19.5-21.5	29.4	94.4	93.2	96.9	1.0	1.0	0.79	0.40	0.37	-	3	74	171	(11)
CR-15	P15	ST10	31.0-33.0	19.5	94.1	93.3	96.2	1.5	1.5	1.69	0.56	0.46	-	1	1	2	(11)

Table 8 (continued)
SUMMARY OF CYCLIC TRIAXIAL TESTS

Test No.	Boring No.	Sample No.	Depth ft.	Initial Water Content %	Dry Unit Weight (s)			Eff. Confining Press.	Consol. Stress Ration	Cyclic Deviator Stress	Cyclic Stress Ratio	Octa-hedral Shear Stress Ratio	Number of Cycle to Reach Maximum Compressive Strain equal to (s)			% Finer than #200 Sieve %	
					In the Tube (6) γ_d pcf	Triaxial Specimen											
						Initial γ_{di} pct	Consol. γ_{dc} pct										
CR-16	SWR11	ST1	19.5-21.5	32.3	89.3	88.5	92.1	1.0	1.0	0.94	0.47	0.44	-	1	4	19	(11)
CR-17	SWR13	ST9	47.5-49.5	36.9	74.2	73.3	75.9	1.5	1.5	1.30	0.43	0.35	-	1	1	2	(11)
CR-18	SWR13	ST9	47.5-49.5	33.3	73.7	73.5	76.0	1.5	1.5	0.85	0.28	0.23	-	6	6	13	(11)

Notes:

1. Due to high mica content, the specimens swelled after extrusion from the tube and therefore, the initial dry unit weights of the triaxial specimen are lower than the dry unit weights in the tube.
2. At no point during any test did the effective confining pressure reach zero.
3. In test CR-1 and CR-2, the specimens reached a double amplitude stain of 2.5% in the cycle preceding the one listed.
4. In test CR-7, the specimen reached a double amplitude stain of 2.5% in 17 cycles.
5. In all tests except those noted, the maximum compressive strain of 2.5%, 5%, and 10% occurred at the same time or earlier than the double amplitude strain of 2.5%, 5%, and 10% respectively.
6. Calculated from tube inside diameter.
7. Annular space of approximately 0.03 mm unit weight not valid.
8. Test not reported error during load application.
9. Test aborted - Membrane leakage.
10. Test aborted - cell malfunction.
11. Sieve analyses incomplete as of June 11, 1976.

DESCRIPTION OF UNDISTURBED SAMPLES

BORING NO. SWR7

Project North Anna Power Station

Project No. 75260
Page 1 of 1

Sample No. and Depth ft.	Section No.	Length of Section in.	Description
ST5 42.5- 43.1	-	7.0	<p>Tan micaceous very silty medium to fine sand. Minerals vary from black to white and appear in spots and streaks throughout the specimen. Fines are non-plastic. (Residual Soil)</p> <p>Specimen swelled after extrusion from the tube due to the large mica content.</p> <p>Failure occurred in compression by developing 2 shear planes in the top half of the specimen.</p>

N03EA120

DESCRIPTION OF UNDISTURBED SAMPLES

BORING NO. SWR9

Project North Anna Power Station

Project No. 75260

Page 1 of 1

Sample No. and Depth ft.	Section No.	Length of Section in.	Description
ST2 22.5- 23.1	-	7.0	<p>Mottled gray, tan, rust orange and black micaceous silty fine sand. Coloring occurs in streaks, pockets and zones throughout the specimen showing structure of parent rock. (Residual Soil)</p> <p>Specimen swelled after extrusion from the tube due to the large mica content.</p> <p>Failure occurred in compression primarily by bulging and shearing in the top half of specimen.</p>

N03EA121

DESCRIPTION OF UNDISTURBED SAMPLES

BORING NO. P11

Project **North Anna Power Station**

Project No. 75260
 Page 1 of 1

Sample No. and Depth ft.	Section No.	Length of Section in.	Description
ST3	-	6.9	<p>Multicolored micaceous silty medium to fine sand. Minerals are rust orange, brown, black, white and green in color. Some banding of light and dark minerals at about 30° from horizontal. Fines non-plastic. (Residual Soil)</p> <p>Specimen swelled after extrusion from the tube due to the large mica content.</p> <p>Failure occurred in compression by developing a shear plane at about 45° in the lower half of the specimen.</p>

N03EA122

DESCRIPTION OF UNDISTURBED SAMPLES

BORING NO. P12

Project **North Anna Power Station**

Project No. 75260

Page 1 of 1

Sample No. and Depth ft.	Section No.	Length of Section in.	Description
<p>ST2 17.5- 18.1</p>	<p style="text-align: center;">-</p>	<p style="text-align: center;">7.0</p>	<p>Tan to black brown micaceous silty medium to fine sand. Minerals occur in bands and streaks at approximately 45°. Grains are subangular. Top half of specimen is predominantly dark minerals. Bottom half is predominantly tan-white minerals. (Residual Soil)</p> <p>Specimen swelled after extrusion from the tube due to the large mica content.</p> <p>Failure occurred in compression in bottom half of specimen by developing a shear plane at approximately 45°, parallel to banding of minerals.</p>

N09EA123

DESCRIPTION OF UNDISTURBED SAMPLES

BORING NO. SWR3

Project **North Anna Power Station**

Project No. 75260
Page 1 of 1

Sample No. and Depth ft.	Section No.	Length of Section in.	Description
ST3	-	7.2	<p>Tan slightly micaceous silty medium to fine sand. Minerals vary from black to white and are banded at approximately 40° from the vertical. One very prominent band of intact quartz crystals up to 16 mm wide is located in the bottom half of the specimen (Residual Soil).</p> <p>The specimen swelled after extrusion from the tube due to the mica content of the soil.</p> <p>Failure occurred in compression by developing 2 shear planes in the top half of the specimen.</p>

N03EA216

DESCRIPTION OF UNDISTURBED SAMPLES

BORING NO. SWR5

Project North Anna Power Station

Project No. 75260
 Page 1 of 1

Sample No. and Depth ft.	Section No.	Length of Section in.	Description
ST5	-	7.2	<p>Multicolored silty micaceous medium to fine sand. Colors range from black to white and green to brown. Minerals are banded at approximately 45°. (Residual Soil)</p> <p>The specimen swelled after extrusion from the tube due to the mica content of the soil.</p> <p>Failure occurred in compression by developing one well defined shear plane parallel to foliation of minerals.</p>

N08EA217

DESCRIPTION OF UNDISTURBED SAMPLES

BORING NO. SWR9

Project North Anna Power Station Project No. 75260
Page 2

Sample No. and Depth ft.	Section No.	Length of Section in.	Description
ST1	-	7.0	<p>Mottled tan, light brown and black very micaceous silty fine sand. Coloring of minerals occurs in spots and streaks and generally trend 45° from vertical. Bottom half of specimen contains one streak of black silty fine sand up to 10 mm wide and 45° from vertical. (Residual Soil)</p> <p>The specimen swelled after extrusion from the tube due to the mica content of the soil.</p> <p>Failure occurred in compression by developing a shear plane in the top 2/3 of the specimen parallel to banding of minerals.</p>

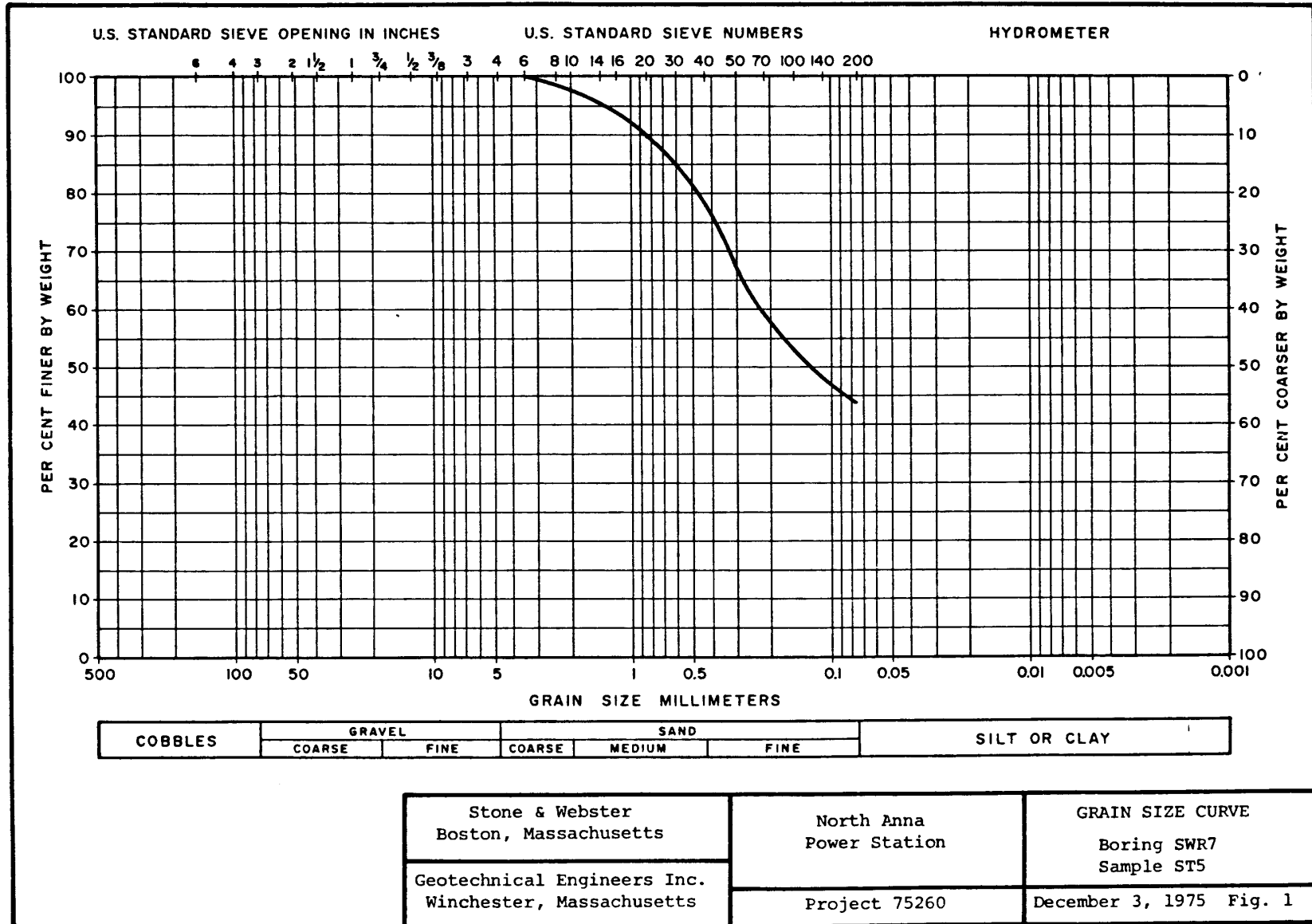
N03EA218

Table 9
PRELIMINARY VISUAL DESCRIPTIONS OF CYCLIC TRIAXIAL TEST SAMPLES^a

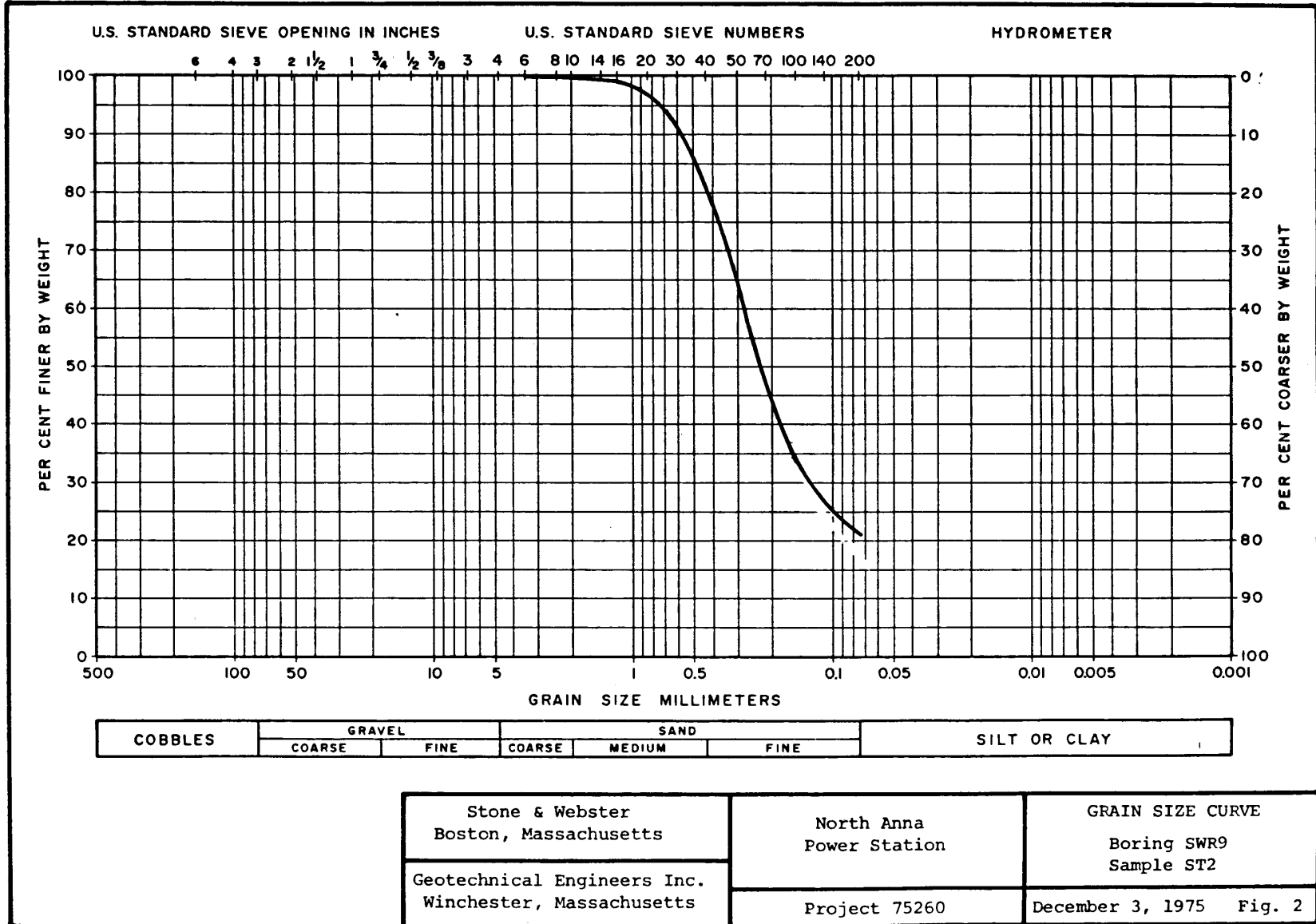
Test Number ^b	Description
CR-10	Grey/white saprolite breaks down to fine sand with silt, fine mica flakes throughout, top 3.5 cm, layered black and white, white layers clayey, foliation dips at 56°.
CR-11	Brown saprolite, fine silty sand, contains 3mm wide layer of med. sand size quartz particles, foliation dips at 45° for top 1/4 of sample, then bends around to dip 60° in opposite direction.
CR-13	Orange-brown saprolite, silty fine to medium sand, band of orange-white clayey med. to coarse sand, foliation dips at 60°, possible failure plane at 35° in top 1/3 of sample.
CR-14	Yellowish-green saprolite, fine to med. sand, 2 to 3 mm layers of very fine mica flakes, foliation dips at 34°.
CR-15	Orange-brown saprolite, silty fine to med. sand, micaceous, contains occasional angular quartz particles to 5 mm, contains zones that are slightly plastic, foliation dips at 45°.
CR-16	Mottled yellow-green saprolite mostly fine to med. sand, slightly silty, fine to med. mica flakes.
CR-17	Mottled orange-brown saprolite, silty fine to med. sand, foliation dips at 43°.
CR-18	Mottled orange-pink saprolite silty sand, foliation at 53°.

a. Sample descriptions are preliminary pending completion of laboratory classification tests.

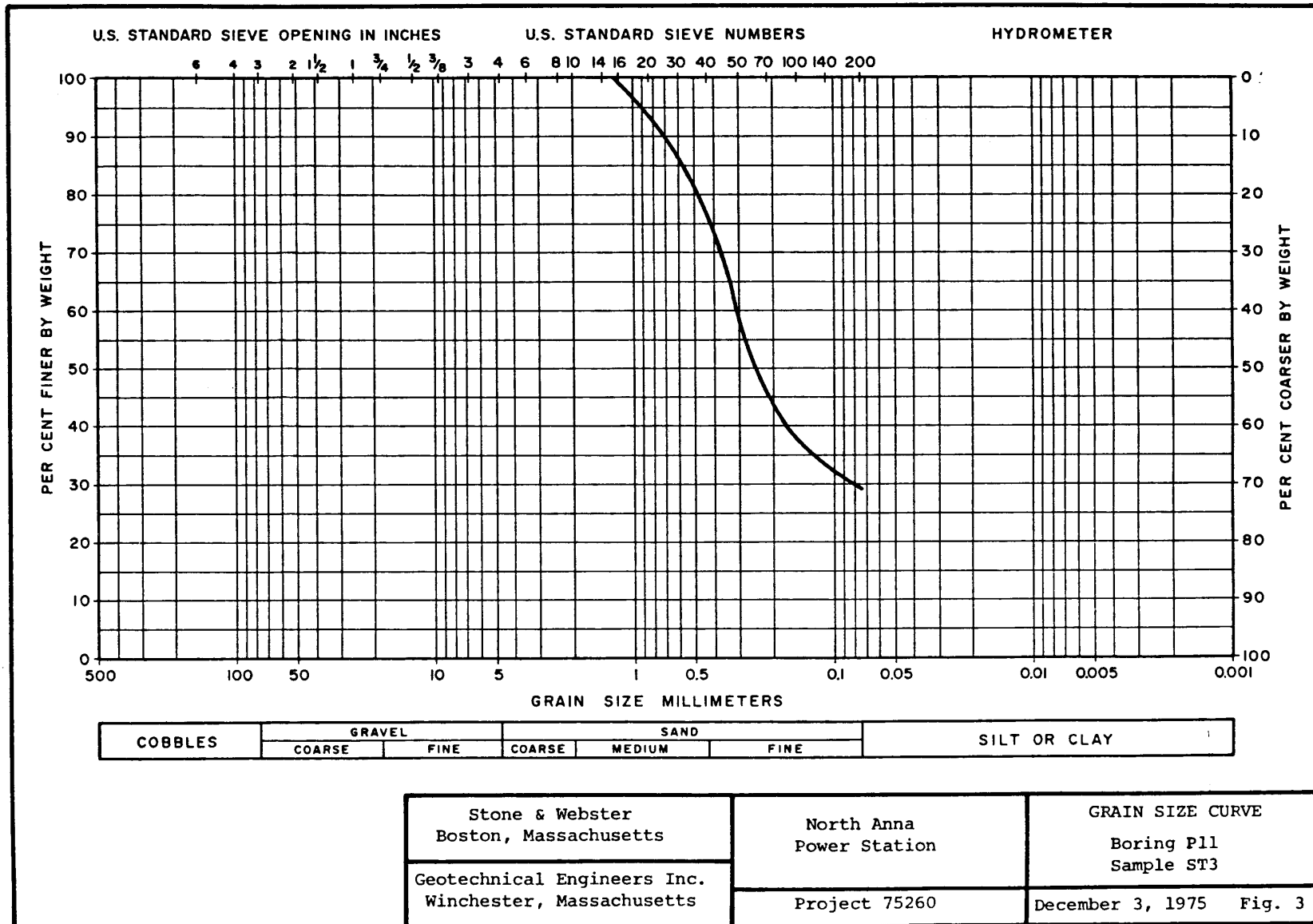
b. Descriptions for aborted tests are not included.



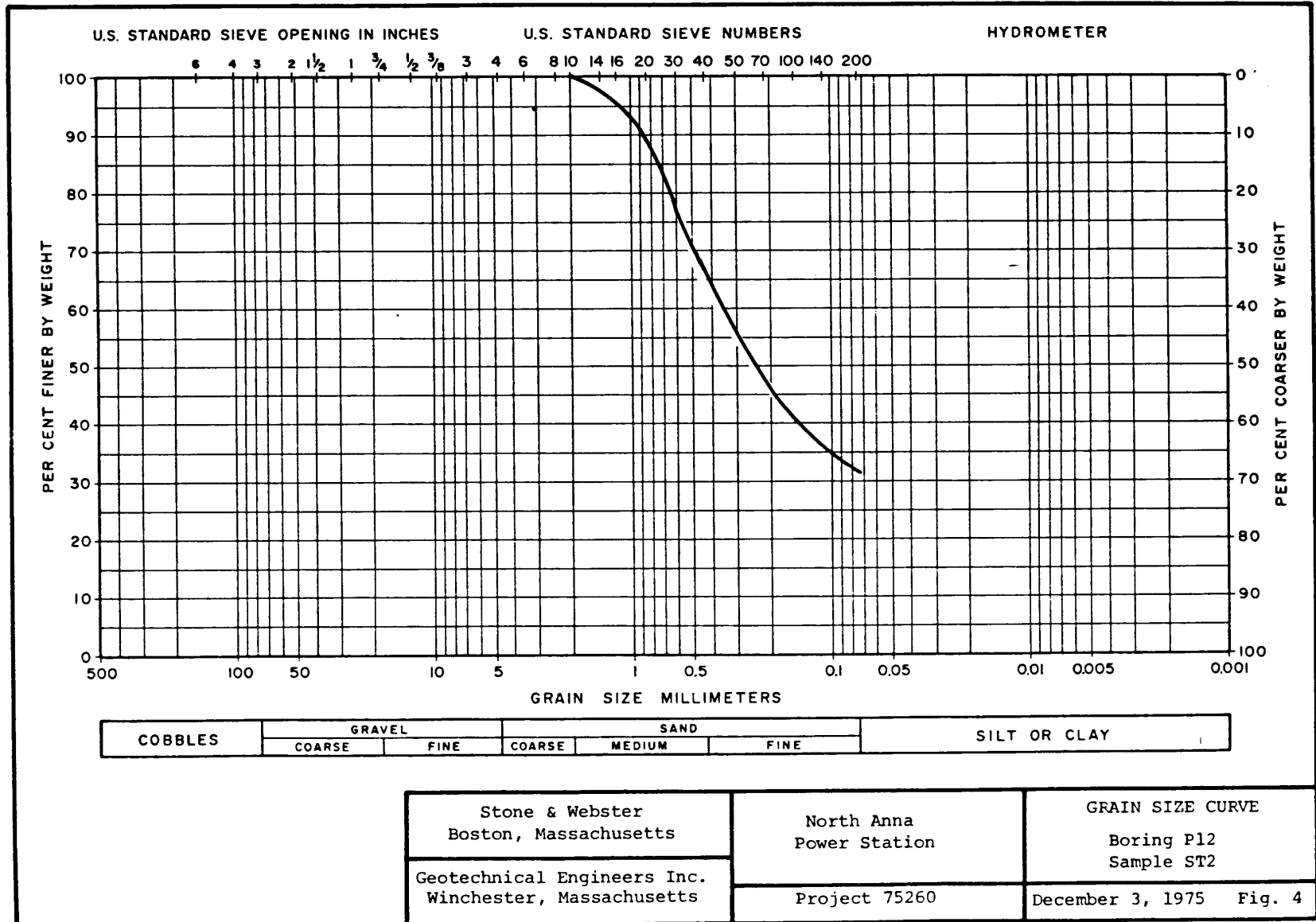
N03EA109



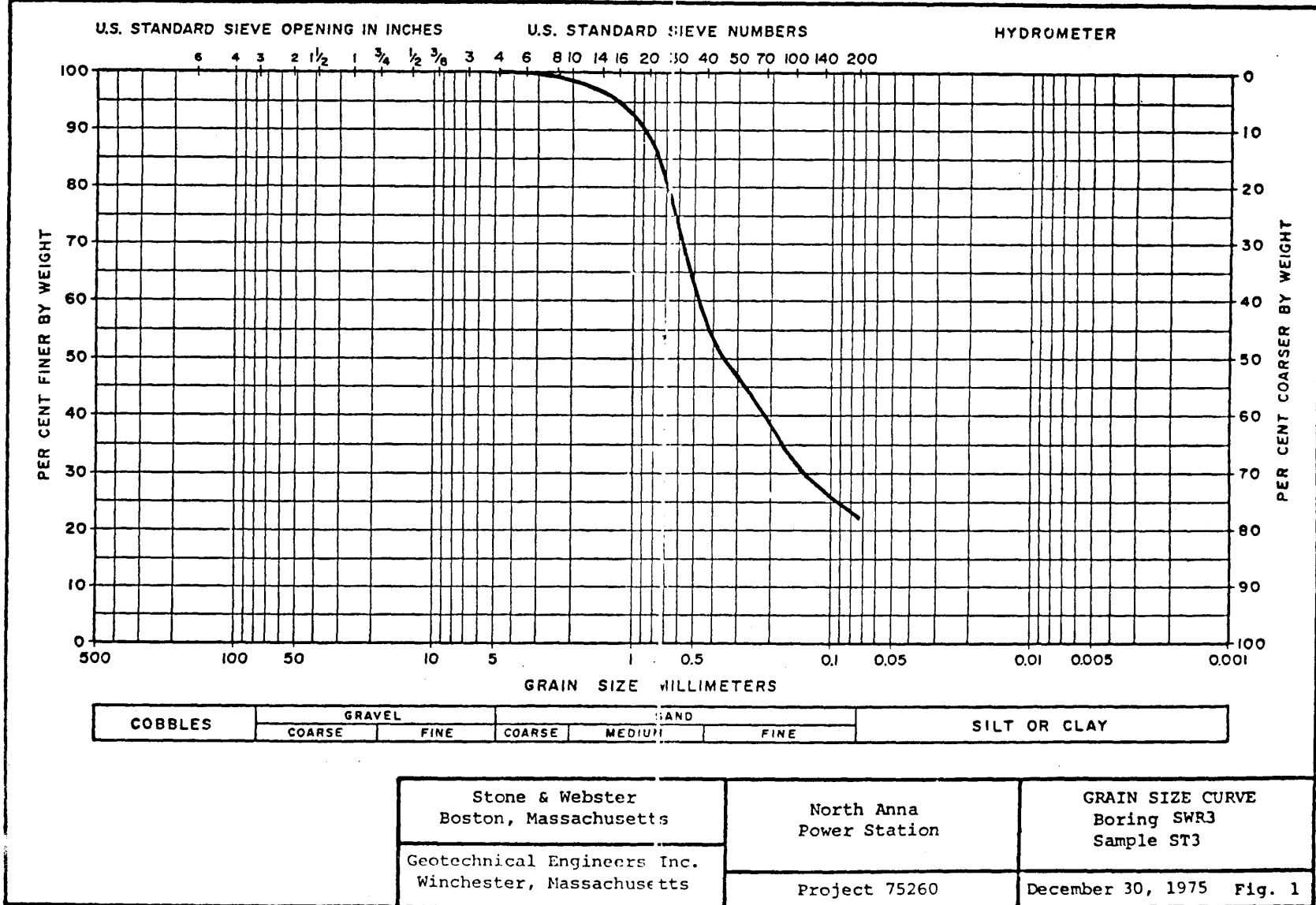
N03EA110



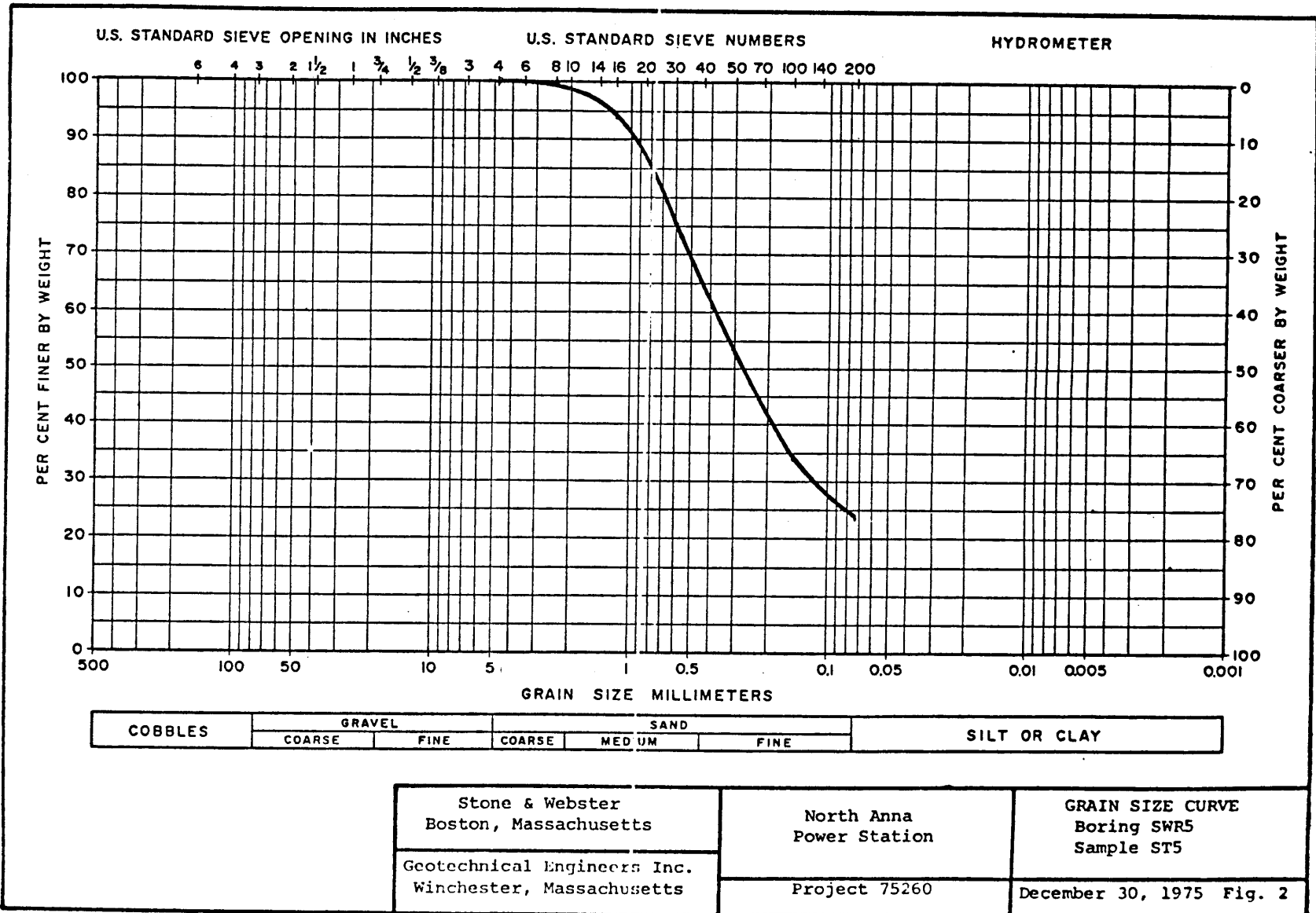
N03EA111



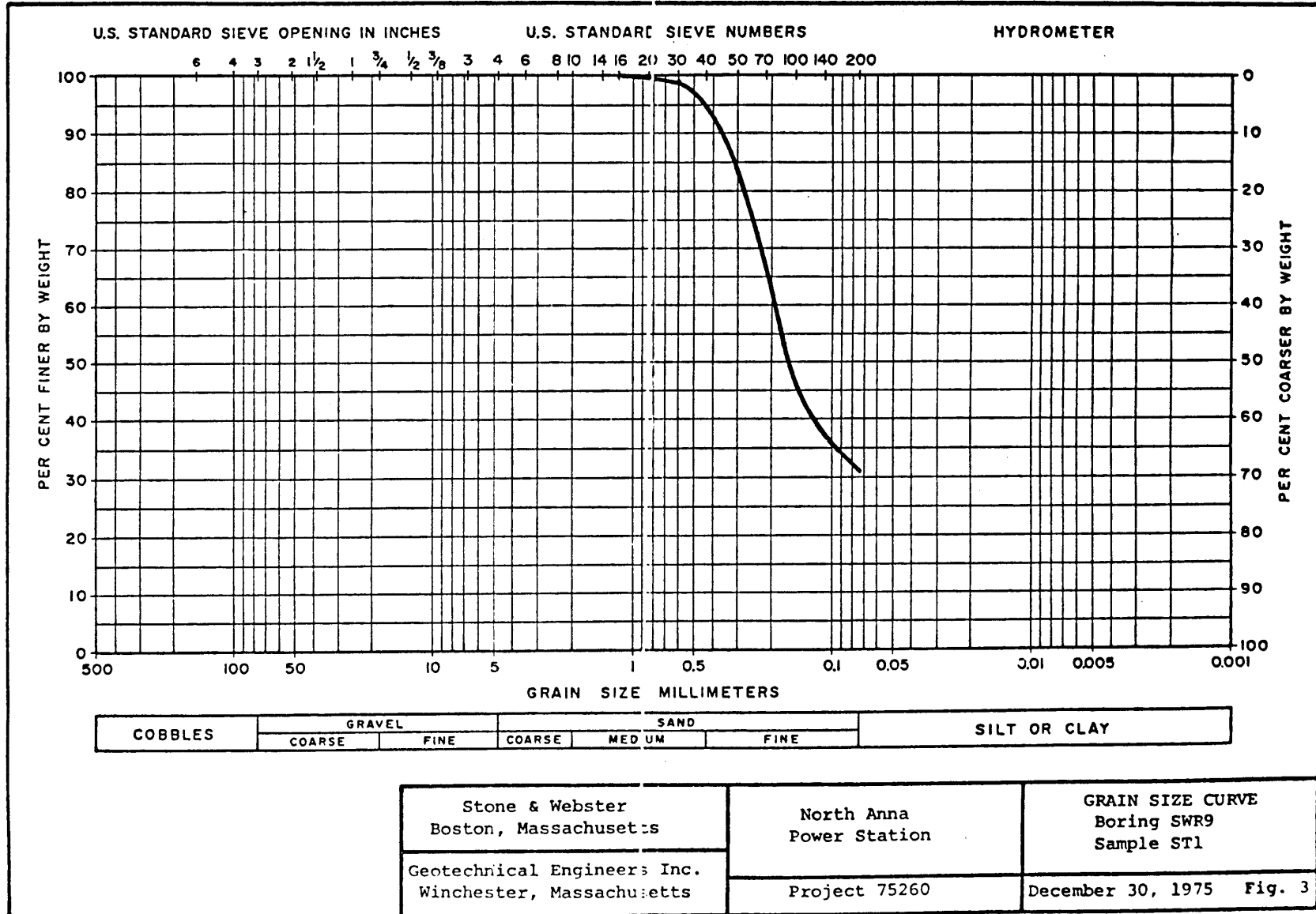
N03EA112



N08EA205



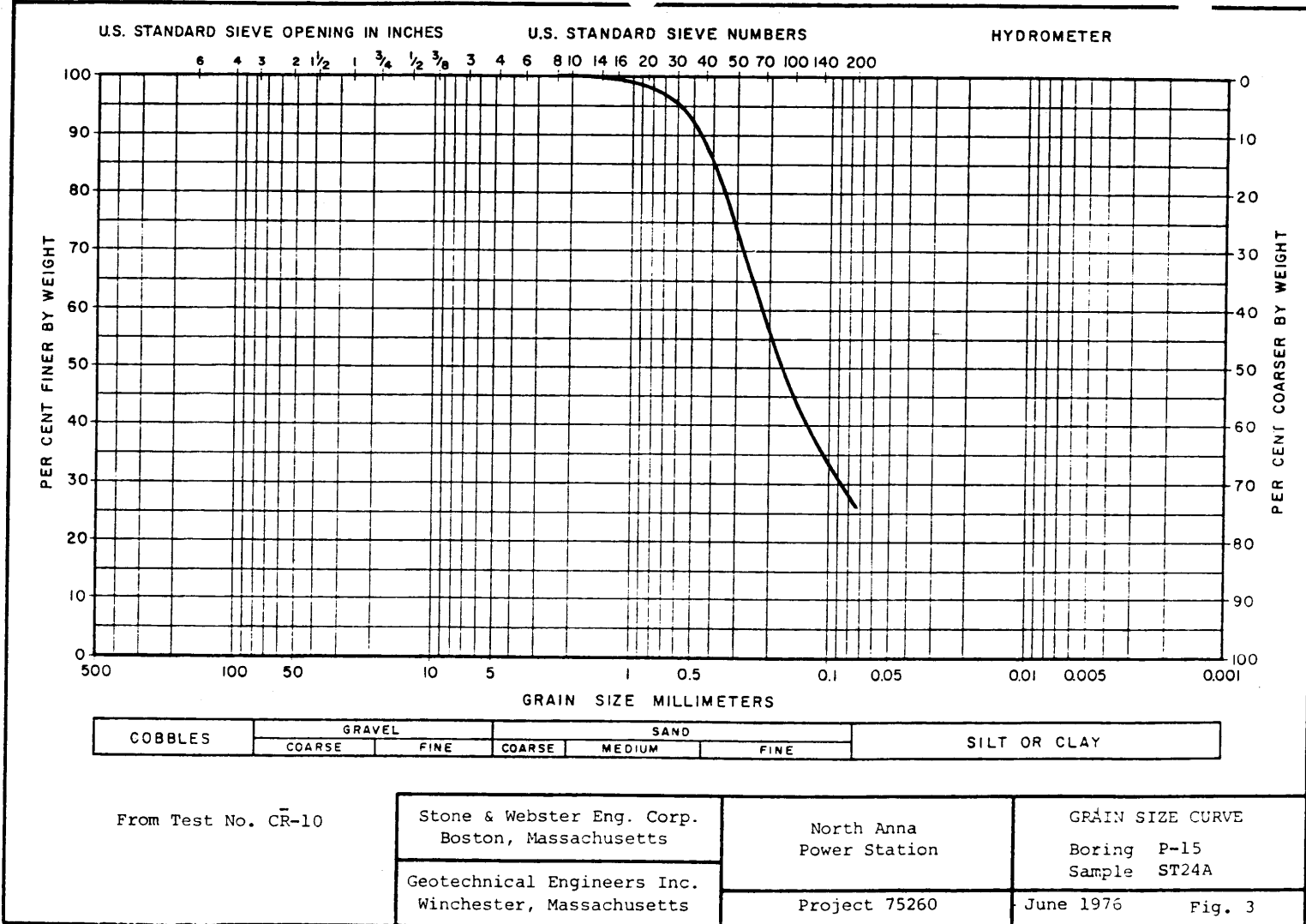
N03EA206



N08EA207

N03EA319

Lab. 4 rev. 0 28 May 74



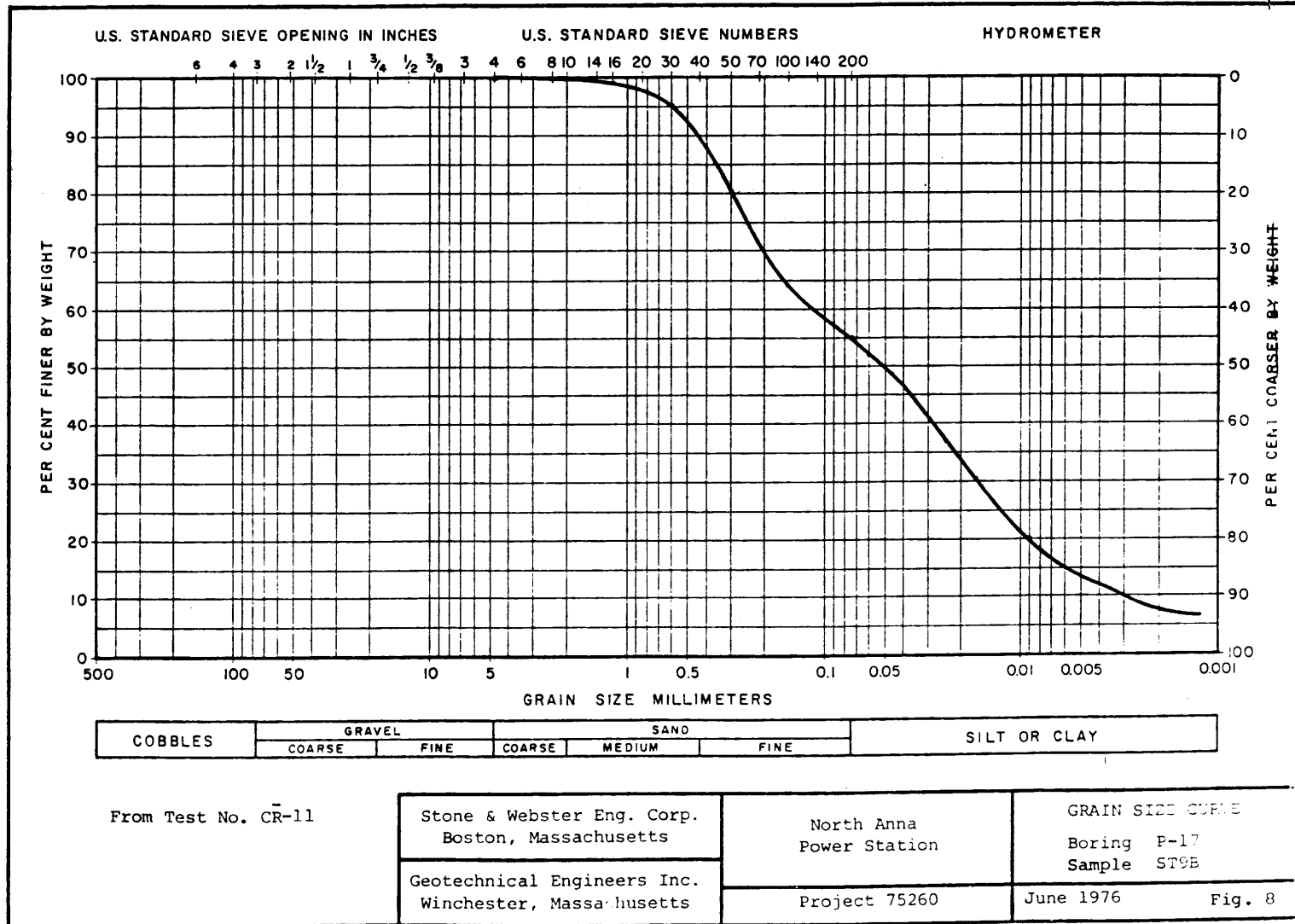
COBBLES	GRAVEL		SAND			SILT OR CLAY
	COARSE	FINE	COARSE	MEDIUM	FINE	

From Test No. CR-10

Stone & Webster Eng. Corp. Boston, Massachusetts	North Anna Power Station	GRAIN SIZE CURVE	
Geotechnical Engineers Inc. Winchester, Massachusetts		Boring P-15 Sample ST24A	
	Project 75260	June 1976	Fig. 3

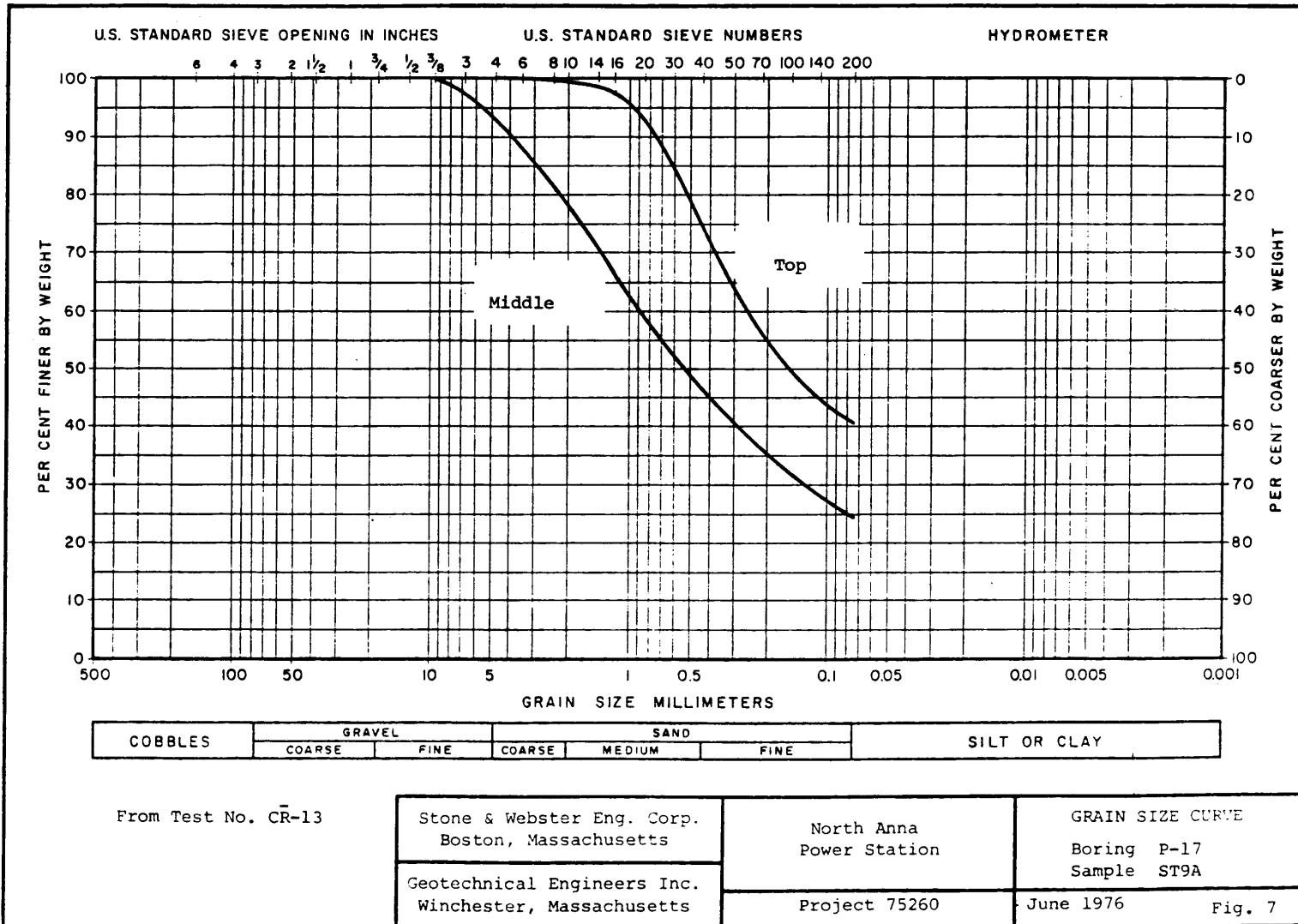
N03EA324

Lab. 3 rev. 0 28 May 74



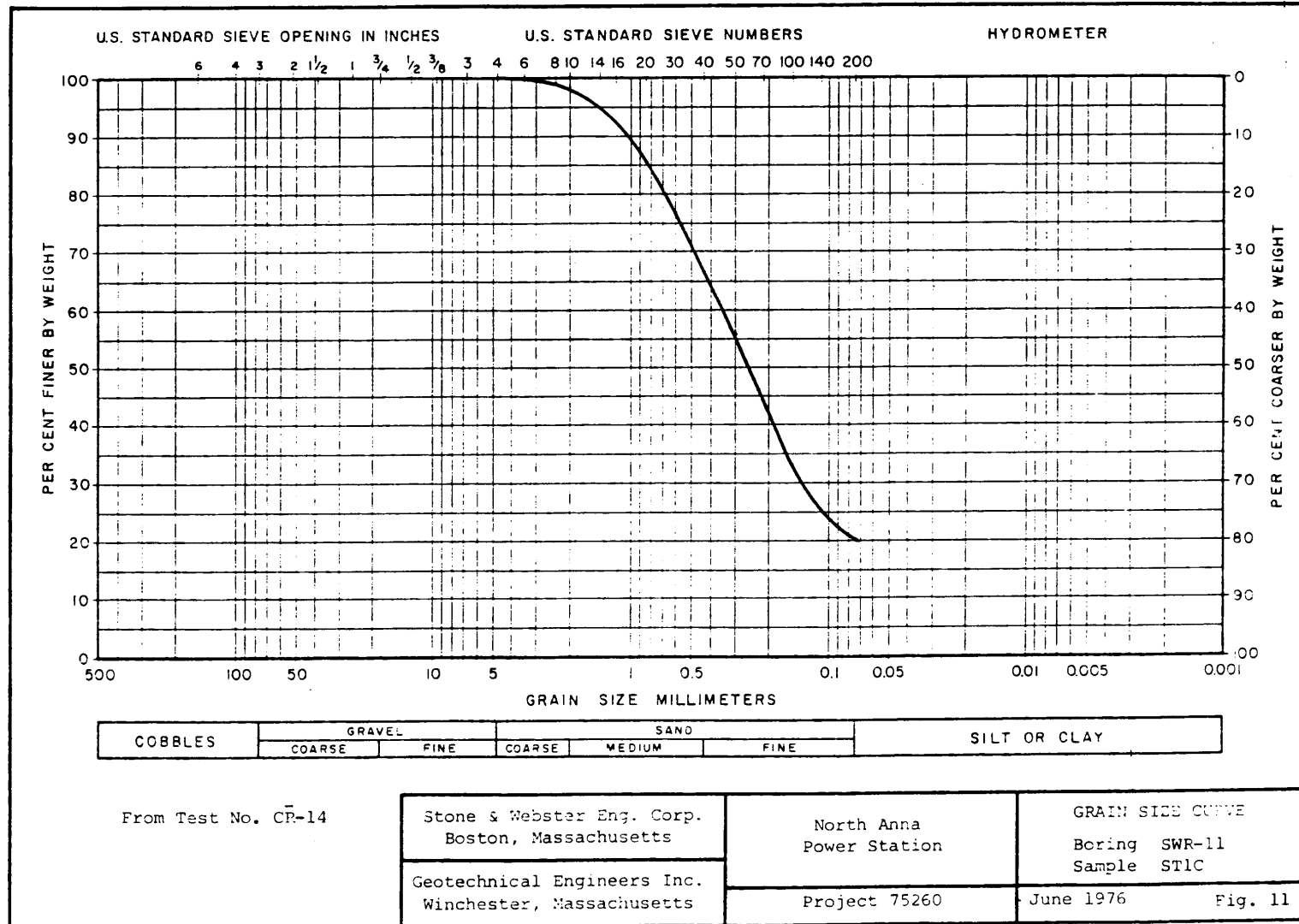
N03EA323

Lab. 4 rev. 0 28 May 74



N03EA327

Lab. rev. 0 28 May 74



From Test No. CP-14

Stone & Webster Eng. Corp.
Boston, Massachusetts

Geotechnical Engineers Inc.
Winchester, Massachusetts

North Anna
Power Station

Project 75260

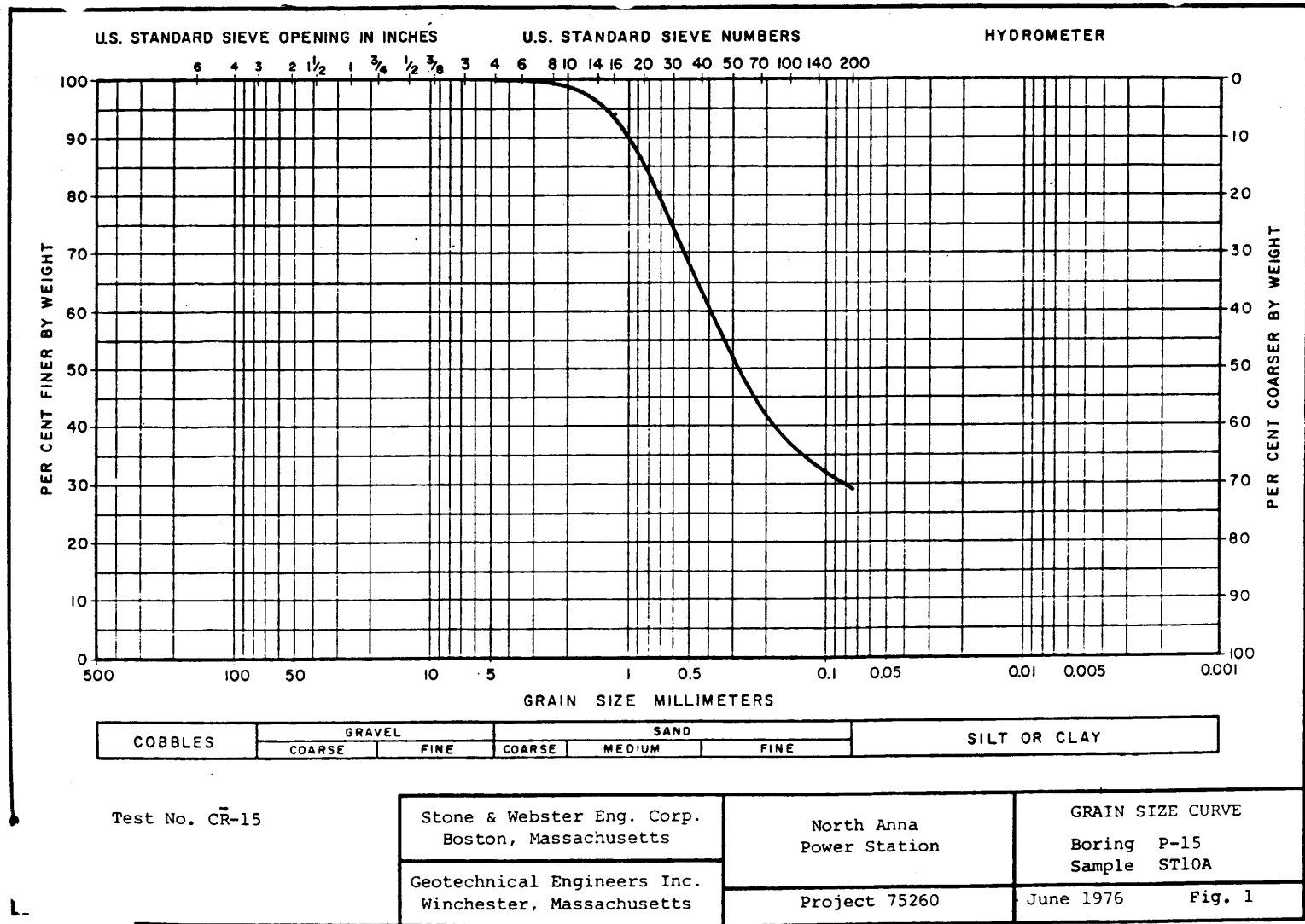
GRAIN SIZE CURVE

Boring SWR-11
Sample ST1C

June 1976 Fig. 11

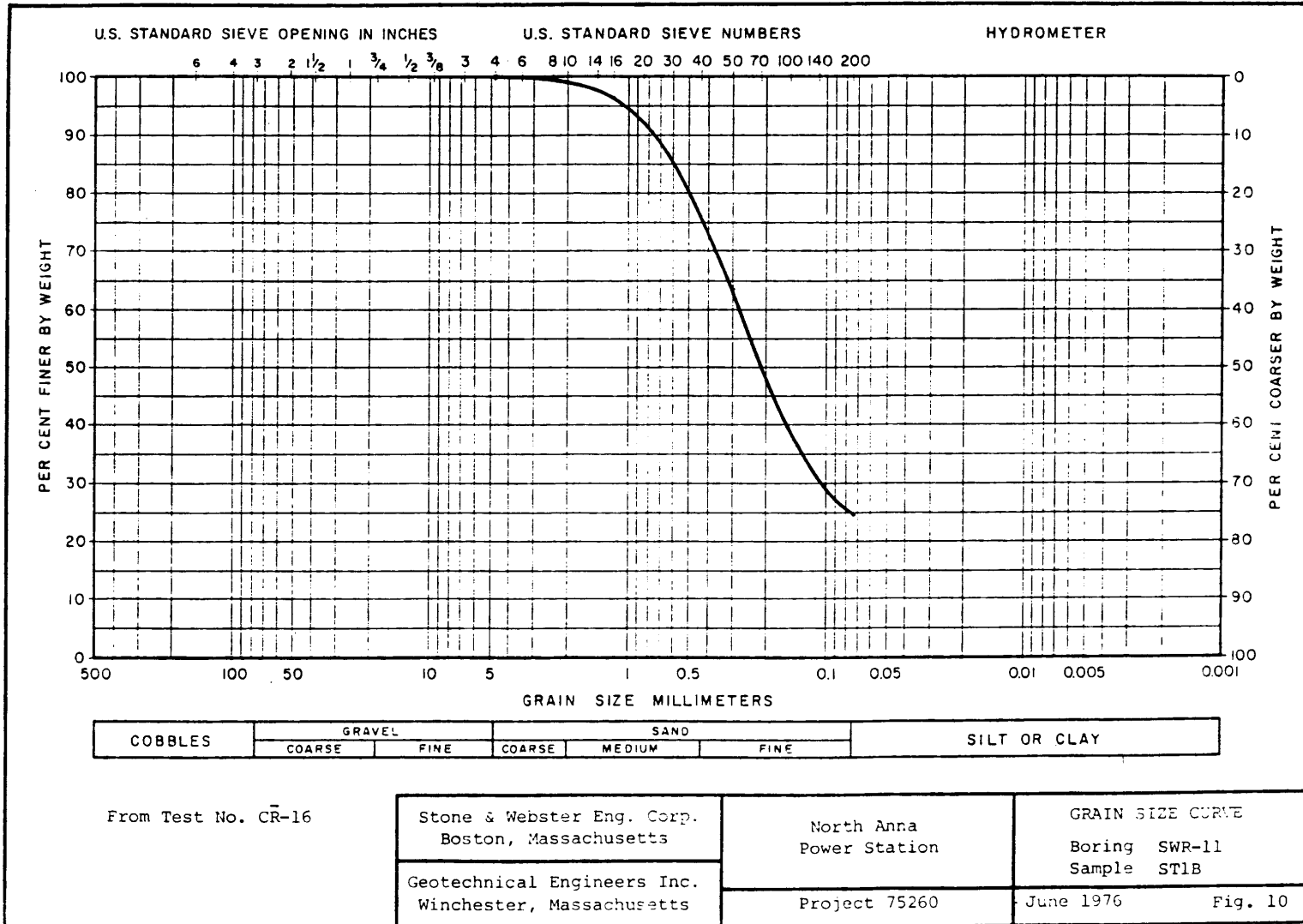
N03EA317

Lab. rev. 0 28 May 74



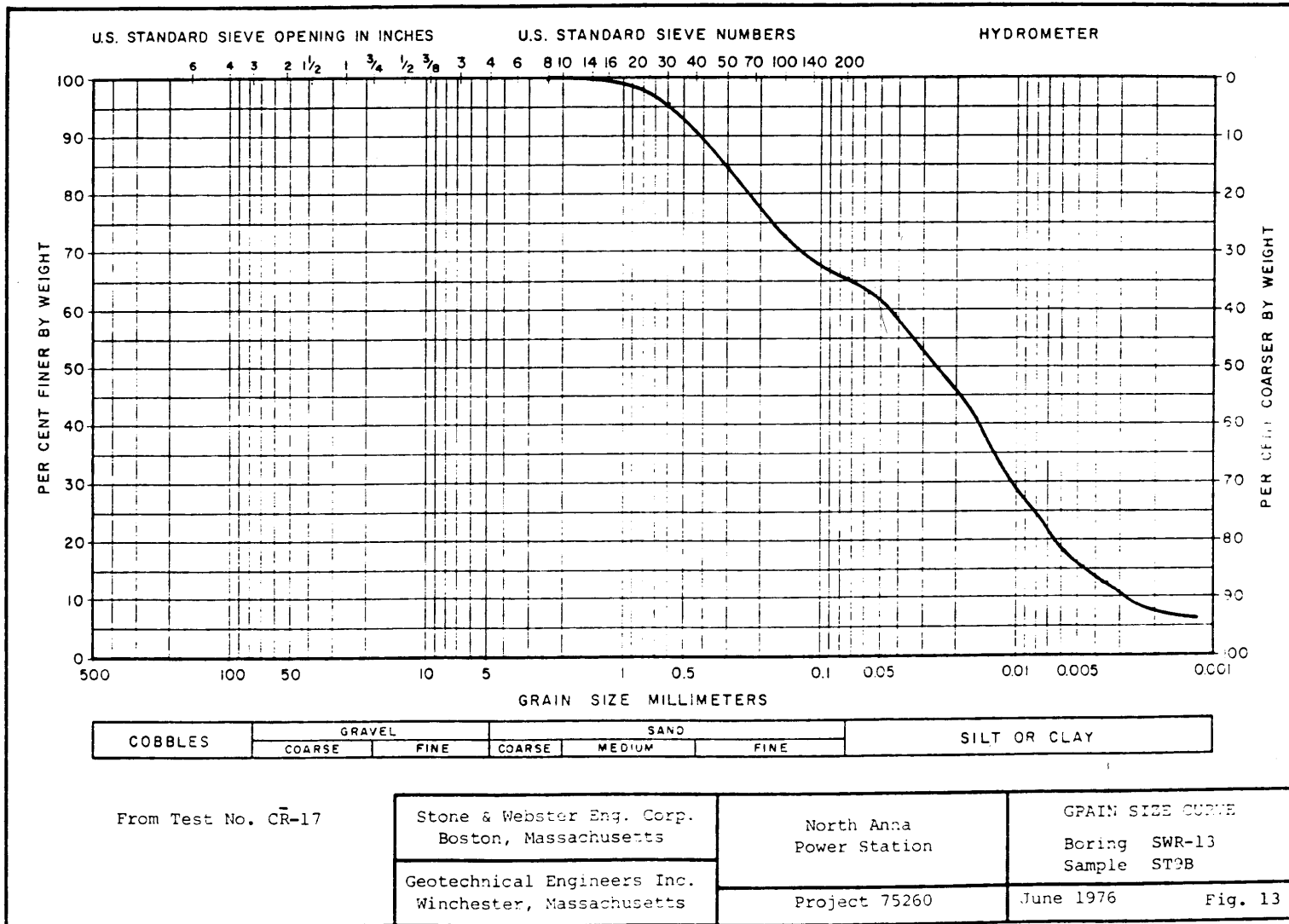
N03EA326

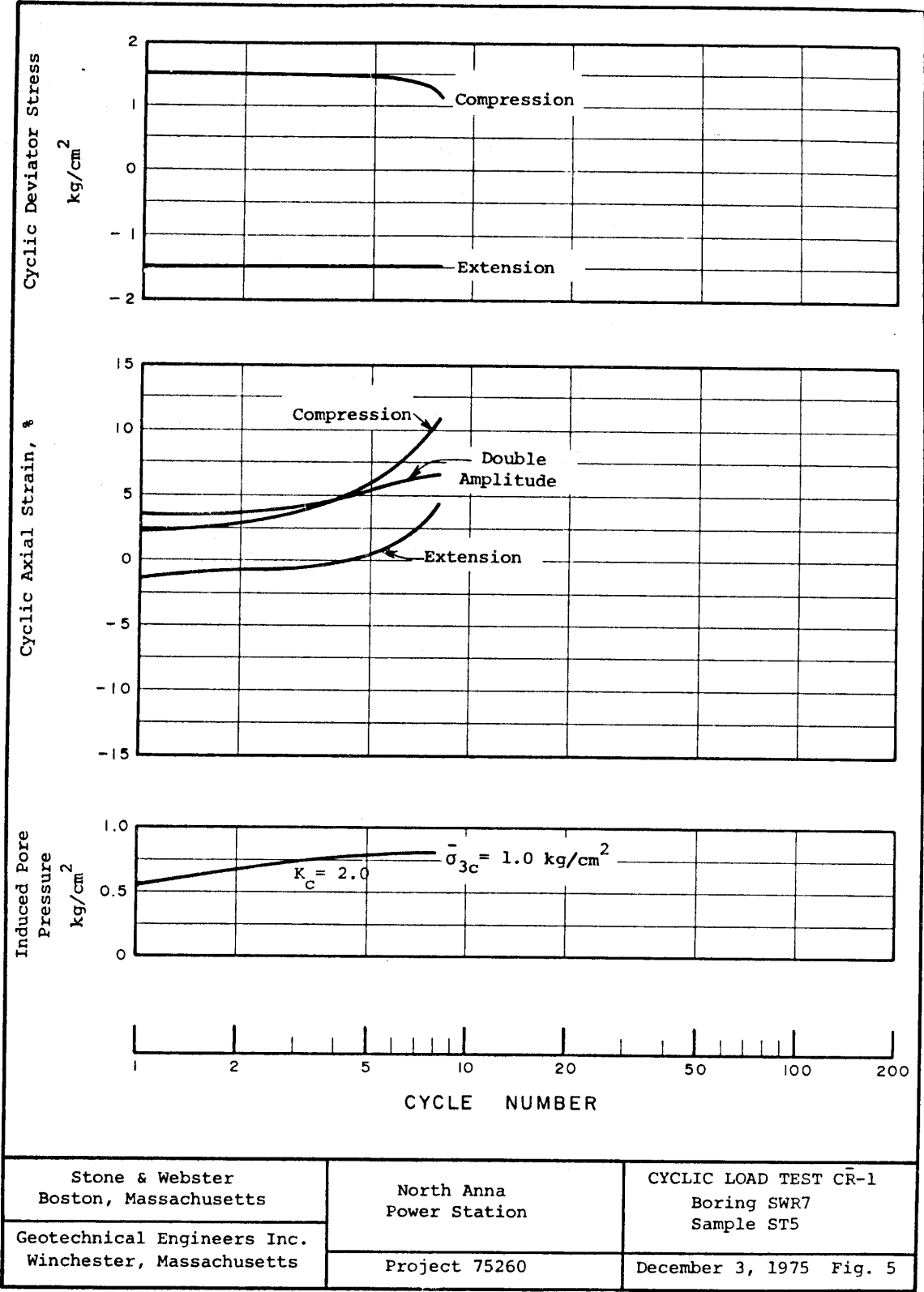
Lab. rev. 0 28 May 74



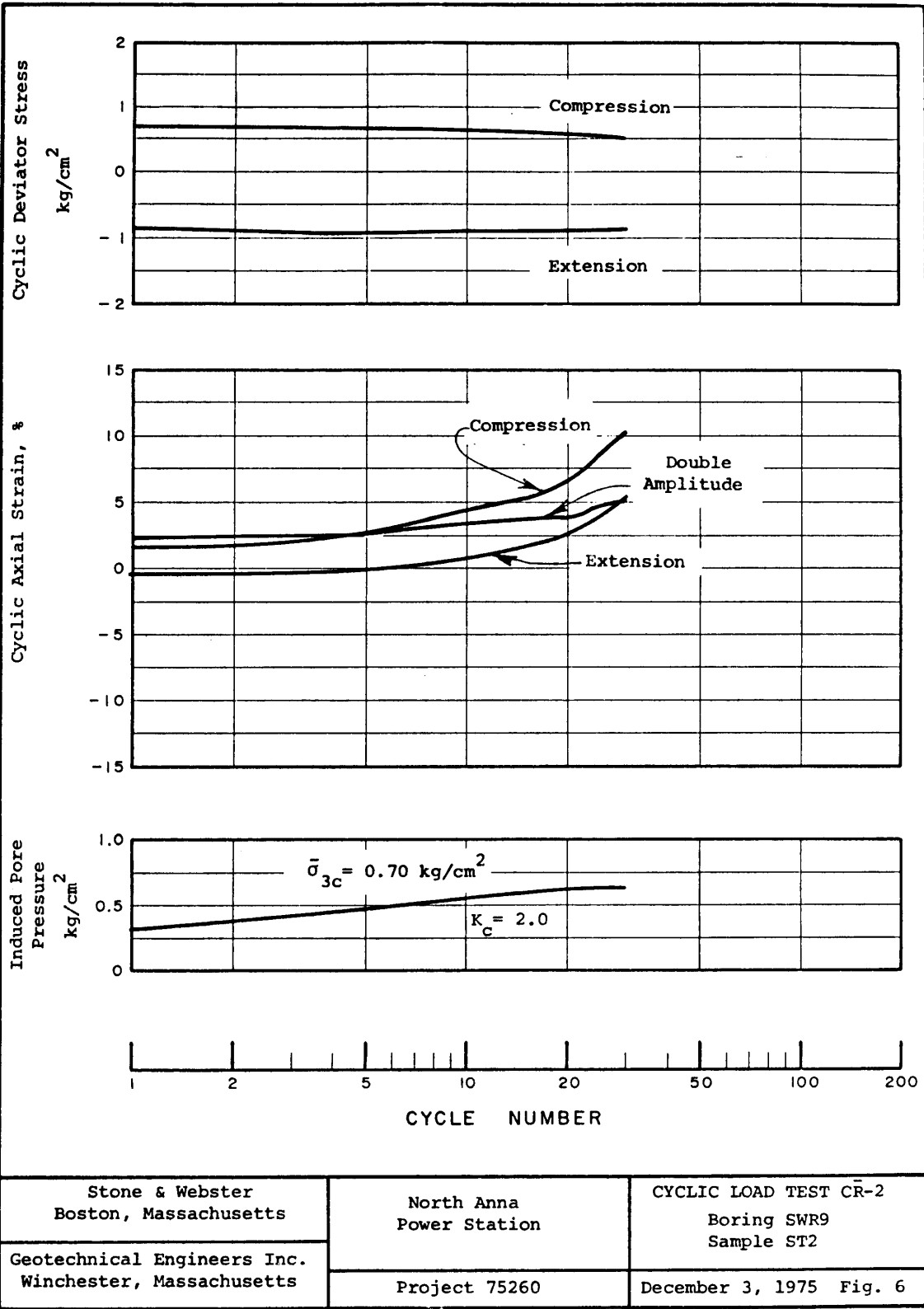
N03EA329

Lab. rev. 0 28 May 74

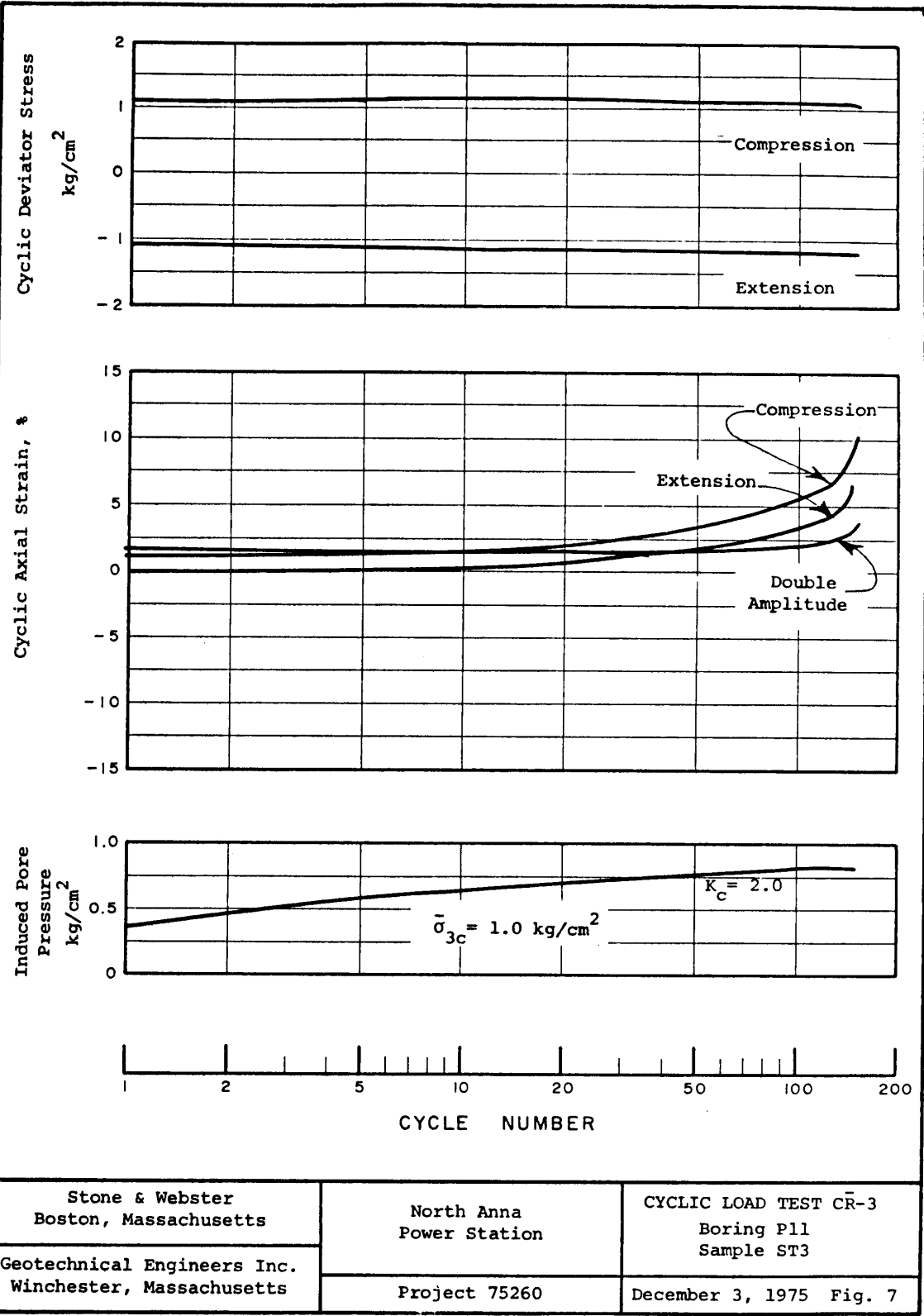




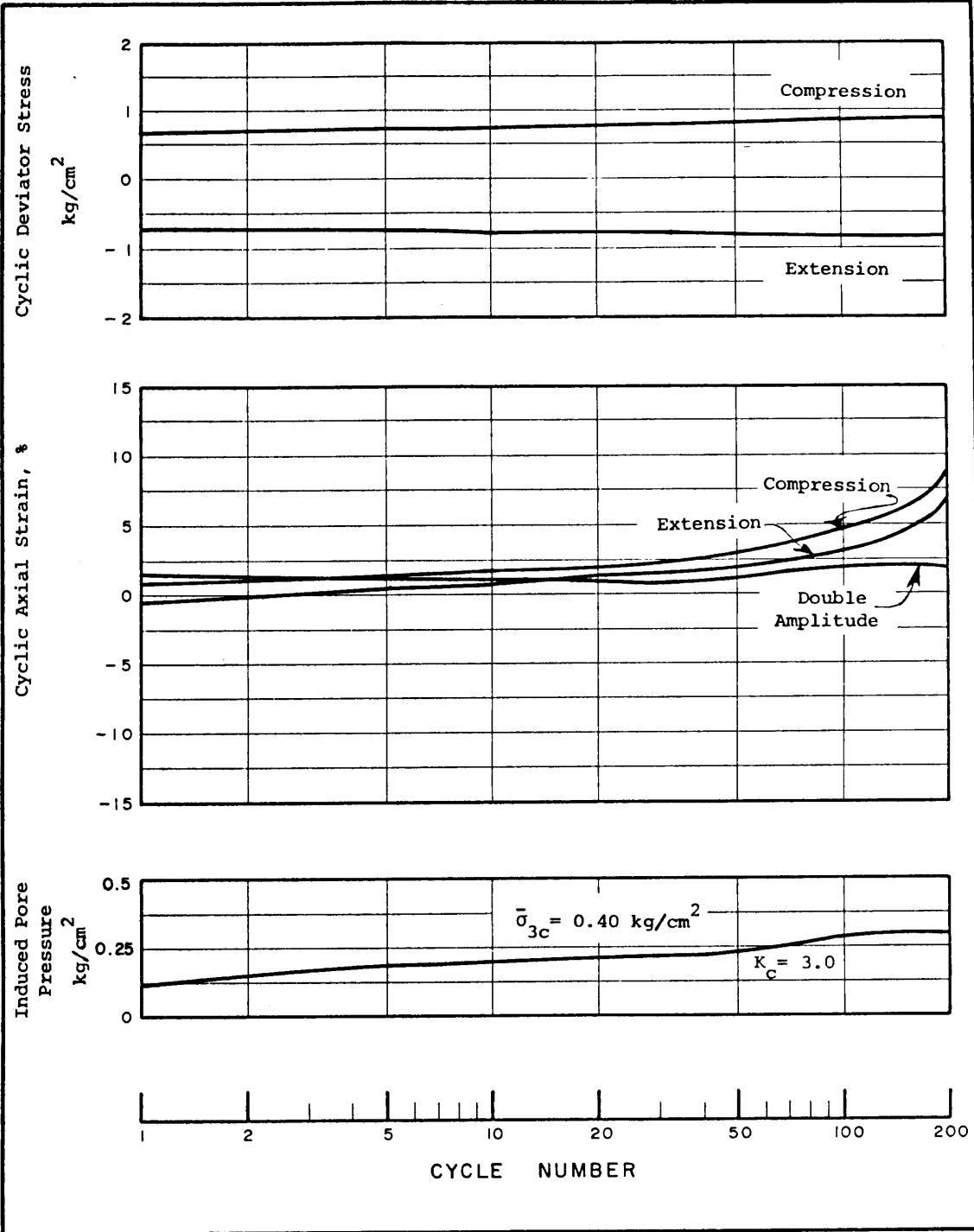
N03EA113



N03EA114

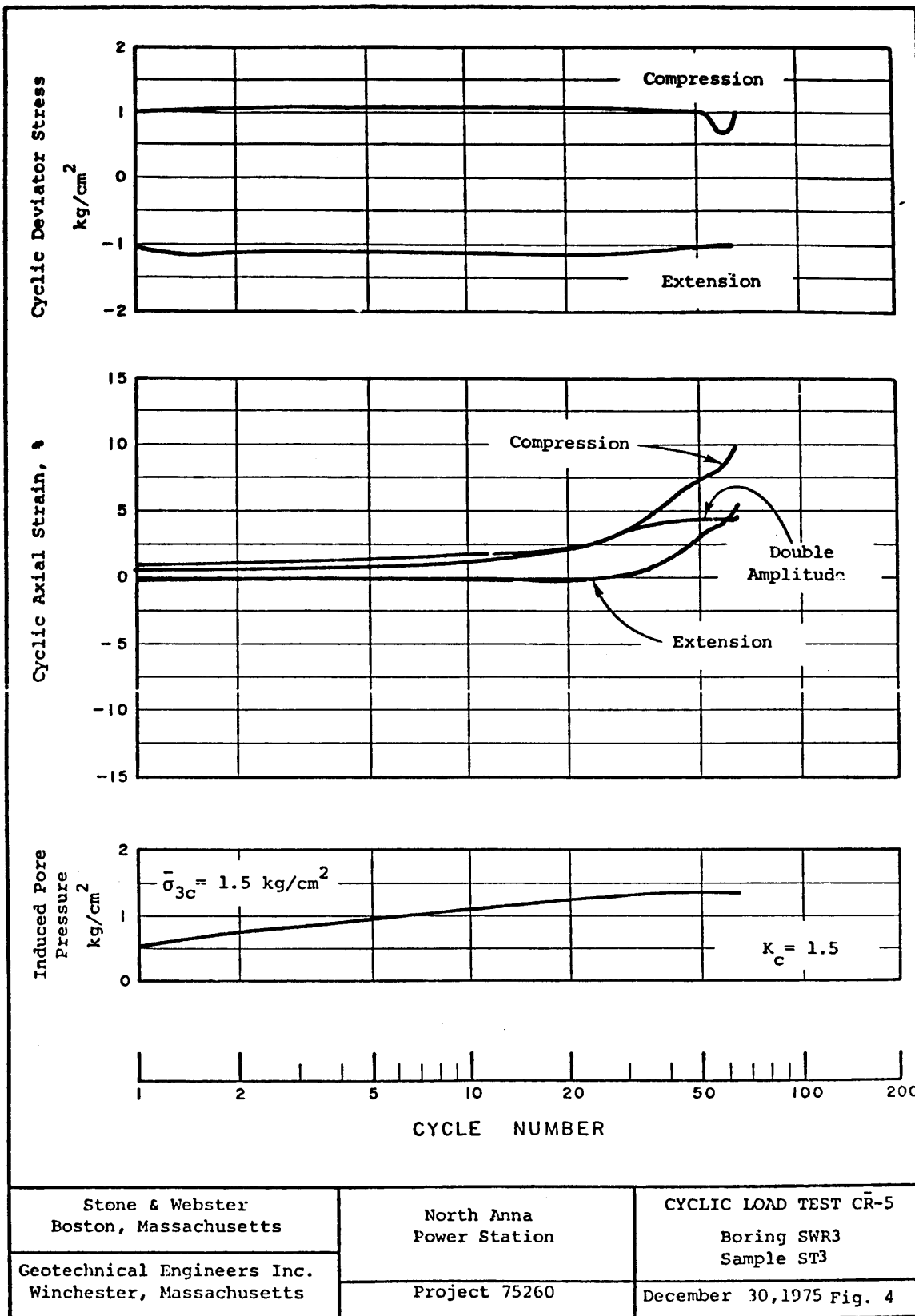


N03EA115



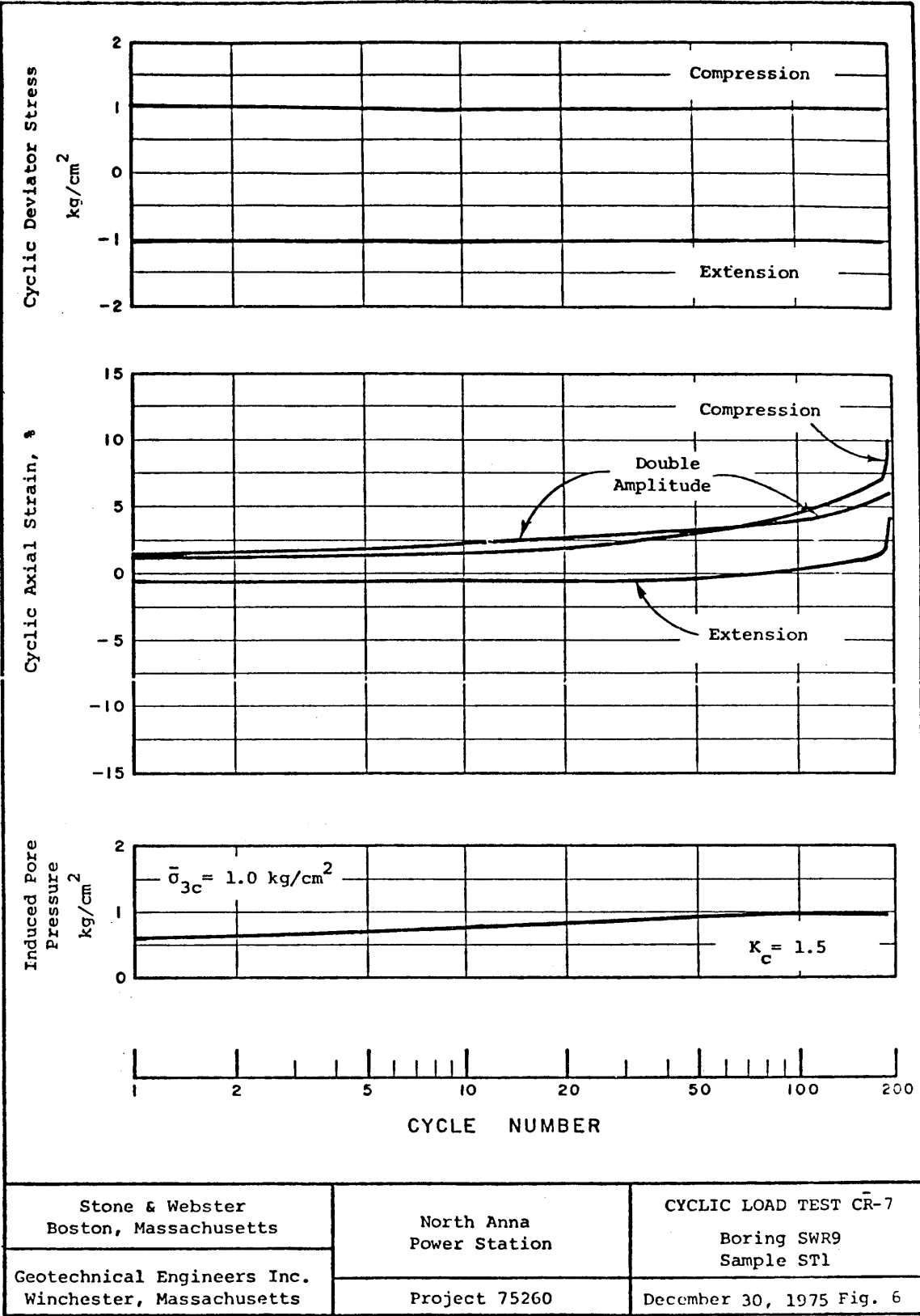
N03EA116

Stone & Webster Boston, Massachusetts	North Anna Power Station	CYCLIC LOAD TEST CR-4 Boring P12 Sample ST2
Geotechnical Engineers Inc. Winchester, Massachusetts	Project 75260	December 3, 1975 Fig. 8

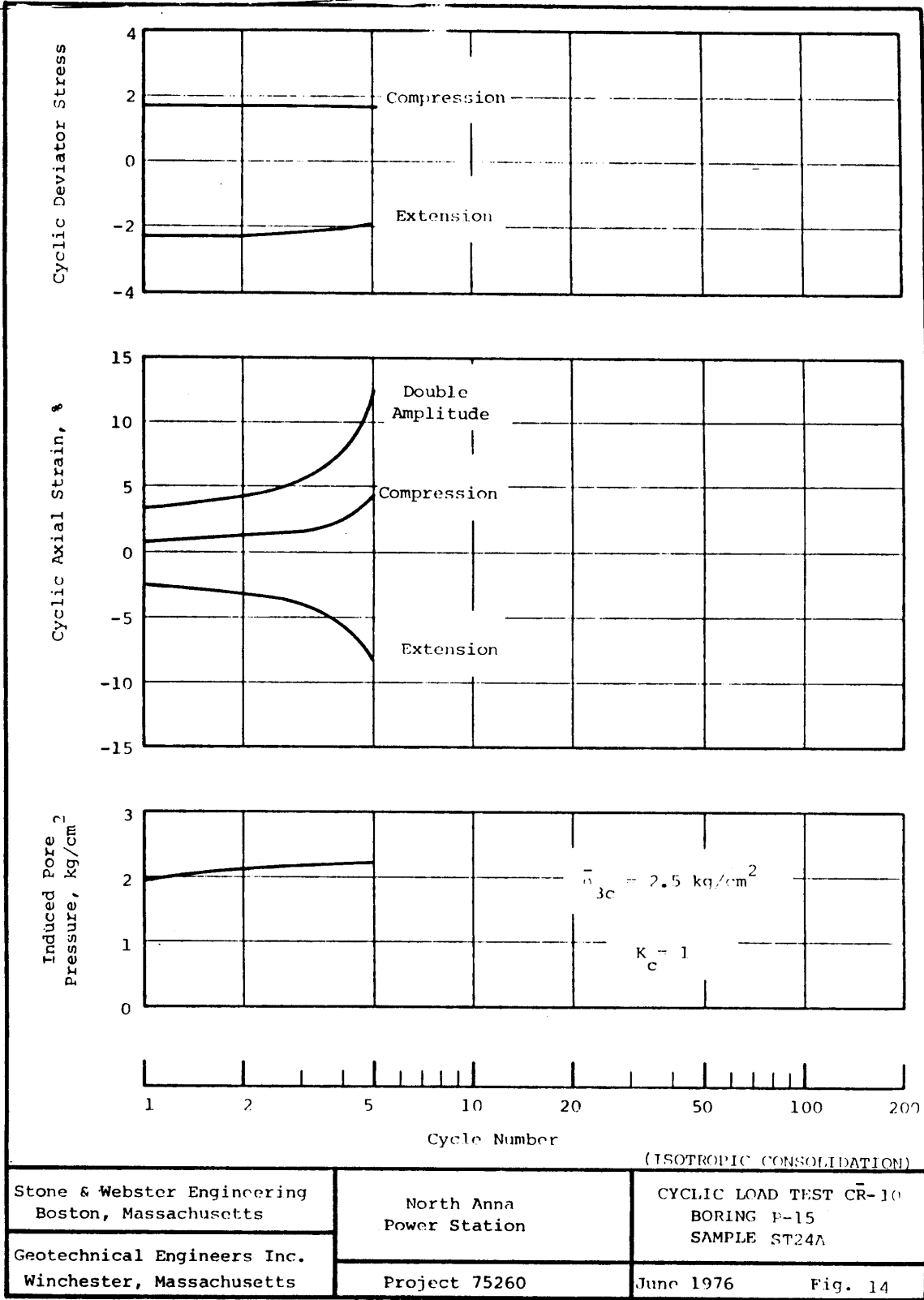


N03EA208

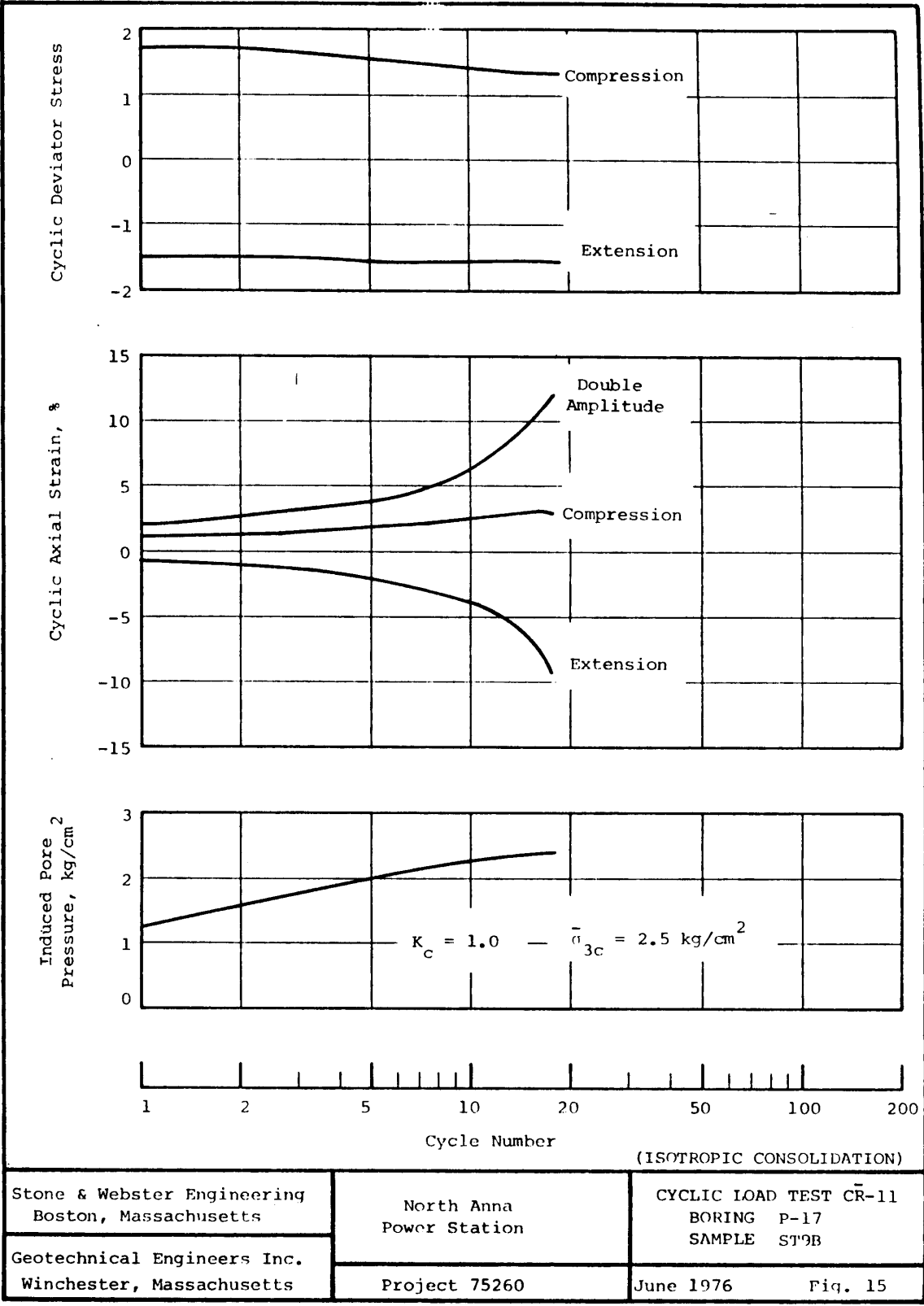
Stone & Webster Boston, Massachusetts	North Anna Power Station	CYCLIC LOAD TEST CR-5 Boring SWR3 Sample ST3
Geotechnical Engineers Inc. Winchester, Massachusetts	Project 75260	December 30, 1975 Fig. 4



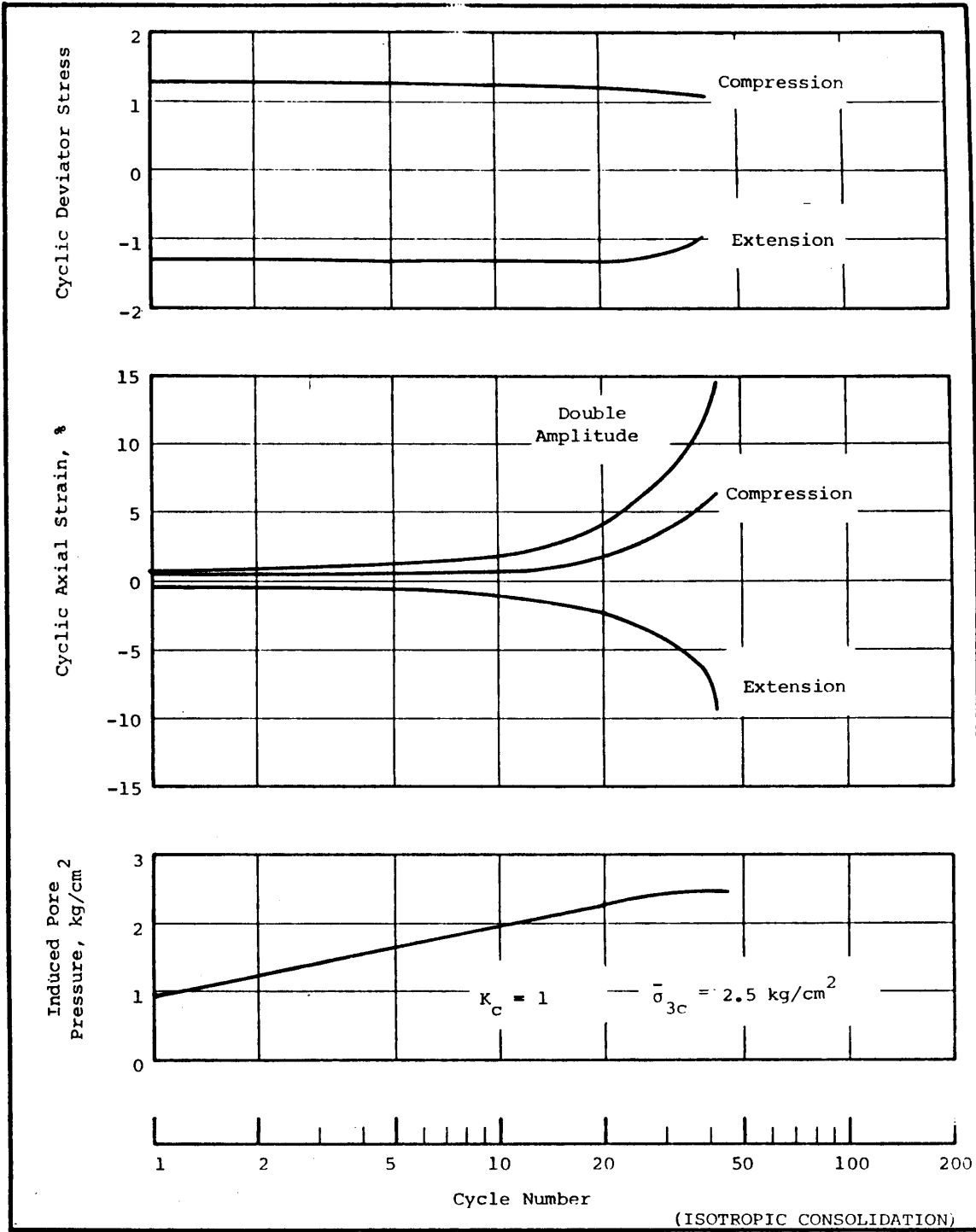
N03EA210



N03EA330



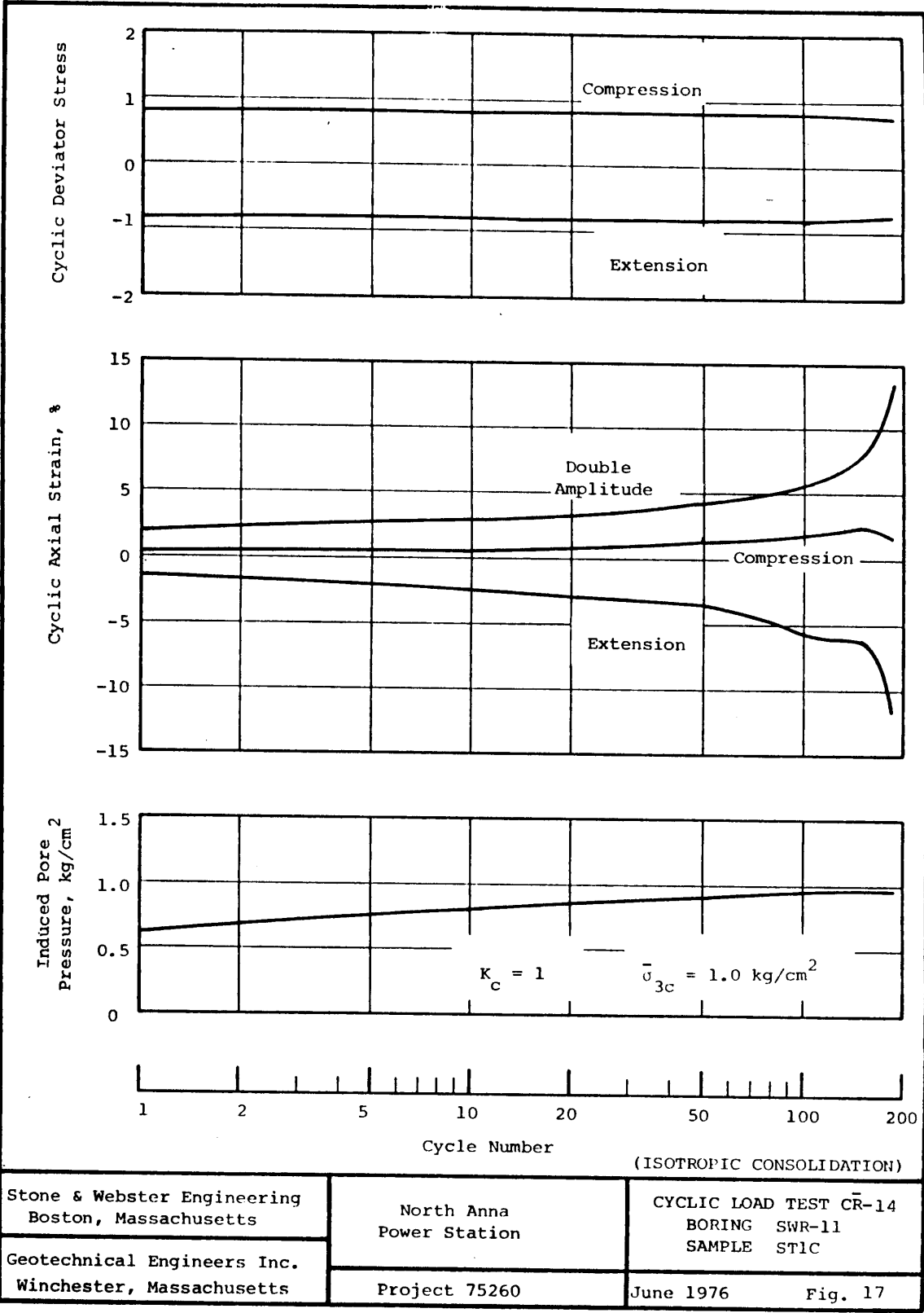
N03EA331



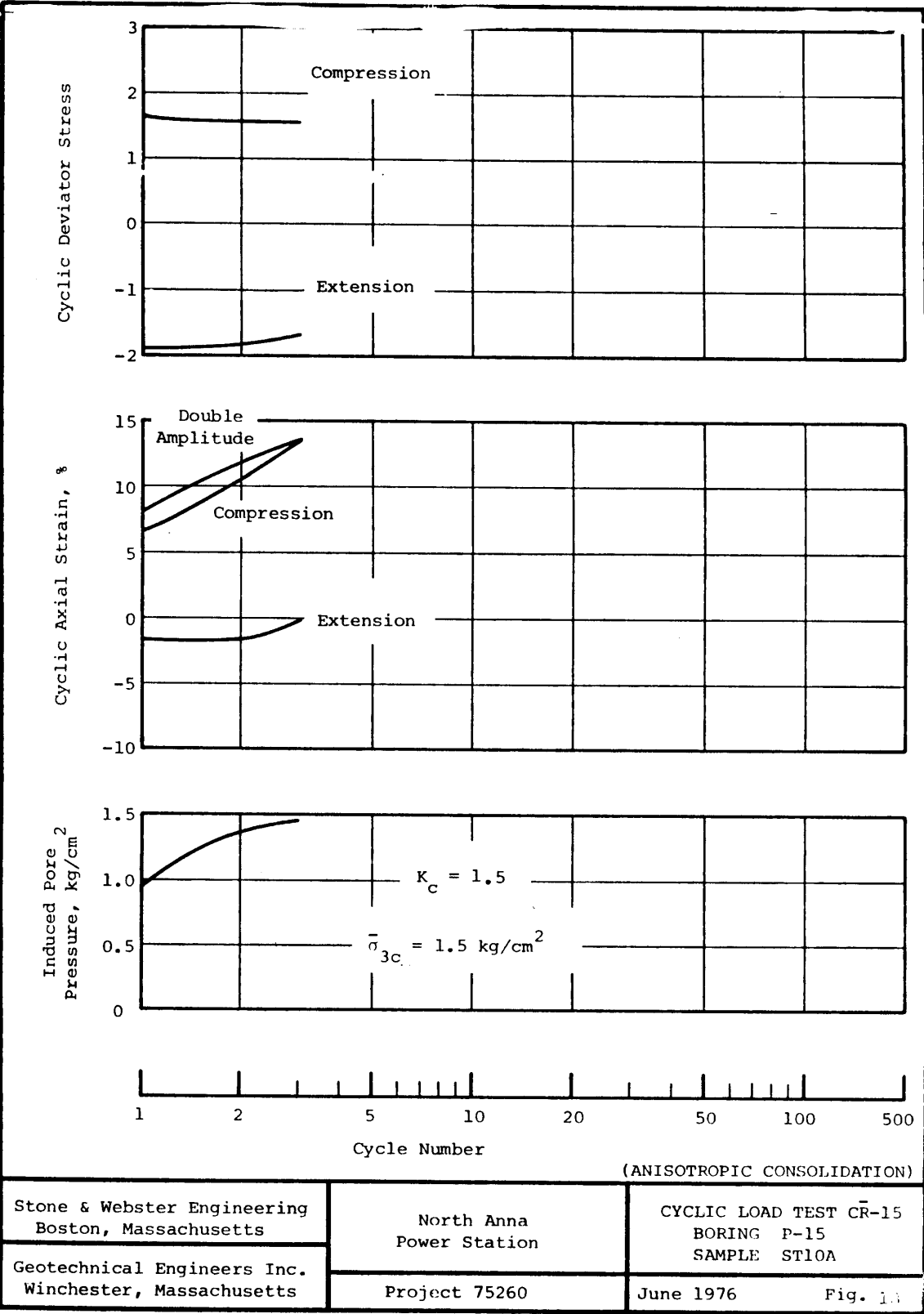
(ISOTROPIC CONSOLIDATION)

Stone & Webster Engineering Boston, Massachusetts	North Anna Power Station	CYCLIC LOAD TEST CR-13 BORING P-17 SAMPLE ST9A
Geotechnical Engineers Inc. Winchester, Massachusetts	Project 75260	June 1976 Fig. 16

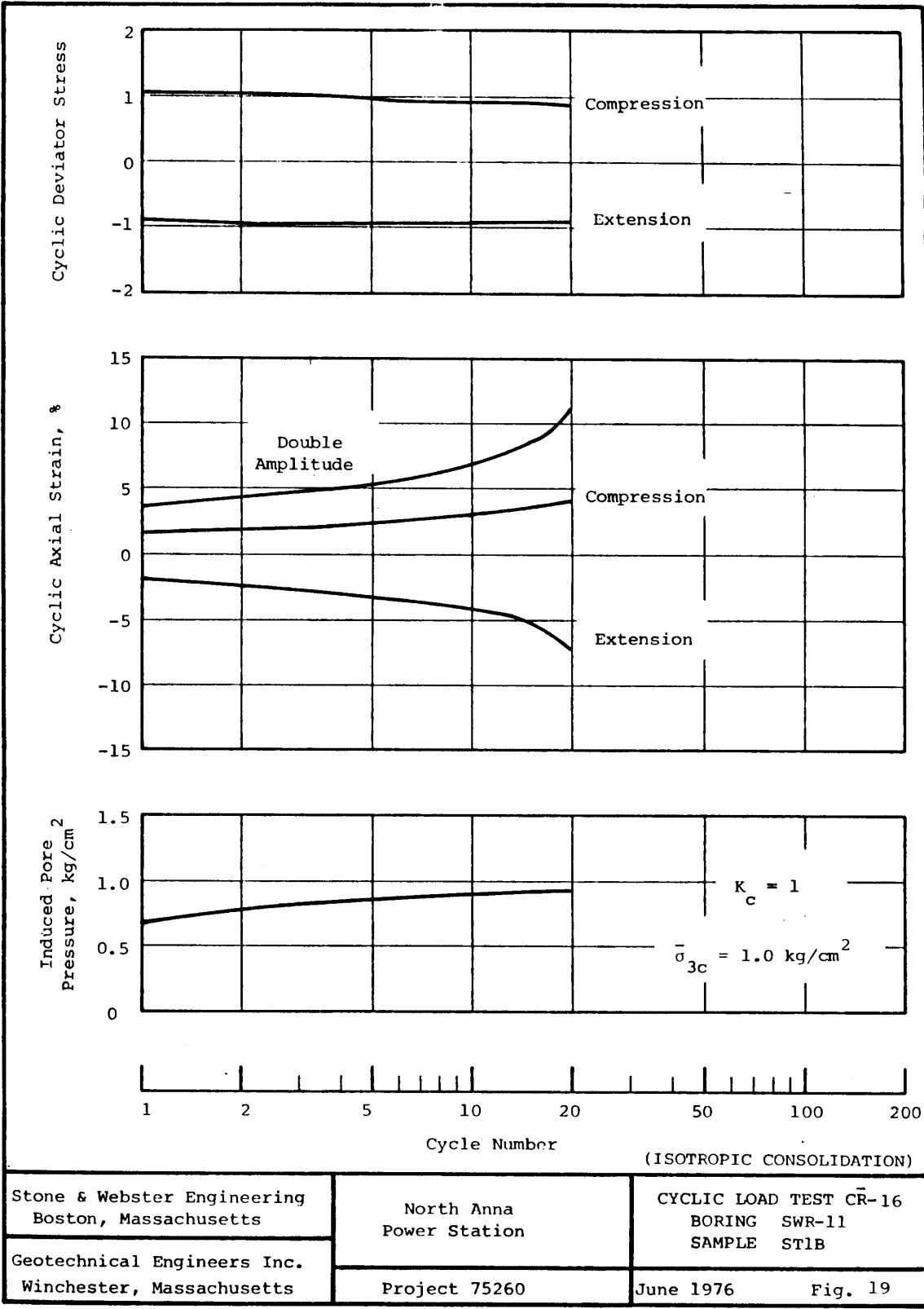
N08EA332



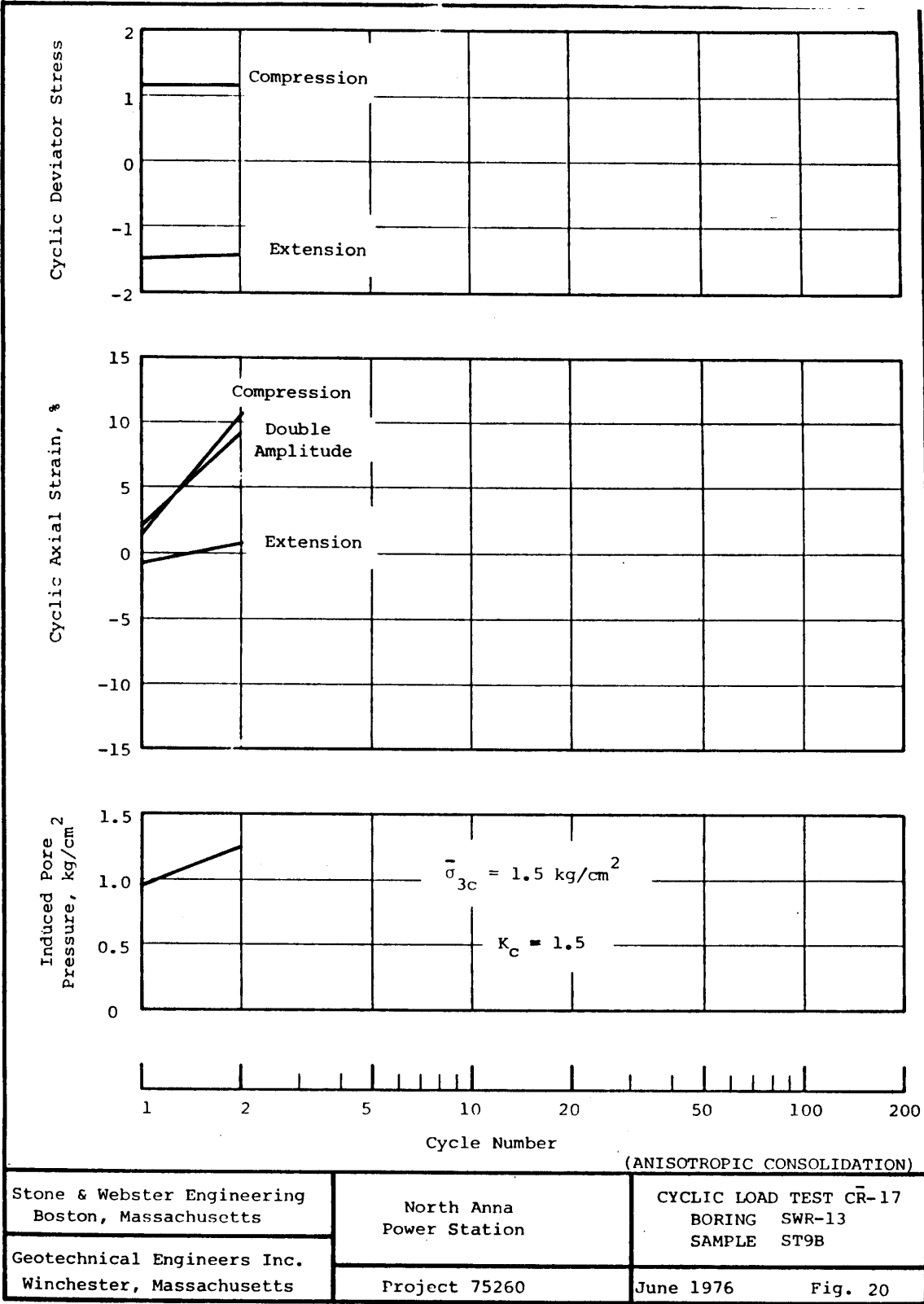
N03EA333



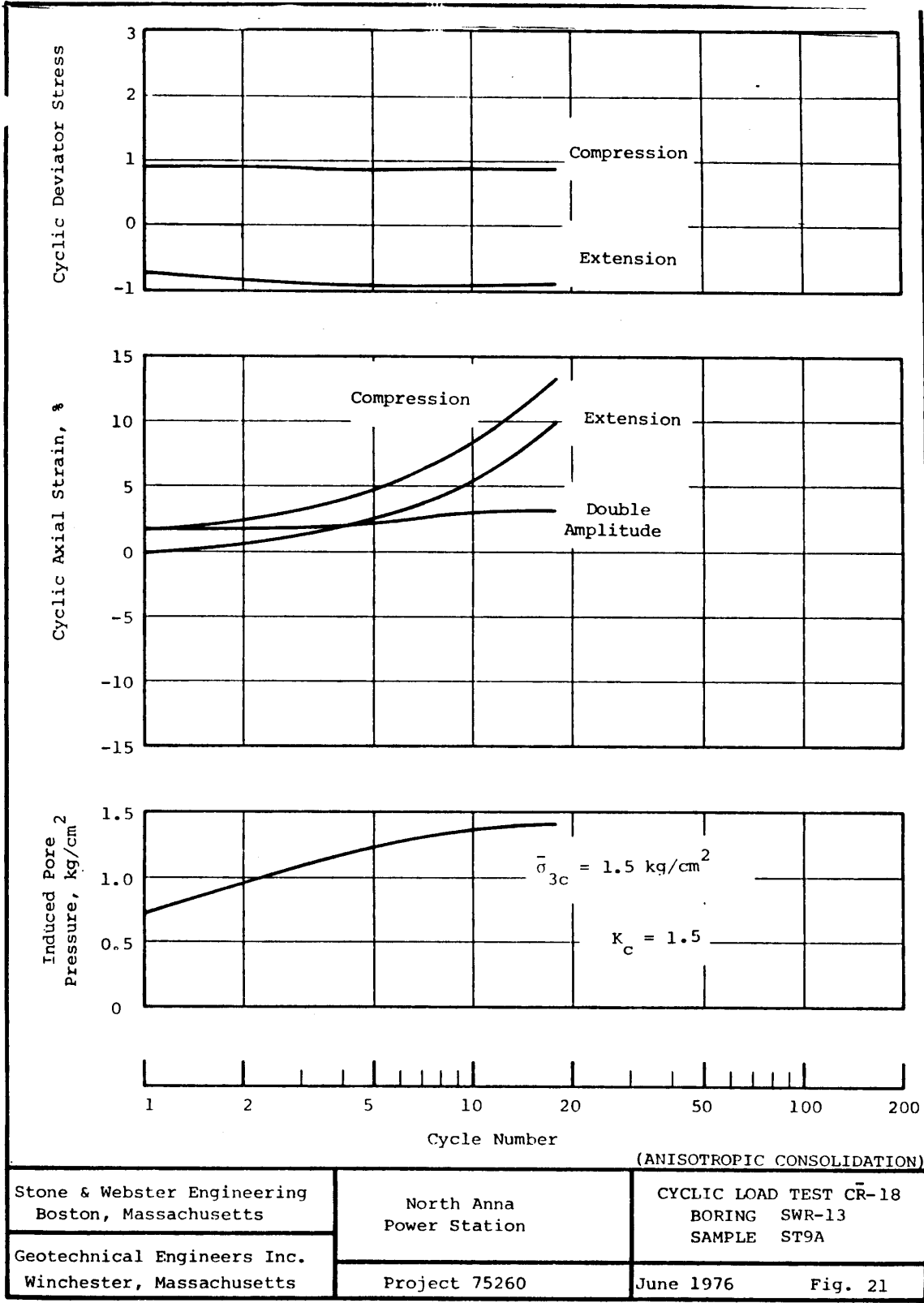
N03EA334



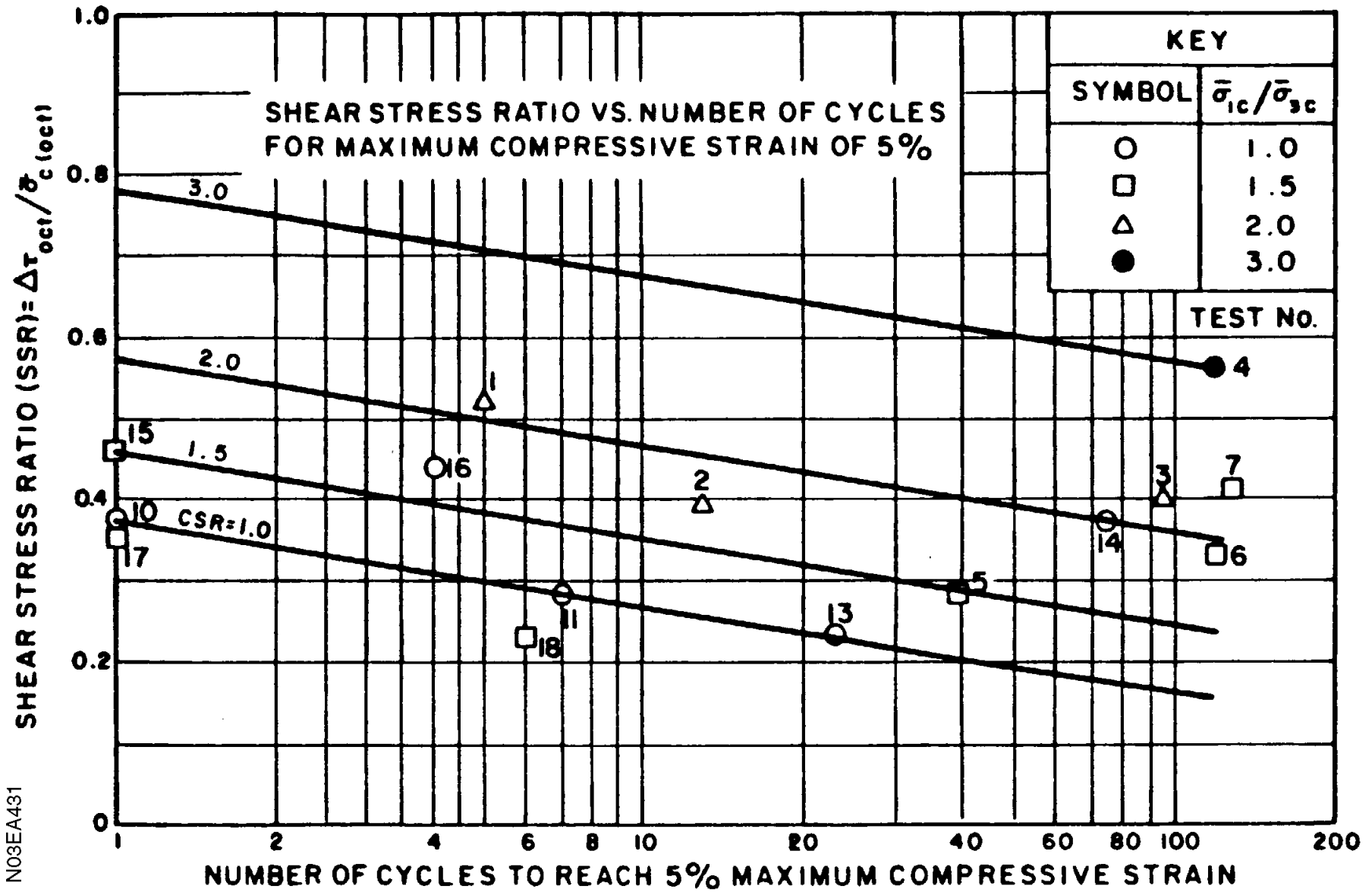
N03EA395



N03EA936

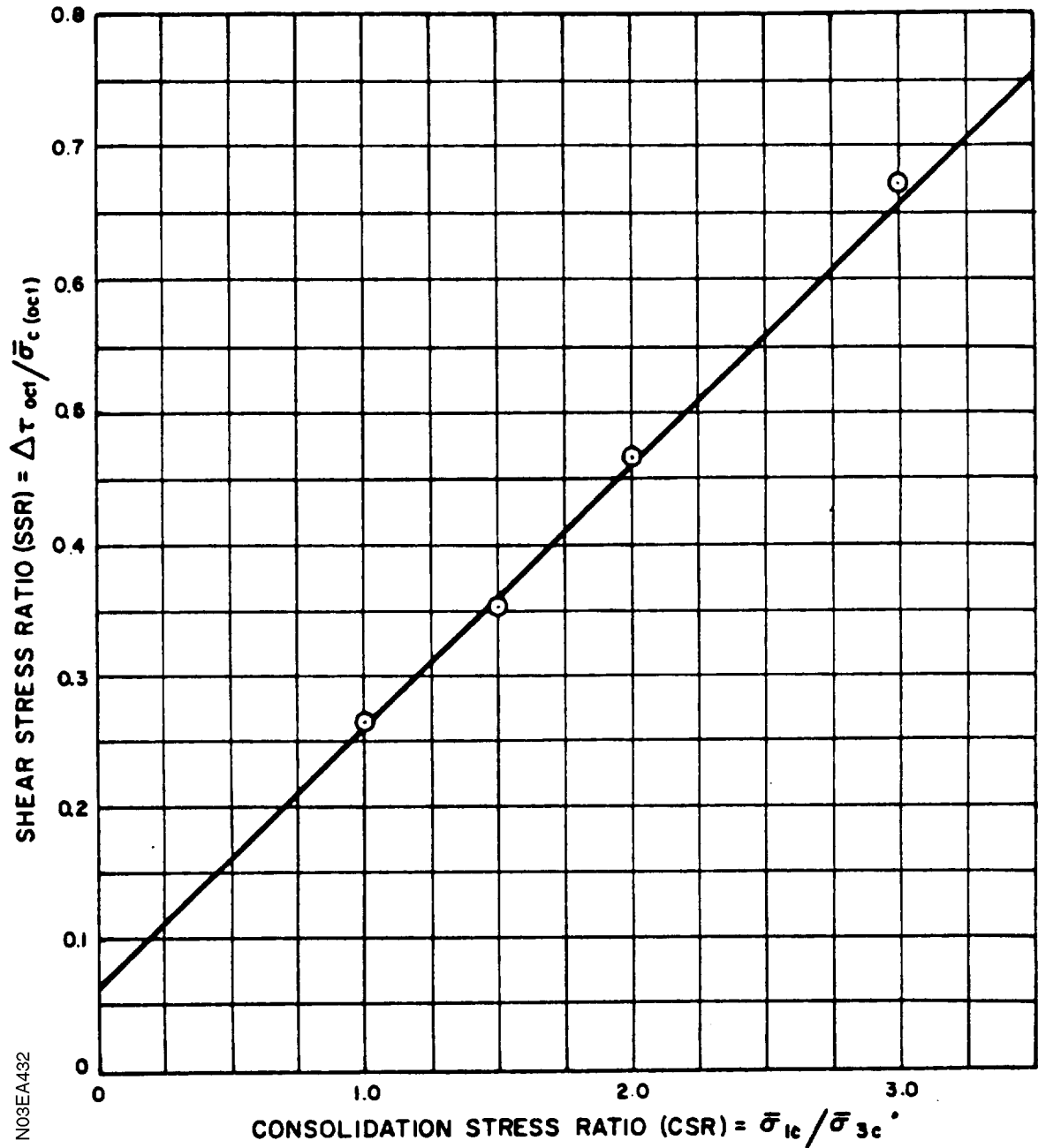


N03EA337



N03EA431

SHEAR STRESS RATIO (SR) VS. CONSOLIDATION
STRESS RATIO (CSR) FOR 5% MAX COMPRESSIVE
STRAIN IN 10 CYCLES



N03EA492

Table 3E-3
RESULTS OF CONSOLIDATION TESTS

Test Number	1	2	3	4	5	6	7	8	9	10	11	12	13	14	15
Boring number	P-11	P-11	P-11	SI-1	SI-1	SI-1	P-12	P-12	SI-2	SWR-6	P-10	SWR-4	SWR-4	SWR-4	SWR-4
Sample number	2F	3F	5F	3B	5F	6E	1F	2F	1F	4G	2B	2D	3E	5D	6
Depth, ft	24.0	37.9	48.8	40.1	52.7	63.0	8.5	18.1	13.3	58.5	22.1	28.3	39.9	63.2	77.5
Group symbol	ML-SM	SM	SM	SM	SM	SM	CH-SC	SM	SM	SM	SM	SM	SM	SM-ML	SM
Percent fines	54	29	24	30	15	31	57	25	18	33	18	36	25	48	34
Initial w_o , %	28.4	21.8	21.9	27.2	15.7	31.0	21.2	14.6	11.1	46.3	22.1	23.5	24.4	22.3	19.9
Initial d_o , pcf	90.9	95.6	95.8	86.4	104.2	90.3	103.0	98.8	99.2	66.4	112.5	92.5	93.2	91.9	96.8
Initial e_o	0.869	0.776	0.771	0.965	0.625	0.879	0.648	0.719	0.712	1.561	0.507	0.808	0.823	0.828	0.755
Type of loading	I	CRS	I	CRS	I	I	CRS	I	I	I	I	CRS	I	CRS	I
Rate of loading ^a	1000	0.079	1	0.096	1000	1000	0.090	1000	I	1000	1000	0.070	1000	0.096	1000
Maximum $\bar{\sigma}_v$, ksf	58.6	51.9	39.9	59.4	3.2	3.2	38.5	3.2	44.6	8.1	3.2	42.4	3.2	43.0	3.2
C_c	0.306	0.237	0.225	0.375	-	-	0.280	-	0.123	-	-	0.279	-	0.234	-
C_s , 10^{-2}	-	1.55	-	3.25	-	-	1.80	-	-	-	-	2.20	-	2.22	-
C , $\times 10^{-4}$	7.05	-	-	-	8.83	5.67	-	2.51	-	42.2	14.4	-	7.32	-	7.07

a. For incrementally loaded tests (I), elapsed time in min for load increments; for constant rate of strain tests (CRS), rate of vertical strain in percent strain per min.

Table 3E-4
RESULTS OF CONSOLIDATED-UNDRAINED TRIAXIAL COMPRESSION TESTS

Type of Material	Dike Fill			Foundation		Foundation with Foliation		
Test Number	1	2	3	4	5	6	7	8
Boring number	P-12	SWR-6	SWR-6	SI-2	SWR-4	SWR-6	SWR-6	SWR-4
Sample number	1D	1D	2E	1D	3D	3D	4F	1F
Depth, ft	7.9	12.7	23.6	12.1	42.2	43.1	57.2	12.9
Group symbol	CH-SC	SM-MH	MH-SM	SM	SM	SM	SM	ML-SM
Percent fines	57	48	58	18	25	31	33	57
Initial $w_o, \%$	24.6	24.8	34.1	14.3	23.5	39.8	36.2	28.9
Initial $\sqrt{d_o}, \text{pcf}$	93.9	92.5	82.0	89.7	95.5	83.3	72.3	85.6
Initial e_o	0.783	0.808	1.042	0.865	0.752	1.135	1.314	0.954
Consolidated $w_c, \%$	22.3	23.5	30.8	9.4	21.0	33.7	27.6	27.1
Consolidated $\sqrt{d_c} 1, \text{pcf}$	97.2	94.3	85.7	93.1	99.2	80.5	79.5	87.8
Consolidated e_c	0.722	0.774	0.952	0.797	0.686	1.079	1.104	0.906
$v_o, \text{kips/ft}^2$	6.5	8.6	9.4	23.1	14.4	8.6	9.4	7.9
$\bar{\sigma}_c, \text{kips/ft}^2$	3.00	2.00	4.00	5.00	4.50	5.00	8.00	2.50
At $(\bar{\sigma}_1/\bar{\sigma}_3) \text{ max}$								
$\bar{\sigma}_3, \text{ksf}$	1.60	1.22	2.23	2.65	3.01	3.69	3.27	1.75
$\bar{\sigma}_1 - \bar{\sigma}_3, \text{ksf}$	3.40	3.31	5.85	5.66	6.19	3.14	4.29	1.66
$\bar{\sigma}_1/\bar{\sigma}_3$	3.13	3.71	3.63	3.14	3.06	1.85	2.31	1.95
$(v - v_o)/(\sigma_1 - \sigma_3)$	0.41	0.24	0.30	0.42	0.24	0.42	1.10	0.45
$\theta, \%$	4.8	2.8	3.3	9.9	5.7	1.6	7.8	1.2
$\phi', \text{degrees}^a$	31.1	35.1	34.7	31.1	30.5	17.3	23.3	18.8

a. $\phi' = \arcsin \frac{(\bar{\sigma}_1/\bar{\sigma}_3) - 1}{(\bar{\sigma}_1/\bar{\sigma}_3) + 1}$.

Table 1
SUMMARY OF LABORATORY TESTING OF UNDISTURBED SAMPLES FROM BORING P-15

Sample Number	Depth (ft)	Elevation (ft)	USCS Group Symbol	Fines (%)	Water Content (wt %)	Dry Unit Weight γ_d				Void Ratio e		Saturation S		Unconsolidated-Undrained Compression Test						Condition of Tube Cutting Edge
						A (pcf)	B (pcf)	C (pcf)	D (pcf)	A	E	A (%)	E (%)	Specimen Diameter (in.)	σ_c (kef)	q_u (max) (kef)	ϵ_f (%)	ϵ_u At 8% (kef)	Mode of Failure Specimen	
ST-1A	7.4	312.6	CH-SC	60	26.3	—	—	—	—	—	—	—	—	—	—	—	—	—	—	Bent
ST-1B	7.6	312.4	SC-CH	48	25.4	98.8	97.0	96.1	—	0.693	0.740	98.3	92.0	—	—	—	—	—	—	deeply inward
ST-1F	8.0	312.0	Preserved in tube																	
ST-1G	8.5	311.5	SM-ML	34	24.1	—	—	—	—	—	—	—	—	—	—	—	—	—	—	
ST-2A	10.0	310.0	SC-CH	47	28.2	—	—	—	—	—	—	—	—	—	—	—	—	—	—	Good
ST-2B	10.2	309.8	Preserved in tube																	
ST-2E	10.4	309.6	CH-SC	55-65	28.4	96.2	94.3	93.8	93.0	0.738	0.798	103.1	95.4	2.54	1.35	4.13	8.9	2.06	—	Shearing
ST-2F	10.9	309.1	CH-SC	59	28.0	97.7	95.9	91.7	—	0.712	0.824	105.4	91.1	2.89	1.35	5.65	10.2	2.78	—	Shearing
ST-2G	11.3	308.7	CH-SC	54	22.6	—	—	—	—	—	—	—	—	—	—	—	—	—	—	
ST-3A	13.0	307.0	CH-SC	61	26.3	—	—	—	—	—	—	—	—	—	—	—	—	—	—	Many small dents
ST-3D	13.2	306.8	Preserved in tube																	
ST-3E	13.7	306.3	CH-SC	65-75	22.9	104.5	102.4	—	100.4	0.600	0.666	102.3	92.2	2.57	1.73	8.51	11.0	4.06	—	Shearing
ST-3F	14.2	305.8	CH-SC	55-65	22.8	104.4	102.4	101.3	—	0.602	0.651	101.5	93.9	2.88	1.73	4.89	7.8	2.44	—	Shearing
ST-3G	14.8	305.2	CH-SC	61	35.7	—	—	—	—	—	—	—	—	—	—	—	—	—	—	
ST-4A	15.5	304.5	CH SC	64	30.2	—	—	—	—	—	—	—	—	—	—	—	—	—	—	Good
ST-4D	15.7	304.3	Preserved in tube																	
ST-4E	15.8	304.2	CH-SC	57	22.5	104.7	102.8	101.2	100.8	0.597	0.659	101.0	91.5	2.54	1.98	8.34	6.1	4.22	—	Shearing and bulging
ST-4F	16.3	303.7	SC-CH	48	22.9	103.7	101.7	94.5	—	0.613	0.770	100.1	79.7	2.88	1.98	6.89	10.4	3.26	—	Shearing
ST-4G	16.9	303.1	CH-SC	52	19.4	—	—	—	—	—	—	—	—	—	—	—	—	—	—	
ST-5A	18.0	302.0	CH-SC	58	22.5	—	—	—	—	—	—	—	—	—	—	—	—	—	—	One deep inward dent
ST-5B	18.2	301.8	CH-SC	52	19.9	109.8	107.8	104.8	—	0.523	—	102.0	—	—	—	—	—	—	—	
ST-5F	18.7	301.3	Preserved in tube																	
ST-5G	19.2	300.8	SM	26	12.9	—	—	—	—	—	—	—	—	—	—	—	—	—	—	
ST-6A	21.0	299.0	SC-CH	45	27.5	—	—	—	—	—	—	—	—	—	—	—	—	—	—	Bent
ST-6B	21.2	298.8	SC-CH	44	30.1	—	—	—	—	—	—	—	—	—	—	—	—	—	—	deeply inward
ST-6F	21.7	298.3	Discarded																	
ST-6G	22.4	297.6	CH-SC	51	35.9	—	—	—	—	—	—	—	—	—	—	—	—	—	—	
ST-7A	23.5	296.5	SC-CH	47	28.1	—	—	—	—	—	—	—	—	—	—	—	—	—	—	Two large dents
ST-7E	23.8	296.2	CH-SC	53	24.1	100.2	98.3	95.8	95.3	0.669	0.755	96.5	85.5	2.49	2.90	5.80	9.2	2.87	—	Shearing
ST-7F	24.3	295.7	CH-SC	50	22.7	104.6	102.6	102.8	—	0.599	0.627	101.6	97.0	2.85	2.90	7.25	15	3.43	—	Shearing
ST-7G	24.8	295.2	CH-SC	52	27.8	—	—	—	—	—	—	—	—	—	—	—	—	—	—	

Table 1 (continued)
SUMMARY OF LABORATORY TESTING OF UNDISTURBED SAMPLES FROM BORING P-15

Sample Number	Depth (ft)	Elevation (ft)	USCS Group Symbol	Fines (%)	Water Content (wt %)	Dry Unit Weight γ_d				Void Ratio e		Saturation S		Unconsolidated-Undrained Compression Test						Condition of Tube Cutting Edge
						A	B	C	D	A	E	A	E	Specimen Diameter (in.)	σ_c (kef)	q_u (max) (kef)	ϵ_f (%)	s_u At 8% (kef)	Mode of Failure Specimen	
						(pcf)	(pcf)	(pcf)	(pcf)	(%)	(%)	(%)	(%)							
ST-8A	26.0	294.0	ML	85-90	31.3															—
Interface between embankment and foundation at about elevation 292.5																				
ST-9A	28.5	291.5	SC-CL	48	19.7	—	—	—	—	—	—	—	—	—	—	—	—	—	—	Good
ST-9E	28.6	291.4	Preserved in tube																	
ST-9F	29.7	290.3	SM	30-40	17.3	98.5	96.6	93.1	—	0.698	0.796	66.4	58.2	2.87	3.54	6.94	11.5	3.28	With foliation at 50°	
ST-9G	30.3	289.7	SM	33	16.8	—	—	—	—	—	—	—	—	—	—	—	—	—	—	
ST-10A	31.0	289.0	SM	10-15	23.5	—	—	—	—	—	—	—	—	—	—	—	—	—	—	Not viewed
ST-10B	31.1	288.9	SM	30	22.8	93.8	92.0	91.1	—	0.783	0.836	78.0	73.1	—	—	—	—	—	—	
ST-10D	31.5	288.5	Provided to Geotechnical Engineers, Inc., for cyclic triaxial testing																	
ST-11A	33.5	286.5	SM	30	20.0	—	—	—	—	—	—	—	—	—	—	—	—	—	—	Good
ST-11E	33.7	286.3	Preserved in tube																	
S-11F	34.6	285.4	SM	20-25	14.9	102.6	100.7	96.4	—	0.630	0.735	63.4	54.3	2.88	4.15	7.74	12.9	3.68	Shear across foliation	
ST-11G	35.2	284.8	SM	23	13.3	—	—	—	—	—	—	—	—	—	—	—	—	—	—	
ST-12A	36.0	284.0	SM	10-15	17.9	—	—	—	—	—	—	—	—	—	—	—	—	—	—	One very small dent
ST-12B	36.1	283.9	SM	10-15	17.0	100.1	98.2	97.2	—	0.671	0.720	67.9	63.3	—	—	—	—	—	—	
ST-12E	36.4	283.6	Preserved in tube																	
ST-12F	36.9	283.1	SM	20-25	16.1	107.2	105.1	97.6	—	0.560	0.713	77.0	60.5	2.89	4.45	8.00	>15	3.86	With foliation at 45°	
ST-12G	37.4	282.6	SM	21	15.0	—	—	—	—	—	—	—	—	—	—	—	—	—	—	
ST-13A	38.5	281.5	SM	26	18.0	—	—	—	—	—	—	—	—	—	—	—	—	—	—	Fair
ST-13E	38.7	281.3	Preserved in tube																	
ST-13F	39.6	280.4	SM	15-25	13.3	106.0	104.0	95.5	—	0.578	0.751	61.7	47.5	2.89	4.78	9.51	10.4	4.52	Shear across foliation	
ST-13G	40.2	279.8	SM	22	13.8	—	—	—	—	—	—	—	—	—	—	—	—	—	—	
ST-14A	41.0	279.0	SM	10-20	16.7	—	—	—	—	—	—	—	—	—	—	—	—	—	—	Very good
ST-14B	41.1	278.9	SM	10-20	15.9	101.7	99.8	97.4	—	0.644	0.717	66.2	59.4	—	—	—	—	—	—	
ST-14E	41.4	278.6	Preserved in tube																	
ST-14F	42.0	278.0	SM	20-25	15.4	108.2	106.1	99.4	—	0.546	0.682	75.6	60.5	2.89	5.08	8.77	9.4	4.35	Slip along clay seam	
ST-14G	42.5	277.5	SM	23	13.8	—	—	—	—	—	—	—	—	—	—	—	—	—	—	
ST-15A	43.5	276.5	SP	4	13.2	—	—	—	—	—	—	—	—	—	—	—	—	—	—	Good
ST-15E	43.6	276.4	Preserved in tube																	

Table 1 (continued)
SUMMARY OF LABORATORY TESTING OF UNDISTURBED SAMPLES FROM BORING P-15

Sample Number	Depth (ft)	Elevation (ft)	USCS Group Symbol	Fines (%)	Water Content (wt %)	Dry Unit Weight γ_d				Void Ratio e		Saturation S		Unconsolidated-Undrained Compression Test						Condition of Tube Cutting Edge
						A	B	C	D	A	E	A	E	Specimen Diameter (in.)	σ_c (kef)	q_u (max) (kef)	ϵ_f (%)	s_u At 8% (kef)	Mode of Failure Specimen	
						(pcf)	(pcf)	(pcf)	(pcf)	(%)	(%)	(%)	(%)							
ST-15F	44.5	275.5	SM	20-25	17.1	110.7	108.5	99.3	—	0.511	0.684	89.7	67.0	2.88	5.39	8.85	>15	3.84	With foliation at 45°	
ST-15G	45.0	275.0	SM	23	15.7	—	—	—	—	—	—	—	—	—	—	—	—	—	—	
ST-16A	46.0	274.0	SM	10-20	17.2	—	—	—	—	—	—	—	—	—	—	—	—	—	—	Fair, but out-of-round
ST-16B	46.2	273.8	SM	10-20	19.7	100.9	99.0	97.3	—	0.657	0.719	80.4	73.4	—	—	—	—	—	—	
ST-16E	46.5	273.5	Preserved in tube																	
ST-16F	47.0	273.0	SM	19	13.9	117.0	114.8	108.3	—	0.429	0.544	86.8	68.5	2.89	5.70	10.17	7.6	5.06	With foliation at 55°	
ST-16G	47.6	272.4	SM	10-20	15.0	—	—	—	—	—	—	—	—	—	—	—	—	—	—	
ST-17A	48.5	271.5	SM	10-20	18.1	—	—	—	—	—	—	—	—	—	—	—	—	—	—	Very good
ST-17D	48.7	271.3	Preserved in tube																	
ST-17E	49.1	270.9	SM	15-20	16.5	112.2	110.0	103.5	—	0.490	0.616	90.2	71.8	2.88	5.96	9.34	>15	3.60	With foliation at 40°	
ST-17F	49.7	270.3	SM	15-20	15.3	116.0	113.7	106.6	—	0.442	0.569	92.8	72.1	2.89	6.04	4.99	3.4	2.56	Slip along clay joint	
ST-17G	50.2	269.8	SM	18	16.9	—	—	—	—	—	—	—	—	—	—	—	—	—	—	
ST-18A	51.0	269.0	SM	10-20	16.2	—	—	—	—	—	—	—	—	—	—	—	—	—	—	Very good
ST-18B	51.2	268.8	SM	10-20	17.0	109.6	107.5	103.4	—	0.526	0.617	86.6	73.8	—	—	—	—	—	—	
ST-18E	51.5	268.5	Preserved in tube																	
ST-18F	52.2	267.8	SM	30-35	21.1	107.3	105.3	99.2	—	0.599	0.686	101.2	82.4	2.88	6.35	3.40	8.2	1.69	With foliation 50°	
ST-18G	52.7	267.3	SM	39	37.5	—	—	—	—	—	—	—	—	—	—	—	—	—	—	
ST-19A	53.5	266.5	SM	35-45	41.9	—	—	—	—	—	—	—	—	—	—	—	—	—	—	One deep
ST-19D	53.7	266.3	SM	15-20	17.8	108.9	106.9	105.2	—	0.536	0.590	89.0	80.9	2.88	6.56	6.95	>15	2.72	With foliation at 45°	
ST-19E	54.1	265.9	SM	18	17.2	—	—	—	—	—	—	—	—	—	—	—	—	—	—	
ST-19F	54.2	265.8	SM	15-20	18.8	110.4	108.3	103.9	—	0.515	0.610	97.8	82.6	2.89	6.61	2.24	13.6	1.10	In clean sand layer	Inward dent
ST-19G	54.7	265.3	SM	30	17.8	—	—	—	—	—	—	—	—	—	—	—	—	—	—	
ST-20A	56.0	264.0	SM	25-35	23.0	—	—	—	—	—	—	—	—	—	—	—	—	—	—	Fair
ST-20B	56.2	263.8	SM	25-35	28.0	98.4	96.5	94.9	—	0.699	0.762	67.4	98.5	—	—	—	—	—	—	
ST-20E	56.5	263.5	Preserved in tube																	
ST-20F	57.2	262.8	SM	26	20.0	109.8	107.8	101.3	—	0.523	0.651	102.5	82.3	2.87	6.96	4.08	3.8	1.35	With foliation at 50°	
ST-20G	57.7	262.3	SM	31	25.0	—	—	—	—	—	—	—	—	—	—	—	—	—	—	
ST-21A	58.5	261.5	SM	21	21.8	—	—	—	—	—	—	—	—	—	—	—	—	—	—	Very good
ST-21D	58.7	261.3	Preserved in tube																	
ST-21E	59.3	260.7	SM	15-20	20.1	109.6	107.6	102.0	—	0.526	0.640	102.4	84.2	2.89	7.24	4.25	9.3	2.00	With foliation at 40°	
ST-21F	59.8	260.2	SM	15-20	21.1	108.9	106.9	102.7	—	0.536	0.628	105.5	90.0	2.89	7.31	5.64	8.2	1.80	With foliation at 55°	

Table 1 (continued)
SUMMARY OF LABORATORY TESTING OF UNDISTURBED SAMPLES FROM BORING P-15

Sample Number	Depth (ft)	Elevation (ft)	USCS Group Symbol	Fines (%)	Water Content (wt %)	Dry Unit Weight γ_d				Void Ratio e		Saturation S		Unconsolidated-Undrained Compression Test						Condition of Tube Cutting Edge				
						A	B	C	D	A	E	A	E	Specimen Diameter (in.)	σ_c (kef)	q_u (max) (kef)	ϵ_f (%)	s_u At 8% (kef)	Mode of Failure Specimen					
						(pcf)	(pcf)	(pcf)	(pcf)			(%)	(%)											
ST-21G	60.3	259.7	SM	17	22.0	—	—	—	—	—	—	—	—	—	—	—	—	—	—	—	—	—	—	—
ST-22A	61.0	259.0	SM	20-30	20.6	—	—	—	—	—	—	—	—	—	—	—	—	—	—	—	—	—	—	Good
ST-22B	61.2	258.8	SM	20-30	22.0	107.1	105.1	101.6	—	0.561	0.646	105.1	91.3	—	—	—	—	—	—	—	—	—	—	—
ST-22D	61.5	258.5	Preserved in tube																					Good
ST-22E	61.7	258.3	SP-SM	5-10	19.4	113.3	111.1	104.7	—	0.476	0.597	109.2	87.1	2.90	7.54	3.55	8.1	1.76						Shearing
ST-22F	62.2	257.8	SM	17	18.2	119.2	116.9	115.7	—	0.403	0.445	121.0	109.6	2.87	7.59	6.54	5.0	2.90						Shear across foliation
ST-22G	62.7	257.3	SM	31	29.7	—	—	—	—	—	—	—	—	—	—	—	—	—	—	—	—	—	—	—
ST-23A	63.5	256.5	SP-SM	8-12	23.0	—	—	—	—	—	—	—	—	—	—	—	—	—	—	—	—	—	—	Good, one small dent
ST-23B	63.7	256.3	Preserved in tube																					
ST-23D	64.3	255.7	SP-SM	8-12	27.1	—	—	—	91.3	—	0.832	—	87.3	Constant-volume direct shear test										
ST-23E	64.5	255.5	Preserved in tube																					
ST-23F	64.7	255.3	SM	18	18.9	119.2	116.9	114.8	—	0.403	0.457	125.7	110.8	2.87	7.92	2.77	3.2	1.40						With foliation at 60°
ST-23G	65.8	254.2	SP-SM	8-12	21.1	—	—	—	—	—	—	—	—	—	—	—	—	—	—	—	—	—	—	—
ST-24A	66.0	254.0	SM	15-25	—	—	—	—	—	—	—	—	—	—	—	—	—	—	—	—	—	—	—	Not viewed
ST-24B	66.2	253.8	SM	24	37.9	92.5	90.7	89.9	—	0.808	0.860	125.7	118.1	—	—	—	—	—	—	—	—	—	—	—
ST-24D	66.5	253.5	Provided to Geotechnical Engineers, Inc., for cyclic triaxial testing																					
ST-25A	69.5	250.5	SM	10-15	23.1	—	—	—	—	—	—	—	—	—	—	—	—	—	—	—	—	—	—	Fair
ST-25D	69.7	250.3	Preserved in tube																					
ST-25E	70.2	249.8	SM	10-15	27.0	98.3	96.5	91.4	—	0.701	0.830	103.2	87.2	2.88	8.60	4.37	7.6	2.18						Shearing and bulging
ST-25F	70.8	249.2	SM	31	25.6	104.2	102.2	95.1	—	0.605	0.758	113.4	90.5	2.87	8.67	2.48	>15	0.82						Along thin clay layer
ST-25G	71.4	248.6	SM	25-30	14.3	—	—	—	—	—	—	—	—	—	—	—	—	—	—	—	—	—	—	—

Table 2
SUMMARY OF LABORATORY TESTING OF UNDISTURBED SAMPLES FROM BORING P-16

Sample Number	Depth (ft)	Elevation (ft)	USCS Group Symbol	Fines (%)	Water Content (wt %)	Dry Unit Weight γ_d				Void Ratio e		Saturation S		Unconsolidated-Undrained Compression Test					Condition of Tube Cutting Edge	
						A (pcf)	B (pcf)	C (pcf)	D (pcf)	A	E	A (%)	E (%)	Specimen Diameter (in.)	σ_c (kef)	q_u (max) (kef)	ϵ_f (%)	s_u At 8% (kef)		Mode of Failure Specimen
ST-1A	7.5	312.5	Empty																	Good
ST-1B	7.5	312.5	CH-SC	65-75	24.5	—	—	—	—	—	—	—	—	—	—	—	—	—	—	
ST-1C	7.7	312.3	CH-SC	65-75	25.5	97.3	95.4	—	—	0.719	—	95.0	—	—	—	—	—	—	—	
ST-1F	8.0	312.0	Preserved in tube																	
ST-1G	9.0	311.0	CH-SC	78	37.6	—	—	—	—	—	—	—	—	—	—	—	—	—	—	
ST-2A	12.5	307.5	CH-SC	56	25.5	—	—	—	—	—	—	—	—	—	—	—	—	—	—	Fair
ST-2E	12.6	307.4	Preserved in tube																	
ST-2F	13.5	306.5	CH-SC	55-60	20.6	109.0	107.0	103.3	—	0.534	0.619	103.4	89.2	2.87	1.66	6.59	14.8	3.00	Bulging and shearing	
ST-2G	14.0	306.0	CH-SC	52	19.6	—	—	—	—	—	—	—	—	—	—	—	—	—	—	
ST-3A	17.5	302.5	ML-SM	55-65	20.0	—	—	—	—	—	—	—	—	—	—	—	—	—	—	Very good
ST-3B	17.6	302.4	ML-SM	55-65	—	—	—	—	—	—	—	—	—	—	—	—	—	—	—	
ST-3C	17.7	302.3	ML-SM	55-65	25.7	101.1	99.1	98.9	—	0.654	0.691	105.3	99.7	—	—	—	—	—	—	
ST-3F	18.1	301.9	Preserved in tube																	
ST-3G	19.1	300.9	SM	27	21.9	—	—	—	—	—	—	—	—	—	—	—	—	—	—	
ST-4A	22.5	297.5	ML-SM	54	29.6	—	—	—	—	—	—	—	—	—	—	—	—	—	—	Good
ST-4E	22.7	297.3	Preserved in tube																	
ST-4F	23.7	296.3	ML-SM	50-55	23.7	99.2	97.3	95.6	—	0.686	0.749	92.6	84.8	2.87	2.82	6.12	9.9	3.00	Shearing	
ST-4G	24.3	295.7	ML-SM	50	25.0	—	—	—	—	—	—	—	—	—	—	—	—	—	—	
ST-5A	27.5	292.5	ML-SM	65-75	32.7	—	—	—	—	—	—	—	—	—	—	—	—	—	—	Fair
ST-5B	27.7	292.3	ML-SM	65-75	31.5	87.9	86.2	84.6	—3	0.90	0.977	93.5	86.4	—	—	—	—	—	—	
ST-5E	28.0	292.0	Preserved in tube																	
ST-5F	28.7	291.3	ML-SM	55-65	23.0	102.6	100.6	98.6	—	0.630	0.696	97.8	88.6	2.87	3.41	7.85	14.4	3.71	Shearing	
ST-5G	29.2	290.8	ML-SM	61	23.9	—	—	—	—	—	—	—	—	—	—	—	—	—	—	
ST-6A	32.5	287.5	ML-SM	55-60	18.5	—	—	—	—	—	—	—	—	—	—	—	—	—	—	Good
ST-6E	32.7	287.3	Preserved in tube																	
ST-6F	33.7	286.3	ML-SM	70-80	31.0	86.9	85.2	84.8	—	0.924	0.972	89.9	85.5	2.87	4.00	6.19	12.0	2.98	Shearing	
ST-6G	34.4	285.6	SM	10-15	19.9	—	—	—	—	—	—	—	—	—	—	—	—	—	—	
Interface between embankment and foundation at exactly elevation 285.9 (near bottom of test specimen)																				
ST-7A	37.5	282.5	SM	10-20	34.4	—	—	—	—	—	—	—	—	—	—	—	—	—	—	Not viewed
ST-7B	37.7	282.3	SM	10-20	31.2	88.2	86.4	86.1	—	0.896	0.942	93.3	88.8	—	—	—	—	—	—	
ST-7C	38.0	282.0	Provided to Geotechnical Engineers, Inc., for cyclic triaxial testing																	

Table 2 (continued)
SUMMARY OF LABORATORY TESTING OF UNDISTURBED SAMPLES FROM BORING P-16

Sample Number	Depth (ft)	Elevation (ft)	USCS Group Symbol	Fines (%)	Water Content (wt %)	Dry Unit Weight γ_d				Void Ratio e		Saturation S		Unconsolidated-Undrained Compression Test					Condition of Tube Cutting Edge	
						A (pcf)	B (pcf)	C (pcf)	D (pcf)	A	E	A (%)	E (%)	Specimen Diameter (in.)	σ_c (kef)	q_u (max) (kef)	ϵ_f (%)	$^s u$ At 8% (kef)		Mode of Failure Specimen
ST-8	42.5	277.5	Provided to USAE Waterways Experiment Station for cyclic triaxial testing												Not viewed					
ST-9A	47.5	272.5	SM	10-20	33.2	—	—	—	—	—	—	—	—	—	—	—	—	—	—	Fair
ST-9B	47.7	272.3	SM	10-20	30.8	91.2	89.4	89.2	—	0.834	0.875	99.0	94.3	—	—	—	—	—	—	
ST-9D	48.0	272.0	Provided to USAE Waterways Experiment Station																	
ST-9E	48.4	271.6	SM	10-20	31.0	92.9	91.2	88.5	—	0.800	0.890	103.8	93.3	—	—	—	—	—	—	
ST-9F	48.9	271.1	SM	10-20	29.8	93.7	91.9	88.6	—	0.785	0.887	101.7	90.0	—	—	—	—	—	—	
ST-9G	49.3	270.7	SM	20	30.7	—	—	—	—	—	—	—	—	—	—	—	—	—	—	
ST-10	52.5	267.5	Provided to USAE Waterways Experiment Station for cyclic triaxial testing												Not viewed					
ST-11A	57.5	262.5	SM	10-15	22.5	—	—	—	—	—	—	—	—	—	—	—	—	—	—	Bent
ST-11B	57.7	262.3	SM	10-15	20.4	106.8	104.7	104.4	—	0.566	0.602	96.6	90.8	—	—	—	—	—	—	deeply inward
ST-11E	58.0	262.0	SM	10-15	22.3	—	—	—	—	—	—	—	—	—	—	—	—	—	—	
ST-11F	58.4	261.6	SP-SM	8-12	21.0	107.2	105.1	101.7	—	0.560	0.644	100.5	87.4	2.87	7.09	5.67	13.5	1.91	Bulging	
ST-11G	59.0	261.0	SM	21	23.4	—	—	—	—	—	—	—	—	—	—	—	—	—	—	
ST-12A	62.5	257.5	SM	17	23.1	—	—	—	—	—	—	—	—	—	—	—	—	—	—	Large inward dent
ST-12E	62.6	257.4	SM	15-20	23.4	104.0	101.9	98.9	—	0.608	0.691	103.1	90.8	—	—	—	—	—	—	
ST-12F	63.1	256.9	SM	15-20	19.1	109.5	107.4	—	—	0.527	—	97.1	—	—	—	—	—	—	—	
ST-12G	63.9	256.1	SM	15	15.6	—	—	—	—	—	—	—	—	—	—	—	—	—	—	
ST-13A	67.5	252.5	SM	20-30	20.4	—	—	—	—	—	—	—	—	—	—	—	—	—	—	Very good
ST-13B	67.8	252.2	SM	20-30	20.8	108.9	106.6	106.0	—	0.536	0.578	104.0	96.4	—	—	—	—	—	—	
ST-13E	68.1	251.9	Preserved in tube																	
ST-13F	68.4	251.6	SM	25-30	20.2	109.5	107.3	101.1	—	0.527	0.654	102.7	82.8	2.88	8.34	2.35	6.8	1.17	Shearing	
ST-13G	69.0	251.0	SM	26	22.1	—	—	—	—	—	—	—	—	—	—	—	—	—	—	

Table 3
SUMMARY OF LABORATORY TESTING OF UNDISTURBED SAMPLES FROM BORING P-17

Sample Number	Depth (ft)	Elevation (ft)	USCS Group Symbol	Fines (%)	Water Content (wt %)	Dry Unit Weight γ_d				Void Ratio e		Saturation S		Unconsolidated-Undrained Compression Test						Condition of Tube Cutting Edge
						A (pcf)	B (pcf)	C (pcf)	D (pcf)	A	E	A (%)	E (%)	Specimen Diameter (in.)	σ_c (kef)	q_u (max) (kef)	ϵ_f (%)	s_u At 8% (kef)	Mode of Failure Specimen	
ST-1A	7.5	312.5	CH-SC	55-60	18.1	—	—	—	—	—	—	—	—	—	—	—	—	—	—	Not viewed
ST-1B	7.8	312.2	CH-SC	55-60	26.2	97.4	95.6	—	—	0.717	—	97.9	—	—	—	—	—	—	—	Not viewed
ST-1F	8.1	311.9	Preserved in tube				—	—	—	—	—	—	—	—	—	—	—	—	—	—
ST-1G	—	—	—				—	—	—	—	—	—	—	—	—	—	—	—	—	—
ST-2A	12.5	307.5	CH-SC	66	33.5	—	—	—	—	—	—	—	—	—	—	—	—	—	—	Bent deeply inward
ST-2F	12.6	307.4	Preserved in tube				—	—	—	—	—	—	—	—	—	—	—	—	—	—
ST-2G	13.9	306.1	SC-CH	44	22.1	—	—	—	—	—	—	—	—	—	—	—	—	—	—	Bent deeply inward
ST-3A	17.5	302.5	MH	70-80	30.4	—	—	—	—	—	—	—	—	—	—	—	—	—	—	Good
ST-3B	17.8	302.2	MH-SM	55-65	22.2	105.6	103.5	104.2	—	0.584	0.605	101.9	98.3	—	—	—	—	—	—	Good
ST-3F	18.1	301.9	Preserved in tube				—	—	—	—	—	—	—	—	—	—	—	—	—	—
ST-3G	19.3	300.7	CH-SC	54	16.2	—	—	—	—	—	—	—	—	—	—	—	—	—	—	Good
ST-4A	22.5	297.5	Preserved in tube				—	—	—	—	—	—	—	—	—	—	—	—	—	—
ST-4F	23.8	296.2	SM-ML	40-50	23.9	100.7	99.8	96.0	—	0.661	0.742	105.8	94.3	—	—	—	—	—	—	Very good
ST-4G	24.2	295.8	SM-ML	45	26.1	—	—	—	—	—	—	—	—	—	—	—	—	—	—	Very good
ST-5A	27.5	292.5	MH-SM	55-60	24.0	—	—	—	—	—	—	—	—	—	—	—	—	—	—	Deeply dented
ST-5F	27.6	292.4	Preserved in tube				—	—	—	—	—	—	—	—	—	—	—	—	—	—
ST-5G	28.1	291.9	ML-SM	55	24.4	—	—	—	—	—	—	—	—	—	—	—	—	—	—	Deeply dented
Interface between embankment and foundation at about elev. 288.0																				
ST-6A	32.5	287.5	SC-CH	40-48	17.6	—	—	—	—	—	—	—	—	—	—	—	—	—	—	Very good
ST-6E	32.7	287.3	Preserved in tube				—	—	—	—	—	—	—	—	—	—	—	—	—	—
ST-6F	33.6	286.4	SC-CH	35-40	13.9	114.4	112.2	110.6	—	0.462	0.512	80.6	72.8	2.88	3.99	11.19	9.0	5.50	Shearing	Very good
ST-6G	34.1	285.9	SC-CH	38	15.1	—	—	—	—	—	—	—	—	—	—	—	—	—	—	Very good
ST-7A	37.5	282.5	SM-ML	40-48	29.9	—	—	—	—	—	—	—	—	—	—	—	—	—	—	Very good
ST-7B	37.8	282.2	SM-ML	40-48	34.0	88.1	86.4	86.6	—	0.898	0.931	101.5	97.9	—	—	—	—	—	—	Very good
ST-7E	38.2	281.8	Preserved in tube				—	—	—	—	—	—	—	—	—	—	—	—	—	—
ST-7F	38.7	281.3	SM-ML	35-45	31.9	86.1	84.5	83.4	—	0.942	1.005	90.8	85.1	2.87	4.63	3.40	14.6	1.59	Shearing	Very good
ST-7G	39.2	280.8	SM-ML	44	36.4	—	—	—	—	—	—	—	—	—	—	—	—	—	—	Very good
ST-8	42.5	277.5	Provided to USAE Waterways Experiment Station for cyclic triaxial testing				—	—	—	—	—	—	—	—	—	—	—	—	—	—
ST-9A	47.5	272.5	SM-ML	30-45	45.5	—	—	—	—	—	—	—	—	—	—	—	—	—	—	Not viewed
ST-9B	47.8	272.2	SM-ML	30-40	38.4	86.3	84.6	82.9	—	0.938	1.017	109.7	101.2	—	—	—	—	—	—	Not viewed
ST-9C	48.1	271.9	Provided to Goetechnical Engineers, Inc., for cyclic triaxial testing				—	—	—	—	—	—	—	—	—	—	—	—	—	—

Table 3 (continued)
SUMMARY OF LABORATORY TESTING OF UNDISTURBED SAMPLES FROM BORING P-17

Sample Number	Depth (ft)	Elevation (ft)	USCS Group Symbol	Fines (%)	Water Content (wt %)	Dry Unit Weight γ_d				Void Ratio e		Saturation S		Unconsolidated-Undrained Compression Test						Condition of Tube Cutting Edge
						A (pcf)	B (pcf)	C (pcf)	D (pcf)	A	E	A (%)	E (%)	Specimen Diameter (in.)	σ_c (kef)	q_u (max) (kef)	ϵ_f (%)	s_u At 8% (kef)	Mode of Failure Specimen	
ST-10	52.5	267.5	Provided to USAE Waterways Experiment Station for cyclic triaxial testing																	
ST-11A	57.5	262.5	SM	12-22	27.4	—	—	—	—	—	—	—	—	—	—	—	—	—	—	Very good
ST-11B	57.8	262.2	SM	12-22	38.8	95.6	93.7	93.0	—	0.749	0.798	110.2	103.4	—	—	—	—	—	—	
ST-11E	58.1	261.9	SM-ML	40	40.2	83.5	81.8	81.4	—	1.043	1.054	107.4	102.2	2.87	7.07	2.28	10.7	1.09	With foliation at 60°	
ST-11F	58.7	261.3	SM-ML	40-45	46.5	77.5	76.0	74.6	—	1.158	1.242	107.6	100.3	2.87	7.13	2.41	10.5	1.18	Shearing	
ST-11G	59.2	260.8	SM-ML	44	49.4	—	—	—	—	—	—	—	—	—	—	—	—	—	—	
ST-12A	62.5	257.5	GP	3-8	—	—	—	—	—	—	—	—	—	—	—	—	—	—	—	One small dent
ST-12B	62.6	257.4	SM	20-30	27.4	—	—	—	—	—	—	—	—	—	—	—	—	—	—	
ST-12D	62.7	257.3	Preserved in tube																	
ST-12E	62.9	257.1	SM	25-35	21.9	105.0	130.0	97.9	—	0.593	0.708	99.0	82.9	2.88	7.65	8.07	14.5	3.24	Bulging	
ST-12F	63.5	256.5	SM	10-20	31.1	93.6	91.8	87.3	—	0.787	0.916	105.9	91.0	2.90	7.74	4.51	12.1	2.04	Shearing	
ST-12G	64.0	256.0	SM	28	31.9	—	—	—	—	—	—	—	—	—	—	—	—	—	—	
ST-13A	67.5	252.5	SM	15-20	22.3	—	—	—	—	—	—	—	—	—	—	—	—	—	—	One deep inward dent
ST-13B	67.8	252.2	SM	15-20	20.6	110.4	108.4	105.7	—	0.515	0.582	107.2	94.9	—	—	—	—	—	—	
ST-13F	68.1	251.9	SM	15-20	23.3	106.0	104.0	101.5	—	0.578	0.648	108.0	96.4	2.88	8.31	3.19	7.2	1.54	With foliation at 55°	
ST-134G	68.6	251.4	EMPTY																	
ST-14A	72.5	247.5	SM	15-25	26.6	—	—	—	—	—	—	—	—	—	—	—	—	—	—	Badly dented
ST-14F	72.6	247.4	SM	—	—	Sample disturbed: void in center due to separation on horizontal plane											—	—		
ST-14G	73.6	246.4	SM	18	26.9	—	—	—	—	—	—	—	—	—	—	—	—	—	—	

Table 4
SUMMARY OF LABORATORY TESTING OF UNDISTURBED SAMPLES FROM BORING SWR-11

Sample Number	Depth (ft)	Elevation (ft)	USCS Group Symbol	Fines (%)	Water Content (wt %)	Dry Unit Weight γ_d				Void Ratio e		Saturation S		Unconsolidated-Undrained Compression Test						Condition of Tube Cutting Edge
						A	B	C	D	A	E	A	E	Specimen Diameter (in.)	σ_c (kef)	q_u (max) (kef)	ϵ_f (%)	s_u At 8% (kef)	Mode of Failure Specimen	
						(pcf)	(pcf)	(pcf)	(pcf)	(%)	(%)	(%)	(%)							
ST-1	19.5	276.5	Provided to Geotechnical Engineers, Inc., for cyclic triaxial testing												Not viewed					
ST-2A	25.0	271.0	SM	25-35	42.5	—	—	—	—	—	—	—	—	—	—	—	—	—	—	Very good
ST-2B	25.2	270.8	SM	25-35	43.7	79.9	78.4	78.6	—	1.093	1.128	107.2	103.8	—	—	—	—	—	—	Very good
ST-2E	25.7	270.3	Preserved in tube																	
ST-2F	26.1	269.9	SM	20-30	32.8	93.6	1.8	90.7	—	0.787	0.844	111.7	104.2	2.89	3.41	1.40	>15	0.51	In clay seam at 65°	—
ST-2G	26.8	269.2	SM	20-30	25.6	—	—	—	—	—	—	—	—	—	—	—	—	—	—	—
ST-3A	30.5	265.5	SM	15-20	37.0	—	—	—	—	—	—	—	—	—	—	—	—	—	—	Very good
ST-3B	30.7	265.3	SM	15-20	33.1	101.0	99.0	96.5	—	0.656	0.733	135.2	121.0	—	—	—	—	—	—	Very good
ST-3G	31.0	265.0	SM	29	24.2	—	—	—	—	—	—	—	—	—	—	—	—	—	—	—

Table 6
SUMMARY OF LABORATORY TESTING OF UNDISTURBED SAMPLES FROM BORING SWR-13

Sample Number	Depth (ft)	Elevation (ft)	USCS Group Symbol	Fines (%)	Water Content (wt %)	Dry Unit Weight γ_d				Void Ratio e		Saturation S		Unconsolidated-Undrained Compression Test						Condition of Tube Cutting Edge		
						A (pcf)	B (pcf)	C (pcf)	D (pcf)	A	E	A (%)	E (%)	Specimen Diameter (in.)	σ_c (kef)	q_u (max) (kef)	ϵ_f (%)	s_u At 8% (kef)	Mode of Failure Specimen			
ST-1A	13.9	275.1	SM	10-15	41.3	—	—	—	—	—	—	—	—	—	—	—	—	—	—	—	Fair	
ST-1B	14.1	274.9	SM	10-15	27.7	90.2	89.0	90.1	—	0.842	0.856	88.2	86.7	—	—	—	—	—	—	—	—	—
ST-1E	14.3	274.7	Preserved in tube																			
ST-1F	14.9	274.1	SM	10-15	40.3	82.8	81.3	80.5	—	1.020	1.077	105.9	100.3	—	—	—	—	—	—	—	—	
ST-1G	15.3	273.7	SM	10-15	—	—	—	—	—	—	—	—	—	—	—	—	—	—	—	—	—	
ST-2A	16.0	273.0	Preserved in tube																			Very good
ST-2F	16.6	272.4	SM	20-25	48.5	77.2	75.8	—	70.0	1.166	1.389	111.5	93.6	1.43	2.24	1.19	12.7	0.55	Bulging and shearing	—	good	
ST-2G	17.0	272.0	SM	19	40.5	—	—	—	—	—	—	—	—	—	—	—	—	—	—	—	—	—
ST-3A	18.0	271.0	Empty																			Very good
ST-3B	18.0	271.0	SM	15-25	38.9	—	—	—	—	—	—	—	—	—	—	—	—	—	—	—	—	good
ST-3C	18.4	270.6	SM	15-25	45.4	79.2	77.8	76.8	—	1.111	1.177	109.5	103.4	—	—	—	—	—	—	—	—	—
ST-3F	18.6	270.4	SM	15	41.9	81.5	79.9	78.9	—	1.052	1.120	106.7	100.3	2.88	2.50	1.36	>15	0.55	With foliation at 50°	—	—	
ST-3G	19.1	269.9	SM	15	42.0	—	—	—	—	—	—	—	—	—	—	—	—	—	—	—	—	—
ST-4A	20.1	268.9	Preserved in tube																			Very good
ST-4F	21.1	267.9	SM	15-20	42.4	81.3	79.6	78.2	74.9	1.057	1.233	107.5	92.2	1.44	2.80	1.39	>15	0.57	Bulging in weak zone	—	good	
ST-4G	21.3	267.7	SM	17	42.0	—	—	—	—	—	—	—	—	—	—	—	—	—	—	—	—	—
ST-5A	22.1	266.9	Empty																			Good
ST-5B	22.3	266.7	SM	10-20	40.0	—	—	—	—	—	—	—	—	—	—	—	—	—	—	—	—	—
ST-5C	22.6	266.4	SM	10-20	43.7	80.0	78.4	79.0	—	1.090	1.117	107.4	104.8	—	—	—	—	—	—	—	—	—
ST-5F	22.8	266.2	SM	30	49.2	74.9	73.5	71.3	—	1.233	1.345	106.9	98.0	2.89	3.01	1.38	7.3	0.66	With foliation at 50°	—	—	
ST-5G	23.3	265.7	SM	25-30	36.2	—	—	—	—	—	—	—	—	—	—	—	—	—	—	—	—	—
ST-6A	24.2	264.8	SM	15-20	55.3	—	—	—	—	—	—	—	—	—	—	—	—	—	—	—	—	Very good
ST-6B	24.4	264.6	SM	15-20	57.3	69.4	68.1	—	—	1.410	1.456	108.9	105.5	—	—	—	—	—	—	—	—	good
ST-6E	24.6	264.4	Preserved in tube																			
ST-6F	25.2	263.8	SM	18	39.0	86.0	84.3	81.3	—	0.945	1.057	110.6	98.9	2.89	3.31	1.32	12.4	0.59	In clean sand layer	—	—	
ST-6G	25.6	264.4	SM	15-20	40.5	—	—	—	—	—	—	—	—	—	—	—	—	—	—	—	—	—
ST-7A	26.2	262.8	SM	10-15	37.9	—	—	—	—	—	—	—	—	—	—	—	—	—	—	—	—	Very good
ST-7B	26.4	262.6	SM	10-15	47.5	76.3	74.8	—	—	1.192	—	106.8	—	—	—	—	—	—	—	—	—	good
ST-7E	26.7	262.3	Preserved in tube																			
ST-7F	27.2	261.8	SM	29	40.6	83.7	82.1	79.7	—	0.998	1.098	109.0	99.1	2.89	3.55	1.32	12.7	0.63	With foliation at 40°	—	—	
ST-7G	27.6	261.4	SM	25-30	38.7	—	—	—	—	—	—	—	—	—	—	—	—	—	—	—	—	—

Table 6 (continued)
SUMMARY OF LABORATORY TESTING OF UNDISTURBED SAMPLES FROM BORING SWR-13

Sample Number	Depth (ft)	Elevation (ft)	USCS Group Symbol	Fines (%)	Water Content (wt %)	Dry Unit Weight γ_d				Void Ratio e		Saturation S		Unconsolidated-Undrained Compression Test						Condition of Tube Cutting Edge	
						A (pcf)	B (pcf)	C (pcf)	D (pcf)	A	E	A (%)	E (%)	Specimen Diameter (in.)	σ_c (kef)	q_u (max) (kef)	ϵ_r (%)	s_u At 8% (kef)	Mode of Failure Specimen		
ST-8A	28.3	260.7	SM	15-20	30.3	—	—	—	—	—	—	—	—	—	—	—	—	—	—	—	Very good
ST-8D	28.4	260.6	Preserved in tube																		
ST-8E	28.8	260.2	SM	15-20	23.9	91.1	89.3	87.6	—	0.836	0.909	105.5	97.0	2.89	3.76	1.32	12.0	0.58	With foliation at 60°	—	
ST-8F	29.2	259.8	SM	15-20	30.2	94.4	92.8	90.8	—	0.772	0.842	104.8	96.1	—	—	—	—	—	—	—	—
ST-8G	29.5	259.5	SM	20	27.9	—	—	—	—	—	—	—	—	—	—	—	—	—	—	—	—
ST-9A	47.5	272.5	SM-ML	35-45	36.0	—	—	—	—	—	—	—	—	—	—	—	—	—	—	—	Not viewed
ST-9B	47.8	272.2	SM-ML	35-45	35.6	76.9	75.4	74.6	—	1.175	1.242	81.2	76.8	—	—	—	—	—	—	—	—
ST-9C	48.1	271.1	Provided to Geotechnical Engineers, Inc., for cyclic triaxial testing																		
ST-10A	52.2	267.5	Empty																		
ST-10D	52.6	267.4	Preserved in tube																		
ST-10E	53.2	266.8	SM-ML	40-45	39.9	77.0	75.5	74.4	—	1.172	1.248	91.2	85.7	2.87	6.48	3.79	10.9	1.88	Slip on weak seam	—	
ST-10F	53.7	266.3	SM-ML	40-45	39.2	75.7	74.3	73.4	—	1.209	1.278	86.9	82.2	2.87	6.54	5.43	5.7	2.68	Bulging	—	
ST-10G	54.2	265.8	SM-ML	46	42.4	—	—	—	—	—	—	—	—	—	—	—	—	—	—	—	—
ST-11A	57.5	262.5	SM	30-40	32.5	—	—	—	—	—	—	—	—	—	—	—	—	—	—	—	Few small dents
ST-11B	57.8	262.2	SM	30-40	32.0	90.8	89.1	86.9	—	0.842	0.924	101.9	92.8	—	—	—	—	—	—	—	—
ST-11D	58.1	261.9	Preserved in tube																		
ST-11E	58.4	261.6	SM	10-15	15.4	113.7	111.5	108.7	—	0.471	0.538	70.6	76.7	2.88	7.14	5.84	4.6	2.54	Shear in quartz vein	—	
ST-11F	59.0	261.0	SM	30-40	28.8	93.2	90.9	88.9	—	0.794	0.881	97.2	87.6	—	—	—	—	—	—	—	—
ST-11G	59.3	260.7	SM	30-40	24.6	—	—	—	—	—	—	—	—	—	—	—	—	—	—	—	—
ST-12A	62.5	257.5	SM	20-30	23.3	—	—	—	—	—	—	—	—	—	—	—	—	—	—	—	Fair
ST-12C	62.6	257.4	Preserved in tube																		
ST-12D	63.3	256.7	SM-ML	45	37.3	—	—	—	79.4	—	1.106	—	90.4	Constant-volume direct shear test						—	
ST-12E	63.5	256.5	Preserved in tube																		
ST-12F	63.8	256.2	SM	35-40	41.3	80.8	79.3	76.9	—	1.070	1.175	103.4	94.2	2.87	7.81	2.51	12.0	1.19	With foliation at 60°	—	
ST-12G	64.4	255.6	SM	40	42.4	—	—	—	—	—	—	—	—	—	—	—	—	—	—	—	—
ST-13A	67.5	252.5	SM-ML	40-45	47.8	—	—	—	—	—	—	—	—	—	—	—	—	—	—	—	One small dent
ST-13B	67.7	252.3	SM-ML	43	37.4	—	—	—	—	—	—	—	—	—	—	—	—	—	—	—	—
ST-13C	68.0	252.0	SM-ML	40-45	42.0	82.3	80.7	—	1.032	—	109.1	—	—	—	—	—	—	—	—	—	—
ST-13D	68.3	251.7	SM-ML	40-45	—	—	—	—	—	—	—	—	—	—	—	—	—	—	—	—	—
ST-13E	68.4	251.6	SM-ML	40-45	36.6	86.1	84.4	82.2	—	0.942	1.034	104.1	94.9	2.87	8.39	2.27	13.8	1.00	With foliation at 60°	—	

Table 6 (continued)
 SUMMARY OF LABORATORY TESTING OF UNDISTURBED SAMPLES FROM BORING SWR-13

Sample Number	Depth (ft)	Elevation (ft)	USCS Group Symbol	Fines (%)	Water Content (wt %)	Dry Unit Weight γ_d				Void Ratio e		Saturation S		Unconsolidated-Undrained Compression Test					Condition of Tube Cutting Edge	
						A (pcf)	B (pcf)	C (pcf)	D (pcf)	A	E	A (%)	E (%)	Specimen Diameter (in.)	σ_c (kef)	q_u (max) (kef)	ϵ_r (%)	s_u At 8% (kef)		Mode of Failure Specimen
ST-13F	69.0	251.0	SM-ML	50	47.4	75.5	74.1	72.2	—	1.215	1.316	104.6	96.5	—	—	—	—	—	—	—
ST-13G	69.4	250.6	SM-ML	40-45	36.4	—	—	—	—	—	—	—	—	—	—	—	—	—	—	—

Table 5
SUMMARY OF LABORATORY TESTING OF UNDISTURBED SAMPLES FROM BORING SWR-12

Sample Number	Depth (ft)	Elevation (ft)	USCS Group Symbol	Fines (%)	Water Content (wt %)	Dry Unit Weight γ_d				Void Ratio e		Saturation S		Unconsolidated-Undrained Compression Test						Condition of Tube Cutting Edge
						A (pcf)	B (pcf)	C (pcf)	D (pcf)	A	E	A (%)	E (%)	Specimen Diameter (in.)	σ_c (kef)	q_u (max) (kef)	ϵ_f (%)	s_u At 8% (kef)	Mode of Failure Specimen	
ST-1A	7.5	312.5	ML-SM	55-65	24.5	—	—	—	—	—	—	—	—	—	—	—	—	—	—	Good
ST-1B	7.9	312.1	ML-SM	55-65	27.8	—	94.1	94.2	—	0.744	0.775	100.1	96.1	—	—	—	—	—	—	
ST-1E	8.2	311.8	Preserved in tube																	
ST-1F	9.0	311.0	SM	29	19.3	—	—	—	—	—	—	—	—	—	—	—	—	—	—	
ST-1G	9.2	310.8	CH-SC		29.7	—	—	—	—	—	—	—	—	—	—	—	—	—	—	
ST-2A	12.5	307.5	ML-SM	60-70	26.1	—	—	—	—	—	—	—	—	—	—	—	—	—	—	Fair
ST-2E	12.6	307.4	Preserved in tube																	
ST-2F	13.5	306.5	SM-ML	45-50	20.4	—	—	103.8	—	0.533	0.611	102.6	89.5	—	—	—	—	—	—	
ST-2G	14.0	306.0	SM-ML	48	20.3	—	—	—	—	—	—	—	—	—	—	—	—	—	—	
ST-3A	17.5	302.5	ML	70-80	25.6	—	—	—	—	—	—	—	—	—	—	—	—	—	—	Not viewed
ST-3B	17.8	302.2	ML	70-80	24.3	—	—	—	—	—	—	—	—	—	—	—	—	—	—	
ST-3C	18.1	301.9	SM-ML	20-30	23.9	102.0	100.1	100.1	—	0.640	0.671	100.1	95.5	—	—	—	—	—	—	
ST-3F	18.4	301.6	Preserved in tube																	
ST-3G																				
ST-4A	22.5	297.5	SM-ML	49	25.6	—	—	—	—	—	—	—	—	—	—	—	—	—	—	Fair
ST-4E	22.7	297.3	Preserved in tube																	
ST-4F	23.8	296.2	SM-ML	40-45	26.0	97.6	95.8	92.1	—	0.713	0.816	97.7	85.4	2.87	2.84	4.90	6.6	2.31	Shearing	
ST-4G	24.3	295.7	CH-SC	62	28.5	—	—	—	—	—	—	—	—	—	—	—	—	—	—	
Interface between embankment and foundation at exactly elevation 295.8 (near bottom of test specimen)																				
ST-5A	27.5	292.5	SM-ML	30-40	21.4	—	—	—	—	—	—	—	—	—	—	—	—	—	—	Few small dents
ST-5B	27.8	292.2	SM-ML	30-40	31.2	77.3	75.8	74.9	—	1.163	1.233	71.9	67.8	—	—	—	—	—	—	
ST-5E	28.2	291.8	Consumed for visual-manual examination																	
ST-5F	29.0	291.0	SM-ML	30-40	34.3	71.0	68.7	—	—	1.355	—	67.8	—	—	—	—	—	—	—	
ST-5G	29.3	290.7	SM-ML	30-40	35.8	—	—	—	—	—	—	—	—	—	—	—	—	—	—	
ST-6A	32.5	287.5	SM	20-30	19.4	—	—	—	—	—	—	—	—	—	—	—	—	—	—	Very good
ST-6D	32.7	287.3	SM	31	23.5	89.3	87.5	84.9	—	0.873	0.970	72.1	64.9	2.87	3.92	5.17	6.0	1.92	With foliation at 50°	
ST-6E	33.3	286.7	ML-SM	53	33.3	71.9	70.5	—	—	1.326	—	67.3	—	—	—	—	—	—	—	
ST-6F	33.8	286.2	CH	90-95		73.6	70.8	—	—	1.323	—	78.8	—	—	—	—	—	—	—	
ST-6G	34.3	285.7	ML	70-80	36.1	—	—	—	—	—	—	—	—	—	—	—	—	—	—	

Table 5 (continued)
SUMMARY OF LABORATORY TESTING OF UNDISTURBED SAMPLES FROM BORING SWR-12

Sample Number	Depth (ft)	Elevation (ft)	USCS Group Symbol	Fines (%)	Water Content (wt %)	Dry Unit Weight γ_d				Void Ratio e		Saturation S		Unconsolidated-Undrained Compression Test					Condition of Tube Cutting Edge	
						A (pcf)	B (pcf)	C (pcf)	D (pcf)	A	E	A (%)	E (%)	Specimen Diameter (in.)	σ_c (kef)	q_u (max) (kef)	ϵ_f (%)	ϵ_u At 8% (kef)		Mode of Failure Specimen
ST-7A	37.5	282.5	SM	10-15	—	—	—	—	—	—	—	—	—	—	—	—	—	—	—	Few small dents
ST-7B	37.7	282.3	SM	10-15	29.0	79.4	77.9	—	—	1.106	—	70.3	—	—	—	—	—	—	—	
ST-7E	38.0	282.0	Preserved in tube																	
ST-7F	38.9	281.1	SM	10-15	16.5	85.8	84.2	75.3	—	0.949	1.221	46.6	36.2	—	—	—	—	—	—	
ST-7G	39.3	280.7	SM	10-15	18.0	—	—	—	—	—	—	—	—	—	—	—	—	—	—	
ST-8A	42.5	266.5	SM	33	23.2	—	—	—	—	—	—	—	—	—	—	—	—	—	—	Good
ST-8E	42.6	277.4	Preserved in tube																	
ST-8F	43.6	276.4	SM	30-35	23.5	84.1	82.5	80.8	—	0.988	1.070	63.7	58.9	2.88	5.30	6.04	15.0	2.65	—	Shear across foliation
ST-8G	44.2	275.8	SM	34	22.7	—	—	—	—	—	—	—	—	—	—	—	—	—	—	
ST-9A	30.3	258.7	Empty																	
ST-9B	30.6	258.4	SM	10-20	24.3	—	—	—	—	—	—	—	—	—	—	—	—	—	—	Very good
ST-9C	30.9	258.1	SM	10-20	23.5	108.1	101.1	99.9	—	0.622	0.674	101.3	98.6	—	—	—	—	—	—	
ST-9F	31.2	257.8	SM	10-15	22.0	100.2	104.2	101.0	—	0.575	0.656	102.5	89.9	2.88	4.06	4.29	>15	1.43	—	Bulging
ST-9G	31.6	257.4	SM	10-15	21.8	—	—	—	—	—	—	—	—	—	—	—	—	—	—	
ST-10A	32.4	256.6	SM	24	30.9	—	—	—	—	—	—	—	—	—	—	—	—	—	—	Very
ST-10D	32.5	256.5	Preserved in tube																	
ST-10E	32.7	256.3	SM	20-25	22.4	105.4	103.2	101.5	—	0.587	0.648	104.6	94.7	2.88	4.25	2.20	15.0	0.90	—	With foliation at 50°
ST-10F	33.2	255.8	SM	15-20	24.0	104.0	102.0	97.8	96.1	0.608	0.740	105.8	86.9	1.42	4.31	4.40	11.3	1.91	—	Bulging
ST-10G	33.5	255.5	SM-ML	43	34.2	—	—	—	—	—	—	—	—	—	—	—	—	—	—	
ST-11A	34.8	254.2	SM	15-25	26.4	—	—	—	—	—	—	—	—	—	—	—	—	—	—	
ST-11B	35.0	254.0	SM	15-25	26.1	98.5	96.6	96.7	—	0.698	0.729	102.9	98.5	—	—	—	—	—	—	
ST-11E	35.2	253.8																		
ST-11F																				
ST-11G																				

Table 5 (continued)
SUMMARY OF LABORATORY TESTING OF UNDISTURBED SAMPLES FROM BORING SWR-12

Sample Number	Depth (ft)	Elevation (ft)	USCS Group Symbol	Fines (%)	Water Content (wt %)	Dry Unit Weight γ_d				Void Ratio e		Saturation S		Unconsolidated-Undrained Compression Test						Condition of Tube Cutting Edge	
						A (pcf)	B (pcf)	C (pcf)	D (pcf)	A	E	A (%)	E (%)	Specimen Diameter (in.)	σ_c (kef)	q_u (max) (kef)	ϵ_f (%)	s_u At 8% (kef)	Mode of Failure Specimen		
ST-12A	36.5	252.5	Preserved in tube																		
ST-12E	36.7	252.3	SM	25-35	31.5	94.2	92.4	91.3	—	0.775	0.832	108.9	101.5	2.87	4.75	1.54	11.3	0.74	With foliation at 45°	Bent deeply inward	
ST-12F	37.2	251.8	SM	29	31.8	94.2	92.3	90.3	86.6	0.775	0.931	110.0	91.5	1.43	4.80	2.18	>15	0.96	Shearing		
ST-12G	37.5	251.5	SM	15-20	29.3	—	—	—	—	—	—	—	—	—	—	—	—	—	—		

respectively) gave stress-strain curves (Figure 11 Sheets 6-7) showing a relative freedom from disturbance.

3. Composition of Saprolite

Thin sections of samples from borings SWR-3, SWR-4, SWR-5, SWR-7, and P-10 (Table 7) were examined in order to determine in a qualitative manner the fabric, texture, and mineralogy of the saprolite beneath the service water reservoir dike (see boring location plan, Figure 12).

The analysis was undertaken to clarify some of the results of soil classification and laboratory analyses, and to clarify the engineering behavior of the saprolite. Twenty-seven thin sections were examined under plane and polarized light at various magnifications up to 400x.

Sections were cut at various angles to the visible banding in undisturbed samples. Part a of Figure 13 shows a section cut perpendicular to the plane of foliation. Other sections were cut parallel to the foliation in both felsic (quartz- and feldspar-rich) layers and mafic (biotite-rich) layers to see if any minerals were oriented in the plane of foliation. Large sections (1.75-inch x 2-inch) were cut horizontally across six of the samples, and small sections (1-inch x 1.75-inch) were cut vertically at the ends of the large sections. A wide range of orientations of section to foliation resulted from the procedure.

Percentage of minerals present in the thin sections was estimated by scanning the sections under low magnification or by projection of the thin section onto a screen using a slide projector. Size of grains was estimated by using a micrometer eyepiece in the polarizing microscope. Major minerals were identified by standard optical petrographic techniques; accessory and trace minerals were ignored for this analysis.

Fabric

The fabric of the saprolite is shown in Part a of Figure 13. The fabric is that of the parent rock, a biotitic granite gneiss. The saprolite consists of irregular planar bands of light-colored minerals in interlocking grains and irregular bands of dark-colored minerals in elongate grains. The strong foliation evident in the saprolite dips at angles of about 50 degrees from the horizontal. Some elongation of feldspar and quartz in the plane of the foliation occurs in one section, but no elongation is apparent in the direction perpendicular to the strike. Within the gneissic bands, the felsic grains are well interlocked and not strongly oriented. The biotite grains are strongly oriented with basal planes parallel to the plane of foliation. There is no apparent preferred alignment or elongation of the biotite within the plane of foliation. The biotite layers appear to be planes along which slippage could take place more readily than along the intervening well-interlocked felsic layers.

The fabric of the saprolite contrasts strongly with that of a sand (Part b of Figure 13). The sand shows no foliation and no interlocking of grains, even though the grains are quite angular.

The sand thin section also shows a well-developed void network unlike that of the saprolite. The fabric of saprolite is therefore not one of a transported soil but one of the parent rock material. The fabric is anisotropic; that is, it has strongly directional properties.

Texture

The textural relationships of the North Anna saprolite are shown in Parts a and c of Figure 13. Visual estimates of grain size in the thin sections yields a range of 0.05 to 10 mm. However, most of the grains fall in a much narrower range of about 0.1 to 2 mm. These size ranges are for discrete mineral grains observable under the microscope. Many “grains” with very sharp boundaries are composed of minute particles of clay minerals. The size of the individual clay minerals is too small to ascertain under the magnification available, but is smaller than 0.010 mm in most cases.

Therefore, although the grain size of the clay mineral aggregations or parent “grains” are similar to surrounding minerals in the interlocked fabric, the size of the clay within the “grains” is much smaller.

The most striking textural feature of the saprolite is the angularity and interlocking nature of the grains. There is no indication that individual grains are arranged so as to be able to reorient. On the contrary, any change in orientation of one grain would affect the surrounding grains because they are so completely locked geometrically in the overall fabric. The interlocking nature of the grains is shown in Part c of Figure 13.

The textural relationship of void space to grains is difficult to ascertain in the thin sections studied. There is no apparent volumetrically identifiable void network extensive enough to allow reorientation of grains (compare Parts a and b of Figure 13). Void space must occur along grain interfaces and within clay mineral aggregates as well as irregular joints and partially filled fractures. Many of the grains are fractured, but it is not known how much of the fracturing is due to the thin sectioning process. Clearly, some of the fractures are geologic because they are stained by weathering products.

The geometric interlocking of the grains and the lack of a void network that would allow reorientation of grains indicates that the saprolite could not liquefy.

Mineralogy

The mineralogy of the saprolite reflects to a large degree the mineralogy of the parent gneiss. The parent rock is composed mostly of quartz, microcline (potassium feldspar), and plagioclase (sodium-calcium feldspar), with minor to moderate amounts of biotite (brown to black mica). Other constituents are of minor importance and were ignored for the purposes of this investigation.

The mineralogy of the saprolite in thin section is seen to consist of quartz, microcline, clay minerals (unidentified as to type), and biotite. Much of the biotite is bleached and shows low birefringence. This is no doubt due to weathering and incipient hydration of the biotite. Quartz and microcline are clear and unaltered in thin section. There has been no significant corrosion of the grain boundaries. Plagioclase was identified only in one section, SWR-4 sample 6A2 from a depth of 77 feet (see Table 7). This grain is shown in Part c of Figure 13. Even at a depth of 77 feet, the plagioclase is nearly 50% altered to clay minerals. Clay aggregations in other thin sections retain the polygonal form of plagioclase grains and are therefore interpreted to be alteration products of plagioclase. The mineralogy of the clay aggregates are discussed in another section of this report.

The mineralogy of the saprolite therefore reflects a weathering process in which plagioclase feldspar has been converted to clay minerals, biotite has been bleached and partially hydrated, and quartz and microcline have remained unaffected. The weathering and change in mineral composition has not disrupted the relic fabric or significantly increased visible void space.

Visual estimates of mineral percentages yield the following:

Quartz	30% - 40%
Microcline	20% - 30%
Clay minerals	25% - 40%
Biotite	5% - 20%

Depth Relationships

Section P-10 sample 1 taken from a depth of 3 feet is not saprolite. No relic rock fabric is preserved. Each grain is an individual in a matrix of biotite and clay minerals with no apparent preferred orientation. The mineralogy is similar to that of the saprolite but the original fabric has been destroyed. This sample is interpreted to have been disturbed by near surface activity, either climatic or man-induced.

The saprolite from the greatest depth (77 feet) is somewhat less altered than that from samples above. Plagioclase is still recognizable and biotite is relatively fresh. Little iron oxide staining occurs at this depth. As depth decreases, the only apparent change is that plagioclase is entirely altered to clay, biotite becomes progressively more bleached, and straining is more abundant and pervasive. No significant change in fabric or texture occurs with decreasing depth until near the surface.

Clay Mineralogy

Dr. R. Torrence Martin has studied the clay mineralogy of samples taken just above those used for thin sectioning in the borings listed in Table 7. Previously he had also reported on the

Table 7
DATA FOR SAMPLES THIN SECTIONED

Boring Number	Sample Number	Depth Below Original Ground, ft	Percent Fines	Percent Water Content
P-10	1E	3	26	19
SWR-5	4B ^a	26	35	26
SWR-7	7B	26	38	23
SWR-4	2A1 ^a	27	36	24
SWR-3	4E	60	23	15
SWR-4	6A2 ^a	77	34	20

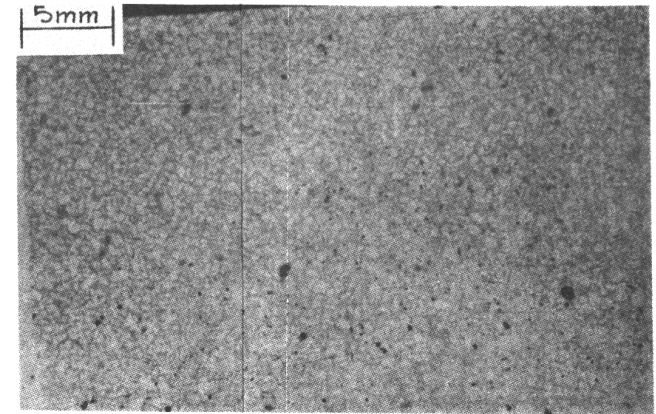
a. Oriented sections obtained.

a. Saprolite thin section cut perpendicular to relict foliation (SWR-4-6A2). Light bands composed of quartz, feldspar and clay minerals. Dark bands are biotite. Fabric and texture identical to parent rock. (plane light)



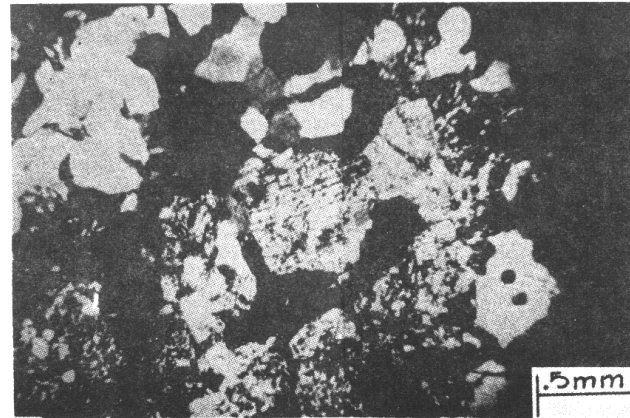
(a)

b. Thin section of sand. Grains are separate and void space is readily apparent. Dark grains are opaque minerals, gray is epoxy cement (void space) and white grains are mostly quartz with some feldspar. (plane light)



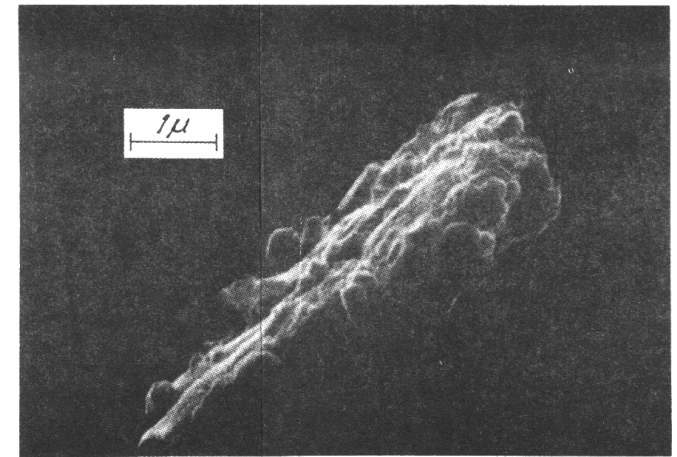
(b)

c. Photomicrograph of saprolite (SWR4-6A2) showing interlocking grains of quartz, microcline, plagioclase and clay after plagioclase. The grain with the striped appearance is plagioclase feldspar. The very fine grained white material is clay. Light and dark grains not mottled with clay specks are quartz and microcline. Note retention of polygonal outline of grains which have been altered to clay. (Polarized light)



(c)

d. Photomicrograph of halloysite (SWR-3-4F) under scanning electron microscope. Note small plates and tube arrangement of particles. Void space within the aggregate of clay particles is large. Size corresponds to fine silt range. (plane light)



(d)

N03EA430